Russian-German Cooperation: Laptev Sea System

Edited by
Heidemarie Kassens, Dieter Piepenburg,
Jörn Thiede, Leonid Timokhov,
Hans-Wolfgang Hubberten and
Sergey M. Priamikov

Ber. Polarforsch. 176 (1995)
ISSN 0176 - 5027

Russian-German Cooperation: Laptev Sea System

Edited by

Heidemarie Kassens
GEOMAR Research Center for Marine Geosciences, Kiel, Germany

Dieter Piepenburg
Institute for Polar Ecology, Kiel, Germany

Jörn Thiede
GEOMAR Research Center for Marine Geosciences, Kiel, Germany

Leonid Timokhov
Arctic and Antarctic Research Institute, St. Petersburg, Russia

Hans-Wolfgang Hubberten
Alfred-Wegener-Institute for Polar and Marine Research, Potsdam, Germany

and

Sergey M. Priamikov
Arctic and Antarctic Research Institute, St. Petersburg, Russia

TABLE OF CONTENTS

Preface i

Liste of Authors and Participants v

Modern Environment of the Laptev Sea 1

J. Afanasyeva, M. Lamakin and V. Timachev
Investigations of Air-Sea Interactions Carried out During the Transdrift II Expedition 3

V.P. Shevchenko , A.P. Lisitzin, V.M. Kuptzov, G.I. Ivanov, V.N. Lukashin, J.M. Martin, V.Yu. Rusakov, S.A. Safarova, V.V. Serova, R. van Grieken and H. van Malderen
The Composition of Aerosols over the Laptev, the Kara, the Barents, the Greenland and the Norwegian Sea 7

V.Yu. Alexandrov, H. Eicken and J. Kolatschek
Satellite Radar Monitoring of Ice Drift in the Laptev Sea 17

J. Kolatschek, T. Viehoff, H. Eicken, E. Nägelsbach and V. Alexandrov
Ice dynamics in the South-western Laptev Sea as Derived from ERS-1 SAR Images 20

Yu. Gorbunov, Z. Gudkovich and S. Losev
Full-Scale Field Experiment Carried out by the AARI in the South-eastern Laptev Sea (1976) and its Main Results 25

A.N. Darovskikh
Surface-Based Studies of Microwave Arctic Sea Ice Signatures During End of Summer and Early Autumn 28

A.P. Makshtas and I. Podgornyy
Calculation of Spectral Albedo for a Melt Pond 32

P.V. Bogorodskiy
Solution and Stability Criteria of Natural Convective Flow in a Melt Puddle 38

I.M. Ashik and Yu.A. Vanda
Catastrophic Storm Surges in the Southern Part of the Laptev Sea 43

I.M. Ashik
Numerical Prediction of Sea Surges and Ice Conditions in the Laptev and the East Siberian Seas 47

Yu.V. Nalimov
The Ice-Thermal Regime at Front Deltas of Rivers of the Laptev Sea 55

H. Eicken, T. Viehoff, T. Martin, J. Kolatschek, V. Alexandrov and E. Reimnitz
Studies of Clean and Sediment-laden Ice in the Laptev Sea 62

E. Reimnitz, H. Kassens and H. Eicken,
Sediment Transport by Laptev Sea Ice 71

D. Dethleff
Sea Ice and Sediment Export from the Laptev Sea Flaw Lead during 1991/92 Winter Season 78

U. Schauer, B. Rudels, R.D. Muench and L. Timokhov
Circulation and Water Mass Modifications along the Nansen Slope Basin 94

P.N. Golovin, V.A. Gribanov and I.A. Dmitrenko
Macro- and Mesoscale Hydrophysical Structure of the Outflow Zone of the Lena River Water to the Laptev Sea 99

V.N. Churun and L.A. Timokhov
Cold Bottom Water in the Southern Laptev Sea 107

I.A. Dmitrenko and TRANSDRIFT Shipboard Scientific Party
The Distribution of River Run-off in the Laptev Sea: The Environmental Effect 114

C. Hass, M. Antonow and Shipboard Scientific Party
Movement of Laptev Sea Shelf Waters During the TRANSDRIFT II Expedition 121

S.V. Pivovarov and V.M. Smagin
Distribution of Oxygen and Nutrients in the Laptev Sea in Summer 135

V.V. Ivanov and A.A. Piskun
Distribution of River Water and Suspended Sediments in the River Deltas of the Laptev Sea 142

V.P. Gordeev and V.P. Shevchenko
Chemical Composition of Suspended Sediments in the Lena River and its Mixing Zone 154

H. Erlenkeuser and TRANSDRIFT Shipboard Scientific Party
Stable Carbon Isotope Ratios in the Waters of the Laptev Sea/ Sept. '94 170

A.F. Anoshkin, I.K. Popov and I.E. Ushakov
Hydrooptical Measurements in the Laptev Sea: Spatial Distributions of Light Attenuation and Chlorophyll Fluorescence 178

V.V. Petryashov, E.L. Markhaseva, A.I. Pinchuk and S.D. Stepanjants
Zooplankton of the Laptev Sea Coastal Waters 187

K. Kosobokova, H. Hanssen, E. Markhaseva, V. Petryashov and A. Pinchuk
Composition and Distribution of Summer Zooplankton in the Laptev Sea 192

S.F. Timofeev
Distribution, Biomass and Production of *Thysanoessa longicaudata* Krøyer, 1846 (Crustacea, Euphausiacea) in the Arctic 200

M.K. Schmid and K. Hinz
Benthic Studies in the Laptev Sea 206

B.I. Sirenko, V.V. Petryashov, E. Rachor and K. Hinz
Bottom Biocoenoses of the Laptev Sea and Adjacent Areas 211

N.V. Chernova and A.V. Neyelov
Fish Caught in the Laptev Sea During the Cruise of RV "Polarstern" in 1993 222

A.Yu. Gukov
Hydrobiological Research in the Lena Polynya 228

A.Yu. Gukov
Trophic Structure of the Benthos of the Lena Polynya 230

Environmental History of the Laptev Sea 233
O. Naidina:
Holocene Climatic, Vegetation and Pollen Data of Siberia Adjacent to the Laptev Sea 235

C. Siegert, S.F. Khrutsky and A.Yu. Derevyagin
Paleogeographical Sudies of Permafrost in the Eastern Taymyr Lowland 254

J. Boike, W. K. P. van Loon, C. Kopsch and H. W. Hubberten
The use of TDR for Studying Seasonal Water and Solute Movement in the Active Layer in a Continuous Permafrost Setting - Preliminary Results From Siberia 257

A.M. Alabyan, R.S. Chalov, V.N. Korotaev, A.Yu. Sidorchuk and A.A. Zaitsev
Natural and Technogenic Water and Sediment Supply to the Laptev Sea 265

V. Rachold
Geochemistry of Lena River Suspended Load and Sediments - Preliminary Results of the Expedition in July/ August 1994 272

F. Lindemann, H. Kassens and E. Reimnitz
Sediment Reworking by Ice Gouging in the Western Laptev Sea 280

R. Stein and D. Nürnberg
Productivity Proxies: Organic Carbon and Biogenic Opal in Surface Sediments from the Laptev Sea Shelf and the Adjacent Continental Slope 286

J.A. Hölemann, M. Schirmacher, A. Prange and TRANSDRIFT I Shipboard Scientific Party
Transport and Distribution of Trace Elements in the Laptev Sea: First Results of the TRANSDRIFT Expeditions 297

M. Wahsner
Mineralogical and Sedimentological Characterization of Surface Sediments from the Laptev Sea 303

J. Dehn, H. Kassens and TRANSDRIFT II Shipboard Scientific Party
Regional and Temporal Changes in the Sediments of the Laptev Sea: Initial Results of the TRANSDRIFT II Cruise 314

A.V.Yakovlev
Lithological-Geochemical Features of Modern Bottom Sediments of the Laptev Sea Shelf 324

H. Bauch, M. Kubisch-Popp, T. M. Cronin, B. Rossak and TRANSDRIFT I Shipboard Scientific Party
A Study of the Calcareous Microfauna from Laptev Sea Sediments 334

C. Langner and TRANSDRIFT I Shipboard Scientific Party
Distribution of Fe and Mn in Pore Waters and Sediments of the Laptev Sea - Results of the Expedition TRANSDRIFT I 340

D.S. Yashin and V.A. Kosheleva
Holocene Sediments of the Russian East-Arctic Seas 344

S.S. Drachev, L.A. Savostin and I.E. Bruni
Structural Pattern and Tectonic History of the Laptev Sea Region 348

H.A. Roeser, M. Block, K. Hinz and C. Reichert
Marine Geophysical Investigations in the Laptev Sea and the Western Part of the East Siberian Sea 367

H.-J. Paech
The Aim of Planned Geological On-Shore Investigations on the Novosiberian Islands Within the Project "Correlation of Circum-Arctic Alpine Structural Events" (CASE) 378

V.I. Kim and V.V. Verba
The Geological Structure of the Laptev Shelf and Adjacent Parts of the Eurasian Subbasin (in the Context of Planned Drilling) 383

PREFACE

The Laptev Sea System

The Arctic Ocean, in particular the wide Eurasian shelf seas comprise some of the most sensitive elements of the global environment which are believed to respond at a very early time to Global Change. The renewed interest in the Arctic, the large scale international research efforts devoted to the Arctic, as well as the presently available new technology to carry out research in ice-infested areas, have opened many new avenues to conduct investigations on the variability of the depositional environments of the Eurasian shelf seas. The Laptev Sea is of particular importance in the string of the Eurasian shelf seas because feeding the Transpolar Drift of the Arctic sea-ice cover it exports relatively the largest amounts of sea ice into the open Arctic Ocean, because it is farthest away from the influence of the Atlantic and Pacific waters, and because it is under the influence of rapidly changing fresh water fluxes from the Siberian hinterland (Fig. 1). The morphology of the seafloor, the rapidly changing coast lines of the fragil Lena Delta Island frame work as well as the presence of submarine permafrost are examples for the dynamics of the entire Laptev Sea System.

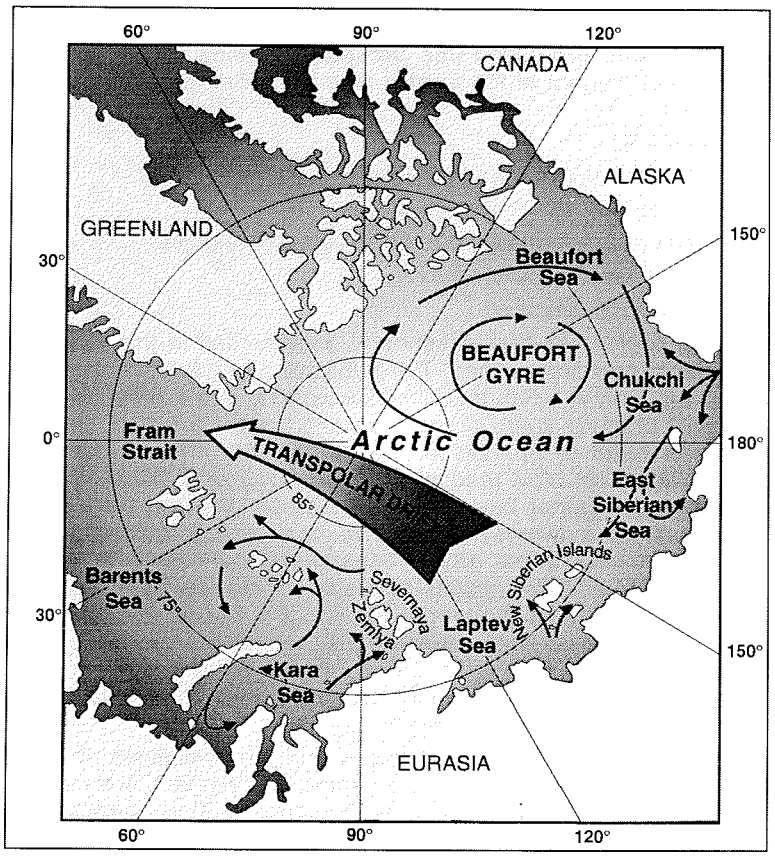

Fig. 1: Sea ice drift paths in the Arctic Ocean

In order to address the natural properties of the Laptev Sea System a joint research project is carried out between a number of Russian and German research institutions under the framework of the "Laptev Sea System Project" (Fig. 2). Every year expeditions are carried out in the area on Russian or German research vessels where multi-disciplinary and binational working groups are addressing some of the identified scientific themes. Results from these joint investigations are then discussed in a series of Russian/German workshops which are held alternatively in Russia or Germany.

The second workshop 'Russian-German Cooperation: Laptev Sea System' was held in November 1994 in St. Petersburg in order to assess (1) the state of knowledge of the Laptev Sea and the adjacent continental margin of the deep Arctic, and (2) to develop a research strategy for the marine geosciences in the Laptev Sea and terrestrial work in East Siberia.

The workshop brought together more than 100 scientists, among them meteorologists, sea ice physicists, oceanographers, biologists, chemists, geologists and geophysicists from various Russian and German research institutions. The main goal of the workshop was to promote and coordinate scientific collaboration among scientists from Russia and Germany. Main emphasis have laid on first scientific results of the expeditions within the scope of the interdisciplinary Russian-German research project 'Laptev Sea System', that is present and past oceanography, ecology, and climatology of the Laptev Sea.

The workshop was organized into serveral sessions which followed various themes of the environment of the Laptev Sea from their present situation to their geological record:

(I) Climate and Ice
(II) Modern Environment of the Laptev Sea
(III) Environmental History of the Laptev Sea
(IV) From Siberia to the Arctic Ocean: Land-Sea Connection
(V) Strategy and Plans for Future Work
(VI) Mid-long Term Perspectives

The scientific content of this workshop is documented in this report containing most of the results and discussions. The publication of this volume serves various purposes. It is primarily a forum for scientists working in the Siberian shelf seas, in which the results of many years of research and preliminary shipboard results can be presented. In order to provide all the participants in the workshop with the opportunity for reporting their results, a speedy way of publication was chosen. Thus, each individual author has presented his opinions and views as he or she sees them, reflecting the diversity and complexity of the Laptev Sea system. On the other hand, this volume offers many researchers the possibility of acquainting themselves with methods and results of research into the East Siberian seas as carried out in other parts of the world. Finally, it is hoped that this collection of papers will function as another step toward joint research projects and are base for the expeditions to be carried out in 1995 and the following years. Many of the papers published identify major scientific problems, thus offering new perspectives for future scientific research in polar regions.

The nature of the papers, the discussions and the disciplines of the attendees clearly demonstrate that the study of the Laptev Sea System is a multidisciplinary one in an interesting key area involving all branches of the natural sciences, such as ice physics, oceanography, biology and geology, in particular. It thus remains an important example for GLOBAL CHANGE and CLIMATE IMPACT research within international research efforts, e.g. International Arctic Science Committee (IASC),

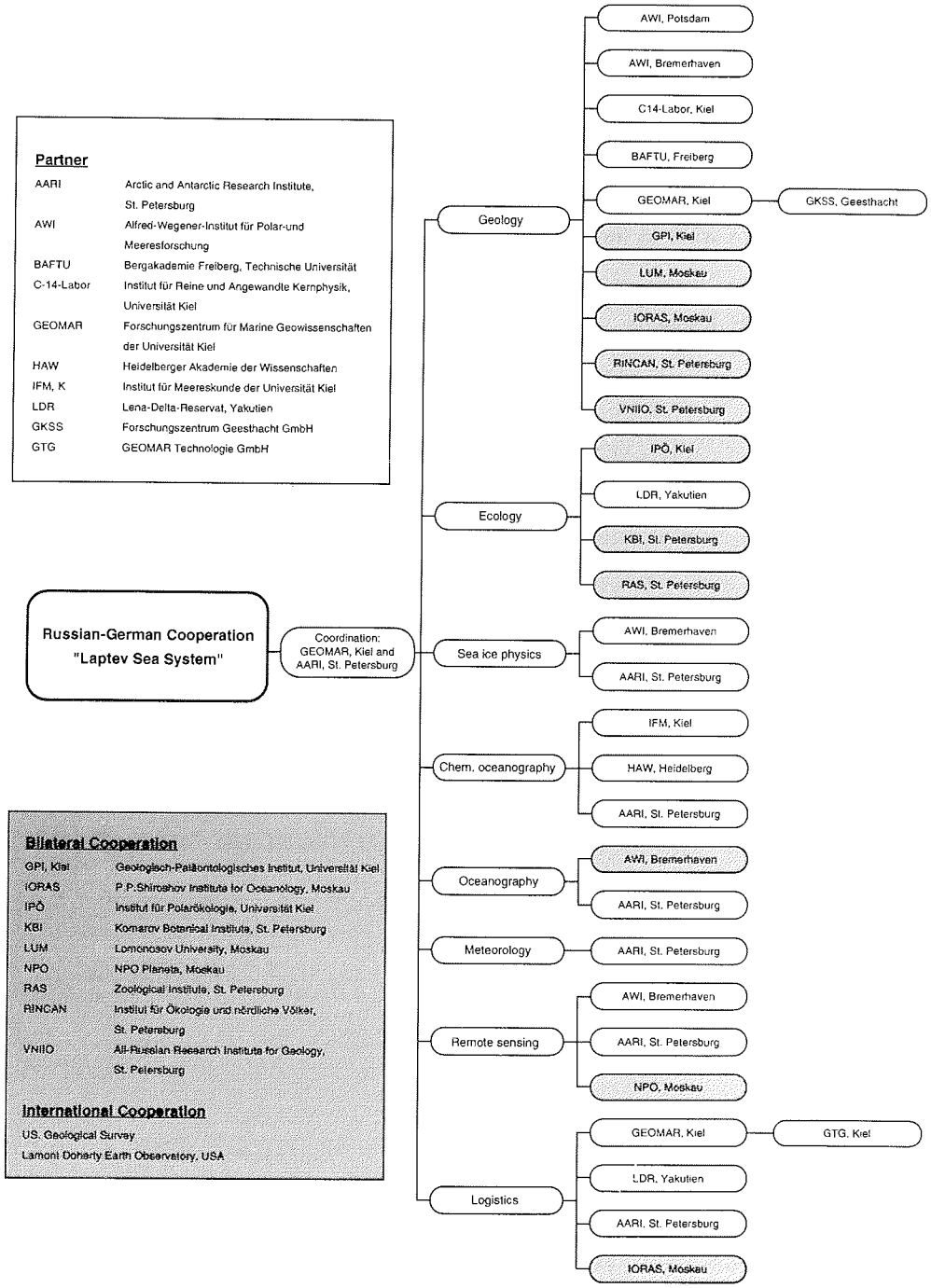

Fig. 2: Research institutions under the framework of the "Laptev Sea System Project"

Arctic Ocean Sciences Board (AOSB) or the Nansen Arctic Drilling Programme (NAD).

The editors also made an effort, probably not wholly successful, to edit manuscripts by non-English-speaking authors to make them easier to understand. In this process, we hope we have not changed the meanings of the original papers. Above all we thank Bettina Rohr and Daniel Krüger who kindly assisted in editing the papers. The workshop has been sponsored by the German and Russian Ministries for Research and Technology and the meeting was held from the 21st to the 14th of November in 1994 in the Arctic and Antarctic Research Institute in St. Petersburg. We wish to thank these organizations for their financial and logistic support.

J. Thiede and H. Kassens

LIST OF AUTHORS AND PARTICIPANTS

Abramova, E., Lena Delta Nature Reserve, 28, Ak. Fedorova, 678400 Tiksi, Tel.: 22 6 14

Afanasyeva, Yu., AARI Arctic and Antarctic Research Institute, 38, Bering Street, 199397 St. Petersburg, Fax: +812-352-2688, E-Mail: aaricoop@sovam.com

Alabyan, A., Lab. of Erosion & Channel Processes, Geographical Faculty, Moscow State University, Vorobyovy Gory, GSp 3, 119899 Moscow, Tel.: +095-939-1709, Fax: +095-932-8836, E-Mail: alabyan@river.geogr.msu.su

Alexandrov, V., AARI Arctic and Antarctic Research Institute, 38, Bering str., 199397 St. Petersburg, Tel.: +812-352-2037, Fax: +812-352-2688, E-Mail: aaricoop@sovam.com

Alexeev, G., AARI Arctic and Antarctic Research Institute, 38, Bering str., 199397 St. Petersburg, Tel.: +812-352-1911, Fax: +812-352-2688, E-Mail: aaricoop@sovam.com

Anisimov, M., AARI Arctic and Antarctic Research Institute, 38, Bering str., 199337 St. Petersburg, Tel.: +812-352-2231, Fax: +812-352-2688, E-Mail: aaricoop@sovam.com

Anoshkin, A., Krylov Shipbuilding Research Institute, 44, Moskovskoye Shosse, 196158 St. Petersburg, Tel.: +812-291-9614, Fax: +812-127-9349

Antonow, M., TU Bergakademie Freiberg, Fachbereich Geowissenschaften, Institut für Geologie, Bernd-von-Cotta-Str. 2, 09596 Freiberg, Tel.: +3731-39-3336, Fax: +3731-39-3599, E-Mail: antonow@tu-freiberg.de

Are, F., University of Communication Ways, 9, Moskovsky Pr., 190031 St. Petersburg, Tel.: +812-168-8318, Fax: +812-315-2621, E-Mail: root@cell.spb.su

Arjakova, S., Department of Geography, Yakutian State University, 58, Belinskogo str., 677891 Yakutsk

Ashik, I. M., AARI Arctic and Antarctic Research Institute, 38, Bering Street, 199397 St. Petersburg, Fax: +812-352-2688, E-Mail: aaricoop@sovam.com

Bauch, H., GEOMAR Forschungszentrum für marine Geowissenschaften, Wischhofstraße 1-3, Geb. 4, 24148 Kiel, Tel.: +431-7202-400, Fax: +431-725391, E-Mail: hbauch@geomar.de

Boetius, A., Alfred-Wegener-Institut für Polar- und Meeresforschung, BIO II, Postfach 120161, 27515 Bremerhaven, Tel.: +471-4831-471, Fax: +471-4831-149

Bogdanov, V., Roshydromet, 12, Novovagankovsky, Moscow, Fax.: +095-255-2030, E-Mail: aarcisea@sovam-com

Bogorodsky, P. M., AARI Arctic and Antarctic Research Institute, 38, Bering Street, 199397 St. Petersburg, Fax: +812-352-2688, E-Mail: aaricoop@sovam.com

Boike, J., Alfred-Wegener-Institut für Polar- und Meeresforschung, Forschungsstelle Potsdam, Postfach 600149, 14401 Potsdam, Tel.: +331-288-2131, Fax: +331-288-2137, E-Mail: boike@awi-potsdam.de

Bolshiyanov, D. Yu., AARI Arctic and Antarctic Research Institute, 38, Bering str., 199397 St. Petersburg, Tel.: +812-352-2231, Fax: +812-352-2688, E-Mail: aaricoop@sovam.com

Borodachev, V., AARI Arctic and Antarctic Research Institute, 38, Bering str., 199337 St. Petersburg, Tel.: +812-352-2143, Fax: +812-352-2688, E-Mail: aaricoop@sovam.com

Chernova, N., Zoological Institute, Lab. of Ichthyology, Russian Academy of Sciences, 1, Universitetskaya nab., St. Petersburg, Tel.: +812-218-0612, Fax: +812-218-2941, +812-114-0444, E-Mail: sbi@zisp.spb.su

Churun, V., AARI Arctic and Antarctic Research Institute, 38, Bering str., 199337 St. Petersburg, Tel.: +812-352-3159, Fax: +812-352-2688, E-Mail: aaricoop@sovam.com

Cremer, H., GEOMAR Forschungszentrum für marine Geowissenschaften, Wischhofstr. 1-3, Geb. 4, 24148 Kiel, Tel.: +431-7202-139, Fax: +431-725391, E-Mail: hcremer@geomar.de

Danilov, A., AARI Arctic and Antarctic Research Institute, 38, Bering str., 199397 St. Petersburg, Tel.: +812-352-1587, Fax: +812-352-2688., E-Mail: aaricoop@sovam.com

Darovskikh, A., AARI Arctic and Antarctic Research Institute, 38, Bering str., 199397 St. Petersburg, Tel.: +812-352-2231, Fax: +812-352-2688, E-Mail: aaricoop@sovam.com

Dehn, J., Geological Survey of Japan, Hokkaido Branch, Kita-8, Nishi-2, Kita-ki Sapporo 060, Tel.: +11-709-1814Fax: +11-709-1817, E-Mail: jdehn@gsj.go.jp

Denisov, D., Murmansk Marine Biological Institute, 17, Vladimirskaya, 183010 Murmansk, Tel.: +815-57 91 76

Dmitrenko, I., AARI Arctic and Antarctic Research Institute, 38, Bering str., 199397 St. Petersburg, Tel.: +812-352-3159, Fax: +812-352-2688, E-Mail: aaricoop@sovam.com

Drachev, S., L.P. Zonenshain Lab. of Geodynamics, P.P. Shirshov Institute of Oceanology, Russian Academy of Sciences, 23, Krasikova, 117218 Moscow, Tel.: 007-095-124-7949, Fax: 007-095-124-5983, 124-7942, E-Mail: paleogeo@sovam.com

Eicken, H., Alfred-Wegener-Institut für Polar- und Meeresforschung, Postfach 120161, 27515 Bremerhaven, Tel.: +471-4831-348, Fax: +471-4831-149, E-Mail: heicken@awi-bremerhaven.de

Erlenkeuser, H., Institut für Reine und Angewandte Kernphysik, Christian-Albrechts-Universität Kiel, 24098 Kiel, Tel.: +431-880-3896, Fax: -431-880-1647, E-Mail: pke@rz.uni-kiel.d400.de

Fahl, K., Alfred-Wegener-Institut für Polar- und Meeresforschung, Postfach 120161, 27515 Bremerhaven, Tel.: +471-4831-560, Fax: +471-4831-149, E-Mail: kfahl@awi-bremerhaven.de

Frolov, I., AARI Arctic and Antarctic Research Institute, 38, Bering str., 199397 St. Petersburg, Tel.: +812-352-1520, Fax: +812-352-2688, E-Mail: aaricoop@sovam.com

Golovin, P. N., AARI Arctic and Antarctic Research Institute, 38, Bering Street, 199397 St. Petersburg, Fax: +812-352-2688, E-Mail: aaricoop@sovam.com

Gorbunov, Yu., AARI Arctic and Antarctic Research Institute, 38, Bering Street, 199397 St. Petersburg, Fax: +812-352-2688, E-Mail: aaricoop@sovam.com

Gordeev, V., P.P. Shirshov Institute of Oceanology, Russian Academy of Sciences, 23, Krasikova str., 117218 Moscow, Tel.: +095-124 1836, Fax: +095-124 5983

Grikurov, G. E., All-Russian Research Inst. for Geology and Mineral Resources of the World Ocean, 1, Angliysky Pr., 190121 St. Petersburg, Tel.: +812-113-8379, Fax: +812-114-1470, E-Mail: garrik@g-ocean.spb.su

Gukov, A. Yu., Hydrometeorological Department Tiksi, 678400 Tiksi

Hannsen, H., Institut für Polarökologie, Christian-Albrechts-Universität Kiel, Wischhofstraße 1-3, 24148 Kiel, Tel.: +431-72087-37, Fax: +431-72087-20, E-Mail: npf02@rz.uni-kiel.d400.de

Hass, C., TU Bergakademie Freiberg, Fachbereich Geowissenschaften, Institut für Geologie, Bernd-von-Cotta-Str. 2, 09596 Freiberg, Tel.: +3731-39-2435, Fax: +3731-39-3599

Heyckendorf, K., Forschungszentrum Jülich GmbH, Projektträger BEO, Bereich Meeresforschung, Postfach 301128, 18112 Rostock, Tel.: +381-5197-293, Fax: +381-51509

Hinz, K., Institut für Polarökologie, Christian-Albrechts-Universität Kiel, Wischhofstraße 1-3, 24148 Kiel, Tel.: +431-72087-37, Fax: +431-72087-20, E-Mail: npf01@rz.uni-kiel.d400.de

Hölemann, J., GEOMAR Forschungszentrum für marine Geowissenschaften, Wischhofstraße 1-3, Geb. 4, 24148 Kiel, Tel.: +431-7202-266, Fax: +431-725391, E-Mail: jhoelema@geomar.de

Hubberten, H.W., Alfred-Wegener-Institut für Polar- und Meeresforschung, Forschungsstelle Potsdam, Postfach 600149, 14401 Potsdam, Tel.: +331-288-2100, Fax: +331-288-2137, E-Mail: hubbert@awi-potsdam.de

Ivanov, G. I., All-Russian Research Institute for Geology and Mineral Resources of the World Ocean, 1, Angliyksy pr., 190121 St. Petersburg, Tel.: +812-219-5972, 210-9954, 210-9384, Fax: +812-232-6690, 114-1470, E-Mail: givanov@sovamsu.sovusa.com

Ivanov, V. L., All-Russian Research Institute for Geology and Mineral Resources of the World Ocean, 1, Angliysky Pr., 190121 St. Petersburg, Tel.: +812-114-0266, Fax: +812-114-1470

Ivanov, V., AARI Arctic and Antarctic Research Institute, 38, Bering str., 199337 St. Petersburg, Fax.: +812-352-2688, E-Mail: aaricoop@sovam.com

Johnson, G. L., GERG Geochemical and Environmental Research Group, Texas A&M University, 4601 North Fairfax Drive, Suite 1130, Arlington, Va. 22203, Tel.: +703-525-7201, Fax: +703-525-7206, E-Mail: Gljgerg1@aol.com

Karpiy, V. Y., AARI Arctic and Antarctic Research Institute, 38, Bering str., 199397 St. Petersburg, Tel.: +812-352-2372, Fax: +812-352-2688, E-Mail: aaricoop@sovam.com

Kassens, H., GEOMAR Forschungszentrum für marine Geowissenschaften, Wischhofstraße 1-3, Geb. 4, 24148 Kiel, Tel.: +431-7202-113, Fax: +431-725391, E-Mail: hkassens@geomar.de

Khrutsky, S. F., Department of Permafrost Studies, Moscow State University, 119899 Moscow, Tel.: +095-939-2648

Kim, V. I., 1, Angliysky Pr., 190121 St. Petersburg, All-Russian Research Institute of Geology and Mineral Resources of the World Ocean

Kolatschek, J., Alfred-Wegener-Institut für Polar- und Meeresforschung, Postfach 120161, 27515 Bremerhaven, Tel.: +471-4831-549, Fax: +471-4831-149, E-Mail: kolatsch@awi-bremerhaven.de

Korotaev, V., Lab. of Erosion and Channel Processes, Geographical Faculty, Moscow State University, 119899 Moscow, Tel.: +095-932-8836, Fax: +095-437-6688

Kosheleva, V., All-Russian Research Institute for Geology and Mineral Resources of the World Ocean, 1, Angliysky pr., 190121 St. Petersburg, Tel.: +812-210-9973, Fax: +812-114-1470

Kosobokova, K., P.P. Shirshov Institute of Oceanology Russian Academy of Sciences, 23, Krasikova str., 117218 Moscow, Tel.: +095-124-5983, E-Mail: mitpan@synapse.ru

Kunz-Pirrung, M., GEOMAR Forschungszentrum für marine Geowissenschaften, Wischhofstr. 1-3, Geb. 4, 24148 Kiel, Tel.: +431-7202-139, Fax: +431-725391, E-Mail: mpirrung@geomar.de

Langner, C., Alfred-Wegener-Institut für Polar- und Meeresforschung, Forschungsstelle Potsdam, Postfach 600149, 14401 Potsdam, Fax: +331-288-2137

Lazurkin, D., All-Russian Research Institute for Geology and Mineral Resources of the World Ocean, 1, Angliysky pr., 190121 St. Petersburg, Tel.: +812-210-9973, Fax: +812-114-1470

Levitan, M. A., P.P. Shirshov Institute of Oceanology, Russian Academy of Sciences, 23, Krasikova str., 117218 Moscow, Tel.: +095-129-2163, Fax: +095-124-5983

Lindemann, F., GEOMAR Forschungszentrum für marine Geowissenschaften, Wischhofstraße 1-3, Geb. 4, 24148 Kiel, Tel.: +431-7202-178, Fax: +431-725391, E-Mail: flindemann@geomar.de

Lisitzin, A. P., P.P. Shirshov Institute of Oceanology, Russian Academy of Sciences, 23, Krasikova str., 117218 Moscow, Tel.: +095-124-8528, Fax: +095-124-5983, E-Mail: apl659lfgi@glas.apc.org

Makeyev, V., Institute of Nature Conservation and Reserves of the Arctic and North, 10 Solidarnosti ave., 193312 St. Petersburg, Tel.: +812-263-2331, Fax: +812-352-2688, E-Mail: makeyev@rincan.spb.su

Makshtas, A., AARI Arctic and Antarctic Research Institute, 38, Bering str., 199337 St. Petersburg, Tel.: +812-352-3354, Fax: +812-352-2688 aaricoop@sovam.com

Mangini, A., Institut für Umweltphysik, Universität Heidelberg, Im Neuenheimer Feld 366, 69120 Heidelberg, Tel.: +621-563-350, Fax: +621-563-405

Morison, J. H., University of Washington, Applied Physics Laboratory, 1013 NE 40th Street, Seattle, Washinton 98105-6698, Tel.: +206-543-1394, Fax: +206-543-6785, E-Mail: morison@apl.washington.edu

Musatov, E. E., All-Russian Research Institute for Geology and Mineral Resources of the World Ocean, 1, Angliysky pr., 190121 St. Petersburg, Tel.: +812-210-9803, Fax: +812-114-1470

Nägelsbach, E., Alfred-Wegener-Institut für Polar- und Meeresforschung, Postfach 120161, 27515 Bremerhaven, Tel.: +471-4831-348, Fax: +471-4831-149

Naidina, O. D., Institute of the Lithosphere, Russian Academy of Sciences, Staromonetny per. 22, 109180 Moscow Tel.: +095-233-5588, Fax: +095-233-5590

Nalimov, Yu., AARI Arctic and Antarctic Research Institute, 38, Bering str., 199337 St. Petersburg, Tel.: +812-352-2762, Fax: +812-352-2688, E-Mail: aaricoop@sovam.com

Novikov, G., Moscow State University, 119899 Moscow, Tel.: +095-939-1333, Fax: +095-939-1545

Nürnberg, D., Alfred-Wegener-Institut für Polar- und Meeresforschung, Postfach 120161, 27515 Bremerhaven, Tel.: +471-4831-238, Fax: +471-4831-149, E-Mail: dnuernbe@awi-bremerhaven.de

Paech, H., Bundesanstalt für Geowissenschaften und Rohstoffe, Postfach 510153, 30631 Hannover, Tel.: +511-6432713

Peregovich, B.: GEOMAR Forschungszentrum für marine Geowissenschaften, Wischhofstr. 1-3, Geb. 4, 24148 Kiel, Tel.: +431-7202-131, Fax: +431-725391, E-Mail: bperegovich@geomar.de

Petrova, V., All-Russian Research Institute for Geology and Mineral Resources of the World Ocean, 1, Angliysky pr., 190121 St. Petersburg, Tel.: +812-210-9174, Fax: +812-114-1470

Petryashov, V., Zoological Institute, Russian Academy of Sciences, 1, Universitetskaya Nab., 199034 Petersburg, Tel.: +812-218-1311, Fax: +812-218-2941, 114-0444, E-Mail: sbi@zisp.spb.su

Piepenburg, D., Institut für Polarökologie, Christian-Albrechts-Universität Kiel, Wischhofstraße 1-3, 24148 Kiel, Tel.: +431-72087-64, Fax: +431-72087-20, E-Mail: npf32@rz.uni-kiel.d400.de

Pivovarov, S., AARI Arctic and Antarctic Research Institute, 38, Bering str., 199397 St. Petersburg, Tel.: +812-352-3021, Fax: +812-352-2688, E-Mail: aaricoop@sovam.com

Priamikov, S. M., AARI Arctic and Antarctic Research Institute, 38, Bering str., 199397 St. Petersburg, Tel.: +812-352-0096, Fax: +812-352-2685, E-Mail: aaricoop@sovam.com

Rachold, V., Alfred-Wegener-Institut für Polar- und Meeresforschung, Forschungsstelle Potsdam, Postfach 600149, 14401 Potsdam, Tel.: +331-288-2141, Fax: +331-288-2137, E-Mail: vrachold@awi-potsdam.de

Rachor, E., Alfred-Wegener-Institut für Polar- und Meeresforschung, Postfach 120161, 27515 Bremerhaven, Tel.: +471-4831-310, Fax: +471-4831-149, E-Mail: erachor@awi-bremerhaven.de

Reimnitz, Erk, US Geological Survey, 345 Middlefield Road MS 999, Menlo Park CA 94025, Tel.: +415-354 3049, Fax: +415-354-3363

Roeser, H.-A., Bundesanstalt für Geowissenschaften und Rohstoffe, Postfach 510153, 30631 Hannover, Tel.: +511/643-2799

Rohr, B., GEOMAR Forschungszentrum für marine Geowissenschaften, Wischhofstr. 1-3, Geb. 4, 24148 Kiel, Tel.: +431-7202-152, Fax: +431-725391, E-Mail: brohr@geomar.de

Romanovskiy, N. N., Geocryology Department, Faculty of Geology, Moscow State University, 119899 Moscow, Tel.: +095-939-1937, Fax: +095-938-0192, E-Mail: nromanovsky@glas.apc.org

Sadikov, M., All-Russian Research Institute for Geology and Mineral Resources of the World Ocean, 1, Angliysky pr., 190121 St. Petersburg, Tel.: +812-113-8379, Fax: +812-114-1470

Savatiugin, L., AARI Arctic and Antarctic Research Institute, 38, Bering str., 199397 St. Petersburg, Tel.: +812-352-1057, Fax: +812-352-2688, E-Mail: aaricoop@sovam.com

Schauer, U., Alfred-Wegener-Institut für Polar- und Meeresforschung, Postfach 120161, 27515 Bremerhaven, Tel.: +471-4831-817, Fax: +471-4831-149

Shevchenko, V.P., P.P. Shirshov Institute of Oceanology, Russian Academy of Sciences, 23, Krasikova str., 117218 Moscow, Tel.: +095-124-7737, Fax: +095-124-5983

Shuliatin, O., All-Russian Research Institute for Geology and Mineral Resources of the World Ocean, 1, Angliysky pr., 190121 St. Petersburg, Tel.: +812-210-9147, Fax: +812-114-1470

Sidorchuk, A., Lab. of Erosion and Channel Processes, Geographical Faculty, Moscow State University, 119899 Moscow, Tel.: +095-202-6922, 939-5697, Fax: +095-932-8836

Siegert, C., Alfred-Wegener-Institut für Polar- und Meeresforschung, Forschungsstelle Potsdam, Postfach 600149, 14401 Potsdam, Tel.: +331-288-2131, Fax: +331-310621

Sirenko, B., Zoological Institute, Russian Academy of Sciences, 1, Universitetskaya Nab., 199034 Petersburg, Tel.: +812-218-1311, Fax: +812-218-2941, 114-0444, E-Mail: sbi@zisp.spb.su

Smagin, V., AARI Arctic and Antarctic Research Institute, 38, Bering str., 199397 St. Petersburg, Tel.: +812-352-1347, Fax: +812-352-2688, E-Mail: aaricoop@sovam.com

Smirnov, V., AARI Arctic and Antarctic Research Institute, 38, Bering str., 199397 St. Petersburg, Fax: +812-352-2688, E-Mail: aaricoop@sovam.com

Sokolov, V., AARI Arctic and Antarctic Research Institute, 38, Bering str., 199397 St. Petersburg, Fax: +812-352-2688, E-Mail: aaricoop@sovam.com

Spektor, V., Permafrost Institute, Siberian Branch of the Russian Academy of Sciences, 677018 Yakutsk, Tel.: +8411-51486

Stein, R., Alfred-Wegener-Institut für Polar und Meeresforschung, Postfach 120161, 27515 Bremerhaven, Tel.: +471/4831-232, Fax: +471/4831-149, E-Mail: rstein@awi-bremerhaven.de

Strobl, C., Institut für Umweltphysik, Universität Heidelberg, Im Neuenheimer Feld 366, 69120 Heidelberg, Tel.: +621-563-314, Fax: +621-563-405, E-Mail: str@uphys1.uphysn.uni-heidelberg.de

Thiede, J., GEOMAR Forschungszentrum für marine Geowissenschaften, Wischhofstraße 1-3, Geb. 4, 24148 Kiel, Tel.: +431-7202-115/116, Fax: +431-725391, E-Mail: jthiede@geomar.de

Timofeev, S., Murmansk Marine Biological Institute, 17, Vladimirskaya, 183010 Murmansk, Fax: 47-789-10288

Timokhov, L. A., AARI Arctic and Antarctic Research Institute, 38, Bering str., 199397 St. Petersburg, Tel.: +812-352-3179, Fax: +812-352-2688, E-Mail: aaricoop@sovam.com

Tormirdiaro, S., Agricultural Academy, St. Petersburg, Tel.: +812-470-0510

Ushakov, I., North West Polytechnical Institute, St. Petersburg, Tel.: +812-110-6338

Vanda, Yu., AARI Arctic and Antarctic Research Institute, 38, Bering str., 199397 St. Petersburg, Tel.: +812-352-1922, Fax: +812-352-2688, E-Mail: aaricoop@sovam.com

Viehoff, T., Alfred-Wegener-Institut für Polar- und Meeresforschung Bremerhaven. - Deceased

Volkov, V., AARI Arctic and Antarctic Research Institute, 38, Bering str., 199397 St. Petersburg, Tel.: +812-352-3129, Fax: +812-352-2688, E-Mail: aaricoop@sovam.com.

Wahsner, M., Alfred-Wegener-Institut für Polar- und Meeresforschung, Postfach 120161, 27515 Bremerhaven, Tel.: +471-4831-238, Fax: +471-4831-149

Yakovlev, A., All-Russian Research Institute for Geology and Mineral Resources of the World Ocean, 1, Angliysky pr., 190121 St. Petersburg, Tel.: +812-114-5772, Fax: +812-114-1470, E-Mail: yakovlev@g-ocean.spb.su

Yashin, D., All-Russian Research Institute for Geology and Mineral Resources of the World Ocean, 1, Angliysky pr., 190121 St. Petersburg, Tel.: +812-210-9973, Fax: +812-114-1470

Zaitsev, A., Lab. of Erosion and Channel Processes, Geographical Faculty, Moscow State University, 119899 Moscow, Fax: +095-932-8836

Zakharov, V.F., AARI Arctic and Antarctic Research Institute, 38, Bering str., 199397 St. Petersburg, Fax.: +812-352-2688, E-Mail: aaricoop@sovam.com

Zelenskiy, V., Tiksi Hydromet, 678400 Tiksi

Zimichev, V., AARI Arctic and Antarctic Research Institute, 38, Bering str., 199397 St. Petersburg, Tel.: +812-352-2561, Fax: +812-352-2688, E-Mail: aaricoop@sovam.com

In Memoriam

Thomas Viehoff
(1957-1994)

The untimely and sudden death of our colleague and friend Thomas Viehoff is a great loss to us all. Thomas will be remembered for his scientific vigour and his contributions to remote sensing in the polar regions, which proved to be an important asset even at the starting stage of the Russian-German Laptev Sea System project. Just as much we will miss him as a warm-hearted, open personality and a friend who always found the time to listen and help.

THE MODERN ENVIRONMENT OF THE LAPTEV SEA

INVESTIGATIONS OF AIR-SEA INTERACTIONS CARRIED OUT DURING THE TRANSDRIFT II EXPEDITION

J. Afanasyeva, M. Lamakin and V. Timachev
State Research Center of the Russian Federation the Arctic and Antarctic Research Institute, St. Petersburg, Russia

The non-uniform field of surface temperature in the Laptev Sea (frontal zone, sea ice drift) determines the significant spatial and temporal variability of the air-sea interactions. On the other hand, the heat of the sea surface layer in summer determines in general the beginning of sea-ice formation and its thickness. Thus, the main aim of the meteorological investigations during the expedition was to estimate long- and short-wave radiation constituents of the surface heat balance which, together with turbulent heat fluxes, are one of the most important physical parameters responsible for the accumulation and loss of heat in the sea.

Scope of the observations

The program of meteorological observations included a set of hourly meteorological standard observations and the continuous registration of global solar radiation. The observations were carried out according to the "Manual for Hydrometeorological Stations and Posts", issue 9, part 3, books 1 and 2 (St.Petersburg, Hydrometeoisdat, 1993). Air temperature, humidity, pressure, surface temperature, wind direction and speed were measured by ship weather station MIDAS-321. For the registration of global solar radiation, pyranometers CM-5 and automatic recorder KSP-4 were used. Cloudiness, atmospheric appearance, swell and ice conditions were determined visually. In order to control measurements intercallibration of different methods and instruments was carried out.

Preliminary Results

During the expedition in the Laptev Sea, synoptic processes and weather conditions were considerably non-uniform. From 3 to 8 September, the weather was determined by the eastern part of a small-gradient narrow gully spreading in the direction North Pole - Taimyr. Habitual fogs and a weak wind of southern direction were observed. From 9 to 15 September, a slightly mobile anticyclone had determined habitual down-pour snow and south-east wind of up to 12 m/s. From 16 to 20 September, the weather in the Laptev Sea was determined by depression. Wind speed was 14-16 m/s with south-west direction, the height of waves was about 3 m. From 20 to 24 September, east-south-east wind speed was no more than 7-9 m/s. The height of waves was 1-2 m. This period was characterized by a pressure crest of an anticyclone with its center in Western Siberia.

As mentioned above the aim of the meteorological investigations in the Laptev Sea was to estimate the intensity of energy-mass exchange in the upper sea layer. It is well known that it is short-wave solar radiation determining the total heat supply of the upper layer in summer. The total heat supply in the layer of maximum temperature and salinity gradients is also greatly influenced by the distribution of solar radiation. Numerous measurements of solar and long-wave atmospheric radiation were an important part of the expedition schedule. As a result the daily average values of all heat balance components have been calculated (Tab. 1).

Table1: Daily average values of heat balance components of the Laptev Sea surface. (September, 1994.)

Day	Turbulent fluxes		Incoming short-wave radiation	Long-wave radiation balance	Heat flux through sea surface
	Sensible	Latent			
4.9	5.3	-32.2	106.4	-53.6	25.6
5.9	4.8	-4.6	87.3	-68.1	19.4
6.9	-1.7	-1.0	25.8	-54.6	-31.5
7.9	1.5	-0.6	36.5	-38.2	-0.8
8.9	-23.9	-17.3	35.1	-47.4	-53.5
9.9	-25.2	-20.5	42.9	-51.2	-54.0
10.9	-33.8	-38.9	31.9	-45.2	-86.0
11.9	-57.6	-71.4	27.2	-54.4	-156.2
12.9	-49.4	-55.9	42.9	-56.1	-118.5
13.9	-16.8	-36.3	36.6	-46.3	-62.8
14.9	-3.8	-19.8	35.6	-55.0	-43.0
15.9	-19.6	-37.9	16.8	-54.6	-95.3

The negative values in Tab.1 mean that the sea surface lost heat. Unfortunately, the data about the vertical distribution of absorbed short-wave radiation were not completely collected due to unfavourable weather conditions. Thus, only episodical soundings of the surface layer were executed. These soundings have shown that, if the altitude of the sun was no more than 25 deg.(as it was during the expedition), 75% of solar radiation are absorbed in the first meter of the water column (Fig. 1).

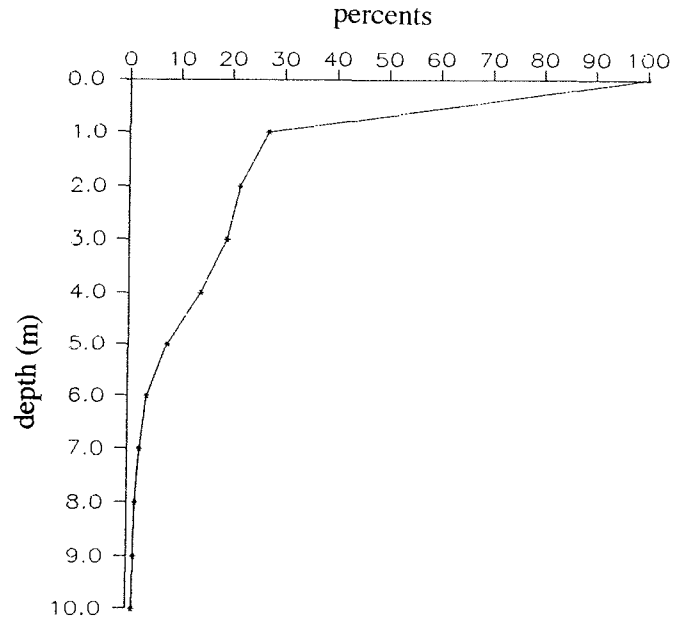

Fig 1. Absorption of solar radiation with depth in the Laptev Sea. September 4-5, 1994.

Aerosol investigations

During the TRANSDRIFT II expedition, the quantity of particles contained in the lower layer of the atmosphere was measured for the Kara and the Laptev Sea. These measurements were taken for defining atmospheric aerosol particle volume contents and its size distribution .

The aerosol counter AZ-5 was used which measures the quantity of particles with sizes from 0.4 - 0.5, 0.5 - 0.6, 0.6 - 0.7, 0.7 - 0.8, 0.8 - 0.9, 0.9 - 1.0, 1.0 - 1.5, 1.5 - 2.0, 2.0 - 4.0, 4.0 - 7.0, to 7.0 - 10.0 mkm. It was necessary to exclude the influence of ship smoke, atmospheric precipitation and fogs during the measurements. For this purpose, we have taken into account meteorological conditions, wind direction and the ship's course.

Fig. 2 shows the interannual change of aerosol contents for Severnaya Zemlya where observations have been continuosly performed for a few years. Obviously, this parameter varies seasonally. It becomes apparent that our observations were carried out in the period of minimum values of aerosol contents. This seasonal variation is connected with different ais-mass motions and conditions for stratification in summer and winter observed in the whole Arctic region. For particles, the size of which is about 0.45 mkm (largest quantity), the average is almost 500 particles per liter whereas in winter this number was more than 8000 per liter.

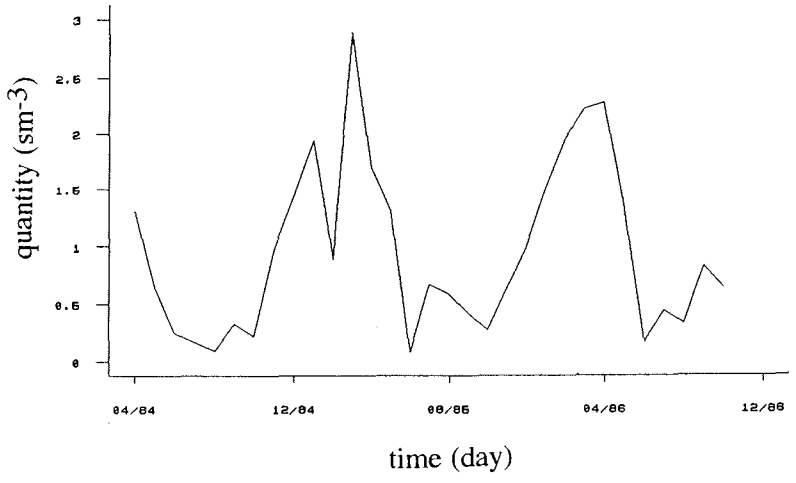

Fig 2: Interannual change of aerosol contents.

The function for particle-size distribution is presented in Fig. 3. For comparison, data from Obninsk (100 km from Moscow) and Franz Josef Land are shown together with TRANSDRIFT II results. We can see that these functions are generally of the same character in spite of a different surface character: forest in the Moscow province, snow on Franz Josef Land and water surface during the TRANSDRIFT II expedition. Thus, we can assume that the same processes form atmospheric aerosols in these different regions.

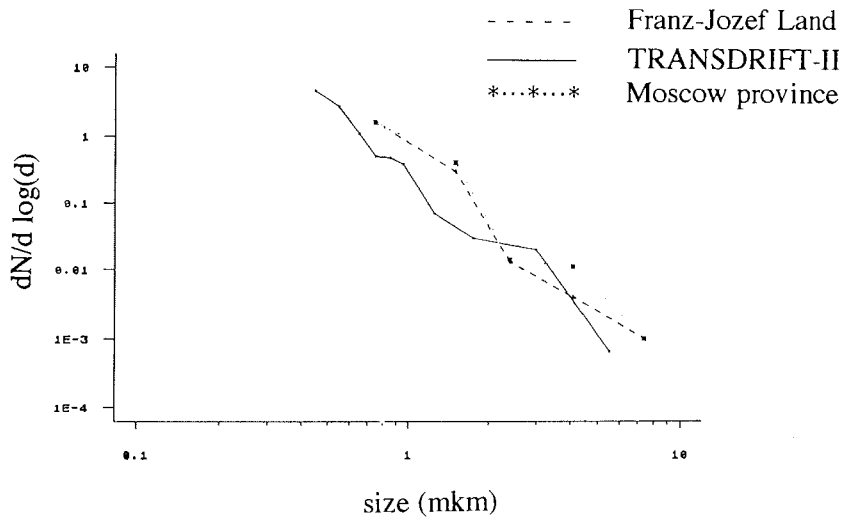

Fig 3. Distribution function for particle sizes (at various stations).

THE COMPOSITION OF AEROSOLS OVER THE LAPTEV, THE KARA, THE BARENTS, THE GREENLAND AND THE NORWEGIAN SEA

V. P. Shevchenko* , A. P. Lisitzin*, V. M. Kuptzov*, G. I. Ivanov°,V. N. Lukashin*, J. M. Martin+, V. Yu. Rusakov*, S. A. Safarova*,V. V. Serova*, R. Van Grieken◊ and H. Van Malderen◊

* P. P. Shirshov Institute of Oceanology, Moscow, Russia

° VNIIOKEANGEOLOGIA, St. Petersburg, Russia

\+ Institut de Biogeochimie Marine, Montrouge, France

◊ Chemical Department of the University of Antwerpen, Belgium

Introduction

The atmospheric input of particulate matter into surface waters plays an important part in the oceanic biogeochemical cycling of many chemical elements (Buat-Menard and Chesselet, 1979; Chester and Murphy, 1990; Duce et al., 1991). Usually riverine input was assumed to be the main geochemical pathway on which terrestrial compounds and compounds of anthropogenical origin are transferred from their sources to the aquatic environment, but there is much evidence that atmospheric inputs contribute particulate matter to marine areas to an appreciable extent (Lisitzin, 1978; Duce et al., 1991). Several efforts have been made to assess the sources and major pathways of the pollutants in the Arctic air (Pacyna and Ottar, 1989). Up to now aerosols of the Russian sector of the Arctic have been studied little (Rovinsky et al., 1989; Vinogradova, 1993).

Sampling and Analytical Methods

Altogether 55 aerosol samples were taken with meshes during the following expeditions and cruises: the SPASIBA-91 expedition on board the R/V *Yakov Smirnitzky* in August and September 1991, the 49th cruise of the R/V *Dmitry Mendeleev* from August to October 1993, the 31th cruise of the R/V Akademik *Mstislav Keldysh* in September 1993, the 9th cruise of the R/V *Professor Logachev* from August to October 1994. The sampling was carried out in the Laptev, the Kara, the Barents, the Greenland and the Norwegian sea (Fig. 1). In September 1993 during the 49th cruise of the R/V *Dmitry Mendeleev*, 14 aerosol samples were taken by means of air filtration with Whatman-41 filters (Table 1). During the 9th cruise of the R/V *Professor Logachev*, 10 samples were taken by means of filtration with AFA-HA-20 filters. In addition, filtration was carried out with meshes, which enables us to compare the results of both methods. The results of the SPASIBA-91 aerosol studies are discussed in the paper of Shevchenko et al. (in prep.).

In order to collect the aerosols, 5 to 10 nylon meshes (1 m^2 each; pores of 0.8 μm) were raised on the mast above the bow of the ship. After 5 to 24 hours the meshes were fetched down, and we removed the particles by washing the meshes in bidistilled water. Then the water with the particles was passed through nuclear filters (0.45 μm), and the filters with the samples were dried at 40-45 °C. In more detail this sampling method is described by Chester and Johnson (1971).

The composition of the particles was studied with a scanning electron microscope JSM-U3 of Jeol (Tokyo, Japan; magnification up to 10,000 times) in the Institute of Oceanology, Moscow. The single-particle analysis of the SPASIBA-91 samples was carried out in the University of Antwerpen. It was performed with a JXA-733 superprobe of Jeol (Tokyo, Japan) according to the electron probe X-ray microanalysis (EPXMA) (Shevchenko et al., in prep.). This superprobe is equipped

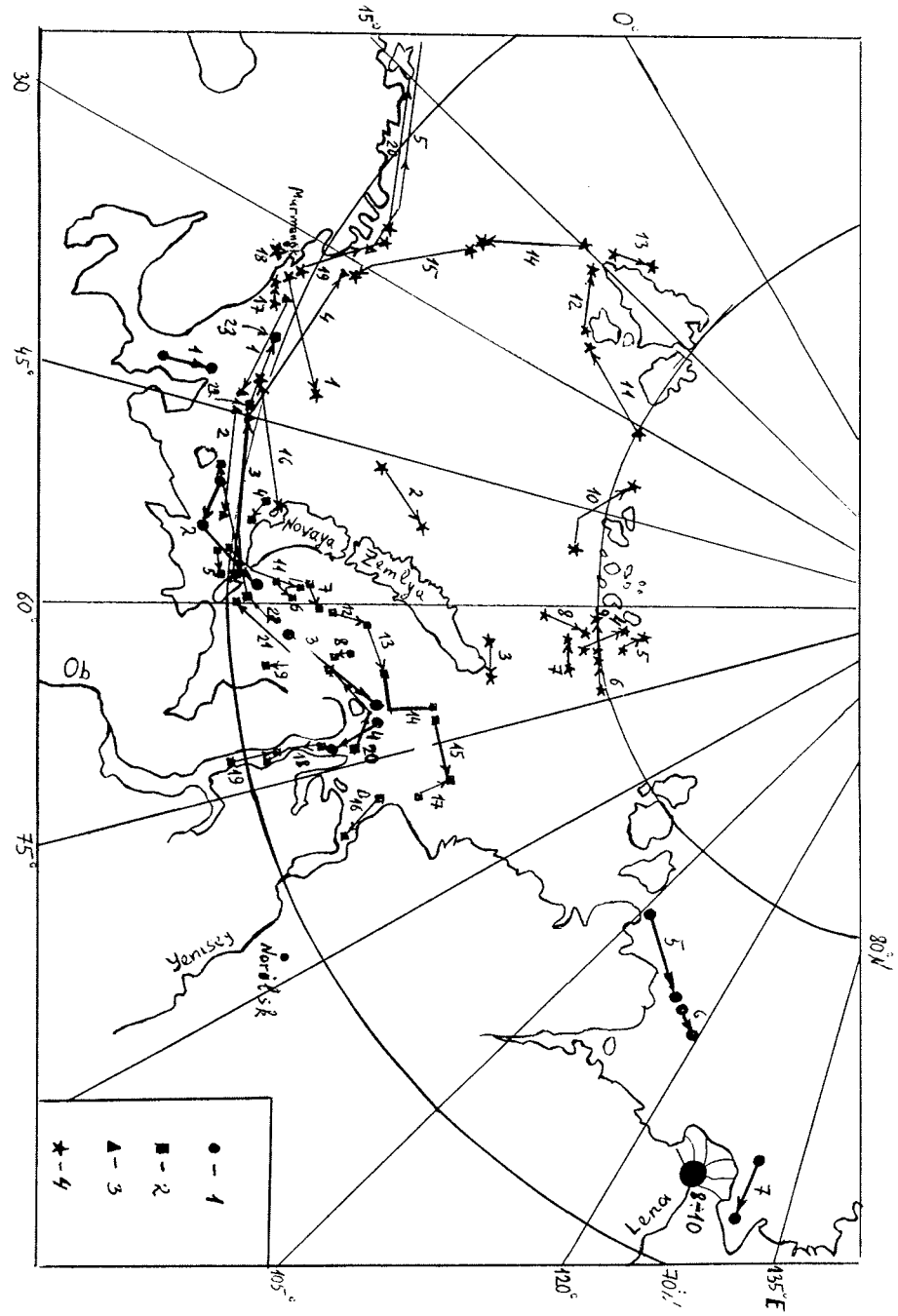

Fig.1: Station map of the cruise 49 on board R/V *Dmitry Mendeleev* in 1993

Tab. 1: Aerosol samples taken during the cruise 49 on board R/V *Dmitry Mendeleev* in 1993

No.	Beginning of sampling			End of sampling			Volume of air.	Wind	
	Time	Coordinates		Time	Coordinates			Direction.	Velocity.
	Date	GMT	Lat.(N)	Lon.(E)	Date	GMT	Lat.(N)	Lon.(E)	m³	grad.	m/s
1	13.09	7:30	70°06.5'	155°10.2'	13.09	20:00	71°42.6'	159°04.7'	530	0	3.8
2	13.09	20:10	71°42.6'	159°04.7'	14.09	14:00	73°26.7'	161°57.8'	461	0	4.5
3	14.09	13:00	73°26.7'	161°37.8'	15.09	5:30	74°16.0'	172°54.2'	762	340	4.7
4	15.09	8:40	74°14.8'	173°01.2'	15.09	23:30	76°00.0'	173°00.0'	547	0	5.8
5	16.09	2:20	75°58.8'	173°36.3'	16.09	19:30	74°59.9'	180°00.6'	645	180	3.6
6	16.09	21:40	74°59.9'	180°00.6'	17.09	15:15	73°30.6'	179°59.6'	783	180	4.0
7	17.09	17:30	73°30.6'	179°59.6'	18.09	12:20	72°06.3'	182°12.5'	570	190	7.0
8	18.09	12:30	72°04.3'	182°12.5'	19.09	14:30	71°02.0'	183°13.2'	470	190	10.5
9	20.09	6:00	71°48.7'	183°10.3'	21.09	7:10	72°28.8'	180°02.2'	793	230	6.0
10	21.09	12:00	72°28.8'	180°02.2'	22.09	18:10	74°31.5'	180°35.4'	614	90	6.7
11	22.09	18:10	74°31.5'	180°35.4'	23.09	10:40	76°00.0'	179°57.9'	408	110	7.5
12	23.09	14:40	76°00.0'	179°57.9'	24.09	16:10	74°59.7'	173°05.2'	582	250	8.3
13	25.09	3:00	74°59.7'	173°05.2'	26.09	4:40	72°21.9'	173°42.4'	685	180	10.0
14	26.09	4:40	72°21.9'	173°42.4'	27.09	6:20	70°03.5'	173°26.2'	801	70	12.0

with energy- and wavelength-dispersive X-ray spectrometers, a secondary and transmission electron detector, and two simultaneously operating backscattered electron detectors for topographic and compositional imaging. Further information on the single particle analysis can be found in Van Malderen et al. (1992) and in Rojas and Van Grieken (1992).

According to the R. W. Rex and B. Murrey (1969) method, the mineral composition of the coarse fraction of aerosols was studied by means of X-ray difractometry on a DRON-2 device. This analysis was performed in the Institute of Oceanology, Moscow. The instrumental neutron activation analysis (INAA) of the samples collected with meshes and by means of filtration was carried out in the Institute of Geochemistry and Analytical Chemistry, Moscow. After the SPASIBA-91 samples were mixed with acids ($HF+HNO_3+HClO_4$) at a temperature of 130-140 °C in a closed teflon system, Al was spectrophotometrically determined with eriochromcyanine -R. Na, K, Mg, Ca were determined by means of atomic flame absorption spectrophotometry (Perkin-Elmer 272) and Mn, Co, Cu, Zn, Cd, Pb by means of graphite furnace atomic absorption spectrophotometry (GFAAS) on Perkin-Elmer 3030 with a HGA-500 furnace block. These studies were carried out in the Institut de Biogeochimie Marine, Montrouge.

Results and Discussion

In August and September 1991, the mass concentrations of the coarse fraction of aerosols which are not soluble in distilled water varied from 0.08 to 0.46 $\mu g/m^3$ (0.27 $\mu g/m^3$ on average, n=7 samples), in August, September and October 1993 from 0.017 to 0.48 $\mu g/m^3$ (0.15 $\mu g/m^3$ on average), and in August, September and October 1994 from 0.026 to 0.58 $\mu g/m^3$ (0.19 $\mu g/m^3$ on average, n=20 samples).

In most of the samples, organic matter (fibres of the vegetation, pollens, diatoms) is the main component (Fig. 2). The main source of these particles is situated on land about 20-120 km from the route of the ship. Pollens of *Camfanulacea, Cyperacea, Cruciferae and Rosaceae* (*Ruleus chamaemorus L.*) were found. In some samples (for example in samples NN 10 and 12 from the 49th cruise of the R/V *Dmitry Mendeleev*) more than half of the particles are pollens. Diatoms could be transported from the sea surface to the air by wind. A number of investigations carried out in the recent years confirm that organic matter is one of the main components of the atmospheric aerosols. C_{org} can sometimes exceed 60% of the total mass of the particles (Isidorov, 1990).

The X-ray difractometry shows that quartz dominates in the mineral not-amorphous part of the coarse fraction of aerosols. In August and September 1991 the content of quartz was 48-72% (62% on average). The highest content (72%) was registered in the Laptev Sea. In August, September and October 1993 the content was 15-56% (33% on average). The average content of feldspar in the samples was the same on both expeditions (12%), while the content of clay minerals was much higher in 1993. The average content of illite was 14% in 1991 and 23% in 1993. The average content of the sum of chlorite and kaolinite was 13% in 1991 and 31% in 1993. This difference can probably be explained with the different origin of the air masses of the investigated area.

The organic particles and soot carbon have no major X-ray intensity. In the automatic regime of the electron microprobe, however, only particles with major X-ray intensities were studied. These particles are mainly:

1) aluminosilicates, both mineral particles and fly-ash (spherical particles originating from high-temperature combustion processes);

2) quartz;

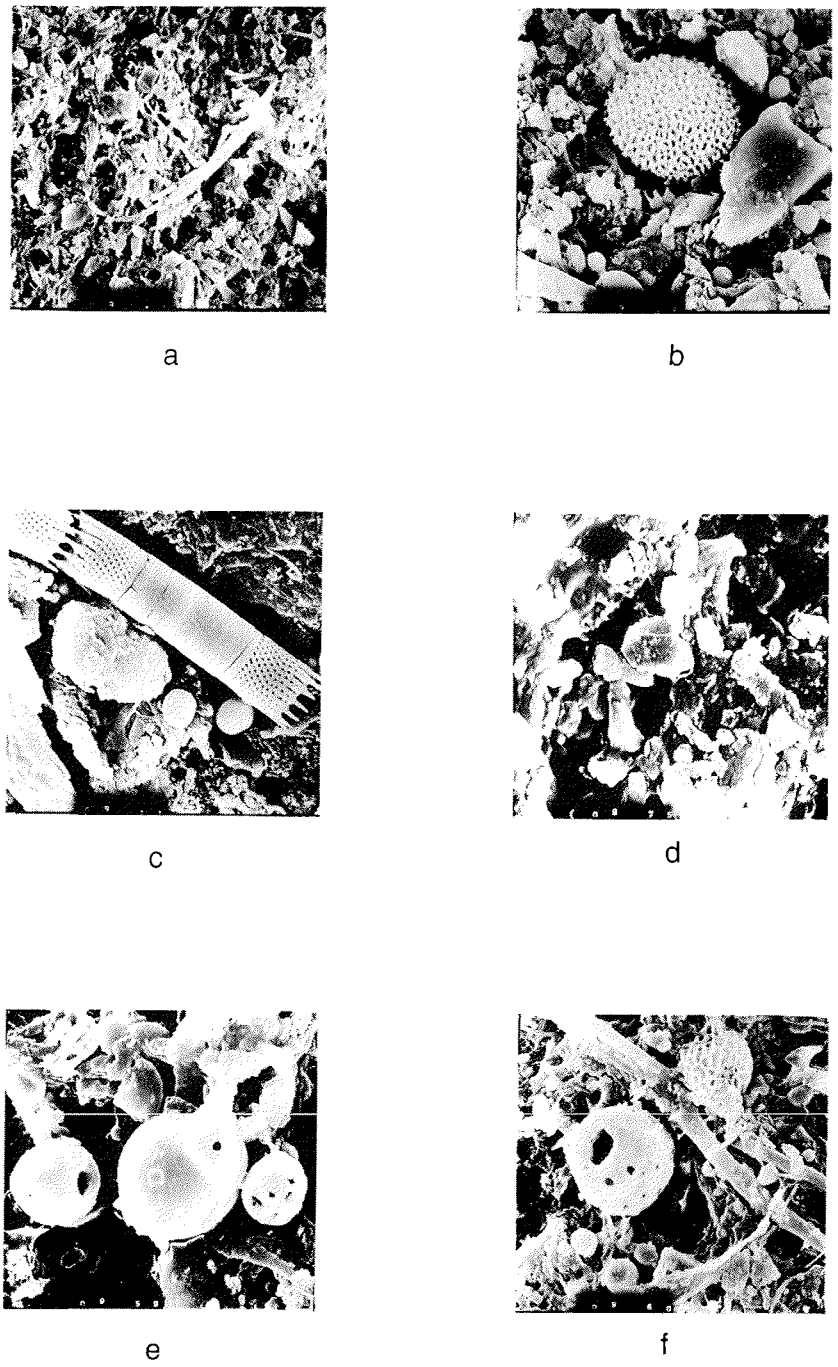

Fig. 2: Scanning electron microscope photos of aerosol samples.

3) particles rich in Si-Fe (maybe also fly-ash).

4) fly-ash particles consisting mainly of Fe, P, Cl and trace metals.

The crustal aluminosilicate particles (1) with a diameter of 1-5 µm (on average 1.7 µm, but sometimes to 20 µm) are shaped irregulary. They could be regarded as windblown mineral soil particles. The quartz particles (2) with a diameter of 1-3 µm (on average 1.5 µm) are nearly round. The variations in the content of aluminosilicates and quartz seem to be connected with the composition of the soils where the particles come from.

The combustion spheres rich in Fe, P, Cl and trace metals (4) have diameters of 0.3-3 µm (Fig. 2) and their concentrations in thesamples are less than 1%. Their composition differs from sample to sample. In the manual regime of the electron microprobe, combustion spheres which are rich in Fe, Ni, Cu, Cr, Zn, Ca, Mn, Sb were found in the samples. The spectrum of a combustion sphere (1.5 µm) which was collected over the Laptev Sea and which is rich in Fe, Si, Mn, K, Cr, Al is presented in Fig. 3. Spheres which originate from high-temperature combustion processes can usually be transported by air masses over a long distance. They were found in Arctic aerosols.

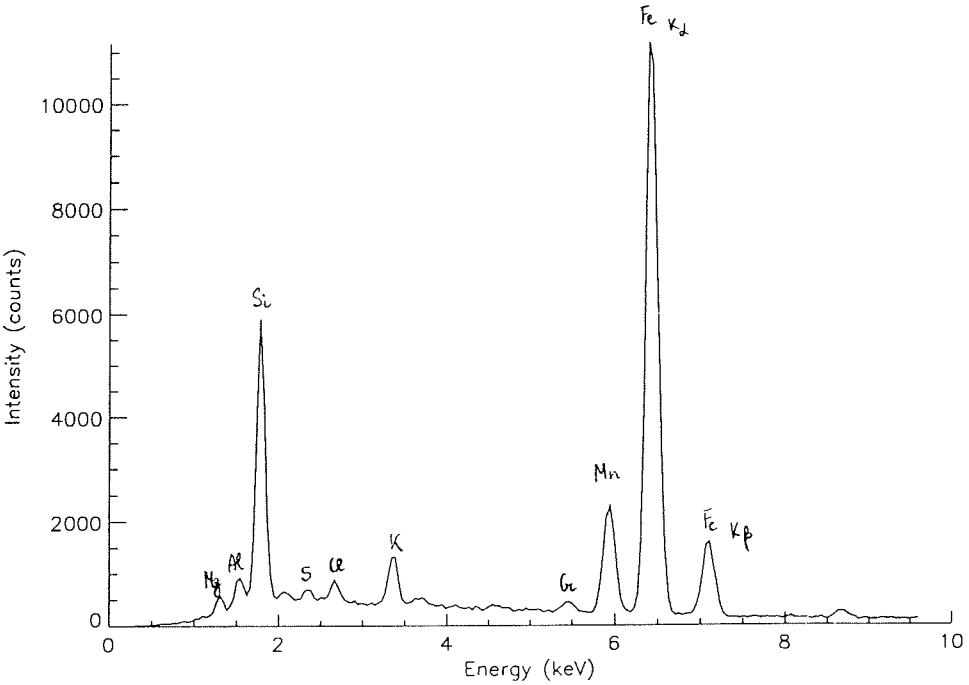

Fig. 3: Typical composition of combustion spheres collected over the Laptev Sea

In order to determine the sources of the elements, so-called enrichment factors (crustal) (EF) were calculated for each element, with

EF = (El/Al)sample/(El/Al)rocks,

where El and Al are the concentrations of the given elements in the sample and in the rocks respectively (Martin and Whitfield, 1983). According to the EF, the elements can be divided into two groups:

1) crustal: Na, Mg, Al, K, Ca, Sc, Mn, Fe, Co, Ni, As, Rb, Cs, Ba, REE (rare earth elements), Hf, Ta, Th, U (EF<10);

2) anthropogenic (EF>10): Cr, Cu, Zn, Se, Br, Ag, Cd, Sb, W.

Marine sources were not taken into account because the meshes were washed in distilled water. The highest EFs for Cr, Cu, Sb, Pb were found in samples collected not far from Norilsk and Murmansk (large centers of mining and metallurgic industry). Even the EFs for Ni in the sample N 6 and N5 from the SPASIBA-91 expedition are >10 (12.3 and 13.5 respectively) while the average for all samples is 4.9.

The total atmospheric fluxes of a few elements were estimated assuming according to Rahn (1981) that in the Arctic the dry deposition is 1/4 of the total deposition (dry and wet). The riverine and atmospheric inputs of a few metals to the Laptev Sea were compared. To calculate the atmospheric input, we assume that the total flux of aerosols to the sea surface is 620 $mg/m^3/yr$ (this study) and the surface of the Laptev Sea is 500,000 km^2. Riverine input was estimated assuming that the Lena run-off is 505 km^3/yr (Telang et al., 1991), and the Lena discharge of solids 17.6 million t/yr (Martin et al., 1993). The concentrations of these metals were taken from Martin et al. (1993). Riverine input evidently dominates for Al, Fe, Ni,Cu, Zn, Cd. The ratios of atmospheric to riverine input are less than 0.2. But the atmospheric input of Pb is comparable with the riverine one, and in remote areas atmospheric input dominates. As early as in 1981, Rahn showed the dominance of the atmospheric input of Pb in the Arctic Ocean.

The concentrations of the chemical elements in the air over the Kara Sea in September 1993 were filtered through Whatman-41 data and then compared with the concentrations of other areas (Table 2). The former range at the same levels like the concentrations in the Arctic in summer. The concentrations of the anthropogenic elements in our samples are lower than those in the aerosols of the Arctic in winter (Maenhaut et al., 1989; Landsberger et al.,1990; Li and Winchester, 1990) because in winter a polar atmospheric front is situated south of the industrial region. In summer, however, the polar front is located in the Arctic and the atmospheric circulation is essentially confined to the Arctic itself (Heidam, 1986). The concentrations of heavy metals in the aerosols of the Kara Sea are higher than those in the Antarctic and in remote ocean regions, but they are much lower than those in highly industrialized regions (for example, the North Sea, the Baltic Sea, the Black Sea and the Mediterranean Sea).

The comparison of the enrichment factors of aerosols collected with meshes and Whatman-41 filters over the Kara Sea shows that in the most cases the enrichment factors for the filtration samples are 1-2 orders higher than those for the mesh samples. This is probably due to the circumstance that sea salt and submicron particles are collected by the filters. Earlier it was shown that the concentrations of many chemical elements are higher in finer aerosol particles (Duce et al., 1976). So it is usefull to collect aerosols according to both methods in order to obtain more detailed information on the composition of aerosols.

Conclusions

1. The coarse fraction (>1 um) of the aerosols mainly consists of biogenic particles of continental origin (rests of plants, pollens etc).

2. The inorganic part of the aerosols consists usually of aluminosilicates (both minerals and combustion spheres) and quartz. Little combustion spheres (0.3-1.5 μm) rich in trace metals could also be found in the samples.

3. The concentrations of heavy metals are near to the world average and much lower than in highly industrialized regions.

Tab. 2: Atmospheric concentration of chemical elements (ng/m^3) in the Kara Sea in September of 1993.

NN	Na	Sc	Cr	Fe	Co	Zn	Sb
1	19.0	0.00011	0.051	2.95		2.0	0.0044
2	20.3	0.000084	0.051			0.4	0.0019
3	2.9	0.0002	0.01		0.0005	5.3	0.0011
4	7.9	0.000085	0.03	1.8	0.001	0.63	0.0049
5	8.1	0.000073	0.027	0.94		0.97	0.0037
6	4.5	0.00002	0.018	1.0		0.27	0.0016
7	13.5	0.00019	0.047	2.78	0.0093	0.97	0.0029
8	7.3	0.000582	0.130	5.99	0.0067	2.56	0.0050
9	4.2	0.000173	0.032	2.51	0.0075	0.66	0.0019
10	7.0	0.000017		0.89		0.65	0.0025
11	59.2	0.000633	0.045	4.94	0.0014	1.52	0.0028
12	107.9	0.000466	0.073	5.13	0.0035	1.97	0.0062
13	78.4	0.000144		1.26	0.0019	0.45	
14	8.9	0.000278	0.046	3.56	0.0052	3.75	0.0026
average	24.9	0.000219	0.044	2.81	0.0041	1.58	0.0032
standard deviation	32.7	0.000201	0.032	1.78	0.0032	1.46	0.0016
Other areas:							
Tropical S.Pacific[1]				0.21	0.0004	0.07	
Antarctica[2]	3.3	0.00016	0.04	0.62	0.00049	0.033	0.00084
West Black Sea[3]	1400.0	0.08	9.0	420.0	0.25	46.0	0.6
North Sea[4]			3.1	231.0	0.19	26.0	
Arctica:							
Spitsbergen, summer[5]	66.0	0.0012	0.56	5.6	0.004	0.15	0.0024
Vrangel Is., spring[6]	240.0	0.022	7.7	88.0	0.05	12.0	0.11

[1]Arimoto et al., 1987

[2]Maenhaut et al., 1979

[3]Hacisalihoglu et al., 1992

[4]Chester and Bradshaw, 1991

[5]Maenhaut et al., 1989

[6]Vinogradova et al., 1993

Acknowledgement

The authors thank A. A. Burovkin (Institute of Oceanology, Moscow) for taking part in the sampling, A. Z. Miklishansky (Vernandsky Institute of Geochemistry and Analytical Chemistry, Moscow) for carrying out INAA, W. W. Huang (Institut de Biogeochimie Marine, Montrouge, France) for helping with the atomic absorption analyses, V. A. Karlov (Institute of Oceanology, Moscow) for the scanning electron microscopy, Z. N. Gorbunova and G. V. Ivanov (Institute of Oceanology, Moscow) for helping with the X-ray difractometry. This work was supported by the Russian Fund of Fundamental Researches (grant RFFR N 93-05-9280).

References

Buat-Menard, P.; R. Chesselet. Variable influence of atmospheric flux on trace metal chemistry of oceanic suspended matter. Earth Planet. Sci. Lett., 1979, v. 42. P. 399-411.

Chester, R.; L. R. Johnson. Atmospheric dust collected off the West African coast. - Nature, 1971. v. 229. P.105-107.

Chester, R. and K. J. T. Murphy. 1990. Metals in the marine atmosphere. - In: R. W. Furness and P. H. Rainbow (Editors), Heavy Metals in the Marine Environment, CRC Press, Boca Raton, FL. P. 27-49.

Duce, R. A.; P. S. Liss; J. T. Merrill et al.. The atmospheric input of trace species to the world ocean. Global Biogeoch. Cycles, 1991, v. 5. P. 193-259.

Duce, R. A.; B. J. Ray; G. L. Hoffmann; P. R. Walsh. Trace metals concentration as a function of particle size in marine aerosols from Bermuda. - Geoph. Res. Lett., 1976, v. 3. P. 339-342.

Heidam, N. Z. Trace metals in the arctic aerosols. - In: J. O. Nriagu and C. I. Davidson (Editors), Toxic Metals in the Atmosphere. Wiley and Sons, 1986. P. 267-293.

Isidorov, V. A. Organic Chemistry of the Earth´s Atmosphere. Springer-Verlag, Berlin-Heidenberg, 1990. 210 p.

Landsberger, S.; S. J. Vermette; L. A. Barrie. Multielemental composition of the Arctic aerosols. - J. Geoph. Res., 1990, v. 95. P. 3509-3513.

Li, S. M.; J. M. Winchester. Haze and other aerosol components in late winter Arctic Alaska, 1986. - J. Geoph. Res., 1990, v. 95. P. 1797-1810.

Lisitzin, A. P. Processes of oceanic sedimentation. M., Nauka, 1978. 392 p. (in Russian).

Maenhaut, W.; P. Cornille; J. M. Pacyna and V. Vitols. Trace element composition and origin of the atmospheric aerosol in the Norwegian Arctic. - Atmos. Environ., 1989, v. 23. P. 2551-2569.

Martin, J. M.; M. Whitfield. The significance of the river input of chemical elements to the ocean. In: Wong, Boyle, Bruland, Burton and Goldberg (Editors), Trace Metals in Sea Water, Plenum Publishing Corporation , 1983. P. 265-296.

Martin, J. M.; D. M. Guan; F. Elbaz-Poulichet; A. J. Thomas and V. V. Gordeev (1993): Preliminary assessment of the distributions of some trace elements (As, Cd, Cu, Fe, Pb and Zn) in a pristine aquatic environment: the Lena River estuary (Russia). - Mar. Chem. 43, p. 185-199.

Pacyna, J. M.; B. Otar. Origin of natural constituents in the Arctic aerosols. Atmos. Environ., 1989, v. 23. P. 809-815.

Rahn, K. A. 1981. Atmospheric, riverine and oceanic sources of seven trace constituents to the Arctic ocean. Atmos. Environ., 15: 1507-1516.

Rex, R. W.; B. Murrey. Initial reports of the Deep-Sea Drilling Project. Wash. (DC) US: Gov. Print. off., 1969, v. IV, Appendix III.

Rojas, C. and R. Van Grieken. 1992. Electron microprobe characterization of individual aerosol particles collected by aircraft above the southern bight of the North Sea. Atmos. Environ., 26: 1231-1237.

Rovinsky, F. Ya.; V. A. Petrukhin; Yu. P. Cherkhanov; L. A. Lapenko; L. B. Burtzeva; M. I. Afanasiev; B. V. Pastukhov and V. A. Ivanov. Background pollution of the arctic atmosphere: observations and estimates. In: Yu. A. Izrael, F.Yu. Rovinsky (Editors), Monitoring of background pollution of environments, N5. Leningrad, Gidrometeoizdat, pp. 88-97 (in Russian).

Shevchenko, V. P.; V. M. Kuptzov; A. P. Lisitzin; H. Van Malderen; J. M. Martin; R. Van Grieken; W. W.Huang; H. Cachier; G. Cauwet. Composition of the coarse fraction of aerosols collected in the Russian sector of the Arctic (in prep.).

Telang, S. A.; R. Pocklington; A. S. Naidu; E. A. Romankevich; I. I. Gitelson and M. I. Gladyshev. 1991. Carbon and mineral transport in major North American, Russian Arctic, and Siberian rivers: the St Lawrence, the Mackenzie, the Yukon, the Arctic Alaskan rivers, theArctic basin rivers in the Soviet Union, and the Yenisei. In: E. T. Degens, S. Kempe and J. E. Richey (Editors), Biogeochemistry of Major World Rivers. John Wiley and Sons, pp. 75-104.

Van Malderen, H.; C. Rojas and R. Van Grieken. 1992. Individual giant aerosol particles above the North Sea. Environ. Sci. Technol., 26: 750-756.

Vinogradova, A. A.; I. P. Malkov; A. V. Polissar; N. N. Khramov. Elemental composition of the surface atmospheric aerosol in the Arctic regions of Russia. - Izvestiya, Atmospheric and Oceanic physics, 1993, v. 29, N2. P. 149-157.

SATELLITE RADAR MONITORING OF ICE DRIFT IN THE LAPTEV SEA

V. Yu. Alexandrov*, H. Eicken° and J. Kolatschek°

* State Research Center of the Russian Federation the Arctic and Antarctic Research Institute, St. Petersburg, Russia

° Alfred-Wegener-Institut für Polar- und Meeresforschung, Bremerhaven, Germany

The Laptev Sea is an area from which ice is exported to the Arctic Basin. The study of ice drift in this area is important both for regional research and for a more accurate determination of sea ice dynamics in the Arctic Ocean. Large-scale ice circulation in the Arctic Ocean, including the Laptev Sea, has been studied by using data of drifting buoys (Colony at al. 1991). Meso-scale and small-scale sea ice dynamics in the Laptev Sea, however, has been studied comparatively little. This is due to a limited number of drifting buoys. At present meso-scale ice drift can be calculated either by means of numerical models or by means of remote sensing data. This paper deals with the problem how sea ice dynamics can be studied by analyzing successive satellite images.

The algorithms and software elaborated in the AARI allow us to determine ice drift in interactive mode with the aid of successive images which cover the same area. Satellite images, geolocated with the aid of orbital data and ground control points, are visualised on the screen of a computer and the geographical coordinates of any point can be determined in interactive mode. As a rule giant ice floes and fractures are delineated on these images. Some characteristic elements are recognized on both images, and their geographical coordinates are determined.

Sea ice dynamics can be determined with visual, IR and radar satellite images. We studied the possibility of a regular ice drift determination by means of successive AVHRR NOAA images (Alexandrov at al.,1994). After the images which RV *Polarstern* received for the Laptev Sea during August and September 1993 were analysed, ice drift patterns could be determined. The interval between the successive images varied between 2 and 42 days, but a considerable number of ice drift vectors was received for intervals from two days to two weeks. The results of a comparison with ARGOS buoy data showed a good coincidence both in velocity and direction. It was shown, that a southward and southeastward ice drift predominated in this period. In their paper from 1994, Gorbunov and Losev came to the same conclusions. Good spatial coverage of ice drift data was obtained for the eastern and western Laptev Sea in August and September. But it was impossible to calculate the ice drift for the central Laptev Sea because clouds covered this area.

Satellite radar images are very useful for sea ice monitoring because they are independent of light and weather conditions. Detailed ice drift patterns can be derived from successive ERS-1 SAR images, but only for limited areas (100 x 100 km). Besides, the ERS-1 images do not cover the central part of the Laptev Sea. At present only radar images from the "Okean" satellite can be used for a regular ice drift study of all of the Laptev Sea. These images provide us with information on areas of mainly old ice, on leads and fractures, on flaw and shore leads, on the position and size of giant ice floes, and on the velocity and direction of ice drift.

For an analysis, we selected the satellite radar images of the Laptev Sea and nearby areas which were received at the drifting station "North Pole - 28" in the period from September 1987 to June 1988. The aim of this analysis is to determine the variations of sea ice conditions and ice drift for this period, to show the

possibility of a regular radar satellite monitoring of the Laptev Sea, and to estimate total ice export and sediment transport for the period from the beginning of freeze-up to summer melting. Digital processing of these images was carried out, including the digitizing of the images, their geolocation and the determination of sea ice parameters in an interactive mode. Preliminary visual analysis showed that the selected images cover all of the Laptev sea. So the main sea ice parameters, including ice drift, can be calculated for this period.

The example of ice drift determination with successive "Okean" images for the period from 10.01.1988 to 30.01.1988 is presented in Fig. 1. Both images cover the central part of the Laptev Sea. A northward ice drift predominated in the Laptev Sea during this period. Near the Taymyr peninsula, however, there was a northeastward ice drift. The analysis showed that in the Laptev Sea a regular ice drift monitoring with SLR "Okean" images is possible. The results obtained will be used in oder to verify the numerical ice drift models.

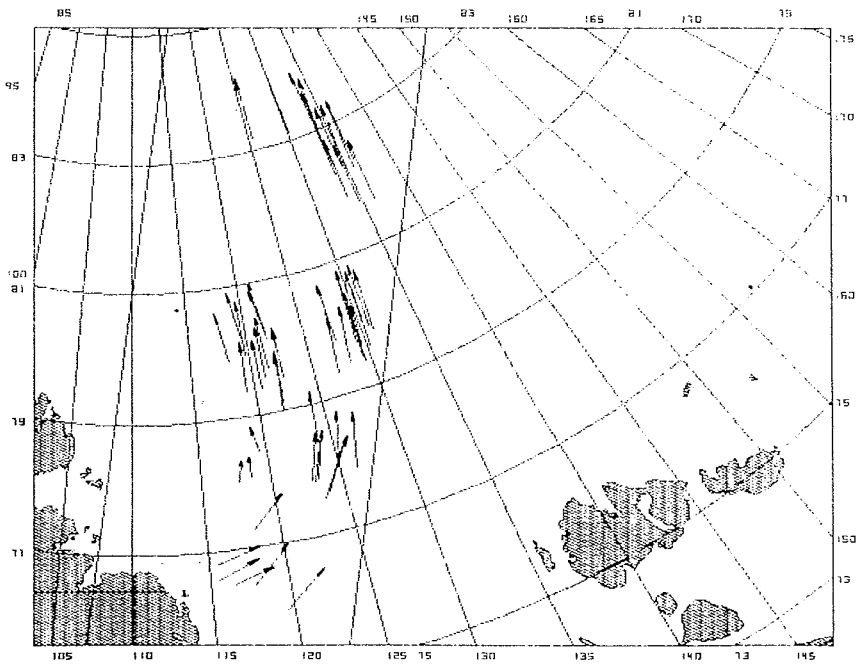

Fig.1: Ice drift in the Laptev Sea for the period from 10.01.1988 to 30.01.1988, determined by analysing successive "Okean" radar images.

References

Alexandrov, V. Yu., Eicken, H., Martin, T. 1994. Determination of ice drift in the Laptev Sea from satellite images and buoys data. - In: The scientific results of the LAPEX-93 expedition, St.Petersburg, AARI, p. 174 - 179.

Colony, R.L., Rigor, I.,Runciman-Moore, K. 1991. A summary of observed ice motion and analysed atmospheric pressure in the Arctic Basin, 1979-1990. Final Report, APL-VW TM13-91. Seattle, 25p.

Gorbunov, Yu., Losev, S. 1994. Ice drift features in the northern regions of the

Laptev and East-Siberian Seas and the adjacent Arctic Basin in July-September 1993 - In: Tthe scientific results of the LAPEX-93 expedition, St.Petersburg, AARI, p. 180-192.

ICE DYNAMICS IN THE SOUTH-WESTERN LAPTEV SEA AS DERIVED FROM ERS-1 SAR IMAGES

J. Kolatschek*, T. Viehoff* †, H. Eicken*, E. Nägelsbach* and V. Alexandrov°

* Alfred-Wegener-Institut für Polar- und Meeresforschung, Bremerhaven, Germany

° State Research Center of the Russian Federation the Arctic and Antarctic Research Institute, St. Petersburg, Russia

† deceased

The Laptev Sea represents an important source area of sea ice, exported into the Arctic Ocean and entering into the Transpolar Drift. As previous studies suggest, much of this ice is produced during autumn freeze-up and within a system of coastal polynyas and shore leads. Time series of images from the Advanced Very High Resolution Radiometer (AVHRR, see Table 1 in Massam, 1991) flown on board the NOAA Satellite series are used to determine the large-scale sea-ice motion field. The resulting motion patterns show high temporal and spatial variability, in particular along the eastern coast of Severnaya Zemlya.

Table 1: Data of the NOAA-Satellites and the AVHRR-Sensor (Massam, 1991)

Orbital height	:	808-867 km approx
Inclination	:	98.75° – 98.925°
The Advanced Very High Resolution Radiometer	(AVHRR/2)	
Ground Resolution	:	1 km at nadir
Swath	:	2580 km
Band 1	:	0.55-0.90 μm
Band 2	:	0.725-1.10 μm
Band 3	:	3.55-3.93 μm
Band 4	:	10.50-11.50 μm
Band 5	:	11.50-12.30 μm

In order to investigate this area more thoroughly, several images of the high resolution Synthetic Aperture Radar (SAR) on board the European Remote Sensing Satellite ERS-1 (see Table 2 in Massam, 1991) have been analysed.

Table 2: Data of the ERS-1-Satellite and the SAR-Sensor (Massam, 1991)

Launch	:	May 1991
Orbital height	:	780 km approx
Inclination	:	98.52°
The Synthetic Apertur Radar (SAR)		
Frequency	:	5.3 GHz (C-band, wavelength 5.7cm)
Ground Resolution	:	30 m
Incident angle mid-swath	:	23°
Swath	:	80-100 km

SAR data allow far more detailed investigations of the distribution and dynamics of different sea ice types, identified through their characteristic backscatter signature (Carsey, 1992). Due to the high resolution it is also possible to identify single icebergs with SAR. This identification is also possible during the summer melt season when different sea ice types cannot be distinguished due to meltwater accumulation in puddles and within the upper ice and snow layers. The low liquid-water content of firn and lower temperatures result in significant higher backscatter from iceberg surfaces.

In this study we analysed a series of SAR images from the western Laptev Sea (along the coast of Severnaya Zemlya). The data cover the period of the joint German expedition with "Ivan Kireyev" and "Polarstern" in August/September 1993 (with supplementary glaciological ground-truth work), extending into December 1993. An ERS-1 SAR image from Sept. 21 1993 is shown in Figure 1. On the left

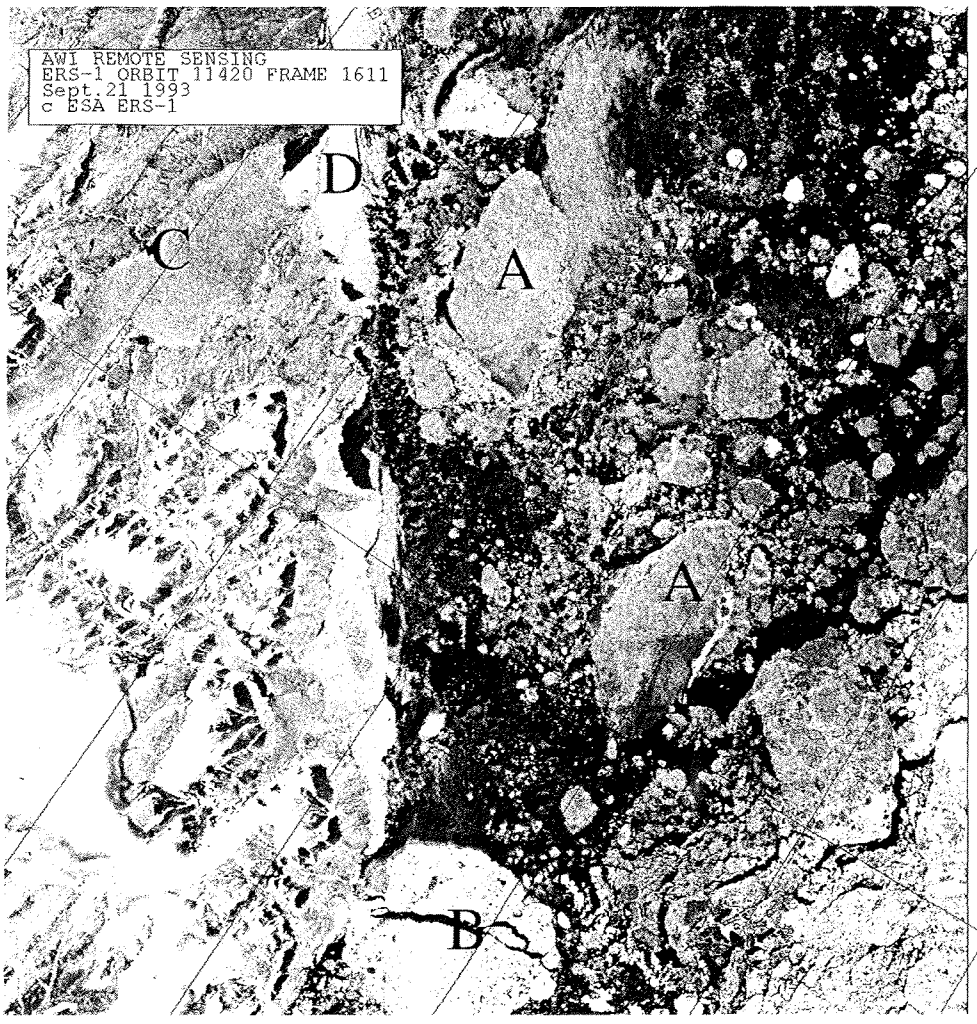

Fig.1: ERS-1 Orbit 11420 Frame 1611 from Sept. 21, 1993, uncalibrated. Centerpoint located at 79.10 N, 104.99 E.

side part of Bol'shevik Island is visible. Several classes of ice floes appearing in different grey shades and texture are discernible: The dark grey floes (marked A) consist of young ice, the brighter ones (B) of old, possibly multiyear ice. The dark area in the center of the frame corresponds to thin new ice, indicating the onset of freezing conditions in the second half of September. This is also confirmed by temperature measurements on board the RV "Polarstern". Attached to the coast some fast ice (C) is visible. The bright triangular patch to the right of the fast ice (D) mostlikly corresponds to open water with high backscatter due to roughing of the surface by wind.

In Figure 2 the extend and margin of the ice dome on Oktyabr'skoy Revolyutsii Island in the upper right of the image (marked A) are clearly delineated in the data. Dispersed in the large patch of ice floes east of the coast numerous icebergs (small

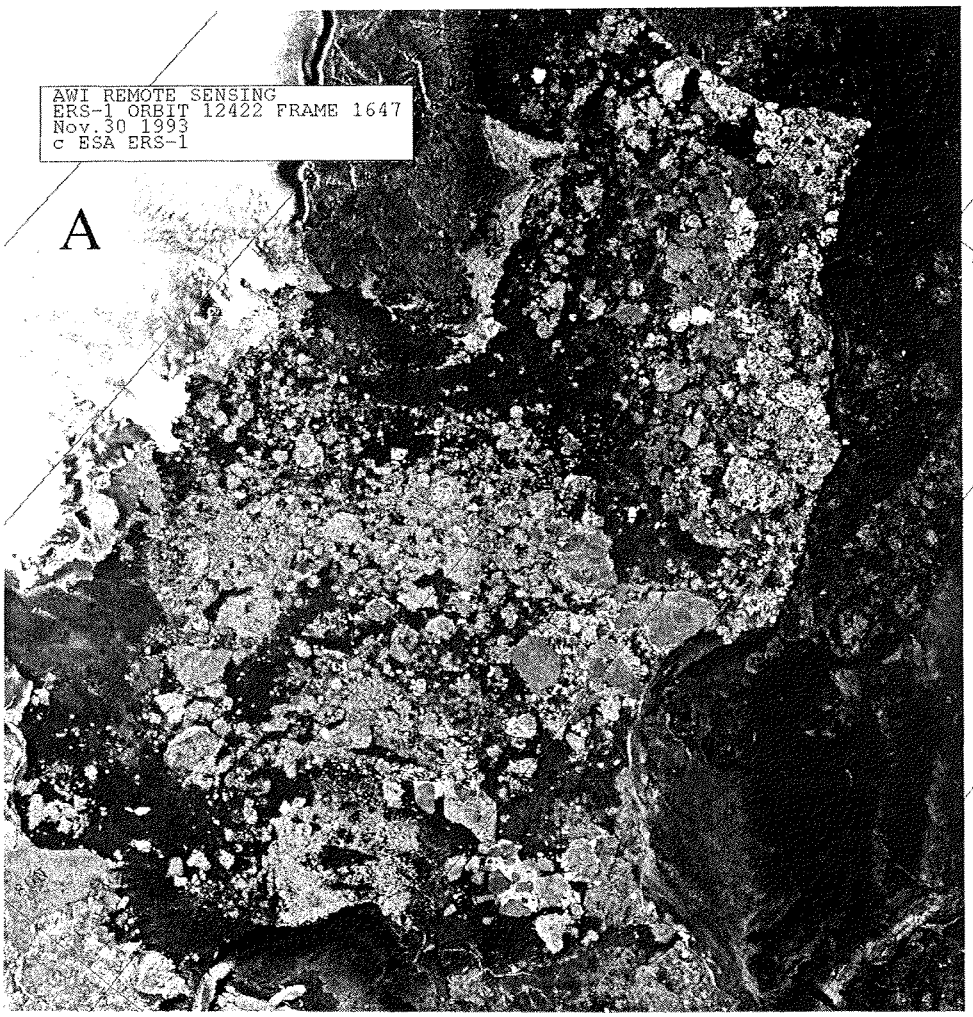

Fig.2: ERS-1 Orbit 12322 Frame 1647 from Nov. 30, 1993, uncalibrated. Centerpoint located at 80.55 N, 99.00 E.

white spots in Fig.) originating from the ice cap have been identified at the southern margin of the ice field which is attached to the coast throughout the period September - October some lee polynias are visible. The highly inhomogenous ice in this area gives further evidence for complex motion and drift patterns in the area east of the Severnaya Zemlya archipelago.

Ice drift vectors were derived from tracked ice floes and icebergs, indicating complex motion patterns (Figure 3, 4). Between Oct. 16 1993 and Nov. 1 1993 strong shear along the south-eastern edge of the Oktyabr'skoy Revolyutsii Island is evident (Figure 3). The direction of the drift is southward, The length of the displacement vectors ranges from about 17 km to 0.6 km. The average displacement is ca. 11 km, corresponding to a velocity of about 0.7 km/day.

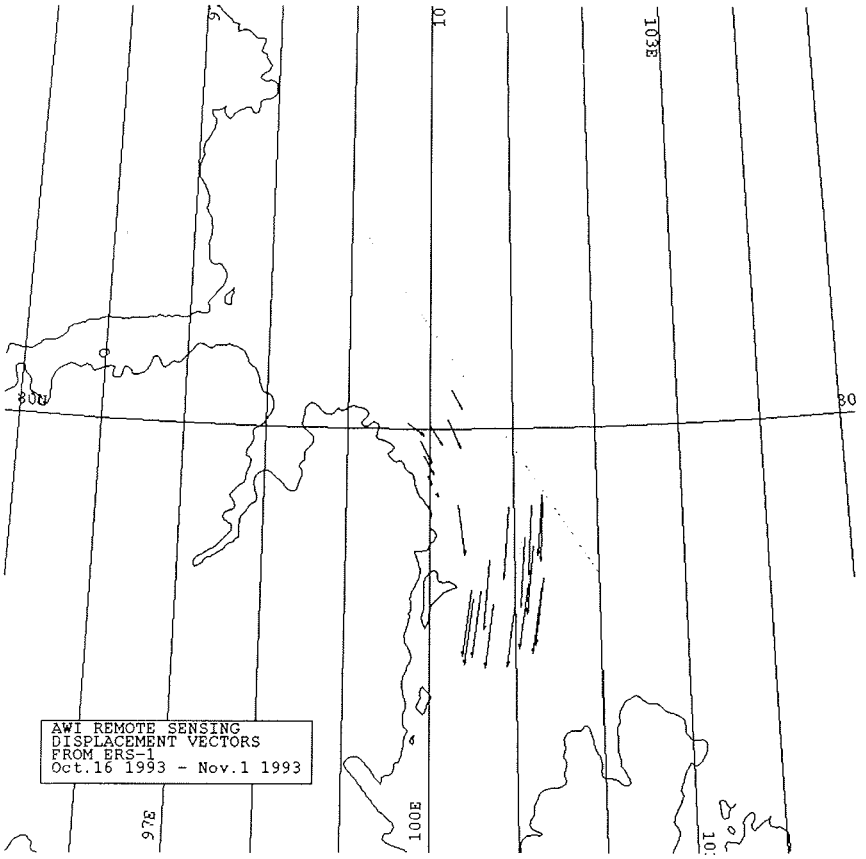

Fig.3: Displacement vectors of ice floes as derived from two ERS-1 SAR frames. The vectors were derived from the ERS-1 image Orbit 11778 Frame 1629 from Oct. 16 1993 and Orbit 12007 Frame 1629 from Nov. 1, 1993. The grey area indicates the position of the first frame.

Between Nov. 30, 1993, and Dec. 19, 1993, an ice eddy (diameter ca. 50 km, rotation counterclockwise) was detected on the eastern entrance of Shokals'kogo Strait (Figure 4), sligthly east of the area of Figure 3. The length of the displacement vectors ranges from about 26 km to 3 km.

By analysing several ERS-1 SAR frames it was demonstrated, that the area along the eastern coast of the Severnaya Zemlya archipelago is a region of complex ice dynamics. As a result of divergence, large patches of new ice occur side by side with older ice floes. Convergence and shear produce heavily riged ice zones, as testified by field observations. These deep-draft ridges may also play an important role in seafloor/sea-ice interaction in the shallow areas of the southern Laptev Sea. Icebergs calving from the ice caps of the Oktyabr'skoy Revolyutsii and the Komsomolets Islands can be distinguished. Further studies will show how to determine their importance for stabilisation of a fast ice cover and seafloor morphology.

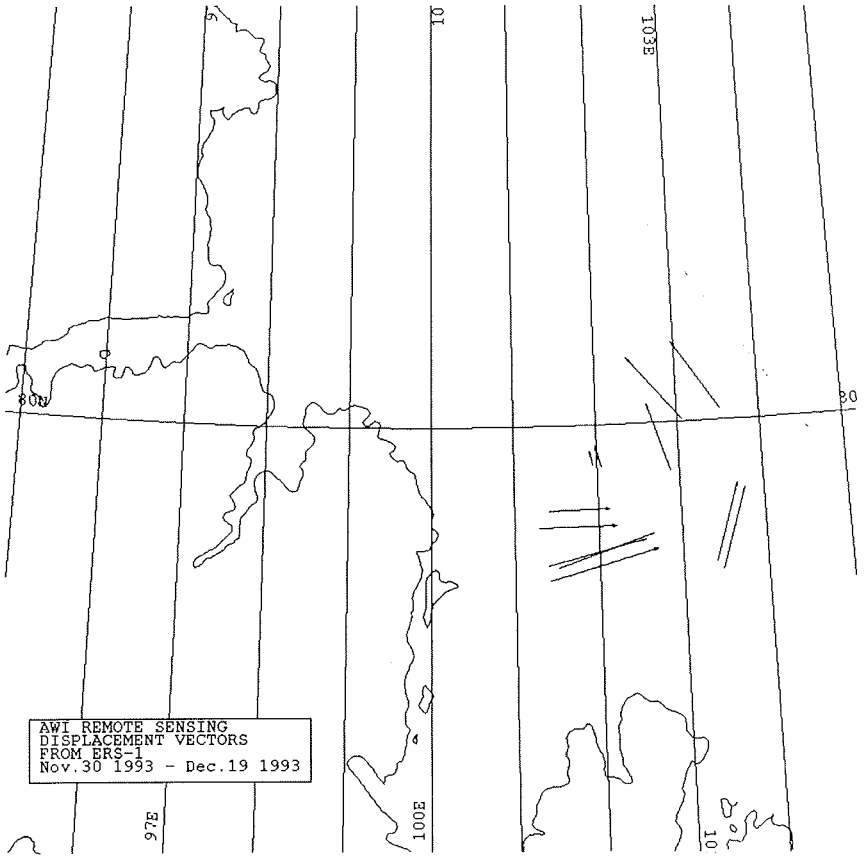

Fig.4: Displacement vectors of ice floes as derived from two ERS-1 SAR frames. The two frames are from Nov. 30 1993 (Orbit 12422, Frame 1629) and from Dec. 19 1993 (Orbit 12694, Frame 1629). The grey area indicates the position of the first frame.

References

Massam, R. 1991. Satellite Remote Sensing of Polar Regions. London, Belhoven Press.

Carsey, F. D. 1992. Microwave Remote Sensing of Sea Ice. American Geophysical Union.

FULL-SCALE FIELD EXPERIMENT CARRIED OUT BY THE AARI IN THE SOUTH-EASTERN LAPTEV SEA (1976) AND ITS MAIN RESULTS

Yu. Gorbunov, Z. Gudkovich and S. Losev
State Research Center of the Russian Federation the Arctic and Antarctic Research Institute, St. Petersburg, Russia

The aim of the experiment is to assess the influence of heat and dynamic processes on changing ice cover characteristics in spring and summer.

The following goals were set:

- to reveal the spatial and temporal changes of ice cover characteristics (thickness, concentration, concentration of ridges and hummocks, melting stages, reflection);
- to determine the patterns for ice drift velocity and their changes during the melting stage;
- to study the distribution of water temperature and salinity below the ice cover;
- to determine the horizontal heat fluxes and peculiarities of ice motion near the ice edge.

The experiment was carried out in the south-eastern Laptev Sea because neither a strong ice cover heterogeneity nor an intensive ice exchange with other regions etc. complicate the processes to be studied there.

The full-scale field experiment was divided into two stages.

At the first stage (in April), ice observations and hydrological surveys of fast ice were carried out during the landing of the aircraft "AN-2" on ice at 23 points.Visual airborne survey of ice, measurements of water temperature and salinity, ice thickness, snow depth and density, ice salinity and durability, ice thickness in hummocks, the determination of ice texture and structure were carried out.

At the second stage of the experiment (during the melting and destruction of ice) the following activities were performed:

- airborne survey, thermal survey and actinometric observations aboard the aircraft "IL-14" along the standard routes;
- customary radar survey (on the average: every three days) of the ice cover by means of side-looking radar aboard the aircraft "AN-24";
- ice and oceanological observations carried out by means of the helicopter "MI-8";
- ice and oceanological observations in fast ice aboard an icebreaker and research vessel.

The scheme of the field activities is shown in Fig. 1. The main results of the investigations are briefly given below. Vast zones of low ice thickness (Fig. 2) were revealed during the spring stage of the expedition. They are caused by heat fluxes penetrating from below into the pycnocline in summer.

It has been found that about 50% of the fresh water stored in fast ice originate from the annual Lena river discharge. The ice volume in hummocks amounts up to 20% of the volume of level ice. Having processed the data of the second stage, it turned out that, in comparison with the total ice volume, the volume of hummocks increased up to 75% during the melting (that is, first of all, more level and thin ice plots were melting). The analysis of ice samples with respect to the distribution of pollution allowed to conclude that the distribution depends on the presence and intensity of storms in the period before the beginning of ice growth. Ice pollution has

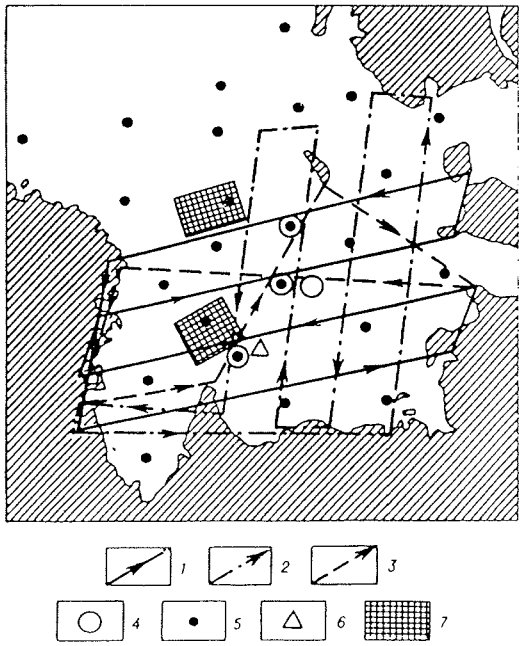

Fig. 1: Scheme of the field activities in the south-eastern Laptev Sea. 1,2 - Location of tacks of radar surveys (aircraft "AN-24"); 3 - Routes of the aircraft "IL-24"; 4 - Ice and oceanological observations on ice in summer ("MI-8" helicopter); 5 - The same in April ("AN-2" aircraft); 6 - Ice and oceanological observations aboard an icebreaker; 7 - Regions of observations aboard an research vessel at the ice edge.

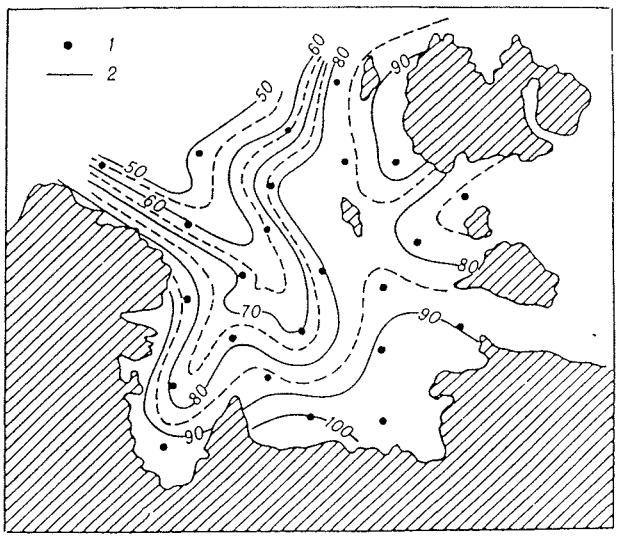

Fig. 2: Pattern of ice thickness distribution at the end of May 1976. 1 - Places of landings on ice; 2 - Isolines of ice thickness (in percent relative to maximum thickness).

a profound effect on the albedo of the surface and on the intensity of destruction during the melting period. In June, the area of puddles on fast ice was, for the polluted plots, 1.5 as large as the area of plots without pollution. The area of water on the ice surface was estimated using the data of airborne survey. Changes of the relative area of puddles in summer, spatial differences of the area of puddles, caused by different terms of the beginning of melting, the concentration of ridges and hummocks, and ice as well as sizes of floes were studied. It was found out that the convection caused by an increasing water density during the heating near 273K played an important role in the rapid deepening of puddles and the appearance of thaw holes. In summer 1976, the study area was to a greater extent exposed to diverging than to compaction. Side melting, transformation of thaw holes into fractures during ice-cover crushing as well as "diffusion" of floes in the zone of the ice edge were crucial to diverging.

Using the data of the radar surveys, 12 consecutive patterns for the drift velocity were completed, extending from 2 to 6 days. Considerable spatial changes of the drift velocity were found caused by a strongly jagged coastal line, the presence of islands, straits, and banks. The distribution of dry land and shallows as well as the direction of prevailing winds have a great impact on the location of compacting zones. Ice exchange through the Novosibirsk Straits was calculated by means of the data on ice drift and ice concentration. The volume of ice transported out of the Laptev Sea in summer 1976, was about 6 km^3 (2% of the initial ice volume in fast ice). Consequently, the main ice mass had melted at the place of its origin. The approximation of patterns of ice-drift velocity allowed to calculate div W. The analysis of the distribution of average values of div W showed that a positive divergence, caused by processes of turbulent diffusion, occurred even for prevailing coastward winds. The assessment of the coefficient of diffusion was 10 cm/s. For 3-day periods, the displacement of the ice edge to the ice-free water area was about 30% from the mean value for the region affected by drift, and for 2-week periods about 45%.

In comparing the observed ice-drift velocities with the baric gradient it was possible to determine the main parameters of the dependence between these values and also to find out the spatial scales of coasts effect for ice drift with tangent and normal to coast wind direction.

A lot of grounded hummocks (more than 200) were found using the data of radar surveys of the ice-cover. Their characteristics (length, draught, time of existence) were determined. The partial areas of ice occupied by floes of different sizes were calculated by means of the data of instrumental surveys carried out for different periods. It also turned out that the intensity of ice crushing rapidly increased after the fracturing of fast ice. In the first half of June, the velocity, with which the total area of floes less than 100m in diameter increased, while their average diameter decreased, was about twice as much as in the second half of July. The intensity of fast-ice crushing was 2.5 - 3 times as much as in the ice massif outside the fast-ice zone. The increasing of ice crushing correlated with a decrease in its total concentration. Big horizontal gradients of water density were observed providing evidence of marked baroclinic gradient currents. These currents increase in summer due to an increasing river discharge and change under the influence of prevailing winds as well.

The results of the investigations obtained during the full-scale experiment were issued in greater detail in "Poleks-Sever-76" Proceeding, part 2, "The Arctic region" part, L.: Hydrometeoizdat, 1979, p.7-110 (in Russian). The main part of them was used for modeling of the Arctic sea ice cover.

SURFACE - BASED STUDIES OF MICROWAVE ARCTIC SEA ICE SIGNATURES DURING END OF SUMMER AND EARLY AUTUMN

A.N. Darovskikh
State Research Center of the Russian Federation the Arctic and Antarctic Research Institute, St. Petersburg, Russia

Emissivities at frequency of 37 GHz were measured from sea ice, open water and freezing melt puddles during the joint Russian - German cruise ARK IX/4 to the Northern Barents Sea and Laptev Sea. The Radiometer was mounted on a sled, 2.5 m above the ice surface. The angle of incidence varied from 0 (nadir) to 65 degrees. The paper describes of the evolution of microwave sea ice signatures during the end of summer and early autumn.

Introduction

In the last decade microwave passive remote sensors have been widely used to provide qualitative information pertaining to the polar sea ice. Satellite, airborne and ground-based microwave measurements, made in conjunction with electrical and physical property measurements of snow and ice, have determined the basic microwave properties of sea ice Microwave remote sensing of sea ice 1992. It was found that microwave arctic sea ice signatures have significant fluctuations in summer and early autumn.

The emissivities presented in this paper were measured from sea ice, open water and freezing melt puddles during the joint Russian-German cruise ARK IX/4 to the Northern Barents Sea and Laptev Sea in 1993.

Radiometric measurements

A 37-GHz radiometer was mounted on the port side of the ship, 16.1 m above the sea surface for measuring the emission from open water or thin ice. The angle of incidence could be changed from about 20-25 to 180 degrees by mechanically rotating the radiometer. The same equipment could also be used directly on the ice while on a station. In this case, it was mounted on a sled, 2.5 m above the ice surface where theangle of incidence could be changed from 0 (nadir) to 65 degrees. The construction of the sled permitted to change the angle of incidence while the antenna of the radiometer continues to point at the stationary object.

From August 12 to 21 measurements were carried out in the Northern Barents Sea. During this period, air temperatures were above zero. We had typical summer conditions. Ice thicknesses were from 2 to 4 meters, the temperature of upper layers of ice was about zero, salinity was < 0.5%. The surface of ice floes consisted of wet ice areas and extensive areas of open melt puddles. It should be noted that ice emissivity was very high (> 0.95) and polarization ratios, defined as PR = (TBV - TBH)/(TBV + TBH), were < 1.4%. TBV and TBH are vertical and horizontal brightness temperatures, respectively. Open melt puddles were "cold" points on the background of "hot" ice. Their emissivities are about the theoretical values calculated by means of the Fresnel reflection theory. Figure 1 shows the dependencies of brightness temperatures of multi-year ice and water in puddles on the angle of incidence.

The second group of measurements were carried out in the Laptev Sea from September 3 to 21. During this period, the air temperatures were below zero and reached -12 °C. The ice thickness varied from 80 to 220 cm. There was a snow

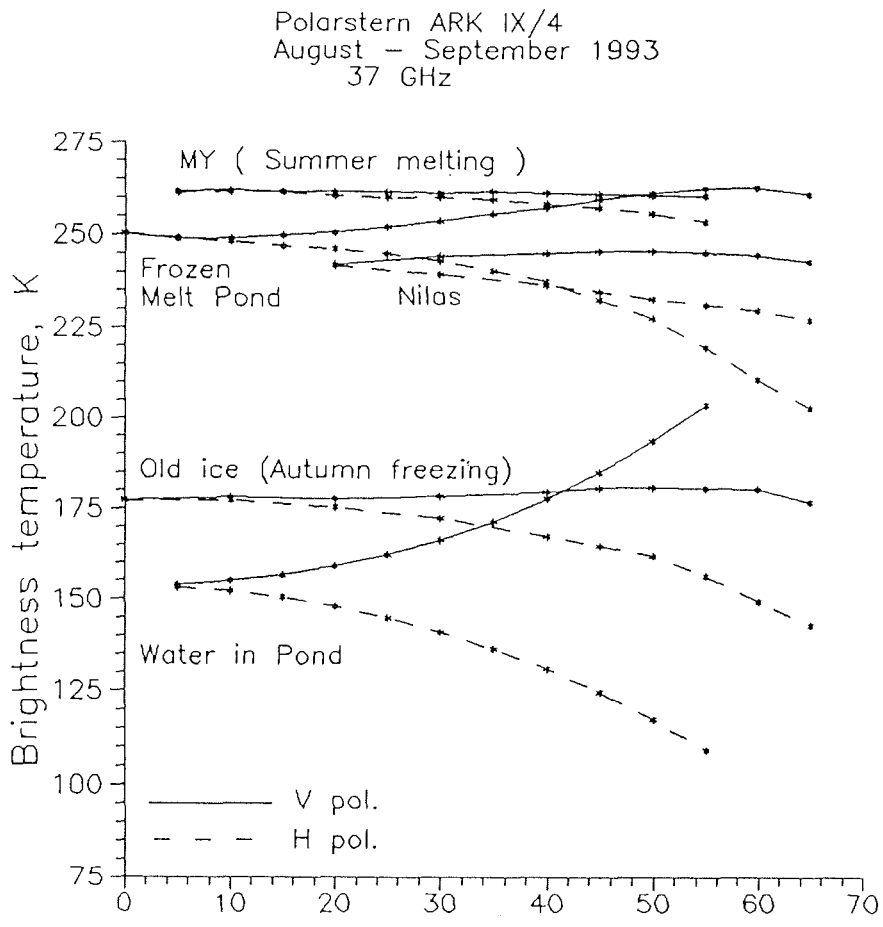

Fig.1. Brightness temperature as a function of the angle of incidence for sea ice and melt puddles.

cover on sea ice varying from 0.5 to 30 cm depth. The brightness temperature of old ice decreased to values typical for winter. As puddles were freezing, their emissivity increased to very high values. Frozen melt puddles became "hot" points on the ice surface. Frozen melt puddles had 10 to 23 cm of new fresh ice on the surface and 10 to 30 cm of liquid water remaining between the puddle ice and the underlying sea ice. The emissivity reached saturation because the fresh ice was optically thick. Figures 1 and 2 demonstrate these relations.

Research summary

1. Emissivities of all objects investigated are shown in Figure 2 and Table 1. Table 1 also shows ice thicknesses, snow depths, ice and snow temperatures.

2. Measured emissivities form four clusters: open water, multi-year ice (summer melting, frozen melt puddles and old ice (autumn freezing)).

3. Emissivities of melt puddles are equal to emissivities of calm water in nearby leads or the ocean, therefore melt puddles are indistinguishable from nearby leads

or ocean water.

4. Due to flooding and wicking brine is drawn up into snow. This causes the formation of a slush layer which can significantly decrease emissivities of ice. Cluster A in Figure 2 illustrates the effect of slush layer (points 2 and 3 in Table). When the ice temperature decreased, slush layers froze and formed frazil ice layers. Emissivities of ice increased a little (cluster B in Figure 2).

5. In both summer and autumn, the emissivities of ice are influenced by the spatial distribution of melt puddles.

Tab. 1: Emissivities, ice thicknesses, snow depths, ice and snow temperatures of all investigated objects

No. point	Date	E Vpol.	E Hpol.	Hice cm	Hsnow cm	tice h=0.2cm	tair/ snow	tsnow/ ice
			MY ice (summer melting)					
1	18.08.93	0.955	0.936	190	0	-0.1		
			Old ice (autumn freezing)					
2	03.09.93	0.593	0.479	80	5.5-7	-0.1	-3.2	-0.36
3	03.09.93	0.603	0.488	80	7	-0.1	-3.8	-0.36
4	07.09.93	0.625	0.573	130	11	-0.1	-1.5	-0.1
5	10.09.93	0.578	0.536	150	18	-0.5	-3.5	-1.7
6	11.09.93	0.618	0.593	220	20-21	-0.4	-3.1	
7	12.09.93	0.672	0.603	150	3	-4.5	-7.4	
8	13.09.93	0.685	0.635	190	5	-2.2	-3.7	
9	14.09.93	0.661	0.605	140	2	-8.0	-10.4	
10	15.09.93	0.656	0.601	220	5-10	-4.6		
11	18.09.93	0.720	0.688	150	30	-0.6		
			Frozen melt ponds					
12	12.09.93	0.972	0.846	10	0	-4.8	-5.2	
13	14.09.93	0.979	0.845	17	0.5	-6.7	-6.9	
14	15.09.93	0.973	0.870	20	0.5	-5.0	-6.3	
15	18.09.93	0.961	0.886	20	0.5-1.0.	-0.63	-0.5	-0.55
16	21.09.93	0.845	0.784	23	1.0-1.5	-5.1		

Ice thicknesses of old ice were taken from Dr.H.Eicken'cruise report

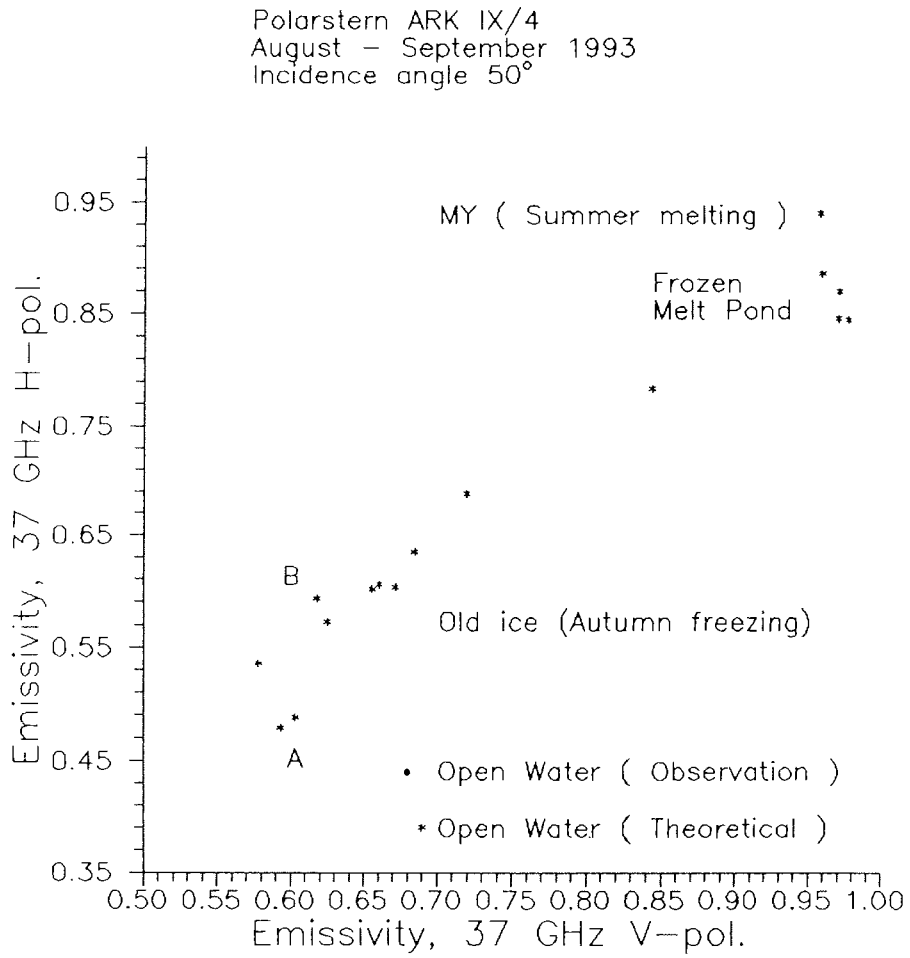

Fig.2. Scatter diagram for emissivities at 37 GHz at H-polarization versus 37 GHz at V-polarization for all objects investigated.

References

Carsey, F. D. (ed.) 1992. Microwave remote sensing of sea ice. - Geophysical monograph 68, 1-462.

CALCULATION OF SPECTRAL ALBEDO FOR A MELT POND

A. Makshtas and I. Podgornyy
State Research Center of the Russian Federation the Arctic and Antarctic Research Institute, St. Petersburg, Russia

Abstract

Two algorithms are proposed: (1) to calculate spectral albedo and (2) to derive the bottom spectral albedo from measurements of spectral albedo of a melt pond. To achieve this goal, an analytical approximate solution of the radiative transfer equation is used. The accuracy of the method is evaluated for the 0.4-to-0.7-μm-wavelength region in the cases of direct and diffuse illumination. The results of the computations and of the data of integral albedo sampled in the Arctic correspond to each other to a satisfactory extent at small melt pond depths.

Method of calculation

The method of calculating spectral albedo is elaborated for an idealized melt pond modelled on a plane - a parallel homogeneous water layer of the depth H lying on flat ice. Ice thickness is suggested to be large enough. The melt pond bottom is a Lambertian reflector whereas the optical properties of the water layer are assumed to be quite similar to those of clearest water.

Unpolarized radiation, reaching the air-water interface from above with the angle of incidence arccos(μ), is partially reflected according to the Fresnel law and enters, after refraction, the melt pond with the angle arccos(ξ). According to the Snell law

$$\sqrt{1-\mu^2} = n\sqrt{1-\xi^2}, \qquad (1)$$

where n is the refractive index of water.

At first an approximate solution of the radiative transfer equation is found under the assumption of small scattering in comparison with absorption. In this case, an expression for $A(\tau_0,\mu)$, spectral albedo (at the wavelength λ, omitted for brevity) for the melt pond of the optical thickness τ_0 illuminated by collimated irradiance, is given by

$$A(\tau_0,\mu) = R(\mu) + \frac{2\alpha(1-R(\mu))\left(E_3((1-\Lambda)\tau_0) - R_3((1-\Lambda)\tau_0)\right)}{1-2\alpha R_3(2(1-\Lambda)\tau_0)}\exp\left(-\frac{(1-\Lambda)\tau_0}{\xi}\right), \qquad (2)$$

$$R_3(t) = \int_0^1 R(\eta)\exp\left(-\frac{t}{\eta}\right)\eta d\eta, \qquad (3)$$

$$E_3(t) = \int_0^1 \exp\left(-\frac{t}{\eta}\right)\eta d\eta. \qquad (4)$$

Here α is spectral albedo for the melt pond bottom, $\tau_0=(\kappa+\sigma)H$, $R(\eta)$ is the Fresnel reflection coefficient, κ and σ are the beam absorption and total scattering coefficients correspondingly, Λ is scattering-to-attenuation ratio.

In the case of diffuse illumination, it follows from Eq. (2) that

$$\overline{A}(\tau_0)=\overline{R}+\frac{4n^2\alpha\left(E_3((1-\Lambda)\tau_0)-R_3((1-\Lambda)\tau_0)\right)^2}{1-2\alpha R_3(2(1-\Lambda)\tau_0)}, \qquad (5)$$

where

$$\overline{R}=2\int_0^1 \mu R(\mu)\,d\mu. \qquad (6)$$

To find an "exact" solution for the radiative transfer equation, the Monte Carlo sampling technique is employed. First the errors which arise owing to scattering in the water layer are estimated. Then the applicability of the parameterization given by Eqs. (2) and (5) to the calculations of spectral albedo for a melt pond for the wavelength region of interest is evaluated. Although the computations are carried out in the case of Rayleigh scattering, the presence of hydrosols is unlikely to modify radiative transfer in the melt pond significantly as they scatter radiation primarily in forward direction.

Fig. 1 shows the values of albedo $A(\tau_0,\mu)$ for a melt pond as dependent on τ_0 for $\Lambda=0.5$, $\alpha=0.8$, and for the angle of incidence being equal to 60° ($\mu=0.5$). The results of three different methods are presented, namely, those obtained by means of the Monte Carlo sampling technique and by means of the calculations using Eq. (2) directly and Eq. (2) with $E_3(t)$ and $R_3(t)$ approximated by the first five terms of power series on t. As shown in Fig.1, scattering may not be neglected for τ_0 less than 1, even for $\Lambda=0.5$, whereas the maximum value of Λ for clearest fresh water does not exceed the value of 0.26 in the 0.4-to-0.7-μm-wavelength region according to data compiled by Smith & Baker (1981).

Inverse Problem

The inverse problem is formulated as follows. Let $A(\tau_0,\mu)$, μ and $\tau_0 \le 1$ be given. Accuracy when determining α (spectral albedo for the melt pond bottom) has to be evaluated depending on accuracy in the determination of $A(\tau_0,\mu)$, μ and τ_0 (or depending on $\overline{A}(\tau_0)$ and τ_0 in the case of diffuse illumination). Making use of Eqs. (2) and (5) yields

$$\alpha=\frac{G}{1+2GR_3(2(1-\Lambda)\tau_0)}, \qquad (7)$$

where G is expressed by

$$G(\tau_0,\mu)=\frac{A(\tau_0,\mu)-R(\mu)}{2(1-R(\mu))\left(E_3((1-\Lambda)\tau_0)-R_3((1-\Lambda)\tau_0)\right)}\exp\left(\frac{(1-\Lambda)\tau_0}{\xi}\right) \qquad (8)$$

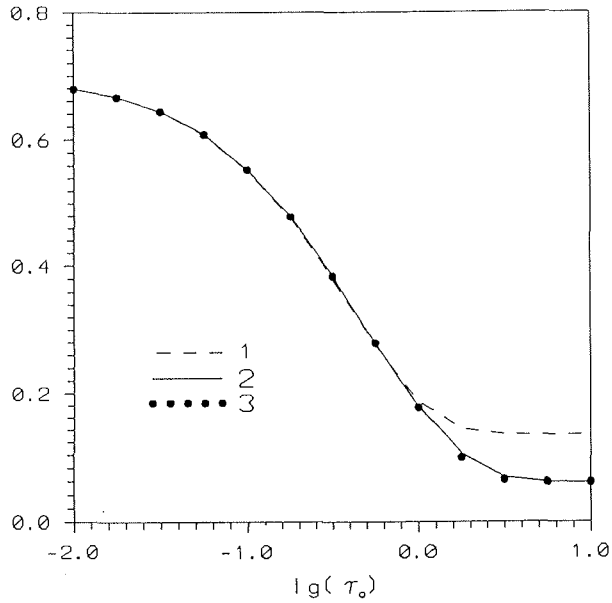

Fig. 1. Albedo for a melt pond of the optical thickness t_0 determined with the Monte Carlo sampling technique (1), together with that derived from Eq. (2) directly (2) and from Eq. (2) with $E_3(t)$ and $R_3(t)$ approximated by the first five terms of power series on t (3) (the angle of incidence is 60°). The values L=0.5, n=1.33 are used.

in the case of direct illumination and by

$$\overline{G}(\tau_0) = \frac{\overline{A}(\tau_0) - \overline{R}}{4n^2\left(E_3((1-\Lambda)\tau_0) - R_3((1-\Lambda)\tau_0)\right)^2} \qquad (9)$$

in the case of diffuse illumination. Parameter β (the sensitivity of α to X) is introduced as follows:

$$\beta = \left| X \frac{\partial \alpha}{\partial X} \right|. \qquad (10)$$

Briefly, if X is known with the relative error Δ_X, the relevant contribution to the absolute error when calculating α is the product of β and Δ_X.

The values of β have been calculated under the condition of direct illumination for μ=0.5 and X corresponding to $A(\tau_0,\mu)$, $\arccos(\mu)$ and τ_0. It has to be emphasized that accuracy in the evaluation of τ_0 depends on both H and beam absorption coefficient κ since $(1-\Lambda)\tau_0 = \kappa H$. For the calculations, the value of α=to 0.4 (an estimate of spectral albedo for a contaminated melt pond) has been used. It has been found out that the values of β differ by no more than 1% for $\overline{A}(\tau_0)$ and 6% for

τ_0 for both modes of illumination. Some results of the calculations are presented in Table 1.

Tab. 1: Sensitivity β (direct illumination, μ=0.5) for a melt pond of a depth of 1 m depending on wavelength λ (α=0.4).

l (mm)	k (m^{-1}) (Smith & Baker 1981)	X=A	X=arccos(m)	$X=t_0$
0.4	0.0171	0.416	0.268	0.011
0.5	0.0257	0.423	0.281	0.017
0.6	0.244	0.569	0.666	0.204
0.7	0.650	0.989	2.24	0.614

To conclude, let us consider, for example, the calculations for H=1m, λ=0.5 μm, α=0.4 and μ=0.5. According to Table 1, 10% relative accuracy in the determination of A, arccos(μ) and τ_0 results in absolute errors when determining α being equal to 0.042, 0.028 and 0.002 respectively. Thus, the least contribution to errors is due to parameter τ_0, which is known, as a rule, with the maximum relative error (about 10% owing to κ and about 10% owing to H).

Calculated Integral Albedo and Observations

The data used below have been collected during the R/V *Lance* cruise in the northern part of the Barents sea in August 1993. On 12 August 1993, special measurements of integral melt pond albedo were carried out on a multi-year ice floe, which had the coordinates 78.8° N, 34.8° E and with linear dimensions about 100 m. A Quantum sensor LI-190 SB with a spectral window of 400-700 nm was employed to measure both downwelling and upwelling irradiances. The thickness of the ice floe was more than 2 m.

All measurements of albedo were performed at noon (with the sun angle being about 30°) when the sky was clear. Every melt pond was tested for contaminants on its bottom, and only contaminant-free ponds (subjective appraisal) were selected to measure albedo. Besides, every evaluation was repeated three to five times in order to acquire statistics (mean values and standard deviation). The results of the measurements are presented in Table 2.

With respect to the conditions under which the observations were made, we apply an uncomplicated model to describe the shortwave radiative transfer in the atmosphere. First, the atmosphere is suggested to be cloudless and aerosol-free. Second, the absorption of solar radiation by O_3 and Rayleigh scattering are assumed to take place in the stratosphere and troposphere respectively. Absorption by water vapour and other gases is ignored owing to their insignificant effect on the spectral region of interest. As a result, the troposphere is reduced to a conservatively scattering layer with optical thickness depending on wavelength.

The optical melt pond model used for the simulations contains the absorption coefficients $\kappa(\lambda)$ (cf. Smith & Baker, 1981) and the values for spectral albedo of melting multi-year ice $\alpha(\lambda)$ (cf. Grenfell & Maykut, 1977). The absorption of solar

radiation by O_3 in the Chappuis band is taken into account for a total ozone content which is equivalent to 0.5 cm.

Tab. 2: Measured integral albedo for the melt ponds in the Barents sea (0.4-to-0.7-μm-wavelength region).

Depth (m)	Albedo	Square mean deviation
0.00	0.84	0.05
0.02	0.54	0.02
0.10	0.53	0.01
0.19	0.56	0.02
0.35	0.59	0.02
0.50	0.35	0.02

Integral albedo for a spectral region (λ_1,λ_2) is introduced as follows

$$<\tilde{A}>=\frac{\int_{\lambda_2}^{\lambda_2}\tilde{A}(\tau_0(\lambda),\mu_0,N)F(\lambda)d\lambda}{\int_{\lambda_2}^{\lambda_2}F(\lambda)d\lambda}, \qquad (11)$$

where $F(\lambda)$ is spectral incidence irradiance just at the top of the troposphere (already corrected for absorption in the Chappuis band) and N is the pond area ($0<N<1$).

Integration is performed from 0.4 to 0.7 μm with steps of 0.01 μm for a sun angle of 30° (air mass of 2), N being equal to 0.5 and H being from 0 to 1 m. The value of integral albedo which is relevant to a non-scattering troposphere also evaluates to what extent Rayleigh scattering may affect the value of $<\tilde{A}>$.

The results of the calculations are presented in Fig. 2. Empirical and calculated values of integral albedo are in reasonable correspondence for small H. In particular, both observed and calculated integral albedo change sharply near H=0. Then, however, they keep their values. The results do not significantly depend on the presence of the atmosphere.

As soon as H reaches the value of 0.5 m, observed and calculated albedos begin to deviate from each other. Although the dependence of $<\tilde{A}>$ on depth should be rather weak according to the theory developed, the albedo measured at H=0.5 m is as low as 0.35 in comparison with the value of 0.59 at H=0.35 m. As mentioned above, this is probably due to the influence of contaminants on spectral albedo for the melt pond bottom.

So direct measurements of spectral bottom albedo for melt ponds (especially for mature ones) are believed to be extremely important for further progress in this field. In particular, that must yield a parameterization of albedo for a melt pond in

terms of bottom contaminants that are likely to be the most significant factor among those affecting the albedo of mature melt ponds in the 0.4-to-0.7-μm-wavelength region.

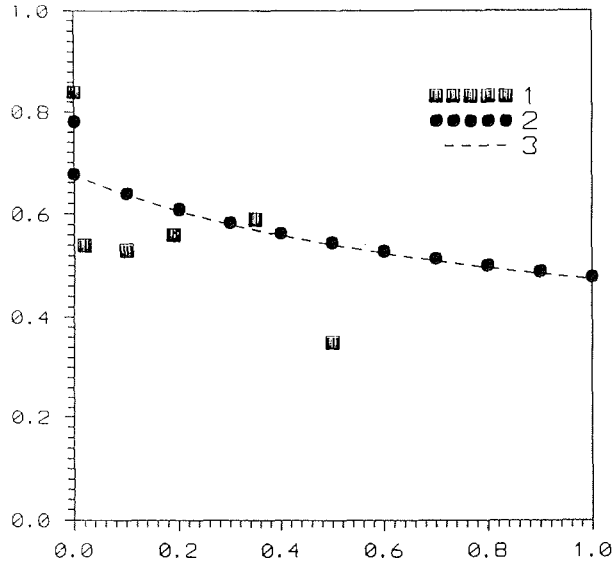

Fig. 2. Integral albedo for a melt pond in the 0.4-to-0.7-μm-wavelength region (i_0=30°) derived from measurements (1) and calculated for the realistic (2) and for a non-scattering atmosphere (3).

Reference

Grenfell, T.C., Maykut, G.A. 1977. The optical properties of ice and snow in the Arctic basin. *J. Glaciol.* 18 (80): 445-463.

Smith, R.C. , Baker, K.S. 1981. Optical properties of the clearest natural waters (200-800 nm). *Appl. Opt.* 20 (2): 177-184.

SOLUTION AND STABILITY CRITERIA OF NATURAL CONVECTIVE FLOW IN A MELT PUDDLE

P. V. Bogorodskiy
State Research Center of the Russian Federation the Arctic and Antarctic Research Institute, St. Petersburg, Russia

Interest in convection in a melt pond is defined by the obvious influence of mixing processes on the rapidity of the Arctic sea ice melting (Appel and Gudkovich, 1979; Moritz et al., 1993). The physical basis for this phenomenon consists in the increase of the melt water density, with the water being heated almost to the freezing point. If the heat balance at the surface is positive, this effect results in a hydrostatic instability.

1. Let us consider a horizontal layer of a two-component fluid bounded by a free upper and a hard lower surface. The axes x and y are horizontal, the origin of the coordinates is on the lower boundary. Driven by wind, the fluid moves stationarily in the x-direction with the typical velocity U and the profile $f(z)$. The peculiarity of the task can be expressed by the equation of state in the form $\rho = \rho_0(1 + \alpha T + \beta S)$, where ρ is water density, T temperature, S the concentration (salinity), and α and β are the thermal expansion and the density concentration coefficients. Convection equations in Boussinesq approximation in a dimensionless, linear form follow:

$$\begin{aligned}
(\frac{\partial}{\partial t} - \nabla^2 + Re f \frac{\partial}{\partial x})\mathbf{v} &= -\nabla p - Re f' v_3 \mathbf{e}_1 - (RaT + RsS)\mathbf{e}_3 \\
(Pr\frac{\partial}{\partial t} - \nabla^2 + RePrf\frac{\partial}{\partial x})T &= v_3 \\
(Sc\frac{\partial}{\partial t} - \nabla^2 + ReScf\frac{\partial}{\partial x})S &= v_3
\end{aligned} \qquad (1)$$

$$div\,\mathbf{v} = 0$$

$$Ra = \frac{g\alpha\Delta T h^3}{\chi\nu},\ Rs = \frac{g\beta\Delta S h^3}{D\nu},\ Re = \frac{Uh}{\nu},\ Pr = \frac{\nu}{\chi},\ Sc = \frac{\nu}{D}$$

$$\mathbf{v} = (v_1, v_2, v_3), (\quad)' = \frac{d}{dz}, \nabla = (\frac{\partial}{\partial x}, \frac{\partial}{\partial y}, \frac{\partial}{\partial z})$$

Here Ra and Rs are the conventional and the concentration Rayleigh numbers, Pr and Sc the conventional and the diffusion Prandtl numbers, Re is the Reynolds number, ΔT and ΔS are the overfall of temperature and salinity, h is the layer thickness, v is velocity, p is pressure, g is gravity acceleration, t is time, and $\mathbf{e}_1$ and $\mathbf{e}_3$ are the basic vectors of the axes x and z. If we introduce small periodic disturbances of velocity, temperature and salinity proportional to $exp(-\omega t)\,exp(i\,\mathrm{kx})$ (where ωt is the complex-valued decrement, i the imaginary unit, $\mathrm{k} = (k_1, k_2, 0)$ the wave vector, $\mathrm{x} = (x, y, 0)$ the radius vector), we obtain amplitude equations from (1):

$$\begin{aligned}
\omega\delta w + ik_1 Re(f\delta w - f''w) &= \delta^2 w + k^2(Ra\,\theta + Rs\,\sigma) \\
\omega Pr\,\theta + ik_1 RePrf\theta &= \delta\theta + w
\end{aligned} \qquad (2)$$

$$a\delta c\sigma + ik_1 ReSc f\sigma = \delta\sigma + w$$
$$\delta = \frac{d^2}{dz^2} - k^2, \quad k^2 = k_1^2 + k_2^2$$

Here w is the vertical component of velocity. The boundary conditions for the layer which cools from below follow:

$$\begin{aligned} z = 0&: \ w = w' = \theta = \sigma = 0 \\ z = 1&: \ w = w'' = 0, \ \theta' = Bi\theta, \ \sigma' = Sh\sigma \\ Bi = \frac{ah}{\kappa}&, \ Sh = \frac{bh}{D} \quad , \end{aligned} \tag{3}$$

where Bi is the Biot number, Sh the Sherwood number, a, and b are the coefficients of the heat-transfer, the thermal conductivity and the mass-transfer, respectively. In case of the the fluid moving as described above, the directions x and y are disparate. Therefore, the equations (2) are unsymmetrical relative to the wave numbers k_1 and k_2. If $k_1 = 0$ and $k_2 \neq 0$, components which contain undisturbed velocity fall out of the equations. Hence the disturbances are independent of the x-coordinate and represent infinitely long cylinders which extend along the x-axis ("x-rollers"). The critical Rayleigh number for the disturbances of "x-rollers" is independent of the current velocity and coincides with the critical Rayleigh number for the fixed layer. This is correct for any function $f(z)$. If $k_1 \neq 0$ and $k_2 = 0$, the disturbances represent the same cylinders, which, however, extend along the y-axis ("y-rollers").

2. Let us confine ourselves to the case of the "x-rollers". Here the decrements may be considered real (Gershuni et al., 1989) for melt water which is produced by the upper layers of ice with a salinity close to zero (Moritz et al., 1993). Decrements of the value zero define the stability threshold. In this case remaining parts of the equations (2) vanish. We will investigate different modes of long wavelengths $(k \to 0)$, which are extremly significant for a single layer. The form of the equations (2) for neutral monotonous disturbances $(\omega = 0)$ ω allows us to present the disturbance amplitudes and the critical Rayleigh numbers as a power series expansion by the even powers of the dimensionless wave number k:

$$\begin{aligned} (w, \theta, \sigma,) &= (w, \theta, \sigma)^{(0)} + k^2 (w, \theta, \sigma)^{(1)} + o(k^2) \\ (Ra, Rs) &= (Ra, Rs)^{(0)} + k^2 (Ra, Rs)^{(1)} + o(k^2) \end{aligned} \tag{4}$$

For the zeroth-order terms $w^{(0)} = (\theta^{(0)})'' = (\sigma^{(0)})'' = 0$. If (3) is satisfied, we get $\theta^{(0)} = \sigma^{(0)} = const$, which are supposed to be equal to the unit. If we neglect the elements of the $o(k^2)$ order because the values of k are insignificant, the equations for the elements of the first order are

$$\begin{aligned} w^{(1)IV} &= R \\ (\theta^{(1)})'' + w^{(1)} &= 0 \end{aligned} \tag{5}$$

$$(\sigma^{(1)})'' + w^{(1)} = 1 \quad ,$$

where the parameter $R=Ra^{(0)}+Rs^{(0)}$ is the effective number of Rayleigh. The boundary conditions for the expansion elements of the first and the following orders coincide with (3). If we integrate (5) with (3), we obtain

$$w^{(1)} = \frac{R}{48}(2z^4 - 5z^3 + 3z^2) \tag{6}$$

$$(\theta,\sigma)^{(1)} = -\frac{R}{2880}(4z^6 - 15z^5 + 15z^4) + \frac{z^2}{2} - \frac{1440[(Bi,Sh)-2] + R[9-4(Bi,Sh)]}{2880[1-(Bi,Sh)]}z \quad .$$

If we put (6) into (4) and further into (2), we obtain the conditions for the search for the critical numbers R, which define the instability level for long-wavelength disturbances:

$$R = \frac{1440[(Bi,Sh)(1-z)+(z-2)]}{[1-(Bi,Sh)](4z^5 - 15z^4 + 15z^3) + [4(Bi,Sh)-9]} \tag{7}$$

The form of the function R, which is defined by the formula (7), depends on the parameters *Bi* and *Sh*. Numerical calculations show that the polynomial of the sixth order in denominators (7) can have real roots in the interval $0 \le z \le 1$. However, the necessary values of dimensionless parameters are unreal for the problem on hand. If $z \to 1$, the numbers *Bi* and *Sh* fall out of the expressions (7) at all, and therefore *R=280.*

3. From the physical point of view it is obvious that the stability task is symmetrical relative to the cooling from below and the heating from above. If the instability processes in the upper layer of the fluid are the same no matter whether the fluid is heated up or cooled, the parameters of the instability can be evaluated with experimentally verified relations and with the calculated Rayleigh number. These relations, however, were obtained under laboratory conditions with the fluid being heated from below. Furthermore, they did not specifically deal with melting surfaces. Therefore, the results yield only approximate values of the corresponding parameters.

With a cyclic regime of growth and collapse of the boundary layer (Howard, 1966), the collapse period (Fedorov & Ginsburg, 1988) is

$$t^* = 12.1\sqrt{\frac{\nu\rho c_p}{g\alpha Q}} \quad ,$$

where c_p is the heat capacity and Q the density of the heat flux. The critical thickness of the boundary layer (Howard, 1966) is

$$h^* = \sqrt{\pi\chi t^*} \quad .$$

The critical temperature overfall and the plume velocity are (Scorer, 1978)

$$\Delta T = \frac{R\nu\chi}{g\alpha(h^*)^3},$$

$$w^* = 1.2\sqrt{g\alpha\Delta T^* h^*} \quad .$$

If the outflux of heated water from a free surface is uninterrupted in a laminar convection (Gershuni et al., 1989), we have a typical size of a sinking particle :

$$h^* = \frac{R\chi\nu^{1/3}}{g\alpha\Delta T^*} ,$$

where the corresponding temperature overfall (Saunders, 1967) is

$$\Delta T^* = 2.83(Q)^{3/4}\left(\frac{\nu}{g\alpha\chi_p\rho\lambda^2}\right)^{1/4} .$$

Deep z and the velocity w of the small laminar element sinking follow from the Stokes law (Turner, 1973):

$$z^* = \frac{g\alpha\Delta T^*(h^*)^4}{\chi\nu},$$

$$w^* = \frac{R\chi}{h^*} .$$

The parameters of the instability of long-wavelength Rayleigh, calculated with the aid of the mentioned ratios for the molecular coefficients of melt water (Kukulka, 1981), are shown in Fig. 1. The estimates which were calculated according to the two schemes are sufficiently close to each other except for the vertical velocity w^*, which can be explained by the turbulent movement of the fluid in a plume. In spite of the fact that it is questionable whether these estimates correspond to the values under natural conditions, they do not contradict the phenomenological scheme of the process when the rate of air-sea exchange in the Arctic is typical (Moritz, 1993). In fact, they are comparable with the data of laboratory experiments, both with regard to time and space.

References

Appel, I. L., Gudkovich, Z. M. 1979. POLEKS - Sever - 76 (nauchn. rezultati). Hydrometeoizdat, Leningrad, pp. 31-37 (in Russian).

Fedorov, K. N., Ginsburg, A. I. 1988. The subsurface layer of the ocean. Hydrometeoizdat, Leningrad, 303pp. (in Russian).

Gershuni, G. Z., Zhukhovitsky, E. M., Nepomnjashchy, A. A. 1989. Stability of convective flows. Nauka, Moscow, 320pp. (in Russian)

Howard, L. N. 1966. Proc. of the 11th Intern. Congress of Applied Mechanics, Munich. pp. 1109-1115.

Kukulka, D. J. 1981. Thermodynamic and Transport Properties of Pure and Saline Water. M. S. Thesis, Univ. of N. Y. at Buffalo, 268pp.

Moritz, R. E., Curry, J. A., Thorndike, A. S., Untersteiner, N. (Eds.) 1993. SHEBA. A research program of the Surface Heat Budget of the Arctic Ocean. Appl. Phys. Lab.-Univ. of Washington, Seattle, 33pp.

Saunders, P. M. 1967. The temperature at the ocean-air interface. J. Atm. Sci. 24 (3): 269-273.

Scorer, R. S. 1978. Environmental aerodynamics. Ellis Horwood, Chichester, 488pp.

Turner, J. S. 1973. Buoyancy effects in fluids. Cambridge Univ. Press, Cambridge, 357pp.

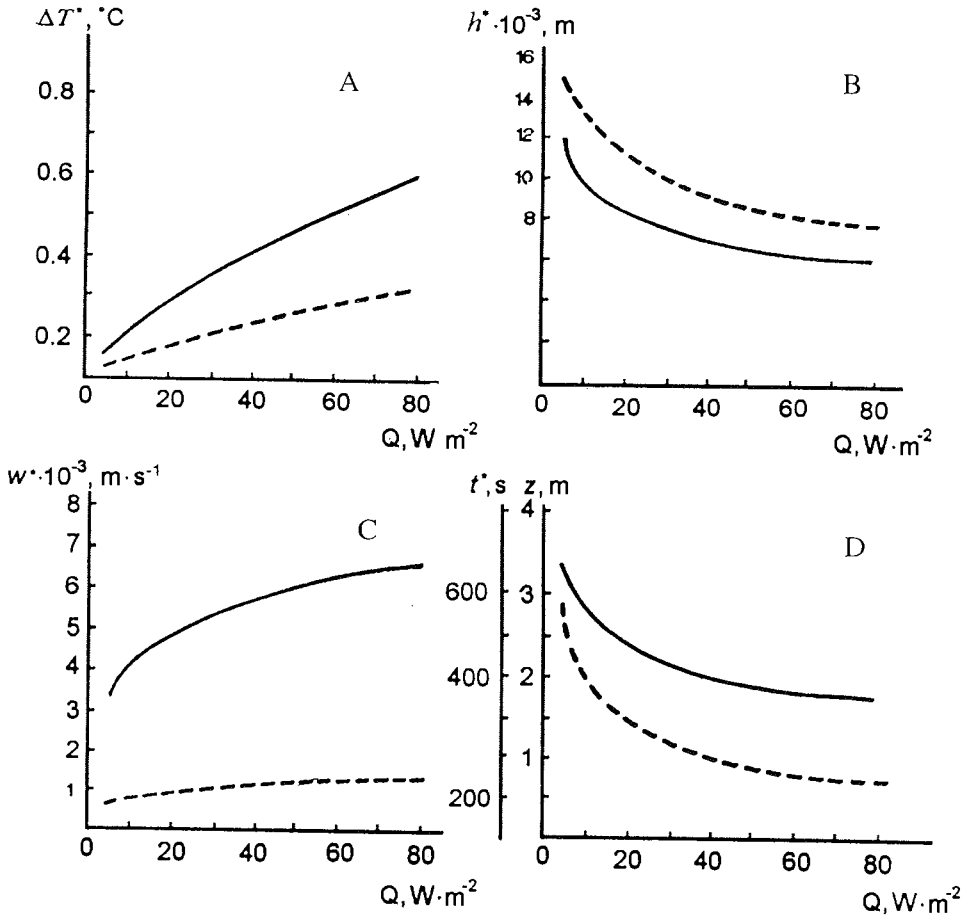

Fig. 1. The critical values of the temperature overfall (a), the thickness of the boundary layer (b), vertical velocity (c), the time and depth of the collapse (d) as a function of the heat flux Q for cyclic (dotted line) and uninterrupted (solid line) processes.

CATASTROPHIC STORM SURGES IN THE SOUTHERN PART OF THE LAPTEV SEA

I.M. Ashik and Yu.A. Vanda
State Research Center of the Russian Federation the Arctic and Antarctic Research Institute, St. Petersburg, Russia

The physical-geographical peculiarities of the Laptev Sea are favourable to the appearance of sufficient level oscillations in its southern part which exert a significant influence on the hydrological conditions of the adjacent water area, on its ecological conditions and economical activity. Meso-and microscale processes connected with the spreading of sea water over great distances into river mouths at a high surge level are also of particular importance. These processes result in dramatic changes in the hydrological and hydrochemical conditions of estuaries. Biological processes in these zones are strongly influenced, too. The quality of drink water is sufficiently deteriorated.

Tidal sea-level oscillations which can exceed 80-100 cm are of great importance for the south-western part of the sea encompassing the Khatanga and the Anabar Bay. Storm surges are of fundamental importance for the eastern part of the Olenek and the Yana Bay and in the Buor-Khaya guba. In this region, they often exceed the danger level and, under certainin conditions, they may be of catastrophic character.

The appearance of significant storm surges in the southern part of the Laptev Sea is most probable in the second half of September and at the beginning of October. Cyclonic activity intensifies in this period and it is connected with seasonal reorganisation of atmospheric processes. For this period the sea is maximum ice-free. So, in contrast to periods when fast ice or immobile close floating ice occurs along the coast, surges are not damped and smoothed by the ice cover.

The maximum catastrophic high level of surges was fixed in the southern part of the Laptev Sea from September 15-16, 1958 when it was by 5.2 m higher than the mean monthly value according to indirect estimates (Mustafin 1961). A period of drastic intensification of gales in the Arctic was noted in the second half of eighties. The highest storm surges were observed from October 9-10, 1985, when the absolute maximum values for the whole period of observations were exceeded at the stations in the south-eastern part of the sea. The absolute maximum values were exceeded at the stations in the Olenek Bay from September 26-27, 1988.

The atmospheric pressure field for the period, preceding the storm surge from October 9-10, 1985, was characterized both by an old high cyclone of low activity which was located above the Laptev Sea and by a thermally inhomogenous cyclone above the middle stream of the Lena river. This cyclone was moving to the north-east keeping its activity. Its centre had moved to the south-eastern part of the Laptev Sea at 6.00 Moskow time (MMT) on October 8. This cyclone united with the old northern one. Powerful advection of cold air took place when they were mixing in their rear part. This advection resulted in the formation and intensification of an atmospheric pressure crest over Yakutiya. Simultaneously with this process, an active frontal wave with great heat storage was displaced in eastern direction along 80° N. This wave has formed a low cyclone in the region of Severnaya Zemlya at 15.00 MMT on October 8. The cyclone, intensely deepening, moved with a velocity of about 70 km/hour eastwards in direction of the Laptev Sea. It met a less active cyclone at 6.00 MMT on October 9 north of Kotel´nyy Island. The less active cyclone came from the region of the Lena river. The first cyclone became more intensive and, due to a supplementary amount of heat, its velocity decreased. From 9.00 to

12.00 MMT on October 10, its atmospheric pressure in the centre was equal to 975 Pa. The interaction of such a deep cyclone and the crest over Yakutiya caused sharp atmospheric pressure gradients over the Laptev Sea and, therefore, an intensification of north-west and west winds. The wind velocity had reached 18-23 m/sec and kept this value until October 9-10. At the end of the first ten-day period of October, the major part of the Laptev Sea was covered by nilas. The south-eastern part of the sea south of 74° N was mainly ice-free. The southern edge of second-year ice was near 76° N.

The meteorological and ice conditions were, therefore, favourable to the development of a high surge level. The sea-level in the Tiksi Bay started to increase at 12.00 MMT on October 9. This increase amounted up to 167 cms during the next 7 hours. An insignificant sinking was followed by a new rising at 22.00 MMT. The sea-level increased by further 127 cms. The maximum value, by 246 cms higher than the mean navigational one, was reached at 6.00 MMT on October 10 (Figure 1). The sea-level in the Tiksi Bay sank during the next 30 hours by 335 cm. At the gauge of the Malyshev Island, located in the mouth of the Bykovskaya branch of the Lena, the rising of the sea-level began at 15.00 MMT on October 9. The sea-level rose by 156 cms after 16 hours. At the gauge Uedey (the mouth of the Yana), the sea-level increase began at 0.00 on October 9. The sea-level exceeded the mean navigational value by 255 cms at 7.00 MMT on October 10. The same type of sea-level changes was observed in this period at all coastal stations in the southern part of the Laptev Sea. If we take into account the intense low surge level, measured from September 30 to October 2 in the south-eastern part of the sea, the sea-level being by 100- 150 cm beneath the mean navigational values, the total amplitude of sea-level oscillations during these 10 days was about 4 meters.

It was a typical feature of this surge that its values in the south-eastern part of the sea sufficently exceeded the values in the south-western part of the sea. This was determined by the fact that the cyclone was deepening while its centre being relatively stable located north of Kotel'nyy Island. The western part of the sea was, to some extent, isolated from the rear part of the cyclone by the atmospheric pressure crest. As a result, the value of the highest surge level in the south-western part of the sea was relatively small. The surge observed nearly along the whole coast from September 26-27, 1988 can also be classified as a catastrophic one. It was generated by a cyclone, which displaced from the west to the east-north-east over the central part of the Laptev Sea. While deepening little by little, the cyclone centre moved towards the Novosibirskiye Islands. A hurricane with a velocity of 35-40 m/sec was registered in its rear part.

The sea-level rising at the Olympiyskaya polar station in the river mouth of the Olenekskaya branch of the Lena began at 3.00 MMT and lasted 18 hours. It exceeded the mean navigational value by 342 cms. The highest surge level was equal to 396 cms. The sea-level rising was observed nearly at all stations along the southern coast, its value in the south-eastern part of the sea being somewhat lower than in the south-western part (200-250 cms). A sufficient sea-level sinking beneath the dangerous marks was observed at some stations before this high level of the surge. A low level of such intensity was registered at the stations of the Tiksi Bay, the Bykov Cape, and Malyshev Island. In comparison with the high surge level in 1985, this surge, though characterized by high intensity, developed in accordance with typical features which have been revealed for storm surges in the south-eastern part of the Laptev Sea (Mustafin, 1961).

A catastrophic storm surge was observed along the southern coast of the Laptev Sea at the end of September and the beginning of October 1989. At the Nayba polar station, the sea-level exceeded the marks of elemental phenomena.

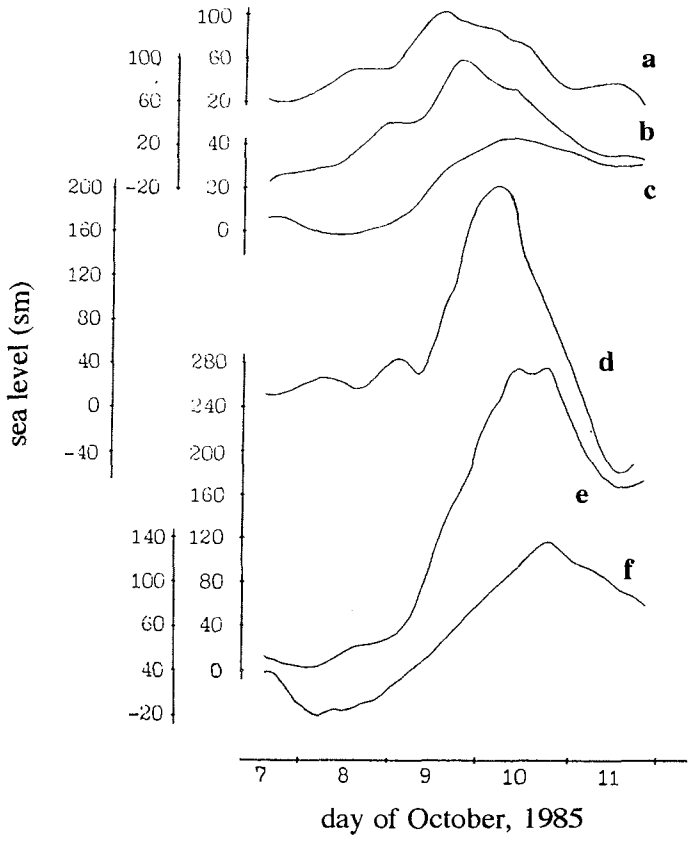

Fig. 1. The sea-level oscillations along the southern coast of the Laptev Sea in October 1985, at the stations Terpyay-Tumsa (a), Ust-Olenek (b), Dunay Island (c), Tiksi Bay (d), Uedey (e), Shalaurov Cape (f).

Powerful cyclonic formations causing gales over the Laptev Sea are not uncommon to the period from November until February. Close floating ice covering the whole sea and fast ice occupying the south-eastern part of the sea prevent, however, the development of an especially high level of surges. Nevertheless, hydrometeorological conditions during this period can turn out in such a way that the consequence of the gales causing the sea-level raising may be catastrophic.

From January 10-12, 1987, the marginal seas were covered by the periphery of a powerful cyclone having been built over the Arctic basin. At this time, hurricanes of western and north-western directions were observed over the Laptev Sea. They caused the maximum surge level in winter. A sea-level rising was measured in this period nearly at all stations along the southern coast being as high as 80-120 cms. The combination of the gales and the propagation of the surge wave resulted in fracturing fast ice along the eastern coast of the Lena delta. Water covered vast areas of fast ice at the bars of the Yana and Indigirka. The same situation was observed in the Tiksi Bay.

The intensification of gales in the Arctic and an increased occurrence of cata-

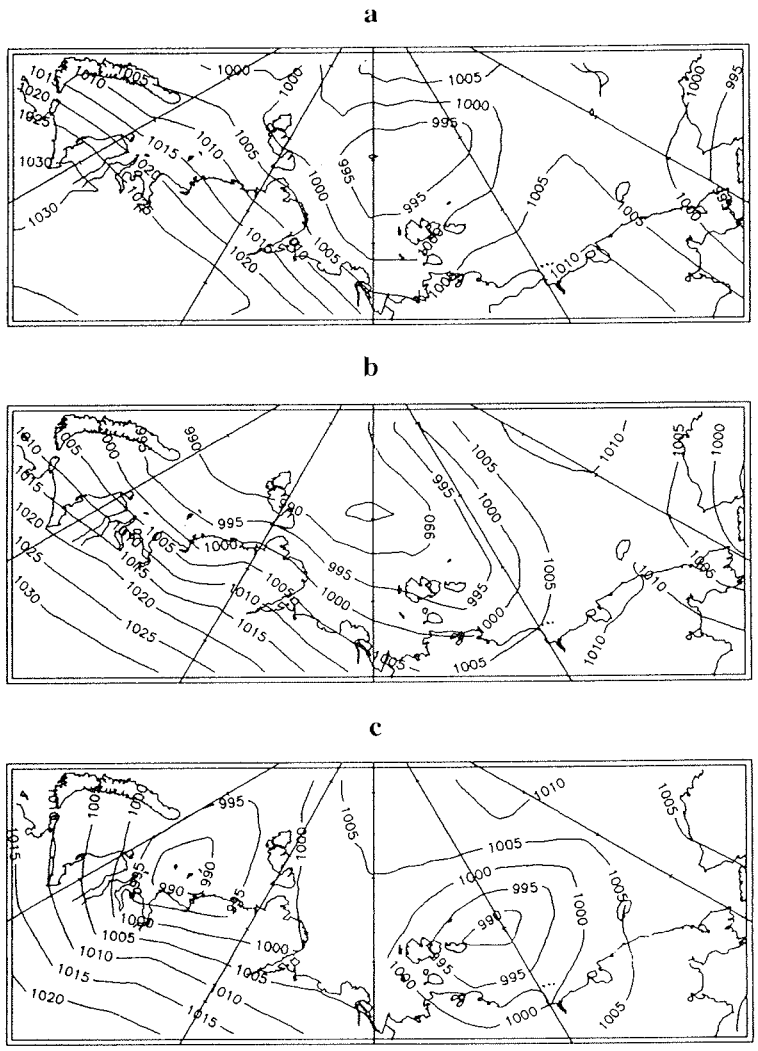

Fig. 2. The atmospheric surface pressure fields during the storm surge in the Laptev Sea in October, 1985: October 9 at 12 GMT (a), October 10 at 12 GMT (b), October, 11 at 12 GMT (c).

strophic storm surges, caused by it, underlines the urgency of further investigation of this phenomenon, of its influence on the hydrological and hydrochemical conditions of the marginal seas and river mouth zones as well as of their ecological conditions. Furthermore, the need of objective and reliable methods of forecasts both of storm-surge oscillations and of their extreme manifestations has become evident.

References

Mustafin, N.V. 1961. On catastrophic storm surges in the south-eastern part of the Laptev Sea. Problems of Arctic and Antarctic, v. 7, pp. 33-36.

NUMERICAL PREDICTION OF SEA SURGES AND ICE CONDITIONS IN THE LAPTEV AND EAST-SIBERIAN SEAS

I.M. Ashik
State Research Center of the Russian Federation the Arctic and Antarctic Research Institute, St. Petersburg, Russia

The physical-geographical conditions of the Arctic Seas favour the forming of well pronounced sea level oscillations that dominate over the tide. These surges are most noticeable, usually, in September - October within ice gone from the sea surface and activation of atmospheric processes. Since the navigation through shoal areas, cargo operations, drilling works and unleakage of the coast living sites should be ensured by correct forecast, improving of the prediction methods for Arctic Seas is becoming an especially important task. The analysis of Russian and foreign works shows that methods of hydrodynamic modelling turn out to be most promising (Lineykin & Ovsienko, 1979; Heaps, 1967).

In the Center of Ice and Hydrometeorological Information at the Arctic and Antarctic Research Institute in 1987 a numerical hydrodynamic model was worked out which permits the calculation of storm-surges forecasts for all Arctic Seas and also its transmission to interested organisations in time (Ashik et. al., 1989). A validity check, performed for these predictions, has shown that the forecasts can be used for practical needs. However, the model takes no account of drifting ice. So, its application was possible only for the navigation period, when the influence of ice on the storm surges is negligible. It was necessary to perform further calibration of the model, and, first of all, to refine the method of the stimulating forces.

So, the two-dimensional model of the storm surges used earlier was improved by adding the terms, taking into account the friction between ice and water

$$\frac{\partial \vec{U}}{\partial t} + 2\vec{\omega}_z \vec{U} = -g(H+\xi)\nabla\xi + \frac{(H+\xi)}{\rho}\nabla P_a + \frac{1}{\rho}((1-C)\vec{\tau}^a + C\vec{\tau}^w - \vec{\tau}^b) \qquad (1)$$

$$\frac{\partial \xi}{\partial t} = -\mathrm{div}(\vec{U}) \qquad (2)$$

and also by the system of equations that describes the dynamics of the ice

$$\frac{d\vec{u}_i}{dt} + 2\omega_z \vec{u} = -g\nabla\xi + \frac{1}{\tilde{\rho}} + (\vec{\tau}^i - \vec{\tau}^w) + \vec{F} \qquad (3)$$

$$\frac{\partial C}{\partial t} = -\mathrm{div}(C\vec{u}_i) \qquad (4)$$

where t is time; $\vec{U} = \int_0^{(H+\xi)} \vec{u}\,dz$ is the vector of the total flow; $\vec{\omega}_z$ is the parameter of Coriolis; g is the free fall acceleration; ξ is the deviation of the sea level from the undisturbed state; H is the undisturbed water depth; P_a is the atmospheric pressure;

ρ is the water density; $\vec{\tau}^a, \vec{\tau}^i, \vec{\tau}^w, \vec{\tau}^b$ tangential friction on the boundaries air-water, air-ice, ice-water, water-sea bottom; $\vec{u}$ and $\vec{u}_i$ are the average by depth vector of the stream speed the vector of ice drifting; $\tilde{\rho} = \rho_i h_i C$ is the surface ice density; ρ_i is the ice density; h_i is the ice thickness; C is the function of consolidation; $\vec{F}$ are the forces of the internal interaction in ice.

The tangential stress on the boundaries ice-water and water-sea floor was calculated according to the traditional dependencies

$$\vec{\tau}^w = R_w \rho (\vec{u}_i - \vec{u}) |\vec{u}_i - \vec{u}| \qquad (5)$$

$$\vec{\tau}^b = K \rho \vec{U} |\vec{U}| \qquad (6)$$

where $K = \frac{K_w}{(H+\xi)^2}; R_w = 5.5 \cdot 10^{-3}$; $R_w = 5.5 \cdot 10^{-3}$ is the friction factor on the boundary ice-water; $K_w = 2.6 \cdot 10^{-3}$ is the friction factor on the boundary water- sea bed.

The tangential stress on the surface of the ice was taken equal to the tangential stress on the surface of the water (Hibler & Bryan, 1987) and was calculated according to the dependence where W is the velocity of the near-water wind in meters per second.

$$\vec{\tau}^a = 12.0(1.0 - \exp(-0.002 W^2)) \qquad (7)$$

In order to introduce the forces of internal interaction into the model, the approximation was used in the form (Rathrock, 1975)

$$\vec{F} = \eta \nabla^2 \vec{u}_i + \lambda \frac{\partial}{\partial x_j} \mathrm{div}(\vec{u}_i) - \frac{\partial P_i}{\partial x_j} \qquad (8)$$

$$P_i = -K_p \mathrm{div}(\vec{u}_i), \quad \text{for} \quad \mathrm{div}(\vec{u}_i)$$

$$P_i = 0 \qquad \text{for} \quad \mathrm{div}(\vec{u}_i) \geq 0$$

where $\lambda = \eta = 10^{10} \mathrm{cm}^2/\mathrm{s}$ are, correspondingly, the factors of volume and shift viscosity; $K_p = 10\eta$ is the compression factor.

On the solid boundaries of the area the condition of unleakage is taken. On the liquid boundaries of the area for the water the condition of irradiation is taken, and for ice the condition of free leakage

$$\left.\frac{\partial \vec{u}_i}{\partial n}\right|_{G_2} = 0 \qquad (9)$$

For initial conditions for water and ice the idle state is taken. The function of consolidation is defined according to real conditions. The width of ice is considered to be constant in time and space and is equal to 2 m.

The area for calculations includes the shelf seas of Russian Arctic from the Kara Sea up to Chukchi Sea. The open boundary approaches the 200 m isobat. The

step of the net area makes Dx=Dy= 55.56 km.

When we perform the finite differences approximation of the assumed system of equations the terms with friction are taken for the middle of the time step, the spatial derivatives are substituted by their central finite differences, and time derivatives - by forward directed differential relations.

The calculations of the ice consolidation are based on the condition that the components of the ice-drift velocity are equal to 0, if they are directed inside the mesh with the consolidation function equal to 1; the corresponding components of velocity on the opposite sides of the mesh are equal to 0.

Calculations using the model assume information on the consequences of the near-earth atmospheric pressure fields, the bay ice distribution and on the consolidation of drifting ice on the sea surface of the calculated area. The real and forecast fields of the near-earth atmospheric pressure calculated in the European Centre of middle-range forecasts (transmitted in GRID code in the nodal points of 5-degree geographical grid with periodicity 24 hours), were interpolated into the nodes of the grid, using the algorithm of the method of finite elements (Segerlind, 1979).

The velocity and direction of wind near the surface of the water are calculated by the dependencies of the type

$$W = k_1 W_g \qquad (10)$$

$$A = A_g - \alpha \qquad (11)$$

where $k_1 = \frac{h}{h+1}, h = 0.25 \cdot 1.212 W^g, \alpha = 41.26\exp(-0.07W_g) - 11.27\exp(-0.48W_g)$

The experimental forecast calculations of the storm surges in the Arctic Seas, using the mentioned model, were started in summer 1991 and are performed since then throughout the year. In order to calculate real oscillations one has to reduce the first forecast value to the real level on the concrete station. The comparison of the diagnostic forecast calculations with real oscillations for some polar stations showed good coincidence of the calculation data with the results of observations with no dependence on the ice conditions.

During the navigation period in 1993, the forecast calculations were carried out as before twice a week. The range of forecasts was up to 6 days. Thus, the forecasts overlapped in time. From July to October 1993, 24 forecasts were made. However, because of malfunctions in communication only a part of them was analysed.

For the navigation period in 1993, oscillations of the sea level were observed in the Laptev Sea and in the western part of the East-Siberian Sea within the average sea level, close to normal, which had smooth character. Nearly for all the navigation period, the sea level deviated in the coastal zone of the Laptev Sea less than 1 m from normal. The same holds for the western part of the East Siberian Sea from July up to October.

By the end of August a large area of enlarged atmospheric pressure was formed above the East-Siberian Sea. It existed up to the first fortnight of September and resulted in a so-called anti-cyclonic surge characterised by a decline of the sea level by 80 - 90 cm below the navigational norm and by stabilisation of this level for 7 - 8 days. Due to a weakening of the anticyclone and transient processes in the atmosphere, the sea level rose back to the normal state later.

By the end of the first fortnight of September, a cyclone had come up to the East-Siberian Sea and moved in general direction from north-west to south-east. The back part of the cyclone was located in the western part of the sea occurred to be in. As a result, the sea level rose by 115 cm above the navigational norm (observed on the polar station in the bay Ambarchic). Thus, the amplitude of water-level oscillations from 28. August to 14. September made 2 m. The whole western part of the East-Siberian Sea was clear of ice. The ice edge lied between 77° and 78° N .

The rising of the sea level along the coast of the East-Siberian Sea and its following reducing were properly enough predicted by the series of consequent forecast calculations (Fig. 1). The average validity of the forecasts with range up to 6 days during this period was 86 % (the estimation by the permissible error) and

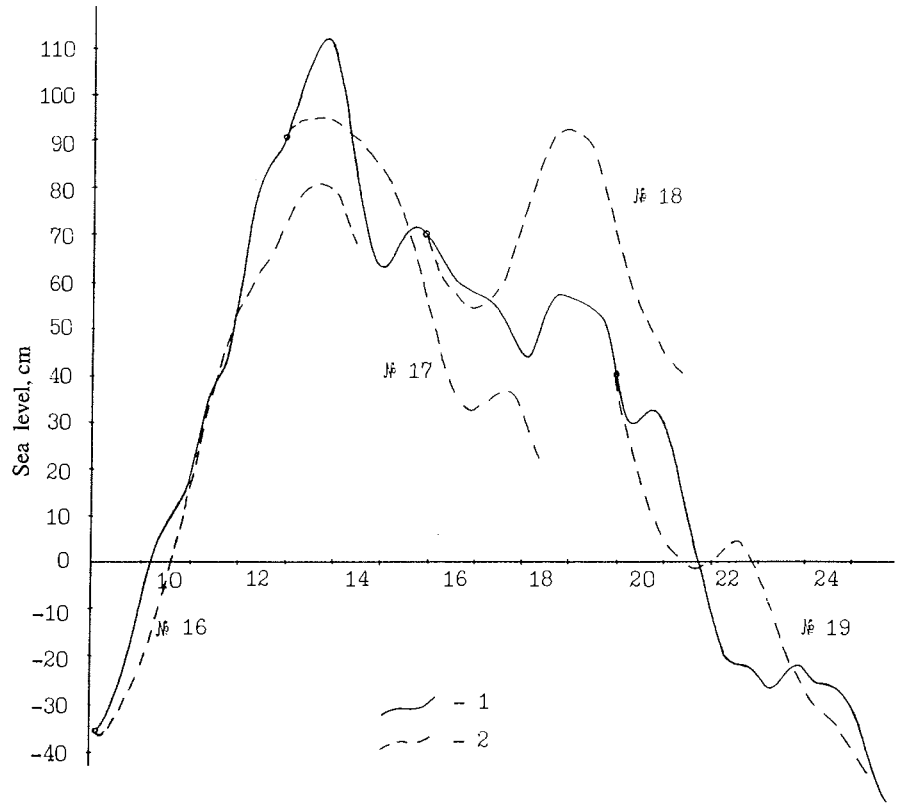

Fig. 1. The oscillations of the sea level, observed by the polar station in Ambarchik bay and the forecast calculations N° 16 - 19 in September 1993: 1 - the observation data, 2 - the forecast.

94 %, when estimating by the sign. Here we can mention good coincidence of the real and the calculated amplitude and phase of oscillations. The forecast No. 18 was not so successful in terms of quantitative prediction, but qualitatively it showed the correct trend of the sea level oscillations.

At the end of October, a sufficient reducing of the water level was observed in the south-eastern Laptev Sea, caused by the front part of a cyclone moving from south-east to north-west by the centre of the Laptev Sea. Starting on October 20, the sea

level decreased by 1m remaining at this level for 24 hours. Then it rose by 110 cm. The surface of the Laptev Sea at this time was covered by ice, while in the coastal areas fast ice was formed.

The forecast calculation No. 23 gave a good description of the final stage of sea-level reducing and of the following rising (Fig. 2) in the Tiksi bay and for the other coast stations. The average validity of the predictions with range up to 6 days made 89% for estimation by the permissible error and 80% for estimation by sign. The calculated amplitudes proved to be close to the real ones. The phase shift was not more than 12 hours.

All in all, the validity of forecast calculations for storm surges much depends on the accuracy of the forecast for fields of atmospheric pressure. In particular, we should have to point out that the quality of the calculations greatly depends on their range, i.e. if the validity of a 1-day forecast is 95% (Tab. 1), with a range increasing by one day, the validity decreases by 10% and stops at the level 50 - 55 % for 5 - 6 day forecast.

Table 1: The validity of the forecasts of the sea level oscillations for the period July-October 1993.

Station	The earliness of forecast, days							
	1	2	3	4	5	6	1-3	1-6
Andrey island	98	83	76	61	41	52	86	70
Terpjy-Tumsa cape	100	92	57	56	44	8	81	57
Tiksi bay	88	63	47	41	53	58	67	58
Kigilakh cape	93	93	95	88	38	50	94	81
Shalaurov cape	100	100	86	88	56	50	96	84
Sannikov strait	89	82	93	81	50	67	87	82
Chetyrekhstolbovoy island	93	72	68	64	61	48	78	69
Ambarchik bay	97	86	67	56	59	61	85	73
Mean	95	82	72	62	54	53	83	71

The same effect is characteristic of other parameters of the forecast quality. The RMS error of the forecast calculations makes 17 cm for a range of three days and increases up to 22 cm for 6-day forecast, the average absolute calculation error is, correspondingly, 13 cm and 17 cm, the quality of the calculations is 0.72 and 0.86 correspondingly (Tab. 2).

The 24-hour discrete (too much) in defining the fields of atmospheric pressure produces negative influence on the quality of the forecast calculations. This leads, first, to a smoothing of the oscillations, and, secondly, makes a phase shift within ±12 hours possible. If all oscillation lasts less then 24 hours, the situations cannot be reproduced correctly. We can propose, that the relatively low quality of forecasts for the Tiksi bay, where the oscillations of the sea level occur often, may be explained, primarily, by this reason.

Though the ice in the described model is taken into account only as an additional factor that influences forming of the storm surges the calculations of the ice drift and of it's consolidation variation can produce good results and be used for diagnostics of the main trends in the dynamics of ice conditions.

Table 2: The estimation of the forecasts of the sea level oscillations for the period July-October 1993.

Station	N	PD	PZ	S	Δ	e	R
	The forecast of 1-3 days						
Andrey island	13	86	87	11.6	8.5	0.76	0.21
Terpjy-Tumsa cape	6	81	74	17.2	12.3	0.82	0.30
Tiksi bay	8	67	66	23.7	18.4	0.99	0.24
Kigilakh cape	7	94	83	13.5	10.1	0.85	0.57
Shalaurova cape	7	96	88	13.3	9.6	0.60	0.64
Sannikova strait	7	87	84	9.0	6.9	0.61	0.76
Chetyrekhstolbovoy island	22	78	87	21.1	16.1	0.75	0.37
Ambarchik bay	22	85	85	18.5	13.8	0.59	0.69
Mean	92	83	83	17.0	12.8	0.72	0.47
	The forecast of 1-6 days						
Andrey island	11	70	81	15.2	12.0	0.85	0.17
Terpjy-Tumsa cape	4	57	56	32.4	24.0	1.20	0.21
Tiksi bay	8	58	70	28.0	24.1	1.07	0.68
Kigilakh cape	4	81	65	18.8	14.7	0.87	0.71
Shalaurova cape	4	84	79	17.0	13.0	0.73	0.72
Sannikova strait	4	82	79	11.3	8.6	0.70	0.91
Chetyrekhstolbovoy island	22	69	75	23.6	19.2	0.91	0.55
Ambarchik bay	22	73	80	25.2	19.6	0.74	0.58
Mean	79	71	75	21.9	17.4	0.86	0.55

Notes: N is the quantity of the forecasts perfomed ; PD is the forecast validity within estimation by permissible error; PZ is the forecastvalidness by the sign; S is the RMS calculation error; Δ is the average absolute calculation error; ε ιϭ the quality of the calculation; R is the correlation factor.

The ice conditions, that occurred from August 5 to 10, 1993, are sketchily shown on Fig. 3a. All the time, the navigational line Cape Dezgneva - Pevek was free of consolidated ice. It permitted to perform navigation without using ice-breakers. On August 14-17 due to strong winds from the northern sector, flowing in the narrow area, a tongue of consolidated ice moved down from the Ayonsky ice massiv. It touched the coast all way between 172° and 176° E and blocked the navigational line (Fig. 3b). The forecast No. 9, made for August 12- 17, predicted this variation of the ice conditions, negative for navigation (Fig. 3c). The forecast calculation showed good agreement with the real conditions in predicting the fact of ice tongue moving, its shape and orientation. The quantitative estimation of calculations which takes no account of a number of characteristics influencing the ice conditions, hardly can be taken as successful, but the qualitative variations are usually reproduced correctly.

Thus, the high quality of numerical forecasts of storm surges with a range less than 3 days permits to apply these data for operative support of different organisations together with physical-statistic methods (Mustafin, 1965). At the same

time, the necessity is evident to improve the base of the forecast and to extend the grid area to the whole Arctic Ocean. That would permit to reduce the negative influence of the neighbourhood of the opened boundary and also to take into account the following items: "outer" surges generated in the open ocean, the detailed and concrete description of the sea floor, the shape of the coast in regions with a well developed morphology, and an improvement of the "ice" part of the model.

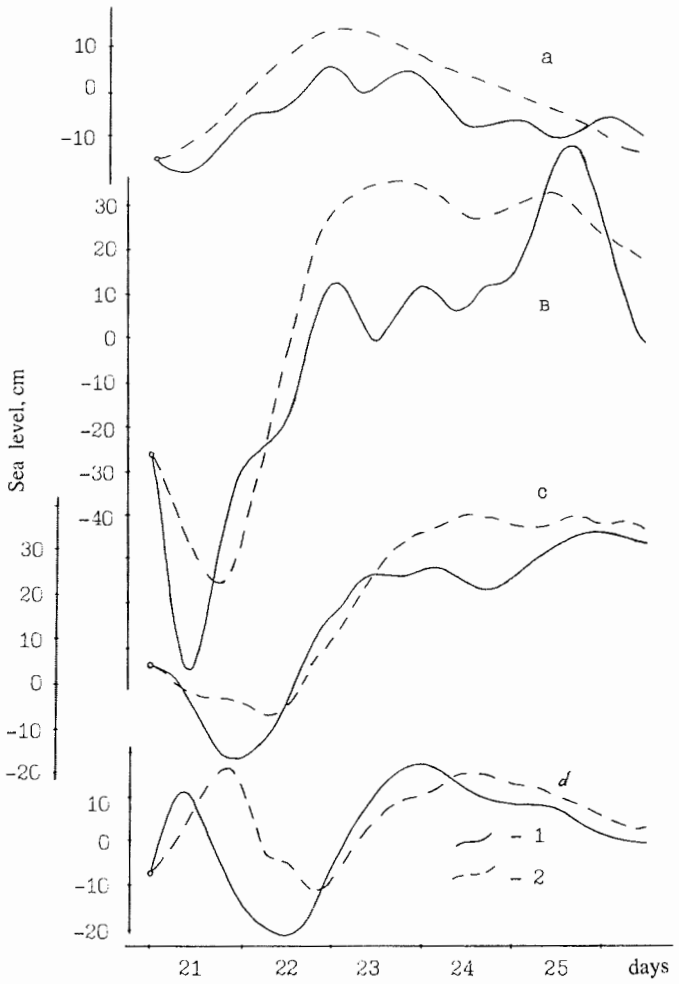

Fig. 2. The oscillations of the sea level and the forecast calculation N° 23 in October 1993 for the Andrey island (a), Tiksi bay (b), Shalaurova Cape (c), Strait of Sannikova (d) polar stations . The other designations are the same as on Fig. 1.

References

Ashik, I.M., Proshutinskiy, A.Yu., Stepanov, V.A. 1989. Some results and outlook of the numerical forecasts of the sea level oscillations in the Arctic Seas. Meteorology and Hydrology., 8, pp. 74-82. (In Russian).

Heaps, N.S., 1983. Storm surges. 1967 - 1982. Geophys. J. Roy. Austr. Soc., Vol.74, pp. 331-376.

Hibler, W.D., Bryan, K.A. 1987. Diagnostic Ice-Ocean Model. J. Phys.Oceanogr. 17, 7, 987-1015.

Lineykin, P.S., Ovsienko, S.N. 1979. The storm surges. Itogi nauki i tehniki. Okeanologiya 5, pp. 117-140. (In Russian).

Mustafin, N.V. 1965. The methodoloogy of the forecast of the surges for the Arctic Seas. Trudy CIP. Issue 142.-p. 86-93. (In Russian).

Rothrock, D.A. 1975. The mechanical behaviour of pack ice. Ann. Rev. Earth and Planetary Sci., 3, 317-342.

Segerlind, L., 1979. The using of a finite element method. Moskva, Mir., 286. (In Russian).

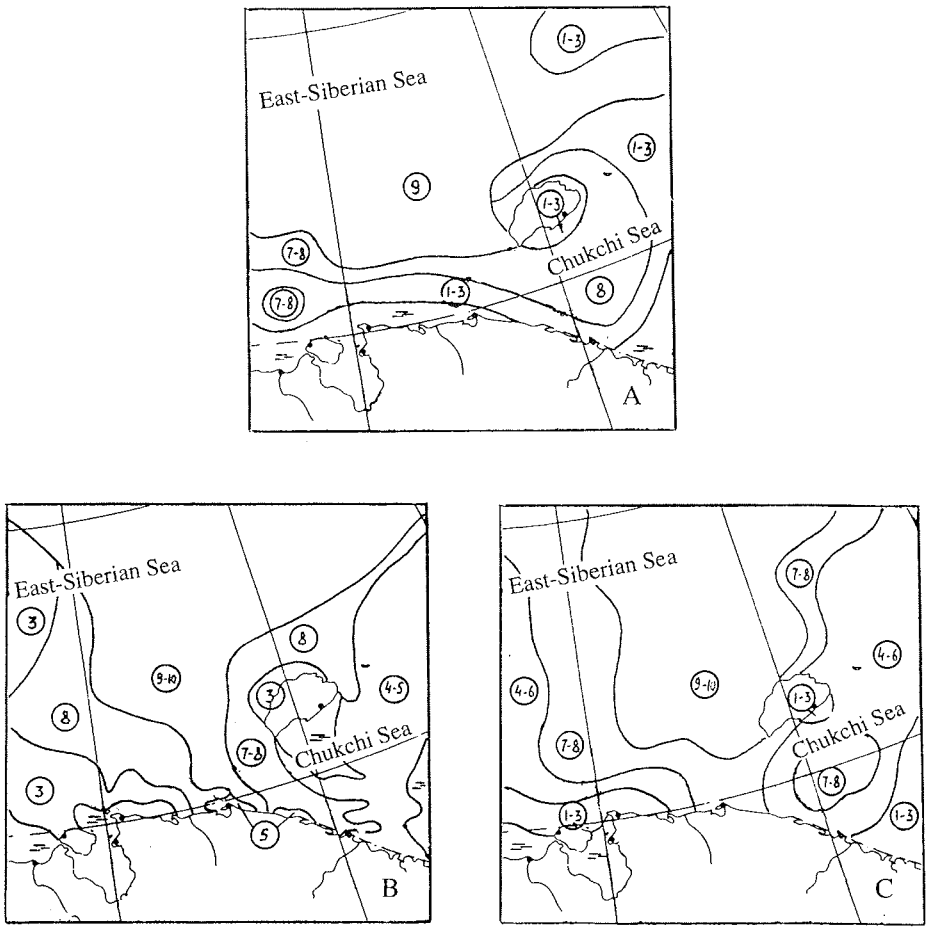

Fig. 3. The ice distribution by its consolidation in the Arctic Seas for the period from 5 to 10 August 1993 (a) and from 14 to 17 August 1993 (b), forecast calculation on 17 of August 1993 (c).

THE ICE-THERMAL REGIME AT FRONT DELTAS OF RIVERS OF THE LAPTEV SEA

Yu. V. Nalimov
State Research Center of the Russian Federation the Arctic and Antarctic Research Institute, St. Petersburg, Russia.

The main sources of information about ice-thermal regime of front deltas at the Laptev Sea are data from polar stations and air studies concerning ice conditions, ice thicknesses, albedo and temperatures of water surface. Data published in [1...30] were also used. According to morphological characters, river mouths of the Laptev Sea basin can be devided into two groups. River mouths regions of estuary type, that is with closed delta fronts, belong to the first group. Those are the Khatangskiy zaliv and the Anabarsky zaliv. The second group includes river mouth regions with developed deltas and opened delta fronts. Those are Olenek, Lena and Yana.

The ice processes at delta fronts of closed and opened types are of different characters [12, 13, 15, 17, 18].

At closed delta fronts of estuary type the ice formation process and fast ice origination begin from shallow bar regions at mean in the past September - middle October. Ice formation propagates from shores to the estuary center and leads to the ice breadge creation at the southern parts of gulfs. Then ice formation spreads to the north and south. The freezing character is presented in Fig. 1 (a, b).

At open front deltas ice formation begins in the middle of September from extensive shallows and bars. Here young coastal ice and fast ice formation begins quickly. There is no ice above channels during long periods, where freezing takes place in the middle of October.

According to the terms and character of ice formations at opened delta fronts Bolshaya Tumatskaya, Malaya Tumatskaya and Bykovskaya branches of Lena river delta are exceptions. Here ice formation begins a little bit later than at exits of other branches to the sea. That phenomena is connected with a relative deep delta fronts of branches considered. The characters of freezing of delta fronts of open type are presented in Fig. 1 (c, d, e).

According to the author's investigation of influence of different factors (in the full range of changing) to the terms of ice formation beginning at delta fronts, the air temperatures play the main role (60%), the next are influence of wind (20-30%), velocity of current and deepness (10%) [7, 23, 25, 26]. In the moment of fast ice formation (mid of October is the mean term for Laptev Sea shoreline) the ice developes to the light nilas stage with a thickness of up to 10 cm, and 15-20 cm for ice rafting.

Then the fast ice growth takes place from sea shoreline to the flaw lead borders as far as the growth of thickness. There are different positions, scales and, thus, the terms of development of the Lena - Anabar flaw lead. In January the mean thickness of the fast ice is up to 1 m and in May 1.7 m.

The maximum ice thickness at Laptev Sea shoreline takes place in June when snow melt floods spread over the delta shorelines where they are connected with the bottom surface of the salt sea and increase their thickness by freezing. The maximum ice thickness at delta fronts is a little more than 2.5 m, and up to 3.0 m at delta branches.

The fast ice morphology at shoreline regions of Laptev Sea is relatively gentle

(hummocks 1/10 - 2/10). Extremely hummocked ice is observed near the fast ice edges and flaw polynya, and at the young ice of flaw polynya. Along the western shoreline of Anabarskiy zaliv between the traverses of Cape Khorgo and Cape Paksa some year-old grounded hummocks are observed. Usually the hummocks at Anabarskiy zaliv is 1/10 - 2/10, at Khatangskiy zaliv up to 2/10 -3/10 [19, 21, 27]. But at these delta fronts the local ice patterns with hummocks of up to 4/10 - 5/10 can be revealed. During the entire winter period there are cracks in fast ice due to the tidal flows.

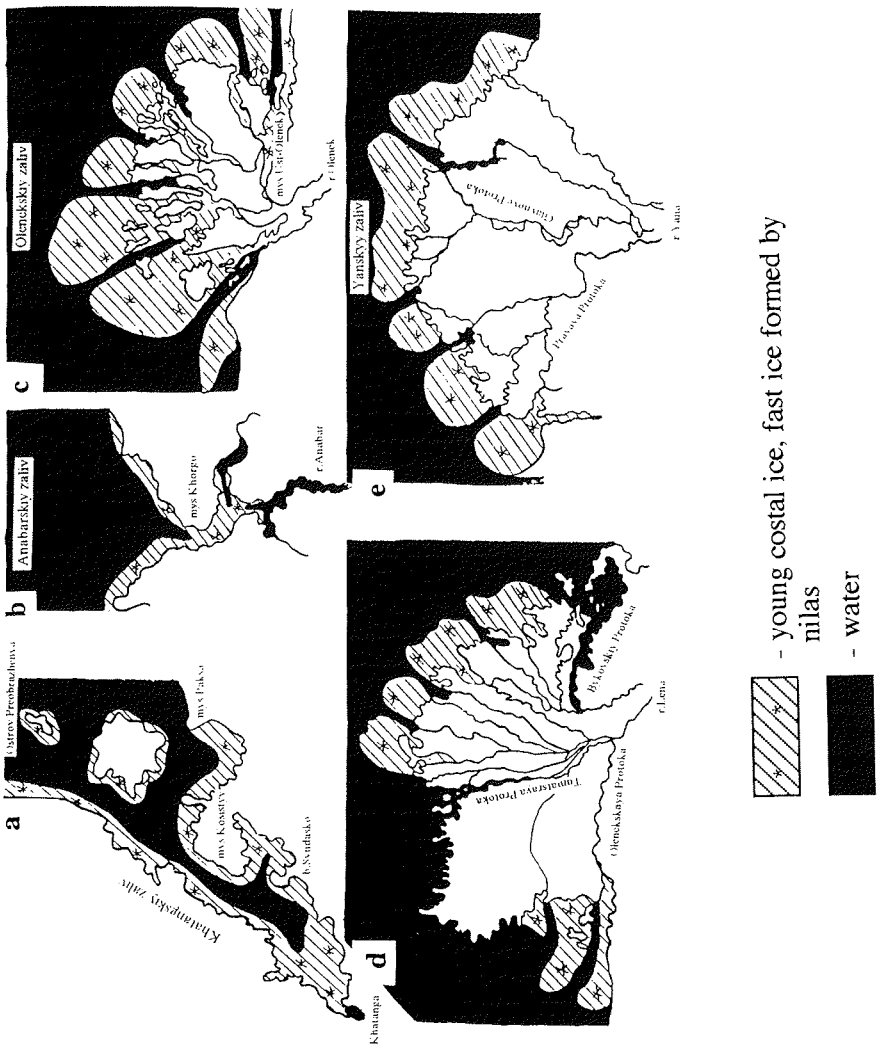

Fig. 1. The character of freezing in estuaries (a, b) and in delta fronts (c, d, e) of Laptev Sea basin's river.

Some studies show that the thermal-physical characters of snow and the air temperatures are the main factors determining the ice thickness [7, 8, 26].

The reflection capabilites of fresh ice without snow for the sea regions and front deltas of Arctic rivers in autumn are presented in the article of A. P. Graevsky, Yu.V.Nalimov and A. A. Timerev [11]. The smallest albedo among all young ices is observed for dark nilas 10-11%, a light nilas albedo - 15%. Weakly snow-covered grey-white ice reflects 37% of the radiations, snow covered - 42%, thin first-year ice - 46% [11].

The process of spring ice destruction at deltas and rivers of Laptev Sea basin was considered in the series of works [4, 5, 6, 8, 10, 12, 14, 15, 16, 17, 18, 19, 20, 21, 27, 29, 30].

But the process of ice destruction at delta fronts and their cleaning from ice is not described practically, while you can find some information on ice processes at delta fronts or rivers Khatanga, Anabar, Lena and Yana in [12, 15, 17, 18, 19, 20, 21, 27]. Spring ice destruction processes at front deltas of opened and closed types are of different character.

At closed delta fronts (e.g. estuaries) ice destruction begins from the southern parts due to the river's water temperature at the end of June. At the northern parts ice ruins mainly result from radiation and temperature factors [17, 18]. The characters of ice break-up at estuaries of rivers Khatanga and Anabar are presented in Fig. 2 (a, b).

The author's calculations for the southern part of Khatangskiy zaliv show that for the mean year ice 61% of heat is needed for destruction through the bottom surface of river water and only 39% from radiation - heat factors. But in the north of Khatangskiy zaliv there is another correlation: 9% by warm water and 91% by radiation heat [26].

In Khatangskiy zaliv the fast ice melting at current line usually spreads to the north up to b. Syndasko traverse and this takes place at the beginning of June. Further to the north the fast ice fracturing occurs up to the Preobrazheniya island in the middle of July. Floes and medium floes are formed in the Khatangskiy zaliv due to the fast ice break-up. At the end of July Khatangskiy zaliv is ice-free (rarely due to the ice carrying out). Ice break-up at delta front of Anabar river differs a bit from that at Khatanga. Here fast ice melting begins at the river flow line at Anabar gulf due to the snow melt flood. The channel created in fast ice spreads to the Lena-Anabar flaw lead up to 15 miles north of cape Khorgo and exists until the fast ice fracturing.

The duration of ice break-up at delta fronts of closed type differs depending on the conditions of spring processes.

In opened delta fronts ice destruction processes begin with puddles formation. By growing these puddles turn to water on ice. Then, while the snow melt flood enters the delta front, the ice above the channels comes to the surface surrounded by extensive water fields above the ice connected with ground. At that time lines of emerged ice ("serpentines") above the deep channels show their positions [3]. Ice break-up character considered above relates to the shallow opened delta fronts with the channels among the shallows (branches of delta of rivers Olenek, Olenekskaya, Saardahskaya, Trofimovskaya and other, branch of river Lena delta, branches of Pravaya and Glavnoye Ruslo of river Yana delta). In the cases of deep delta fronts (branches Malaya Tumatskaya, Bolshaya Tumatskaya and Bykovskaya of river Lena delta) the ice break-up is an analogy of that at estuaries, where fast ice melting at the line of flow takes place. The character of ice break-up at opened delta fronts is presented in Fig. 2 (d, e).

Ice break-up at the delta branches occurs in the mid of June. Fracturing of lines of emerged ice (in "serpentines") takes place at the beginning of July. The fast ice melting at the deep parts of opened delta fronts (exites to a delta front of branches Bolshaya Tumatskaya, Malaya Tumatskaya and Bykovskaya of river Lena delta)

occurs at the end of June - beginning of July. The mean terms of fast ice break-up at Laptev Sea delta fronts are the middle of July, these of cleaning is the middle of August. According the calculations, in the years with about the mean and later terms of development of spring processes near the Muostah island the ice break-up processes depend mainly on radiation-heat factors.

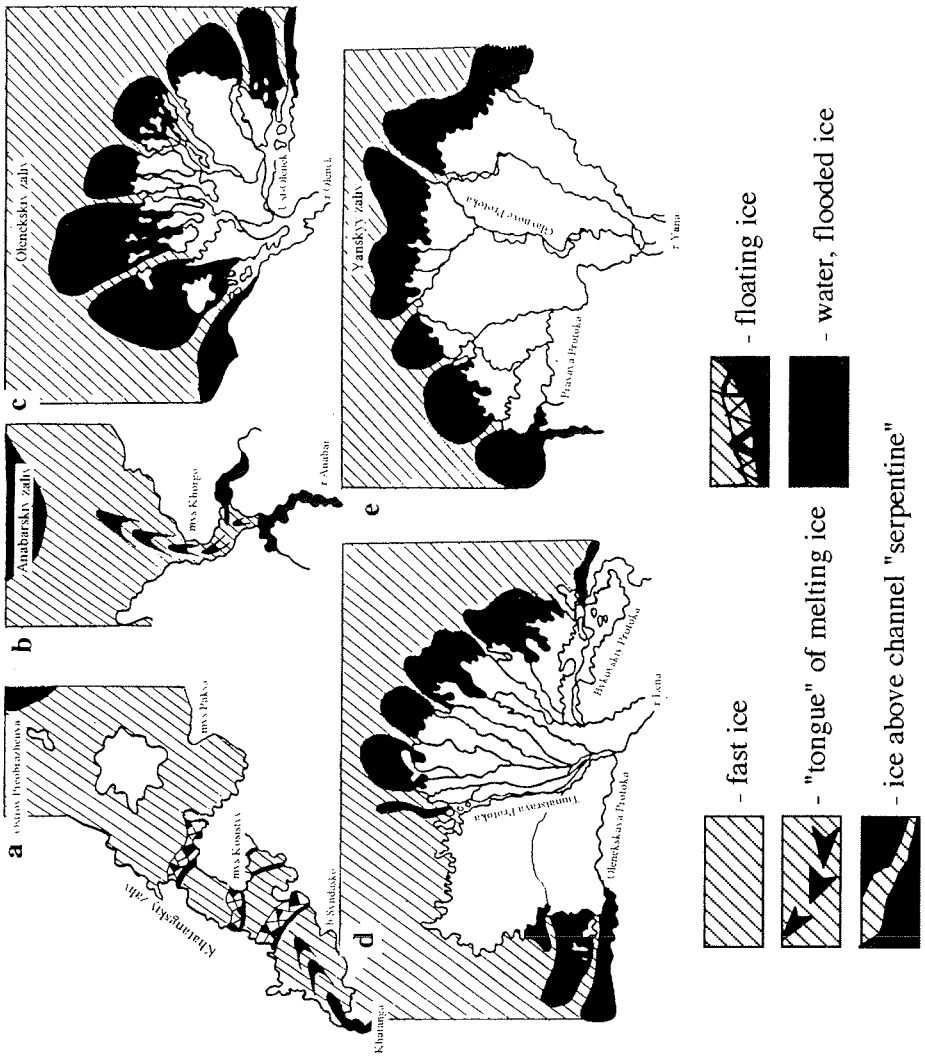

Fig. 2. The character of break-up in estuaries (a, b) and in delta fronts (c, d, e) of Laptev Sea basin's river.

Air studies of albedo show that the albedo of snow at ice changes from 57% to 75% [24] due to the stage of snow melting. The albedo of dry clear ice at delta fronts is 55% and it diminishes during the ice destruction. Ice with the pollution of 30-70% of visible surface has the reflecting capability 15% [24]. Ice air-

investigations in spring and autumn determine only the visible measure of ice surface pollution [28].

The period of ice melting depends from its pollution. Weak polluted ice (1-2 balls) destroys more rapidly than the clear one. Ice covered by thick layer of sediments during the spring snow melt flood term can survives from full summer period and it is considered as second-year ice in next spring and summer [1, 17, 18].

The water temperature regime at river mouth area has poorly been studied up to now. The Arctic and Antarctic Science-Research Institute organized a regular air-thermal study of Russian Arctic river deltas until 1969 [9, 22]. The investigations show that during the break-up period and later the water temperature in cross-sections of the stream is inhomogeneous. The temperature difference between banks is more than 1 °C, and between banks and the center of the river more than 6 °C.

The period of temperature homogeneity established at delta front cross-sections is up to 1 month. In closed delta fronts the water temperature in tongues of ice melting varies between 3.0 °C to 6.0 °C and depends on hydrometeorological conditions (wind bides, tiges). In open delta fronts the temperatures of surface water above the ice that is connected with the ground is 2-4 °C. No temperature measurements were caried out in channels.

According to established flows temperature homogeneity (usually at the beginning of June), the increase in water temperatures at river deltas begins with a maximum in mid-July. Maximum water temperatures (more than 20 °C) were observed in the southern parts of the mouth areas of rivers Anabar, Olenek, Yana, and 18-19 °C in r. Khatanga and in the summit of r. Lena delta. In the second half of July a decreas in water temperature begins in the mouth river areas, and at the end of September in the southern regions of these areas it amounts to 0.3°C at Anabar, 1.5 °C at Olenek and Yana, 3-4 °C at Khatanga and Lena. At the end of September and at the beginning of October the difference of water temperatures between the shores and the middle of the delta fronts is up to 2-4 °C. At this time an intensive process of shore ice formation begins. When water temperature reaches 0.2 °C the ice formations and ice drifts begin.

References

1. Antonov V.S. Residual ice in the delta of Lena. Proc./Arct.and Antarct. Recearch institute. 1963, v.234, p.112-117.
2. Antonov V.S. Mouth area of Lena river (Hydrological outline).-L.: Hydro-meteopublishers, 1967.- 107 p.
3. Antonov V.S., Bushuyev A.V., Nalimov Yu.V. Indication of deepwater furrows through bars of arctic rivers.-Proc./Arct. and Antarct. Research institute, 1970, v.290, p.83-91.
4. Antonov V.S., Ivanov V.V., Nalimov Yu.V. The typical peculiarities of ice conditions of navigable rivers at arctic zone.-Problems Arctic and Antarctic, 1964, issue 11-17.
5. Antonov V.S., Ivanov V.V., Nalimov Yu.V. The distribution of spring ice dams on the rivers of arctic zone of Siberian.-Proc./Arct. and Antarct. Research institute, 1972, v.297, p.116-122.
6. Antonov V.S., Balabayev A.P., Ivanov V.V., Nalimov Yu.V. The distribution of ice dam segments on the rivers of arctic and subarctic zones of Siberian-Proc./Arct. and Antarct. Research institute, 1974, v.308, p.89-96.

7. Belyakov A.G., Nalimov Yu.V., Soloviova Z.S., Usankina G.E. The role of hydrometeorological factors in the formation of ice regime in the mouth areas of larges rivers of Laptev Sea basin.-Proc./Coord.conf.at hydroengineering "Struggle with ice difficulties at the rivers and reservoir on construction and exploitation of hydroengineering structures". Murmansk, 1983, p.74-78.
8. Belyakov A.G., Nalimov Yu.V., Usankina G.E. The investigation of ice proceses in the mouth areas of Khatanga river and methods of their forecasting. Theses of rep. at all-union conference Study of natural conditions at low and mouth arctic zones for hydrolometeorological support providing of national economy. 1985, p.40-41.
9. Bogorodskiy V.V., Ivanov V.V., Martynova E.I., Nalimov Yu.V. Results of infra-red apparatures application for investigation of hydrological objects.-Proc./ 4 allunion hydrolog. congress., v. 6, 1975, p.268-272.
10. Golovina A.P., Golovin V.S. Forecasting of ice dam phenomena at near delta segments of Lena and Yana.-Proc./Arct. and Antarct. Research institute, 1974, v.308, p.143-172.
11. Graevsky A.P., Nalimov Yu.V., Timerev A.A. The reflectance of young ice on the delta front arctic rivers.-Proc./Arct. and Antarct. Research institute, 1980, v.358, p.35-39.
12. Doronina N.A., Ivanov V.V.,Nalimov Yu.V. Results of ice regime research of mouth areas at arctic zone.-Proc./4 allunion hydrological congress, v.6, 1976, p.289-291.
13. Ivanov V.V., Nalimov Yu.V. The ice regime of low Siberian rivers.- River transport, 1964, N1, p. 39-40.
14. Ivanov Yu.V., Soloviova Z.S., Usankina V.V. Revealing of breazing and breaking terms anomalies at low and mouth areas of Siberian rivers.-Proc./Arct. and Antarct. Research institute, 1980, v.358, p.5-24.
15. Ivanov V.V., Nalimov Yu.V. Results of air expeditions in the low and mouth areas of arctic zone rivers.-Problems Arctic and Antarctic, 1981, issue 51, p.79-91.
16. Komov N.I. Spring ice dam in the low Lena. - Proc./Arct. and antarct. Research institute, 1968, v.283, p.136-150.
17. Nalimov Yu. V. Aircraft inspection of breaking-up and freezing of Siberian river mouth and coastal of zone arctic seas.-Problems Arctic and Antarctic, 1960, issue 6, p.93-94.
18. Nalimov Yu.V. Ice airsurvey in the arctic rivers mouth in spring and autumn of 1960.-Problems Arctic and Antarctic, 1961, issue 9, p.95-96.
19. Nalimov Yu.V. Ice regime of Anabar river.-Proc./Arctic. and Antarctic. Research institute, 1967, v.278, p.54-65.
20. Nalimov Yu.V. The hydrological characteristic of Main Bed of Yana river delta arm.-Proc./Arct. and Antarct. Research institute, 1968, v.283, p.136-150.
21. Nalimov Yu.V. Ice Regime of rivers of basin Khatanga river basic.-Proc./Arct. and Antarct. Research institute, 1968, v.283, p.124-135.
22. Nalimov Yu.V. The Radiation thermometer application in Siberian river mouth areas.-Problems Arctic and Antarctic, 1971, issue 38, p.129-132.
23. Nalimov Yu.V. Estimation of ice cover melting factors role in role factor melt cover ice in the arctic river mouths (on the example of Yenisey river mouth).-Proc./Arct. and Antarct. Research institute, 1972, v.297, p.60-68.
24. Nalimov Yu.V., Timerev A.A. Albedo values of snow-ice cover in the low and

mouths of arctic rivers.-Meteorology and hydrology, 1974, N 5, p.64-68.

25. Nalimov Yu.V. Forecasts and calculations of spring ice-thermal processes on the delta fronts of Siberian arctic zone rivers.-Proc./Coord. conference by hydroengineering "Ice-thermal phenomena and their registration on constructing and exploitating of hydrological nodes and hydroengineering constructions", 1979, L., "Energy".
26. Nalimov Yu.V. The heat balance methods of ice regime element calculations of Siberian river delta fronts.-Proc./5 allunion hydrolog. congress, v.9. Mouth rivers, 1990, p.182-188.
27. Romanov I.P. Ice conditions of Khatanga and Khatanga gulf in the spring of 1958.-Problems Arct. and Antarct, 1960,issue 3, p.109-112.
28. Guide for ice airsurvey executing. 1981, p.240.
29. Tasakov P.D. On winter regime and process of Lena mouth breaking-up .-Proc./Arct. and Antarct. Research institute, 1955, v.72, p.105-129.
30. Fedorov M.C. Ice dam and ice jam phenomena and their development on Lena river.-Proc./Arct. and Antarct. Research, 1956, v.204, p.62-89.

STUDIES OF CLEAN AND SEDIMENT-LADEN ICE IN THE LAPTEV SEA

H. Eicken*, T. Viehoff*†, T. Martin*, J. Kolatschek*, V. Alexandrov+ and E. Reimnitz°

* Alfred-Wegener-Institut für Polar- und Meeresforschung, Bremerhaven, Germany

\+ State Research Center of the Russian Federation the Arctic and Antarctic Research Institute, St. Petersburg, Russia

° United States Department of the Interior, Geological Survey, Menlo Park, USA

† deceased

Abstract

During the joint Russian-German expedition into the Laptev Sea with RV Polarstern in 1993, studies of the structure and sediment content of sea ice were carried out. The analysis of sea-ice cores demonstrates that dynamic ice-growth mechanisms play a more important role in the Laptev Sea as compared to the multi-year ice cover of the Arctic Basin. Growth of frazil ice, in particular, is often associated with the entrainment of sediments into the ice cover. Average concentrations of particulate matter in cores taken in such "dirty" ice amounted to 156 g m^{-3}. From series of satellite images, the motion of sediment-laden ice during the study period is derived.

Introduction

The Laptev Sea is a major source area for sea ice produced on the Eurasian shelves, traversing the central Arctic with the Transpolar Drift and eventually exported into the Greenland and Barents Sea (Colony and Thorndike, 1985). Formation and growth of sea ice in the Laptev Sea are dominated by freeze-up of the vast ice-free portion of the Laptev Sea during autumn and export of ice produced throughout the winter in flaw leads (Zakharov, 1966, Martin and Cavalieri, 1989, Dethleff et al., 1993, Reimnitz et al., 1994, Dethleff et al., in press). Due to the small waterdepths - a major fraction of the Laptev Sea is shallower than 30 m - ice formation occurs in close interaction with the seafloor, resulting in entrainment of sediments into the ice cover. Most important in this context are scavenging of suspended material from the water column by frazil ice crystals and uplift of clastics by anchor ice (see Reimnitz et al., 1992, for details of sediment entrainment in the North American Arctic). Studies of the sediment content of multi-year ice in the Transpolar Drift and the Eurasian Arctic suggest that much of the inorganic particulate load in the ice originates from the Siberian and specifically the Laptev Sea shelf (Pfirman et al., 1989a, Wollenburg, 1993, Nürnberg et al., 1994).

Ice dynamics and entrainment of sediment into the ice cover on the Siberian shelves have received comparatively little attention to date. Zakharov (1966) studied ice formation within the coastal zone and the flaw lead of the Laptev Sea. Dethleff et al. (in press) present an extended analysis of ice formation within coastal polynyas and flaw leads based on weather-station data. Timokhov (1994) mentions sediment entrainment in sea ice of the Laptev Sea. Barnett (1991) discusses the ice regime of the Russian Arctic based on satellite imagery and ice charts. Dethleff et al. (1993), Wollenburg (1993), and Reimnitz et al. (1994) were among the first to study sediment dynamics and ice rafting in the Laptev Sea in some detail.

Whereas the previous work had largely focussed on the fast ice and the coastal polynyas, the joint Russian-German cruise onboard the icebreaking RV *Polarstern* during summer 1993 (ARK 9/4) provided an opportunity to study and sample the entire Laptev Sea ice cover (Fig. 1). In addition to field measurements, sea-ice cores were analysed with respect to microstructure and distribution of sediment to

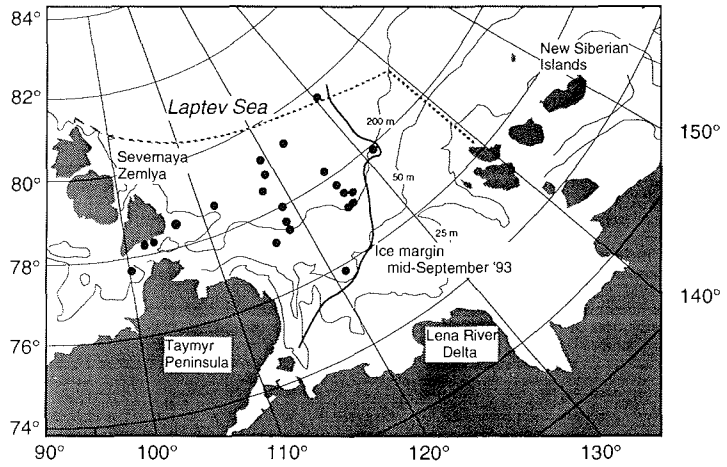

Fig. 1: Study area and sea-ice sampling locations during *Polarstern* -cruise ARK 9/4 in the Laptev Sea and location of ice edge in mid-September as derived from AVHRR imagery. Also shown are locations of weather stations (including WMO identification code) used for analysis of winds and temperatures during freeze-up. The dashed line marks the official boundary of the Laptev Sea according to Treshnikov (1985).

obtain information about ice-growth processes and entrainment of sediment. The large-scale distribution and drift of sea ice during the expedition was studied through satellite data received onboard the ship from the Advanced Very High Resolution Radiometer (AVHRR) onboard the NOAA satellites.

Methods and techniques

Sea-ice cores were drilled within level ice at 23 locations in the Laptev Sea (a few additional cores taken from ridged ice, Fig. 1). At each site, two cores were immediately transferred to the ship and stored at -30 °C. From one of these, thick sections were produced over the entire length of the core. From examination in ordinary light and between crossed polarizers, a textural core stratigraphy was produced, with detailed observations on the distribution, sizes and shapes of pores and grains. Based on the stratigraphy, cores were sectioned into pieces of 0.05 to 0.15 m length, for measurement of salinity, chlorophyll and other parameters (for details of ice-core analysis see Eicken et al., submitted).

At most main sampling sites ice cores of roughly 1 m length were taken for analysis of particulate matter content. Cores which appeared clean were split into upper and lower halves, melted, and measured volumes of meltwater vacuum filtered through pre-weighed 0.4 µm filter papers. Distinct, sediment-rich layers were often sampled, melted, and filtered separately. Filters and condensed/dried residues where inspected under a binocular microscope aboard ship and later dried and weighed. From these weights and water volumes the sediment concentrations were calculated.

Ice velocities were derived for cloud-free areas in NOAA AVHRR satellite images received onboard the ship. After transformation of coordinates into a polar stereographic projection, ice drift vectors were determined by matching features interactively in corresponding images, selected from a series of 30 covering the

period from August 12 till September 23. The satellite data were compared with ice velocities from ARGOS drifting buoys.

Sea-ice stratigraphy and distribution of sediment

Analysis of core stratigraphies indicates that a major fraction of the ice cover of the Laptev Sea sampled in 1993 consisted of columnar ice, formed through congelation of seawater at the bottom of ice floes (Table 1, see Weeks and Ackley, 1986, for nomenclature and ice-formation processes). The fraction of columnar ice f_c within cores was lower, however, than that found in multi-year ice in the Arctic Ocean and in the northern Barents Sea between Svalbard and Franz-Josef-Land (Table 1). This difference would have been more pronounced had the ice been sampled earlier in the season before melting of the top layers, which contain an even higher fraction of ice formed from frazil crystals or through rafting of floes. More distinct is the contrast between the average length of stratigraphic textural units L_{su} for the multi-year ice cover of the Arctic Ocean and the predominantly first-year cover of the Laptev Sea (Table 2). Smaller values of L_{su} indicate that ice growth

Table 1. Average and standard deviation of core length L and fraction of columnar ice f_c (ARCTIC 91 and 93)

Region	L, m	f_c, %	n
ARCTIC 93			
Laptev Sea	1.58 ± 0.54	59 ± 27	23
Barents Sea	2.49 ± 0.39	82 ± 15	6
ARCTIC 91			
Arctic Ocean	2.67 ± 0.95	68 ± 25	51/66

Table 2. Average length (L_{su}) of stratigraphic textural units (ARCTIC 91 and 93)

Textural class	L_{su}, m	st. dev., m	n
ARCTIC 93 (Laptev Sea)			
Columnar	0.38	0.41	60
Granular	0.13	0.12	44
Mixed c/g	0.13	0.15	67
ARCTIC 91 (Arctic Ocean)			
Columnar	0.83	0.68	102
Granular	0.27	0.32	94
Mixed c/g	0.17	0.20	126

is more dynamic on the shallow shelf, with frequent oscillations in the growth regime from undisturbed congelation to dynamic growth with incorporation of frazil ice formed mostly in open water and thickening by deformation, i.e.rafting and ridging (Eicken et al., submitted). The average length of cores corresponds closely with drill-hole measurements (11 profiles, 419 measurements) which yield an

average ice thickness of 1.64 ± 0.59 m.

Ice-core analysis demonstrates that dynamic growth is closely associated with the entrainment of sediment into the ice column. An illustration of the mechanisms involved is given by the exemplary core section shown in Fig. 2. The core had been obtained from a ridged area in an ice floe in the eastern Laptev Sea (Fig. 1). Texture and stable-isotope data indicate the freshwater origin of the upper ice layers. With $\delta^{18}O$ smaller than -12 ‰, this ice is likely to have formed near the mouth of the Lena or another river in the vicinity. While $\delta^{18}O$ of Arctic watermasses and the central Laptev Sea mostly ranges between -10 and 0 ‰ (Létolle et al., 1993, Schlosser et al., in press), $\delta^{18}O$ of water from the Lena and the southern Buorkhaya Gulf east of the river mouth has values below -18 ‰ (Létolle et al., 1993). The stratigraphic layering indicates that freshwater ice is interlaced with true sea ice (identified by higher $\delta^{18}O$ and the typical microstructure) as a result of deformation in a convergent ice regime. In particular the granular ice (i.e. former frazil) is associated with higher sediment concentrations, while the congelation ice layers are virtually devoid of particulate matter. Occurrence of granular ice containing mm-sized patches of sediment within a matrix of congelation ice towards the bottom of the core is attributed to incorporation of frazil or anchor ice. The complex interleaving of ice of different age and origin was also found on larger scales, with adjacent ice floes often greatly differing in structure, thickness and ice properties.

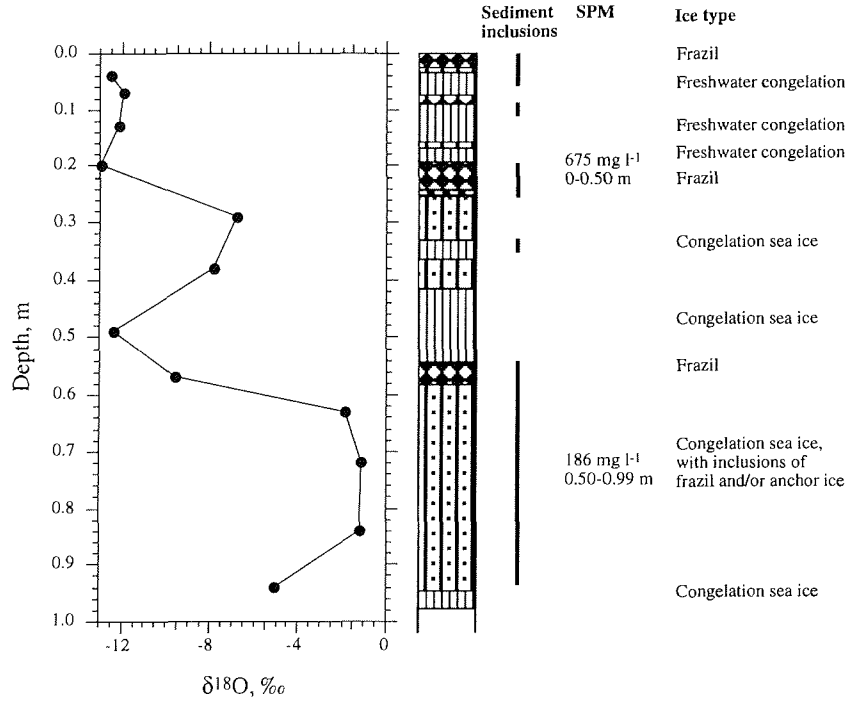

Fig. 2: Textural stratigraphy, distribution of suspended particulate matter (SPM) and $\delta^{18}O$ for a sea-ice core from the eastern Laptev Sea (sample 25311, see Fig. 1). Note high sediment concentrations in rafted segments and within granular/frazil ice. Low $\delta^{18}O$ of freshwater congelation ice suggests an origin near a river mouth and subsequent introduction into an ordinary sea-ice cover through deformation processes in a convergent ice regime.

Table 3 presents data from those ice cores that were suitable for quantifying the sediment load, indicating that generally sediment concentrations are higher in the upper than in the lower section of ice cored. In some samples, e.g. at station 25812, this reflects summer melt processes concentrating sediments from the upper decimeters of ice removed through surface ablation. There are, however, cases where the highest sediment concentrations occur at some depth below the surface layer. Thus, the core from station 25821 has the highest sediment concentrations at about 1.75 m below the surface. Here, a slab of dirty ice has been shover underneath a layer of clean ice.

The average sediment load derived for the upper meter of 10 cores of visibly "dirty ice" amounts to 156±140 g m^{-3} (volume of melted water, Table 3). Maximum SPM concentrations exceeded 600 g m^{-3} (average value for the upper 0.5 m of ice) at two locations. The vast majority of dirty sea ice sampled in the Laptev Sea occurred as turbid ice, with sediment evenly distributed throughout layers of granular ice mostly 0.05 to 0.15 m thick. This indicates that suspension freezing, incorporating particulates into compacted frazil ice is widely occurring in the sediment source area.

Table 3. Suspended particulate matter (SPM) as derived from ice-core measurements (for details see text)

Sample	Location		Core	SPM (g m^{-3})
	Lat. (°N)	Long. (°E)	length (m)	
239-1	87.0	102.4	0.54	28
240-1	77.4	131.9	1.10	346
249-1	77.5	131.2	1.20	53
251-2	77.2	126.1	0.98	190
253-1	77.4	125.5	0.99	433
257-1	87.4	118.4	1.00	13
258-11	87.2	117.5	1.00	94
258-12	87.2	117.5	1.01	58
258-21	78.0	118.1	1.91	163
262-1	77.3	115.6	1.01	182
Average				156 ±140

The spatial distribution of derived sediment load showed no systematic regional trends or patterns, nor was there a pronounced correlation between ice morphology or large-scale characteristics of ice floes and their sediment content. While higher SPM concentrations were often found in ridged areas, we attribute this mainly to the fact that sediments are most conspicuous in such locations and escape the observer when hidden underneath a snow cover accumulating preferentially on low, level surfaces. Concentrations within fast-ice samples at the southeastern tip of Severnaya Zemlya were generally low. Higher values in core 239 most likely represent entrainment with drifting snow from adjacent land surfaces (Reimnitz et al., submitted).

Ice motion in the Laptev Sea during summer 1993

Apart from determinations of sediment load in the ice cover (see above), estimates of the export of sediment-laden ice from the Laptev Sea require data on magnitude and direction of ice drift over the course of the year. Ice-motion patterns during the summer months also affect the redistribution of sediment within the Laptev Sea, since the melting ice loses part and eventually all of its particulate load as it drifts over the shelf and continental slope. Ice velocity vectors for the summer of 1993 as derived from series of AVHRR images received during the course of the expedition are shown in Fig. 3. During the entire study period net motion was to the south-east (i.e. onshore), with an average velocity of 0.04 m s^{-1} for the whole period. The comparatively small ice concentrations during summer result in fast response of the ice pack to changes in the surface wind field, with maximum ice velocities as high as 0.24 m s^{-1} for time intervals of a few days. Along the coast of Severnaya Zemlya, complex patterns of ice motion were detected in time series of AVHRR and radar remote-sensing data, explaining the juxtaposition of different ice types observed in the field. Further analysis of remote-sensing and buoy data is required to arrive at a better estimate of ice motion in the study area.

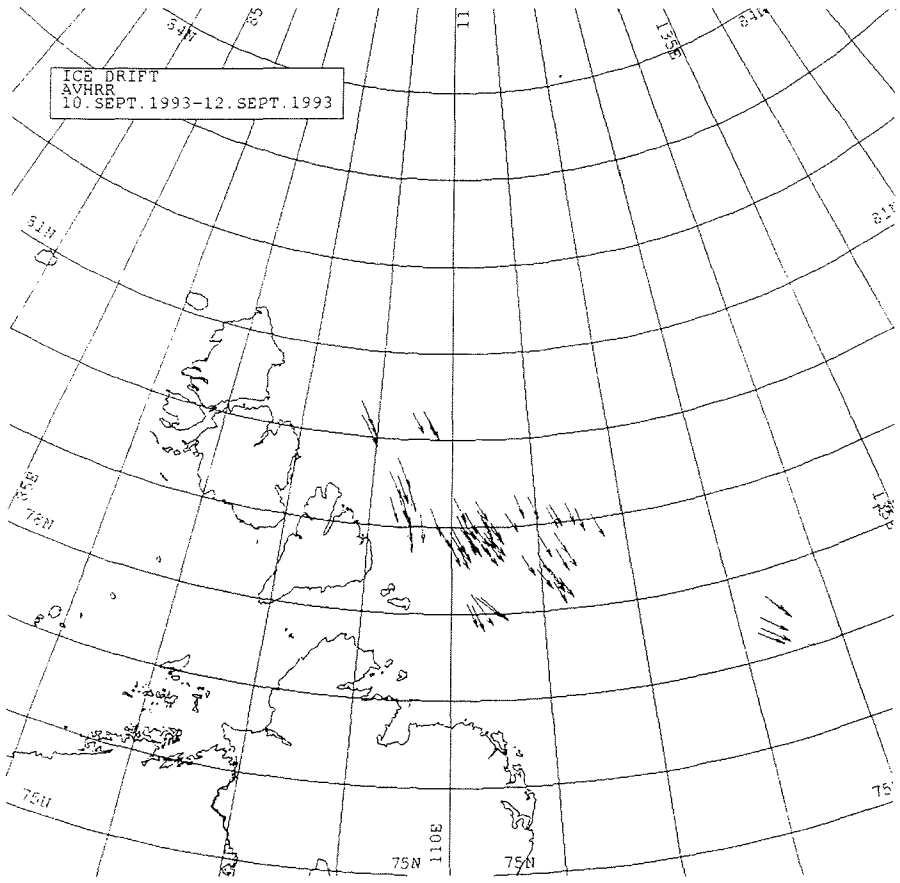

Fig. 3a: Sea-ice dislocation vectors derived from successive AVHRR images for the periods between September 10 and 12.

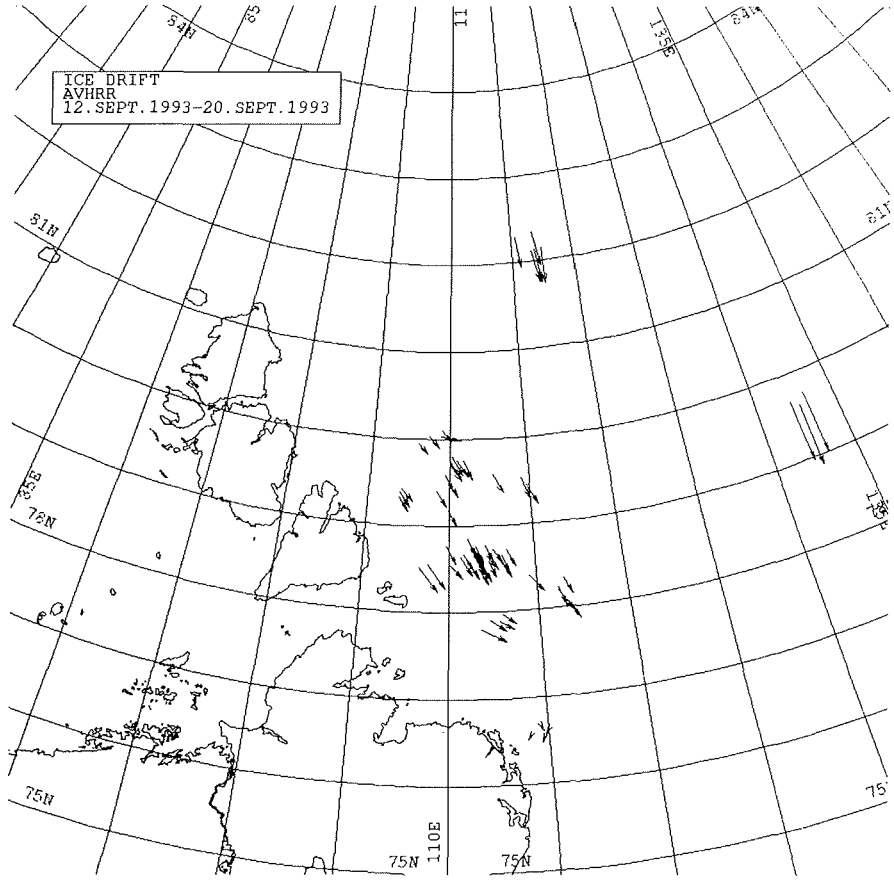

Fig. 3b: Sea-ice dislocation vectors derived from successive AVHRR images for the periods between September 12 and 20.

Conclusions

The analysis of sea-ice cores and ship-bord observations demonstrated that the ice cover of the Laptev Sea as studied during the ARCTIC 93 cruise was far from homogeneous. Stretches of thinner, level congelation ice alternated with highly deformed areas of older ice. In comparison with multi-year ice from the central Arctic, higher fractions of dynamically grown ice (frazil or rafted and ridged ice) were observed, in accordance with earlier findings by Fedotov (1976). Correspondingly, the distribution of ice sediments was also variable. The origin of ice sampled in the Laptev Sea and the processes responsible for the heterogeneity in the ice cover still need to be resolved. Analysis of sea-ice velocities indicates, however, that complex motion patterns along the western Laptev Sea coast play an important role in juxtaposition of different ice types. Sea ice plays a very important role with respect to the sedimentology of the Laptev Shelf and the export of particulate matter into the Arctic Ocean. The value of 156 g m^{-3} for the average sediment load of dirty ice derived from ice cores comes close to the value of 192 g m^{-3} measured in six cores by Osterkamp and Gosink (1984) from the Alaskan

Beaufort Shelf and that of 212 g m^{-3} measured by Kempema et al. (1989) in slush ice during fall freeze-up. From multi-year ice in the central Arctic SPM values ranging between few tens of grams to few hundred grams per cubic meter have been reported (Wollenburg, 1993, Nürnberg et al., 1994).

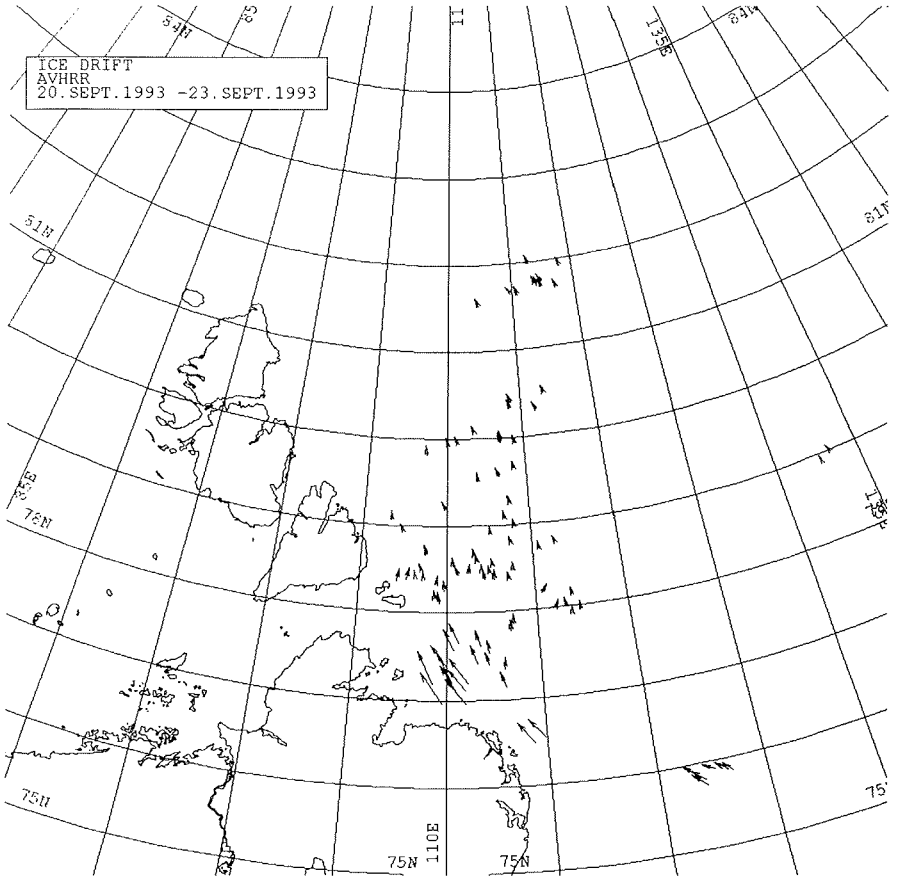

Fig. 3c: Sea-ice dislocation vectors derived from successive AVHRR images for the periods between September 20 and 23.

6. References

Barnett, D., Sea ice distribution in the Soviet Arctic, *in* The Soviet maritime Arctic, edited by L. W. Brigham, pp. 47-62, Belhaven Press, London, 1991.

Colony, R., and A. S. Thorndike, Sea ice motion as a drunkard's walk, *J. Geophys. Res., 90,* 965-974, 1985.

Dethleff, D., E. Kleine, and P. Loewe, Oceanic heat loss, sea ice formation and sediment dynamics in a turbulent Siberian flaw lead, *in* Physics of ice-covered seas - Proc. of Savonlinna summer school, Department of Geophysics, University of Helsinki, in press.

Dethleff, D., D. Nürnberg, E. Reimnitz, M. Saarso, and Y. P. Savchenko, East Siberian Arctic Region Expedition '92: The Laptev Sea - its significance for Arctic

sea ice formation and Transpolar sediment flux, *Ber. Polarforsch., 120,* 3-37, 1993.

Eicken, H., M. Lensu, M. Leppäranta, W. B. Tucker III, A. J. Gow, and O. Salmela, Thickness, structure and properties of level summer multi-year ice in the Eurasian sector of the Arctic Ocean, *J. Geophys. Res.,* submitted.

Fedotov, V. I., Structure of one-year-old ice during spring in the Laptev Sea (in Russian), *Arkt. Antarkt. Nauchno-Issledov. Inst. Trudy, 331,* 151-156, 1976.

Kempema, E. W., E. Reimnitz, and P. W. Barnes, Sea ice sediment entrainment and rafting in the Arctic, *J. Sed. Pet., 59,* 308-317, 1989.

Létolle, R., J. M. Martin, A. J. Thomas, V. V. Gordeev, S. Gusarova, and I. S. Sidorov, 18O abundance and dissolved silicate in the Lena delta and Laptev Sea (Russia), *Mar. Chem., 43,* 47-64, 1993.

Martin, S., and D. J. Cavalieri, Contributions of the Siberian shelf polynyas to the Arctic Ocean intermediate and deep water, *J. Geophys. Res., 94,* 12725-12738, 1989.

Nürnberg, D., I. Wollenburg, D. Dethleff, H. Eicken, H. Kassens, T. Letzig, E. Reimnitz, and J. Thiede, Sediments in Arctic sea ice - implications for entrainment, transport and release, *Mar. Geol., 119,* 185-214, 1994.

Osterkamp, T. E., and J. P. Gosink, Observations and analyses of sediment-laden sea ice, *in* The Alaskan Beaufort Sea: ecosystems and environments, edited by P. W. Barnes, D. M. Schell, E. Reimnitz, pp. 73-93, Academic Press, Orlando, 1984.

Pfirman, S., M. A. Lange, I. Wollenburg, and P. Schlosser, Sea ice characteristics and the role of sediment inclusions in deep-sea deposition: Arctic - Antarctic comparisons, *in* Geological history of the Polar Oceans: Arctic versus Antarctic, edited by U. Bleil, J. Thiede, pp. 187-211, Kluwer Academic Publishers, Dordrecht, 1990.

Reimnitz E., L. Marincovich Jr, M. McCormick, and W. M. Briggs, Suspension freezing of bottom sediment and biota in the Northwest Passage and implications for Arctic Ocean sedimentation, *Can. J. Earth Sci., 29,* 693-703, 1992.

Reimnitz, E., D. Dethleff, and D. Nürnberg, Contrasts in Arctic shelf sea-ice regimes and some implications: Beaufort Sea and Laptev Sea, *Mar. Geol., 119,* 215-225, 1994.

Reimnitz, E., H. Eicken und T. Martin, Multi-year fast ice along the Taymyr Peninsula, Siberia, *Arctic,* in press

Schlosser, P., D. Grabitz, R. Fairbanks, and G. Bönisch, Arctic river-runoff: mean residence time on the shelves and in the halocline, *Deep-Sea Res.,* in press.

Timokhov, L. A., Regional characteristics of the Laptev and the East Siberian seas: climate, topography, ice phases, thermohaline regime, and circulation, *in* Russian-German Cooperation in the Siberian Shelf Seas: Geo-System Laptev Sea, edited by Kassens, H., Hubberten, H. W., Priamikov, S., Stein, R., pp. 15-31, Ber. Polarforsch., 144, 1994.

Weeks, W. F., and S. F. Ackley, The growth, structure and properties of sea ice, *in* The Geophysics of sea ice, edited by N. Untersteiner, pp. 9-164, Martinus Nijhoff Publ., Dordrecht (NATO ASI B146), 1986.

Wollenburg, I., Sedimenttransport durch das arktische Meereis: Die rezente lithogene und biogene Materialfracht, *Ber. Polarforsch., 127,* 1993.

Zakharov, V. F., The role of flaw leads off the edge of fast ice in the hydrological and ice regime of the Laptev Sea, *Acad. Sci. USSR, 6,* 815-821, 1966.

SEDIMENT TRANSPORT BY LAPTEV SEA ICE

E. Reimnitz*, H. Kassens+ and H. Eicken°
* US Department of the Interior, Geological Survey, Menlo Park, California, USA
+ GEOMAR Forschungszentrum für marine Geowissenschaften, Kiel, Germany
° Alfred-Wegener-Institut für Polar- und Meeresforschung, Bremerhaven, Germany

Observations and measurements of sediment in sea ice were made during the Polarstern expedition ARK IX-4 to the Laptev Sea (Fütterer et al., 1992). These sudies cover the place of origin for the Siberian Branch of the Transpolar Drift. The Laptev Sea is considered a major ice factory for the Arctic Ocean, where sedimentary particles along with other foreign substances are entrained into newly forming ice. The stream of pack ice then carries such substances across the Arctic Ocean through Fram Strait into the North Atlantic, where they are released by ice melt. Knowledge about the mechanism of modern ice rafting, requiring about three-years from entrainment to ultimate melting, is necessary for a) understanding the high rates of Arctic coastal retreat and shelf erosion, b) interpreting the polar deep-sea sedimentary record, c) assessing the total sediment budget of the Arctic Ocean, and d) learning about dispersal of hazardous substances in the Arctic.

"Dirty ice" near its source, occurs mainly in the form of turbid ice. Turbid ice contains individual particles dispersed rather evenly throughout an ice layer ranging from .1 to one or more meters in thickness. The formation of turbid ice by suspension freezing is now believed to be the principal entrainment mechanism, but there are others. Wind transport of fine sediments from the Siberian continent onto ice, flooding by river waters, and slumping from coastal cliffs all would be recognizable as distinct surface layers or mounds on first-year ice. Bottom adfreezing on very shallow shelf regions would be revealed by basal sediment accumulations, while the formation of grounded pressure ridges would incorporate internal coarse-sediment pockets.

During transit in the Transpolar Drift the ice undergoes changes that affect the mode in which sediments are carried. These changes gradually mask the original entrainment mechanism to the point where its recognition is impossible. One half meter of seasonal surface melting, greatly enhanced by dark foreign substances, results in the formation of irregular sediment layers on top of the ice and on floors of melt puddles. Various surface processes combine fine particles and biogenic substances into millimeter-size pellets, which become increasingly cohesive with aging through several melt seasons. With slightly acidic conditions prevailing on ice surfaces during summers, calcareous micro-fossils may dissolve with time, making the recognition of sediment entrainment environments increasingly difficult. Not all sediment is retained on ice floes, as some turbid meltwater flows into the sea. Near ice source regions, the pack carries sand and coarser grains, in the Central Arctic and Fram Strait mainly fines have been found, suggesting that coarse grains are lost preferentially. Winter wind-ablation mobilizes exposed sedimentary particles and redistributes them throughout snow drifts. More sediment is lost to open cracks and leads by eolian transport on the ice in winter.

ARK IX-4 reached to the very heart of Siberian ice production area in the Laptev Sea. Because of the above described metamorphosis of the sediment/ice mixture with age and drift distance, the expedition provided a unique opportunity to learn about original entrainment mechanisms, and the fate of sediment in ice.

Objectives

The list of objectives pursued during the expedition includes the following:

- Observe and document the mode of sediment occurrence in ice.
- Compare local observations with those of other parts of the Arctic Ocean.
- Assess likely methods of sediment incorporation, and attempt to evaluate the time or distance from the source region.
- Use regional sediment distribution to evaluate ice dispersal patterns in the Arctic Ocean.
- Collect and process suitable ice samples for sediment load and transport quantification.
- Make albedo measurements at sites where the sediment load is quantified.
- Collect sediment bulk samples for determination of grainsize, clay mineralogy, sand lithology, microfossils, organic carbon/total carbon content, etc..
- Help establish criteria for the recognition of interglacial (sea-ice rafted) layers in deep-sea sediment cores.

Methods of Investigation

Observations, focused on specific objectives listed above, are combined with hourly shipboard ice observations in an attempt to achieve a regional understanding of ice drift patterns and potential sediment sources. All opportunities for actual sample collection were used. In the Laptev Sea, these include 12 ice stations directly from the ship, and 11 helicopter sorties, depending on flight conditions. Where sediment concentrations on the ice permitted, bulk samples were collected by use of spoon, spatula, slurper (when below water), or by chopping and scraping with a spade. Any ice shavings included with sediments were melted and the water decanted. Excess amounts of mud were condensed aboard ship by panning and sieving, and the residues dried in an oven at 60°C. At most sites, about one-meter long ice cores were taken next to other cores taken for ice biology and physical properties studies. Where cores looked clean, they were split into upper and lower halves, melted, and measured volumes of meltwater vacuum filtered through pre-weighed .4 micron filter papers. Where they contained distrinct, sediment-rich layers, these were often sampled, melted, and filtered seperately. Filters and condensed/dried residues where inspected under a binocular microscope aboard ship. Spectral radiation measurements in the visible parts of the spectrum were made, before snow accumulations or low sun angles prevented this, on surfaces of discolored ice or snow. At these sites, ice- or snow-samples of the upper 2-3 cm were also taken, melted, and filtered for later comparisons of sediment content and albedo values.

Shorebased, the filters with sediments were dried and re-weighed, and from these weights and melt-water volumes the sediment concentrations calculated in mg/L. For calculating ice-sediment loads in g per cubic meter, only ice cores, not surface samples were used. An average sediment concentration was calculated from individual values weighted according to the depth interval represented by each sample. These calculated average values are assumed to apply to the upper one meter of ice.

Preliminary Results

During the mid-August work in the Barents Sea, before reaching the Laptev Sea, shipboard and aircraft observations were made without a snow cover soon

obscuring ice and sediment. By August 26 (station #2381), approaching the Laptev Sea through Vilkitski Strait, the melt ponds were freezing and new snow covered the ice. Therefore, percentage estimates of discolored ice from here on were reduced from as much as 30 to just a few percent in the Laptev Sea. Yet, the amounts of sediments collected per site were large, and therefore subsampling for the numerous collaborators was possible. But large fields of clean ice were interspersed with smaller fields of dirty ice.

From excess sediment sample material collected on the ice, the sand fraction was condensed aboard ship and viewed under a microscope. These coarse fractions were found to consist of seemingly well-sorted, fine quartz sand. Except for drift wood, no clasts coarser than sand were found. Most quartz grains had an angular to sub-angular shape. Some diatoms were seen in these coarse fractions on cursory examination, but no foraminifera or ostracodes. Textural analyses show the sand in the Laptev Sea samples to range from 0.01 to 16.6 percent. Clay-size particles dominate the fine fraction.

Table 1 contains data from Laptev Sea ice cores that were suitable for quantifying the sediment load, and figure 1 shows station locations and sediment loads determined. Any ice samples of the upper few centimeters collected by spade or other tools for such purposes as albedo measurements were eliminated in this attempt to quantify sediment load. The table shows that generally sediment concentrations are higher in the upper than in the lower section of ice cored. This reflects in large part summer melt processes concentrating sediments from the upper layer removed. There are, however, cases where the highest sediment concentrations occur at some depth below the surface layer. Thus, cores from station numbers 25821 and 2621 have the highest sediment concetrations at about 175 and 60 cm respectively, below the surface. Here ice compressional events evidently had shoved slabs of dirtier ice under slabs of cleaner ice. Table 1 identifies by * those cores where the ice seemed totally clean to the observer on the ground. Except for the first core listed (2381), which may have been faintly discolored from surficial dust accumulation, all ice with less than 8 mg/L was judged "clean". Filters used for such samples generally contain biogenic material and contamination, such as lint from clothing. They carry very little terrigenous particles. In the following analysis of sediment loads per unit area, SPM values of 8 mg/L and lower serve as background for "clean ice". The average sediment load extrapolated for the upper meter of 10 cores of obviously "dirty ice" is 156 mg/L, which is equivalent to 156 g/cubic meter (Table 1).

The search of clues for sediment entrainment mechanisms in the Laptev Sea revealed the following: A thin, even surface dust cover was not observed on first-year ice, not even at the three coastal sites visited, indicating that eolian transport from land to sea is insignificant overall. No evidence was seen in dirty ice for bottom adfreezing of sediment in shallow water, or for slumping from coastal sites. These mechanisms would be easily recognizable, particulary in vertical fracture faces produced by the ice breaker and observable while in transit. Most important for the Laptev Sea, which is dominated by water and sediment supply from several large rivers, is the fact that no distinct layers that can be attributed to deposition by flood waters, were seen on first-year ice. In particular, the easily identificable freshwater ice mapped off the eastern Lena Delta by the 1992 ESARE study (Dethleff et al., 1993) was not seen during the present expedition.
This suggests that ice which may have been flooded by the Lena River melts in place before entering the Transpolar Drift. However, abundant evidence for suspension freezing in form of turbid ice was seen. Strata of turbid ice sometimes occurred in complex patterns of short layers intersecting at acute angles, where

Tab. 1: Sediment concentrations in sea ice of the Laptev Sea.

Station#	Latitude (°N)	Longitude (°E)	Depth (cm)	Sediment load (mg/l)	Sediment load (g/cubic meter)
2381*	87,1	103,05	0-50	11,8	
			50-100	4,9	8
2391	87,09	102,46	0-10	17,9	
			10-32	39,9	
			32-54	21,3	28
2401	77,4	131,9	0-55	668,7	
			55-110	22,9	346
2461*	79,39	130,36	0-22	2,7	
			22-44	1,6	2
2491	77,57	131,29	0-60	67,5	
			60-120	38,7	53
2501*	77	125,48	0-60	8,0	
			60-120	2,7	5
2511*	77,28	125,53	0-60	2,2	
			60-120	1,6	2
2512	77,24	126,13	0-49	313,3	
			49-98	66,7	190
2521*	77,09	125,54	0-42	2,9	
			42-94	2,6	3
2531	77,41	125,55	0-50	675,3	
			50-99	185,9	433
2541*	78,08	125,02	0-30	10,8	
			30-60	4,6	7
2551*	79,14	122,52	0-50	3,7	
			50-100	4,1	4
2561*	79,11	119,54	0-50	9,7	
			50-100	5,2	7
2571	87,4	118,44	0-50	23,4	
			50-100	2,3	13
25811	87,21	117,54	0-50	109,7	
			50-100	78,2	94
25812	87,21	117,54	0-6	237,6	
			6-23	43,8	
			23-35.5	36,4	
			35.5-45	12,5	
			45-71	51,5	
			71-89	49,7	
			89-92	50,0	
			92-101	77,9	58
25821	78,02	118,13	0-45	181,2	
			45-90	23,0	
			90-140	210,7	
			140-191	223,1	163
25831*	77,78	118,35	0-50	4,9	
			50-100	1,6	3
2601*	77,32	118,28	0-50	1,6	
			50-100	1,1	1

Station#	Latitude (°N)	Longitude (°E)	Depth (cm)	Sediment load (mg/l)	Sediment load (g/cubic meter)
2611*	77,15	118,32	0-50	2,6	
			50-100	4,5	4
2621	77,26	115,58	0-10.5	265,8	
			10.5-18	393,0	
			18-29	321,2	
			29-36	79,9	
			13-46	98,4	
			46-58	243,8	
			58-69	433,2	
			69-85	55,4	
			85-101	8,2	182
2631*	78,19	106,48	0-40	5,3	
			40-80	5,1	5
2641*	78,42	112,32	0-50	1,1	
			50-100	1,8	1

* looks surficially clean to the observer

ARCTIC 93: Sedimentload in pack ice of the Laptev Sea

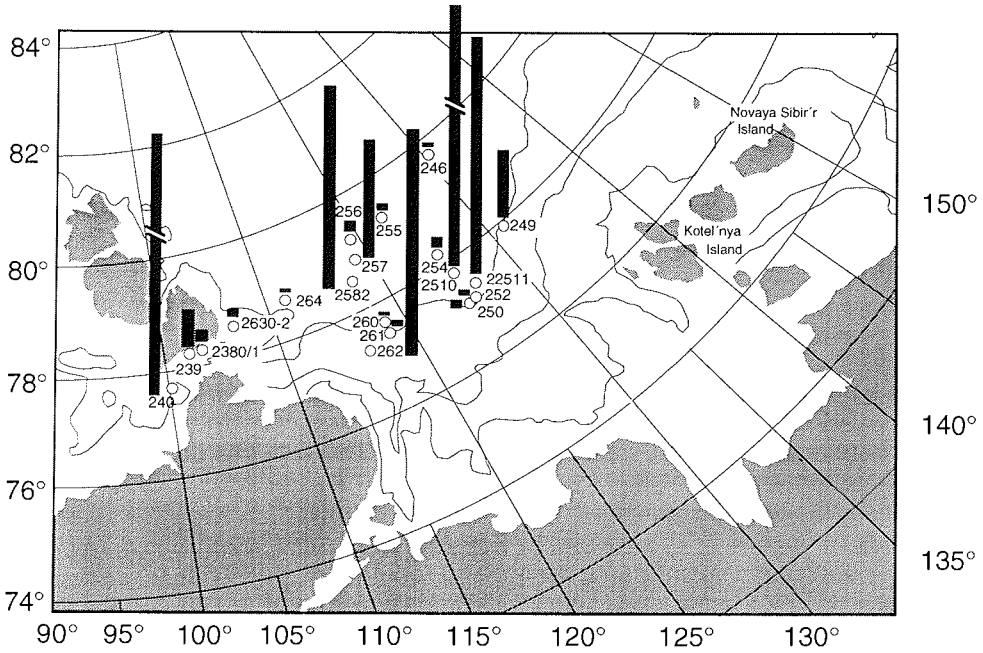

Fig. 1: Locations of ice sampling stations with average sediment loads calculated in g/m^3.

individual layers had been partly condensed by surface melting. Such sediment occurrences therefore indicate that the ice probe had survived at least one melt season and then was compressed into ridges. Individual layers of turbid ice generally were only 5 to 15 cm thick.

Discussion

Fieldwork attempting to quantify the sediment load of sea ice are attracted by dirty ice, because the background load of clean-looking ice is well enough established from numerous expeditions, and because of constraints on station time while on an ice-breaker cruise. The cores taken thus are biased by dirty ice. The cores of "cean ice" collected during ARK-IX-4 represent locations chosen by other scientific disciplines aboard the ship rather than by the ice group. Therefore we must try other means than increasing the number of ice cores to obtain a regional estimate of sediment load. A log of hourly or two-hourly shipboard observations kept aboard the Polarstern recorded the percentage of total ice cover, and the percentage of dirty ice. These records are of questionable quality, because they are made alternately by a number of different people, some of them inexperienced in making pack ice observations. A helicopter with a mounted video camera and GPS navigation was also used in the Barents Sea prior to new snow accumulation, and the resulting data from three flights later interpreted in terms of area-percentage of discolored ice and melt ponds, for example. Comparing these data to shipboard observations showed that area-percentages of dirty ice and melt ponds were greatly overestimated by the observers. For any estimates of sediment transport rates, vertical remote-sensing data properly interpreted for dirty ice-area percentages is advisable.

Preliminary attempts to estimate sediment export rates from the Laptev Sea using summer load measurements, an ice thickness of 1 m, a longterm seaward drift rate of 3 km/day, and percentage estimates of dirty ice observed, were made. These attempts suggest that sediment loss with drifting ice in the Transpolar Drift may approximate sediment supply by the Lena River. In any case, sediment transport by drifting ice is an important component of the overall Laptev Sea sediment budget. The sediment-load averages for the Laptev Sea are higher than those reported by Dethleff et al. (1993) based on winter data.

Conclusions

A large and valuable data set on ice rafted debris in the Laptev Sea was collected during ARK-IX-4, and final analyses will require considerable time. Some preliminary conclusions are listed as follows:

- The summer-sea ice carries a highly variable sediment, with truly dirty ice averaging 156 g/cubic meter.
- Export of this ice in the Transpolar Drift is a significant factor for the Laptev Sea sediment budget and should contribute to the high coastal erosion rates.
- The sediments exported should be recorded in deep sea interglacial deposits mainly as fines, with only a small sand fraction.
- Since anthopogenic pollutants are associated with fine sediments, drift-ice processes are believed important for their dispersal.
- Observations indicate that ice entrainment by river flooding, eolian transport, and the other classic entrainment mechnisms are unimportant relative to the mechanism of suspension freezing in the Laptev Sea.

- The patchy distribution of relatively small regions of dirty ice among large regions of clean ice in the very cradle of the Transpolar Drift reveals intense mixing of ice types by flow eddies over short distances.

References

Dethleff, D., Nürnberg, D., Reimnitz, E., Saarso, M. and Savchenko, Y. P. 1993. The Laptev Sea - Its Significance for Arctic Sea Ice Formation and Transpolar Sediment Flux. - In: Arctic Expeditions: Laptev Sea and Barents Sea. - Ber. Polarforsch. 120: 3-48.

Fütterer, D.K. and Arctic '91 Shipboard Scientific Party 1992. The Expedition ARK-VIII/3 of RV POLARSTERN in 1991. - Ber. Polarforsch. 107: 1-267.

SEA ICE AND SEDIMENT EXPORT FROM THE LAPTEV SEA FLAW LEAD DURING 1991/92 WINTER SEASON

D. Dethleff
GEOMAR Forschungszentrum für marine Geowissenschaften, Kiel, Germany

Abstract

The scientific goal of this research contribution is to estimate the new ice production in the Laptev Sea flaw lead during the 1991/92 winter season. Furthermore, the relative contribution of the lead ice to the sea-ice export from the Laptev Sea to the Central Arctic Basin is quantified. In order to promote a better understanding of the Arctic sea ice as a geological agent, possible mechanisms of sediment re-suspension and entrainment into newly formed ice are discussed. In addition, the mass transport of ice rafted sediment from parts of the Laptev Sea flaw lead to the Arctic Ocean is estimated.

Introduction

The Laptev Sea flaw lead is one of the most extended openings in Arctic sea ice during winter, separating the fast ice from drifting ice. This temporarily over 2000 km long and more than 10 km wide feature was first mentioned by Zakharov (1966) and described in more detail by Dethleff et al. (1993). A recent long-term evaluation of NOAA satellite images, ice atlasses (NAVY/NOAA Joint Ice Center 1981-1992) and unpublished Russian ice charts (Arctic and Antarctic Research Institute, St. Petersburg, Russia) reveals that during early winter (Oct. to Dec.) the lead lies inshore at 5-10 m water depth, bordering a narrow zone of coastal fast ice (Figure 1). This period provides optimum conditions for convection-induced resuspension of bottom material, and thus, for turbulent sediment entrainment into newly formed sea ice. Between December and mid January, the ice cover of the southeastern Laptev Sea expands rapidly to as high as 9-10 tenths of this shelf area and an expanded fast-ice canopy forms within a few days. During that time the formerly inshore flaw lead locally shifts over 500 km from the main land towards water depths ranging roughly between 20-30 m. Turbulent resuspension of bottom material is assumed to be significantly reduced here due to greater water depth. The occurrence and shape of the flaw lead are closely connected to the run of the fast ice edge. Maintainance and width of open water are controlled by regional wind regimes. Initially formed sea ice (frazil- and slush ice) is continuously advected towards the Central Arctic Ocean and, increasing in thickness, constitutes the Laptev Sea tail of the Transpolar Drift-ice stream.

Data and Methods

The Laptev Sea flaw lead exposes the relatively warm water to the cold atmosphere and thus, is an area of significant oceanic heat loss and ice formation during Arctic winter. Heat fluxes and ice production rates are estimated by one-dimensional energy balance calculations employing meteorological data (air temperature, wind direction, wind speed, cloudiness, humidity) that have been collected every 6 hrs at regional Laptev Sea weather stations by the World Meteorological Organization (WMO).

Heat Flux Calculations

The calculations of the ocean/atmosphere energy exchange are based on the

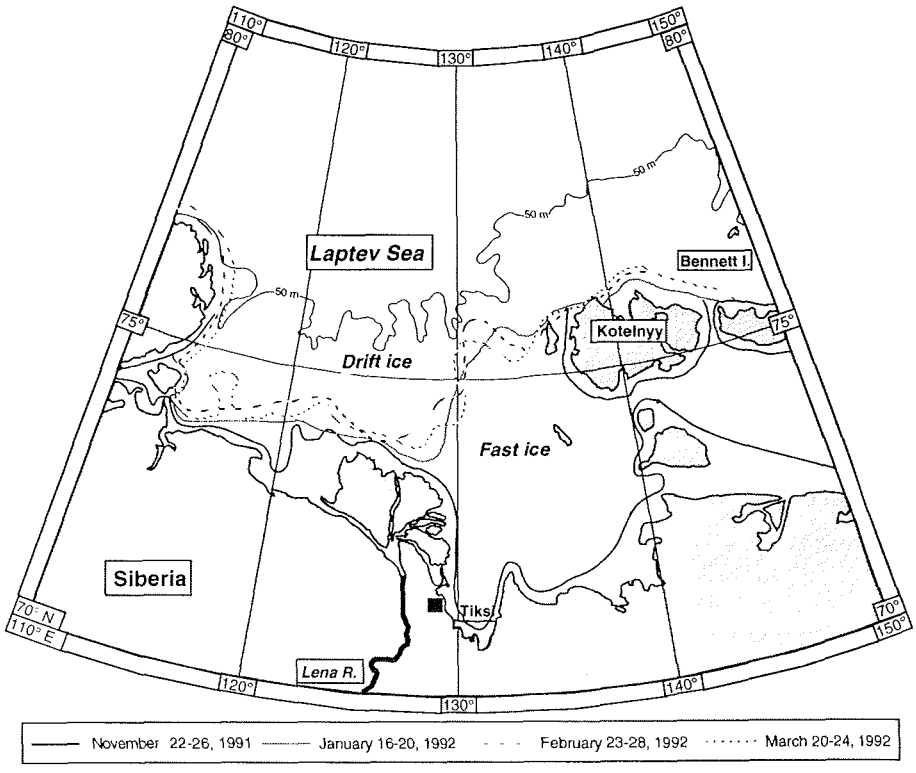

Fig. 1: The edge of fast ice from November 1991 to March 1992 as evaluated by AARI scientists (St. Petersburg, Russia) from satellite images. From January through March 1992 the outer boundary fluctuated, indicating occasional break-aways due to offshore winds and subsequent accretion of new ice. Light stippled area indicates fresh water ice.

following simple heat balance equation:

$$F_{net} = F_s + F_l + R_o + R_a - R_l \qquad (1)$$

where F_{net} is the net heat flux, F_s and F_l are the sensible and latent heat flux, respectively, R_o is the incoming shortwave radiation, R_l is the outgoing longwave radiation, and R_a is the incoming atmospheric longwave radiation. The parameterizations of the individual fluxes in terms of the observed meteorological data are given in detail by Dethleff (1994).

Sea Ice Calculations

Assuming that the entire water column is at its freezing point, the net heat loss ($F_{net}<0$) according to equation (1) has to be set off by ice formation. The new ice forming in the lead area is assumed to be removed instantaneously by continuous leeward advection. Provided that $F_{net}<0$, the maximum possible thickness of stacked-up new ice formed over open water can be obtained by integration of F_{net} over the entire cold season:

$$H_{(tot)} = \int_{\text{Thickness}} dh = -1/L_V \int_{\text{Winter}} F_{net}(t)dt, \qquad (2)$$

where L_V is the volumetric heat of fusion (3.0145×10^8 J/m^3), and the indices h and t represent the ice thickness and time of consideration, respectively.

The meteorological data and consequently F_{net} are known at discrete times only. Thus, to estimate H_{tot} the following sum-formula:

$$H_{tot} = \sum_{i=1}^{n} (\Delta h)_i = -\Delta t/L_V \sum_{i=1}^{n} (F_{net})_i \qquad (3)$$

was employed as an approximation of (2). The index i corresponds to the proper day of the 1991/92 winter season.

The maximum possible volume of new ice formed over open water can be obtained by the following integration:

$$A_f \int_{h_0(t_0)=0}^{h_1(t_1)} dh = -A_f/L_V \int_{t_0}^{t_1} F_{net}(t)dt, \qquad (4)$$

where A_f is the lead area, and $h_0(t_0)=0$ and $h_1(t_1)$ represent the ice thickness at the beginning and the end of a certain period of ice formation.

To estimate V_{tot} for the entire season the following sum-formula:

$$V_{tot} = A_f \sum_{i=1}^{n} (\Delta h)_i = -A_f \Delta t/L_V \sum_{i=1}^{n} (F_{net})_i \qquad (5)$$

was employed as an approximation of (4).

The heat flux and new-ice calculations over open water were based on meteorological data from 5 coastal Laptev Sea weather stations. The sea ice distribution (Figure 1) of the Laptev Sea shelf area and the position of the flaw lead were derived from Russian remote sensing data (provided by the Hydrometeorological Survey of Russia, Tiksi, Russia), unpublished Russian ice charts (AARI, Arctic and Antarctic Research Institute, St. Petersburg, Russia) and own observations during field work in April 1992. Due to the changing orientation of the flaw lead run and regionally varying wind regimes the response of individual lead areas differs from one section to another. For a detailed quantification of the initial ice formation, the band of open water was devided into 14 sub-sections (A_1, A_2, A3, B_1 etc.). The ice calculations for sections A_1-A_3 were carried out using meteorological data of station "Cap Chelyuskin". Sections B_1 and B_2 were associated with meteorological conditions at "Preobrazheniya", C_1-C_4 with data from "Tiksi", and D_1-D_3 and E/F with "Kotelnyy" and "Zhokhova", respectively (Figure 2).

The total seasonal thickness H_{tot} and/or volume V_{tot} of ice produced in a fixed-area lead as obtained from equation (2-5) represent a crude estimate. For a more realistic estimation the following set of rules was applied in the evaluation of new ice formation. For a lead section to be open on day i 1) the wind speed was

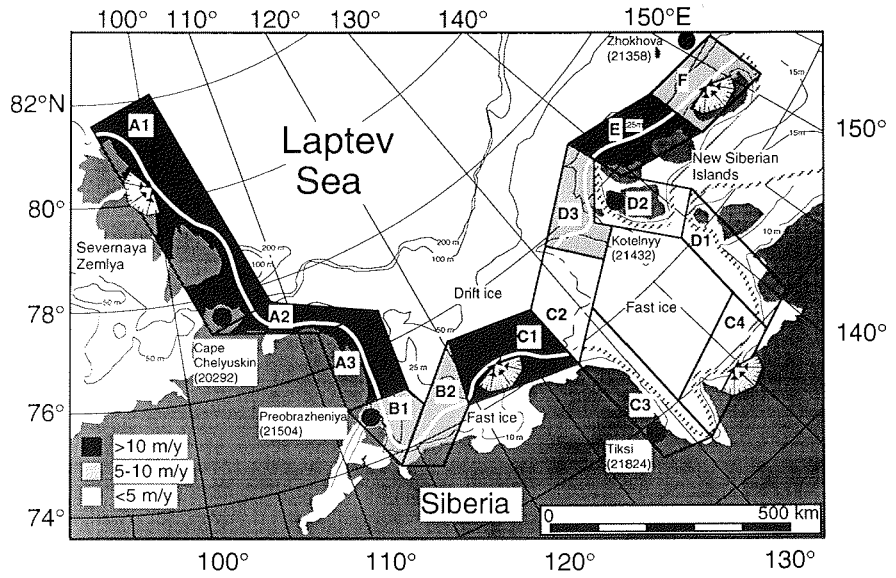

Fig. 2: Chart of the Laptev Sea showing the flaw lead sections A_1, A_2, etc. during mid- and late winter (stippled bold line). Areas C_3, C_4, D_1 and D_2 are located in accordance with the position of the flaw lead during early winter 1991/1992 (dashed bold line) as adapted from unpublished Russian charts and NOAA satellite data. The solid circles indicate the weather stations with their five-digit WMO codes. Seasonal ice thicknesses (m) produced over open water are indicated by shaded sections. Arrows in the polygonal grey stippled areas (e. g. sector A_1) indicate wind directions necessary for lead opening.

required to assume or exceed 4 m/s, and 2) the wind direction had to be offshore and within a range of +/- 70° from a normal to the generalized run of the lead section. If not both conditions applied at the same time the lead was assumed closed. The total seasonal ice thickness H_{tot} and volume V_{tot} were determined for each of the 14 lead sections using equation (3) and (5) under the conditions of 1) and 2), i. e. closed-lead days were excluded from the summation. To obtain the seasonal ice volume V_{tot} the lead area had to be estimated. The length of lead sections was approximated from the average lead run during mid-winter 1992 (Figure 2). Based on mean temperature and wind speed data during the cold season (e. g. Kotelnyy: -21.4°C and 7 m/s) a fixed width of 10 km was assigned to an open lead section. This value corresponds well with modeling results presented by Pease (1987) and Lebedev (1966) and is also supported by the analyses of satellite images and meteorological data (Dethleff et al. 1993).

Ice Formation in the Laptev Sea Flaw Lead

Seasonal Ice Production

The potential seasonal growth of new ice in the flaw lead is displayed by means of an example for the Kotelnyy area (Figure 3). The highest daily rates of ice formation occur during the coldest period from October 1991 to April 1992. According to the model results, the potential thickness of new ice formed over hypothetically permanently open water - continuous leeward advection assumed - amounts to more than 20 m. Real seasonal new-ice production in the Laptev Sea

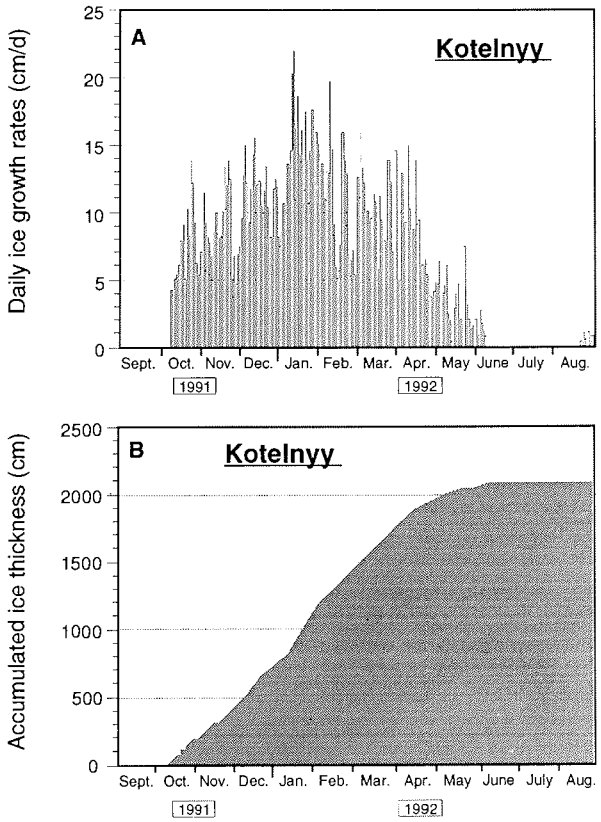

Fig. 3: Daily rates (A) and seasonal total (B) of new-ice formation over hypothetically permanently open water in the Kotelnyy area during cold season 1991/92. Note that according to the model results new ice formation over open water already started again at the end of August 1992.

flaw lead varies significantly from section to section (Table 1, Figure 4) and depends on the areal extent of open water, the number of lead-opening events and finally, on the thickness of ice formed during open-lead periods. Width of the lead and rates of new ice production are mainly steered by regional atmospheric conditions (wind speed and direction) and could additionally be influenced by local oceanic heat input.

In order to improve the classification and comparability of polynyas and leads (flaw lead sections) in respect to their new-ice production, the factor of "sea ice productivity":

$$I_{prod} = H_{tot} \times A_S \qquad (6)$$

is introduced, representing the volume of new ice (in 10^6 m^3) formed in a standardized area of open water A_S ($1km^2 \approx 10^6m^2$) according to the seasonal ice thickness (H_{tot}) in m.

Due to high area-standardized new-ice formation (I_{prod}; Figure 4A) and large areal extent, the flaw lead sections A_1, A_2, A_3, C_1 and E were characterized by

Table 1: Formation of sea ice in the Laptev Sea flaw lead sections depending on regional meteorological conditions during 1991/92 winter season. Geographical position of lead sections is given in Figure 2.

Flaw lead section	Wind direction for occurrence of open water	Estimated areal flaw lead extent (km^2; width of 10 km assumed)	Seasonal sea ice equivalent thickness (cm)	Volume of new ice (km^3) 1.10.91-31.12.91 ** 1.10.91-15.6.92 + 1.1.92-15.6.92 #	Sea ice productivity factor (10^6 m^3/ km^2)
A1	170°-310°	5,300	1,113.90	59.04 +	11.1
A2	130°-270°	2,000	1,085.00	21.70 +	10.9
A3	200°-340°	1,700	1,035.50	17.60 +	10.4
B1	200°-340°	1,300	664.90	8.64 +	6.6
B2	110°-250°	1,600	726.60	11.63 +	7.3
C1	110°-250°	2,500	1,017.20	25.43 +	10.2
C2	50°-190°	2,800	444.00	12.43 #	4.4
C3	190°-330°	3,300	482.10	15.91 *	4.8
C4	110°-250°	3,300	481.40	15.89 *	4.8
D1	30°-170°	3,200	154.50	4.94 *	0.2
D2	20°-160°	2,700	128.10	3.46 *	1.3
D3	70°-210°	2,400	790.60	18.97 #	7.9
E	130°-270°	2,000	1,306.90	26.14 +	13.4
F	130°-270°	1,800	901.80	16.23 +	9.0
Total	-	**35,900**	**10,332.40**	**258.01**	-

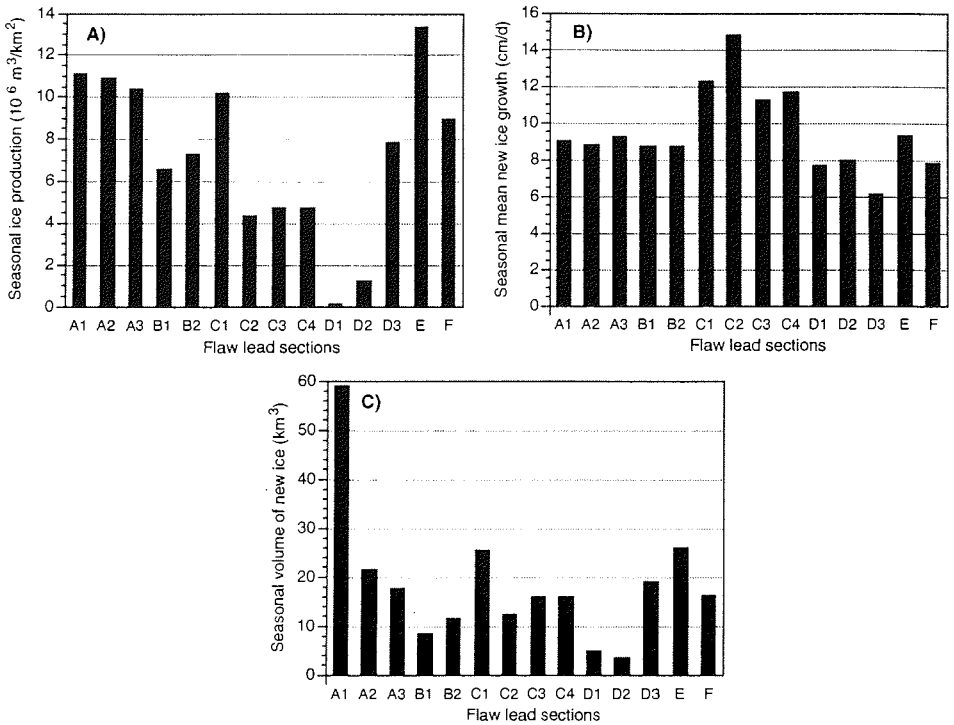

Fig. 4: Depiction of area-standardized seasonal ice production (A), seasonal average of daily new ice growth (B), and total seasonal ice volume (C) of distinct flaw lead sections in the area of investigation.

high production rates of seasonal ice volumes during winter 1991/92 (Figure 4C). In contrast, the (seasonally averaged) daily new-ice rates (Figure 4B) in these lead sections were relatively low. Consequently, high rates of new-ice volumes in the above sections were mainly due to persistent lead opening induced by long periods of regionally offshore winds during December 1991 and January 1992, and temporarily high individual daily ice formation rates (Table 2).

Due to their reduced areal extent and their lower areal-standardized new-ice formation, the lead sections C_2, C_3, C_4, D_1, and D_2 contribute only roughly 20 % (ca. 53 km³) to the entire new ice volume of 258 km³ produced in the Laptev Sea flaw lead during 1991/92 winter season. However, considering their temporally limited occurrence of only 3-5 months the lead sections C_2, C_3, C_4, and D_3 have also to be regarded as areas of high new-ice production rates (Figure 4C). As presented also in Figure 4C, the lead sections A_1, C_1, and E are the main contributors of new ice formed in the Laptev Sea flaw lead during the cold season 1991/92.

Recent "Ice Factory" Laptev Sea Flaw Lead?

The critical question will be raised in this chapter, if the Laptev Sea flaw lead may be regarded as one of the main contributors to seasonally produced Arctic sea ice. To clarify this assumption made e. g. by Dethleff et al. (1993) and Reimnitz et al. (1994), the sea-ice calculations presented here will be interpreted in relation to results gained by different authors.

After Kupetskiy (1959) the seasonal rate of ice formation in the flaw lead east of the Taymyr Peninsula amounts to 8.16 m in case of permanent leeward advection of new ice. Martin & Cavalieri (1989) estimated a 4-year average (1978 - 1982) of 15.7 m of new ice formed in the lead sections K, L, and M in the same area. As derived from sea-ice calculations in the present paper, the mean rate of new-ice formation in the lead sections A_2, A_3, and B_1 east of the Taymyr Peninsula amounts to 9.28 m (Table 1) during winter 1991/92 and thus, compares relatively well to the results presented by Kupetskiy (1959) and Martin & Cavalieri (1989). Mean seasonal new-ice formation in the entire Laptev Sea flaw lead is as high as 7.38 m (this study), well according to the rate of 8.00 m estimated by Zakharov (1966). The above results point to recurring atmospheric and oceanic-cryological conditions during winter in the past decades, at least, in parts of the Laptev Sea.

According to Zakharov (1976) the mean areal ice export from the Laptev Sea amounts to 350,000 km² in the period from 1937 to 1968. Considering a mean thickness of 2.3 m (allowing for hummocking), a seasonal export of 800 km³ of new ice from the Laptev Sea could be estimated. Assuming the same export volume of new ice from the Laptev Sea during 1991/92 winter season, roughly one third (32 % ≈ 258 km³) of the ice advected to the Central Arctic Ocean was generated in the flaw lead. However, the lead represents only 8 % of the entire shelf area available for new ice formation in the Laptev Sea. Consequently, the flaw lead must be regarded as a region of significant new-ice production rates on local and regional scales.

Compared to the entire volume of sea ice (20,000 km³) formed in the northern hemisphere during one winter season (Buzuyev & Gudkovich 1990), the volume of ice exported from the Laptev Sea (800 km³) and the flaw lead (ca. 250 km³, Figure 5), respectively, amounts to 4 % and 1.3 % (Figure 6A). However, the areal extent of the Laptev Sea shelf (ca. 400,000 km²) and the flaw lead (36,000 km²), respectively, represent only 2.7 % and 0.24 % of the entire area of 15x106 km² available for drift ice formation at high northern latitudes. Consequently, especially the Laptev Sea flaw lead does not contribute significantly (only 1.3 %) to the total

Table 2: Periods of regionally offshore winds necessary for lead opening and maintainance and, daily rates of new-ice growth in distinct Laptev Sea flaw lead sections during December 1991 and January 1992. Wind records were obtained from WMO. Ice thickness data are derived from the modeling results according to equation (3).

Jul. Day (1991/92)	Lead Sections A1 to A3		Lead Section C1		Lead Section E	
	Ice growth (cm/d)	Wind direction (°)	Ice growth (cm/d)	Wind direction (°)	Ice growth (cm/d)	Wind direction (°)
333			6.6	200		
334			5.6	210		
335			7.3	230		
336			7.3	210		
337			4.8	180		
338			5.3	220	8.4	200
339	10.3	250	6.7	200	5.8	350
340	14.6	250	6.9	220	7.0	340
341	12.1	260	7.5	200	6.0	250
342	21.1	250	10.0	210	11.4	230
343	20.7	260	17.2	250	13.3	220
344	12.3	240	22.3	250	7.8	230
345	16.0	290	14.8	240	6.0	270
346	13.1	240	11.6	170	11.8	290
347	15.1	240	8.0	200	13.6	270
348	15.2	220	12.1	240	13.0	260
349	11.6	230	23.9	210	12.7	240
350	10.9	270	19.8	230	15.0	110
351	16.3	230	11.5	210	10.1	260
352	16.0	250	17.6	220	11.6	270
353	8.2	210	18.5	230	11.7	270
354	16.2	240	10.3	220	9.5	230
355	18.7	240	14.0	260	12.3	200
356	20.5	240	12.4	230	6.8	310
357	17.3	230	7.7	210	9.0	280
358	13.4	240	16.3	210	10.3	260
359	7.8	200	22.2	210	12.4	230
360	8.5	200	23.3	230	7.5	150
361	5.1	150	19.9	210	7.3	190
362			22.9	230	11.7	220
363			11.8	280	8.9	190
364			14.1	230		
365			11.6	220		
366			17.7	230		
1			16.5	220		
2			14.3	240		
3			19.5	230		
4			20.8	240		

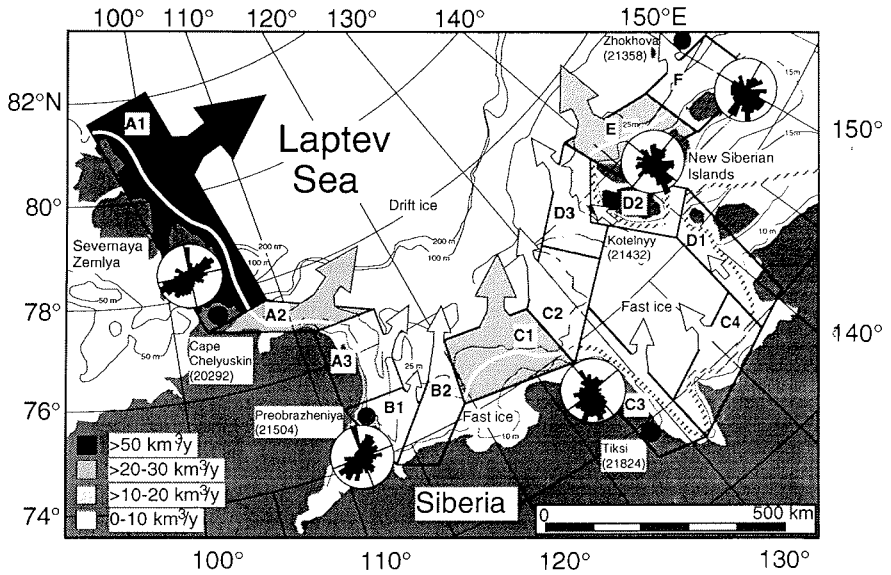

Fig. 5: Chart showing seasonal ice volume production (in km^3) in distinct flaw lead sections (shaded areas). Wind roses indicate the regional dominance of offshore winds during the period from October 1, 1991 to June 15, 1992, blowing from the western to the eastern Laptev Sea increasingly from southerly directions. Size of the arrows and different dot-patterns indicate the volumes of ice exported from the proper lead sections.

ice volume formed in the northern hemisphere during winter, however, it produces large relative amounts of new ice in respect to its limited areal extent. Additonal evidence for high relative sea-ice production in the Laptev Sea flaw lead is given in Figure 6B and 6C.

Sediments in Laptev Sea Ice

Sediment Analyses

According to investigations carried out during the past decade, Arctic sea ice contains regionally significant loads of mainly silt- and clay-sized sediments (e. g. Larssen et al. 1987, Nürnberg et al. 1994, Pfirman et al. 1989, Wollenburg 1993). Coarser material is of minor importance (< 10 %). Results from field studies (carried out in April 1992) show that sediments in the Laptev Sea ice cover and the adjacent Arctic Ocean pack consisted on average of 63 % of silt sized material (Fig. 7), with quartz and feldspar being the main components. The coarse fraction contained both high percentages of quartz and feldspar as well as textile fluffs and plant debris, respectively. The clay fraction contributed more than 30 % to the bulk sediment and partly contained high percentages of illite (> 50%), kaolinite (20-30%), and smectite (partly exceeding 30 %). The characteristics of the Laptev Sea ice-core sediments, such as total- and silt fraction distributions, roundness of silt-sized clastic material, and clay mineral assemblages compare well with regional shelf-bottom and sea-ice surface material. However, they reveal less similarity to suspended particulate matter (SPM) or snow trapped particles. Distribution of sediment content in the Laptev Sea ice cover is displayed in Figure 8.

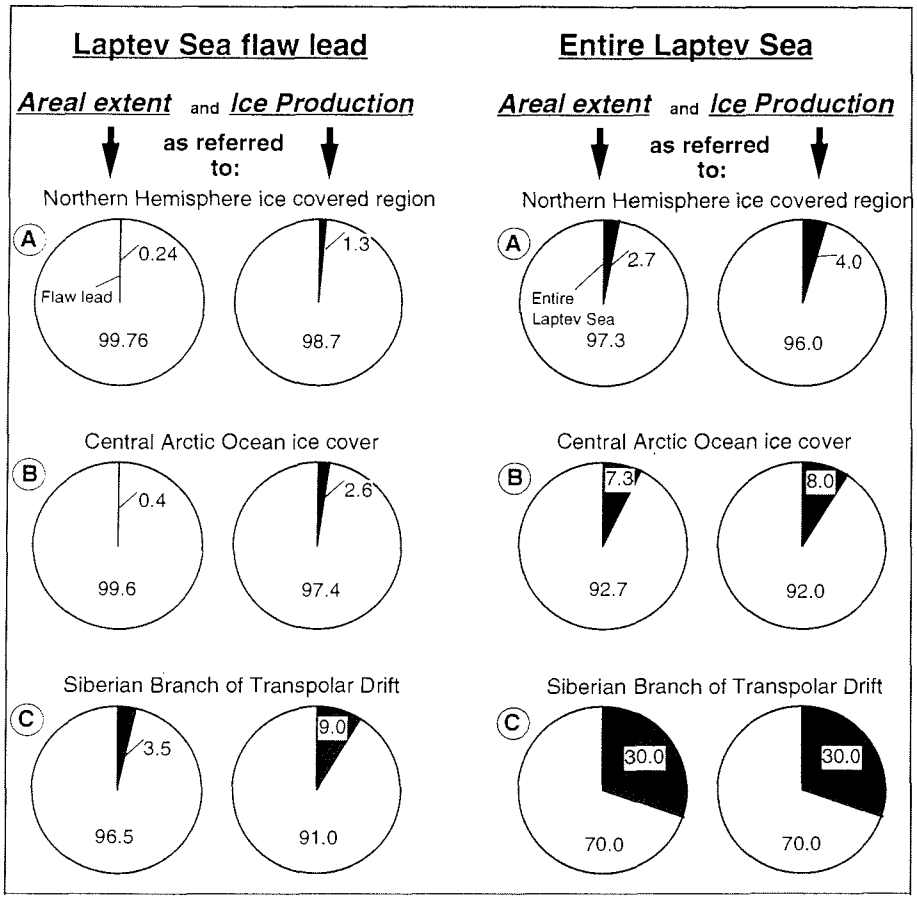

Fig. 6: Areal-percentages and annually produced ice volume of the Laptev Sea flaw lead and the entire shelf area, respectively, as referred to different high northern latitude marine regions (A-C). Black "pie-pieces" represent percentages of the flaw lead and the entire Laptev Sea, respectively.

Ocean and Sediment Dynamics

The ocean beneath the Laptev Sea flaw lead is turbulent and convective. Long, wind-parallel streaks of frazil ice at the water surface indicate convergence zones of oppositely rotating pairs of convective cells in the water column (Fig. 9). Such vortices are initiated by (i) fully developed thermohaline convection and/or (ii) by wind stress and irregular wave fields inducing Langmuir circulation. Both mechanisms continuously clear the water surface for new ice growth. Vortical transport of mass, energy and momentum within the circulation cells can reach water depths greater than 200 m (Backhaus & Harms subm.). Downward velocities can reach 10-15 cm/s. This suggests that convective cells can resuspend unconsolidated fine-grained bottom surface material in the Laptev Sea shallows. Due to interaction with buoyant rising frazil ice crystals (Reimnitz et al. 1993) or lifted by helical oceanic flow, the sediment may be floated upward and collected in the slush-ice rows at the water surface. Additionally, the turbulent water masses may be forced through the wedge-like streaks of frazil and suspended particulate matter can be trapped in the slushy ice cover in areas of downward motion (Fig. 9c). Initial sea ice formation in the Laptev Sea flaw lead may thus be closely

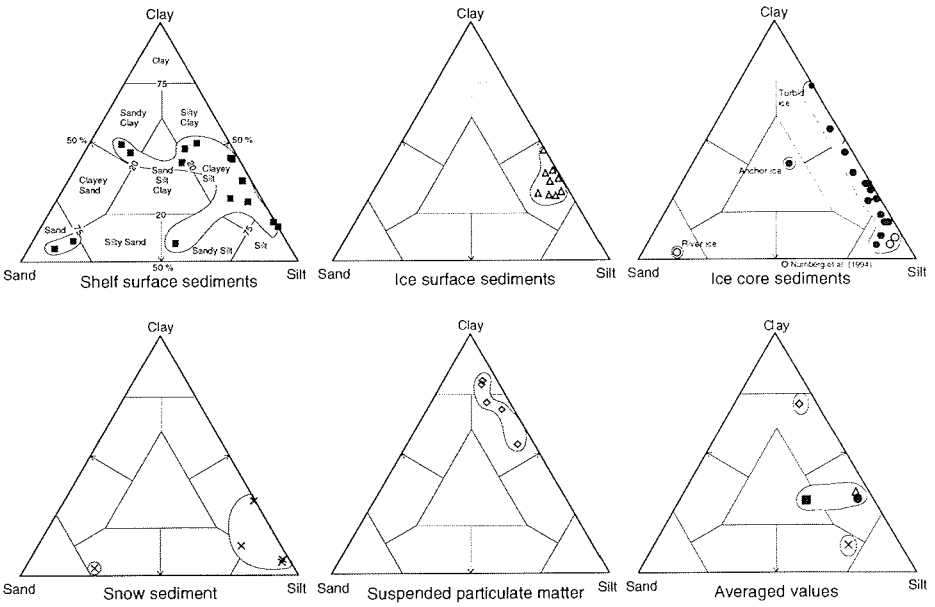

Fig. 7: Ternary grain-size plot of distinct Laptev Sea sedimentary environments. Stippled areas indicate the area of grain size distributions. Averaged values of individual fractions are shown in the lower right triangle.

connected to sediment entrainment into the Arctic pack. Collection efficiency of filtration and scavenging processes in respect to western Arctic shelf areas were modeled and discussed e. g. by Osterkamp & Gosink (1984).

Mineralogical characteristics of sea-ice sediments (e. g. high clay and silt percentages) from various Arctic regions point to similar or identical entrainment processes active in the circumpolar shelf shallows during initial ice formation. The following main mechanisms of turbid-ice formation are discussed in the literature (e. g. Osterkamp & Gosink 1984, Reimnitz et al. 1993): (i) buoyant frazil ice crystals scavenging fine grained suspended particulate matter from the water column and floating to the surface (suspension freezing), (ii) entrainment by upward floating sediment-laden anchor ice, and (iii) discharge of sediment-rich river water over coastal ice canopies. As developed from Osterkamp & Gosink (1984) and detailed here graphically (Fig. 9c), another possibly active mechanism of turbid-ice formation in the Laptev Sea shallows may be the entrainment by trapping sediments in surface streaks of frazil ice, when highly convective sea water is forced through it (filtering).

Sediment Export from the Laptev Sea flaw lead

Based on an average drift- and fast ice sediment content of 40 mg/l and the additional assumption that a volume of ca. 70 km^3 of turbid new ice produced in the sections C_1, C_2, C_3, and D_3 (Table 1, Figure 5) is entirely advected to the Central Arctic Basin, the export of clastic material from the southerly and northeasterly Laptev Sea during one winter season can be estimated at roughly 3-4 million t (Figure 10). Additionally, about 3-4 million t (65 $t/km^2 \approx 40$ mg/l) of sediment,

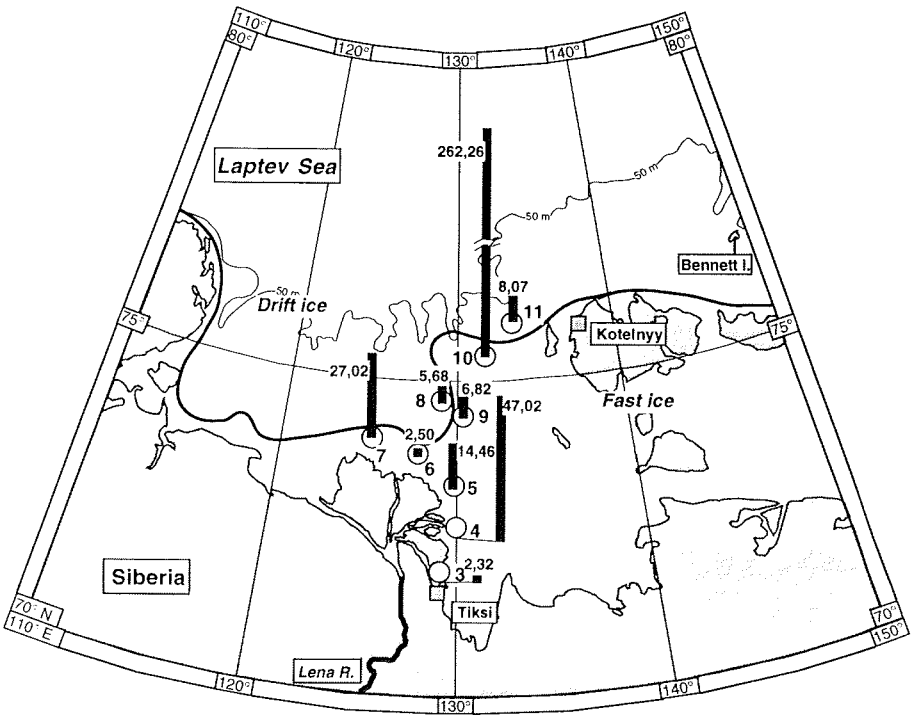

Fig. 8: Average sediment load (mg/l) of several ice-core samples at different locations in the study area.

incorporated into the regional fast ice cover of the same sections, can be released, redistributed and redeposited during the melt season. The corresponding regional fast ice volumes were calculated from the average ice thickness (1.63 m, after Dethleff et al. 1993) of that area (roughly 50,000 km²). Since about 17.6 million t/yr of suspended material is discharged into that part of the Laptev Sea (Létolle et al. 1993), the above numbers are of crucial significance for Arctic Ocean sediment dynamics and mass budget.

Conclusive Remarks

The total ice production in the Laptev Sea during the cold season (October to June) can reach up to 20 m in a body of ocean water permanently maintained by continuous leeward advection. Sea-ice productivity in the flaw lead varies significantly from section to section. In the lead area oceanic turbulences enhance resuspension of bottom material and thus, formation of sediment-laden sea ice. Relatively high amounts of clastic material are evident in Laptev Sea drift- and fast ice. The export of material-laden sea ice from the Laptev Sea to the Central Arctic Basin significantly influence the sediment re-deposition and mass balance on local and regional scales.

In conclusion, the coastal meteorological and oceanographic regime of the Laptev Sea, and in particular the extended flaw lead, is of crucial significance for (i) ocean-to-atmosphere heat flux, (ii) formation of new ice, (iii) regionally varying

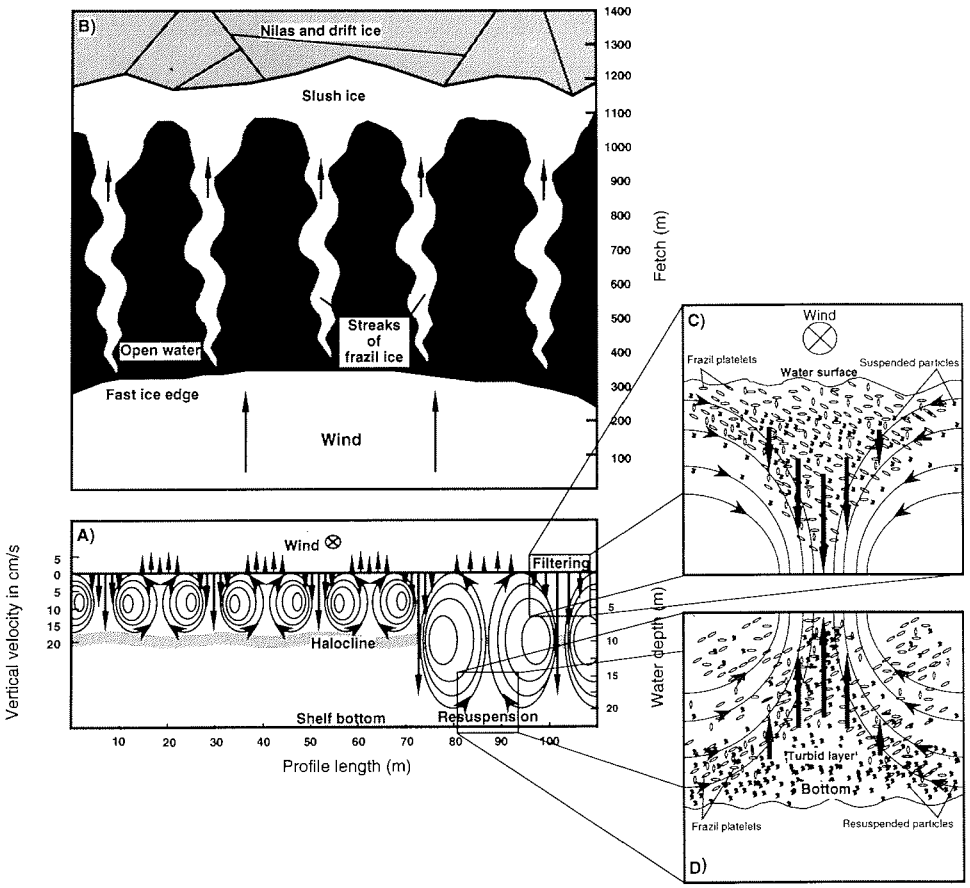

Fig. 9: Hypothetical cross section (A) of Langmuir circulation cells in the Laptev Sea flaw lead as deduced from observed patterns of frazil streaks (B). Vertical section indicates the scale, sense of rotation and speed of the rolls. Explanation of figure (C) is given in the text. Depth of circulation may partly reach the bottom, where sediment is resuspended (D).

rejection of dense brines, (iv) forcing of oceanic convection, (v) resuspension of bottom material, (vi) turbulent sediment incorporation into newly formed ice (suspension-freezing), and (vii) ice and sediment export and redistribution in the Arctic Ocean (Fig. 11).

Acknowledgements

The author would like to thank Peter Loewe and Dr. Eckhardt Kleine of the Bundesamt für Seeschiffahrt und Hydrographie (Hamburg, Germany) for performing the heat flux- and sea ice calculations. Prof. Dr. J. Thiede kindly granted guest status at GEOMAR (Kiel) during preparation of the paper.

References

Backhaus, J. O., Harms, I.H. (submitted to J. Geophys. Res.). Convective Water Mass and Ice Formation in Barents Sea Lee-Polynyas.

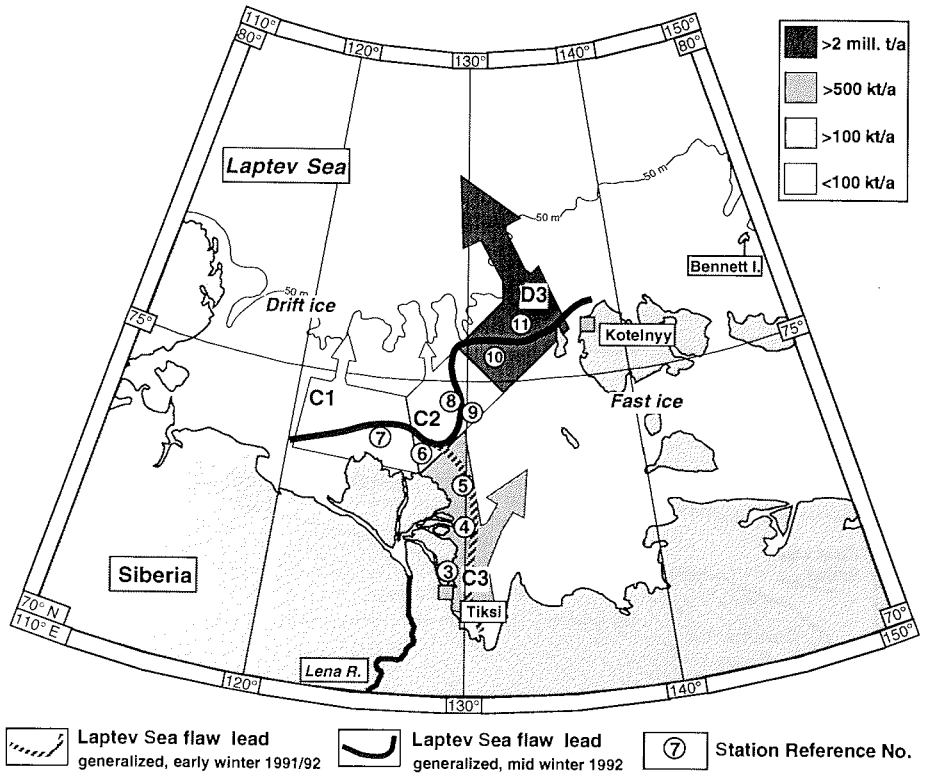

Fig. 10: Sediment export from different Laptev Sea flaw lead sections derived from rates of seasonal new ice production (km^3) and sea ice sediment contents (mg/l). Directions of export correspond to regionally predominating offshore wind regimes under consideration of a slight coriolis deviation to the right (10°).

Buzuyev, A. Y., Gudkovich, Z. M. 1990. Urgent problems in studying sea ice in the Arctic Ocean, Kotlyakov, V. M. & V. E. Sokolov, *in:* Arctic Research: Advances and Prospects. Proceedings of the Conference of Arctic and Nordic Countries on Coordination of Research in the Arctic, Leningrad, December 1988, Moskau "Nauka", 2, pp. 447.

Dethleff, D., Nürnberg, D., Reimnitz, E., Saarso, M., Savchenko, Y. P. 1993. The Laptev Sea - Its significance for Arctic sea-ice formation and transpolar flux of sediments. - Results from East Siberian Arctic Region Expedition `92, Reports on Polar research, Alfred-Wegener-Institut, Bremerhaven, Germany, no. 120, pp. 44.

Dethleff, D., 1994. Polynyas as a Possible Source for Enigmatic Bennett Island Atmospheric Plumes. - *in:* O. M. Johannessen, R. D. Muench & J. E. Overland (eds.). The role of the Polar Oceans in shaping the global environment, Geophysical Monograph Series 85, pp. 475-483.

Kupetskiy, V. N., 1959. Deep Atlantic waters of the thermal regime of the Central Arctic, Problemy Arktiki, 6.

Larssen, B. B., Elverhoi, A., Aagaard, P. 1987. Study of particulate material in sea ice in the Fram Strait - a contribution to paleoclimate research? - Polar Res. 5: 313-315.

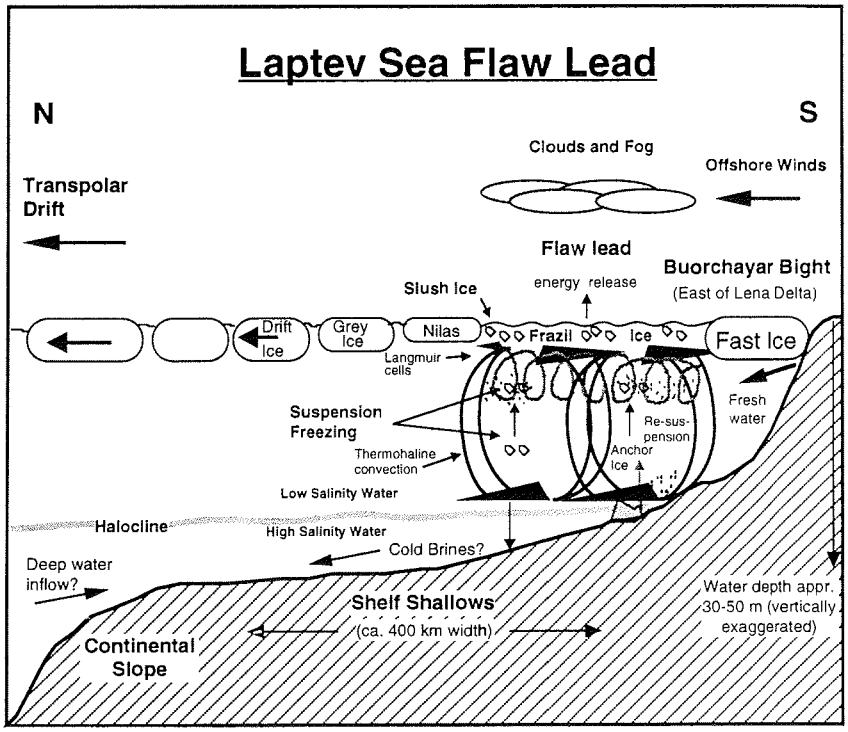

Fig. 11: Hypothetical cross section of the Laptev Sea flaw lead indicating the early winter oceanography, possible mechanisms of sediment resuspension, processes of sea-ice formation and the entrainment of particulate matter into newly formed ice.

Lebedev, V. L. 1966. Maximum Size of a Wind-Generated Lead During Sea Freezing. - Oceanology 8: 313-318.

Létolle, R., Martin, J. M., Thomas, A. J., Gordeev, V. V., Gusarova, S., Sidorov, I.S. 1993. ^{18}O abundance and dissolved silicate in the Lena delta and Laptev Sea (Russia). - Mar. Chem. 48: 47-64.

Martin, S., Cavalieri, D. J. 1989. Contributions of the Siberian Shelf polynyas to the Arctic Ocean intermediate and deep water, J. Geophys. Res. 94(C9): 12725-12738.

NAVY/NOAA Joint Ice Center, 1981-1992, Eastern-Western Arctic Sea Ice Analysis, Naval Polar Oceanographic Center, Suitland, MD, USA.

Nürnberg, D., Reimnitz, E., Dethleff, D., Wollenburg, I., Letzig, T., Eiken, H., Kassens, H., Thiede, J. 1994. Sediments in Arctic Sea-Ice - Entrainment, Transport and Release. - Mar. Geol., Special issue of "ICP-IV-92 Contributions on Arctic Ocean Research, 1992.

Osterkamp, T. E., Gosink, J.P. 1984. Observations and analysis of sediment laden sea ice. - *in*: Barnes, P. W., Schell, D. M. & E. Reimnitz (Eds.). The Alaska Beaufort Sea: Ecosystem and Environment: San Francisco, Academic Press, p. 73-94.

Pease, C. H., 1987. The size of wind-driven polynyas. - J. Geophys. Res. 92(C7): 7049-7059.

Pfirman, S. L., Wollenburg, I., Thiede, J., & Lange, M. A., 1989. Lithogenic sediment

on Arctic pack ice - Potential aeolian flux and contribution to deep sea sediment - *in:* M. Leinen & M. Sarnthein (Eds.), Contribution to the NATO Advanced Workshop; Paleoclimatology and paleometeorology: Modern and past patterns of global atmospheric transport, NATO ASI Series C, Vol. 282, p. 463-491.

Reimnitz, E., Clayton, J. R., Kempema, E. W., Payne, J. R., Weber, W.S. 1993. Interaction of rising frazil with suspended particles: tank experiments with applications to nature. - Cold Regions Science and Technology 21: 117-135.

Reimnitz, E., D. Dethleff, Nürnberg, D. 1994. Contrasts in Arctic shelf sea-ice regimes and some implications: Beaufort Sea versus Laptev Sea, Mar. Geol., 119, Spec. issue, pp. 215-225.

Wollenburg, I. 1993. Sediment transport by Arctic Sea Ice: The recent load of lithogenic and biogenic material. - Rep. Pol. Res. 127: 159.

Zakharov, V. F. 1966. The role of flaw leads off the edge of fast ice in the hydrological and ice regime of the Laptev Sea. - Academy of Sciences of the USSR, Oceanology, No. 6, p. 815-821.

Zakharov, V. F. 1976. Cooling of the Arctic and the ice cover of the Arctic Seas, Arctic and Antarctic Research Institute, Leningrad, Russia, pp. 96.

CIRCULATION AND WATER MASS MODIFICATIONS ALONG THE NANSEN BASIN SLOPE

U. Schauer*, B. Rudels+, R. D. Muench° and L. Timokhov◊

* Alfred-Wegener-Institut für Polar- und Meeresforschung, Bremerhaven, Germany

\+ Institut für Meereskunde, Hamburg, Germany

° Science Applications International Corporation, Washington, USA,

◊ Arctic and Antarctic Research Institute, St. Petersburg, Russia

Introduction

The intermediate and deep circulation in the Nansen Basin is dominated by the inflow of waters from the Norwegian Sea through Fram Strait which spread as a tongue of saline water towards the east (Carmack, 1990) and by the input of waters from the various adjacent shelf seas. The temperature and salinity structures of these shelf waters depend mainly on the fresh water input from continental river runoff, on fresh water extraction due to ice formation and on the intensity of vertical and horizontal mixing. Only the Barents Sea receives in addition a considerable contribution of warm and saline Atlantic derived water from the Norwegian Sea which passes through and leaves the Barents Sea towards the Kara Sea (Rudels, 1987; Blindheim, 1989; Loeng et al., 1993).

This paper presents observations from RV "Polarstern" cruise ARK IX-4 in August and September 1993 over the slope and in the Arctic Basin north of the Barents and Laptev Seas. The influence of shelf water input in the different areas is discussed.

Data

The station positions from the Polarstern cruise ARK IX-4 are shown in Figure 1. Profiles of temperature and conductivity were measured at each station with a Neil Brown Mark III CTD system in combination with a General Oceanics rosette sampler with 24 bottles. The temperature and the pressure probes of the CTD were calibrated before and after the cruise. The salinity obtained from CTD measurements was calibrated by measuring the salinity of water samples with a Guildline Autosal 8400 B.

Results

Warm, saline Atlantic Water which had entered the Nansen Basin through Fram Strait spreads as a boundary current along the continental slope north of the Barents Sea at least until 40=B0E (Fig. 2a and c). In that region, the warm core was situated 30 km off the shelf break with 2.9=B0C and 35.0 as temperature and salinity maximum values. There was a slight eastward decrease in these maxima and in the cross section area covered by the core between the westernmost section and section "W". Beneath the warm saline core, temperature decreased with depth to the bottom and salinity had a weak minimum at 1100 m. The dilution of the core properties of the Atlantic layer in the western Nansen Basin is most likely a result of the admixture of waters from the Barents shelf. Relatively cold, low salinity water overlays the upper slope and the shelf edge at the depth of the Atlantic Water core (Fig. 2a and c). Several tens of meters thick tongues at the slope bottom indicates draining of this water down the slope to about 700 m depth. The cold dense water is expected to be formed in the northern Barents Sea during winter. Its low salinity is caused by the downward mixing of low salinity surface water during winter

convection and by wind-stirring. A patch of shelf water surrounded by warm core water was found at station 25 (Fig. 2a and c) indicating mesoscale mixing processes between shelf water and Atlantic layer.

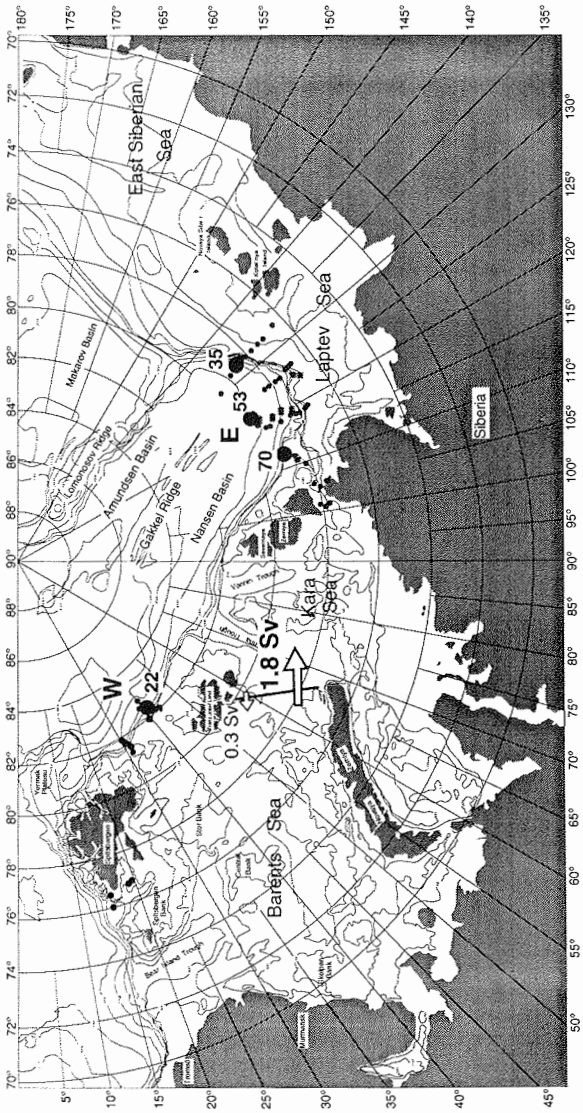

Fig.1: Location of the stations (dots) of the RV "Polarstern" cruise AR= K IX-4 (August-September 1993) to the eastern Arctic. "W" and "E" indicate sections shown in Figure 2. Big dots indicate stations which are referred to in other figures. Arrows depict the mean flow between Barents and Kara Sea from current measurements over twelve months (Loeng et al., 1993).

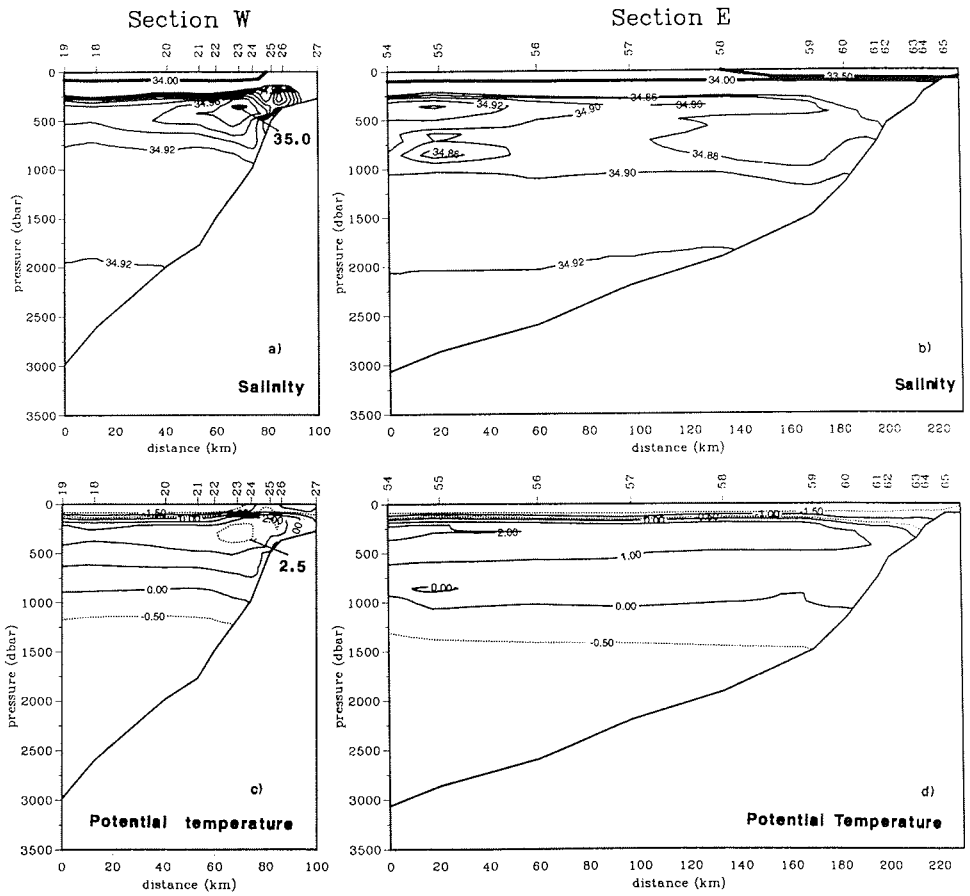

Fig.2: Vertical distribution of salinity and potential temperature along sections at the Nansen Basin continental slope. See Figure 1 for locations.

A comparison between the western sections north of the Barents Sea and the eastern sections north of the Laptev Sea (Figure 2) shows that the continental slope in the east is covered by a 1000 m thick much colder and less saline water mass. The warm, saline core of Atlantic layer originating from Fram Strait appears to have been displaced off the slope towards the interior basin. In addition, the temperature and salinity maxima were less farther east although it is possible that the true maxima were not sampled on the eastern section because of the quite great station spacing. The decrease in T and S values over the slope were consistent with input, north of the Kara Sea, of a substantial volume of Atlantic Water which had been transformed by cooling during its transit over the Barents and Kara shelves. The net inflow of Atlantic Water from the Norwegian Sea to the Barents Sea is estimated to be 1.9 Sv (Blindheim, 1989) and recent current measurements in the passage between Franz Josef Land and Novaya Zemlya indicate that most of this Atlantic Water enters the Kara Sea (Loeng et al., 1993) (Figure 1). It is cooled and freshened during its transit and also interacts with brine enriched water formed in the shallower parts of the Barents Sea. The density of the

Atlantic Water thus increases and when it eventually sinks into the Arctic Ocean, presumably down the St. Anna Trough, it will form a thick cold wedge between the continental slope and the core of the Fram Strait inflow. Lateral interactions and the large property contrasts lead to the formation of inversions, which can induce further mixing through double diffusive processes (Figure 3). Despite its density increase during the transit through the shelf seas, upon entry into the basin, the injected water is less dense than the displaced water column (Figure 4). This leads

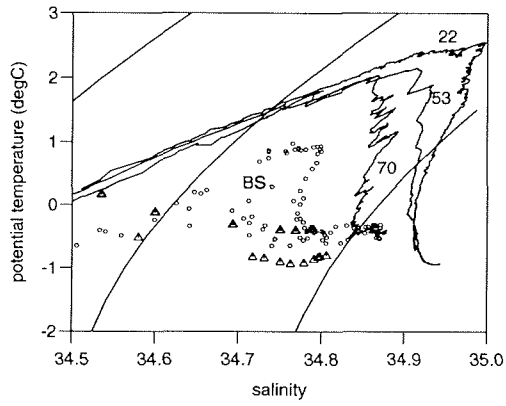

Fig.3: Potential temperature vs. salinity from stations at the slope north of the Barents (22) and Laptev Sea (70) and within the deep basin 200 km north of the Laptev Sea (53). "BS" represents water leaving the eastern Barents Sea towards Kara Sea (Loeng et al., 1993).

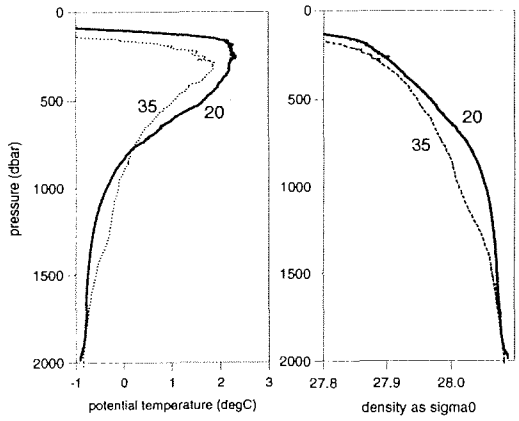

Fig.4: Vertical temperature and density profiles in the western (20) and eastern (35) Nansen Basin. For locations see Figure 1.

to a density decrease of the boundary current to the south. It implies that, if the inflow from the Barents Sea moves towards the east as the observations suggest, it must be driven by a pressure gradient caused by a higher sea level at the

continental slope than in the deep basin and the injection and the layers above move in the same direction.

Summary

All shelf water contributions to intermediate and deep waters observed along the Nansen Basin continental slope were traced back to the Barents Sea. These contributions consist either in local dense winter water plumes leaking from the northern shelf edge or in a broad outflow of Atlantic derived water which enters the Nansen basin continously as a part of the large-scale circulation. Both kinds of shelf water input appear as low salinity water sources for the depth levels of their intrusion in the Nansen Basin.

References

Blindheim, J. 1989. Cascading of Barents Sea bottom water into the Norwegian Sea. Rapp. P.-v. Reun. Cons. Int. Explor. Met. 188, 161-189

Carmack, E.C. 1990. Large-scale physical oceanography of Polar Oceans. In Polar Oceanography, Part A, Ed. W.O. Smith, San Diego, 171-222

Loeng, H., V. Ozhigin, B., D. Landsvik, Sager, H. 1993. Current measurements in the northeastern Barents Sea ICES C.M., 1993/C:41, 22 pp.

Rudels, B. 1987. On the mass balance of the Polar Ocean, with special emphasis on the Fram Strait. Norsk Polarinstitutt Skrifter 188: 1-53

MACRO- AND MESOSCALE HYDROPHYSICAL STRUCTURE OF THE OUTFLOW ZONE OF THE LENA RIVER WATER TO THE LAPTEV SEA

P. N. Golovin, V. A. Gribanov and I. A. Dmitrenko

State Research Center of the Russian Federation the Arctic and Antarctic Research Institute, St. Petersburg, Russia

The studies of the TRANSDRIFT I and II expeditions have shown that in the eastern Laptev Sea, i.e. in the zone of river water outflow and adjacent regions, a specific spatial-temporal macro-, meso- and small-scale hydrophysical structure is formed. Up to now, there is no specific study investigating the mechanisms of its formation in the Arctic shelf zones. Thus, this task requires special investigation. One of the first attempts to analyze these mechanisms as affected by freshwater is made in the present article on the basis of TRANSDRIFT expedition data.

The freshwater discharge and its spreading in the eastern Laptev Sea has a decisive effect on the formation of the hydrological structure. The Lena river occupies the fifth place in the world by its mean annual runoff volume - 650-700 km^3/year (Fedorov 1983). It is the main source of fresh and relatively warm water in the Laptev Sea. 80% of the total runoff fall on two summer months (Doronin 1986) when maximum discharges can run to $100\text{-}120 \cdot 10^3$ m^3/s. Such a powerful factor results in impressive areas of low salinity surface water which significantly transform both surface and lower water layers due to processes of wave-wind-induced mixing and entrainment.

Another result of the intensive river runoff is the formation of hydrological outflow fronts in spring and summer limiting the lens of low salinity water. In accordance with the empirical relationships obtained by Fedorov (1983), the outflow lens area of the Lena is estimated to be about $40 \cdot 10^3$ km^2 with a 14.4 m thick layer of low salinity water. However, as shown by the results of the expedition in 1993 and 1994, river water generelly spreads no deeper than 5-6 m. Then, using a quasi-permanent ratio $h/l=10^{-4}$, where h is the thickness of the freshwater lens, l is the crosssection of the lens by normal from the coast, we obtain l=50-60 km. Hence, by the above estimates the width of the freshwater lens of the Lena will be about 700-800 km, i.e. by 6 times more than the value obtained on the basis of the full-scale observations in 1993-1994. The fact that there is not even an approximate correlation between the actually observed and the estimated parameters of the Lena river outflow lens obviously indicates a more complicated configuration of the outflow lens and the hydrological structure in the river water outflow zone, as compared with traditional representation.

One of the reasons is quite obvious: it is known that the Lena river runoff is distributed among its 4 main branches in a very non-uniform manner. The main portion of the runoff flows from the delta eastwards through the Trofimovskaya and the Bykovskaya branch, and only 10% northwards through the Tumatskaya and 7% westwards through the Olenekskaya branch. As a result of a differently directed inflow of river water to the sea, one can expect a quite complicated configuration of the outflow lens.

The absence of an outflow hydrofront at the periphery of the lens directed seawards, as recorded during the experimental observations of 1993-1994 within the program "Laptev Sea System", allows its identification as an outflow zone of river water formation rather than as a lens. Thus, in 1994 the salinity gradients at the hydrological transects along 130°30' and 134° E did not exceed 0.3 ‰/nm, being on average 0.18 and 0.13 ‰/nm respectively. The latitudinal structure of the

distribution of salinity and other oceanographic characteristics allows the identification of a system of outflow hydrofronts located on both sides of the axes of submarine river valleys: west and east of the Lena and the Yana river as well as in the region of the outflow current formed by river water inflow from the Tumatskaya branch.

The studies of the TRANSDRIFT II expedition aboard the R/V "Professor Multanovskiy", carried out at two transects across the outflow zone of the Lena river water along 74° and 74°30' N, the distance between the stationsbeing 7.5 miles, reveal the main macroscale features of the oceanographic structure of the Lena river water outflow zone:

- The outflow zone is located north-east of the Lena delta approximately from 126°30' E to the Stolbovoy island. Even if the river runoff is weak as recorded in summer 1994, it is well pronounced at 74° and 74°30' N. The western boundary of the outflow zone is formed by the outflow hydrofront confined to the river discharge from the Tumatskaya branch. The eastern boundary is less pronounced and formed by the outflow hydrofront located on the eastern slope of the submarine valley of the Yana;
- In the outflow zone, a significant water layer of low salinity water is formed beneath the surface outflow lens differing from water masses at corresponding depths in adjacent regions in a quasi-isothermal state at a stable salinity stratification (Fig. 1 A, B). There is practically no thermocline related to the spreading of transformed water of river origin in the upper layer. The thickness of the quasi-isothermal water layer amounts to 27 m and significantly depends on the sea-floor relief. The typical vertical temperature gradients are 0.03 °C/m, while corresponding salinity gradients exceed the temperature gradients as a minimum by one order reaching 0.6 ‰/m. An intermediate water layer directly under the outflow cores is characterized by enhanced values of dissolved oxygen (Fig. 1 C), chlorophyl A fluorescence (Fig. 1 D), maximum values of light transmittance coefficients (Fig. 1 F) and absolute minima in the vertical distribution of dissolved silicon (Fig. 1 E);
- The outflow zone is formed by a system of outflow cores of valley axes and local outflow hydrofronts, which are located along the peripheries of the outflow cores. Local outflow hydrofronts are usually 5-7 m deep corresponding to the depth of river water spreading. In the outflow lens, isopycics, isotherms and isohalines intersect with lines of equal pressure (baroclinic front). In the lower quasi-isothermal water layer there is a front formed where isopycnes and isohalines are practically parallel to isobars and intersect with isotherms at an angle of 90° (thermocline hydrofront). This particularly takes place at the periphery of the outflow zone directly under the baroclinic hydrofront at depths of 7-17 m. The terms "baroclinicity" and "thermoclinity" are used here in the sense of isopycnic lines intersecting with lines of equal pressure and temperature (Fedorov 1983).

Hydrological soundings of the water column from surface to bottom, carried out by means of the small-inertia sounding system (OTS-PROBE Serie 3 - Meerestechnik Elektronik GmbH, Germany), have shown the following small-scale features in the vertical distribution of oceanographic characteristics:

- In the subsurface layer located under the low salinity river water lens, as well as in regions adjacent to the outflow zone, isopycnic intrusions of warm and cold waters were observed. The vertical temperature gradients at the upper and lower surfaces of these lenses can reach 2 °C/m. Their vertical scales ranges up to 5-7 m. The studies performed during the TRANSDRIFT II expedition have shown that the spatial dimensions of the outflow hydrofront north of the Tumatskaya branch can reach 4 km.

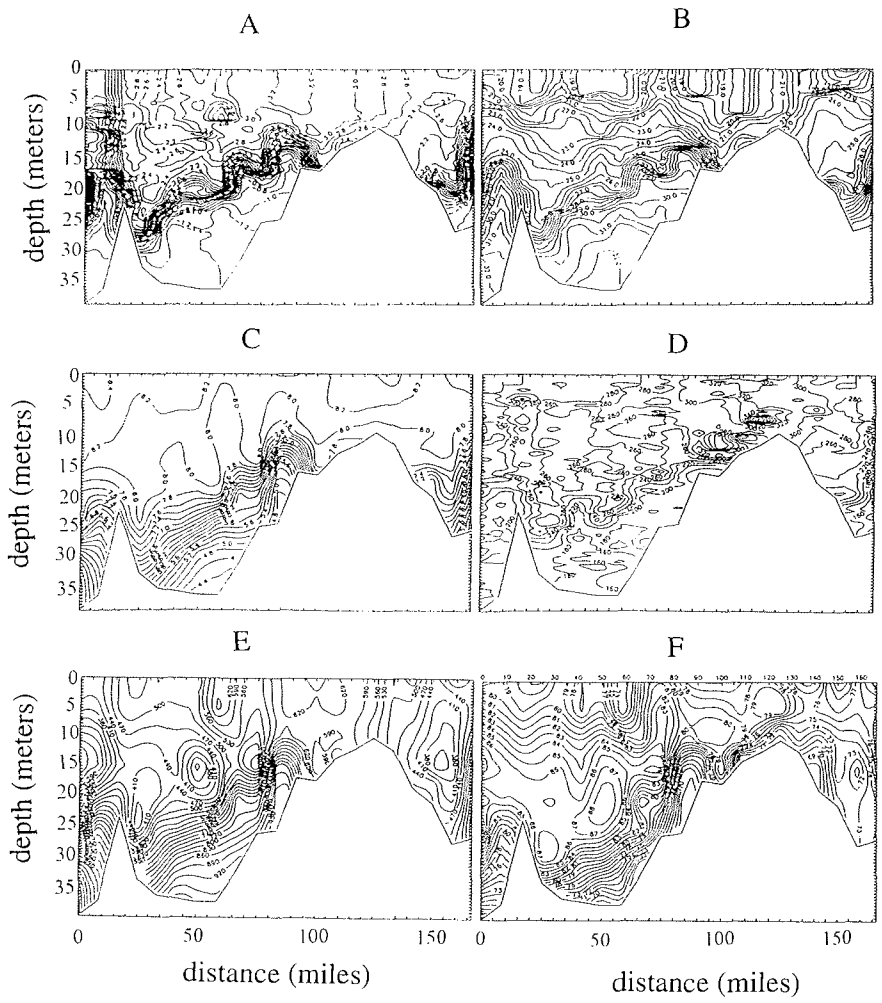

Fig. 1: Distribution of hydrophysical characteristics at the transect across the outflow zone of the Lena river water along 74°30 N from 126° to 136° E.

A: temperature distribution, °C; **B**: salinity distribution, ‰; **C**: distribution of dissolved oxygen, ml/l; **D**: distribution of chlorophyll A fluorescence intensity, arbitrary units; **E**: distribution of dissolved silicon, ml/l; **F**: distribution of light transmittance coefficient at a wave length of 400 nm, %.

The formation of baroclinic hydrofronts at the outflow lens periphery is sufficiently well described in scientific publications. However, the transformation of the baroclinic outflow fronts into sharply thermoclinic ones at the outflow lens periphery in depths of more than 7 m are still not investigated and require special explanations. As shown by experimental studies in the Laptev Sea in summer, such fronts play an important role in the formation of a mesoscale spatial thermohaline structure of the subsurface layer. Isopycnic warm and cold water intrusions are formed here which can spread over considerable distances as affected by advection. Such intrusions were observed everywhere during the TRANSDRIFT I expedition. Any horizontal motions, including motions of inertial and tidal origin, can serve as initial momentum for their formation under conditions of a

sharp hydrofront thermoclinity.

Data on the thermohaline structure, obtained at long-term oceanographic stations in the coastal zone of the Kara and the Laptev Sea from 1956 to 1964, were used to assess water dynamics affected by outflow currents. The stations under analysis were occupied in summer when the river runoff influence is at its maximum. Similar observations in the coastal zone of the East-Siberian Sea, where river runoff is quite insignificant, were also analyzed in order to find features of mesoscale variability of the characteristics. It was assumed with a known probability that the variability of thermohaline characteristics with a frequency ranging from 0.005 to 0.5 Hz is mainly governed by vertical motions. Except for advection of mesoscale structures, advective processes are expressed in the indicated realizations in the form of a third-degree polynomial trend.

The distribution of spectral density of mesoscale fluctuations in correlation with depth permitted estimating the character of vertical motions in the regions being subject to outflow currents. In the coastal zone, in absence of outflow currents, a very well pronounced baroclinicity is found. The spectral structure of processes is characterized by subsurface maxima at inertial and tidal frequencies (Fig. 2 A). A similar structure is observed in deeper regions where maxima of spectral density functions are shifted to water layers of a high gradient. Under the effect of outflow processes on the shallow shelf, spectral maxima are shifted to the surface. A monotone decrease in spectral density values with increasing depth suggests a barotropic character of motions (Fig. 2 B). Since the outflow lens thickness does usually not exceed 5-7 m, a barotropic character of motions can in this case be attributed only to vertical motions, i.e. to entrainment and convergence at the outflow hydrofronts.

The data on the Lena, obtained in the outflow zone during the TRANSDRIFT II expedition, also confirm the supposed convergence of surface water in the outflow hydrofront. In the intermediate layer, directly under the axes of the outflow cores, local minima of dissolved silicon are observed: less than 320 mg/l at the surface layer and from 650 to 980 mg/l at near-bottom levels (Fig. 1 E). Their spatial location coincides with local maxima of the oxygen content, enhanced values of chlorophyl A fluorescence reaching here values typical of the sea surface, as well as with absolute maxima of light transmittance coefficients in water in the range of all wave lengths analyzed, i.e. from 400 to 750 nm (Fig. 1). Water with such characteristics can obviously be of surface origin. It is formed outside the limits of the river water outflow zone (low values of dissolved silicon and high transparency). As a result of near-frontal convergence it, then, sinks to lower water layers forming a sufficiently thick water layer with anomalous hydrochemical and hydrooptical characteristics. Since the river water outflow zone consists of a system of outflow hydrofronts formed at the peripheries of the outflow cores along separate relict river valleys, the distribution of the indicated hydrochemical and hydrooptical characteristics across the outflow zone is characterized by a spatial non-uniformity. Water sinking from the surface to lower layers is, due to convergent processes at the outflow hydrofronts, located directly under the outflow cores its volume probably depending on the "sharpness" of hydrofronts.

The thermohaline water structure repeats in general the hydrochemical and hydrooptical structure. It is characterized by a quasi-isothermal surface layer of considerable thickness that reaches the main thermocline. This results in a complete lack of a seasonal thermocline, while the halocline limiting the river water lens below is present in those regions of the outflow zone where the outflow cores are located along relict submarine valleys. The lower quasi-isothermal layer is characterized by a "dispersed" salinity stratification - from 0.2 to 0.45 ‰/m - while in

A

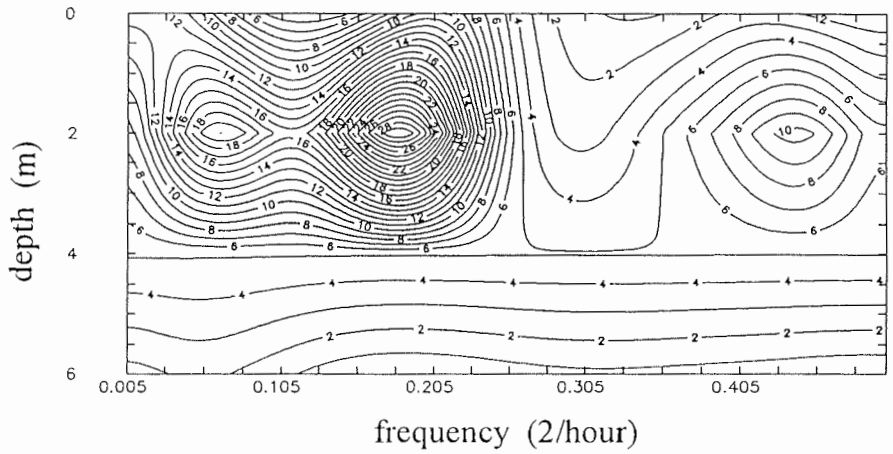

B

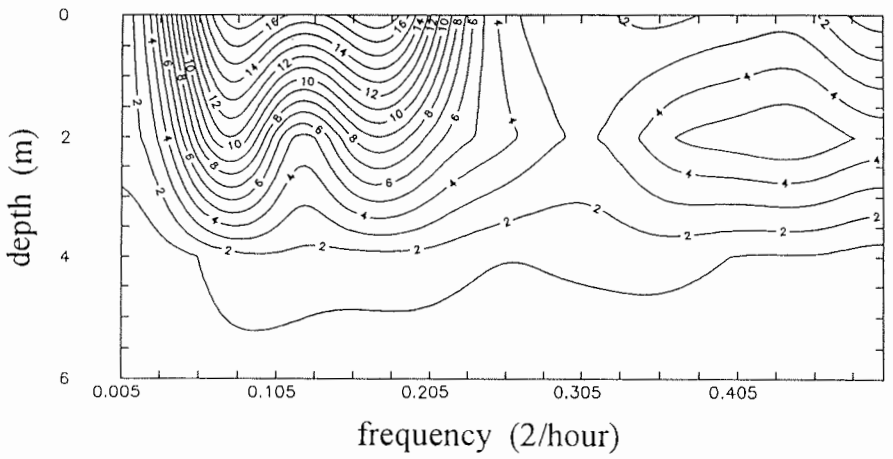

Fig. 2: Spectral density of salinity fluctuations at long-term stations in the coastal zone of the Laptev Sea thermocline front.

the main halocline, coinciding by depth with the main thermocline, the salinity gradients reach 1.1 ‰/m (Fig. 1 B).

The existence of a significant subsurface layer, which is quasi-isothermal but stratified by salinity and density, is probably related to a simultaneous action of two hydrophysical processes. That is, on the one hand, entrainment due to a decay of internal waves at a lower boundary of the outflow lens, resulting in a mutual penetration of river and sea water occurring in two directions (Fig. 3 A). On the

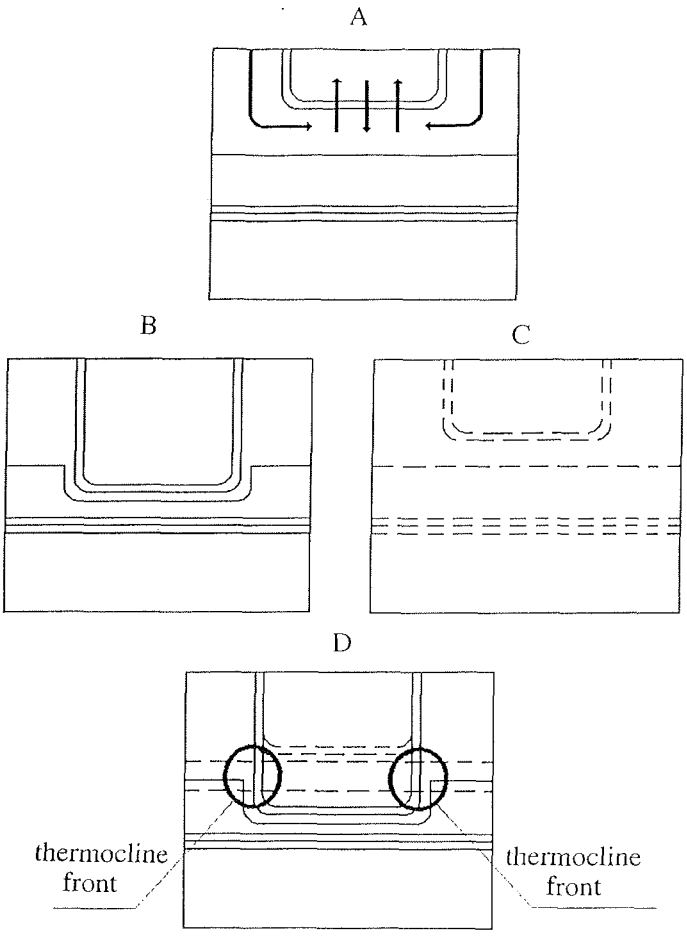

Fig. 3: A scheme of thermocline front formation in the river water outflow zone, as affected by convergence and turbulent entrainment processes; --- - isohalines, ——— - isotherms.

other hand, it is a near-frontal convergence of a more saline water pore in dissolved silicon that leads to a "sucking" of significant volumes of surface water under the outflow lens (Fig. 3 A). The differences in temperature of these water masses and river water in the outflow lens, particularly in the spring period of river runoff, are not as great. Therefore, this process, combined with mixing due to entrainment, results in the hydrophysical structure presented in Fig. 3 B, C. The existing convergence at stationary outflow hydrofronts is indicated in Garvin & Monk (1974). A frontal convergence was also considered as one of the mechanisms resulting in the deepening of the main thermocline and pycnocline in the outflow region of Ob' and Yenisey river water to the Kara Sea (Burenkov & Vasil'kov 1994).

The processes considered above result in a sharp thermocline front under the baroclinic outflow front, at which isotherms and isohalines intersect at an angle reaching 90° (Fig. 3 D). This means that at equal depths on horizontal time scales, which do not exceed the width of the outflow hydrofront, there is water equal in

density but significantly differing in temperature. In this situation, practically any horizontal momentum will result in isopycnic, isolated water volumes (lenses) significantly differing in temperature from ambient water. Inertial fluctuations, well-pronounced practically everywhere in the Arctic seas, can act as initial disturbance (Vertical structure 1989).

Such quasi-isopycnic intrusions of cold and warm water were repeteadly observed during the TRANSDRIFT expeditions at the peripheries of the outflow zones. In all cases, they were recorded in a subsurface water layer at depths corresponding to the scheme suggested in Fig. 3. As a rule, not one but a system of isopycnic temperature intrusions is observed at vertical profiles. Their existence indicates the transformation and splitting of initial intrusions into numerous more thin intrusion layers and interlayers (Fig. 4). A wide spreading of such intrusions over the Laptev Sea (Gribanov & Dmitrenko 1994) can indicate that isopycnic stratification of intrusions at the thermocline outflow fronts can be considered as one of the main mechanisms for assessing a transfrontal exchange. Thus, the results of the studies of the TRANSDRIFT expeditions in the Laptev Sea suggest the following:

- Under the effect of river runoff, a complicated hydrophysical water structure is formed in the outflow zone of the Lena; it is governed by river water spreading from the delta northwards in the direction of relict river valleys. It is formed by a system of local outflow hydrofronts;
- Turbulent entrainment at the lower boundary of the outflow lens and near-frontal convergence at the outflow hydrofronts form a quasi-isothermal intermediate water layer stratified by density under the outflow lens that extends to the main thermo- and pycnocline. It is characterized by anomalous hydrochemical and hydrooptical characteristics;
- Under the effect of near-frontal convergence and turbulent entrainment a sharply thermocline hydrofront is formed under a baroclinic outflow hydrofront;
- The main mechanism of transfrontal exchange at the thermocline outflow fronts is the stratification of intrusions. It results in a wide spreading of isopycnic isolated warm and cold water volumes in adjacent regions which shift in space by advection of the mean current.

The conclusions drawn in this work are preliminary and have to be confirmed on the basis of full-scale observation data and, first of all, detailed measurements of all hydrophysical characteristics in the region of outflow hydrofronts.

Acknowledgments

This work was supported by the Ministry of Science and Technical Policy of the Russian Federation and by the German Ministry for Sciences and Technology.

References

Burenkov, V.I., Vasil'kov, A.P. 1994. On the effect of continental outflow on spatial distribution of hydrological characteristics of the Kara Sea water. MIAK NAUKA, Okeanologiia, v.34, No.5, p.652-661.

Doronin, Yu. P. 1986. Regional oceanography. Leningrad. Gidrometeoizdat: 303 p.

Fedorov, K.N. 1983. Physical nature and structure of oceanic fronts. Leningrad. Gidrometeoizdat: 296 p.

Garvin, R.W., Monk, J.D. 1974. Frontal structure of a river plume. J. Geophys. Res. 79(15): 2251-2259.

Gribanov, V.A., Dmitrenko, I.A. 1994. Types and features of vertical distribution of thermohaline characteristics in the Laptev Sea in summer of 1993. St. Petersburg. Gidrometeoizdat. Scientific results of the LAPEX-93 expedition, pp. 76-82.

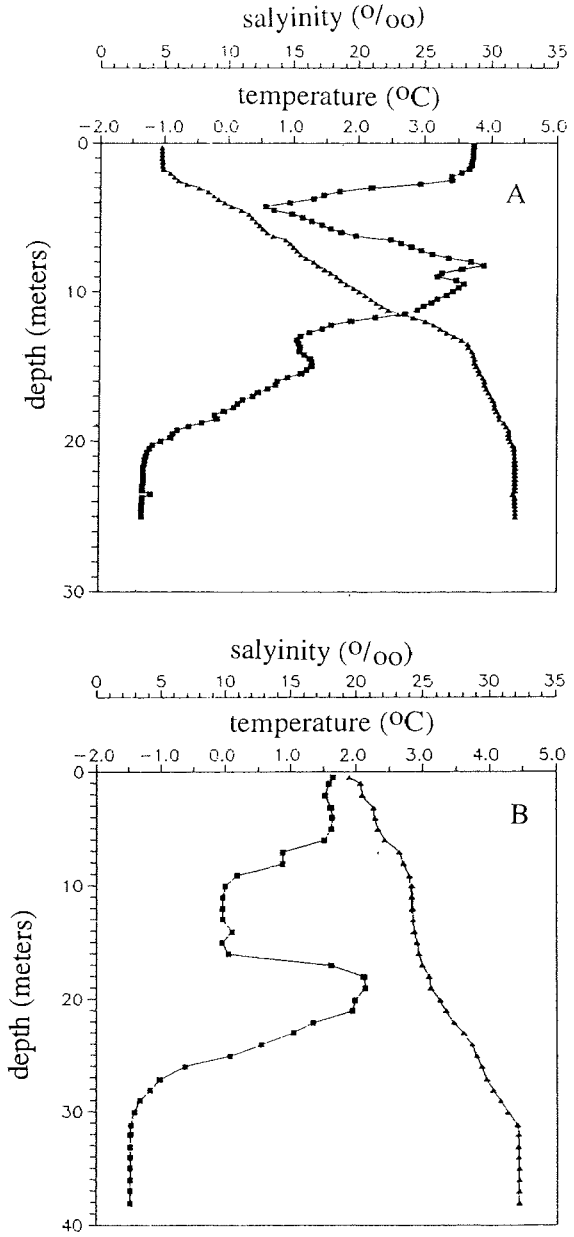

Fig. 4: Vertical distribution of temperature (■, °C), salinity (▲, ‰), typical of the periphery of the outflow zones. A - TRANSDRIFT-I, B - TRANSDRIFT-II.

COLD BOTTOM WATER IN THE SOUTHERN LAPTEV SEA

V. N. Churun and L. A. Timokhov
State Research Center of the Russian Federation the Arctic and Antarctic Research Institute

Abstract

Cold and saline waters with a temperature up to -1.97 °C and a salinity of more than 34‰ are typical features of the oceanographic regime of the Laptev Sea. In the shallow south-western part of the sea, waters with such extreme characteristics form close to flaw leads at a depth up to 40 m. Especially in this part of the Laptev Sea, the drainage decreases sharply, and saline surface water (up to 34‰) from the north of the Laptev Sea can flow in. Oceanographical measurements which were carried out during the expedition TRANSDRIFT I to the Laptev Sea in 1993 have shown that these waters are remaining winter shelf waters which are located in the depressions of the sea floor in summer.

Introduction

During late autumn and winter in the Arctic shelf seas, surface water cools and a salinization takes place due to freezing. As a result, so called shelf waters form. After their formation, these waters leave the shelf and enter the deep Arctic Basin at a depth between cold surface water and warm deep water.

Blinov and Nikiforov (1991) divide shelf waters into Eurasian shelf waters with temperatures between -1.75 and -1.90 °C and a salinity of 32.00 to 33.5‰ and Amerasian shelf waters with temperatures of -1.75 to -1.85 °C and a salinity of 31.00 to 31.50‰. They suggest that the main areas for the formation of shelf waters are regions in which the divergence of sea ice is stable. According to their assessment, shelf waters can cover on average 35 to 50 % of the Arctic Ocean.

In 1985 Midttun observed cold dense water with a temperature below -1.8 °C and a salinity of more than 35.1 ‰ in the depressions to the west of Novaya Zemlya. Thus, he provides direct evidence for dense water formation on the shelf.

In this paper, the extreme values of sea water temperature and salinity are analysed. The data was recorded during the oceanographic expedition SEVER, which was carried out in the south-western Laptev Sea from 1977 to 1989 and in 1993. On the basis of these values, we delineated the most probable regions for the production of cold and saline shelf waters. In addition, we identified the causes for the formation of anomalous cold and saline waters on the shelf of the Laptev Sea in winter.

Methods

Sea water temperature was measured both on the winter and summer expeditions to the Laptev Sea during the last 15 years. The measurements were carried out with high resolution deep-sea mercury thermometers, whose accuracy is ± 0.01 °C. For sea water sampling, Nansen samplers (1.0 l or 0.5 l) were used. Sea water conductivity was determined with a salinometer GM-65 and was then converted to a salinity value on the basis of the equations formulated in International Oceanographic Tables (UNESCO, 1981). The accuracy of salinity determination is ± 0.02‰.

On the basis of the data recorded during the winter expeditions of SEVER, we

chose oceanographic stations where extreme temperature and salinity values were measured and mapped these stations.

Results

During the Russian-German expedition abord R/V *Ivan Kireyev* in the summer of 1993, bottom water with temperatures between -1.77 and -1.82 °C (i. e. one degree colder than the bottom water of the Nansen Trough) and with a high salinity of 34.35 to 34.45‰ was observed north of the Preobrazheniya Island. In this water, the values of dissolved oxygen are very close to saturation, which is indirect evidence for its relatively recent origin. Moreover, the temperature in the cores sampled in this sea region was between -2.0 and -2.2 °C. This turned out to be the lowest temperature in the entire area which was investigated.

Analyses of oceanographic data which was recorded on summer expeditions in the region south of 76° N in the fifties and sixties have shown that the phenomenon described above was observed earlier, too, but not very often. Within a period of 30 years, eight summer expeditions observed cold and saline bottom water with temperatures below -1.50 °C and a salinity of more than 34‰. On 15 expeditions, bottom water was fresher in summer. In August 1967, for example, maximum salinity at the bottom did not exceed 32.47‰. Seven times the summer observations could not be carried out in the south-western sea region. This was due to different reasons (extent of ice cover larger than average, other expedition goals).

As a rule cold and saline shelf water (CSSW) is observed west of 130° E and south of 76° N (Fig.1). The distribution of CSSW is non-uniform. CSSW is located in the area of underwater river valleys. Most often cold bottom water fills the depres-

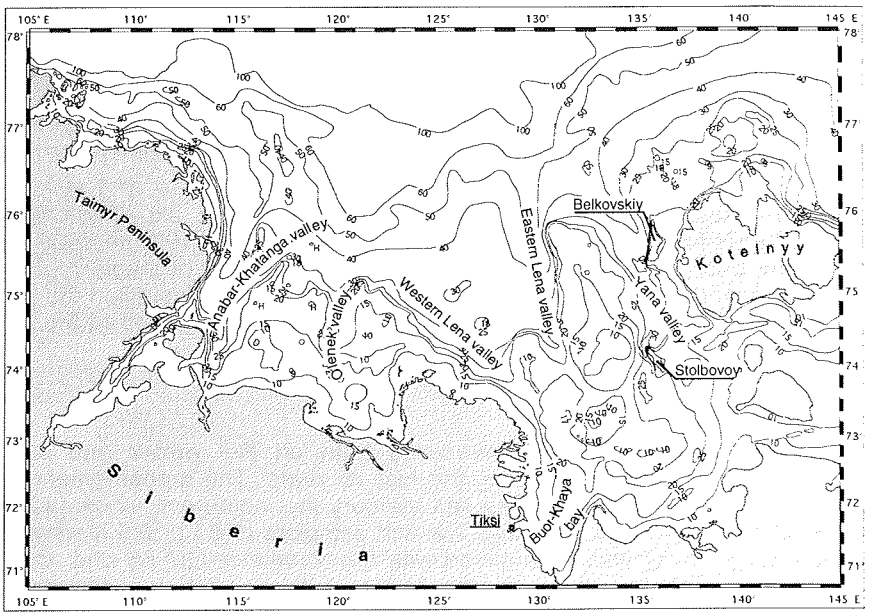

Fig. 1: The bathymetry of the Laptev Sea

sion of the Anabar-Khatanga valley between 74° and 76° N hollows in the West-Lena and East-Lena valleys with the coordinates 75° N, 124°E and 74°35´N, 128°30´E, respectively, and the confluence of the Olenek and West-Lena valleys. The temperature and salinity profiles which are presented in Fig. 2 are most characteristic. For comparison, there are also given the vertical temperature and salinity distributions in the depressions of the eastern sea region, where stagnation effects are observed in summer.

The fact that cold and saline bottom waters are scattered all over the area indicates that local conditions, primarily winter processes, play a dominant part in their formation. Thus, the analyses of the oceanographic observations of the SEVER expedition in April/May 1993 have shown that very cold (-1.98 °C) and very saline (35.79‰) water was recorded in the south-western sea in the winter of that year. This fact caused us to analyse the structure of the winter shelf water of the Laptev Sea.

In order to delineate the most probable regions for the formation of cold and saline shelf water (CSSW), we studied the data of the expedition SEVER from the years 1977 to 1989 and from 1993. Our main attention was directed to the oceanographic observations made in the south-western sea region. Water formed here which was colder and more saline, i.e. denser, than adjacent water. The oceanographic stations were occupied in March and April and, as a rule, from fast ice. A scheme of the location of the oceanographic stations in the south-western Laptev Sea is given in Fig. 3.

Discussion

The main features of ice conditions in the Laptev Sea during March and April are known very well thanks to numerous airborne ice observations and satellite images. A well-developed quasi-stationary flaw polynya is observed in the winter period. It appears in the form of one large or several separate local areas which are covered with nilas or grey and grey-white ice (Fig.4). In particular, there is a polynya near the Peschanyy Island in fast ice. This polynya extends northward along the Anabar-Khatanga river valley. A considerable number of stations where enhanced salinity values were observed belong to the area near to this polynya.

All 40 oceanographic stations can be divided into three groups according to their extreme values of temperature and salinity. The mapping of the stations and the subsequent analysis of these values allowed us to identify three regions in this part of the sea (Fig. 5). These regions can be considered the most probable areas of shelf water formation. The extreme values of temperature, salinity, and silicon for the identified regions are given in Table 1.

Tab. 1: Extreme T (°C), S (‰) and Si (mg/l) characteristics in the delineated regions

Region	T, °C	S, ‰	Si, mg/l
1	-1.84:-1.97	33.63-34.81	150-500
2	-1.80:-1.94	32.38-34.56	-
3	-1.58:-1.80	29.67-32.42	>780

Region I is confined to the depression of the Anabar-Khatanga valley. As shown in Table 1, the most cold and most saline water is recorded here. Water depths reach 40 m. But the formation of cold waters with temperatures below -1.90 °C and a salinity of more than 34‰ was not always observed. Cold waters were observed in 1978, 1979 and 1980, then salinity decreased to 32.40-33.97‰. Water with a

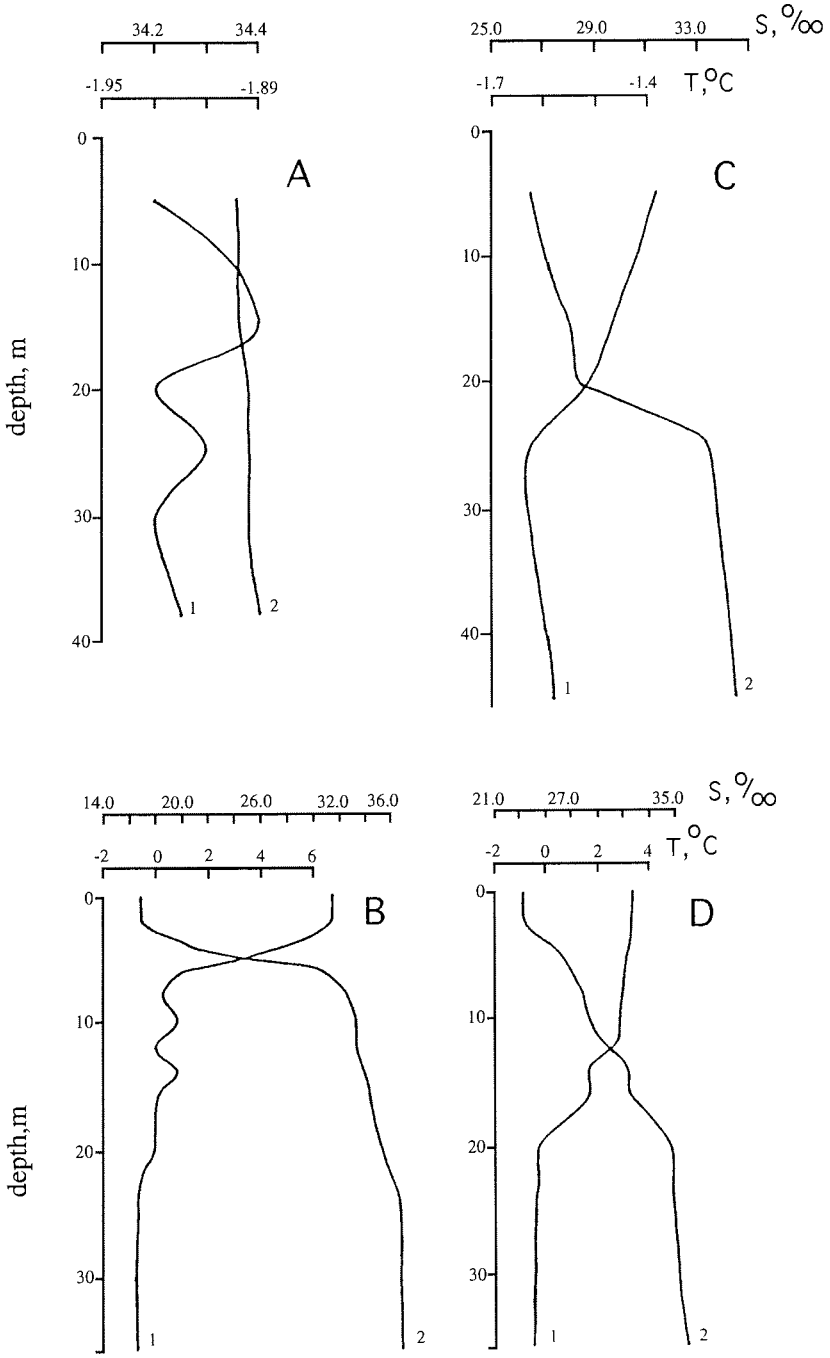

Fig. 2: Characteristic water temperature (1) and salinity (2) profiles for the areas with CSSW in Winter and Summer in the western and eastern (C,D) Laptev Sea.

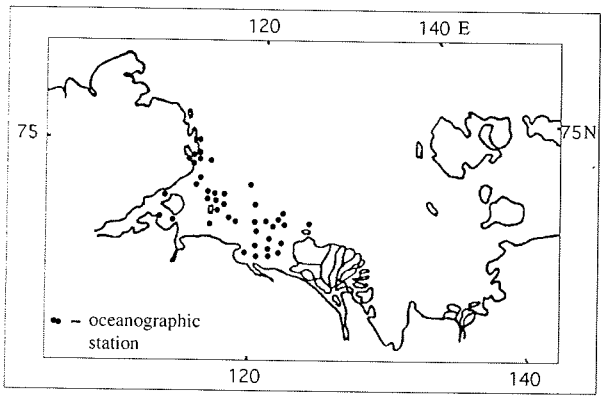

Fig. 3: A scheme of oceanographic stations in the south-western Lapetv Sea occupied by the 'SERVER' expedition in 1977 to 1989 and 1993.

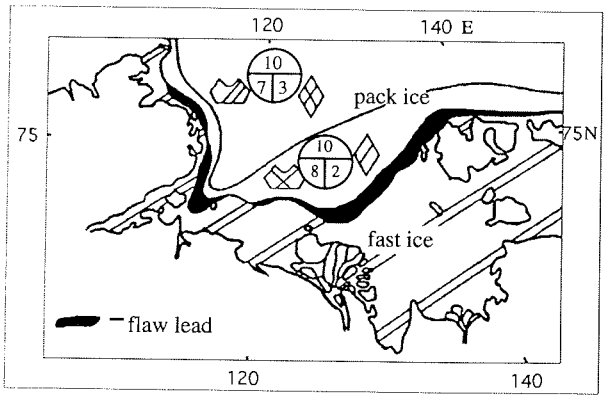

Fig. 4: Mean ice conditions in the Laptev Sea in April.

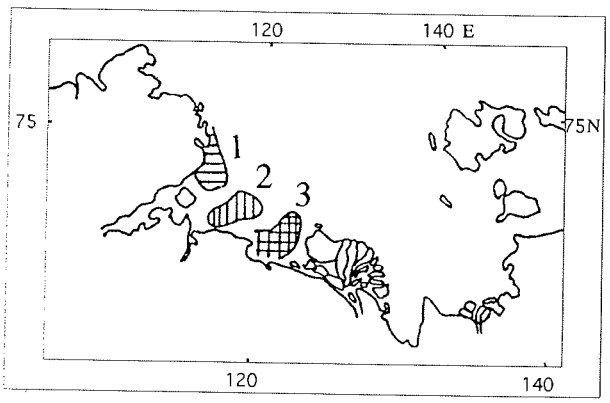

Fig. 5: Scheme of regions in the south-western Laptev Sea identified by extreme temperature and salinity values..

salinity of 34.46 and 34.81‰ was recorded again in 1987 and 1993 respectively.

Region 2 with depths of 8 to 12 m is located east of the local polynya near the Bol´shoy Begichev Island. Here the largest interannual temperature and salinity changes from anomalously low to anomalously high values are observed.

Region 3 is west of the Lena river delta, i. e. it is farthest away from the flaw quasi-stationary polynya. Though sea depths do not exceed 10 m, cold and saline water was observed in this region, too. In the central part of the region, water salinity does not exceed 30‰, and temperature varies between -1.44 and -1.58 °C while at the periphery salinity increases up to 32.42‰ and temperature decreases to -1.80 °C.

In all these regions, a vertical distribution of thermohaline characteristics is typical of the winter period. It is characterized by a homogeneity of the layer. Nevertheless, in winter sea water still preserves some thermal potential, which prevents the water cooling. The thermal potential is determined as the difference between water temperature in situ and its freezing temperature at a given salinity. In our case the values of the thermal potential were between 0.0 and +0.18 °C. The freezing temperature of sea water was calculated according to O. Miyaka (Popov et al.,1979).

What causes govern the appearance of especially cold and saline shelf water in winter in the south-western Laptev Sea? There are three main factors for the formation of CSSW in winter:

(i) the inflow of saline surface water (up to 34‰) from the north to the south-western part;

(ii) intensive ice formation, especially in the polynya zone, which is accompanied by the salinization of the subsurface layer and the occurrence of gravitation convection;

(iii) a significant reduction of the water flow of rivers; some of the rivers in this region freeze over completely in winter.

In fact, if we compare the salinity distribution maps of the winters of 1978 and 1981, we state that in 1978 salinity values up to 34 ‰ were observed at the surface in the western part. Very cold and saline water was recorded in the same year. In 1981 in the same region, the salinity values at the surface were lower (about 33‰), and a bottom water salinity of more than 34‰ was recorded nowhere on the shelf.

During ice formation in the southern part of the sea, salinization was recorded instrumentally: a salt flux from the bottom of the ice cover to sea water is observed at each second to third oceanographic station in winter. The difference between the salinity value at a level of 2 m and the salinity value at a level of 5 m can reach 0.55‰, as it was observed at the point 72°03´ N, 132°50´ E in April 1993.

The effect of rivers on water stratification in winter can easily be illustrated by comparing thermohaline profiles of the western and eastern sea regions. While a homogeneity from the surface to the bottom is often observed in the south-western sea area, a two-layer structure is always preserved in the south- eastern part. This is due to the inflow of fresh water of the Lena river. We would like to emphasize that the existence of the pycnocline even in winter prevents a vertical exchange. As a result, bottom water is low in oxygen in the depressions of the south-eastern part of the sea. Each of the factors contributes to the formation of CSSW. For example, winter salinization can increase the salinity of surface water by 25% in zones exposed to the influence of river water (Panov and Shpaikher, 1963). Evidently, this is not sufficient to increase salinity from the surface to the bottom up to 32-34‰ in the south-western sea region. As a rule surface salinity does not exceed 11-15‰ here in summer. Only the combined effect of three factors (i. e. the inflow of more

saline water from the north to the south-western part in winter, the reduction of river run-off to negligible values and intensive ice formation) create the conditions for the formation of anomalously cold and saline shelf water. In winter CSSW fills the bottom depressions. A part of CSSW probably flows through the troughs in the direction of the shelf edge. But up to now there has been no experimental confirmation that especially cold and saline shelf water reaches the continental slope and - interacting with Atlantic water - forms the bottom water of the Arctic Basin. First, CSSW with a large density forms seldom, and its volume is insignificant. Second, the shelf slope is small in this region, and the distance from the place of CSSW formation to the shelf edge is large. Consequently, it is quite probable that CSSW is transformed while sinking to the continental slope. Winter CSSW flows in the Arctic Basin, mainly over Atlantic water, and forms a layer of intermediate winter water (Blinov and Nikiforov, 1991, Martin and Cavalieri, 1985, Nikiforov and Shpaikher, 1980).

Conclusions

As a result of the analysis of sea water temperature and salinity, three regions of the Laptev Sea were delineated. These regions can be considered the most probable sources for CSSW formation. A flaw polynya which is located near this area is an additional source for maintaining this water in a metastable state. Spring and summer processes significantly transform temperature and salinity in the active layer. Small CSSW volumes, however, are preserved at large depths in the depressions of bottom topography under the pycnocline layer.

Acknowledgments

This work was supported by the Ministry of Science of the Russian Federation as a part of the joint Russian-German project "System Laptev Sea". We wish to thank H.Kassens of GEOMAR for her friendly help and constructive advice for the preparation of the article. The authors thank I.I.Solov´eva and D. Krüger, who translated the paper into English.

References

Blinov, N.I. and Ye. G.Nikiforov, 1991. Structure and hydrological types of water in the Arctic Basin. (In Russian), Problemy Arktiki i Antarktiki, iss.66, p. 211-223.

Gawarkiewicz, G. and D.C.Chapman, 1994. Dense water formation on Arctic shelves. Model tracks coastal ocean response to Arctic ice conditions, Oceanus, Vol. 37, 2, p.14-16.

Martin, S. ang D.J.Cavalieri, 1989. Contribution of the Siberian shelf polynyas to the Arctic Ocean Intermediate and Deep Water, J.Geophys.Res., 94, p.12,725 - 12,738.

Midttun, L., 1985. Formation of dense bottom water in the Barents Sea, Deep Sea Res., 32, p. 1233 - 1241.

Nikiforov, Ye.G. and A.O. Shpaikher,1980. Typical formation features of large-scale fluctuations in the hydrological regime of the Arctic Ocean. (In Russian), L.: Gidrometeoizdat, 270 p.

Panov, V.V. and A.O. Shpaikher,1963. The effect of Atlantic water on some features of the hydrological regime of the Arctic Basin and adjacent Seas. (In Russian), Okeanologiia, Vol. 3, iss.4, p.579-590.

Popov, N.I., K.N. Fedorov and V.M. Orlov, 1979. Sea water. A Handbook.(In Russian), M.: Nauka, 328 p.

THE DISTRIBUTION OF RIVER RUN-OFF IN THE LAPTEV SEA: THE ENVIRONMENTAL EFFECT

I. A. Dmitrenko and the TRANSDRIFT II Shipboard Scientific Party
State Research Center of the Russian Federation the Arctic and Antarctic Research Institute, St. Petersburg, Russia

Introduction

The property of oceanological processes to preserve the main characteristics of the evolution is known from previous observations in the Arctic seas. Nikiforov and Shpaikher (1980) named this property "hydrological inertia". This effect is connected with the distribution and the transformation of river run-off. The prevailing hypothesis that there are three types of distribution patterns in the Laptev Sea which dominate in the central, the western and the eastern part of the sea respectively suppose that the "hydrological inertia" can be traced back not further than 1-2 years (Moretskiy et al., 1994). Nikiforov and Spaikher (1980) suggested that the reason for the "hydrological inertia" is that the distribution of river run-off resists influences of different (in the first place synoptical) origin except for the initial influence. In our opinion, such an important factor like the sea bottom topography has been disregarded here. The sea bottom topography influences the circulation, including the outflow current, in a constant manner and in one direction only. Exactly this factor could determine the "hydrological inertia" in the distribution of fresh waters in the shallow Laptev Sea, including the main river jets. This factor could indirectly influence all possible components of the sea by run-off, from the hydrochemical regime to the features of sedimentation.

In this article, we examine the environment of the Laptev Sea with regard to the distribution and the transformation of run-off.

Methods

In order to investigate the distribution and the transformation of fresh waters, we carried out transects along 74° N and 74°30´ N, with the distance between the stations being 7.5 miles (Fig. 1). Crossing the Laptev Sea from west to east, we carried out a similar transect along 76°30´ N, with the distance between the stations being 15 miles.

Sea water salinity and temperature, pressure and dissolved oxygen were recorded with CTD OTS-Probe Serie 3 of the Meerestechnik Electronik GmbH at each station. The parameters were measured at different depths (every 2 to 10 cm). Each 5 m, beginnig at the sea surface, we measured dissolved oxygen (according to the Winkler method), dissolved silicate (according to the colorimetric method) and the beam transmittance coefficient within the wave range from 400 to 750 nm. In order to record the chlorophyll-A fluorescence intensity, we used the "Variosens" fluorimeter.

Moreover, we used oceanological and hydrochemical data of the TRANSDRIFT I expedition (Kassens and Karpiy, 1994) in order to investigate the distribution and the transformation of fresh waters.

The location of the river jets was determined with the aid of the distribution of thermohaline parameters and of silicate on the transects. The analysis of the spatial distribution, another characteristics of sea water, allows us to determine the influence of river run-off on the environment of the Laptev Sea.

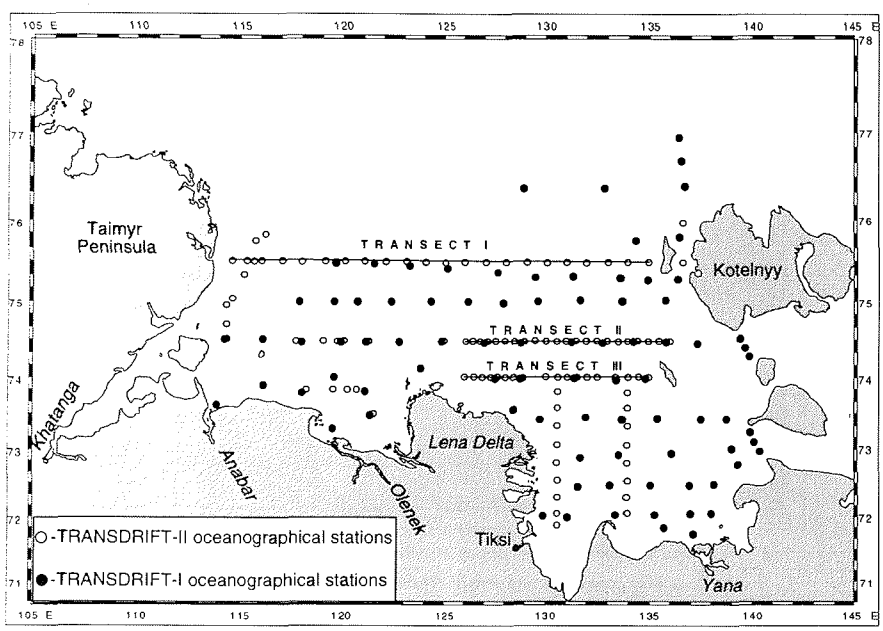

Fig. 1. Plan of the oceanographical stations and transects which were used for the analysis. The stations and transects were carried out during the TRANSDRIFT I and the TRANSDRIFT II expedition.

Results

The analysis of the obtained data suggests that the inflow of fresh water into the Laptev Sea coincides with local sea areas. For the Laptev Sea, these are mainly the eastern and western valley of the Lena river. Moreover these are the valleys of the rivers Yana, Olenek, and Anabar and Khatanga, but to a lesser extent because their run-off intensity is considerably lower. The outflow jets, which form together the outflow zone of river water, roughly coincide with the axes of the underwater valleys (Fig. 2). In fact, a deviation of the river jets from the axes of the underwater valleys was observed for the first time in 1994. At that time the river jets were located 18 to 20 miles to the east of the valleys (Fig. 3).

The outflow of river water in the direction of the river valleys has a decisive effect on the whole complex of natural processes in these sea regions. A specific hydrological-hydrochemical regime is formed in the zone of river water outflow. The outflow jets are characterized by maximum values of silicon dissolved in water, by slightly reduced values of dissolved oxygen, and by maximum values of the light transmission coefficients in sea water. However, much larger silicon concentrations and absolute minima of oxygen dissolved in water are observed in the near-bottom layer at the bottom of the river valleys. Thus, we can conclude that mineral and organic matter which comes from the surface and is transported by river waters is oxidized in the near-bottom water layers which are located under the jets of the river water outflow. Probably, such zones form due to a stable influx of organic matter during several years. Their existence can indicate that in the near-bottom layer, the water advection from the sea in the direction of the river valleys is attenuated considerably. In accordance with the position of the outflow jets at the sea surface, the stagnation zones and the zones with a maximum of dissolved silicon in the near-bottom water layer are deflected to the eastern slopes of the river valleys.

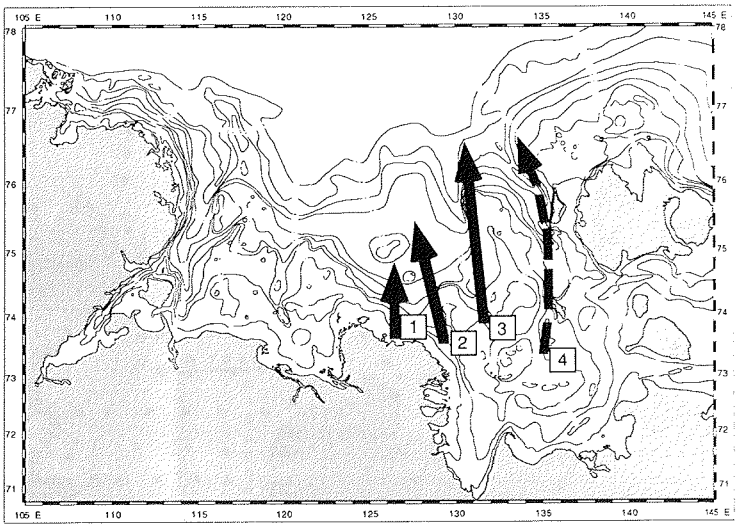

1 - outflow core from Tumatskay branch
2 - outflow core in the direction of Western Lena Valley
3 - outflow core in the direction of Eastern Lena Valley
4 - outflow core in the direction of Yana Valley

Fig. 2. A schematic diagram of the distribution of the outflow jets in the direction of the river valleys in accordance with the bottom geomorphology.

The observations during the TRANSDRIFT II expedition suggest a certain scheme for the distribution of the hydrochemical, hydrooptical and hydrological characteristics presented in Fig. 4. This scheme is typical of the outflow jets and reflects the influence of river run-off on the hydrophysical characteristics of the water medium in the outflow zones.

Discussion

The prevailing depths in the regions of the Laptev Sea which are exposed to the effect of river run-off most, i.e. in the regions to the north and north-east of the Lena delta river, are 20 to 40 m. Hence, according to the Ekman theory with modifications of Shtockman (1953) and Fedorov (1955), the sea bottom relief has a significant influence on the distribution of river water in this region, since the sea depth H<2D, where D is the friction depth:

$$D=\pi/(\omega\rho \, \mathrm{Sin}\, \varphi \, \mu^{-1})^{-1/2}.$$

Here μ is the turbulent friction coefficient, ω is the angular speed of the rotation of the Earth, ρ is water density, and φ is the location latitude. An estimate of D for the Laptev Sea latitude is about 40 m, with μ= 500 g/(cm·s). Consequently, in the regions where the sea depth exceeds 70 to 80 m, only the geostrophic flow component depends on the bottom relief. In accordance with the theoretical conclusions, the experimental studies in the Laptev Sea in 1993 and 1994 have shown that water of river origin spreads - according to the bottom geomorphology - from the mouth of the main rivers northward in the direction of the river valleys (Fig. 2, 3).

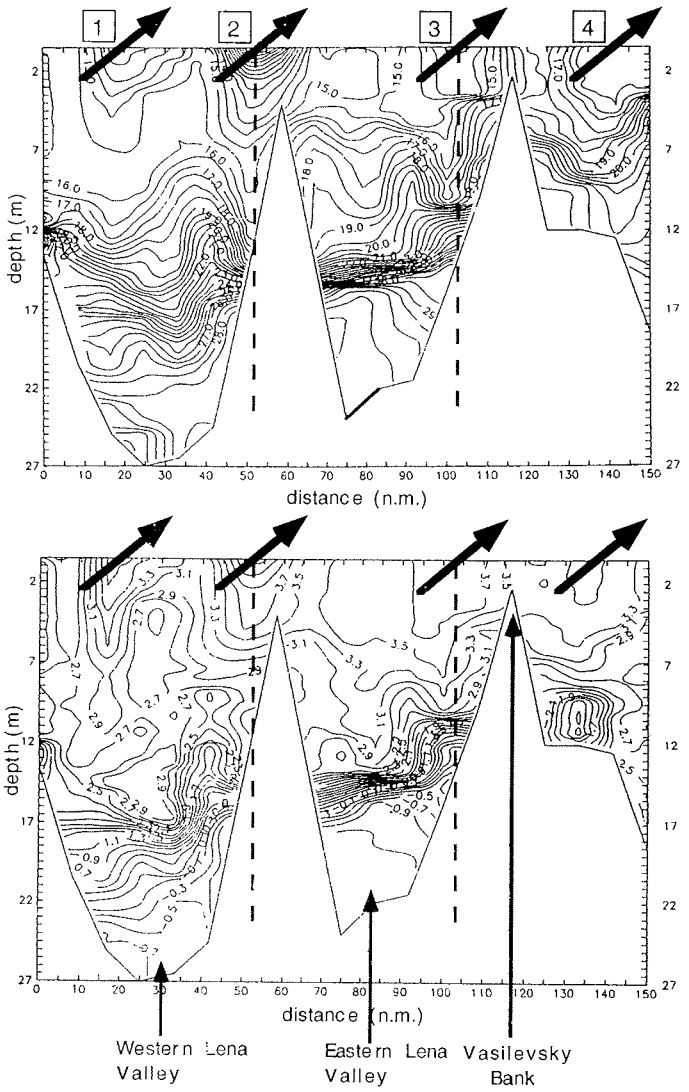

Fig. 3. Distribution of salinity ($^{o}/_{oo}$) (A) and temperature (^{o}C) (B) on transect III (TRANSDRIFT II).

In our opinion, the deviation of the river jets from the axes of the underwater valleys to the east is connected with the rotation of the Earth. In accordance with the conclusions of Fedorov (1955) concerning the typical features of the formation of currents in a sea with variable depths, the Coriolis force influences the distribution of river water by deflecting the outflow jets. The influence of the Coriolis force begins at a depth of about H, with $H\ (\omega\rho\ \mathrm{Sin}\ \varphi\ \mu^{-1})^{-1/2} = 0.4$. For the Laptev Sea, H is 10-12 m. Beginning at these depths, a cross circulation forms under the effect of the Coriolis force in the outflow. As a result, the current regime is significantly complicated here.

Under the effect of river run-off, a lens of desalinated water forms in the outflow zone. This lens is 5 to 7 m thick. As can be seen in Fig. 5, the configuration of the

lens, which was determined on the basis of TRANSDRIFT I expedition data (Karpiy et al., 1994), correlates with the distribution of bottom sediments (Fig. 6) (Benthien, 1994). It is obvious that such coincidences are not occasional. On the one hand, they confirm that the mean climatic direction of the river water outflow is quasi-permanent. On the other hand, they reflect the influence of river run-off on the sedimentation processes.

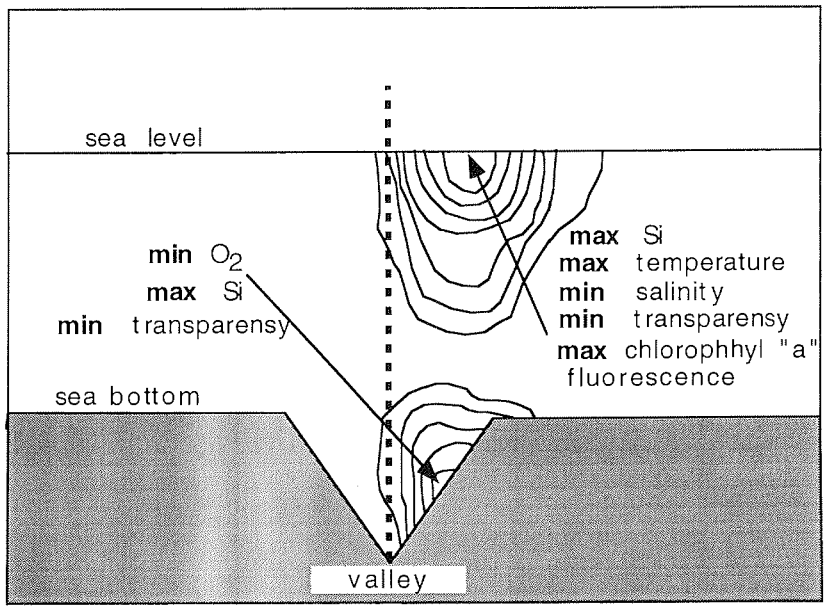

Fig. 4. Oceanographical conditions forming under the influence of river run-off in the water column above the river valleys.

The hydrobiological studies during the TRANSDRIFT II expedition have shown that biocenocis of macrofauna which is typical of freshwater sea regions can be found at the bottom of the river valleys. Thus, the distribution of river water in the sea surface layer towards the river valleys must be so stable that specific hydrochemical conditions form here. These conditions contribute to the development of biological communities of organisms which are not typical of the adjacent sea regions.

Conclusions

In accordance with the results of our analyses, we can draw the preliminary conclusion that the distribution of river water from the river mouths northward is quite stable in shallow Arctic Seas with an irregular sea bottom relief. This is primarily the case in the south-western Laptev Sea. Moreover, the direction of the distribution is governed by the sea bottom relief. The distribution of river water influences all components of the environemtal system and forms a unique natural subsystem in the outflow zones.

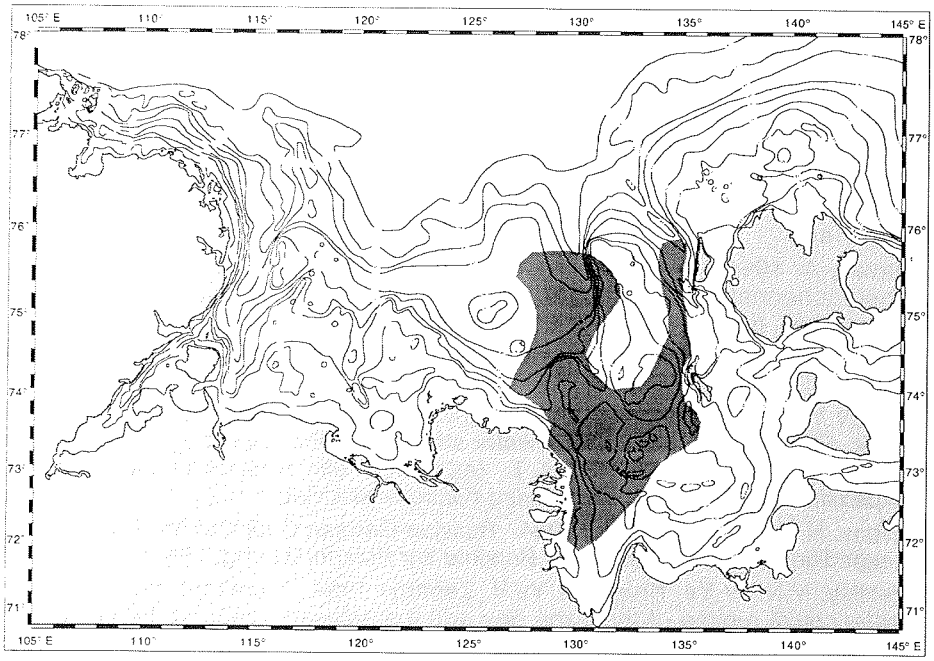

Fig. 5. A schematic diagram of the distribution of surface water which formed under the influence of river run-off in the summer season of 1993 (Karpiy et all., 1994).

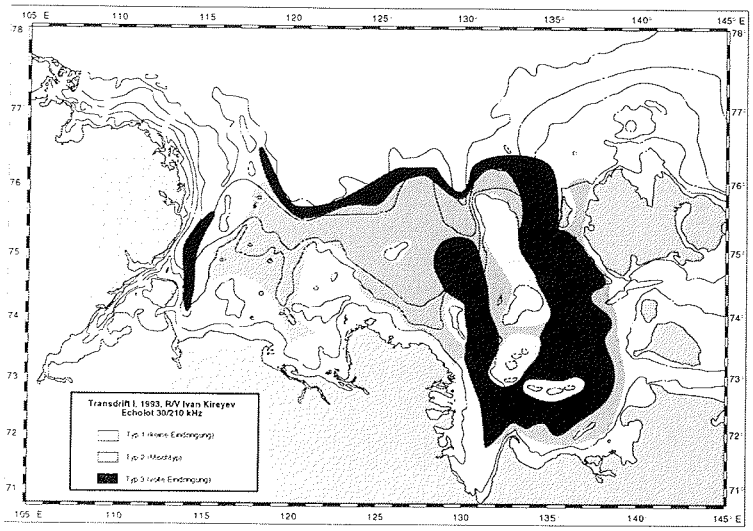

Fig. 6. The distribution of echo types in the Laptev Sea (Benthien, 1994)

Acknowledgements

This work was supported by the Ministry of Science and Technical Policy of the Russian Federation. The author is most grateful to Dr. H. Kassens, A. Benthien and F. Lindemann, who provided the sedimentological data of the expeditions TRANSDRIFT I and II. The author thanks Dr. H. Kassens and Prof. L. Timokhov (AARI) for the effective discussion of the results of the joint investigations.

References

Benthien, A. 1994). Echographiekartierung und physikalische Eigenschaften der oberflächennahen Sedimente in der Laptevsee. - Diplomarbeit, Teil II. Laborarbeit. 80 p.; Kiel (Christian-Albrechts-Universität).

Fedorov, K.N. 1955. Wind-driven currents in the sea of variable thickness (Russia). -Izv. AN SSSR, ser. geof. No. 3.

Karpiy ,V.Yu.; N.V. Lebedev; A. Luchetta; L.A. Timokhov; V.N. Churun; U. Schauer 1994. Features of thermohaline water structure of the Laptev Sea in summer of 1993 (Russia). - In: Timokhov, L. (ed.): Scientific Results of the LAPEX-93 expedition: pp. 66-75; St. Petersburg (Gidrometeoizdat).

Kassens, H.; V.Y. Karpiy (eds.) 1994. Russian-German Cooperation: The Transdrift I expedition to the Laptev Sea. - Berichte zur Polarforschung. 168 p.

Moretskiy, V.N.; V.Ye. Kruglova; Yu.V. Zaharov 1994. A present-day state of the hydrological regime of the Yana Bay and the adjacent areas of the Laptev Sea (Russia). - In: Timokhov, L. (ed.): Scientific Results of the LAPEX-93 expedition: pp. 132-141; St. Petersburg (Gidrometeoizdat).

Nikiforov, E.G.; A.O. Shpaikher 1980. Formation regularity of the Arctic ocean hydrological regime large scale variations (Russia). - 269 p.; Leningrad (Gidrometeoizdat).

Shtokman, V.B. 1953. Effect of bottom relief and cross homogeneity of wind on horizontal circulation in the shallow sea or water reservoir (Russia). - Meteorologiya & gidrologiya. No. 8.

MOVEMENT OF LAPTEV SEA SHELF WATERS DURING THE TRANSDRIFT II EXPEDITION

H.C. Hass, M. Antonow and Shipboard Scientific Party
Technische Universität Bergakademie Freiberg, Institut für Geologie, Freiberg, Germany

Abstract

Current speed and current direction throughout the water column was measured during the joint Russian-German expedition TRANSDRIFT II in late summer 1994. The results show the typical cyclonic circulation system. Kara Sea and Arctic Ocean water masses enter the Laptev Sea in the west then follow the coastline to the east until the Lena Delta. East of the Lena Delta part of the main easterly current branches to the south in order to follow the coastline in this area. The data suggest that great bays such as the Buor-Khaya and Yana Bays have their own counter-clockwise circulation systems. The northeastern part of the Laptev Sea is characterized by ENE directed currents. Current directions generally remained stable throughout the water column; only few deeper locations revealed changes. Current speed did not exceed 5cm/s.

Introduction

In late summer 1994 the joint Russian-German expedition TRANSDRIFT II to the Laptev Sea (Siberian Arctic) aboard the Russian research vessel "Professor Multanovsky" took place in the framework of the project "Laptev Sea System". The goal of this multidisciplinary project is to investigate the role of the Laptev Sea within the broad Global Change picture.

The shelf of the Laptev Sea does not exceed 50 m water depth, thus, major parts of the shelf area were dry land from at least the Last Glacial Maximum until the first half of the Holocene. Therefore, river erosion superimposed this area, and the action of Khatanga, Anabar, Olenyok, Lena, and Yana created (at present submarine) river valleys (Holmes and Creager, 1974).

Tidal, wind-driven and storm-wave processes affect the inner shelf water mass exchange of the Laptev Sea (Holmes, 1967). In modern times a regular cyclonic circulation pattern controls the water mass distribution. Kara Sea and Arctic Ocean water masses enter the Laptev Sea in the NW and the W, respectively. Currents generally follow the coast line and leave the Laptev Sea again in the northeastern part. Fluctuating amounts of fresh water enter the system via big rivers like Lena or Khatanga. From the area off the Lena Delta northerly directed "freshwater jets" were described (see Karpyi et al., 1994). These occur in periods of strong Lena discharge into the Laptev Sea in combination with northerly winds.

Besides great amounts of fresh water most of the fine grained sediment occurring in the Laptev Sea derive from the big rivers (see Létolle et al., 1993). Part of the sediment remains in front of the deltas or river mouthes another part is distributed via bottom currents. Hence, the current patterns in the Laptev Sea link water mass circulation and sediment distribution. Therefore, for investigation of sediment dynamics and for reconstruction of former sedimentary environments, the evaluation of present day processes is necessary.

Due to the severe climatic conditions in this area ice is an important geological agent. Ice gouging is responsible for the redeposition of sediment within large parts of the Laptev Sea inner shelf (Antonow and Lindemann, 1994). Part of the fine-

grained sediment , however, will be incorporated (suspension freezing) into the sea ice and carried away by the Transpolar Drift (e.g. Dethleff et al., 1993).

Methods

Oceanographic investigations were carried out using a computerized modular probe system ("MUM") which contained a piezoresistive pressure-gauge, a Pt 100 temperature sensor, a 7 pin conductivity cell, an AANDERAA INSTRUMENTS compass, a piezoelectrical ultrasonic oscillator device for measurements of the current velocity in X, Y and Z directions, a calorimetric thermistor for current velocity measurements, and three optical backscatter systems to measure the amount of suspended matter in the water column. Function and deployment routines of the system has thoroughly been described by Antonow et al. (in press).

Continuous measurements were performed at 78 stations (9 transects) throughout the entire Laptev Sea (Fig. 1, Tab. 1). The transects mainly cross the submarine valleys mentioned above. Every station was measured at least in 2m often in 1m depth intervals. For further descriptions and interpretations data were combined and averaged for the 0-5m, 5-10m, 10-20m, and the >20m water levels. The measurements were hooked on oceanographic transects taken by the Russian shipboard scientific party in order to gain a most complete insight into the Laptev Sea system by means of oceanographic and in situ sedimentological studies (see Kassens & Dmitrienko, in press).

Results

Current directions

Surface current directions (Figs. 2-6) at the northwesternmost stations are directed to the south. In the reach of the Khatanga they turn to easterly and northeasterly directions. With only a few exceptions the currents are heading east on the 74.5° N latitude. However, a slight southern component is visible throughout Transects VII and IV. Data of Transect VIII suggest that surface currents basically follow the coastline in the area of the Yana bight. East of the 125° E longitude currents are directed away from the Lena Delta. While Transect IV data yield a slight southerly component the parallel Transect III at 74.0° N is characterized by a strong northerly component. This is most obvious at 130.5° E.

Transects V and VI were taken perpendicular to Transects IV and III at 130.5° and 134° E. Both transects are characterized by southerly current directions. In the direct vicinity of the Lena Delta currents flow away from the coast whereas at least in the upper part of Transect VI currents show a westerly component. In the southern part of Transect VI currents are easterly directed. Transect II is characterized by straight easterly directed surface currents. Station 24 at 76° N reveals northeasterly surface currents.

At the 5-10m water depth level (Fig. 3) current direction data basically reveal the same features as in the surface (0-5m) water layer. However Transect V suggests turbulent conditions as current directions appear to change from station to station and with water depth.

At the 10-20m level (Fig.4) Transect IX data yield that current directions change slightly from SSW to WSW. While there is no remarkable change in the Yana bight (Transect VIII) Transect VII suggests that current directions begin to parallel the submarine Yana valley direction flowing in SSW direction below 10m water depth. The eastery component increases with depth at Transect IV. Transect III and II reveal a general trend to more uniform northeasterly current directions whereas

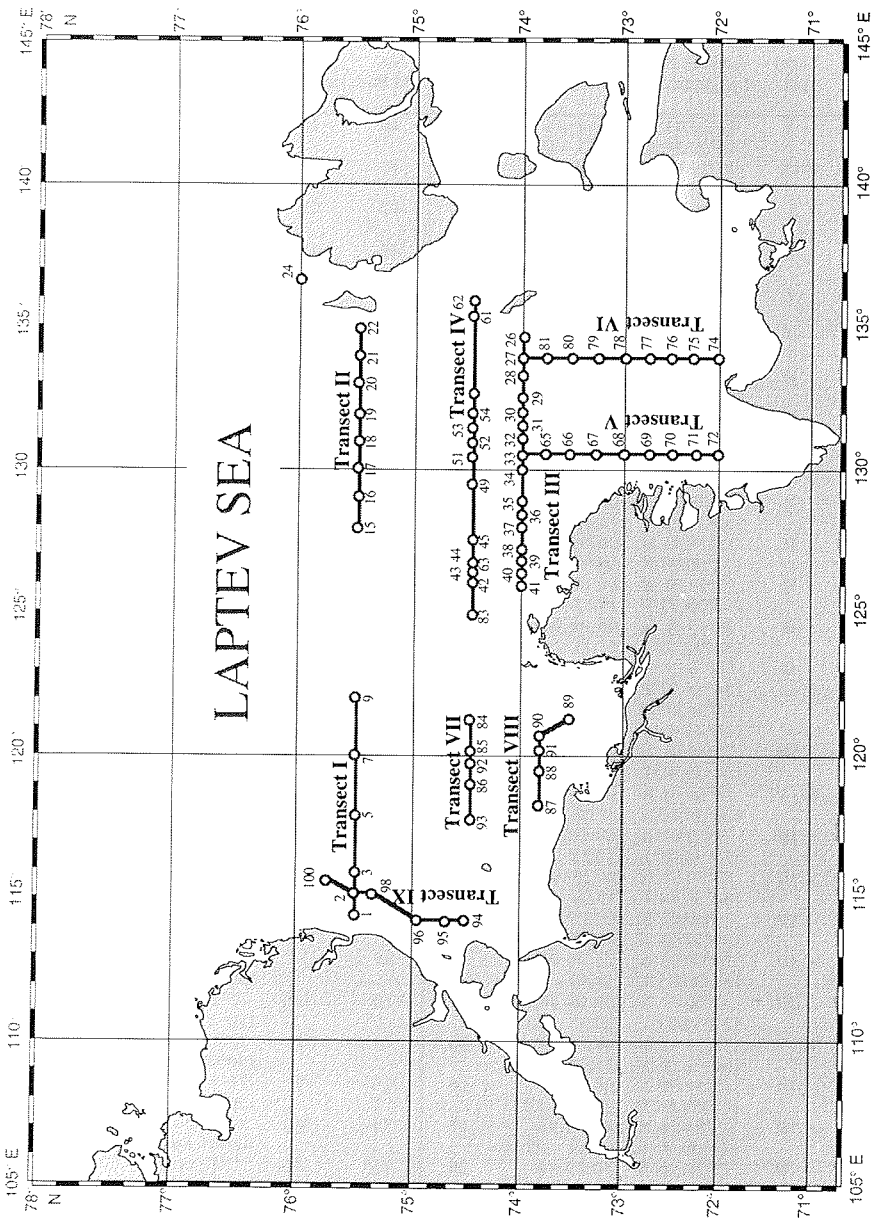

Fig. 1: TRANSDRIFT II station map. Circles mark "MUM" deployments, lines mark transects (station numbers are indicated without prefix *PM 94*).

Tab.1: Station list of "MUM" deployments.

Station No. PM 94-	Tran-sect	Latitude (N) Longitude (E)	Date Moscow Time	Water Depth [m]	Station No. PM 94-	Tran-sect	Latitude (N) Longitude (E)	Date Moscow Time	Water Depth [m]
01	I	75°29.93'N 114°30.34'E	03.09.94 23:33 - 00.23	39	40	III	73°59.99'N 126°29.83'E	10.09.94 09:40 - 10:02	21
02	I - IX	75°29.97'N 115°14.65'E	04.09.94 02:46 - 03:30	48	41	III	? 74°00.00'N 125°59.29'E	10.09.94 11:18 - 11:34	14
03	I	75°30.18'N 116°00.38'E	04.09.94 08:12 - 08:42	24	42	IV	74°30.12'N 125°59.88'E	10.09.94 16:25 - 16:47	40
05	I	75°30.00'N 118°00.07'E	04.09.94 14:39 - 15:11	29	43	IV	74°30.05'N 126°30.00'E	10.09.94 19:15 - 19:51	38
07	I	75°29.99'N 119°59.34'E	04.09.94 18:49 - 19:27	45	44	IV	74°30.21'N 127°00.27'E	10.09.94 21:00 - 21:24	19
09	I	75°30.31'N 122°00.47'E	04.09.94 23:33 - 00:18	52	45	IV	74°59.99'N 127°30.18'E	10.09.94 22:32 - 23:07	35
15	II	75°29.99'N 128°00.94'E	05.09.94 19:45 - 20:49	45	49	IV	74°29.89'N 129°29.57'E	13.09.94 12:54 - 13:20	38
16	II	75°29.96'N 129°00.97'N	05.09.94 22:17 - 22:55	45	51	IV	74°30.02'N 130°29.53'E	13.09.94 02:00 - 02:30	26
17	II	75°30.04'N 130°00.84'E	06.09.94 01:40 - 02:20	50	52	IV	74°29.87'N 130°59.63'E	13.09.94 00:50 - 01:07	30
18	II	75°29.98'N 130°59.82'E	06.09.94 14:13 - 14:35	18	53	IV	74°29.95'N 131°29.61'E	12.09.94 23:35 - 23:55	18
19	II	75°29.93'N 132°00.38'E	06.09.94 16:39 - 17:00	19	54	IV	74°29.95'N 131°59.99'E	12.09.94 22:28 - 22:43	18
20	II	75°29.86'N 132°59.35'E	06.09.94 19:53 - 20:14	20	57	IV	74°30.10'N 133°29.99'E	12.09.94 17:56 - 18:10	11
21	II	75°59.98'N 134°00.08'E	06.09.94 22:11 - 22:46	34	61	IV	74°29.90'N 135°30.04'E	12.09.94 14:07 - 14:26	28
22	II	75°30.38'N 134°58.77'E	07.09.94 01:01 - 01:42	41	62	IV	74°30.08'N 136°00.07'E	12.09.94 09:05 - 09:27	28
24		75°56.80'N 136°44.82'E	07.09.94 22:02 - 22:32	21	63	IV	74°30.07'N 126°35.06'E	13.09.94 19:56 - 20:20	36
26	III	73°59.96'N 134°29.40'E	09.09.94 09:55 - 10:20	14	83	IV	74°29.91'N 125°00.30'E	20.09.94 18:10 - 18:30	34
27	III - VI	73°59.98'N 133°59.85'E	09.09.94 11:16 - 11:35	13	65	V	73°44.98'N 130°29.87'E	15.09.94 14:35 - 14:59	25
28	III	73°59.83'N 133°30.01'E	09.09.94 12:32 - 12:52	12	66	V	73°29.96'N 130°29.91'E	15.09.94 16:42 - 17:00	26
29	III	73°59.91'N 132°30.54'E	09.09.94 15:36 - 15:58	11	67	V	73°14.87'N 130°29.92'E	15.09.94 19:15 - 19:30	25
30	III	74°00.02'N 131°59.84'E	09.09.94 17:07 - 17:29	16	68	V	72°59.97'N 130°29.98'E	15.09.94 21:30 - 21:56	22
31	III	74°00.03'N 131°30.05'E	09.09.94 18:33 - 18:57	22	69	V	72°44.97'N 130°29.61'E	16.09.94 00:02 - 00:16	19
32	III	74°00.01'N 130°59.87'E	09.09.94 20:02 - 20:30	22	70	V	72°29.97'N 130°29.93'E	16.09.94 02:12 - 02:25	15
33	III - V	73°59.92'N 130°30.06'E	09.09.94 21:37 - 22:11	26	71	V	72°14.94'N 130°29.60'E	16.09.94 04:45 - 04:59	14
34	III	73°59.99'N 129°59.80'E	09.09.94 23:17 - 23:37	16	72	V	71°59.84'N 130°31.01'E	16.09.94 06:57 - 07:15	17
35	III	73°59.96'N 129°00.00'E	10.09.94 02:49 - 02:18	15	74	VI	72°00.20'N 133°59.80'E	18.09.94 17:07 - 17:30	17
36	III	73°59.96'N 128°30.23'E	10.09.94 03:21 - 03:50	26	75	VI	72°15.00'N 133°59.70'E	18.09.94 21:05 - 21:35	21
37	III	73°59.95'N 127°59.64'E	10.09.94 04:54 - 05:21	27	76	VI	72°30.76'N 133°59.72'E	19.09.94 00:25 - 00:46	22
38	III	74°00.00'N 127°29.87'E	10.09.94 06:30 - 07:01	28	77	VI	72°45.05'N 133°59.66'E	19.09.94 02:40 - 03:10	16
39	III	74°00.00'N 126°59.96'E	10.09.94 08:00 - 08:32	26	78	VI	73°00.17'N 133°59.99'E	19.09.94 04:47 - 05:03	18

Tab.1: Station list of "MUM" deployments.

Station No. PM 94-	Tran-sect	Latitude (N) Longitude (E)	Date Moscow Time	Water Depth [m]	Station No. PM 94-	Tran-sect	Latitude (N) Longitude (E)	Date Moscow Time	Water Depth [m]
79	VI	73°15.08'N 133°59.08'E	19.09.94 06:43 - 06:58	15	85	VIII	74°30.11'N 120°00.27'E	21.09.94 04:00 - 04:33	38
80	VI	73°30.17'N 133°59.78'E	19.09.94 09:02 - 09:16	16	86	VIII	74°29.88'N 118°59.45'E	21.09.94 07:16 - 07:47	18
81	VI	73°45.00'N 134°00.25'E	19.09.94 11:50 - 12:15	17	92	VIII	74°30.06'N 119°50.48'E	22.09.94 17:55 - 18:25	33
87	VII	73°52.50'N 118°17.52'E	22.09.94 01:20 - 01:35	13	93	VIII	74°29.91'N 117°44.96'E	23.09.94 01:00 - 01:20	19
88	VII	73°50.07'N 119°29.87'E	22.09.94 03:59 - 04:20	14	94	IX	74°30.06'N 114°17.05'E	23.09.94 08:02 - 08:35	37
89	VII	73°29.65'N 121°30.44'E	22.09.94 08:33 - 08:52	13	95	IX	74°42.98'N 114°14.08'E	23.09.94 12:50 - 13:20	39
90	VII	73°50.07'N 120°40.06'E	22.09.94 11:44 - 12:01	16	96	IX	74°58.24'N 114°15.11'E	23.09.94 17:23 - 17:56	42
91	VII	73°50.18'N 120°10.38'E	22.09.94 13:25 - 13:50	27	98	IX	75°21.64'N 115°05.46'E	23.09.94 22:25 - 22:55	46
84	VIII	74°30.15'N 121°15.00'E	21.09.94 01:00 - 01:25	15	100	IX	75°42.14'N 115°44.37'E	24.09.94 09:41 - 10:14	49

conditions remain turbulent at Transect V. Transect VI also shows only slight changes compared to the upper water levels.

Most of the stations showed less than 20m water depth. Thus, measurements could only be made where water depths were sufficient (less than 50%; Fig. 5). No changes were recorded at Transects II, III, IV, V and VI. However, data from Transect IX (Stations 98-100) suggest that currents turned north by some 45° in the westernmost part of the Laptev Sea. Transect VII also shows that currents turn north (in the reach of the Yana submarine valley).

Current speed

Current speed was generally low (below 3.5 cm/s) during TRANSDRIFT II. Peak values measured at the very surface may have been influenced by strong winds during the deployment. At Transect II (75.5° N) current velocities range generally around 1.5 cm/s (Fig. 7). The deeper Stations 15,16 and 17 and Station 24 reveal slightly increased velocities up to 2cm/s. These stations show generally uniform current velocities throughout the water column whereas the shallower Stations 18-22 reveal a very slight trend to increasing velocities to the surface.

Transect IV (74.5° N) is characterized by generally uniform current velocities between ca. 1.5 and 2 cm/s. There is, however, an increase of surface current speed from west to east until Stations 54 an 53. Peak surface current velocities are at Station 54 (4.53 cm/s). At Transect III (74° N) there is also a zone of increased surface current velocities (Stations 34, 53, 36). These are situated slightly further west when compared to those of Transect IV. Station 36 yields peak values at 4.52 cm/s. Stations 31, 32, 33 and 41 reveal a trend to increasing current speed with water depth. Mean current velocities of Transect III are between 1.5 and 2 cm/s.

Transect V (130.5° E) and VI (134° E) reveal mean current velocities around 1.5 cm/s without significant fluctuations (Fig. 8). Only Station 74 which is the southernmost station of Transect VI shows increased surface current speed (4.52 cm/s). Thus, mean current velocities of the two meridional transects appear to be

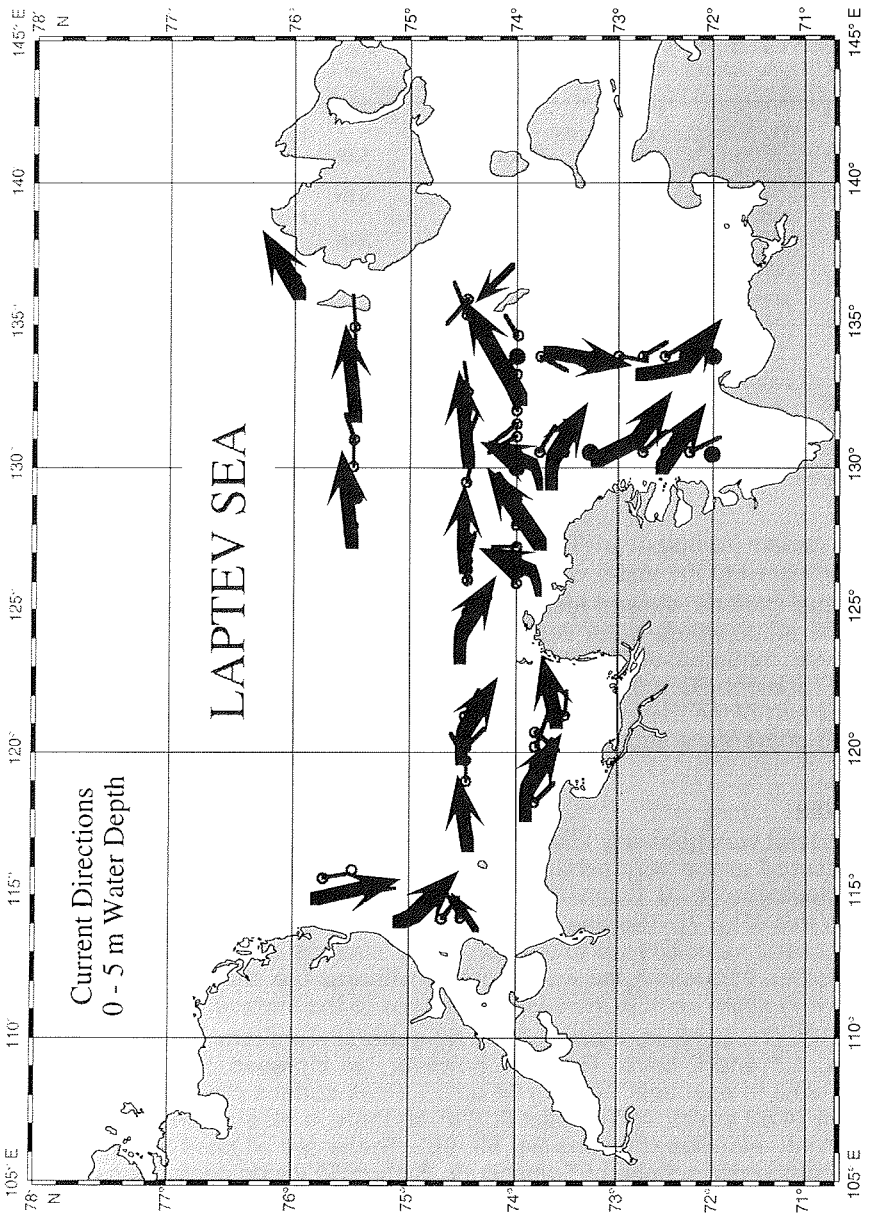

Fig. 2: Current directions at the surface layer (0-5m water depth).

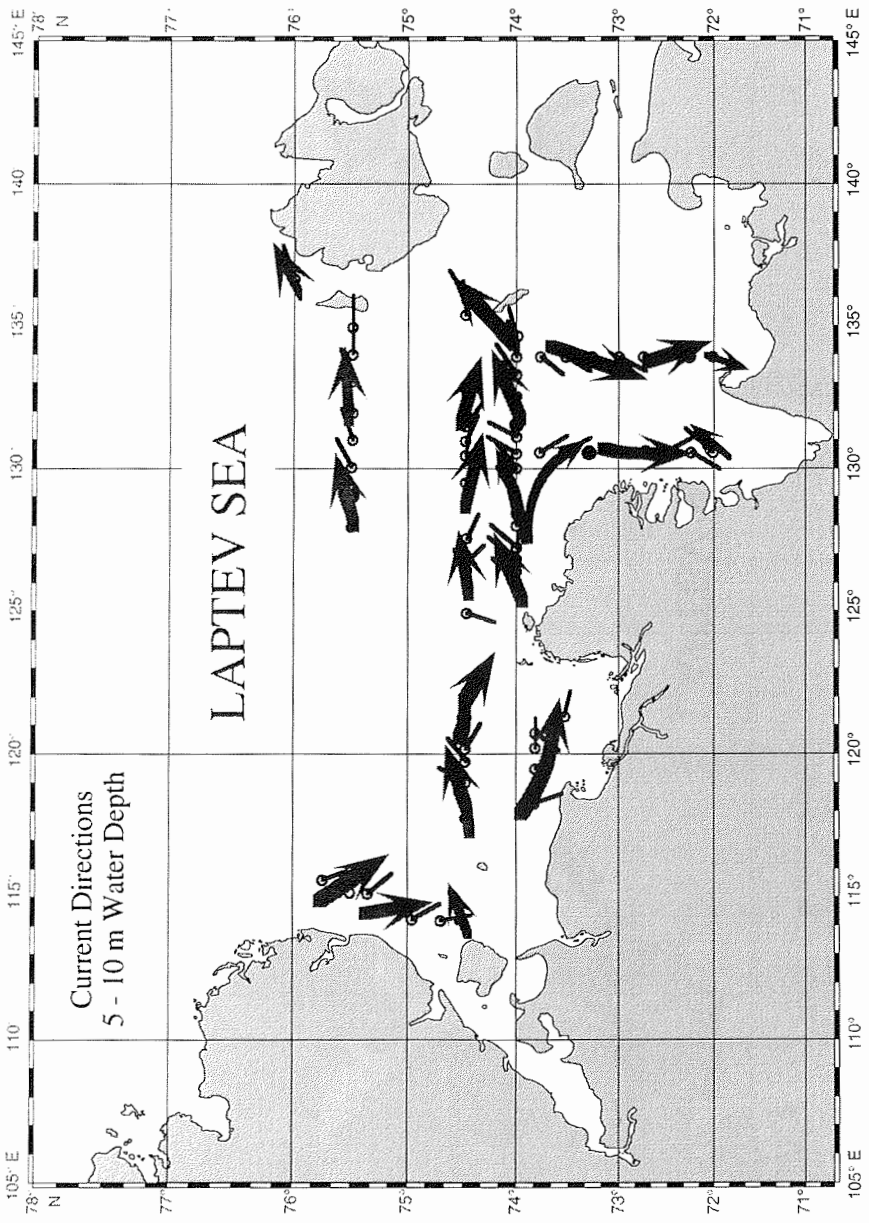

Fig. 3: Current directions in 5-10m water depth.

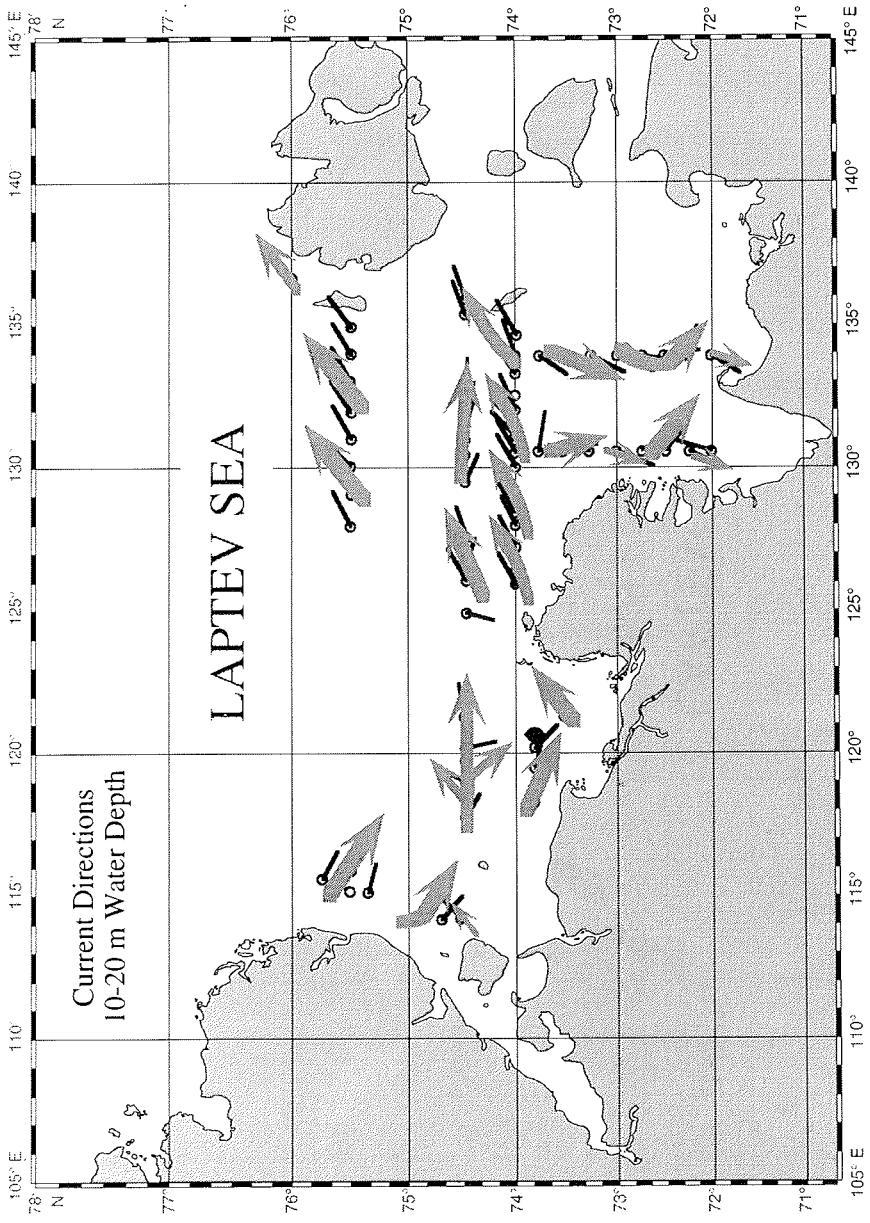

Fig. 4: Current directions in 10-20m water depth.

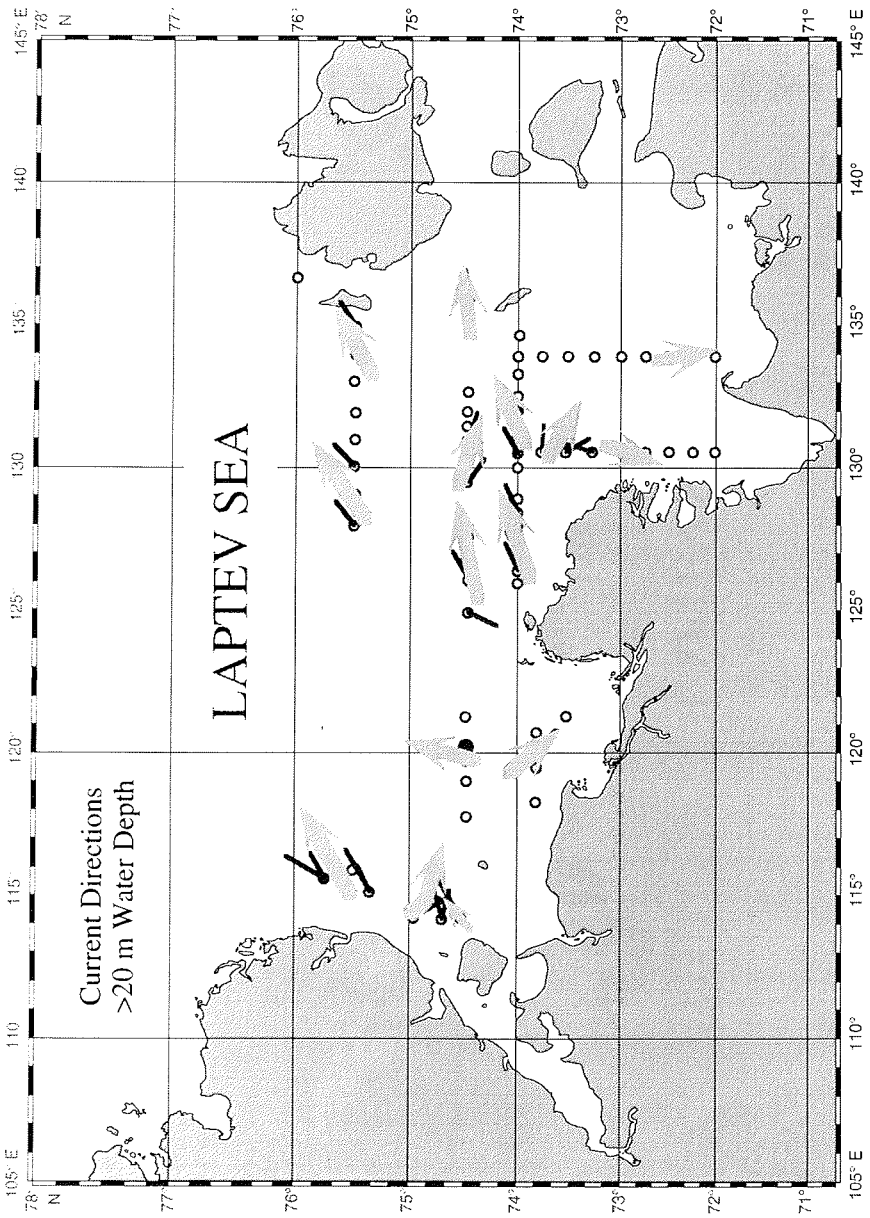

Fig. 5: Current directions in >20m water depth

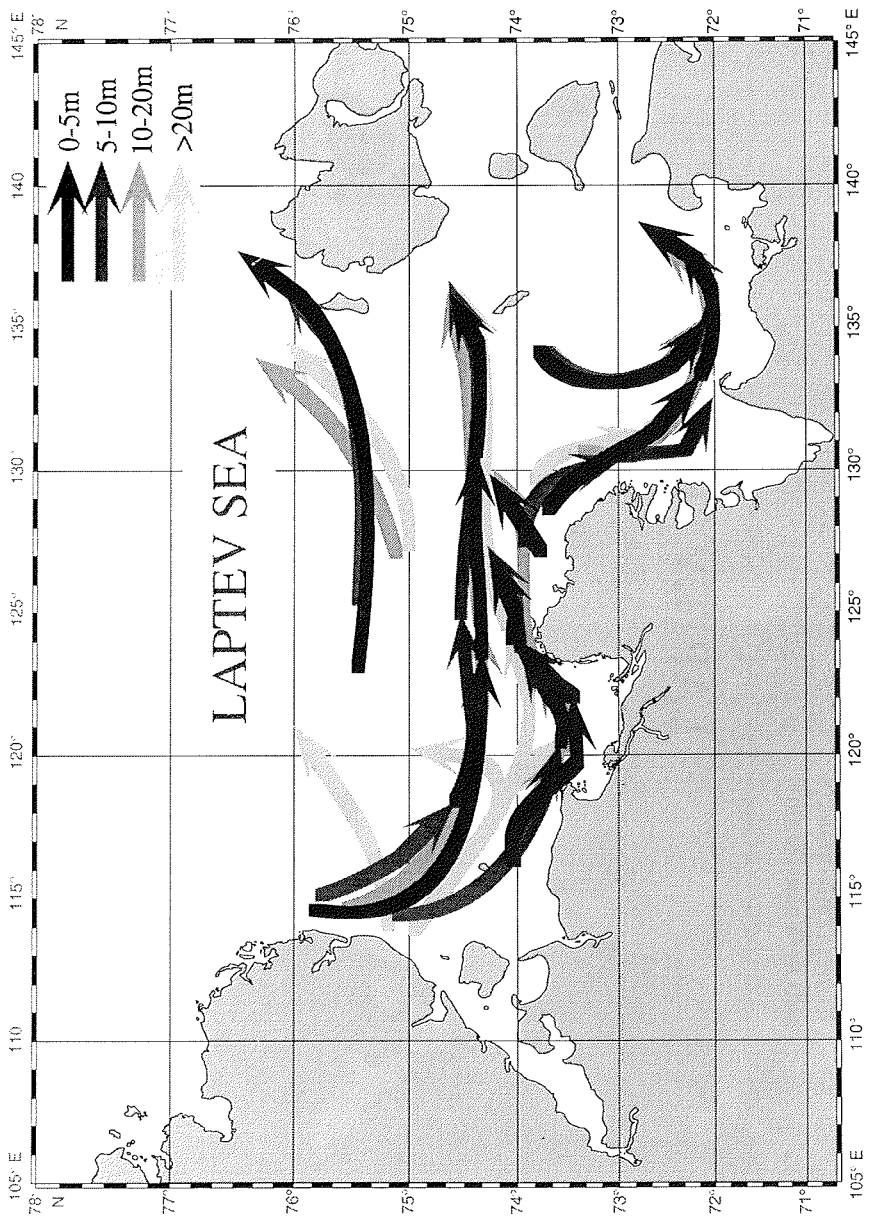

Fig. 6: Interpretation of current directions in 4 depth intervals

slightly decreased compared to Transects II, III and IV. Transect VII (across the submarine Yana valley at 74.5° N) and Transect VIII (Yana Bight area) show current speed values around 1.5 cm/s without significant changes. Only Station 92 (Transect VII) is characterized by increasing current velocity with depth. Transect IX (direction of the submarine Khatanga valley) reveals current velocities around 1.5 cm/s. Except Station 98 which shows a trend of increasing current speed to the surface, current velocities are stable throughout the entire water column.

Water mass movement in the Laptev Sea

The results generally show the regular sluggish cyclonic circulation system basically dependent on the Coriolis force (Fig. 6). Kara Sea and Arctic Ocean water masses enter the Laptev Sea in the west then follow the coastline to the east until the Lena Delta. East of the Lena Delta part of the main easterly current branches to the South to follow the coastline in this area. It appears that great bays have their own counter-clockwise circulation systems (Buor-Khaya and Yana Bays). Although the main Laptev Sea current heads further east it cannot be from the obtained data concluded whether it flows through the New Siberian Islands or whether it turns north west of 140° E. The northeastern part of the Laptev Sea is characterized by ENE directed currents. The direction of the measured currents was stable at least until 10m water depth. At the deeper stations the currents turn slightly to more northerly directions. North of the Lena Delta, however, the northerly component measured at the surface diminishes slightly with depth. Most interestingly the currents in the western Laptev Sea turn gradually from SSE at the upper levels to ENE below 10m water depth. Surface and bottom water mass in this area are marked by a vertical temperature inversion between ca. 10 and 25 m where conductivity values suggest a transition from stable lower to stable higher salinities. Temperatures in this transitional layer were increased by partly more than 1.5 K (unpubl. data). Probably higher saline Arctic water masses which flow into the Laptev Sea in this area become covered by lower saline riverine waters from the Khatanga, sink down and leave the Laptev Sea again heading NE partly through the submarine Khatanga valley (see also Karpyi et al., 1994; Antonow et al., in press). A similar thermo-haline process seems to be active over the submarine Yana valley.

Based on the horizontal and vertical distribution of current directions and current velocities it can be inferred that during TRANSDRIFT II measuring period (September 1994) no exceptional river discharge events such as the so-called "freshwater jets" (see also Karpyi et al., 1994) of the Lena occurred. This is possibly due to an extrem short summer and the early advent of the winter 1994 over Siberia preventing strong river discharge.

Outlook

First results of oceanographic (current speed and direction) measurements yield a thorough insight into the Laptev Sea system. Since data of the TRANSDRIFT and former Russian expeditions and interpretations of this investigation suggest a high variability of oceanographic features of the Laptev Sea further expeditions are desirable in order to gather more information about water mass circulation and properties under different seasonal and weather conditions. Only a complex oceanographic model taking as many weather conditions as possible into account can provide a basis for the interpretation of the paleoceanographic conditions and thus for the paleoclimate and related processes of ice erosion on the sea floor. Forthcoming interpretations of optical backscatter (OBS) data which were measured parallel to the oceanographic parameters during TRANSDRIFT II and

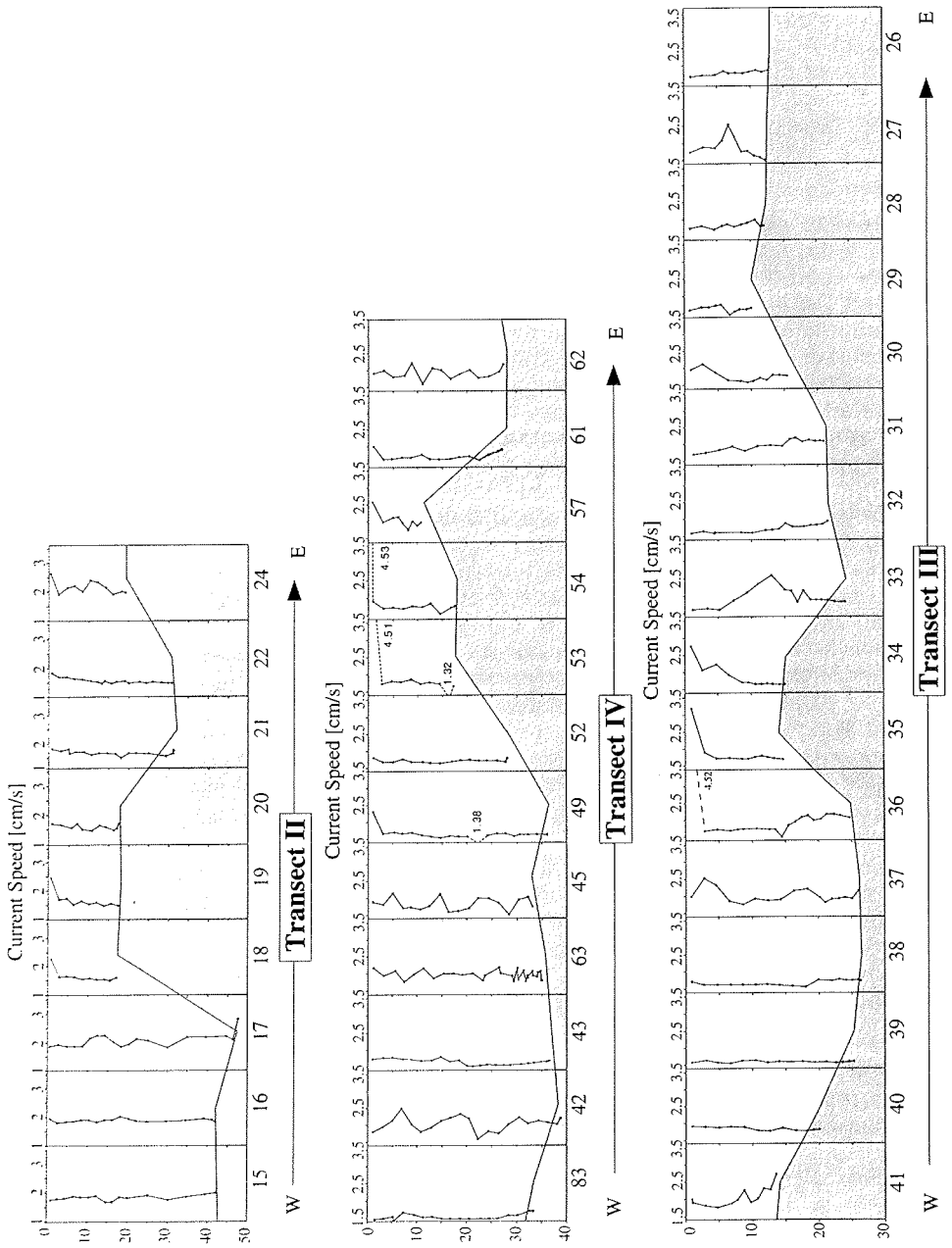

Fig. 7: Current speed vs. water depth [m]: Transect II, Transect III, Transect IV (grey area: simplified sea floor, not true to horizontal scale)

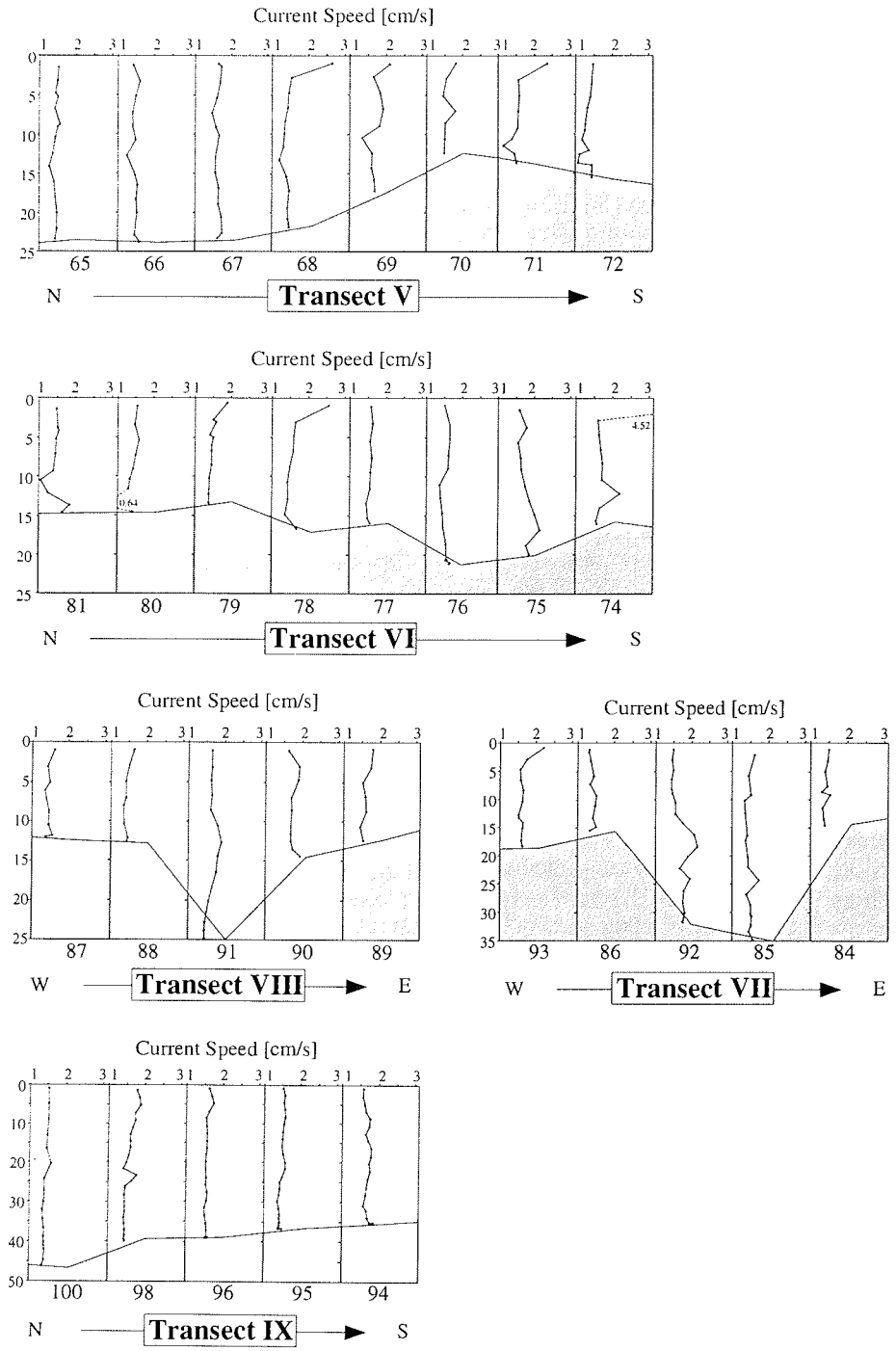

Fig. 8: Current speed vs. water depth [m]: Transect IX, Transect VIII, Transect VII, Transect V, Transect VI (grey area: simplified sea floor, not true to horizontal scale)

detailed granulometric studies of sediments (grain size distribution, sinking velocities) will provide the basis for interpretations of in situ sedimentary processes (e.g. sediment transport in different water layers) and their relation to water mass properties and oceanographic features of the Laptev Sea.

Acknowledgements

We thank Veit Haase (TU Bergakademie Freiberg) for his professional help during TRANSDRIFT II and ADM Elektronik GmbH (Warnau, Germany) who constructed the MUM multi-sensor probe. Discussions with colleagues from the joint Russian-German scientific party are much appreciated. We thank Captain V. V. Danilenko and the crew of RV "Professor Multanovsky" for good teamwork during a 2 months expedition to the Siberian Arctic. Many thanks to H. Kassens, J. Thiede (Geomar Kiel) and the Russian responsibles for making the expedition possible. Financal support by the German Ministry of Research and Technology (BMFT) is kindly acknowledged.

References

Antonow, M.; Lindemann, F. 1994. Dynamic Geological Shelf Processes - Implications from Side Scan Sonar Observations. In: Kassens, H. and Karpiy, V. (ed.) Russian-German Cooperation: The Transdrift I Expedition to the Laptev Sea. Ber. Polarforsch. 151: 64-66.

Antonow, M.; Hass, H.C.; Haase, V. Preliminary results of multi probe suspension and current speed measurements on the Laptev Sea shelf. - In: Kassens, H. and I. A. Dmitrienko (ed.): Russian-German Cooperation: The Transdrift II Expedition to the Laptev Sea. Ber. Polarforsch., in press.

Dethleff, D; Nürnberg, D.; Reimnitz, E.; Saarso, M.; Savchenko, Y.P. 1993. East Siberian Arctic Region Expedition '92: The Laptev Sea - its significance for Arctic sea ice formation and transpolar sediment flux. Arctic Expeditions: Laptev Sea and Barents Sea, Ber. Polarforsch. 120: 3-44.

Holmes, M.L. 1967. Late Pleistocene and Holocene history of the Laptev Sea.- MSc-Thesis, University of Washington , 99 pp.

Holmes, M.L.; Creager, J.S. 1974. Holocene history of the Laptev Sea continental shelf. In: Herman, Y. (ed.) Marine Geology and Oceanography of the Arctic Seas, Springer, Berlin, pp. 211-229.

Karpiy, V.; Lebedev, N.; Ipatov, A. 1994. Oceanographic studies - Thermohaline and Dynamic Water Structure in the Laptev Sea. In: Kassens, H. and Karpiy, V. (ed.) Russian-German Cooperation: The Transdrift I Expedition to the Laptev Sea. Ber. Polarforsch. 151: 16-47.

Kassens, H.; Dmitrienko, I. A. (ed.). Russian-German Cooperation: The Transdrift II Expedition to the Laptev Sea. Ber. Polarforsch., in press.

Létolle, R.; Martin, J.M.; Thomas, A.J.; Gordeev, V.V.; Gusarova, S.; Sidorov, I.S. 1993. ^{18}O abundance and dissolved silicate in the Lena delta and Laptev Sea (Russia). Mar. Chemistry 43 : 47-64.

THE DISTRIBUTION OF OXYGEN AND NUTRIENTS IN THE LAPTEV SEA IN SUMMER

S.V. Pivovarov and V.M. Smagin

State Research Center of the Russian Federation the Arctic and Antarctic Research Institute, St. Petersburg, Russia

During the expedition aboard the R/V *Ivan Kireyev* in August and September 1993, dissolved oxygen and the concentration of silicon and phosphates were determined. In September 1994 aboard the R/V *Professor Multanovskiy*, the observation program was expanded and, in addition to the parameters mentioned above, nitrates and nitrites were determined at those stations where hydrobiological observations were carried out.

The main goal of the studies was to determine the distribution features of hydrochemical elements in the zones of river outflow and the variability of the concentration of transported substances.

Dissolved oxygen and silicon quite well indicate the origin of water masses and their spreading over the sea area. Together with other nutrients, they also allow us to assess the surface layer productivity and the direction of biological and biochemical processes at different depths. That is why an important objective of the studies was to find out the relationships between hydrophysical, hydrobiological and hydrochemical parameters of water masses.

The dissolved oxygen concentration was determined according to the Winkler method. For this analysis, an automatic electronic burette ABU 80 was used. According to the colorimetric method, the silicate concentration was determined with ascorbic acid for the reduction of the silicomolybdic complex. The phosphate concentration was determined according to the colorimetric method by Murphy and Riley. Before we started our work, calibrating plots were constructed with sea water with a low concentration of phosphates and silicate. All analyses were carried out according to the Manual on chemical analysis of sea waters (1993).

The nitrite and nitrate concentrations were determined with an automatic analyzer AKEA according to the colorimetric method by Wood, Armstrong and Richards. The calibrating of the device with standard solutions was carried out before the analysis of each sampling group.

While in 1993 the influence of river run-off to the sea was below mean values (Buynevich et al.,1980, Pivovarov & Smagin, 1994), it was anomalously low in September 1994. River run-off was probably restricted by the water mass inflow from the north-west. This is confirmed by the existence of a very large zone with a minimum silicon supply in the north-western zone of the sea (Fig. 1).

The correlation coefficients between salinity and silicon concentration at the sea surface were calculated on the basis of the expedition data of the last five years. In these five years, their values vary between -0.80 and -0.95. The survey of 1994, which was carried out with smaller intervals, allowed us to specify this dependency. It was found out that some regions have their own dependency between salinity and silicon, which is, as a rule, a non-linear one (Fig.2). The general character of the dependency is broken at extreme values of silicon and salinity in the north-western sea zone, near the river mouths, and in the region located to the north of the New-Siberian Islands. The causes for the deviation from the relationship in this region, however, should be investigated separately.

The influence of rivers is revealed in the distribution of oxygen in the surface

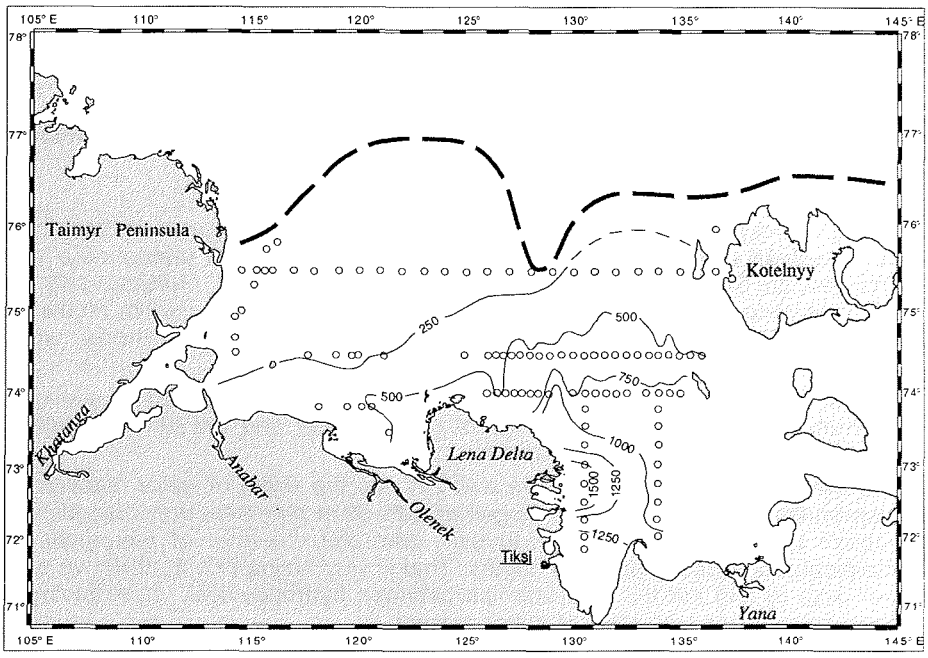

Fig. 1. The distribution of silicate (μg/l) at the surface of the Laptev Sea in September 1994.

layer. In the outflow zone, the saturation of surface water usually does not exceed 100%. This is attributed to an oxygen loss. On the one hand the loss is due to the oxidation of organic and mineral substances flowing out of the rivers, on the other hand it is due to a sharp cooling of the water masses which move northward over a cooled underlying surface (Fig. 3). A saturation minimum (about 95%) is observed near the mouths of large rivers. Maximum oxygen saturation is usually observed near the ice edge in summer (105-110%) and in the regions of phytoplankton blooming. In regions freshened by melting ice, maximum oxygen concentrations of 9.0 to 9.4 ml/l are observed in the surface layer.

During a survey in September 1994, oxygen concentration at the sea surface varied only between 8.06 and 8.75 ml/l, and the change in surface layer saturation did not exceed 5%. The mean value was 99.2% and standard deviation was 1.0%. And general typical features of oxygen distribution were preserved while anomalies were observed in places of intensive vertical mixing (both wind-driven and convective), in the zones of intermediate water upwelling, and in the zones of the blooming of weeds.

The supplies of phosphates and nitrates during the observation period were almost completely used up in the river outflow zone. In 1993 enhanced levels of phosphates (10 to 15 μg/l) were recorded only directly near the mouths of large rivers, near the so-called hydrochemical barriers, where fresh and saline waters meet and probably death and decomposition of freshwater plankton occurs. In September 1994, the mean concentration of phosphates in the zone influenced by river water was only 3 μg/l, which is half the concentration of all of the rest of the sea.

Enhanced concentrations of nutrients in the active layer in the northern region

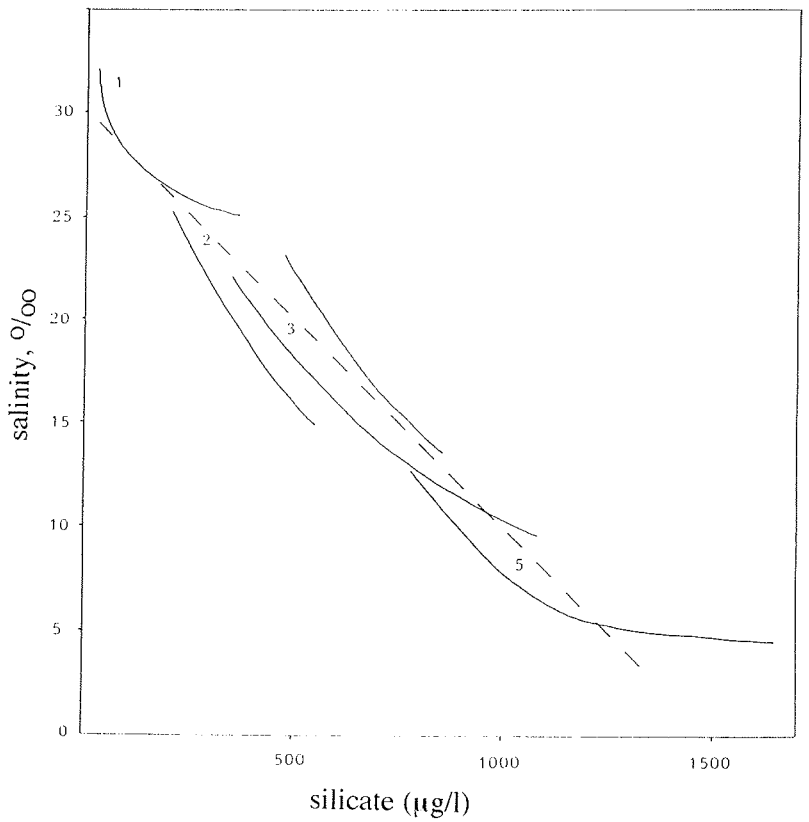

Fig. 2. Correlation between salinity and silicate at the surface of the Laptev Sea in September 1994 (1 - northwestern; 2 - southwestern; 3 - central; 4 - estern part; 5 - southern part of the sea).

led to an intensive development of phytoplankton, which was recorded by Anoshkin et al.,1995. An anomalous oxygen concentration of 101-103 % was observed here, too.

Water freshened by river run-off spreads over the sea surface in a thin film, which is 5 to 10 m thick. At the same time, however, it governs the hydrochemical characteristics of all lower layers. The point is, that a large amount of dissolved and suspended organic matter is discharged with the river run-off. And the concentrations of oxygen, silicon, phosphates, nitrates and other parameters in deep water depend on the oxidation intensity of this organic matter.

A 5 m surface layer in the zone of river outflow is uniform with regard to hydrochemical parameters, but in regions where the influence of rivers is absent the upper quasi-uniform layer is several times thicker. In 1994 in the north-western part of the sea, the upper quasi-uniform layer was usually very thick (20-25 m). At the extreme station of the transect along 75°30' N, practically the whole water column from the surface to the bottom was uniform at a depth of 38 m.

A characteristic feature of the vertical oxygen distribution in the western sea region appears to be a layer of maximum concentration at a depth of 15 to 25 m. In 1994, however, the maximum was not well-pronounced - the difference in the saturations of the layers was not more than 2%. There are two hypotheses explain-

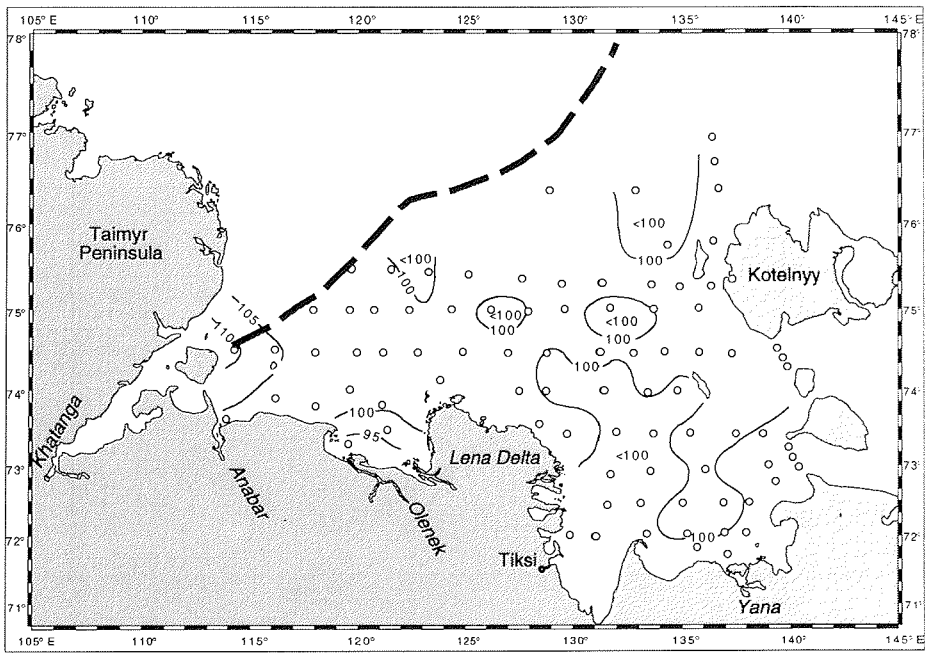

Fig. 3. The distribution of oxygen (%) at the surface of the Laptev Sea in August and September 1993.

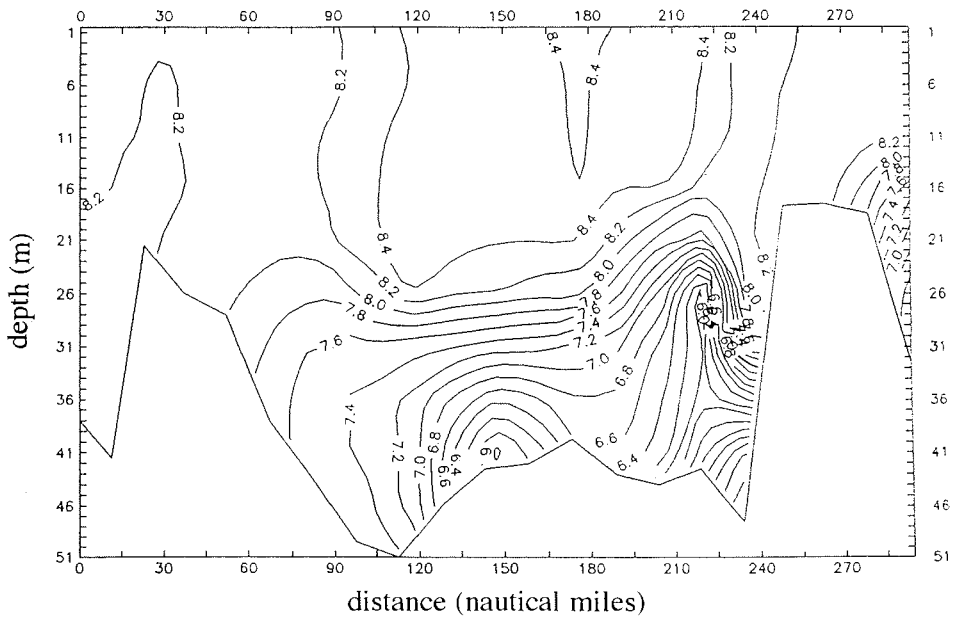

Fig. 4. The distribution of oxygen (ml/l) along the transect 74°30′N across the Laptev Sea in September 1993.

ing the subsurface oxygen maximum in the Arctic Seas. Either this is a remaining phenomenon after the formation of a new summer upper quasi-uniform layer or it is a result of the phytoplankton photosynthetic activity. These hypotheses do not exclude each other, but joint studies of biologists, opticians and chemists will evidently give a precise answer to the question on which of the factors is a deciding one.

At almost all stations (except for shallow ones) in the zone influenced by river run-off, a minimum concentration of silicon was quite distinct between levels of 10 and 15 m . This corresponds, as a rule, to temperature anomalies in the upper part of the main halocline. It may be suggested that this minimum is governed by water spreading from the north and compensating the water outflow at the surface.

Intermediate maxima of nitrate concentrations in the interlayers with decreased temperatures were recorded in the zone of the hydrological front.

The existence of a zone of stagnant water, which fills bottom depressions in the regions influenced by river run-off, is a very important and dangerous component of the hydrochemical structure of the Laptev Sea for the inhabitants of the bottom and near bottom levels. Detailed surveys of the past expeditions allowed us to map the location of these water masses and, on the basis of the oxygen deficit, to estimate to what extent they are subjected to stagnation (Fig. 5). Sidorov & Gukov (1992) have shown that in winter in the stagnation sources (Buor-Khai Gulf, Tiksi Bay, etc.), oxygen almost completely disappears and hydrogen sulphide forms. By means of regular observations, the annual cycle of this water transformation, water changing in the near-bottom levels and the oxygen consumption rate can be traced.

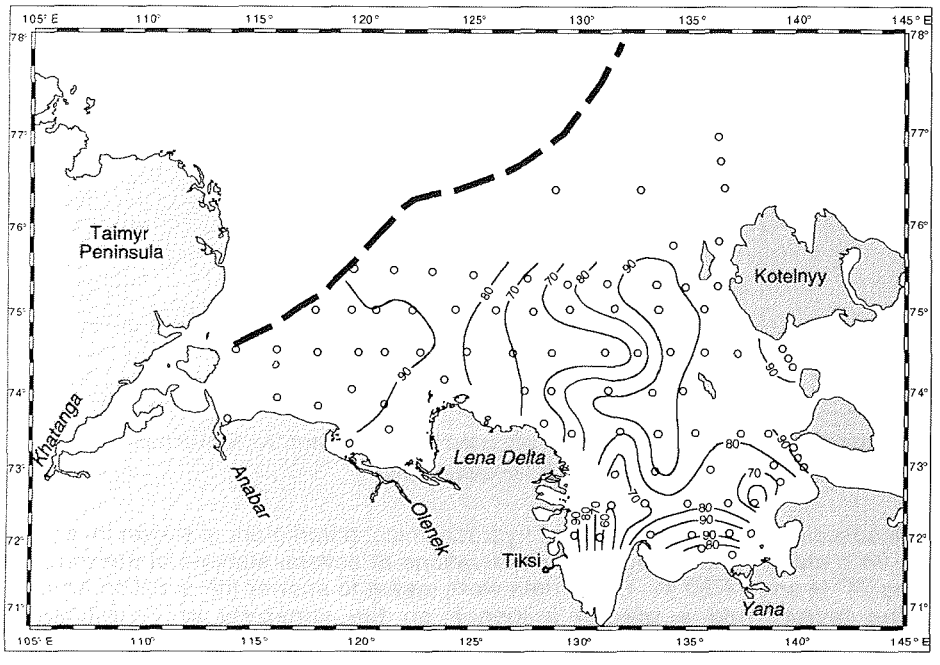

Fig. 5. The distribution of oxygen (%) at the bottom of the Laptev Sea in August and September 1993.

In September 1994, a minimum oxygen saturation (45%) was observed at a depth of 36 m in a small valley between two underwater hills at 74°30' N between 125° and 127° E. Obviously, with stagnant water spreading, two processes of opposite directions occur in it: (1) an oxygen loss owing to oxidation and (2) ventilation when the water mixes with surrounding water masses.

There is a stable relationship between hydrochemical parameters in stagnant water. The relationship between phosphates and nitrates is close to a linear one and concentrations of these parameters are inversely propotional to the oxygen level. The silicon and oxygen concentrations correlate well if the area of stagnant water spreading is arbitrarily divided into three parts according to the transects. In this case three relation lines converging at minimum oxygen values are well-pronounced in the field of points (Fig. 6).

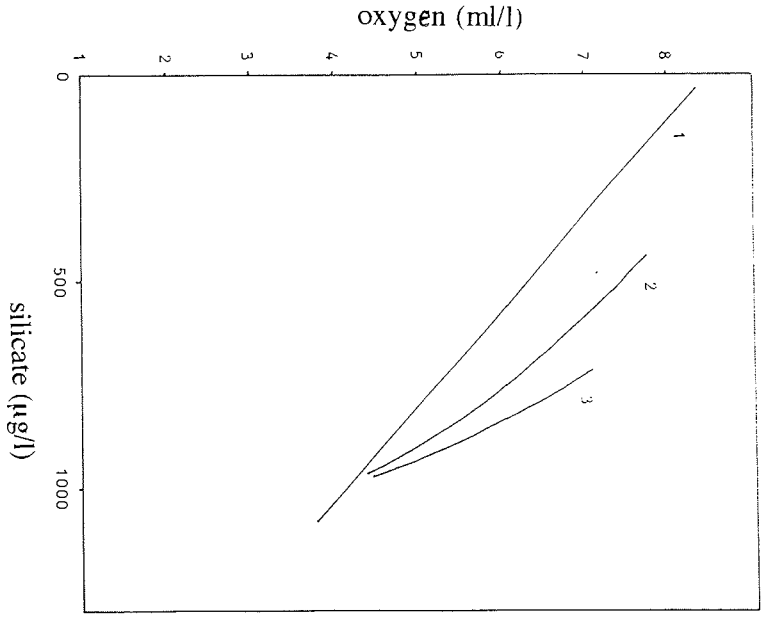

Fig. 6. Correlation between oxygen and silicate in the bottom waters in September 1994 (1 - northern; 2 - central; 3 - southern part of the Laptev Sea).

Mesoscale temporal variability of hydrochemical parameters is shown in the data of a 24 h station and in repeated observations at several stations of the transects along 74° N and 74°30' N. These data were meant to answer the question on which of the factors had a greater influence on the variability of hydrochemical parameters: daily photosynthesis variations or advection.

A 24 h station was occupied under quiet weather conditions. Here no significant changes in the concentrations of all elements were observed, except for the halocline layer where large gradients of the parameters were observed and errors

were possible when the samples were taken. That is why it can be said that daily variations of hydrochemical parameters are insignificant even in the hydrofront region if there is no strong wind and phytoplankton activity is low. However, at repeated stations with an interval from 1 to 3 days, large changes in the silicon and oxygen concentrations were recorded throughout the whole water column. These changes were governed by the influence of hydrological factors.

Thus, the new data obtained during the implementation of the"Laptev Sea System" Program allowed us to specify the distribution features of the main biohydrochemical parameters in the zone influenced by river water. The data confirms the stability of the hydrochemical sea structure, while the concentrations of oxygen and nutrients vary significantly through the years.

References

Anoshkin, A.F., Petryashev, V.V., Pivovarov, S.V., Ushakov, I.Ye. 1995. Study of the relationship between biota distribution and hydrooptical and hydrochemical parameters in the Laptev Sea in September of 1994 (in press).

Buynevich, A.G., Rusanov, V.P., Smagin, V.M. 1980. Spreading of river water in the Laptev Sea by the distribution of hydrochemical elements. - Proc. of the AARI. - v.358. p.116-125.

Manual on chemical analysis of sea waters.//St.P.,Gidrometeoizdat,1993,-264 p.

Pivovarov, S.V., Smagin, V.M. 1994. Hydrochemical studies in the Laptev Sea in 1993. Scientific results of the LAPEX-93 expedition. - St.Petersburg; Gidrometeoizdat, - p.210-221.

Sidorov, I.S., Gukov, A.Yu. 1992. Influence of the oxygen regime on the zoobenthos existence conditions in the coastal regions of the Laptev Sea - Oceanologiia.-v.32. - Iss.5., p.902-904.

DISTRIBUTION OF RIVER WATER AND SUSPENDED SEDIMENTS IN THE RIVER DELTAS OF THE LAPTEV SEA

V.V. Ivanov and A.A. Piskun
State Research Center of the Russian Federation the Arctic and Antarctic Research Institute, St. Petersburg, Russia

River run-off significantly influences the water balance of the Laptev Sea and the water exchange between its zones, ice thermal processes, the formation of the structure and the chemistry of water and bottom sediments. This influence is especially strong in the outflow zones of the rivers among which the Lena river is the largest. The Lena run-off is distributed along numerous delta arms and flows off to the sea in a wide front, its extent being about 450 km. Separate coastal regions are affected not only by the run-off of the delta arms of the Lena, but also by the total run-off of its branches and the adjacent Olenek and Yana rivers. In turn, for the studies of the regime of the south-eastern Laptev Sea and especially of the Yana Bay it becomes equally important to know the typical features of the run-off distribution by the arms of the Yana delta the coast line of which extends over about 130 km.

Systematic run-off observations at the downward measuring sections of the rivers Lena, Yana, and Olenek were initiated in different years by wintering expeditions of the AARI and the Main Administration of the Northern Sea Route (Table I). The longest series of continuous observations are available for the sections of Kusyur of the Lena river and Dzhangky of the Yana river. However, as a result of the accumulation of data on the hydrological regime as well as of the development of principles for the optimal location of the hydrometeorological network in the river mouth areas /12/, downward measuring sections at these rivers were set up closer to the actual river boundaries of the mouth areas. This permis to take their run-off into account more fully and reliably.

The organization of a network of permanent hydrometric sections at the head and in the arms of the Lena delta was preceded by winter expeditions of the AARI studying the Ust'-Lena from 1950 until 1955 /1,6-10, 16/. This expedition has laid the foundation for complex geodetic, hydrological, hydrochemical and geomorphological studies throughout the year on which subsequent expeditions and a permanent network were based. The Ust'-Lena expedition set up hydrometric sections in all main arms at the head of the Lena delta as well as a serie of hydrometric sections in the system of the navigable Bykovskaya branch (Fig.1). At the sections in the Glavnoye ruslo (I) and Bykovskaya branch (II) observations of the river outflow were carried out from 1950 to 1955, for Trofimovskaya (III),Tumatskaya (IV), Olenekskaya (V) from 1951 to 1953 and in the lower reaches of the Bykovskaya branch (sections 1-8) from 1953 to 1955. Sediment observations were carried out in the upper reaches of the Bykovskaya branch from 1950 to 1955 and in its lower reaches from 1952 to 1955. According to the data of this expedition for the first time discharge curves were plotted and water run-off and sediment discharge in the arms calculated /6-10/. After the end of the expedition the run-off observations in the delta arms were of episodical character. Only after 1978 the sections at the delta head started to operate as permanent ones.

The expedition studies in the Yana delta were carried out by the Arktikproyekt in 1941-1942 and 1952-1954 and continued by the AARI on a new basis in 1960. This allowed for the first time to estimate the distribution of water run-off and

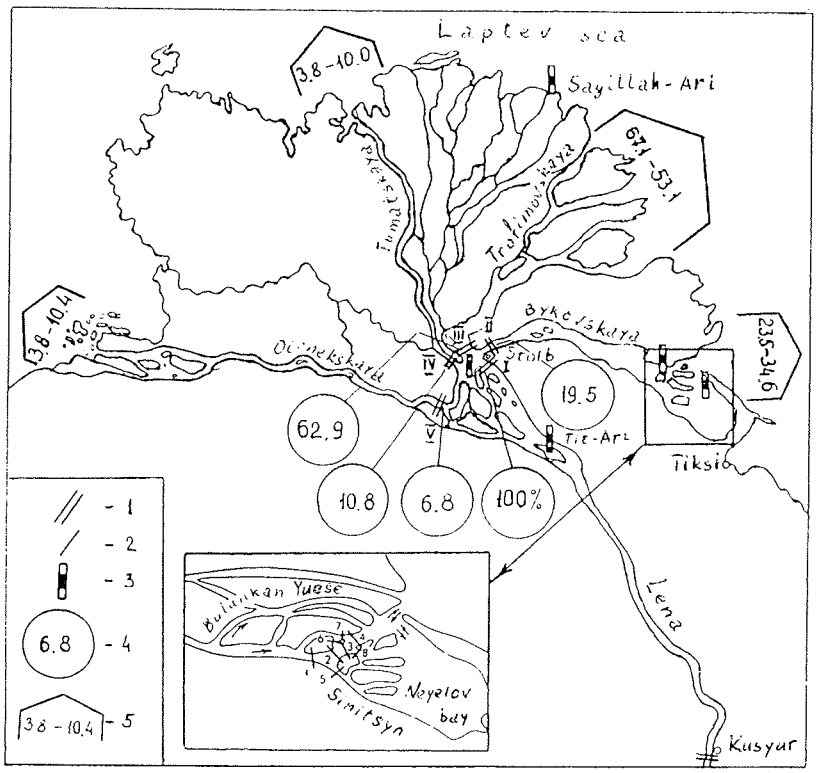

Fig. 1. Location scheme of the hydrometric sections in the Lena delta. I - permanent hydrosection; 2 - expedition hydrosections; 3 - level measuring stations; 4 - annual sediment discharge in % of the total mean multiyear run-off of the branches equal to 19 400 000 tons; 5 - range of values of mean monthly water run-off in % of the total run-off of the branches for a multiyear period.

sediment discharge by the main delta arms /14/. Later on, these estimates were significantly supplemented by the MGU expeditions from 1971 to 1973 and from 1985 until 1987 /3,15/.

The expedition data of the AARI served as a basis for further studies of the run-off distribution and levels as well as for the schemes of surface and bottom currents using small-scale aerodynamic models of some segments of the Lena and Yana deltas. By means of these models missing data for the univestigated areas, required for numerical calculations /11/, were obtained. Variants for improving navigation conditions on limiting bars and crossovers were also tested /4,5/ (Table 2).

The observations of water discharge in the Lena delta accumulated up to now allow to revise the characteristics of run-off distribution by its arms. The run-off inflow to the delta is best of all characterized by the sum of water discharges of all delta branches. As shown by the comparison of mean monthly values of water discharge in the main channel (4.7 km upstream of the Stolb island) with those near Kusyur, the discharges in the main channel from October to April are much larger than those near Kusyur (the difference reaches 4.9 in per cent ratio and 2200

m^3/s as an absolute value). In other months it is less. At the same time, the intensity of the decrease in mean monthly discharge by the main channel in winter is more than on the segment upstream. This is a result of the run-off losses due to the formation of a thick ice cover in the lower reaches and in the delta of Lena. Because of a smoothing of the flood wave and water accumulation on the flood-plain at the delta head, a decrease in water discharges is observed at the beginning of the spring flood, if compared with the river segment upstream.

Table 1: Run-off observation at downstream measuring sections of the Lena, Yana and Olenek rivers

River	Section	Distance from the mouth, km	Water catchment area, sq. km	Run-off observation period, years (water)	Run-off observation period, years (sediments)
Lena	Kusyur	211	2.430.000	1934-present	1960,1962, 1973,1976-present
Lena	4.7 km upstream of Stolb Island	4.7	2.460.000	1950-present	1970-1973, 1976-present
Olenek	8 km upstream of Purmouth	226	181.000	1951-1964	
Olenek	7.5 km downstream of Purmouth	210	198.000	1964- present	1978-present
Yana	Dzhangky	391	216.000	1938-present	
Yana	Yubileynaya	158	224.000	1972-present	

On the other hand, the sum of mean monthly discharges of the delta branches during stable ice conditions is generally below (by 1-20%) the discharge of the main channel, but above that near Kusyur (by 3-45%). During the period of an open channel an inverse ratio is observed. The fact that the total run-off of the branches exceeds the run-off in the main channel from June to August is attributed to the water outflow from the flood-plain to the branches, the melting of snow and ice which is accumulated in large amounts on the flood-plain and in the delta. Only the water that flows onto the flood-plain and into the Bulkurskaya branch is measured at the Stolb measuring station. Parts of the run-off that flows into the delta are not taken into account. As noted in /8/, a similar phenomenon also occurs at the hydrometric sections of Trofimovskaya and Tumatskaya branches. That is why, strictly speaking, neither water discharge in the main channel nor total discharge of the branches can be assumed to be water discharge incoming to the delta for this period. In the opinion of Burdykina /8/ the influx of the Lena flood water through the Leno-Anabarsky depression into the basins of the Olenek and Anabar rivers can also serve as an explanation of the water discharge decrease.

Because of a large natural control of the Lena river run-off, its multiyear variability is small. Mean annual discharge of water flowing into the delta changes from 10.600 to 20.200 m^3/s with a mean value of 15100 m^3/s. The largest discharge of the spring flood exceeds by 380 times the lowest discharge during the winter low-water period. On average the flood lasts about two months. Rain floods are observed when the spring flood is on the decrease.

Table 2: Studies of the deltas of the Lena and Yana by means of aerodynamical models

Object	Final year of studies	Dimension of the object under study	Range of water discharges studied, m^3/s	Number of regimes studied	
				natural	design
Crossover zone in the Lena delta	1957	10*5.5	2000-6500	3	11
Bar of the Glavnaya branch of the Yana	1967	24*20	200-1500	2	3
Delta head of the Lena	1968	14*15	14000-40000	2	-
Mouth and bar of the Bykovskaya branch of the Lena delta	1970	40*30	2000-6000	2	5

An analysis of water run-off distribution by the arms at the head of the Lena delta, based on mean daily discharges of equal probability, indicates that, with an increasing water content, the share of the run-off of the Bykovskaya, the Olenekskaya and the Tumatskaya branches increases due to a decreased share of the Trofimovskaya branch run-off. A similar feature is observed for the seasonal run-off distribution. On annual average, 61.5% of the total run-off of the branches comes from the Trofimovskaya branch, 25.3% from the Bykovskaya branch, 6.8 and 6.4% from the Olenekskaya and Tumatskaya branches, respectively (Table 3).

Interannual distribution of the water run-off in each of the delta branches shows a seasonal character of the Lena river run-off varying with respect to percentage. Thus, in the Trofimovskaya branch which has the largest water content the run-off increases by 15.8% during the transition from winter to spring and in the Tumatskaya branch with the lowest water content by 46.0%. The run-off in fall as compared with that in summer is by 15.8% less in the Trofimovskaya branch, and by 21.3% in the Tumatskaya branch. On the whole, the Lena delta is characterized by the following typical feature: the lower the water content of the branch is, the larger is the difference in its run-off (in % of the annual) at the turn of the seasons.

The considered run-off distribution refers to the heads of main branches. In approaching the mouth their run-off gradually decreases being distributed between the side branches. On the basis of observation data of the Ust'-Lenskaya hydrological expedition it was found that from the water discharge at the head of the Bykovskaya branch being equal to 20000 m^3/s only one third reaches the Sinitsyn branch (83 km from the head of the Bykovskaya branch) and only one quarter of it passes the crossover Dashka which is the main shipping limiting zone. With the decrease of water discharge at the head of the branch its share in the lower reaches increases in percent ratio /8/. At water discharges below 6000 m^3/s a simple relation is observed to be slightly broken due to the effect of alternating backwater from the sea.

During the period of an open channel, from 6 to 15% of the total discharge of the Bykovskaya branch flow into the Sinitsyn branch while the Ispolatov branch takes from 27 to 81%. During the low-water period of summer and fall the discharge in the Ispolatov branch ranges from 60 to 81% at the head of the Bykovskaya branch.

Due to a substantial decrease of the water run-off in winter, the water level in the Lena delta drops. Most of the side branches become dry or freeze to the bottom already in early winter. This could explain why there is no water outflow to the side

branches in the segment from the head of the Bykovskaya branch up to the separation of the Sinitsyn branch in winter.

Table 3: Seasonal distribution of water run-off and water rations of the main Lena delta arms for 1977-1990.

	Season				Naviga-tion period VI-IX	Year	
	winter XI-V	spring VI	summer VII-VIII	fall IX-X		m^3/s	%
In % of the annual run-off of the branch							
Bykovskaya	7.5	38.9	34.8	18,2	85.5	4050	100
Trofimovskaya	14.9	30.7	35.6	19.8	79.0	9840	100
Tumatskaya	1.2	47.2	35.0	13.7	91.5	1030	100
Olenekskaya	7.6	43.9	34.9	15.5	89.0	1080	100
In % of the seasonal total run-off of the branches							
Bykovskaya	17.3	28.5	25.0	24.7	26.4	4050	25.3
Trofimovskaya	77.4	54.2	61.9	65.0	59.0	9840	61.5
Tumatskaya	0.7	8.8	6.5	4.7	7.3	1030	6.4
Olenekskaya	4.6	8.5	6.6	5.6	7.3	1080	6.8
Mean water discharges for a season, m^3/s							
Total run-off of the branches	3020	66700	34000	18000	39500	16000	
Main channel	2720	62200	32500	17600	37500	15100	
Kusyur	2910	73800	33600	19200	41400	16700	

The distribution of water discharges along the channels and branches in the area of the crossover Dashka has been considered in detail in /6,7/. Downstream of the crossover Dashka (at 89 km) the branch D'aardaasyn Yuese separates from the Ispolatov branch and falls into the Neyelov Bay. This branch takes from 8 to 10% of the total discharge by the hydrometric section 1.

Further to the sea, water discharges of the Ispolatov branch slightly increase because of the fall of several small branches flowing out of the upper zone of the Bykovskaya branch. Near the Bykov Cape the water discharge increases even more due to the water inflow from the Neyelov Bay which is approximately equal to the discharge of water flowing through the Sinitsyn and the D'aardaasyn Yuese branches.

Sediment load of the Lena changes with variations in the water content of the river. As shown by Table 4, in comparison with water run-off, about half of the annual sediment discharge or more occurs at most sections in June and only about one third during July-August. The distribution of transported suspended matter between the arms indicates a well pronounced (with regard to water run-off) fraction of solid discharge in the Tumatskaya branch with a small water content. In the Bykovskaya branch the share of sediment load in winter is a little bit larger while during the navigation period it is smaller than water run-off. Considerung the annual discharge the main mass of sediments passes the section of the Trofimovskaya branch.

Table 4: Distribution of suspended sediment discharge by the main arms at the head of the Lena delta

	Season				Naviga-tion period VI-IX	Year	
	winter XI-V	spring VI	summer VII-VIII	fall IX-X		thous. tons	%
Mean seasonal sediment discharge, kg/s							
Bykovskaya	2.11	830	212	67.6	338	3780	19.5
Trofimovskaya	19.9	2280	847	247	1080	12200	62.9
Tumatskaya	1.30	524	138	42.8	217	2100	10.8
Olenekskaya	0.85	317	67.8	20.9	120	1330	6.8
In % of the annual discharge at a given hydrometric section							
Bykovskaya	1.1	59.1	30.2	9.6	96.2	3780	100
Trofimovskaya	3.0	49.5	36.8	10.7	93.8	12200	100
Tumatskaya	1.0	58.6	30.9	9.5	97.1	2100	100
Olenekskaya	1.2	63.3	27.1	8.4	95.8	1330	100
In % of the seasonal total discharge of the branches							
Bykovskaya	8.7	21.0	16.8	17.9	19.2	3780	19.5
Trofimovskaya	82.4	57.7	66.9	65.3	61.5	12200	62.9
Tumatskaya	5.4	13.3	10.9	11.3	12.4	2100	10.8
Olenekskaya	3.5	8.0	5.4	5.5	6.9	1330	6.8
Mean multiyear sediment discharge, thous. tons							
Total discharge of the branches	445	10200	6780	1980	18400	19400	
Main channel	316	9180	5580	1650	15900	16700	
Kusyur	379	9950	6340	1700	17400	18400	

The observed differences between the water content of the arms and the fraction of suspended matter transported by them are governed by the channel morphometry and associated distribution features of surface and bottom current at hydrometric sections found by means of aerodynamic models (Fig.2, Table 5).

It should be stressed that the data in Table 4 characterize the discharge of suspended load at the top of the Lena delta. They cannot serve as a direct indication of the amount of suspended matter flowing into the sea. This has been substantiated by the observations of the Ust'Lenskaya expedition of the AARI /9, 10/. As is known /1,2,9,10/, the suspended load in the Lena delta is composed of particles transported from the upper river segments and of products of the destruction of shores. Shores with polygonal formations and thick veins of ground ice are destroyed especially intensively. In this case, as affected by the river flow, caves of several meters depth are built in the lower part of the shore bench. If the direction of the caves coincides with the direction of the axes of the ice veins, then large rock blocks usually fall down along the contacts of the ice veins and frozen masses of the inner parts of the polygons. Thus, between 6 and 8 m of such shores in the Bykovskaya Branch are annually destroyed, sometimes even more /10/. The products of these processes during the period of the open channel are the main source for sediment transport to the branch. In addition sedimend load is supplemented when polluted ice (transported and local) melts. During floods, anchor ice transports downstream 10-15 cm thick layers of ground frozen to it.

Moving ice scours flooded shoal and low islands. On the shores where ice rubble is observed every year, gradually near-channel sand-pebble barriers up to 4 m height are formed /10/. Ice rubble on the flooded shoals and islands and ice jams in the side branches result in increased channel transformations, especially in the segments where the bottom is not composed of frozen ground.

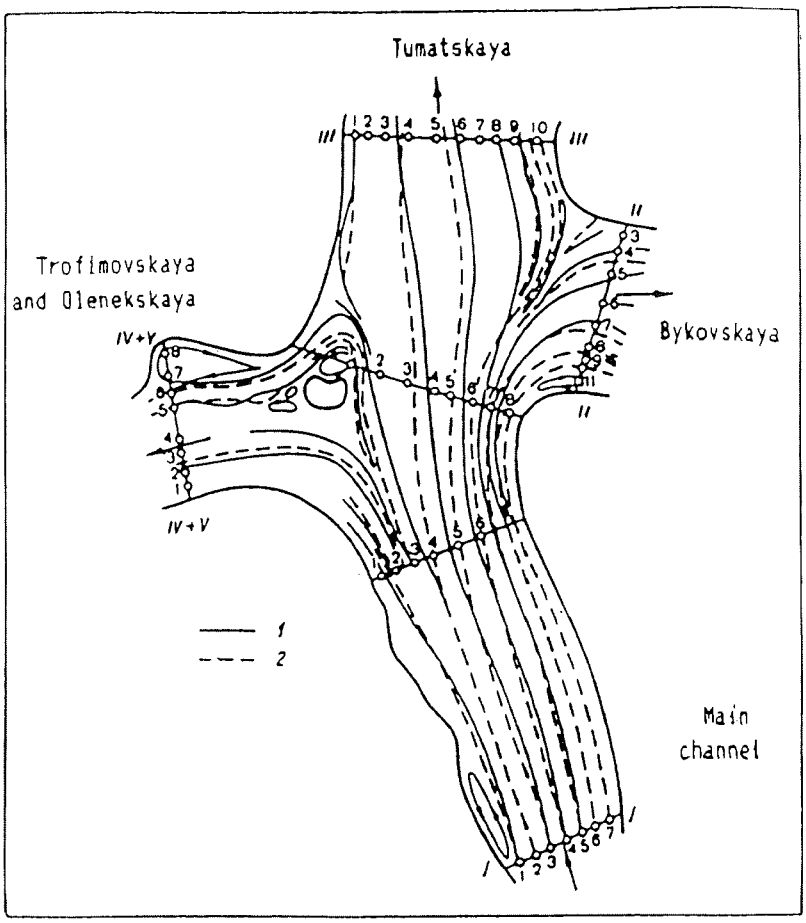

Fig. 2. Plan of the current trajectories at the surface (I) and in the near-bottom layer (2) at the head of the Lena delta according to the data of aerodynamical modelling.

Wind-driven transfer supplies additional sediment load to the delta. At strong and persistent winds over the delta large masses of dry sand are transported from the shores into the water, thus contributing to suspended load. Due to this an enhanced turbidity in the surface water layer of the delta branches compared with the upper zones is observed /2/. Significant swell at strong winds also contributes to increased concentration of suspended particles, especially relatively shallow areas.

Depending on the ratio of the enumerated factors both decreased and increased

Table 5: Distribution of liquid run-off and sediment load in the surface and near-bottom layer at the head of the Lena delta according to the results of aerodynamic modelling

Arm name and section number	According to field data of 1954 (at a 265 cm level)		According to model measurements (at a 200 cm level) Water discharge, m^3/s Calculated sediment load, kg/s						
	Water dis., m^3/s	Sediment dis., kg/s	Along the whole section	Including the layers upper	bottom	By av. arithmetical turbidity	Proportion of water run-off in the arms	Including the layers upper	bottom
Main channel (I)	19800	332	14500	6600 / 6600	7900 / 7900	-	-	99.0 / 99.0	145.0 / 145.0
Bykovskaya branch (II)	4950	54	3770	1690 / 1112	2000 / 2658	42.7	39.8	16.6 / 10.9	25.6 / 32.7
Trofimovskaya branch (III)	13300	257	9650	4350 / 4795	5300 -- / 4855	183.0	188.0	73.0 -- / 81.5	109.0 / 100.0
Olenekskaya and Tumatskaya branches (IV+V)	1510	14.9	1080	536 / 693	544 / 387	16.8	11.0	7.5 / 9.7	9.3 / 6.6

Notes:

1) In the numerator are the results without taking into account cross flow circulation, in the denominator those with cross flow circulation;

2) The flow was subdivided into surface and near-bottom layers along the line of the location of zero values of the cross components of the flow speed by depth;

3) Depth profiles of the turbidity obtained by the Ust'-Lena expedition were used to calculate the sediment load velocity.

(relative to the delta head) concentration of suspended mater can be observed in the lower reaches of the delta. The main mass of transported suspended matter is redeposited in locations of a considerable channel widening to which, for example, the crossover Dashka in the lower reaches of the Bykovskaya branch is confined, and at the exit of the branches to the sea forming bar shoals with underwater channels. The Neyelov Bay serves as a significant accumulator of sediment discharge in the lower reaches of the Bykovskaya branch.

More detailed data on the distribution of sediment discharge, the amount of sediments and deformations of the lower reaches of the Bykovskaya branch are presented in /9, 10/. It should be noted that in spite of substantial deformation of the shores and the channel in the Lena river delta, a comparison of the results of stationary hydrometric observations in its branches over a 20-year period showed a relative stability in the water run-off distribution by the arms /13/. This can be attributed to the fact that channel deformations for the indicated time period remain to be quite small on the background of large crosssections of the channel.

As has already been mentioned, the run-off of separate branches of the Lena delta is distributed over the sea area mixing with the run-off of the Olenek and Yana rivers due to which it seems to be important to estimate their joint contribution to the freshwater balance of the sea areas adjacent to the mouths of these rivers.

An analysis of multiyear data on the water run-off at the downstream measuring sections of the Olenek and Yana shows the annual run-off of each of them being equal to the water run-off of such Lena delta branches as Tumatskaya or Olenekskaya. Nevertheless, it constitutes only about 6% of the full Lena run-off which in turn provides 72 % of the freshwater run-off to the Laptev Sea. Considering the multiannual distribution of the run-off of Olenek, Yana and Lena, the largest volumes of water and sediments fall on June. In October-April and June, the multiyear mean monthly water run-off of the Olenek slightly prevails over the Yana run-off. The sediment discharge at the downward measuring sections of the Olenek and Yana is approximately equal only in June constituting 1250 000 and 1730 000 t, respectively. In July, the sediment discharge of the Olenek decreases to 127 000 t. In August and September it is at the level of 40 000 t. The mean monthly sediment discharge at the Yubileynaya section of the Yana gradually decreases from June to September up to 272 000 t reachinga value of 10 000 t in October. During the period of the open channel 1460 000 t of suspended load pass on average the downstream measuring section of the Olenek and 4050 000 t that of the Yana. Mean annual sediment discharge through these sections is 1480 000 and 4190 000 t, respectively, or 7.6 and 21.6% of the total sediment discharge of the Lena delta branches.

It is not possible to estimate the distribution of the run-off in the Olenek delta because there are no hydrometric observations at the sites located below the downstream measuring section at this river.

According to available sufficiently detailed studies, the Yana river delta differs in the distribution of discharge water masses and sediment load /2, 14, 15/. The results of these studies indicate that, regarding water content, Glavnoye Ruslo and Pravaya are the main branches. And while during the low water period these branches transport only about 80% of the river run-off, at high levels only about a half, the remaining portion is distributed by small branches. At the sea side of the delta some arms combine their run-off again falling into the Yana Bay in comparatively combined groups. Fig. 3 shows the contribution of some groups of the arms to the volumes of the liquid discharge transported by the Yana to the delta front.

The hydraulic calculations made for the Yana delta by means of the method developed at the AARI /11/ for the whole range of natural variability of boundary conditions on the side of the river and the sea, allowed us to obtain analytical dependencies in form of polynomials of second degree for calculating water run-off in the delta arms (Q_i) depending on the water content of the river (Q_p) and the height of the position of the background sea level (Z_m). Water discharges (Q_p) prescribed for the calculations, changed from 400 to 7900 m^3/s with an interval of 1500 m^3/s. The sea level marks (Z_m) from -0.8 to 0.2 with an interval of 0.15 m. The dependencies have the form

$$Q_i = a_{00} + a_{10} Q_p + a_{20}Q_p^2 + a_{01}Z_m + a_{11}Q_pZ_m + a_{21}Q_p^2Z_m + a_{02}Z_m^2$$

$$+ a_{12}Q_pZ_m^2 + a_{22}Q_p^2Z_m^2$$

The coefficients of the polynomials for some branches of the Yana delta are given in Table 6.

The distribution of sediment load by the arms of the Yana river delta in fractions of the total sediment discharge to the delta is shown in Fig. 3. During floods the largest share of sediment discharge goes to the Samandon branch which takes

about 3/4 of suspended matter /15/. As the content of river water decreases, it is the Glavnoye Ruslo carrying the major part of suspended matter. The amount of sediment discharge of the branches Pravaya, Ilin Shar, Kochevaya, and Kamelek increases, too. The amount of suspended matter carried by the Yana into the sea differs from the values given here as the main sediment mass is deposited at the mouth of the branches to the front forming shallow bars.

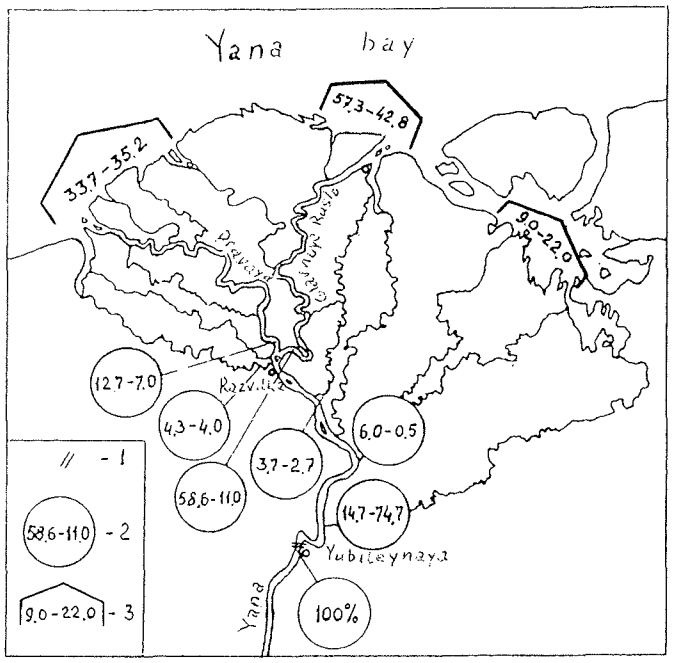

Fig. 3. Scheme of the channel network of the Yana delta network. I - downward measuring section; 2 - range of values of mean daily discharge of sediments (%) during the open channel at the sediment discharge change at the downward measuring section from 30 to 3000 kg/S /15/; 3 - range of values of mean daily water runoff (%) in summer at the water discharge change at the downward measuring section from 845 to 6900 m^3/s /3/.

In conclusion it is necessary to stress that the water run-off measured at the downstream measuring sections of the Olenek, Lena, Yana and their deltas characterizes quite accurately the share of the liquid run-off carried by them to the sea (Table 7), while the discharge of sediments transported by river water to the sea significantly differs from the values recorded in the delta arms and moreover at the downstream measuring sections. A reliable estimate of the amount of suspended matter transported to the open sea by river water can be given on the basis of specially organized full-scale studies.

Table 6: Coefficients of polynomials for calculating water discharges in the Yana delta arms at different combinations of river water content and sea level height

Coef-ficient	Arm above the separation node of Pravaya and Glavnoye ruslo branches	Pravaya branch after separating from Glavnoye ruslo	Glavnoye ruslo branch before exiting to the bar	Kiselev branch
a_{00}	$1.456*10^{2}$	$1.690*10^{2}$	$1.953*10^{2}$	$-4.342*10^{1}$
a_{10}	$6.451*10^{-1}$	$2.796*10^{-1}$	$3.045*10^{-1}$	$2.625*10^{-1}$
a_{20}	$-4.455*10^{-7}$	$-1.653*10^{-7}$	$8.351*10^{-5}$	$-3.286*10^{-6}$
a_{01}	$-5.204*10^{1}$	$-5.468*10^{1}$	$2.295*10^{1}$	$-1.754*10^{2}$
a_{11}	$-3.607*10^{-2}$	$-4.385*10^{-2}$	$-9.795*10^{-2}$	$1.467*10^{-1}$
a_{21}	$1.034*10^{-5}$	$4.220*10^{-5}$	$9.606*10^{-6}$	$-1.464*10^{-5}$
a_{02}	$-1.015*10^{2}$	$1.315*10^{2}$	$-9.851*10^{1}$	$-7.709*10^{1}$
a_{12}	$6.853*10^{-2}$	$9.543*10^{-2}$	$9.324*10^{-2}$	$5.926*10^{-2}$
a_{22}	$-1.693*10^{-6}$	$7.480*10^{-5}$	$-7.136*10^{-6}$	$-6.253*10^{-6}$

Table 7: Interannual distribution of river run-off (km^3) according to measurements at the downward measuring sections of the Olenek, Yana rivers and in the Lena delta

	I	II	III	IV	V	VI	VII	VIII	IX	X	XI	XII	Year
Olenek river and Olenek-skaya branch	0.322	0.185	0.091	0.332	2.08	33.7	13.8	7.18	6.35	2.74	0.65	0.44	63.9
Tumatskaya branch	0.074	0.027	0.011	0.003	0.01	15.1	7.53	4.04	2.98	1.46	0.17	0.10	31.5
Trofimov-skaya branch	6.46	5.08	4.55	3.84	11.2	93.8	65.9	46.9	38.9	22.4	57.3	6.16	310
Bykovskaya branch and Yana river	1.40	0.92	0.70	0.54	4.35	59.6	36.5	24.5	19.1	8.98	1.91	1.54	160

References

1. Antonov, V.S. Lena river delta (Brief hydrological description). - Proc./Ocean. Commiss., 1960, v.VI, M., izd. AN SSSR, p.25-34.
2. Antonov, V.S. Mouth area of the Lena river (Hydrological description). - L. Gidrometeoizdat, 1967. -107 p.
3. Babich, D.B. Hydrological-morphological processes in the Yana delta river and their anthropogenic changes. Author's summary of the thesis... cand. of geographical sciences. - M., 1992. - 24 p.
4. Gilyarov, N.P., Ivanov V.V. Study of the regime of levels and currents of the river mouths in the zone of the sea effect by means of models. - Proc./AARI, 1963, v.254, p.155-162.
5. Gulyarov, N.P., Ivanov V.V. Modelling of the mouths of Arctic rivers. Problemy Arktiki i Antarktiki, 1960, No.2, p.35-42.
6. Ivanov, V.V. Features of the regime of crossover zone of the Lena delta in the sea effect zone. - Proc./AARI, 1961, v.256, p.89-103.

7. Ivanov, V.V. Regime of the levels of Bykovskaya branch of the Lena delta in the zone of the sea influence. - Proc./AARI, 1961, v.213, p.164-178.
8. Ivanov, V.V. Run-off and currents of the main branches of the Lena river delta. - Proc./AARI, 1963, v.234, p. 76-85.
9. Ivanov, V.V. On the discharge of suspended and entrained sediments of the main branches of the Lena delta. - Problemy Arktiki i Antarktiki, 1964, vyp. 18, p.31-39.
10. Ivanov, V.V. Bottom sediments and dynamics of the bottom of the Bykovskaya branch in the Lena delta. - Problemy Arktiki i Antarktiki, 1967, v. 278, p.128-141.
11. Ivanov, V.V. Method for hydraulic calculation of the water regime elements in the river deltas. - Proc./AARI, 1968, v.283, p.30-63.
12. Ivanov, V.V. Main principles for hydrological-morphological zonation of the mouth areas of the Arctic rivers. - In: Factors and principles of the physical-geographical zonation of the polar regions of the Earth. - L., 1974, p.108-120.
13. Ivanov, V.V., Piskun A.A., Korabel' R.A. Run-off distribution by the main arms of the Lena delta. - Proc./AARI, 1983, v.378, p.59-71.
14. Nalimov, Yu.V. Hydrological characteristics of the Glavnoye ruslo branch of the Yana river delta. - Proc./AARI, 1965, v.268, p.57-77.
15. Sidorchuk, A. Yu. Processes of delta formation in the mouth area of the Yana river. Author's summary of the thesis, cand. of geograph. sciences. - M., 1975. 25 p.
16. Tasakov, P.D. On the winter regime and process of ice break-up in the Lena river mouth. - Proc./AARI, 1955, v.72, p.105-129.

CHEMICAL COMPOSITION OF SUSPENDED SEDIMENTS IN THE LENA RIVER AND ITS MIXING ZONE

V. V. Gordeev and V. P. Shevchenko

P.P. Shirshov Institute of Oceanology, Russian Academy of Sciences, Moscow, Russia

Abstract

In the suspended particulate material (SPM) of the lower reach and some of the small tributaries of the Lena a total of 29 chemical elements was analyzed. As compared to the world's large rivers the data show a significant depletion of calcium in SPM and an enrichment by sodium that is most probably connected with carbonate weathering in the Lena drainage basin and the abundance of K-Na feldspars in SPM. The SPM is slightly depleted of Cd, Ta, Cu, Ni and enriched by Ce, Pb, Th. The shale-normalized rare earth element (REE) pattern of the Lena River SPM is enriched by light and intermediate REEs relative to heavy REEs ((La/Lu) normalized ratio = 2.2). Small tributaries show a large degree of variation in chemical composition but the trend of light REE enrichment is maintained. LREE (La, Ce) contents have a tendency to decrease slightly with increasing salinity. In the mixing zone the concentrations of Sc-normalized elements do not significantly vary relative to the values for river water. The shale-normalized REE pattern is preserved in the suspension of near bottom waters of the Laptev Sea with a salinity of up to 31 pro mille.

Introduction

The river input of dissolved and suspended parcticulate matter is the most important source of terrigenous deposit supply to the World Ocean. The knowledge of the chemical composition of river suspension is important because, firstly, the river input is one of the main links between geochemical cycles of many elements. Secondly, by determining the chemical composition of SPM it is possible to evaluate the level of chemical weathering in a river drainage basin. Rivers are thirdly the most important source of pollutant fluxes into a coastal zone.

At the present time, there are abundant data on the chemical composition of river suspension (Gordeev, Lisitzin, 1978; Martin, Meybeck, 1979; Thomas, Martin, 1982; Gordeev, 1983; Martin, Whitfield, 1983; Meybeck, 1984,1988; Martin, Gordeev, 1986; Martin, Windom, 1991). At the same time, there are only scarce according data about the large rivers on the territory of the former Soviet Union flowing into in the Arctic Ocean. In the fifties and sixties, some works were published in the USSR (Konovalov, 1959; Nesterova, 1960; Konovalov at al., 1968; Kontorovich, 1968; Morozov et al., 1974). At present, it is necessary to investigate the SPM of Arctic rivers applying modern methods of sampling and analysis. In 1989, the Russian-French-Dutch Scientific Programme on Artic and Siberian Aquatorium (SPASIBA) has started. The results of the first expedition SPASIBA-1 into the Lena delta and the adjacent part of the Laptev Sea are published (Gordeev, Sidorov, 1993; Letolle et al., 1993; Martin et al., 1993). In September 1991, the second expedition SPASIBA-2 was carried out in the same region. The results of the analysis of SPM sampled during the latter expedition are presented in this paper. The aim of the study is: (i) to obtain data on the distribution of a large number of chemical elements in the suspension of the Lena's lower reach; (ii) to distinguish specific features of the element distribution in SPM in the mixing zone between river and sea waters in an area of cold Arctic climate.

The Lena Drainage Basin

The area of the Lena drainage basin is 2.49 million sq. km, the length of the river is 4400 km. The surface of the delta (about 32000 sq. km) takes second place in the world after the Mississippi delta (Antonov, 1967). The Lena basin is characterized by a severe continental climate. The annual temperature averages 7.6° C (Letolle et al., 1993) and the range of temperature may reach 100° C in some years. About the half of the drainage basin (north of Yakutsk) is situated in the zone of complete and continuous permafrost. Precipitation is scarce. In the Lena delta, precipitation only amounts to 90 mm per year; in its middle reach (the Lena-Vilyui plain) it is about 200 mm per year. The mountainous regions of the south are the only ones where precipitation rises up to 800-1000 mm per year (Antonov, 1967).

The main part of the drainage basin (in middle and lower reaches of the Lena) is characterized by outcrops of carbonate rocks, occasionally salt and gypsum-containing Paleozoic rocks, of terrigenous deposits, including coal-bearing deposits of the Jurassic, Cretaceous and Neogene ages, as well as Quaternary lacustrine-glacial and alluvial deposits. It also contains different calcareous rocks. In the upper basin crystalline and metamorphic rocks of the Archaean and Proterozoic ages are spreaded. Karst of carbonate and evaporites is abundant in the western and southern parts of the central area of the basin. More information is given by Gordeev and Sidorov (1993).

Materials and Methods.

Samples of river water (Fig. 1a) were taken in two legs aboard the river ship "Olkhon" by a plastic pump (stations labelled L-n) in one case and by a plastic bucket from the surface in other cases (station 0-n). The samples were filtered on board by vacuum filtration using *Millipore* filtrations with *Nuclepore* filters (0.4 μm pore size; 47 mm diameter). 6 samples (table 1) were collected by means of sedimentation from 30 l water in 3-4 days. In the Laptev Sea (R/V "Yakov Smirnitskiy", Fig. 1,b) water was sampled by a plastic pump from 2 to 7 m depth and by a Go-flo bottle (5 l) from greater depths. Sedimented samples were analyzed by flame and graphite-furnace AAS (Perkin-Elmer 3030, HGA-500). Al was determined by eriochromcyanine - R method. The analyses were carried out in the Institute of Marine Biogeochemistry (Montrouge, France).

18 elements (Fe, Sc, Cr, Cs, Co, Hf, Th, Ta and 10 rare-earth elements) in filtered river and marine SPM were determined by instrumental neutron-activation analysis (INAA) in the Vernadsky Institute of Geochemistry and Analytical Chemistry in Moscow. Details of the INAA method are given in Gordeev et al. (1985). The reference samples (TB-shale and SD-M2/TM - bottom sediment (IAEA)) were used to evaluate the precision and accuracy of the determinations. Standard deviations for INAA measurements observed in a duplicate analysis of reference rock-samples were 3-6% for Fe and Co, 5-10% for Sc, Cr, Hf, Th, Ce, Eu, Gd and 10-15% for Cs, La, Sm, Tb, Lu.

Results and Discussion

1. RIVER DATA: Short description of mineralogical composition

The mineral composition of SPM and bottom sediments of the Lena River and the Laptev Sea was studied during the expedition SPASIBA-2 (Serova, Gorbunova, 1995). X-ray diffraction analyses of bulk samples of the Lena SPM has shown an abundance of quartz (52-60%), feldspars (20-25%) and clay minerals (15-20%). Feldspars were probably represented as K-Na species. The quarz/feld-

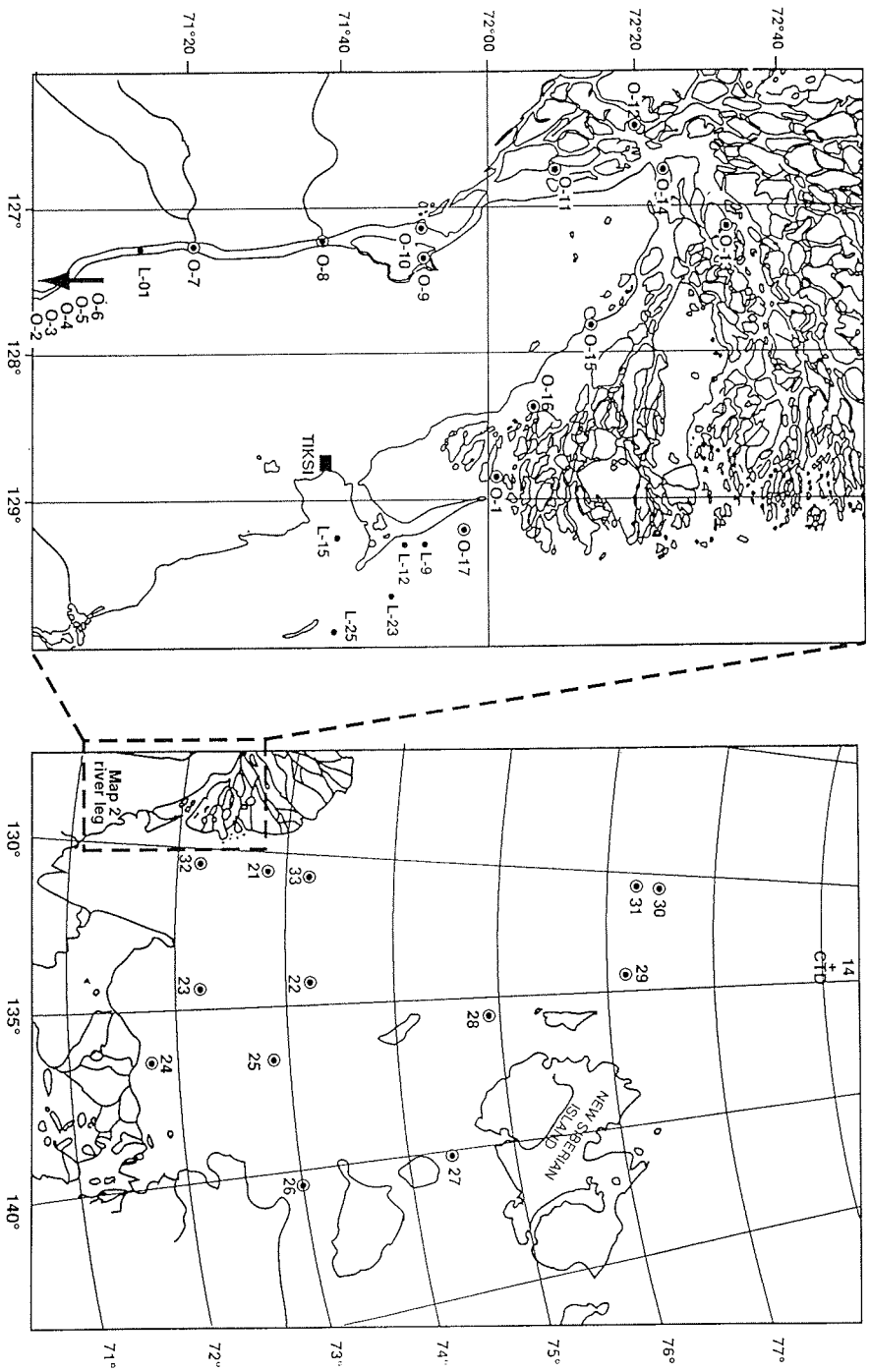

Fig.1. The Lena River delta (a) and the Laptev Sea (b): locations of the sampling stations

spars ratio was very constant (2.0-2.3). As clay minerals, illite, chlorite and kaolinite were found at a illite/(chlorite+kaolinite) ratio of nearly 1.2. In general, the mineralogical composition of the SPM of the Lena is very homogeneous and typical of rivers in cold climatic zones (Darby et al., 1989).

Major elements and weathering

The contents of major elements and of a group of trace elements in the same 6 samples are given in Table 1. The concentration of SPM in river waters varies between 10 and 30 mg/l. The waters of small tributaries (Beris, Tegis, Khatystakh) were exceptionally clear (turbidity was about 1 mg/l and less); this did not allow to sample SPM by sedimentation. The comparison with the average chemical composition of surface rocks (52% shales, 15% sandstones, 7% carbonates and 26% igneous rocks (Martin, Meybeck, 1979)) has shown (Fig. 2) that the SPM of the Lena is enriched by sodium by 2.5 times and depleted of calcium almost by one order (Al-normalization is not necessary because of the low variation of major elements and organic carbon contents in the samples analyzed). The POC content (3.4%) is very similar to average POC values in rivers with a turbidity of about 30-40 mg/l (Meybeck, 1988).

Ugolini (1986) noticed that in polar regions a majority of weathering processes were practically the same as in humid zones, while the rates of weathering were by one or a few orders lower. Low temperatures make the reactions of mineral dissolution very difficult except for carbonates. Chemical weathering occurs even under temperatures below zero because unfrozen water is still present in a frozen soil.

Drever (1988) underlines that even in a glacial environment chemical weathering can be rapid. Two important factors are: (i) a high rate of physical erosion reexposing the bedrock; (ii) a high annual precipitation (the South Cascade Glacier area represents an example). Both factors are not characteristic of the Lena River basin. Thus, high rates of chemical weathering are hardly to expect in the basin. In a previously published paper (Gordeev, Sidorov,1993) it was shown that carbonate weathering predominates over silicate weathering in the Lena basin and that the rate of annual chemical denudation for the entire Lena basin (19.7 t/sq.km) is about half of the current annual world average (36 t/sq.km).

Carbonate dissolution and abundance of K-Na feldspars probably explain the specific chemical composition of the SPM of the Lena.

It is well known that the suspension of tropical rivers is enriched by Al and Fe and depleted of Na, Ca, Mg and K (Fig. 2). Excluding Na-anomaly, the ratios between El(Lena SPM) and El(bedrock) indicate the existence of chemical weathering in the Lena basin with more or less similar intensity as in other rivers in cold and temperate zones.

As we noted above, a cold climate and a carbonate type of chemical weathering results in a predominant leaching of calcium from the source rocks with small effect on silicate rocks (Al/Fe is about 1) (Fig. 2).

Rare-earth elements and other trace elements

The results of AAS and INAA determinations of Fe and trace elements in the SPM of the Lena River, its delta and some small tributaries are presented in Table 1 and 2. With respect to salinities (0.01 pro mille), turbidity and the chemical composition, the samples L-23-2, L-23-3, L-25-2 and 0-17 taken near the delta edge (Fig. 1,b) are practically undistinguishable from the river samples. Therefore they were attributed to the river proper. Fig. 3 shows the variations in the ratios of

Table 1
Content of major, minor elements (AAS data) and POC in the surface suspended sediments of the Lena River and its tributary Ayakit

Sample	Location	Al	Fe	Na	K	Mg	Ca	Mn	POC	Cu	Zn	Co	Ni	Pb	Cd
		%								ppm					
O-2	Lena, Sikstyah	5.84	3.36	1.73	2.38	1.35	0.44	0.134	3.69	28	103	13.8	28	32	<0.1
O-3	Lena, Govorovskiy shoal	4.25	2.77	2.13	2.43	0.94	0.48	0.085	2.06	18	106	10.4	20	24	<0.1
O-12	Lena, Bykovskaya branch	10.31	3.36	1.82	2.26	1.35	0.30	0.121	3.74	28	185	13.6	59	81 *	0.39
O-13	Lena, Trofimovskaya branch	7.83	3.52	1.62	2.32	1.32	0.34	0.154	3.52	31	147	13.2	33	26	0.24
O-1	Lena, Bykovskaya branch	5.44	3.58	1.62	2.41	1.37	0.53	0.131	3.78	33	262	15.3	30	62	0.54
O-6	Ayakit	6.08	3.57	1.71	2.21	1.04	0.52	0.062	3.55	38	196	12.9	35	61	0.18
Lena River, average This work (n = 5)		6.73 +/- 2.12	3.32 +/- 0.29	1.78 +/- 0.19	2.36 +/- 0.06	1.27 +/- 0.16	0.42 +/- 0.09	0.125 +/- 0.022	3.36 +/- 0.65	27.6 +/- 5	160 +/- 59	13.3 +/- 1.6	34 +/- 13	36 +/- 15	0.25 +/- 0.19
Lena River (Martin et al., 1993)		7.4	-	-	-	-	-	-	3.80	28	143	-	31	23	-
World Rivers, cold and temperate zones (Meybeck, 1988)		7.5	4.66	0.80	2.30	1.25	3.15	0.11	-	-	-	-	-	-	-
World Rivers, tropical and warm arid zones (Meybeck, 1988)		11.4	6.17	0.51	1.83	0.96	0.75	0.089	-	-	-	-	-	-	-
Surface continental rocks (Martin and Meybeck, 1979)		6.93	3.59	0.71	2.44	1.64	4.5	0.072	-	32	127	13	49	16	0.2

* not include to average

Table 3
Content of Fe, REEs and other trace elements in the mixing zone of river and sea waters

Salinity S °/°°	Number of samples	Horizon M	Turbidity mg/l	La	Ce	Nd	Sm	Eu	Gd	Tb	Tm	Yb	Lu	Sc	Cr	Cs	Co	Hf	Th	Fe	(La/Lu)n
				ppm																%	
0	13	0 - 30	10 9 - 28 6	40	93 8	31 7	5 9	1 06	4 85	0 80	0 35	1 60	0 27	12 5	78	3 3	18	2 4	10 8	4 35	2 2
0 25	1	2 5	9 3	45	78	33	6 0	0 70	2 7	0 50	0 23	1 2	0 20	14	79	5 0	17	3 2	11	5 0	3 3
3 0 - 3 7	2	2 5 - 3 5	3 0 - 6 6	38	73	28	6 1	0 75	< 3	< 1 3	< 0 2	< 3	< 0 5	12	82	4 7	16	3 2	10	2 84	-
7 1 - 8 0	2	2 - 3	0 9 - 3 7	26	38	< 54	5 8	< 5	< 3	< 3	< 0 2	< 3	< 1	13 6	63	4 9	< 20	3 1	6 2	2 42	-
9 9 - 13 3	5	2 - 4	0 55 - 2 7	31	69	< 140	6 7	0 97	< 3	< 4	< 0 2	< 3	< 1	10	73	< 7	16	3 2	7 1	3 16	-
16 5 - 16 6	2	6	0 35 - 0 40	24	42	< 33	3 9	0 80	< 3	< 9	< 0 3	< 10	< 0 5	7 5	50	4 5	9	< 10	< 10	1 86	-
21 1	1	9	1 2	42	65	< 67	7 0	< 5	< 3	< 3	< 0 2	< 3	< 1	17	53	4 0	12	5 6	10	4 48	-
29 9	1	5	0 5	30	43	< 150	6 2	< 9	< 3	< 5	< 0 2	< 6	< 2	9 7	< 95	< 9	< 20	< 8	8	2 96	-
21 1 - 22 9	3	8 - 14	3 8 - 5 1	33	63	30	4 9	1 0	3 6	0 8	0 26	1 5	0 26	15 6	88	5 9	14	2 3	11	4 76	2 0
30 0 - 31 8	2	20 - 25	2 8 - 2 9	33	63	33	6 4	0 95	5	0 9	0 31	2 0	0 31	16	86	6 5	15	7 5	13	5 24	1 6

Tab. 2: Content of Fe, REEs and other trace elements in suspended sediments of the Lena River

Station	Location	Sample depth M	Turbidity mg/l	La	Ce	Nd	Sm	Eu	Gd	Tb	Tm	Yb	Lu
				ppm									
L-01-1	Lena, main stream	3	17.5	46	86	32	6.2	1.3	5.0	0.63	0.33	1.8	0.29
L-23-2	Lena, below delta	2	24.0	47	85	36	7.0	1.2	5.4	1.0	0.45	2.4	0.37
L-23-3	Lena, below delta	2	28.6	42	83	36	7.1	0.5	5.8	1.1	0.54	3.0	0.50
L-25-2	Lena, below delta	3	10.9	45	79	36	7.0	1.5	5.4	0.91	0.41	1.9	0.31
O-1	Lena, Bykovskaya branch	0	-	56	112	44	7.4	1.6	6.4	0.95	0.37	1.4	0.29
O-2	Lena, Sikstyah	0	-	34	91	-	4.8	1.0	-	-	-	-	-
O-3	Lena, Govorovskiy shoal	0	-	44	115	36	6.5	1.2	4.8	0.90	0.29	1.0	0.26
O-4	tr Beris	0	1.0	19	60	< 57	4.7	0.8	-	< 2.6	-	< 1.8	< 0.4
O-5	tr Bulun	0	2.1	43	89	39	7.5	1.3	5.2	0.98	0.42	2.2	0.36
O-6	tr Ayakit	0	4.0	27	56	28	5.9	1.1	4.5	0.85	0.26	1.4	0.24
O-7	tr Tegis	0	0.7	79	133	< 74	8.7	1.4	-	-	-	< 5	-
O-8	tr Khatystakh	0	0.6	54	95	< 200	6.7	< 0.8	-	-	-	< 6	-
O-9	tr Kengdey	0	3.4	34	77	< 70	5.9	0.87	-	-	-	< 2	-
O-10	Lena, main stream	30	-	31	80	25	4.4	0.65	2.9	0.55	0.15	0.8	0.14
O-12	Lena, Bykovskaya branch	0	-	41	108	34	6.3	1.2	4.1	0.76	0.18	0.76	0.16
O-13	Lena, Trofimovskay branch	0	-	37	110	32	6.0	1.1	4.3	0.74	0.37	1.8	0.28
O-14	Lena, Bykovskay branch	0	-	31	85	23	4.2	0.96	-	0.62	-	0.95	0.15
O-15	Lena, Bykovskay branch	0	-	35	96	26	5.7	0.60	-	0.88	-	2.1	0.20
O-16	Lena, Bykovskay branch	0	-	27	73	22	4.1	0.79	-	0.52	-	0.48	0.12
O-17	Lena, below delta	0	-	45	96	30	6.0	1.3	4.4	0.88	0.40	2.3	0.39
Average content of Lena River suspended sediments		0-3	20.3	40.0 +/- 7.6	93.8 +/- 13	31.7 +/- 6.1	5.9 +/- 1.0	1.06 +/- 0.32	4.85 +/- 0.9	0.80 +/- 0.17	0.35 +/- 0.11	1.60 +/- 0.73	0.27 +/- 0.1
Average content of the world river suspended sediments (1)		-	-	45	80	42	7.0	1.5	5.7	1.0	0.4	3	0.5
Average content of surface continental rocks (2		-	-	41	86	35	7.1	1.2	6.5	1.05	0.5	3.5	0.45
REEs in shale used for normalization (3)				41	83	38	7.5	1.61	6.35	1.23	0.63	3.51	0.61

Station	Location	Sample depth M	Turbidity mg/l	Sc	Cr	Cs	Co	Hf	Th	Ta	Fe	(La/Lu)n	(Ce/Ce*)
				ppm							%		
L-01-1	Lena, main stream	3	17.5	15	75	5.2	15	-	1	-	5.18	2.3	1.01
L-23-2	Lena, below delta	2	24.0	16	83	5.6	17	3.7	14	-	5.35	1.9	0.96
L-23-3	Lena, below delta	2	28.6	15	81	5.2	17	2.0	10	-	5.07	1.2	1.00
L-25-2	Lena, below delta	3	10.9	14	-	4.2	15	3.0	13	-	4.90	2.2	0.90
O-1	Lena, Bykovskaya branch	0	-	14	100	-	17	1.1	14.3	0.35	4.61	2.7	1.07
O-2	Lena, Sikstyah	0	-	18	130	4.0	20	4.5	7.2	0.20	3.58	-	-
O-3	Lena, Govorovskiy shoal	0	-	12	110	3.0	22	1.1	12.7	0.34	4.46	2.5	1.35
O-4	tr Beris	0	1.0	14	140	< 5.0	< 10	-	6.8	< 1.2	4.80	-	-
O-5	tr Bulun	0	2.1	15	140	3.7	10	1.8	12.2	< 0.6	7.06	1.8	1.03
O-6	tr Ayakit	0	4.0	6.2	48	0.9	5	< 1.5	6.5	< 0.6	-	1.7	0.98
O-7	tr Tegis	0	0.7	21	133	< 7	< 10	< 2.8	18.4	< 1.8	5.33	-	-
O-8	tr Khatystakh	0	0.6	14.5	86	< 8	< 18	< 4	< 9	< 2	4.91	-	-
O-9	tr Kengdey	0	3.4	12.8	67	4.3	10.3	3.1	12	< 0.6	5.00	-	-
O-10	Lena, main stream	30	-	7.5	75	1.9	17	1.3	8.5	0.27	2.92	3.3	1.32
O-12	Lena, Bykovskaya branch	0	-	10.3	76	2.2	21	2.6	4.2	0.41	4.40	3.8	1.00
O-13	Lena, Trofimovskay branch	0	-	12.1	63	2.2	21	2.3	13.7	0.28	4.45	2.0	1.51
O-14	Lena, Bykovskay branch	0	-	8	50	2.2	17	0.8	8.4	< 0.6	3.30	3.0	1.44
O-15	Lena, Bykovskay branch	0	-	10.4	45	1.9	17	2.1	11.2	< 0.6	4.05	2.6	1.46
O-16	Lena, Bykovskay branch	0	-	7.5	49	1.8	17	< 2	7.3	0.21	3.28	3.3	1.43
O-17	Lena, below delta	0	-	14.8	84	4.0	19	4.0	14.4	0.78	5.36	1.7	0.85
Average content of Lena River suspended sediments		0-3	20.3	12.5 +/- 3.2	78 +/- 23	3.3 +/- 1.4	18 +/- 2.1	2.4 +/- 1.1	10.8 +/- 3.1	0.35 +/- 0.17	4.35 +/- 0.78	2.2 +/- 0.7	1.18 +/- 0.23
Average content of the world river suspended sediments (1)		-	-	20	100	5.2	20	6	10	1.2	4.8	1.35	0.87
Average content of surface continental rocks (2		-	-	10.3	71	3.6	13	5	9.3	0.8	3.59	1.35	1.07
REEs in shale used for normalization (3)				-	-	-	-	-	-	-	-	-	-

(1) Gordeev, 1983, Martin, Gordeev, 1986
(2) Martin, Meybeck, 1979
(3) Shelkovitz, 1988

the elements to scandium in the SPM of the Lena and its tributaries normalized according to the ratios in SPM of average world rivers. The normalized ratios of practically all the elements show an overall constancy, the enrichment by Ce, Pb, Th and the depletion of Cd, Ta, Cu, Ni being within a factor of 2 (except Cd). The constancy of Sc-normalized ratios was reported by Thomas and Martin (1982) for other large rivers of the world (Yangtse, Mackenzie, Indus, Orinoco and Parana). It is worth noting the tendency that the SPM is slightly enriched by the LREE Ce and La whereas it is depleted of heavy rare-earth elements.

A relatively large range of variations of the normalized ratios characterizes the small tributaries, parcticularly the Ayakit. A very low content of Sc (about 6 ppm) is responsible for the fact that the ratios of the Ayakit exceed the ones of the Lena (Fig. 3).

There is a difference between the results of the AAS and INAA determinations for Fe and Co (Tables 1 and 2). The contents of both elements are on average by 30% higher in the filtered sediment samples (4.35% against 3.32% for Fe and 18 ppm against 13.3 ppm for Co). The most probable reason for this difference is that more

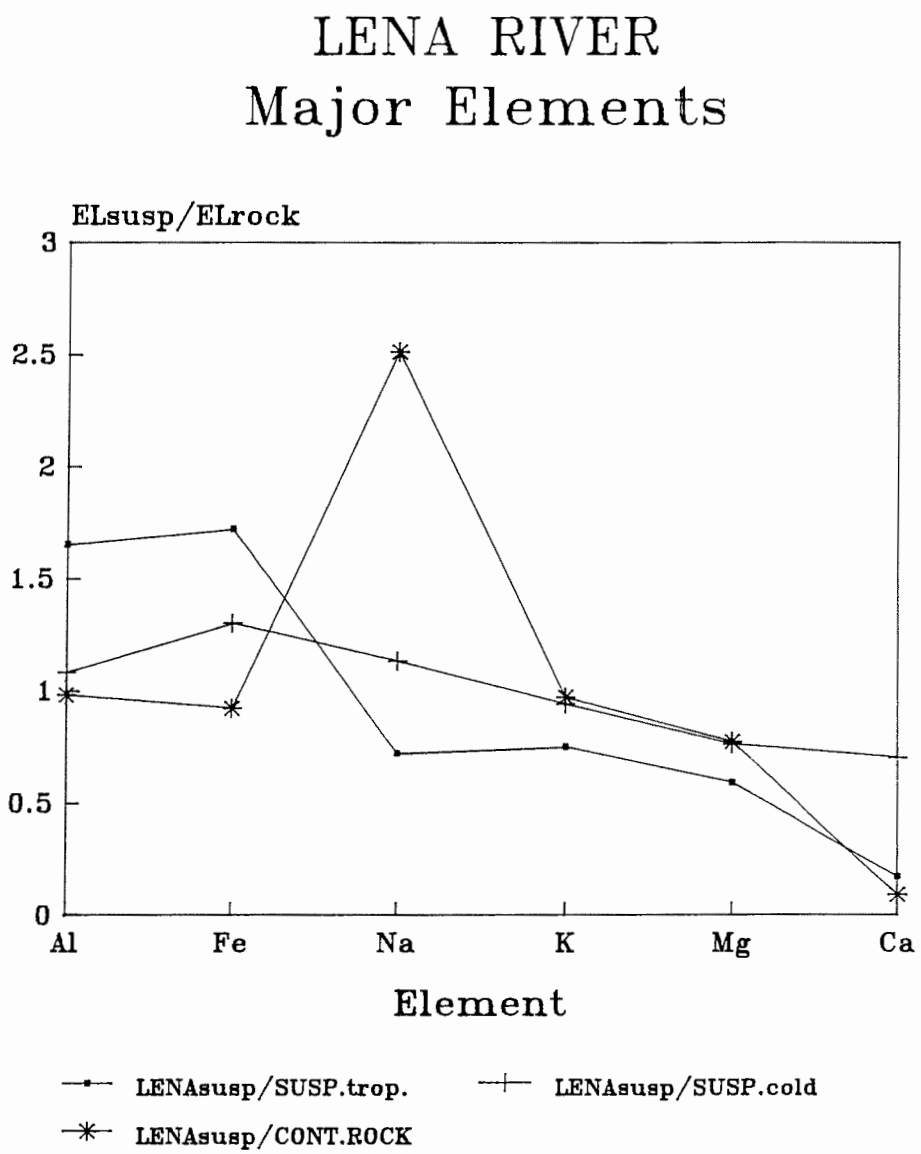

Fig.2. Ratios of major elements in the Lena River SPM (Lena susp.) to the same elements in the SPM of average world rivers, cold and temperate zones (Susp. cold.), tropical and warm arid zones (Susp. trop.) and surface continental rocks (CONT.ROCK).

fine SPM was retained on filters. Metal enrichment in the smallest grain size fractions is well known (Morozov et al., 1974; Gordeev, 1983).

Let us consider the behaviour of REEs in more detail. The shale-normalized REE pattern for the SPM of the Lena is shown in Fig. 4. It is apparent that river suspension does not have flat REE pattern relative to shales.The LREE enrichment factor defined as La shale-normalized ratio divided by Lu shale-normalized ratio (La/Lu)n is equal to 2.2 +- 0.7 for the Lena River. This value is in the range of LREE

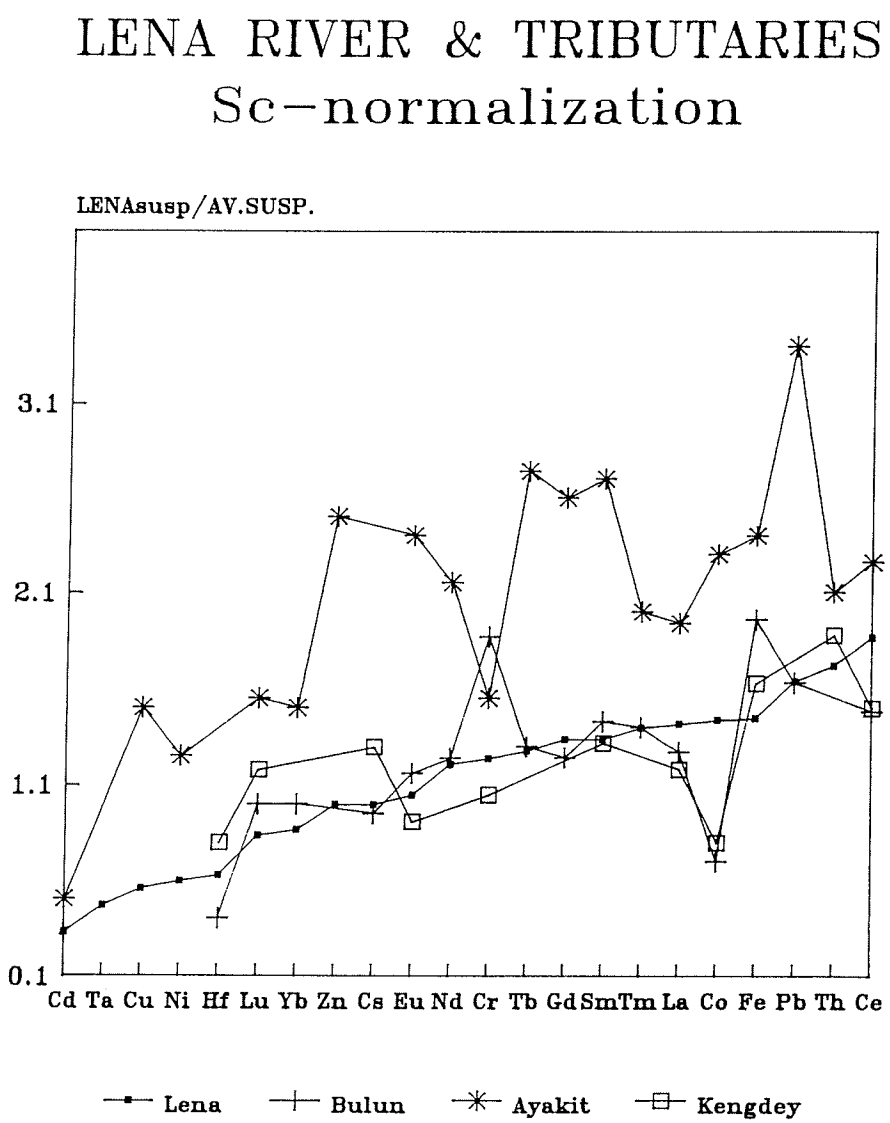

Fig.3. Sc - normalized elements in the Lena River SPM and its small tributaries (Bulun, Ayakit and Kengdey)

enrichment factors for many large rivers (Sholkovitz, 1988; Goldstein, Jacobsen, 1988; Elderfield et al., 1990). The same tendency is observed for the small tributaries although analytical data about them are incomplete (Table 2).

Again, the small tributaries show a relatively large range in the absolute abundance of elements. A large degree of variation in the REE patterns for the smaller rivers was demonstrated by Goldstein and Jacobsen (1988). These authors attributed the variations to the variability of the mineralogy of SPM in small rivers. Fig. 5 illustrates this situation very well for the small tributaries of the Lena. The

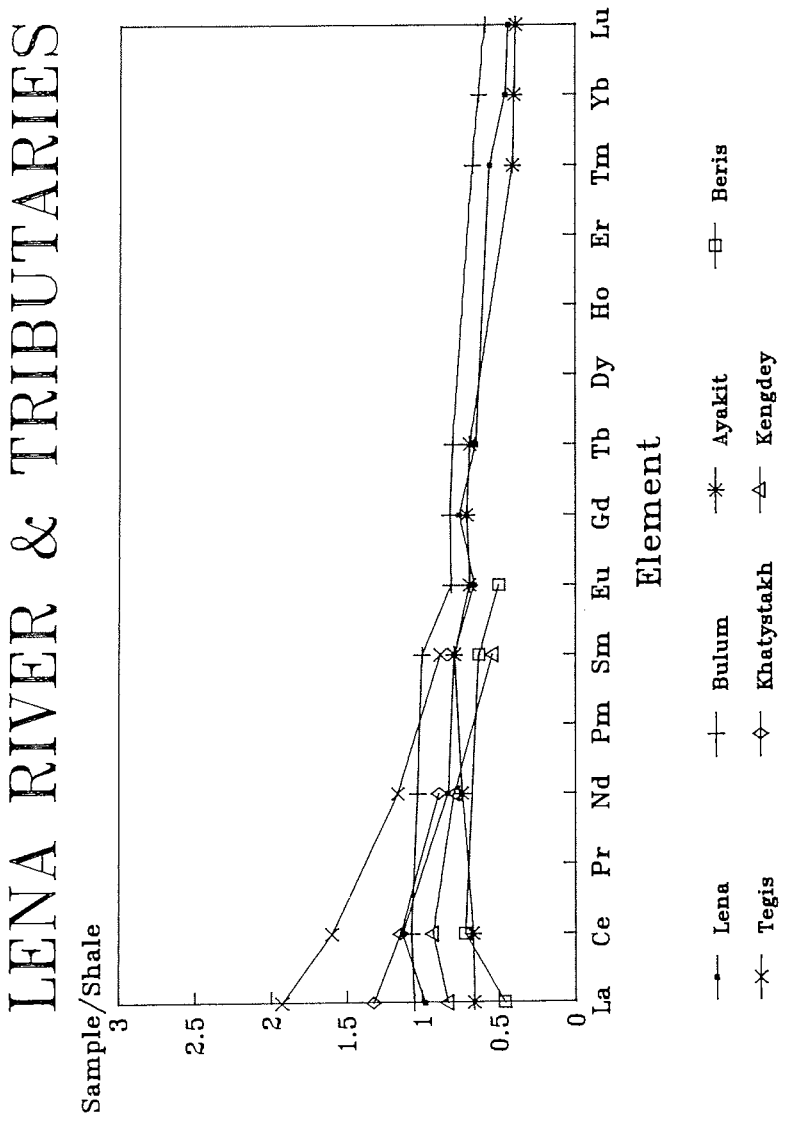

Fig.4. Shale-normalized REE patterns for the Lena River SPM and its small tributaries (Bulun, Ayakit, Beris, Tegis, Khatystakh and Kengdey).

Fe/La ratio for the Lena is different from the one for the tributaries. The dot for the Ayakit is the nearest to the Lena line due to the similarity of the SPM mineralogy of both rivers (Serova, Gorbunova, 1995). The average SPM composition shows for the Lena a slight positive anomaly of cerium ($Ce/Ce^* = 3Ce(n)/2La(n)+Sm(n) = 1.18+- 0.23$). It is worth noting that only 6 samples among 13 show an apparent positive Ce anomaly (4 samples - 0-13, 0-14, 0-15, 0-16 - in the delta) (Table 2). It is difficult to say at present whether this fact is regular or accidental.

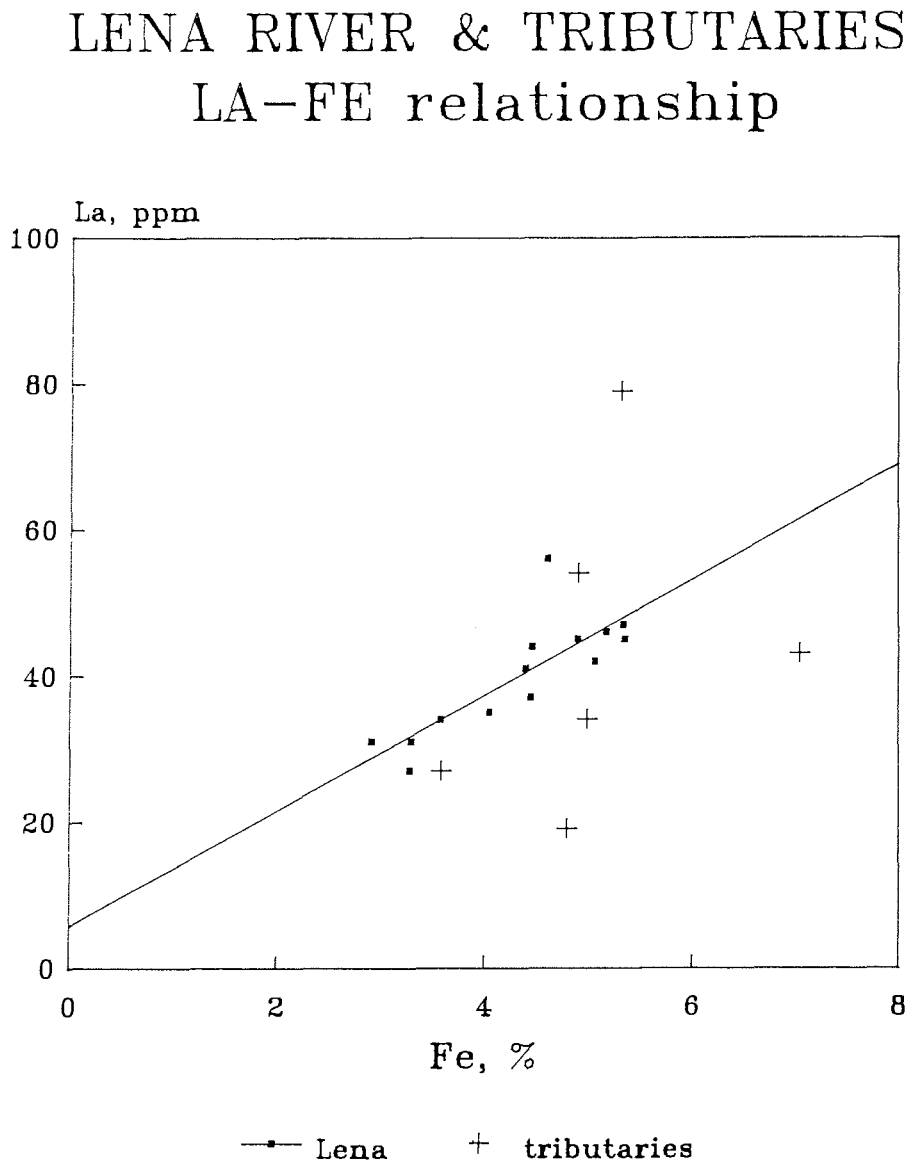

Fig.5. Parcticulate La versus parcticulate Fe in the SPM of the Lena River and its small tributaries

2. MIXING ZONE BETWEEN RIVER AND SEA WATERS.

Table 3 and Fig. 6 and 7 summarize the available data on the mixing zone. In the main mixing zone of the Lena River a three-layer stratification was defined with a 4-13 m thick brackish surface layer overlying intermediate and bottom water masses (Letolle et al., 1993). Deep waters have a higher salinity. At the same salinity, however, the bottom water contains more SPM than surface water. A high turbidity of near-bottom waters is a result of sedimentation from upper waters and

resuspension caused by bottom currents.

Unfortunately, very low contents of SPM in brackish surface waters did not allow to determine the concentrations of many trace elements, parcticulary of HREE at high salinities.

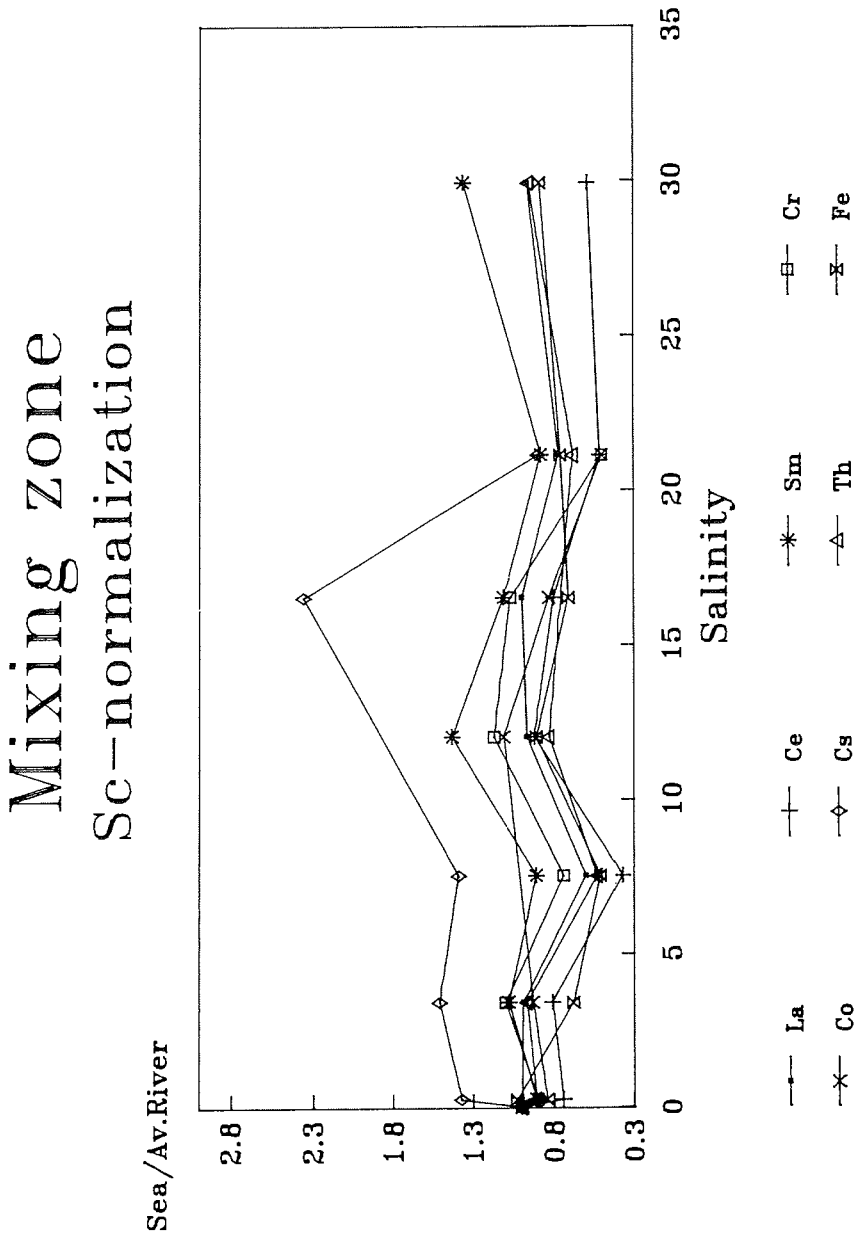

Fig.6. Sc - normalized elements in the mixing zone versus salinity

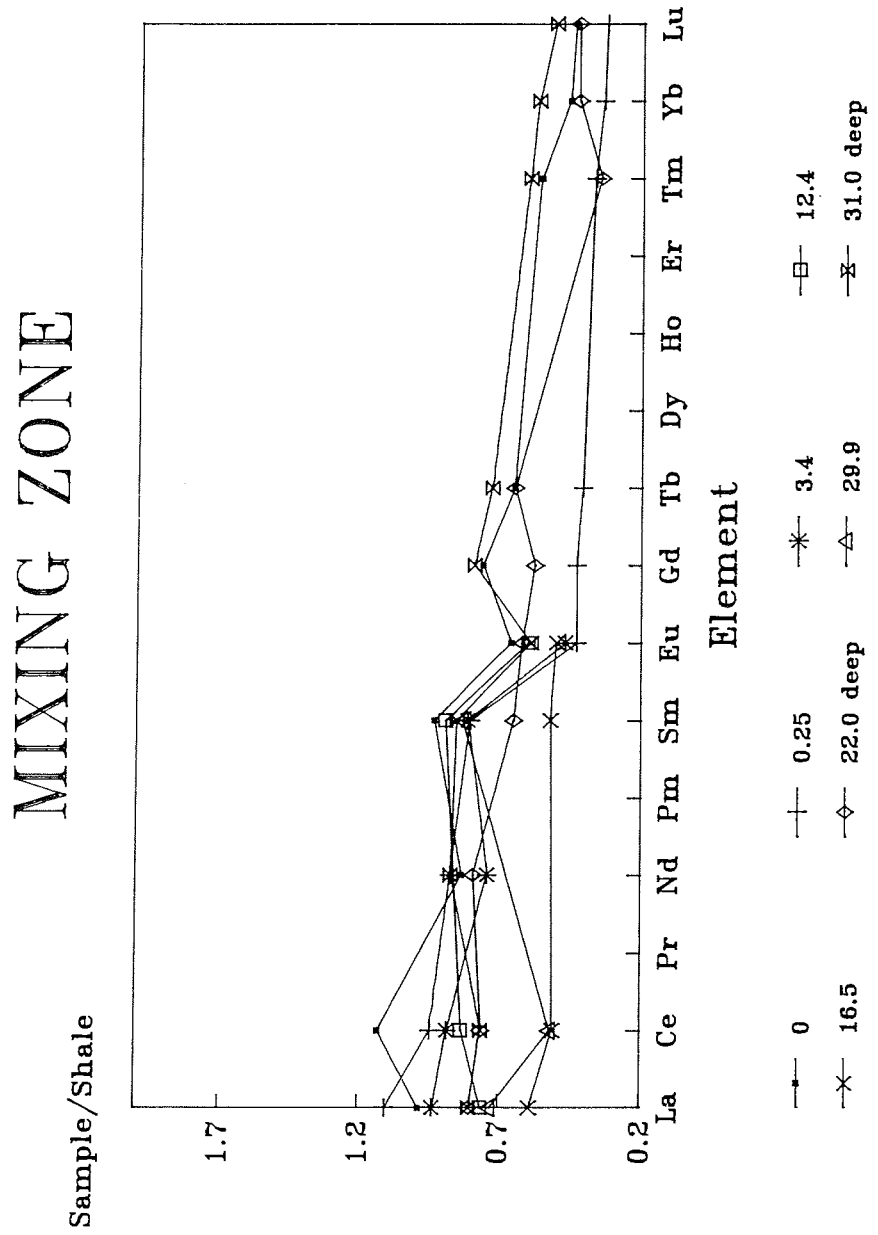

Fig.7. Shale - normalized REE patterns in the mixing zone.

In general, the element concentrations slightly decrease with increasing salinity (Table 3). This parcticularly holds true for the LREE (La, Ce). The same trend was found in the estuarine zones of other rivers (Martin et al., 1976; Somajalulu et al., 1993). It is a more likely explanation that particles in fresh water are diluted by

particles in sea water having lower contents of trace elements and a higher content of POC.

Cauwet and Sidorov (1995) reported the following results for POC contents: SPM in rivers amounts to 3.1-5.9% (3.36% - Table 1). In brackish surface waters with a salinity of 10-20% it ranges from 12 to 20 %, and in saline bottom waters from 3.0 to 4.3%.

The fact that the content of Sc slightly decreased with increasing salinity confirms this conclusion as well. The Sc-normalized metals (Fig. 6), although scattered, do not show significant variations with increasing salinity. This behaviour possibly indicates a low affinity of the analyzed trace elements for marine biogenic material.

A different picture was found in the Amazon estuary where light and medium lantanides (La, Ce, Sm) are accumulated in SPM at a salinity of 10-15 pro mille (plankton bloom) with an enrichment factor of about 2.0-2.5 as compared to river values (Gordeev et al., 1985). All ten REE were only determined in near-bottom SPM at high salinities up to 31 pro mille (two bottom lines in Table 3). The shale-normalized REE pattern for near-bottom SPM at salinities of about 22 pro mille and 31 pro mille is very similar to the river pattern (Fig. 7) although the enrichment factor for LREE decreases from 2.2 to 1.6. Though it is not quite correct to compare the REE patterns for surface water samples with a low salinity with the near bottom patterns because of different water masses, the very close similarities between them indicate at least a river source for near-bottom SPM. The admixture of resuspended bottom sediments is a possible explanation for the (La/Lu)n decrease in the near-bottom suspension as compared to river SPM.

Available data show that the Ce/Ce* ratio is nearly equal in surface suspension at low salinities and in near-bottom sediments at a salinity of 22-31 pro mille.

One should also note that dissolved heavy metals (Cu, Zn, Pb, Cd, Ni) are practically conservative in the Lena mixing zone and even dissolved iron shows a very slow removal process (Martin et al., 1993).

Conclusions

Geochemical studies of the SPM of one of the largest Arctic rivers - the Lena River - in its lower reach, some of its small tributaries and in the mixing zone with the Laptev Sea waters have shown that:

1. The mineralogical composition of the river SPM is a very typical one of rivers in cold climatic zones (50-70% of quartz and feldspars and clay minerals with a predominance of illite, chlorite and kaolinite).

2. The contents of the major elements of the SPM are characterized by a two-fold Na enrichment and by a depletion of Ca by one order as compared to surface continental rocks. Carbonate weathering in the basin and the abundance of Na-K feldspars are supposed to be the main reasons of the Ca depletion.

3. The analysis of 21 trace elements including 10 REEs has revealed that the suspension of the Lena is depleted of Cd, Ta, Cu and Ni whereas it is enriched by Ce, Pb and Th, if compared to average concentrations in the world's major rivers. Both the enrichment and the depletion are well within a factor of 2, except Cd. Relatively large variations were found in the small tributaries. The data show that the scattering is probably attributable to variations in the mineralogy of bedrocks in the drainage sub-basins, whereas the enormous Lena River basin integrates geological variations and averages the composition of water-borne materials.

4. The shale-normalized REE pattern is not flat. The river SPM has a relatively uniform REE pattern and is HREE depleted relative to shales with an enrichment

factor (La/Lu)n = 2.2 +- 0.7. Previously published REE patterns for the SPM of the Amazon, Ganges, Mekong, Congo, Gironde and other rivers (Gordeev et al., 1985; Sholkovitz, 1988; Goldstein, Jacobsen, 1988; Elderfield et al., 1990) have shown a roughly similar overall pattern.

5. Our limited data for the mixing zone between river and sea water show a nearly constant trend for Fe and some trace elements. The Sc-normalized metals do not show significant variations with increasing salinity, that means a low affinity of the analyzed trace elements for the marine biogenic material.

6. The shale-normalized REE pattern for the near-bottom SPM in the Laptev Sea with a salinity of 22-31 pro mille is very similar to the river pattern. It is probably an indicator for the river source of the near-bottom SPM.

Acknowledgments

The authors are very grateful to Prof. A.P. Lisitsyn and Dr. V.M. Kuptsov for providing a part of the SPM samples of the Lena River and its small tributaries. We also express our gratitude to Prof. J.-M. Martin and Dr. W.W. Huang from the Institute of Marine Biogeochemistry (France) for the help in the AAS determinations. Funds for this work were provided by the Russian Foundation for Fundamental Research under grant no 94-05-16766.

References

Antonov, V.S., 1967. The Mouth Area of the Lena (the Hydrographic Review). Gidrometeoizdat, Leningrad, 107 pp. (in Russian).

Cauwet, G., Sidorov I.S., 1995. Biogeochemistry of the Lena River: organic carbon and nutrients distribution. Mar. Chem. (in press).

Darby, D.A., Naidu, A.S., Mowatt ,T.C. Jones, G., 1989 Sediment composition and sedimentary processes in the Artic Ocean. In: Y.Herman (Editor), The Arctic Seas. Van Nostrand, New York, pp.657-720.

Drever, J.I., 1988. The Geochemistry of natural waters. Second Edition. Prentice Hall, Englewood Cliffs, New Jersey, 438 pp. Elderfield H., Upstill-Goddard R. and Sholkovitz E.R., 1990. The rare earth elements in rivers, estuaries and coastal seas and their significance to the composition of ocean waters. Geochim. Cosmochim. Acta, 54: 971-991.

Goldstein, S.J., Jacobsen, S.B., 1988. Rare earth elements in river waters. Earth Planet. Sci. Lett., 89: 35-47.

Gordeev, V.V., 1983. River Run-off into the Ocean and its Geochemical Aspects. Moscow, Nauka. 160 pp. (in Russian).

Gordeev, V.V., Lisitzin, A.P., 1978. Average chemical composition of suspended sediments in the rivers of world and the river supply of sediment materials to the ocean. Dokl. Akad. Nauk, SSSR, T. 238: 225-228. (in Russian).

Gordeev, V.V., Miklishansky, A.Z., Migdisov, A.A., Artemyev, V.E., 1985. Rare Element Distribution in the Surface Suspended Material of the Amazon River, some of its Tributaries and Estuary. In: E. Degens, S. Kempe and H. Herrera, eds. Transport of Carbon and Minerals in Major World Rivers. Mit. Geol.Palaeont.Inst. Univ. Hamburg, 58: pp 225-244.

Gordeev, V.V., Sidorov, I.S., 1993. Concentrations of major elements and their outflow into the Laptev Sea by the Lena River. Mar. Chem., 43: 33-45.

Konovalov, G.S., 1959. Trace elements outflow by the main rivers of the USSR. Dokl. Akad. Nauk SSSR, T.129: 912-915. (in Russian).

Konovalov, G.S., Ivanova, A.A., Kolesnikova, T.Kh., 1968. Dispersed and rare elements dissolved in water and contained in suspended materials of the main rivers of the USSR. In: N.M.Strakhov (Editor), Geochemistry of sedimentary rocks and ores. Nauka, Moscow, pp.72-87. (in Russian).

Kontorovitch, A.E., 1968. Migration forms of elements in rivers of humidic zone (after data for the Western Siberia and other regions). In: N.M. Strakhov (Editor), Geochemistry of sedimentary rocks and ores. Nauka, Moscow, pp. 88-102. (in Russian).

Letolle, R., Martin, J-M., Thomas, A.J., Gordeev, V.V., Gusarova, S.P., Sidorov, I.S., 1993. O-18 abundance and dissolved silicate in the Lena delta and Laptev Sea (Russia). Mar. Chem., 43: 47-64.

Martin, J.-M., Hogdahl, O., Philippot, J.C., 1976. Rare earth element supply to the Ocean. J.Geophys. Res., 81: 3119-3124.

Martin, J.-M., Meybeck, M., 1979. Elemental mass-balance of material carried by major world rivers. Mar.Chem., 7:173-206.

Martin, J.-M., Whitfield, M., 1983. The significance of the river input of chemical elements to the ocean. In: C.S.Wong, E.Boyle, K.W.Bruland. J.D.Burton and E.D.Goldberg (Editors). Trace Metals in Seawater. New York and London: Plenum Press, pp.265-296.

Martin, J.-M., Gordeev, V.V., 1986. River input to ocean systems: a reassessment. In: Estuarine Processes: An Application to the Tagus Estuary. Proc. UNESCO/IOC/CNA workshop. Paris, UNESCO, pp.203-240.

Martin, J.-M., Windom, H.L., 1991. Present ant Future Roles of Ocean Margins in Regulating Marine Biogeochemical Cycles of Trace Elements. In: R.F.C.Mantoura, J.-M. Martin and R.Wollast (Editors), Ocean margins processes in Global Change. John Wiley and Sons, Ltd., pp.45-67.

Martin, J.-M., Guan, D.M., Elbaz-Poulichet, F., Thomas, A.J., Gordeev, V.V., 1993. Preliminary assessment of the distributions of some trace elements (As, Cd, Cu, Fe, Ni, Pb and Zn) in a pristine aquatic environment: the Lena River estuary (Russia). Mar. Chem., 43: 185-199.

Meybeck, M., 1984. Les Fleuves et le cycle geochimique des elements. These de Doctorat d'Etat, Univ. Paris VI, 500pp.

Meybeck, M., 1988. How to establish and use world budgets of riverine materials. In: A.Lerman and M. Meybeck (Editors), Physical and Chemical Weathering in Geochemical Cycles. Kluver Academic Publishers, pp.247-272.

Morozov, N.P., Baturin, G.N., Gordeev, V.V., Gurvich, E.G., 1974. About composition of suspended matter and bottom sediments in the mouths of the North Dvina, the Mezen, the Pechora and the Ob Rivers. Hydrochemical Materials, 60: 60-73. (in Russian).

Nesterova, I.L., 1960. Migration forms of elements in the Ob river. Geochemistry, N4: 355-362. (in Russian).

Serova, V.V., Gorbunova, Z.N., 1995. Mineral composition of soils, aerosols, suspended sediments and bottom sediments from the Lena River basin and the Laptev Sea. Oceanology (in press) (in Russian).

Sholkovitz, R.E., 1988. Rare earth elements in the sediments of the North Atlantic Ocean, Amazon delta and East China Sea: reinterpretation of terrigenous input patterns to the oceans. Amer. J. Sci. 288: 236-281.

Somayajulu, B.L.K., Martin, J.-M., Eisma, D., Thomas, A.J., Borole, D.V., Rao, K.S., 1993. Geochemical Studies in the Godavari estuary, India. Mar. Chem., 43: 83-93.

Thomas, A.J., Martin, J.-M., 1982. Chemical Composition of River Suspended Sediment: Yangtse, Mackenzie, Indus, Orinoco, Parana and French Rivers (Seine, Loire, Garonne, Dordogne, Rhone). In: E. Degens and S. Kempe eds., Transport of Carbon and Minerals in Major World Rivers. Mit. Geol. Palaeontol. Inst. Univ. Hamburg, 52: pp.555-564.

Ugolini, F.C., 1986. Processes and rates of weathring in cold and polar desert environment. In: S.M. Coleman and D.P. Dethier (Editors), Rates of Chemical Weathering of Rocks and Minerals. Academic Press, London, pp.193-235.

STABLE CARBON ISOTOPE RATIOS IN THE WATERS OF THE LAPTEV SEA/ SEPT. 94

H. Erlenkeuser and the TRANSDRIFT II Shipboard Scientific Party
Institut für Reine und Angewandte Kernphysik, C14-Lab., Universität Kiel, Germany

Abstract

Surface and bottom water samples from 5 transects in the Laptev Sea were analysed for dissolved inorganic carbon (DIC) and stable carbon isotopes. Both parameters show a pronounced spatial pattern in the surface waters, which is related to salinity and reflects the influence of the riverine waters and the inherent low $^{13}C/^{12}C$-ratio of the DIC discharged into the Laptev Sea. Also the bottom waters of the Laptev Sea respond to the impact of the riverine waters at the surface as the stable carbon isotope composition of the subhalocline waters is significantly affected by remineralization of (isotopically light) organic matter either produced by plankton or discharged by the Lena river. The light isotope signature culminates off the river estuary. All $\delta^{13}C$ values are far from isotopic equilibrium with the atmosphere.

Introduction

The stable isotope ratios of the dissolved inorganic carbon (DIC) in marine waters provide an interesting means to study the relative importance of biological and physical processes which affect the carbon balance in the aquatic environment. The large carbon isotope fractionation upon assimilation of the carbon dioxide by planktonic algae in the surface waters and remineralization and feed-back of this ^{13}C-depleted carbon to the inorganic carbon pool in the deeper layers have great potential for carbon flux studies. In the Laptev Sea, the discharge of isotopically light riverine DIC will exert an additional major influence on the carbon isotopic composition of the waters.

The resulting vertical and lateral isotope pattern is related to the hydrographic settings and oceanographic processes. Understanding the characteristics of this pattern is of a high paleoclimatic interest. First, because the stable carbon isotope situation is preserved in the biogenic carbonate shells of foraminifera, bivalves, and ostracods, thus providing a means to reconstruct the history of the regional hydrography in the past from the sediments. Second, because the Laptev Sea is a significant source of Artic Ocean Surface waters, of which the isotopic characteristics may be traced and used as a paleoclimatic signal 'downstream' through the Fram Strait far to the south.

In this work we present a first set of stable isotope data for dissolved inorganic carbon in the Laptev Sea waters, and briefly discuss the major processes affecting their signature.

Materials and Methods

The water samples were collected from Sept. 9 to 19, 1994, on the cruise TRANSDRIFT II of RV Professor Multanovsky to the Laptev Sea. The sample positions are shown in Fig. 1. Usually, two samples were collected from each station, one from the surface waters at 2 m depth and one below the halocline, which ranged in thickness from a few to more than 20 meters and on the average was found between 7 and 17 m water depth. Actually the stratification of the water column is complex, and the vertical structure of the halocline, which partly revealed several

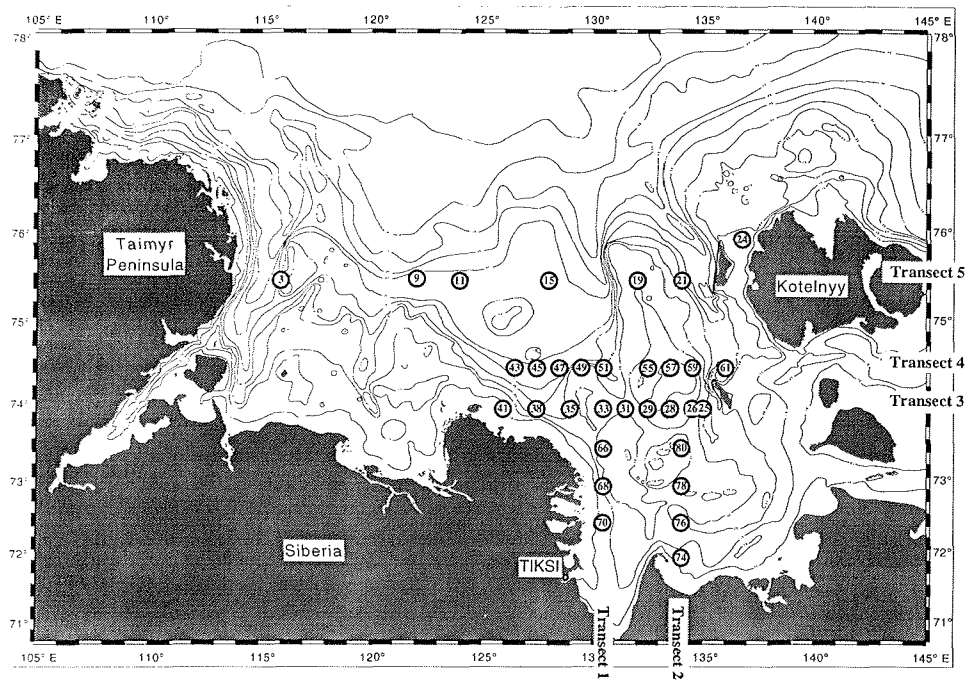

Fig. 1. Water sampling stations in the Laptev Sea during TRANSDRIFT II.

distinct layers, is highly variable, depending on the location (Karpiy et al., 1994). Occasionally, the 'deep' water samples originate from the mixed surface layer or from the lower halocline waters. - Salinities at the sampling stations were measured by the Arctic and Antarctic Research Institute/ Russia.

A water aliquot from the sampler bottle was gently filled into a 100 ml glass flask with ground neck through a plastic tube dipped down to the bottom of the flask to avoid any vigorous agitation of the sample water and entrainment of air bubbles. The samples were poisoned by 0,2 ml of saturated H_9Cl_2 solution (69 g/l at 20°C) in order to stop microbial metabolism. A slightly greased (silicon high vacuum grease) ground stopper (glassware) was used to seal the bottle and was held in position by a tightly wrapped tape. The sample flasks were stored in darkness at about 4°C.

For preparation the sample water was transferred, in a closed system, by means of high purity nitrogen gas at slightly enhanced pressure through a 0,2 µm filter into a glass reactor vessel and acidified with 1 ml of 30% H_3PO_4. CO_2 was stripped with a total of about 1200 ml (NTP) high purity nitrogen supplied at a rate of 100 ml/min at a pressure of 1.1 bar. Water vapour in the outflowing gas was frozen at ca. -70°C in a dry-ice/ ethanol trap, and CO_2 was retained from the stripper gas in a 3-fold curled multiloop trap at liquid nitrogen temperature. Minor CO_2 quantities entrapped at -70°C were distilled from the ice by warming the trap and re-freezing the water vapour under vacuum, and were combined with the main fraction. The total CO_2 yield is better than 99.5 %.

Absolute CO_2 yield was determined by the gas pressure measured with a high

precision solid state pressure gauge in a measuring volume at known temperature. Sample water amount used was determined by weighing the full and emptied flask. Relative accuracy of the inorganic carbon concentration is about 0.5 %.

The sample CO_2 was frozen into a glass flask (ca. 70 ml) with a high-vacuum stop cock, and analysed for $\delta^{13}C$ on a Finnigan-Delta E isotope mass spectrometer equipped with a multiport sample gas inlet facility.

The reproducibility of the analytical process was repeatedly checked using an internal isotope standard for dissolved inorganic carbon. The standard is prepared as a 5 l quantity from distilled water carefully freed of allochthonous CO_2 and a commercial analytical grade Na_2CO_3. For additional isotope control, aliquots of the carbonate powder were analysed on the Carbo Kiel/ MAT 251 carbonate isotope analytical facility. Reproducibility of the $\delta^{13}C$ results from the DIC isotope standard was 0.1 ‰ or better.

Results

The results are presented in Fig. 2. The data are arranged according to their sampling transects, showing the south-western group (transect 1) first and proceeding from south to north. For each transect, the station results are shown from south to north (transect 1 and 2) respectively west to east (transect 3 to 5). For each station, the surface sample is shown first (open circle), followed by the deeper water (triangle). The results from each station are linked by a dotted line, all surface samples of a transect are additionally connected for greater graphical transparency. In the sample information bar below Fig. 2a, station number, sample depth, and for each deepest sample of a station, total water depth are given. Fig. 2a displays the DIC concentrations, Fig.2b the $\delta^{13}C$ results. DIC values of two deep water samples were omitted because of gas losses during preparation which, however, did not affect the isotope ratios. On station 74, the deep water data ($\delta^{13}C$=-16.55‰, DIC=4.5 mMol/l) were probably indicative of a birthday's champagne rather than the natural sample. These data are not shown in the figures.

The DIC concentrations of the surface waters (Fig. 2a) range between 1 mMol/l on SW transect 1 in front of the Lena estuary to about 1.9 mMol/l in the NW (transect 5). DIC in the subsurface samples is generally higher than at the surface. In most of the deep waters below the halocline DIC closely groups around 2.2 mMol/l, but sampling depth was variable and some of the 'deep' waters were actually collected above the halocline.

$\delta^{13}C$ reveals as a general trend higher values with increasing distance from the freshwater source(s). This trend is seen in both the surface and deep water samples. At the southern stations (transects 1 and 2) the ^{13}C-depletion of the surface samples clearly exceeds that of the bottom waters. Lightest values occur off the Lena mouth on transect 1. Further NW, on transects 4 and 5, surface samples tend to be enriched in ^{13}C as compared to the bottom water layer.

Discussion

As the waters of the Laptev Sea are strongly influenced by the discharge of several large rivers with their characteristic DIC content and $\delta^{13}C$ signature, both the DIC and its stable carbon isotope composition will be affected by the relative contributions from marine and riverine sources. Biological carbon consumption and remineralization processes exert another major influence on the pool of dissolved inorganic carbon. Additionally, CO_2 exchange with the atmosphere may alter the

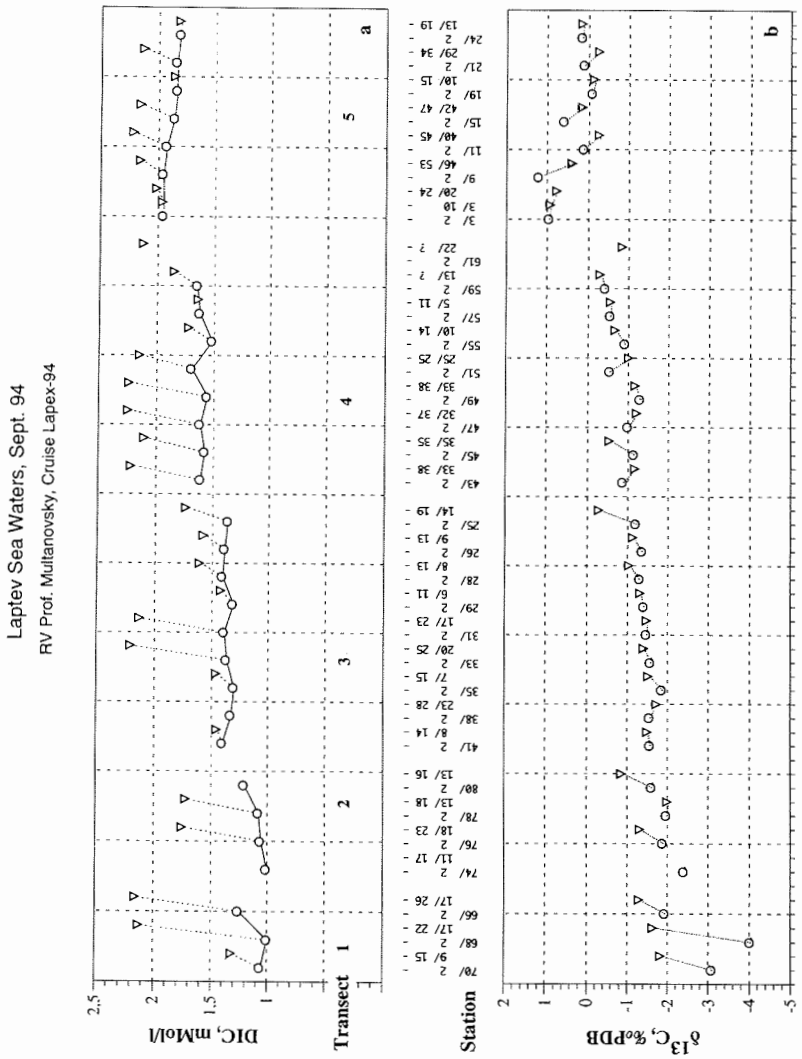

Fig. 2. Dissolved inorganic carbon (DIC; Fig. 2a) and its stable carbon isotope composition ($\delta^{13}C$; Fig. 2b) in the Laptev Sea/ Sept. 94. The station identifier gives the station number, sampling depth (m) of the surface water samples (open circles), sampling depth (m) of the deep water samples (triangles), and total water depth. Transect numbers refer to Fig. 1.

carbon isotope pattern with time and location. The effect of the riverine waters is best displayed in relation to salinity (Fig.3a and b). The DIC values (Fig. 3b) closely group around a linear regression line which intercepts the ordinate at zero-salinity at a DIC value about 0.7 mMol/l. This strong relation between DIC and salinity is thought to reflect the dominant diluting effect of the riverine waters. Dilution by sea ice melting, which should result in an intercept at 0 mMol/l, appears to be of minor importance. Also from a rough mass balance consideration, the effect of, say, 1 m of melted sea ice on 10 m mixed surface waters, would add to the scatter rather than be discernible in our data set.

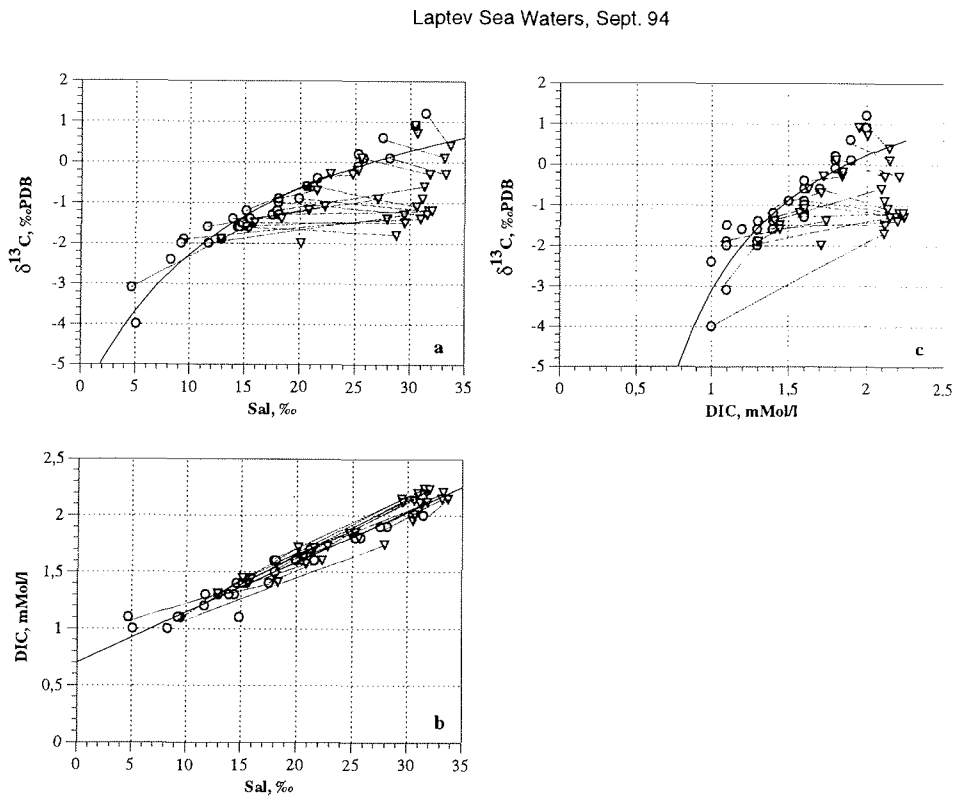

Fig. 3. $\delta^{13}C$ and DIC data from the Laptev Sea waters/ Sep.94, plotted against salinity (Fig. 3a and Fig. 3b), and $\delta^{13}C$ versus DIC (Fig. 3c). Open circles denote surface waters (2 m depth), triangles mark the deeper waters (s. Fig 1 for sampling depths).

The dominance of the riverine waters as diluting agent is also evident from the $\delta^{13}C$ vs. salinity plot (Fig. 3a). Almost all surface waters and about half of the subsurface samples closely relate to a regression line which would intercept the ordinate (sal=0) at $\delta^{13}C$ about -3.5 to -4 ‰ if the regression is considered to be linear.

Low $\delta^{13}C$-values are typical of fresh waters as the DIC commonly forms from dissolution of fossil carbonates of marine origin ($\delta^{13}C$ about 0 ‰) by - isotopically much lighter - soil-CO_2 derived from degradation of organic plant litter with $\delta^{13}C$ about -25 ‰ (e.g., Moser and Rauert, 1980). Subsequent CO_2 exchange of river waters and lakes with the atmosphere makes the $\delta^{13}C$ of the DIC gradually increase towards values as determined by the isotopic equilibrium conditions (Emrich et al, 1970; Mook, 1970). For instance, Mook (l.c.) reports $\delta^{13}C$-figures between -10 ‰ and -6 ‰ for rivers in the Netherlands.

Theoretically, the relation of $\delta^{13}C$ vs. salinity is non-linear for waters mixed from

different sources. Just for illustrating the shape of the model curve, a non-optimized calculation is shown in Fig. 3. The parameters of the source waters of this 2-source mixing model are DIC=2.3 mMol/l, $\delta^{13}C$=0.6 ‰, sal=35 ‰ for the marine source and 0.7 mMol/l, -6 ‰, 0 ‰, respectively, for the riverine source. Dilution of salt content by melting sea ice would not have modified the carbon isotopes and only might have produced some of the small scatter in the (salinity) data.

Interestingly, a number of deep-water samples from all transects (except no. 2) forms a second group of data points distinctly separated from the upper waters. The $\delta^{13}C$ range of this group amounts to about 2 ‰ and is almost as wide as for the first set, though salinity is confined to a much smaller interval (27 to 34 ‰). These data also show a well defined, but much steeper regression with salinity. On closer inspection, the lowest $\delta^{13}C$ values relate to the inner transects (1 and 3) while the outer stations reveal a much lower $\delta^{13}C$ offset from the surface water line. All samples of the second ensemble are closely grouped about the same DIC-value (2.1 mMol/l; Fig. 3c).

As a first explanation of these results, i.e. the comparatively steep relationship of $\delta^{13}C$ vs. salinity and the independence of $\delta^{13}C$ from the DIC content, we hypothesise that the expected variation (according to surface water data) of DIC and $\delta^{13}C$ with the minor variation of salinity still seen below the halocline on approach to the Lena river estuary, is superimposed by an increasing contribution of CO_2 remineralized from organic matter.

Due to the depleted ^{13}C-content of organic carbon, a comparatively small addition of CO_2 from this source to the DIC will effectively lower the $\delta^{13}C$ (and simultaneously increase the DIC content). This contribution of organogenic CO_2 to the bottom water may relate to sample location. It is apparently higher for the inner stations, either because the water renewal is less efficient there, because planktonic productivity responds to the concentration of nutrients, particularly silica, discharged by the Lena and hence relates to surface salinity, or because the contribution of riverine particulate organic matter settling to the sea floor is highest near the mouth. Also the possible release of CO_2 from oxidation of isotopically highly depleted methane, which may form in the sediments by fermentation of organic material, may exhibit a lateral pattern in response to the distribution of the riverine load and affect the inner waters more than the waters at the outer shelf.

A rough numerical estimate may verify the basic idea. Reducing the $\delta^{13}C$ of the DIC from 0 to -2 ‰ by CO_2 from oxidative degradation of planktonic matter (of a presumed $\delta^{13}C$ = -20 ‰) will be paralleled by a DIC increase of 10 %, i.e. roughly by 0.2 mMol/l. This amount just balances the DIC reduction expected on the basis of the DIC-salinity relation for the surface waters (Fig. 3b), when the bottom water salinity change from 34 ‰ at the outer transect 5 to 29 ‰ at the inner stations is taken into account. CO_2 from oxidation of biogenic methane at -40 to -80 ‰ would exert a half to quarter of that effect on the DIC given the same isotope shift (-2 ‰), though it is questionable if the rates are high enough to produce an effect as large as seen in the bottom waters.

Riverine DIC and remineralization of organic matter thus appear to play the major role for the inorganic carbon isotope composition of the surface waters and the sub-halocline waters, respectively, of the Laptev Sea. Isotopic enrichment due to DIC consumption by planktonic algae could have another possibly important effect on the isotopic signature of the surface waters. Since the diagenetic processes in the bottom water appear to be related to the lateral dispersion of the

riverine waters, this factor may control the productivity in the surface layer as well (Petrjaschev, 1994) and make the isotopic effect arising from planktonic productivity, a more or less linear relation of nutrient availability, i.e. salinity. If so, the interference of the two relationships, i.e. fraction of riverine water and productivity, with salinity will hardly allow us to evaluate the isotopic effect of planktonic processes from our data set alone. Indeed, supplementing the mixing model shown in Fig.3, for isotopically fractionated DIC consumption linearly related to salinity, would not generally change the shape of the calculated curves and moreover allows a broad range for the values of the parameter set-up. This situation clearly deserves a closer evaluation. A preliminary result of these simple model calculations is, however, that significantly higher riverine DIC concentrations and lower $\delta^{13}C$-values are allowed than is possible when the planktonic impact is negotiated. For instance, a reasonable fit was obtained with DIC = 1 mMol/l and $\delta^{13}C$ = -10 ‰ for the river water source. However, these figures are mere samples and have no actual significance.

Moreover there are clear systematic deviations from the simple model curves. So higher than expected $\delta^{13}C$ values are found at both ends of the salinity range and probably are indicative of local peculiarities not yet taken into account. One of the effects to consider is CO_2 exchange with the atmosphere. The exchange rate, in the order of 10 Mol/m^2 a for open waters, results in an exchange time of 2 years per 10 m water column, a time probably much too long to be effective, if the seasonal length of the sea ice cover is taken into account. So we expect the gas exchange with the atmosphere to be a less important process. Indeed, all of the $\delta^{13}C$ values found in the Laptev Sea waters are far from isotopic equilibrium with atmospheric CO_2. The expected equilibrium value is about +2.5 ‰ at 0°C (Emrich et al., 1970; regarding the bicarbonate as the overwhelming component of the DIC and assuming $\delta^{13}C$= -8 ‰ for the atmospheric gas).

Conclusions

Due to the riverine waters and the inherent low $^{13}C/^{12}C$-ratio of the DIC discharged to the Laptev Sea, the stable carbon isotope composition of the surface waters is pronouncedly reduced as compared to the Arctic Ocean. The lateral pattern of the surface water $\delta^{13}C$ is related to salinity. This provides the potentiality to study the hydrographical history of the area and the paleoclimatic background from the isotope signature preserved in the shells of shallow-dwelling carbonate producers preserved in the sediments.

Also the bottom waters of the Laptev Sea respond to the impact of the riverine waters at the surface. The stable carbon isotope composition of the subhalocline waters is significantly affected by remineralization of organic matter. The accumulation of organogenic CO_2 in the bottom water layer is highest in the inner (southern) part of the Laptev Sea and may relate to the lateral pattern of either planktonic production or river discharge of particulate organic matter. So also the benthic carbonate producers such as foraminifera or ostracods should provide an attractive signal to follow the development of the hydrography in the Laptev Sea through time.

If the low bottom water $\delta^{13}C$ resulting from degradation of organic matter is exported to the surface layer or halocline waters of the Arctic Ocean at a considerable rate, it may contribute in addition to the light isotope composition of the riverine DIC to the comparatively low carbon isotope ratios in the Arctic ocean.

This low $\delta^{13}C$-level is evidenced by carbonate shells of the planktonic foraminifer *Neogloboquadrina pachyderma* (left coiling variety) from surface sediments (Spielhagen and Erlenkeuser, 1994) which suggest a $\delta^{13}C$ about +1.5 ‰ in the DIC of the Arctic Ocean surface waters in the Transpolar Drift, as compared to a calculated $\delta^{13}C$ in equilibrium with the atmosphere of about +2.5 ‰.

Acknowledgements

I like to thank Meike Wollny for her engaged work in the isotope-chemical preparation of the water samples and for operating the mass spectrometer, Hans H. Cordt for supervising the spectrometer and ensuring the high performance of the instrument, and Pieter M. Grootes for discussion. This study is part of the Joined Research Project System Laptev Sea at Geomar, Kiel and is supported by the 'Bundesminister für Bildung und Forschung'.

References

Emrich, K., D.H. Ehhalt and J.C. Vogel, 1970. Carbon isotope fractionation during the precipitation of calcium carbonate. Earth and Planetary Science Letters, 8: 363-371.

Karpiy, V, N. Lebedev and A. Ipatov, 1994: Thermohaline and dynamic water structure in the Laptev Sea. In: Russian-German Co-operation: The Transdrift I Expedition to the Laptev Sea (H. Kassens, V. Karpiy Eds). Reports on Polar Research 151, p.16-47. Alfred-Wegener-Institute for Polar and Marine Research, Bremerhaven.

Mook, W.G., 1970. Stable carbon and oxygen isotopes of natural waters in the Netherlands. In: Isotope Hydrology 1979, IAEA, Vienna 1970, p. 163-190.

Moser, H. and W. Rauert, 1980. Isotopenmethoden in der Hydrologie. Lehrbuch der Hydrogeologie (G. Matthess Ed.), Vol. 8. Bornträger, Berlin, 1980, pp. 400.

Petryaschev, V., 1994: Hydrobiological investigations in the Laptev Sea. In: Russian-German Co-operation: The Transdrift I Expedition to the Laptev Sea (H. Kassens, V. Karpiy Eds). Reports on Polar Research 151, p.54-59. Alfred-Wegener-Institute for Polar and Marine Research, Bremerhaven.

Spielhagen, R.F. and H. Erlenkeuser, 1994. Stable oxygen and stable carbon isotopes in planktonic foraminifers from Artic Ocean surface sediments: Reflection of the low salinity surface water layer. Marine Geology 119: 227-250.

HYDROOPTICAL MEASUREMENTS IN THE LAPTEV SEA: SPATIAL DISTRIBUTIONS OF LIGHT ATTENUATION AND CHLOROPHYLL FLUORESCENCE

A. F. Anoshkin*, I. K. Popov°, I. E. Ushakov+ and TRANSDRIFT II Shipboard Scientific Party

* Krilov Research Institute, Moscow, Russia
° State Research Center of the Russsian Federation the Arctic and Antarctic Research Institute, St. Petersburg, Russia
+ North-West Polytechnical Institute, St. Petersburg, Russia

Introduction

In sea water, light attenuation is caused by the scatter and absorption generated by both pure water and dissolved and suspended matter. A parameter of light attenuation is the beam transmittence coefficient (BTC) quantifying the decrease of a light beam through a water layer of fixed thickness.

The formation of low transparency layers in a sea environment is caused by an increase of the concentration of dissolved and suspended matters, phyto- and zooplankton. For pure water, light attenuation is smallest in the blue-green range of the light spectrum (wavelengths 460-480 nm). In presence of substances and particles, the minimum shifts to longer wavelengths, i.e. to the yellow range. Therefore, BTC measurements over a range of wavelengths allow to detect dissolved substances and suspended particles.

Chlorophyll *a*, the principal photosynthetic pigment of marine water column algae, can be used to measure phytoplankton biomass. Chlorophyll *a* is a fluorescent substance, i.e. it emits a light quantum when affected by light radiation of a particular wavelength range. The measurement of the flux of the emitted quantums (i.e. the fluorescence intensity) gives an information about chlorophyll *a* quantity.

The vast information available on the hydrooptical characteristics in southern seas and oceans are collected and described in Erlov (1970), Ivanov (1975), Karabashev (1987). However, hydrooptical data for northern seas are are scarce (Matushenko & Ushakov, 1993). Hydrooptical measurements of BTC and of chlorophyll *a* fluorescence intensity (CFI) in the Laptev Sea were carried out in September 1994 during theTRANSDRIFT II expedition. The main goals of these investigations were:

- to outline the spatial distributions of BTC and CFI
- to investigate the influence of river outflow on the hydrooptical characteristics
- to study interrelationships between hydrooptical, hydrological, hydrochemical and hydrobiological characteristics.

Methods

Light attenuation was measured with the laboratory photometer CFC-2 as BTC difference between distilled water and water samples taken from standard depths. BTC were measured at 400, 440, 490, 540, 590, 670, and 750 nm. The submersible fluorometer "Variosens II" was used for *in situ* measurements of water column CFI.

Results

Hydrooptical characteristics were measured along three latitudinal (75°30',

74°30', 74°00'N) and two longitudinal (133°30', 134°00'E) transects throughout the ice-free region of the Laptev Sea and at 16 stations in the Kara Sea.

Figs.1a,b show the distribution of BTC measured at 400 nm (T(400)) and the CFI distribution along the transect at 75°30'N. The water transparencies at the eastern

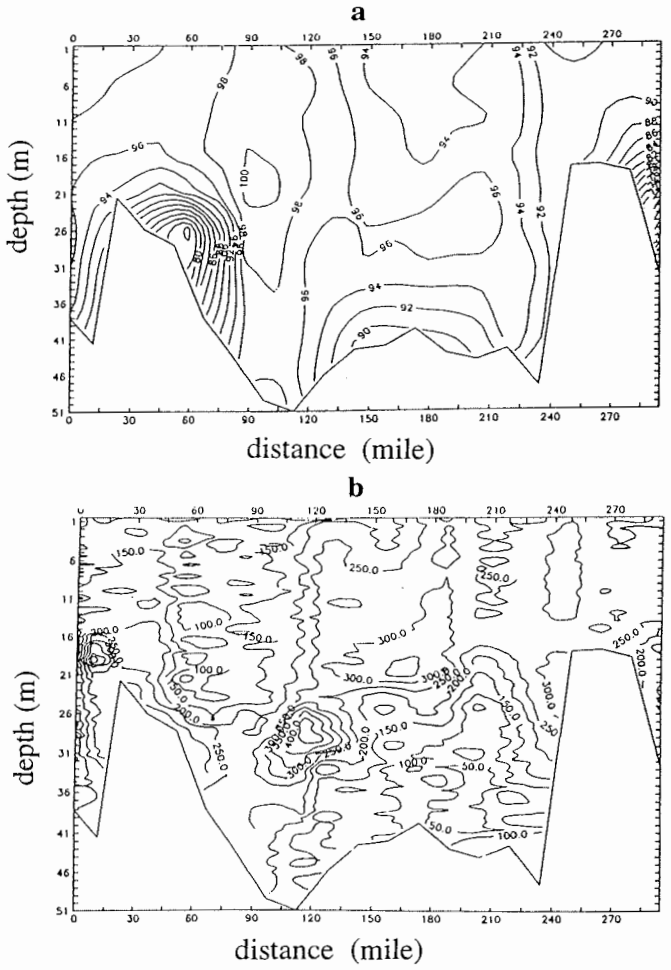

Fig.1: Distribution of beam transmittence coefficient at 400 nm wavelength (a) and of chlorophyll *a* fluorescence intensity (b) along the transect at 75°30'N (3.-7.9.1994).

part of the transect were high, similar to clear sea water. The transparencies decreased in the near-bottom layers at the western slope of the Lena valley, caused mainly by suspended particles. This pattern was in accordance with the silica concentration increase in this region. The decrease of T(400) from 100% to 94% in the upper water layers at distances between 150 and 200 miles was caused by the input of particles during ice melting in this region some days before the measurements. The decrease to 90% in the upper layer over the eastern slope of the Lena valley was probably caused by dissolved and suspended matter originating from the river outflow. The chlorophyll *a* fluorescence profiles (Fig.1b)

revealed several subsurface maximums : at 15 miles in depths between 16 and 21 m, at 90-135 miles in depths of 25-35 m, at 225-240 miles in depths of 19-26 m, and at 120-180 miles in depths of 7-22 m. The first three zones indicated hydrological fronts, the fourth were located in the above mentioned region of recent ice melt.

Figs.2a,b present the distribution of hydrooptical characteristics along the transect at 134°00'E. The BTC distribution (Fig.2a) indicated that the sea water was more transparent at the southern (120-140 miles, at depths of about 15 m) and

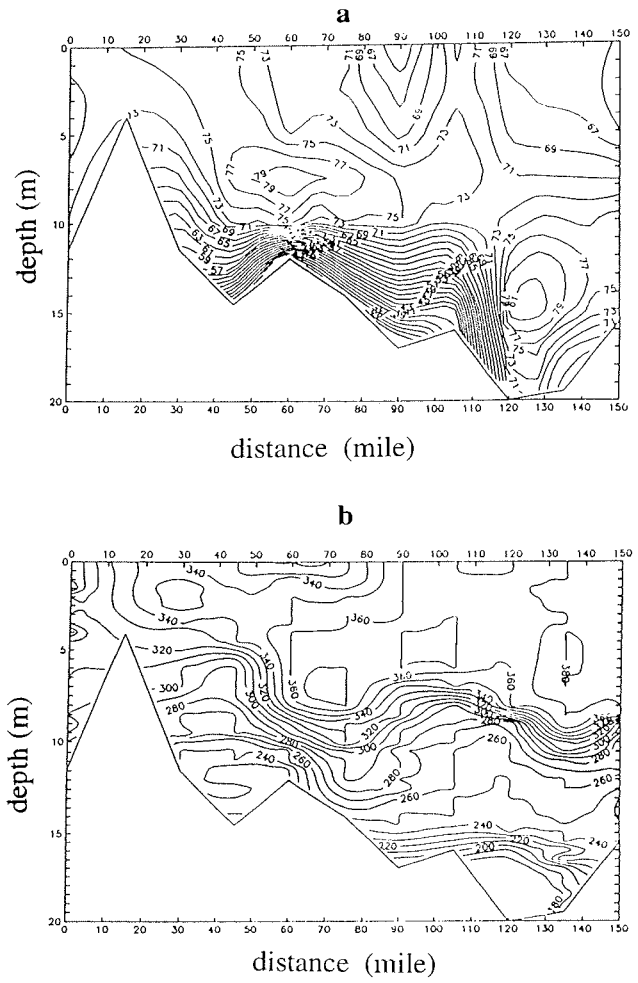

Fig.2. Distribution of beam transmittence coefficient at 400 nm wavelength (a) and of chlorophyll *a* fluorescence intensity along the transect at 134°00'E (18.-19.09.1994).

middle part (45-80 miles, at depths about 10 m) of the transect. This pattern was probably determined by the interaction of sea and river water masses disturbed by sea bottom topography. The comparison with other characteristics distributions showed that the principal river outflow is displayed by the BTC isoline of 71% at the surface of the southern part of the transect (78-100 and 115-150 miles). The CFI

values (see Fig.2b) were highest (350-370 relative fluorescence units) in the upper layer at the southern part (distances 60-150 miles) and decreased towards the north. The vertical distribution of CFI fitted well to the water temperature and salinity profiles. The steepest CFI gradients varied between depths of 8 and 16 m and coincided with the upper and lower pycnoclines. In summary, the river outflow zones were indicated by BTC decrease and CFI increase.

BTC data also allow to estimate the distribution of the dissolved organic matter by calculating of the difference T(750)-T(400) which is positively correlated with the concentration of organic matter. The distribution along the transect 134°00'E is shown at Fig.3. It corroborated the pattern found in the other measurements, indicating that the principal river outflow occurred in the upper layer in the southern part of the transect (T(750)-T(400) > 22%).

The vertical BTC profiles of the BTC at most stations were characterized by a BTC increase at the pycnocline and a BTC decrease in the near bottom layer. Fig.4 shows the vertical profiles measured at different wavelengths at the station 063 (74°30'N, 126°35'E). The pycnocline was at 5-7 m depth. The highest water transparencies were observed below the pycnocline. Near the bottom, suspended matter caused a transparency decrease. The difference T(750)-T(400) was higher in the upper layer, indicating increased dissolved organic matter concentrations.

Spectral BTC distributions were obtained for each water sample. A monotonous BTC increase with wavelengths (400 to 750 nm) was observed for clear sea water. A local BTC decrease was discovered at wavelengths of 540-590 nm, if water transparency is decreased by dissolved and suspended matter. The BTC minimum is observed at 590 nm, and the difference T(540)-T(590) achieves 5% and more. This pattern was found at all stations both in the Laptev Sea and in the Kara Sea. Special BTC measurements were carried out with filtered and unfiltered water samples taken at station 063 (at depths 5, 10, 15, 30, and 35 m) and at stations 064-072 along the longitudinal transect 130°30'E (at depths of 2 m under the sea surface and 5m over the sea bottom). The water samples were filtered through 0.45mm Nucleopore filters. Fig.5 shows the comparison of the BTC spectral distribution for water samples before and after filtration at the station 065. The BTC decrease at the wavelengths of more than 540 nm and the local minimum at 590 nm were observed for unfiltered water samples (solid lines). After the filtration (dashed lines), the local minimum at 590 nm almost disappeared or did not exceed the error of the measurements. Similar results were obtained at all stations. Therefore, it may be concluded that the local decrease of BTC at 540-490 nm is caused by particles with the size more than 0.45mm. A kind of the particles becomes more clear if the chlorophyll-a fluorescence data are considered.

Figs.6a,b show two CFI profiles of the transect along 75°30'N. At station 006 (Fig.6a) in the western part of the transect, the flourescence values increased below the pycnocline, whereas at station 016 in the eastern part they decreased. This transformation of fluorescence profiles is in accordance with the distribution of zooplankton biomass. The intermediate fluorescence vertical profile at station 009 (Fig.7a) displays the phytoplankton acculmulation (solid line) at the pycnocline. In the same layer, a pronounced BTC decrease was observed (Fig. 7a, dashed line) over the entire wavelength range (Fig.7b, 30 m). In addition, it is evident that the most pronounced BTC decrease at 540-590 nm were found at the pycnocline (Fig. 7b), indicating that the typical local BTC minimum at 540-590 nm is primarily caused by phytoplankton cells > 0.45mm.

Fig.8 illustrates the relationship between zooplankton biomass and chlorophyll *a* fluorescence. The relationship between macrobenthos biomass and total chlorophyll *a* fluorescence in the water column is shown in Fig.9. A positive

correlation was distinct for the zooplankton, less well pronounced, however, for the macrobenthos.

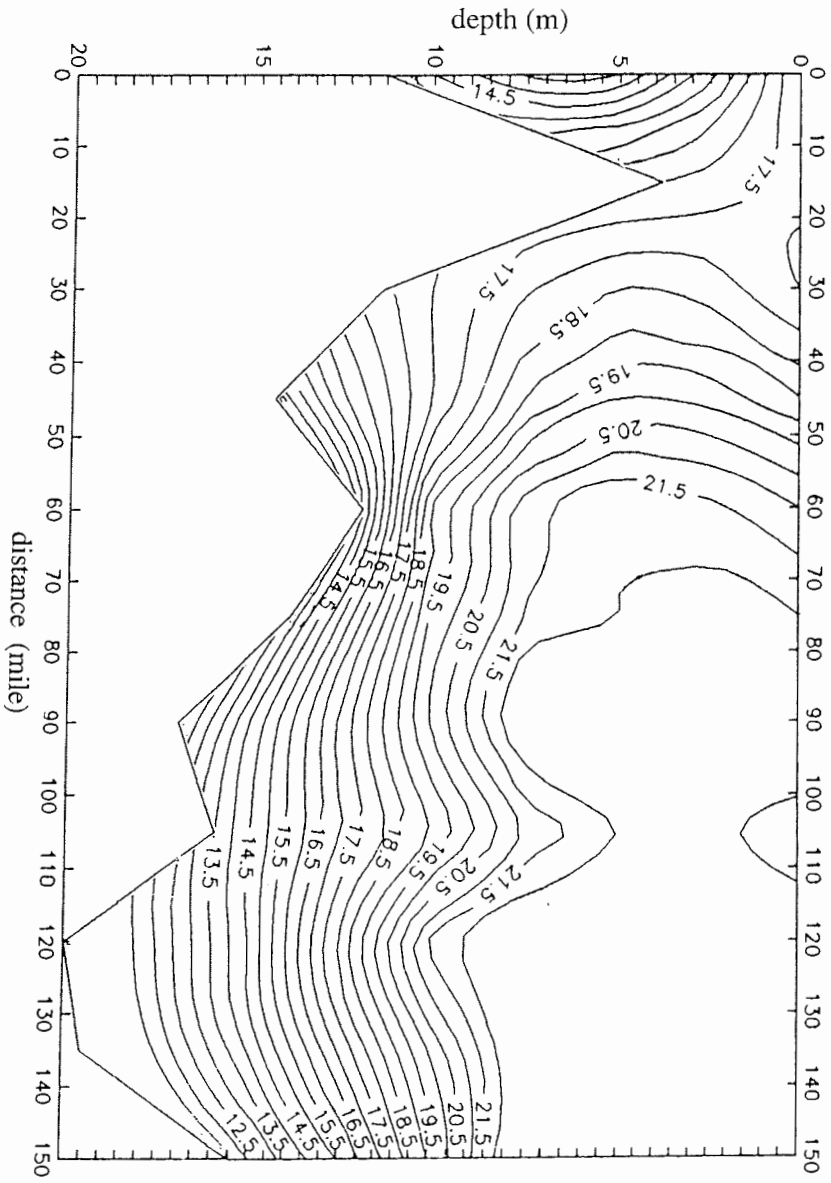

Fig.3. Distribution of the difference of beam transmittence coefficients T(750)-T(400) along the transect at 134°00'E (18-19.09.94).

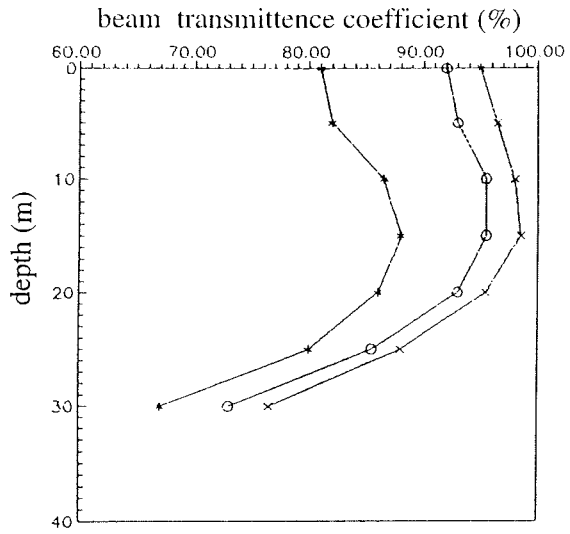

Fig.4. Vertical profiles of beam transmittence coefficient for different wavelengths at st.063 (13.09.94).

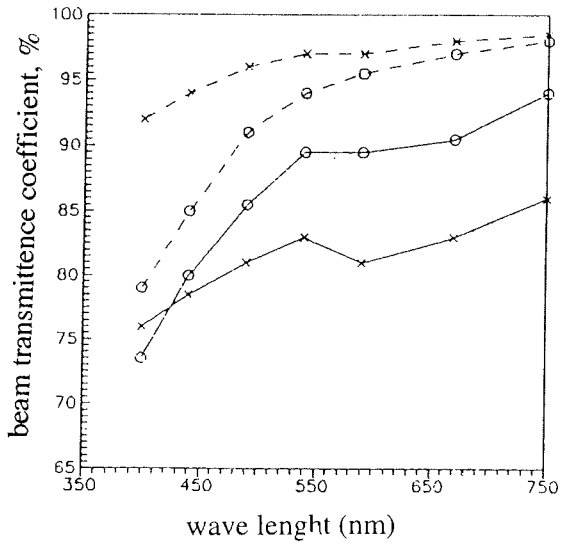

Fig.5. Spectrum of beam transmittence coefficient of unfiltered (solid lines) and filtered water samples (dashed lines) at st.065 (15.09.94) for depths of 2 and 20 m.

Conclusions

1. River outflow zones were discernable in the spatial distributions of hydrooptical characteristics. Their locations coincided with those outlined by other hydrological and chemical measurements.

2. These zones were characterized by an increased content of dissolved organic matter, as determined by the difference T(750)-T(400).

3. A local decrease at 540-590 nm was discovered in the spectral distributions of the beam transmittence coefficient at all stations. This pattern is probably caused by phytoplankton cells.

4. The measurements of the chlorophyll *a* fluorescence intensity indicated the horizontal and vertical distribution of phytoplankton hroughout the Laptev Sea. River outflow zones were characterized by surface fluorescence maxima, whereas in zones with less river influence sub-surface and near-bottom maxima occurred.

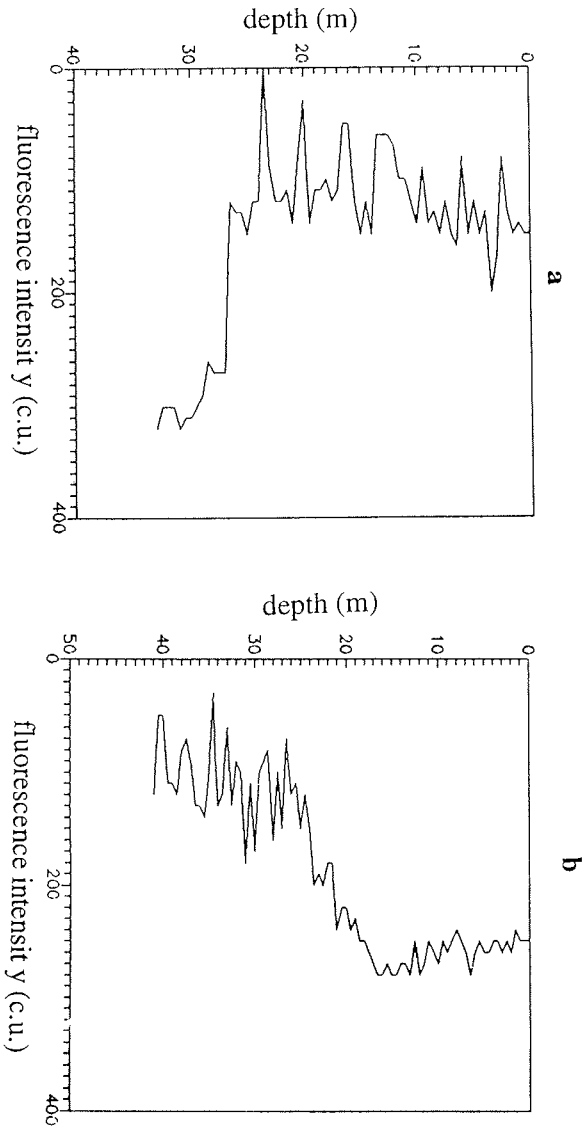

Fig.6. Vertical profiles of chlorophyll *a* fluorescence intensity at st.006 (4.09.94) and st.016 (5.09.94) along the transect at 75°30'N.

Acknowledgements

Dr. J. Hölemann and C. Strobl helped with the water filtrations. We are grateful to them for the collaboration.

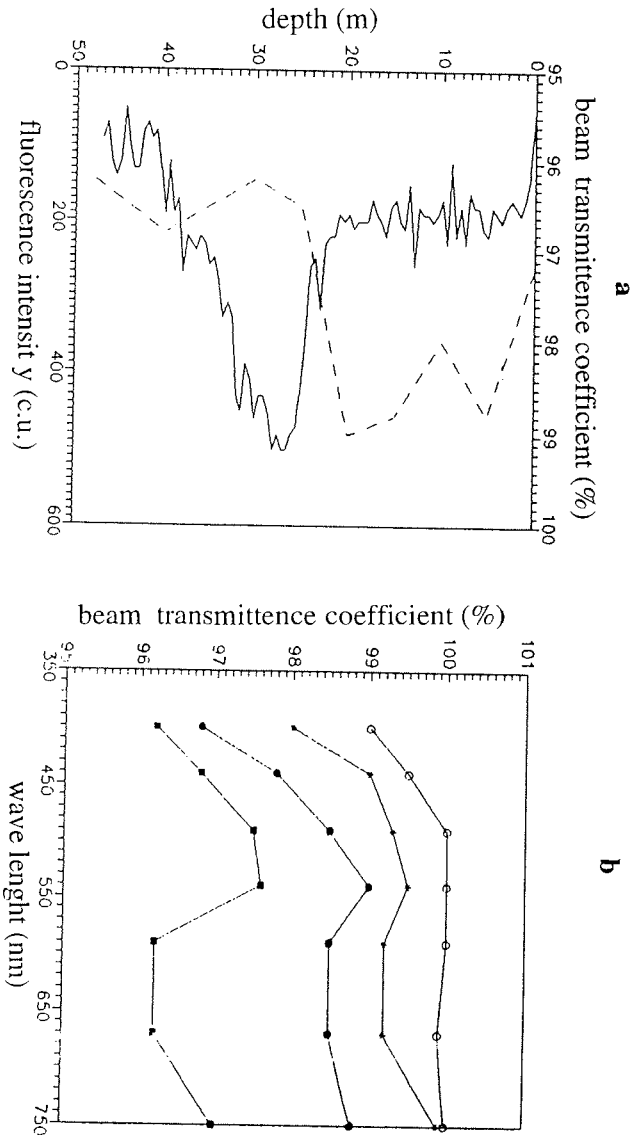

Fig.7. Vertical profiles (a) of chlorophyll *a* fluorescence intensity (solid line) and beam transmittence coefficient (dashed line), and spectrum (b) of beam transmittence coefficient at different depths (st.009, 4.09.94). i - depth 10 m; m - 20 m; n - 30 m; l - 40 m.

References

Erlov, N. G., 1970. Optical Oceanography. "Mir", 224 pp.

Ivanov, A. P., 1975. Physical principles of hydrooptics. Nauka i technica, Minsk, 504 pp.

Karabashev, G. S., 1987. Fluorescence in the Ocean. Gidrometeoizdat, Leningrad, 200 pp.

Matushenko, V. A., Ushakov, I. E., 1993. Ecological express-monitoring of the transparency of littoral sea water near archipelago Novaya Zemlya and in the Barents and Baltic seas. Transactions of complex marine Arctic expedition. v.III. Novaya Zemlya. 2, 132-149.

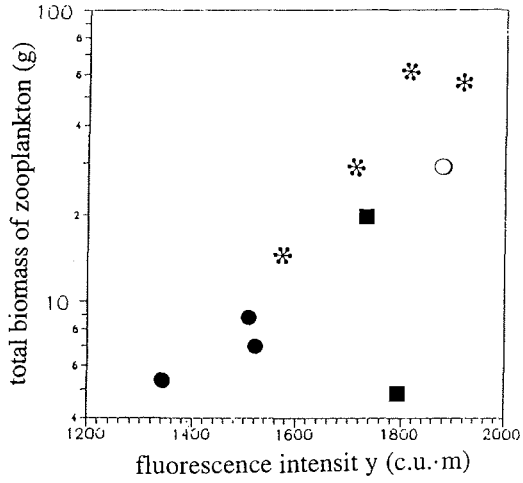

Fig.8. Total zooplankton biomass vs. total chlorophyll *a* fluorescence intensity. i - st.001, 005, 009, 016; n - st.042, 063: l - st.066, 068, 070; m - st.k12 (Kara Sea).

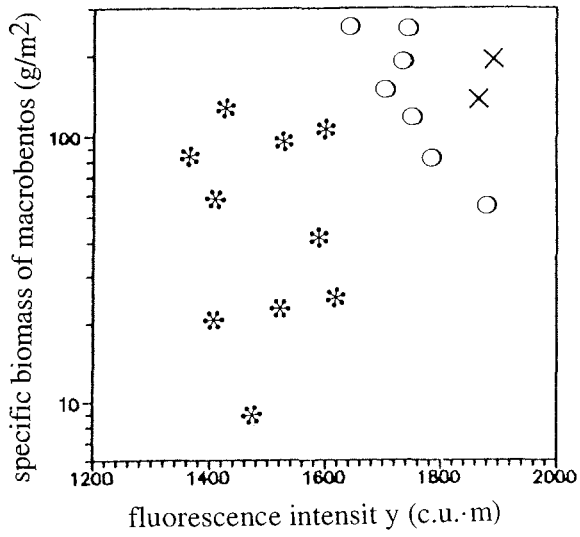

Fig.9. Specific macrobenthos biomass vs. chlorophyll *a* fluorescence intensity. i - depths <25 m; m - depths 25-50 m; 5 - depths >50 m.

ZOOPLANKTON OF THE LAPTEV SEA COASTAL WATERS

V. V. Petryashov, E. L. Markhaseva, A. I. Pinchuk and S. D. Stepanjants
Zoological Institute, Russian Academy of Sciences, St. Petersburg, Russia

Introduction

The study of the zooplankton of the Laptev Sea had started already 100 years ago. The first sampling was carried out by the Russian Polar expedition with the "Zarya" from 1900 - 1903. However, the actual number of zooplankton samples from the Laptev Sea as well as the number of publications on the zooplankton from this area is relatively small to date (Linko 1913; Jaschnov 1940, 1946; Markhaseva 1980; Pavshtiks 1977, 1990; Virketis 1932). While the hydrocoeles, mostly from the coastal south-eastern and eastern parts of the Laptev Sea, were studied quite well, the shallow water zooplankton of the other regions of the Laptev Sea remained poorly known. Therefore, the main goals of the our field studies of the Laptev Sea in 1993 - 1994 were:

1. to describe the species composition of the zooplankton of the southern part of the Laptev Sea
2. to analyse the horizontal distribution of the zooplankton in the study area

Material and Methods

Zooplankton was collected in 1993 from board of RV "Ivan Kireev" at 19 stations in depths between 10 and 46 m (Fig.1) by means of a Nansen net (50 cm diameter, 26 µm mesh size). Two total hauls were made at every station. During the expedition of RV "Professor Multanovsky" in 1994, zooplankton was sampled at 10 stations in depths between 10 and 50 m with a Judey net (37 cm diameter, 26 µm mesh size). Two hauls were usually conducted: one total haul and another above the pycnocline (if a two-layer structure of waters was clearly visible).

Results

Species composition

A total of 34 zooplankton species from 6 types were collected in 1993 (Table 1). Most species (14) were copepods. Other crustaceans were: Ostracoda (1 species), Amphipoda (more than 2 species), *Mysis oculata* (Mysidacea), *Pandalus borealis* (Decapoda), and juveniles of Cirripedia and Copepoda. In addition , other invertebrate taxa such as Hydrozoa (nearly 7 species), Scyphozoa (1 species), Ctenophora (2 species), Appendicularia (1 species) and juvenile stages of Polychaeta and Echinodermata (Asteroidea and Ophiuroidea) were found.

Zooplankton distribution

In 1993, the highest abundances were found north of the Lena delta (Sts. 21, 23: 500-900 ind m^{-3}), north of the Yana delta (St. 9: 1317 ind m^{-3}), and in the deltas areas (400 ind m^{-3} in the Lena delta and 700 ind m^{-3} in the Yana delta) (Fig. 2). The poorest samples (less than 100 ind m^{-3}) were collected in the northern Laptev Sea (at St. 44, 50, 53, 56, 68, 70, 73, 73A, between 74°30'N and 75°30'N), i.e. in the zone where the most transformed waters of the rivers runoff and adjacent typical sea waters mix.

In 1994, the highest seston concentrations were registered on the latitudinal transect along 75°30'N (Fig.3: 0.787-3.451 g wet weight m^{-3}) where also a phyto-

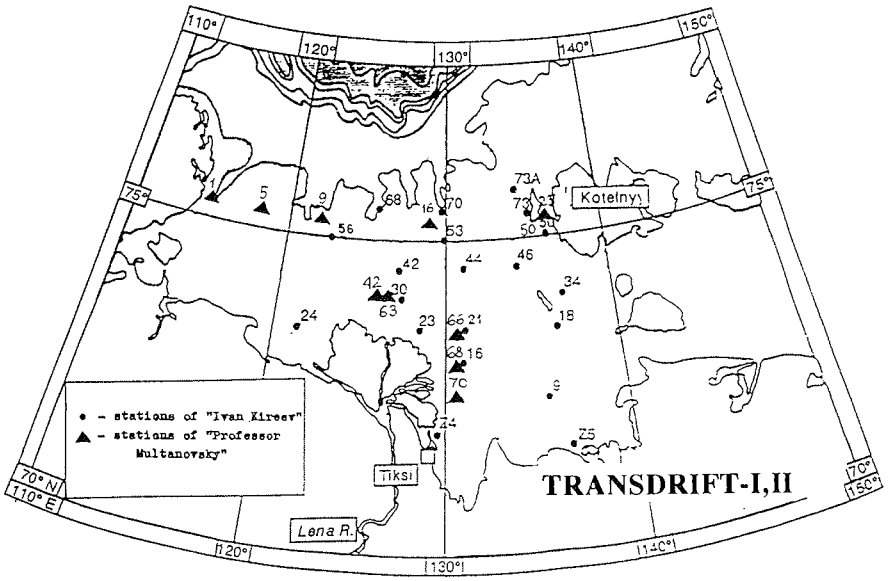

Fig. 1: Plankton stations in the Laptev Sea during the cruises of RV "Ivan Kireev" in 1993 and RV "Professor Multanovsky" in 1994.

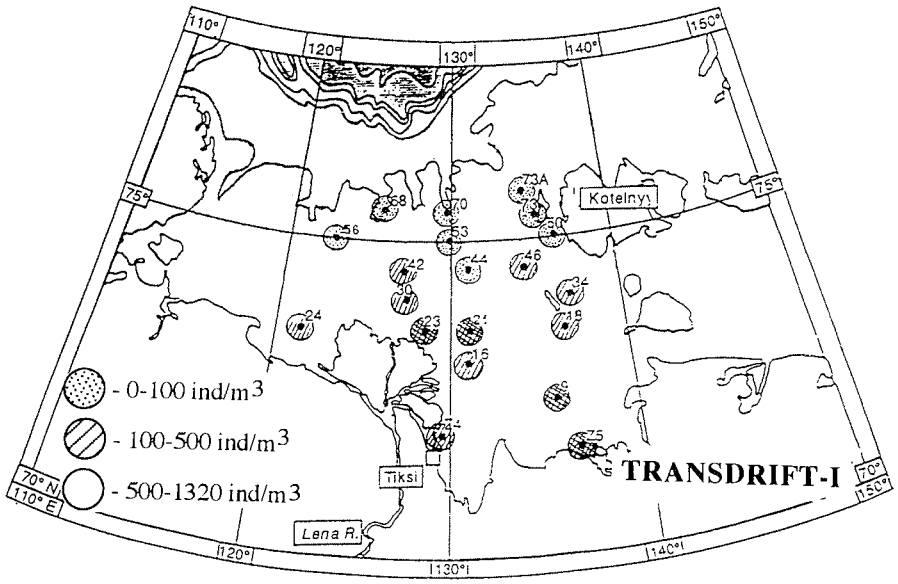

Fig. 2: Abundances of zooplankton (ind m^{-3}) during the cruise of RV "Ivan Kireev" in 1993.

plankton bloom and the zooplankton maximum was registered. The lowest seston concentrations were found east of the Lena delta southward of 74°30' N (St. 42, 66, 68, 70: 0.124 - 0.557 g wet weight m^{-3}). Pavshtiks (1990) reported that the zooplankton was more abundant in the upper quasi-homogenous water layer. In regions where the phytoplankton bloom was not too intensive, the highest seston concentrations were found under the pycnocline.

Tab. 1: Zooplankton species collected in the Laptev Sea during the "Transdrift-I" cruise of RV "Ivan Kireev" in 1993.

Taxa	Station																		
	z4	z5	9	16	18	21	23	24	30	34	42	44	46	50	53	56	68	70	73	73A
Type Cnidaria Class Hydrozoa																				
1.Mitrocomella polydiademata															+				+	+
2.Eumedusa birulai																	+			+
3. Euphysa flammea																			+	
4. Leuckartiara octona													+				+		+	
5. Plotocnide borealis															+					
6. Aeginopsis laurentii			+			+			+	+	+		+	+	+	+	+		+	+
7. Obelia longissima									+		+			+		+	+		+	+
Class Scyphozoa																				
8. Cyanea capillata																				+
Type Ctenophora																				
9. Beroe sp.																				+
10. Pleurobrachia sp.		+	+	+		+					+			+						+
Type Annelida Class Polychaeta																				
11.Polychaeta gen. sp.								+		+		+		+		+	+		+	+
Type Arthropoda Class Maxillopoda																				
12. Acartia longiremis	+		+	+	+	+	+	+	+	+	+	+	+	+	+	+	+		+	+
13. Calanus glacialis								+	+	+	+	+	+		+	+	+	+	+	+
14. C. hyperboreus											+									
15. Drepanopus bungei	+	+	+	+	+	+	+	+	+	+	+	+	+	+		+				+
16. Jaschnovia sp.	+		+	+	+	+	+	+	+	+		+	+							
17. Limnocalanus macrurus grimaldii	+	+	+	+	+	+	+	+	+	+	+	+	+							
18. Metridia longa															+					
19. Microcalanus pygmaeus															+					
20. Pseudocalanus acuspes															+	+				
21. P. minutus														+	+					
22. P. major			+	+	+		+	+	+	+	+	+	+							
23. Oithona similis			+	+		+			+	+	+	+	+		+	+	+		+	+
24. Cyclopoida gen. sp.																			+	
25. Harpacticoida gen. sp.	+		+					+	+	+	+	+	+	+	+	+	+	+	+	+
26. Cirripedia (larva)								+	+	+	+			+						

Table 1: Continued

Taxa	Station																		
	z4	z5	9	16	18	21	23	24	30	34	42	44	46	50	53	56	68	70	73	73A
Class Ostracoda																				
27. Ostracoda gen. sp.																	+		+	
Class Malacostraca																				
28. Mysis oculata			+			+			+		+						+			
29. Gammaridea gen. sp.														+	+	+	+		+	+
30. Hyperiidea gen. sp.			+															+		
31. Pandalus borealis															+					
Type Chaetognatha																				
32. Sagitta elegans			+		+				+	+	+	+	+		+	+	+	+	+	+
Type Echinodermata																				
33. Asteroidea+Ophiuroidea (larva)								+	+				+	+	+	+	+		+	+
Type Chordata																				
34. Oikopleura sp.			+						+	+	+		+	+	+	+	+			+

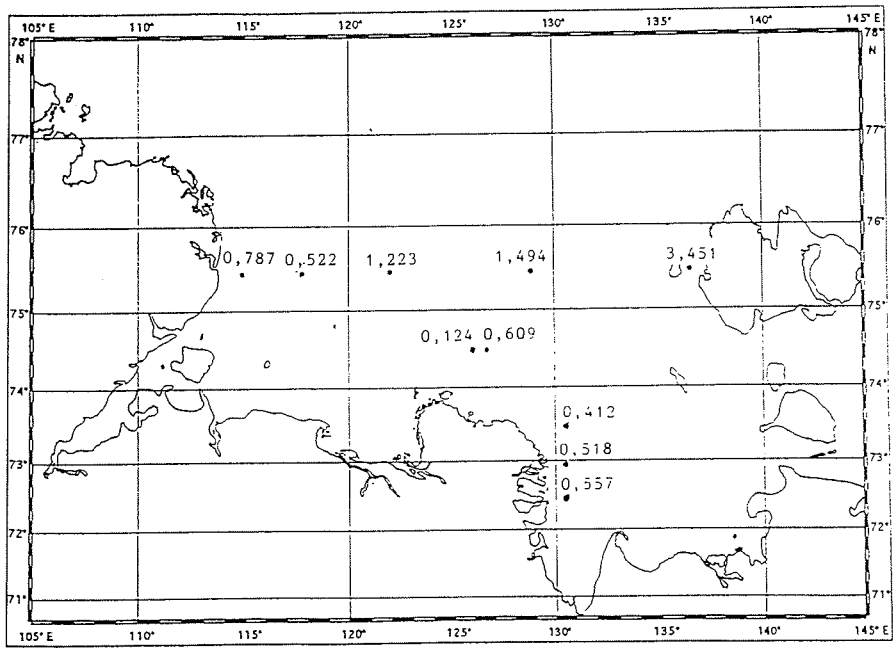

Fig. 3: Seston concentrations (g wet weight m^{-3}) during the cruise of RV "Professor Multanovsky" in 1994.

The majority of the zooplankton species occurred in the entire study area. It is very possible that different water layers were inhabited by a characteristic zooplankton fauna, but the vertical zonation could not be investigated because we did not perform depth-stratified catches. According to our data and information from the literature, distinct zoogeographical boundaries do not exist in the Laptev Sea. The major controlling factor of the zooplankton distribution seems to be the salinity gradient between the river delta areas and the northern region.

References

Jaschnov, V. A., 1940. Plankticheskaya productivnost severnykh morei SSSR. M.: 1-44. (In Russian).

Jaschnov, V. A., 1946. Distribution of the autochthonous pelagic Arctic fauna. Bull. MOIP. Otd. biol. 51 (6): 40-50. (In Russian).

Linko, A. K., 1913. Zooplankton of the Siberian Ice Ocean after collections of the Russian Polar expedition 1900-1903. Zap. Imp. Akad. nauk. S. Pb. 29 (4): 1-54. (In Russian).

Markhaseva, E. L., 1980. Calanoids of the genus *Jaschnovia* nom. nov. (*Derjuginia* Jaschnov, nom. praeocc.) (Calanoida, Aetideidae). Issled. fauny morei. Nauka Leningrad. 25(33): 63-76. (In Russian).

Pavshtiks, E. A., 1977. On the quantitative distribution of *Derjuginia* tolli (Linko) and *Drepanopus bungei* G. O. Sars in August-September 1973 near the New Siberian Islands. Issled. fauny morei. Nauka Leningrad. 19(27): 115-118. (In Russian).

Pavshtiks, E. A., 1990. Composition and quantitative distribution of the zooplankton near the New Siberian Islands. In: Golikov, A.N. (Ed.): Ecosystems of the New Siberian shoals and the fauna of the Laptev Sea and adjacent waters. Issled. fauny morei. Nauka Leningrad. 37 (45): 89-104. (In Russian).

Virketis, M. A., 1932. Some data on the zooplankton of the south-eastern part of the Laptev Sea. Issled. Fauny morei SSSR. 15: 105-125. (In Russian).

COMPOSITION AND DISTRIBUTION OF SUMMER ZOOPLANKTON IN THE LAPTEV SEA

K. Kosobokova[+], H. Hanssen[*], E. Markhaseva[°], V. V. Petryashov[°], A. I. Pintchuk[°]

[+] Institute of Oceanology, Russian Academy of Sciences, Moscow, Russia

[*] Institut für Polarökologie, Universität Kiel, Kiel, Germany

[°] Zoological Institute, Russian Academy of Sciences, St. Petersburg, Russia

Introduction

The marine biology programme of the multi-disciplinary German-Russian Scientific Expedition of RV "Polarstern" and RV "Ivan Kireyev" to the Laptev Sea in September 1993 included the collection of zooplankton and experimental studies of plankton grazing and reproduction. The main objectives of the study were:

1) to characterize the composition and horizontal distribution of major zooplankton assemblages of the area studied,
2) to provide abundance and biomass data for shallow and deep regions of the sea,
3) to characterize distribution patterns and age composition of dominant zooplankton species,
4) to provide data on feeding activity of dominant zooplankton species for a better understanding of the role of zooplankton in transformation of organic matter in the water column,
5) to obtain data on the reproduction rate of the dominant zooplankton species to characterize the secondary production.

Material and Methods

Zooplankton was sampled with a multiple opening/closing net (multinet, mesh size 150 µm) and Bongo nets (mesh sizes 100, 200 and 500 µm) on 27 stations between 76° and 80° N along four transects from the shelf down to the deep sea plains and with a Nansen net on 18 stations in the shelf region (Fig.1). Five successive depth layers from near the bottom or 1500 m to the surface were sampled in the slope region. Unstratified vertical hauls from the bottom to the surface were made in the shallow part of the sea. In such detail, collection of zooplankton in the Laptev Sea was performed for the first time. In this study we present the data from the three deep stations of the easternmost transect along 133° E (transect H) in comparison to the data from the shelf region.

Results and Discussion

Species composition

A total of 48 copepod species (40 calanoids, 6 cyclopoids and 2 harpacticoids) and 15 other taxa from 8 phyla were identified in the present zooplankton collections (Tab.1). Species composition in the shallow and deep regions of the sea differed markedly. Only 15 copepod species and 8 other taxa were found in shallow waters. In the deep region, 44 copepod species, 5 species of Hydromedusae, 1 Scyphomedusae, 4 Ctenophora, 2 Pteropoda, 6 Amphipoda, 1 Euphausiacea, 1 Decapoda, 1 Chaetognatha and 2 Appendicularia were identified. Two copepod species, Xanthocalanus profundus and Xanthocalanus groenlandicus Tupitsky (= Tharybis groenlandica after Andronov, in press), identified from the deep sea, are reported from the Arctic Ocean for the first time. The number of species in the

Atlantic Water in the deep region was much higher than in the overlaying Polar Surface Water (Fig.2).

Zooplankton abundance and biomass

The highest abundance of zooplankton in the shallow waters (532-1317 ind m^{-3}) was recorded on stations with depth 11-22 m located to the north and north-east off the Lena river's delta. The lowest values (less than 100 ind m^{-3}) were found in the northern part of the shallow region. A few coastal brackish-water copepods *Drepanopus bungei*, *Limnocalanus grimaldii*, *Oikopleura* sp. juv. and Echinodermata larvae (Asteroida and Ophiuroidea) dominated abundance and biomass in shallow waters.

In the northern slope region, the greatest abundance of zooplankton up to 2650 ind m^{-3} was observed in the 0-25 m depth layer of the Arctic Surface Water (Fig.3). The small copepods *Oithona similis*, *Oncaea borealis* and copepod nauplii were responsible for this maximum. Below 25 m, zooplankton abundance decreased dramatically and was less than 75 ind m^{-3} in the Atlantic Water layer.

Principal characteristics of the vertical distribution of zooplankton biomass in the northern deep region of the sea were quite similar to those found previously in the Arctic Ocean in the summer season. The bulk of biomass was concentrated in the Arctic surface layer, while the Atlantic layer contained about 30-35 % of the total biomass. Within the Arctic Surface Water, the upper 0-25 m depth layer contained relatively low biomass of 20-40 mg wet weight m^{-3}. Maximum values were recorded in the narrow 25-50 m depth layer (Fig.4).

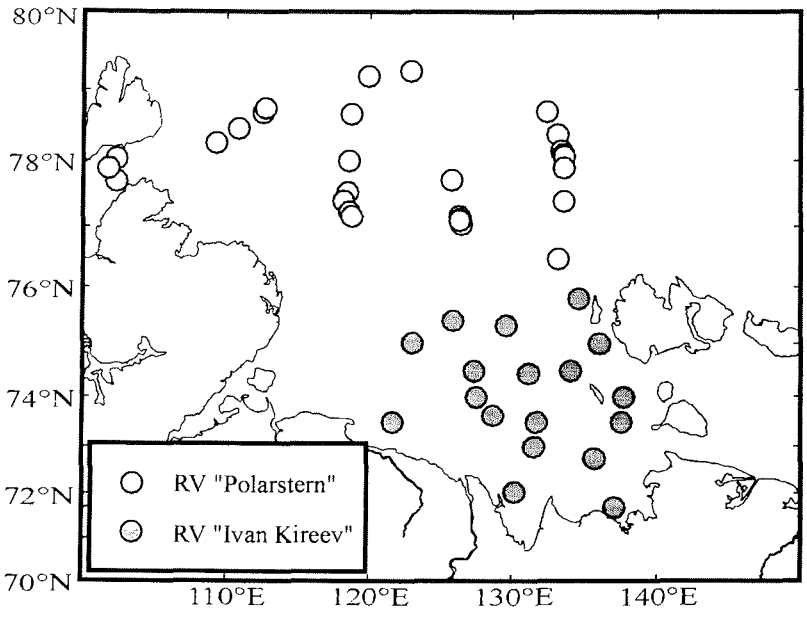

Fig. 1. Station map.

Tab.1: List of zooplankton species caught during ARCTIC'93

Species	Shallow region	Deep region
Copepoda		
Acartia longiremis (Lilljeborg)	*	
Aetideopsis multiserrata (Wolfenden)		*
Aetideopsis rostrata G.O.Sars		*
Augaptilus glacialis G.O.Sars		*
Calanus finmarchicus (Gunnerus)	*	*
Calanus glacialis Jaschnov	*	*
Calanus hyperboreus Kroyer	*	*
Chiridius obtusifrons G.O.Sars		*
Drepanopus bungei G.O.Sars	*	
Gaidius brevispinus (G.O.Sars)		*
Gaidius tenuispinus (G.O.Sars)		*
Haloptilus acutifrons (Giesbrecht)		*
Heterorhabdus compactus (G.O.Sars)		*
Heterorhabdus norvegicus (Boeck)		*
Jaschnovia tolli (Linko)	*	
Limnocalanus grimaldii De-Guerne	*	
Lubbockia glacialis G.O.Sars		*
Metridia longa (Lubbock)	*	*
Microcalanus pygmaeus (G.O.Sars)	*	*
Microsetella norvegica (Boeck)	*	*
Mormonilla polaris G.O.Sars		*
Oithona atlantica Farran		*
Oithona similis Claus	*	*
Oncaea borealis G.O.Sars	*	*
Oncaea minuta Giesbrecht		*
Oncaea notopus (Giesbrecht)		*
Pareuchaeta barbata (Brady)		*
Pareuchaeta glacialis (Hansen)		*
Pareuchaeta norvegica (Boeck)		*
Pseudaugaptilus polaris Brodsky		*
Pseudocalanus acuspes (Giesbrecht)	*	*
Pseudocalanus major G.O.Sars	*	*
Pseudocalanus minutus (Boeck)	*	*
Pseudochirella elongata		*
Scaphocalanus brevicornis (G.O.Sars)		*
Scaphocalanus magnus (T.Scott)		*
Scaphocalanus polaris Brodsky		*
Scolecitricella minor (Brady)		*
Spinocalanus abyssalis Giesbrecht		*
Spinocanus antarcticus Wolfenden		*
Spinocalanus elongatus Brodsky		*
Spinocalanus longicornis G.O.Sars		*
Spinocalanus longispinus G.O.Sars		*
Temorites brevis G.O.Sars		*
Tisbe furcata (Baird)		*
Undinella oblonga G.O.Sars		*
Xanthocalanus groenlandicus Tupitzky		*
Xanthocalanus profundus G.O.Sars		*
Hydromedusae		
Aglantha digitale (O.F. Muller)	*	*
Aeginopsis laurentii Brandt	*	*
Botrynema ellinorae Kramp		*
Catablema vesicarium Agassiz	*	

Tab.1 (cont'd): List of zooplankton species caught during ARCTIC'93

Species	Shallow region	Deep region
Hydromedusae		
Euphysa flammea (Linko)	*	
Halitholus yoldia-arcticae Birula	*	
Homoenema platygonon Maas		*
Paragotoea elegans Margulis		*
Plotocnide borealis Wagner	*	
Sarsia princeps (Haeckel)	*	
Yakovia polinae Margulis		*
Scyphomedusae		
Atolla tenella Hartlaub		*
Siphonophora		
Dimophyes arctica (Chun)		*
Ctenophora		
Bolinopsis infundibulum (O. Muller)		*
Beroe cucumis Fabricius		*
Mertensia ovum (Fabricius)		*
Pleurobrachia pileus O.Muller	*	*
Polychaeta	*	*
Pteropoda		
Limacina helicina Phipps	*	*
Clione limacina Phipps	*	*
Ostracoda		
Conchoecia sp.	*	*
Cirripedia		
Cypris larvae	*	
Mysidacea		
Mysis oculata (Fabricius)	*	
Amphipoda	*	
Apherusa glacialis (Nansen)	*	*
Cyclocaris guilelmi Chevreux	*	*
Pseudalibrotus glacialis G.O. Sars	*	*
Parathemisto abyssorum Boeck	*	*
Parathemisto libellula (Mandt)	*	*
Lanceola clausi Sovallius	*	*
Euphausiacea		
Thysanoessa inermis (Kroyer)		*
Thysanoessa longicaudata (Kroyer)		*
Thysanoessa raschii (M. Sars)	*	
Decapoda		
Hymenodora glacialis (Buchholz)		*
Chaetognatha		
Eukrohnia hamata (Moebius)	*	*
Sagitta elegans Verrill	*	*
Sagitta maxima		*
Appendicularia		
Oikopleura vanhoeffeni Lohmann	*	*
Fritillaria borealis Lohmann	*	*
Echinodermata		
Bipinnaria	*	
Ophioplutei	*	

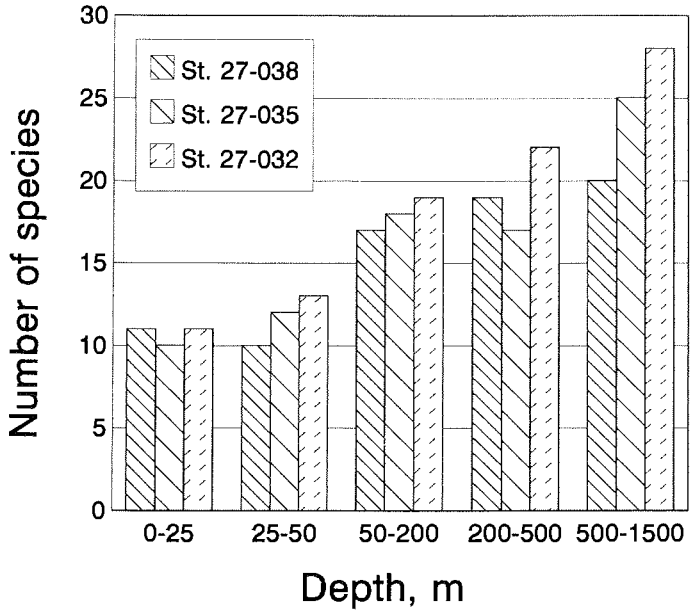

Fig. 2. Transect H. Number of copepod species in each depth interval sampled.

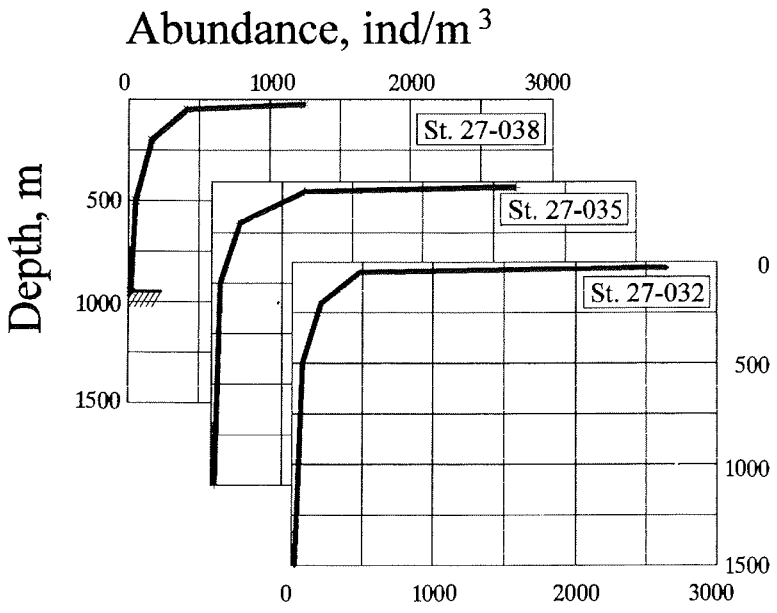

Fig. 3. Transect H. Vertical distribution of zooplankton abundances.

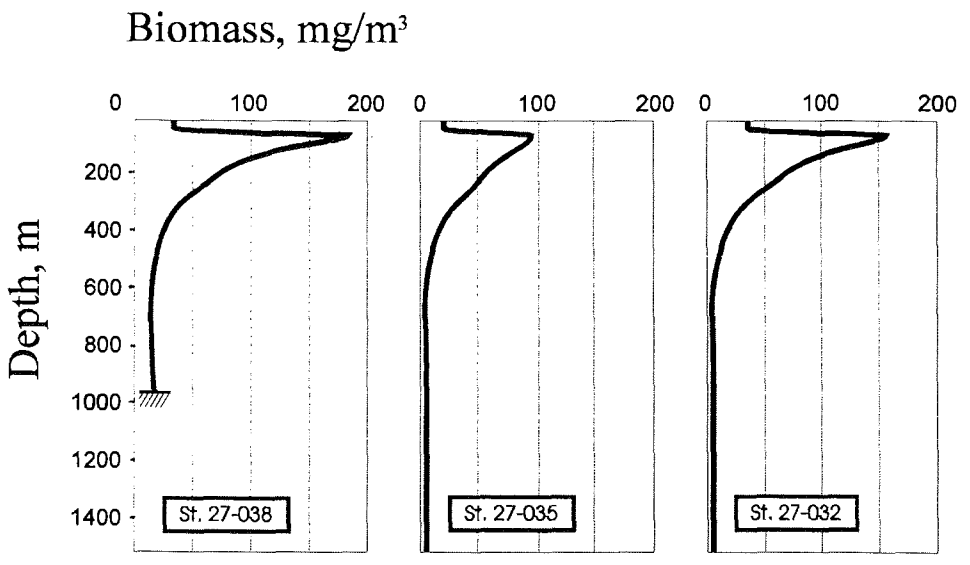

Fig. 4. Transect H. Vertical distribution of copepod biomass.

Copepods dominated in the deep region overwhelmingly, comprising more than 80% of a total zooplankton abundance and biomass. Four calanoid species *Calanus glacialis, C. hyperboreus, Metridia longa* and *Pareuchaeta glacialis* accounted for 82-87% of the copepod biomass. The highest biomass of the two *Calanus* species and *P. glacialis* found in the depth layer 25-50 m were responsible for the maximum of the total copepod biomass at these depths (Fig. 4). Population structure and vertical distribution of the dominant copepod species were typical for the Arctic summer season.

Egg production

Egg production and state of gonadal maturation of *Calanus glacialis, C. hyperboreus, C. finmarchicus* and *M. longa* were studied. Neither *C. hyperboreus* nor *C. finmarchicus* reproduced during the studied period. The state of gonadal maturation indicated that all females of both species were unripe. The absence of juvenile stages and unripe gonads in all adult females of *C. finmarchicus* confirm the conclusion of V.A. Jaschnov (1970) that this species is not able to reproduce in Arctic waters, thus being an expatriate species. *C. glacialis* demonstrated relatively low *in situ* egg production rates of 3-8 eggs·fem^{-1}·d^{-1}. Reproduction of this species was clearly positively correlated to phytoplankton availability (Fig.5). Egg laying of *M. longa* was observed at the most stations located deeper than 200 m. Egg production rates ranged from 2 to 4 eggs·fem^{-1}·d^{-1}. Egg laying ceased completely after 6-7 days of starvation in *C. glacialis* (Fig.6) and 10-11 days in *M. longa* (Fig.7).

References

Springer, K., 1994. Phytoplantkon and particle flux. Ber. Polarforsch. 149: 79-84.

Jaschnov, W. A., 1970. Distribution of *Calanus* species in the seas of the northern hemisphere. Int. Rev. ges. Hydrobiol. 55(2): 197-212.

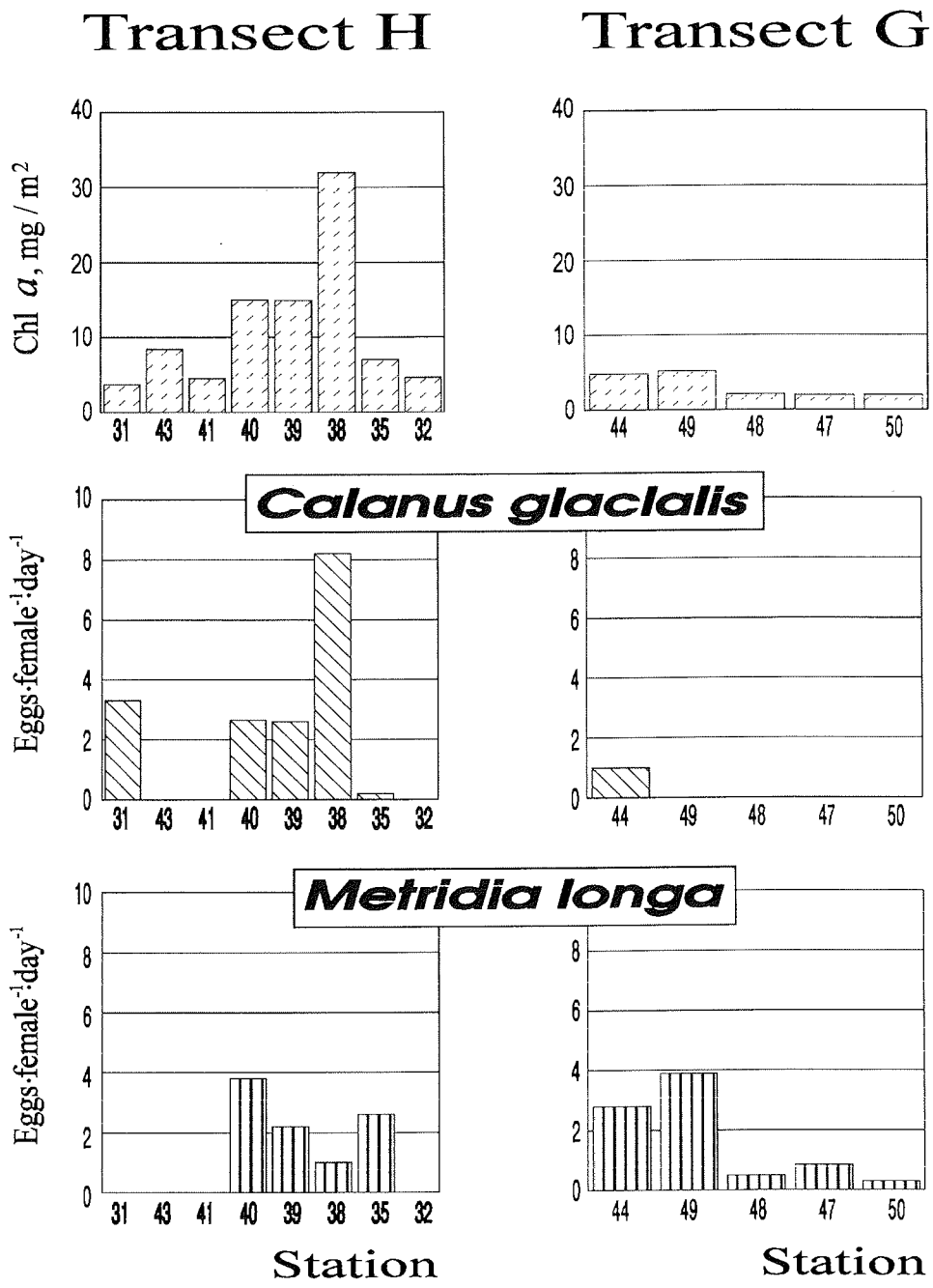

Fig. 5. Chlorophyll *a* concentrations in the 0-30 m depth layer (after Springer, 1994) and copepod egg production rates.

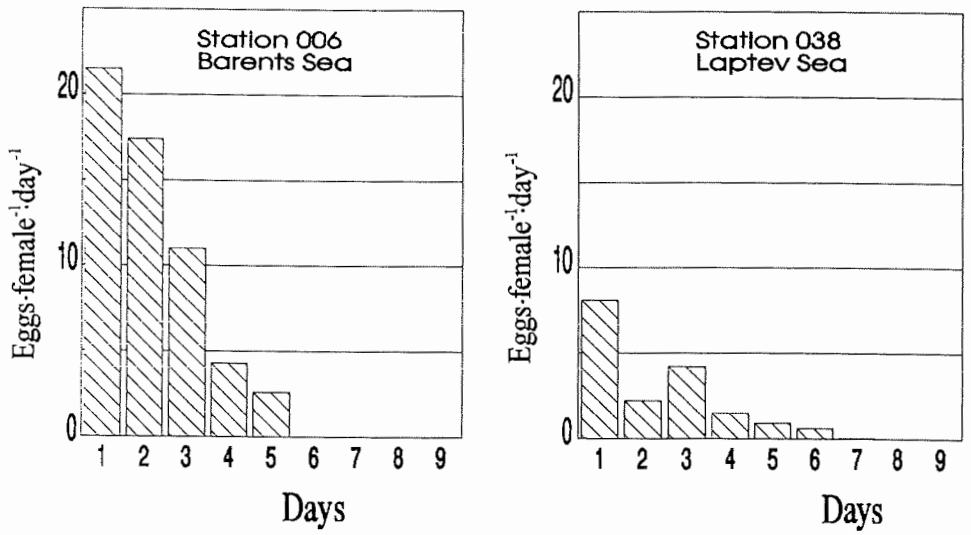

Fig. 6. *Calanus glacialis*. Egg production rate of starving females.

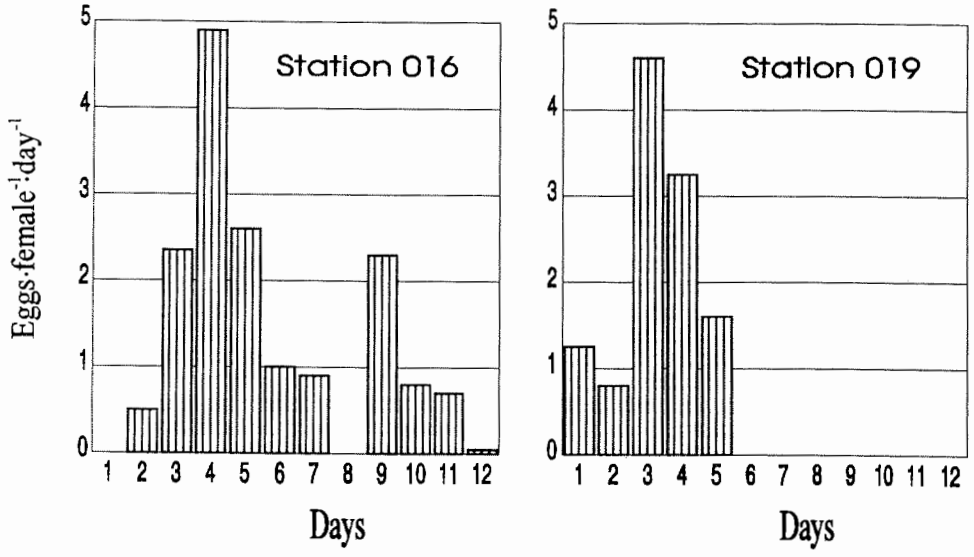

Fig. 7. *Metridia longa*. Egg production rate of starving females.

DISTRIBUTION, BIOMASS AND PRODUCTION OF *THYSANOËSSA LONGICAUDATA* KRØYER, 1846 (CRUSTACEA, EUPHAUSIACEA) IN THE ARCTIC

S. F. Timofeev
Murmansk Marine Biological Institute, Murmansk, Russia

Abstract

Adults of *Thysanoëssa longicaudata*, collected during "Polarstern" expedition ARK IX/4 in August-September 1993, were examined and measured. Samples were obtained from 19 stations, covering an area reaching from Spitsbergen and Franz Joseph Land to the Laptev Sea. The water column from 100 m to surface was sampled by means a vertically towed 61-cm Bongo net (200 μm mesh gauze). The size measurements were converted to biomass using a length/wet weight equation, and net production were calculated from these data. In Spitsbergen - Franz Josef Land area, the abundance of euphausiids ranged from 35.7 to 392.9 ind 1000 m^{-3} (178.6 ind 1000 m^{-3} on average), their biomass from 302.4 to 4016.6 mg 1000 m^{-3} (1817.4 mg 1000 m^{-3} on average). In the Laptev Sea, abundance and biomass of euphausiids was usually between 35.7 and 142.8 ind 1000 m^{-3} (62.6 ind 1000 m^{-3} on average) and 526.7-2735.2 mg 1000 m^{-3} (1388.2 mg 1000 m^{-3} on average). The mortality of euphausiids during the drift from Spitsbergen to the Laptev Sea was calculated to be about 65 %. The annual production was estimated to be 28.5 mg 1000 $m^{-3}a^{-1}$.

Introduction

Thysanoëssa longicaudata Kroyer, 1846 is an oceanic, boreal-Arctic Atlantic species, widely represented in the North Atlantic plankton, from where it penetrates into the Arctic Ocean with the waters of Atlantic origin (Fomin 1966; Lomakina 1978). Single specimens have been found north of Spitsbergen and Franz Joseph Land (Lomakina 1964), in Vilkitsky Strait (Linko 1908,1913), north of the Novosibirsk Islands and even in the Chukchi Sea (Lomakina 1978). *T. longicaudata* does not reproduce in the Arctic regions, however, larvae of older age (furcilia) occur west and north of Spitsbergen. Its maximum age in the Arctic is 2 years (Lomakina 1964,1978)

No information, obtained during one season, on distribution of crustaceans over the vast areas of the Arctic is available. The processes of development of euphausiid assemblages during their drift with Atlantic waters in high latitudinal areas are unknown.

This paper presents new information on the distribution, biomass, length-age composition, and production of *T. longicaudata* assemblages in the area from Spitsbergen to the northeastern Laptev Sea.

Material and Methods

Euphausiids were collected in the upper 100-meter layer during an international Expedition (ARKTIS IX/4) of RV "Polarstern" in August-September 1993. During the investigations the Bongo net (opening 0.28 m^2, mesh gauze 200 μm) was used; samples were fixed in 4-% neutral formalin. Information on stations is given in Table 1.

Euphausiid specimens were identified by species, analysed for sex and maturity stage (according Makarov and Denys 1980), and body lengths from rostrum tip to

Table 1: Abundance of *Thysanoëssa longicaudata* in the Arctic area in summer 1993

Stations	Date	Positions	Depth m	Temperature 0 m	Temperature 100 m	Salinity 0 m	Salinity 100 m	Abundance of euphausiids ind./ 1000 m^3	Abundance of euphausiids mg/ 1000 m^3
To the north-east from Spitsbergen									
27/007	13 Aug.	81°27N, 30°53E	540	-1.6	2.3	33.58	34.76	35.7	302.4
27/014	13 Aug.	81°40N, 30°15E	2681	-1.6	-0.1	32.94	34.50	71.4	799.0
To the north-east from Franz Josef Land									
27/019	18 Aug.	82°45N, 40°12E	2984	-1.8	-1.0	33.61	34.30	250.0	3333.2
27/020	19 Aug.	82°23N, 40°55E	1977	-1.7	-0.6	33.68	34.36	392.2	4016.6
27/024	20 Aug.	82°09N, 42°02E	1003	-1.7	2.1	33.18	34.76	142.9	635.9
Laptev Sea									
27/032	02 Sept.	78°43N, 132°20E	2992	-1.6	-1.6	32.70	34.12	107.1	2735.2
27/038	05 Sept.	78°08N, 133°23E	877	-1.3	-1.2	32.42	34.26	35.7	947.4
27/043	05 Sept.	77°24N, 133°33E	44	-1.2	-1.6	29.05	33.02	117.9	2615.1
27/048	09 Sept.	77°07N, 126°25E	526	-1.4	-1.0	31.81	34.32	142.8	2562.4
27/049	09 Sept.	77°06N, 126°18E	260	-1.6	-0.8	31.70	34.38	35.7	1140.4
27/050	10 Sept.	77°44N, 125°45E	2000	-1.7	0.1	32.49	34.46	35.7	1181.9
27/054	13 Sept.	79°11N, 119°54E	3070	-1.8	-1.7	33.45	34.08	71.4	1670.8
27/056	14 Sept	78°40N, 118°42E	2615	-1.8	-0.6	33.42	34.32	35.7	746.7
27/058	15 Sept.	78°00N, 118°33E	1930	-1.8	-0.4	33.28	34.40	35.7	644.0
27/060	17 Sept.	77°33N, 118°25E	1182	-1.8	-1.1	33.02	34.28	35.7	826.4
27/068	20 Sept.	78°28N, 110°47E	100	-1.7	-1.2	32.11	34.28	44.2	1241.4
27/069	21 Sept.	78°42N, 112°32E	521	-1.7	-0.4	32.50	34.38	107.1	1818.1
27/070	21 Sept.	78°45N, 112°41E	1140	-1.8	0.2	32.60	34.44	35.7	526.7
27/071	22 Sept.	78°34N, 111°22E	235	-1.8	-1.2	32.36	34.40	35.7	777.9

telson end were measured. Wet formalin body weights (W, mg) were calculated applying an equation relating this parameter and body lengths (L, mm) of *T. longicaudata* from the Barents Sea (Timofeev 1990):

$$W = 0.0048\ L^{3.0942}$$

Production of *T. longicaudata* was assessed from growth and mortality estimates according to the approach proposed by LeBlond and Parsons (1977).

Results

The abundances of *T. longicaudata* off Spitsbergen and Franz Josef Land varied from 35.7 to 392.9 ind 1000 m^{-3}, constituting on the average 178.6 ind 1000 m^{-3} for the whole area. Biomass of crustaceans varies from 302.4 to 4016.6 mg 1000 m^{-3} (on average mg 1000 m^{-3})(Tab.1 and Fig.1). The highest values for euphausiid abundance and biomass were recorded at stations over high depths (about 2000 m). No relationship was found between abundances of *T. longicaudata* and hydrography (temperature and salinity).

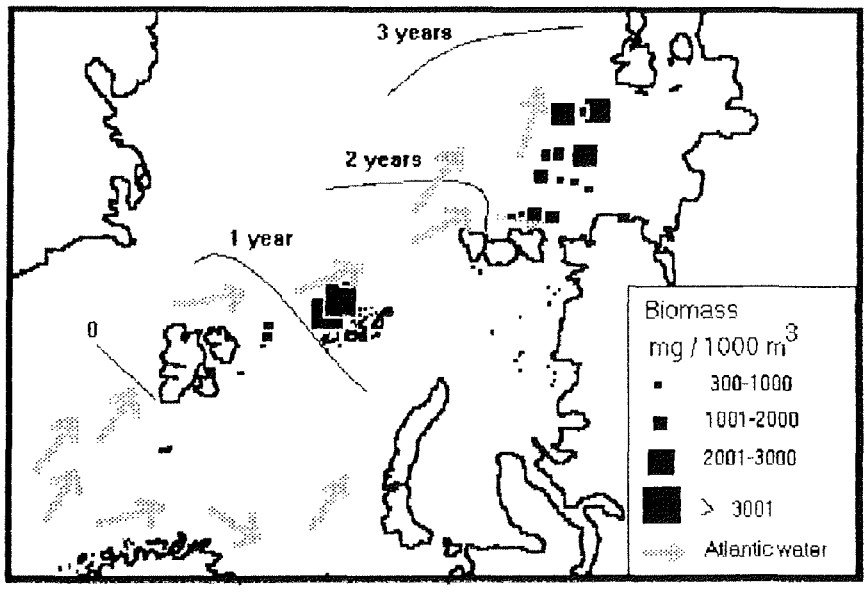

Fig. 1. Biomass distribution of *Thysanoëssa longicaudata* in the Arctic in summer 1993.

The abundances of *T. longicaudata* in the Laptev Sea were much lower and did not exeed 142.8 ind 1000 m^{-3} (minimum: 35.7 ind 1000 m^{-3} , mean: 62.6 ind 1000 m^{-3}). Biomass ranged between 526.7 and 2735.2 mg 1000 m^{-3} (mean biomass: 1388.2 mg 1000 m^{-3})(Tab.1 and Fig. 1). Thus, the biomass values in the Laptev sea were approximately similar to those in the Spitsbergen - Franz Josef Land area, whereas the abundances were nearly three times lower.

This phenomenon resulted from differences in the length-age structure of *T. longicaudata* populations between the regions (Fig. 2). In the west (Spitsbergen - Franz Josef Land) crustaceans were represented by specimens of 6.8-14.5 mm length (mean 11.5 mm), in the east (the Laptev Sea) they ranged between 12.2 and 17.4 mm (mean 15.3 mm) . Such length structures of *T. longicaudata* populations

suggest ages of 1+ in the west and 2+ in the east (Lindley 1978; Drobysheva 1979). It means, that the specimens from the Laptev Sea were 1 year older than those from the western area.

T. longicaudata sex structure is simple. Specimens dominated for which the secondary genital features (Thelycum and petasma) were not developed and ovaries and testis were not pronounced (stage I). Developed secondary genital features have been found only in males (stage IIIA), which accounted for 4 % of the population of the Spitsbergen - Franz Josef Land area and for 29 % of the Laptev Sea stock.

Discussion

The abundances of *T. longicaudata*, found in the Arctic in summer 1993, were comparable to those reported from the "functional basis" of the area (terminology of Beklemishev 1969), i.e. for the areas where euphausiids mature and reproduce, for example, in the Norwegian Sea. In 1959, the mean biomass of the crustacean assemablages of the Norwegian Sea (0-500 m), which were dominated by *T. longicaudata*, was 120-570 kg km^{-2} = 40-1140 mg 1000 m^{-3} (Timokhina 1964). In March 1989, *T. longicaudata* biomass varied from 140 to 3672 mg 1000 m^{-3} (on average 526 mg 1000 m^{-3}) in the central Norwegian Sea (0-50 m; Timofeev 1990). *T. longicaudata* stocks with similar abundances (below 1000 ind 1000 m^{-3}) had also been recorded in the vicinity of the Arctic area, i.e. in the Davis Strait, off Labrador (Huntley et al. 1983) and in the Barents Seas (Drobysheva 1979; Dalpadado and Skjoldal 1991).

The variation in the length-age structure of *T. longicaudata* stocks from Spitsbergen - Franz Josef Land to the Laptev Sea corroborates thehypothesis of a circulation of Atlantic waters in the Arctic. The drift of Atlantic waters from Franz Josef Land to the Laptev Sea are assumed to last one year (Treshnikov 1985). The differences between the mean age of crustaceans caught in the western and eastern regions was also1 year. The mortality and production of *T. longicaudata* during a possible transport from Franz Josef Land to the Laptev Sea could be estimated using the data on abundance, biomass and drift velocity. An abundance decrease from 178.6 ind 1000 m^{-3} in the western area to 62.6 ind 1000 m^{-3} in the Laptev Sea means that about 65 % of the population was eliminated by different reasons during the one-year drift. The annual production would then be 28.5 mg 1000 m^{-3} (growth constant = 0.3839; mortality coefficient = 0.4553; increment of organisms per time interval = 13.04 = 1 year).

This annual production estimate for *T. longicaudata* in the Arctic differs sharply from those estimated in the North Atlantic. *T. longicaudata* production in the northern Atlantic Ocean was assessed to be 100-1000 times higher by Lindley (1978). This difference is probably due to the fact that the production of only adult animals, whose growth rates are relatively low, were estimated in the Arctic area whereas the production of euphausiids in the Atlantic area was calculated including all age stages. Unfortunately, it is impossible to assess the contribution of the adults to the total production of *T. longicaudata* in the Atlantic from Lindley's data. Therefore, the relationship of productive potentials of same age *T. longicaudata* assemblages between the North Atlantic and Arctic area remains unknown.

Conclusions

The following conclusions from this study can be drawn: 1. the abundance, biomass and age composition of *T. longicaudata* in the Arctic area were

determined by the circulation of waters of Atlantic origin; 2. a pronounced elimination of euphausiids (65 %) takes place during the passive drift from the area around Spitsbergen to the Laptev Sea; 3. the yearly production of *T. longicaudata* in the Arctic (28.5 mg 1000 m^{-3}) is by several orders lower than that in the North Atlantic.

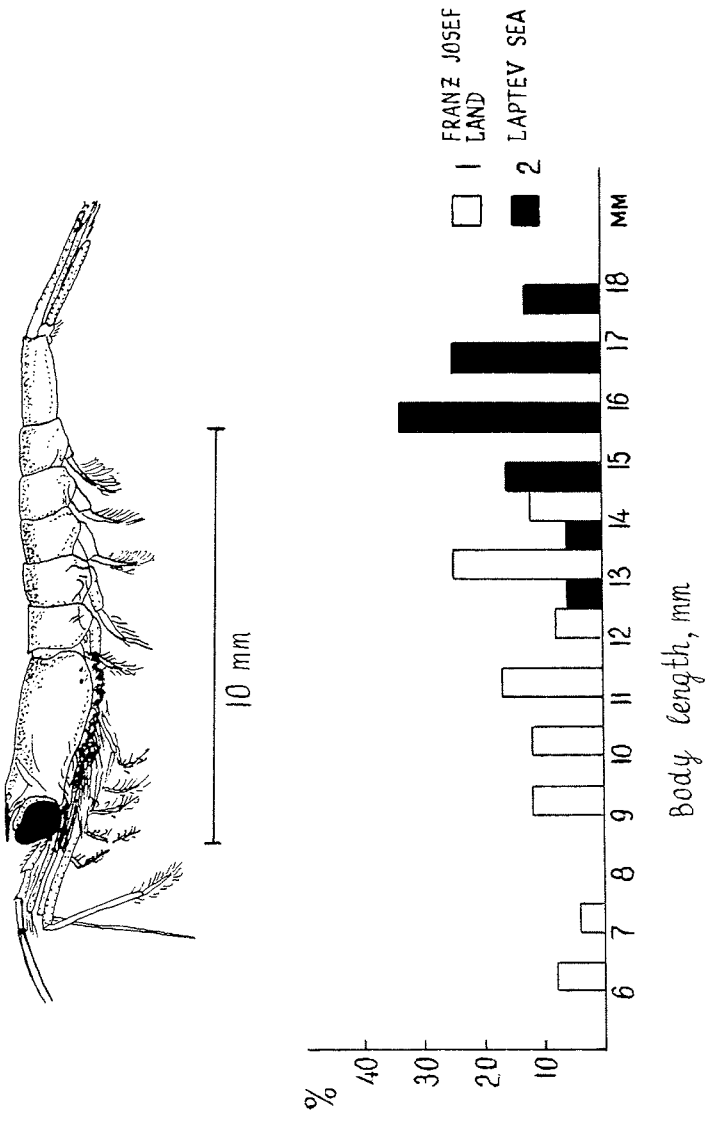

Fig. 2. Size-frequency distribution of *Thysanoëssa longicaudata* in the Arctic in summer 1993.

Acknowledgements

I thank the crew of the RV "Polarstern", H. Hanssen (Kiel) and Dr. K. Kosobokova (Moscow) for ensuring successful field operations without which this work would not have been possible.

References

Beklemishev, K.V., 1969. Ecology and biogeography of the pelagial. Moscow, Nauka, pp. 1-291. (In Russian).

Dalpadado, P., Skjoldal, H. R., 1991. Distribution and life history of krill from the Barents Sea. Polar Res. 102: 443-460.

Drobysheva, S. S., 1979. Euphausiids aggregations in the Barents Sea. In: Dushkina, L A. et al. (eds.): Food, feeding and survival of the Barents Sea's cod. Murmansk, PINRO, pp. 54-76. (In Russian).

Fomin, O. K., 1966. To the relationships between of *Thysanoessa longicaudata* and the Atlantic water. In: Nesis, K. N. (ed.): Materials to the fishery investigations in the northern area. Murmansk. PINRO, pp. 109-113. (In Russian).

Huntley, M., Strong, K. W., Dengler, A. T., 1983. Dynamics and community structure of zooplankton in the Davis Strait and northern Labrador Sea. Arctic 36: 143-161.

LeBlond, P. H., Parsons, T. R., 1977. A simplified expression for calculating cohort production. Limnol. Oceanogr. 22: 156-157.

Lindley, J. A., 1978. Population dynamics and production of euphausiids. I. *Thysanoëssa longicaudata* in the North Atlantic ocean. Mar. Biol. 46: 121-130.

Linko, A. K., 1908. Schizopoda of the Russian northern seas. Trans. Emper. Acad. Sci. 18(8): 1-76. (In Russian).

Linko, A. K., 1913. Zooplankton of the Siberian Polar Ocean by the collections of the Russian Polar Expedition in 1900-1903. Trans. Emper. Acad. Sci. 29(4): 1-54. (In Russian).

Lomakina, N. B., 1964. Mysids, cumaceans and euphausiids (Mysidacea, Cumacea et Euphausiacea) in the materials of the Arctic expedition on RV "F.Litke" 1955, RV "Ob" 1956 and RV "Lena" 1957 and 1958. Trans. Arctic and Antarctic Inst. 259: 241-254. (In Russian).

Lomakina, N. B., 1978. Euphausiids of the World Ocean (Euphausiacea). Leningrad, Nauka, pp. 1-222. (In Russian).

Makarov, R. R., Denys, C. J., 1980. Stages of sexual maturity of *Euphausia superba* Dana. BIOMASS Handbook 11: 1-11.

Timofeev, S. F., 1990. Macroplankton of the Norwegian Sea in March-April 1989. In: Matishov, G. G. (ed.): Structural and functional organization of ecosystems in the Barents Sea. Apatity, Kola Sci. Centre, pp. 121-136. (In Russian).

Timokhina, A. F., 1964. To production of zooplankton in the different water masses of the Norwegian Sea. Trans. PINRO 16: 165-181. (In Russian).

Treshnikov, A.F., 1985. Atlas of the Arctic. Moscow, State Maps Department, pp. 1-204. (In Russian).

BENTHIC STUDIES IN THE LAPTEV SEA

M. K. Schmid and K. Hinz
Institut für Polarökologie, Universität Kiel, Germany

Introduction

The shallow waters of the Laptev Sea have been a main research area of Russian investigations for over 40 years. Therefore, a good knowledge of the species composition and zoogeographical distribution of benthic as well as pelagic animals is available. On the other hand, deeper localities (>100m) of the Laptev Sea, including the continental slope, could not be sampled until recently. Quantitative data of biomass, small scale distribution and community analyses on a statistic basis were still scarce (Golikov 1990).

Our investigations are performed in close cooperation with the Zoological Institute of the Russian Academy of Sciences in St. Petersburg (ZISP) and focuses

a) on the interactions between sympagic fauna, phyto- and zooplankton, and benthos
b) on the impact of the seasonally pulsed fluvial input (fresh water, sediments) on the various biota of the Laptev Sea

Material and Methods

In a first step, the distribution and composition of zooplankton and benthos communties was elucidated during the TRANSDRIFT I cruise of RV "Ivan Kireev" to the shallow southern Laptev Sea in 1993 to complement the data from the past Russian expeditions. These community analyses were based on samples taken at 34 stations along four major transects by means of box corers, dredges, and seabed photography. Those transects have been prolonged with 28 stations during "Polarstern" cruise ARK IX/4 in 1993. They ranged from the shelf region with depths of 39 m down the continental slope to the deep sea with depths of over 3200 m. Various sampling gears have been used to cover a wide spectrum of benthic organisms, i.e. Agassiz-trawl (AGT), epibenthic sledge (EBS), giant box grab (GKG) and multi-box corer (MG).

The faunistic data were added to a biogeographic database of benthic species which is implemented by the ZISP. This database is aimed to monitor longterm changes in the distribution of benthic species assemblages.

Additional laboratory studies on aspects of the autecology of selected abundant species, e.g. respiration experiments, have been carried out in Kiel and during a research stay at the German "Koldewey" station in Ny Ålesund, Svalbard, in 1994.

Results

The results presented in this paper are based on the AGT samples taken during the "Polarstern" cruise. Only the macro- and megafauna (mesh size = 1cm) has been evaluated.

Figure 1 shows the location of the sampling stations of both expeditions. First results on the composition of major taxa on the easternmost transect (Transect I) are given in Fig. 2a. A depth gradient of 39 m to 3028 m is covered by four stations (Sts. 31, 41, 40, 32). At all stations, echinoderms were the most abundant group. Locally, crustaceans reached fairly high numbers but all other taxa were of minor importance in terms of abundance. Abundances were decreasing with depth and salinity. The abundance decline at station 40 corresponded to a sharp increase in

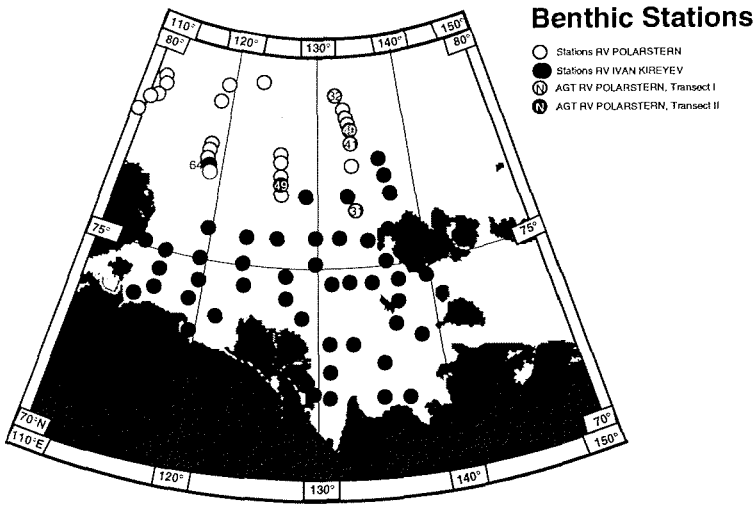

Fig.1: Benthic stations in the Laptev Sea sampled during TRANSDRIFT-I of RV "Ivan Kireev" in 1993 (black dots without numbers) and during the "Polarstern" cruise ARK IX/4 in 1993 (white dots, white and black dots with numbers). Numbers in dots indicate evaluated AGT-stations along the eastern-most transect (Transect I) and along the 200 m depth line from west to east (Transect II). Station 40 is part of both transects (grey dot with number).

temperature. There is, however, no distinct shift in the taxonomic composition of the catches with water depth, salinity and temperature. The composition of the various echinoderm taxa on Transect I is shown in Fig. 2b. Ophiuroids were most important on stations shallower than 233 m. The deep-sea station (3028 m) is dominated by the holothurian *Elpidia glacialis*. Echinoidea, mainly represented by *Pourtalesia jeffreysi*, was another deposit feeding group present at this deep sea station.

Within the Ophiuroids *Ophiocten sericeum* was most important on the two shallow stations (Sts. 31, 41)(Fig. 2c). It reached maximum numbers (5,735 ind 3000 m^{-2}) at station 41. The second important species was *Ophiacantha bidentata,* it dominated in 233 m depth (St. 40), whereas *O. sericeum* was not found on this station. One of the biggest brittle star species, *Ophiopleura borealis*, which is presumed to be confined to Arctic water masses, appeared here on the station with the highest water temperature (+1,44 °C).

The composition and abundance of echinoderms and in more detail of ophiuroids sampled along the 200 m depth line from west to east (Transect II) are presented in Fig. 3a and 3b. Ophiuroids reached the highest abundances within the echinoderms (Fig. 3a) with a maximum density on station 49 in the central Laptev Sea. Asteroids and crinoids were of minor importance, holothurians and echinoids were caught only in very low numbers.

A more detailed analysis of the ophiuroid compositon is presented in Fig. 3b. The three stations indicating a longitudinal gradient were very different in species composition and abundance. Notable were the very high abundances of *O.bidentata* and *O. sericeum* at station 49 in the central Laptev Sea with 5,615 ind 3000 m^{-2} and 2,403 ind 3000 m^{-2}, respectively. The densities of *Ophiopleura borealis* decreased pronouncedly from west to east.

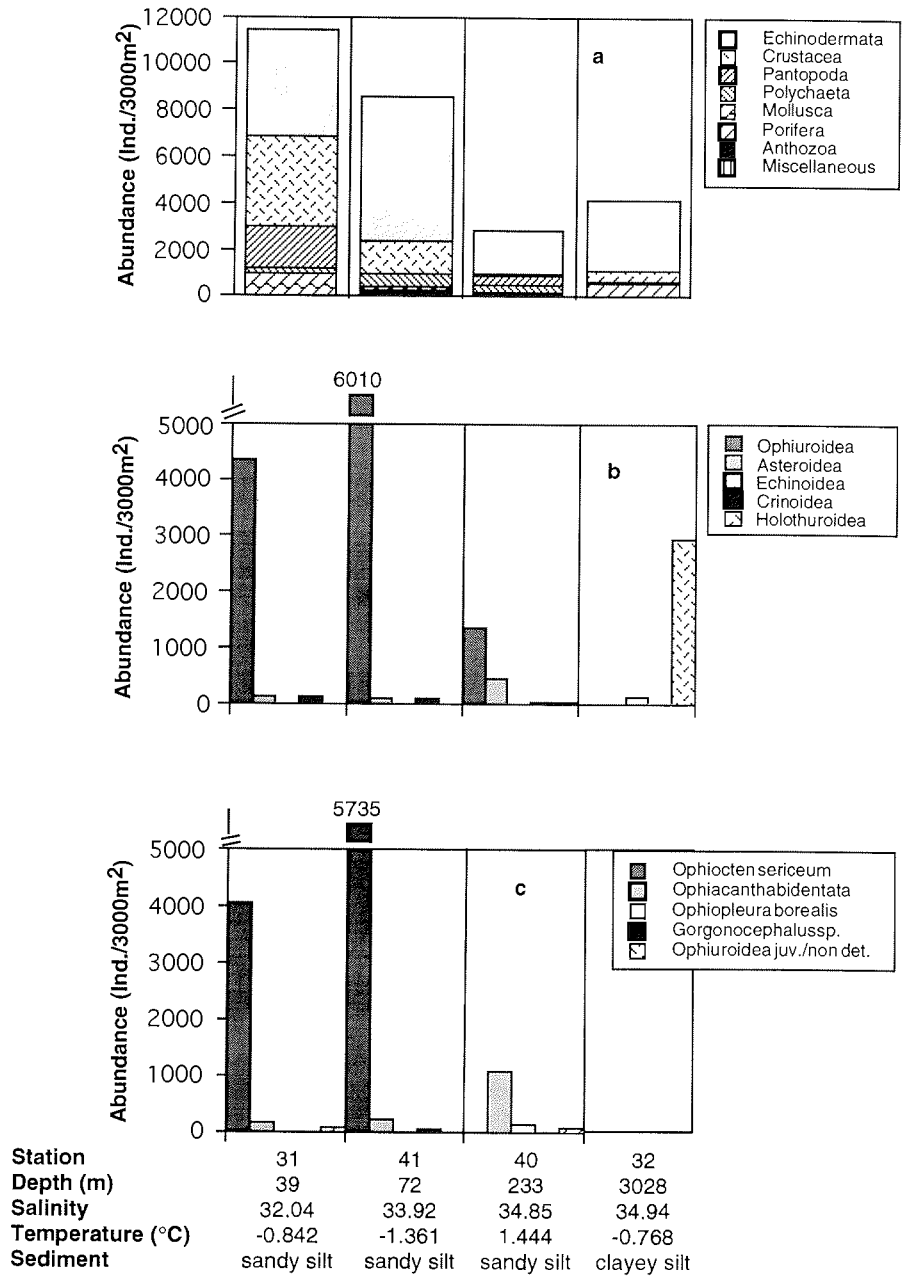

Fig. 2: a) Abundances (ind 3000 m^{-2}) of epibenthic organisms of different taxa found in AGT samples on Transect I (Sts. 31, 41, 40, 32). b) Abundances (ind 3000 m^{-2}) of echinoderms in AGT samples from Transect I (Stn 31, 41, 40, 32). c) Abundances (ind 3000 m^{-2}) of ophiuroid species in AGT samples from Transect I (Sts. 31, 41, 40).

Discussion

First results confirmed the existence of the presumed gradients in species distribution and abundance with increasing water depth, temperature and fresh water influence of the Lena.

The total benthic abundances on Transect I were mainly influenced by depth (Fig. 2a). A second factor is presumably salinity. With increasing depth and salinity, individual numbers were decreasing. The crustaceans and pantopods followed this general trend, whereas the abundances of the other major taxa might be influenced by other parameters, such as food supply, seasonal variation, surface structure, etc. The type of substrate, usually a major factor controlling the composition and distribution of benthic organisms, can be neglected on the shelf stations.

Echinoderms were the dominant benthic taxon. Investigations showed that they are often of high importance in higher latitudes (Piepenburg 1989; Piepenburg and Juterzenka 1994). The more detailed look at the echinoderm community reveals clearer dependencies on depth, salinity and temperature (Fig. 2b). Within the ophiuroids, *O.sericeum* was confined to shallow stations (<100m) where it reached very high numbers (5,735 ind 3000 m^{-2}). Its densitiy decreased drastically in approx. 200 m depth (7 ind 3000 m^{-2}), and it was not found in the deep sea. The 200 m station was dominated by *O.bidentata,* which has been found in lower numbers also at the shallow stations. *O. borealis* was only found on this station (St. 40) of Transect I.

Ophiuroids and asteroids were not found at the deep sea station. We propose that this is mainly due to the lack of food supply in this area. Ophiuroids have been reported to be a major taxonomic group on many deep sea locations (Gage and Tyler 1982).

The distribution and abundance of echinoderms on Transect II (Fig. 3a and 3b), especially the very high numbers of the two ophiuroid species *O. bidentata* and *O. sericeum* cannot be related to the abiotic factors regarded so far. Only *O. borealis* followed an obvious temperature gradient. Other studies also emphasize that this species is strongly restricted to cold water masses with temperatures below 0°C (Blacker 1957).

Further examinations of the remaining stations will emphasize our preliminary findings reported above. In addition, they will reveal the importance of the Laptev Sea area as a transition zone inhabited by species of both Pacific and Atlantic origin as well as the specific adaptions and interactions of the organisms of the different marine compartments.

Acknowledgments

The benthological studies carried out during the TRANSDRIFT-I cruise of RV "Ivan Kireev" and ARK IX/4 of RV "Polarstern" to the Laptev Sea in 1993 were part of the project "German-Russian Investigations on the Ecology of the Marginal Seas of the Eurasian Arctic" (GRIEMSEA), funded by the German Ministry for Research and Technology (BMFT), and is embedded in the multidisciplinary research programme "SYSTEM LAPTEV SEA".

References

Blacker, R. W., 1957. Benthic animals as indicators of hydrographic conditions and climatic change in Svalbard waters. Fisheries Invest. (Ser.2) 20(10): 1-49.

Gage, J. D., Tyler, P. A., 1982. Depth-related gradients in size structure and the bathymetric zonation of deep-sea brittle stars. Mar. Biol. 71: 299-308.

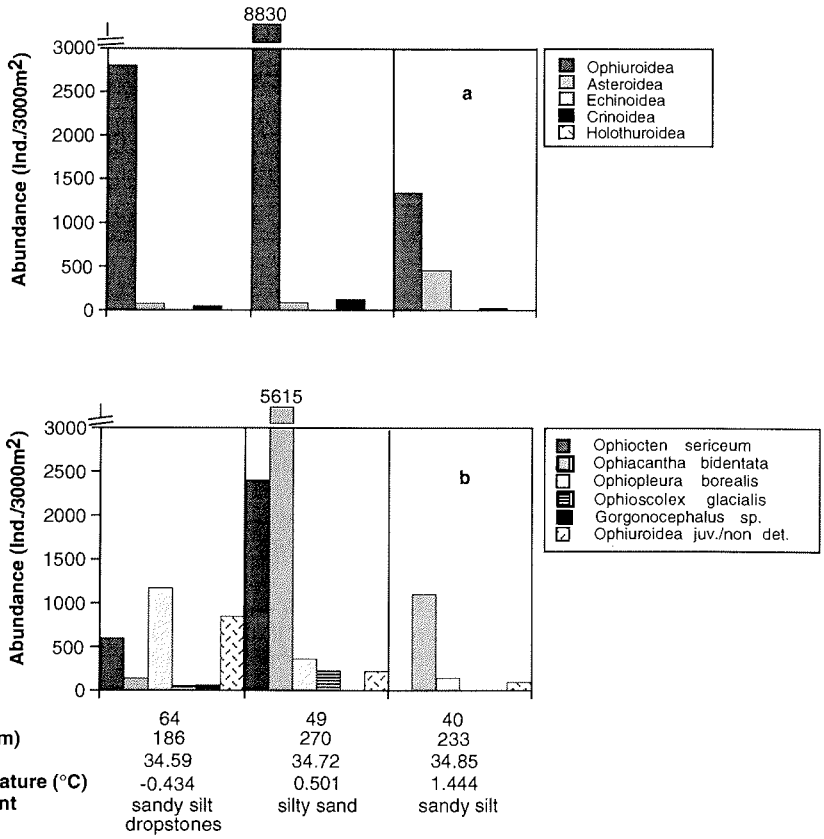

Fig. 3: a) Abundances (ind 3000 m^{-2}) of echinoderms found in AGT samples from Transect II (Sts. 64, 49, 40). b) Abundances (ind 3000 m^{-2}) of ophiuroid species in AGT samples from Transect II (Sts. 64, 49, 40).

Golikov, A. H., 1990. Ecosystem of the New Siberian shoals and the Fauna of the Laptev Sea and adjacent waters. Explorations of the Fauna of the Seas. 37(45): 1-462.

Piepenburg, D., 1989. Absolute densities and spatial distribution patterns of epibenthic species from the Fram Strait. Rapp. P.-v. Réun. Cons. Int. Explor. Mer 188: 188.

Piepenburg, D., Juterzenka, K. v., 1994. Abundance, biomass and spatial distribution pattern of brittle stars (Echinodermata: Ophiuroidea) on the Kolbeinsey Ridge north of Iceland. Polar Biol. 14: 185-194.

BOTTOM BIOCOENOSES OF THE LAPTEV SEA AND ADJACENT AREAS

B. I. Sirenko*, V. V. Petryashov*, E. Rachor+ and K. Hinz°

* Zoological Institute, Russian Academy of Sciences, St. Petersburg, Russia

\+ Alfred-Wegener-Institut für Polar- und Meeresforschung, Bremerhaven, Germany

° Institut für Polarökologie, Universität Kiel , Germany

The history of the investigations

Scientific investigations of aquatic biota of the Laptev Sea have been conducted for more than 120 years. Within this period, organisms were collected by more than 20 expeditions. The most comprehensive ones were the hydrographic expedition of the Arctic Ocean on board of the steamers "Taimir" and "Vaigach" (1912-1914) studying mainly the shallow part of the sea, as well as the expeditions on board of the ice-steamers "Sadko"(1937-1938) and "Litke" (1948) and the Second Arctic Hydrobiological Expedition of the Zoological Instituteof the Russian Academy of Sciences (ZISP) in 1973 studying the south-eastern and eastern parts of the sea using diving equipment. Until 1993, biological samples had been collected in the Laptev Sea at about 360 stations, at 200 stations faunistic material was only collected using dredges and trawls (Fig. 1).

In 1993, expeditions on board the German ice-breaker "Polarstern" and the Russian research vessels "Ivan Kireev" and "Lot" initiated a new stage in the investigations of the Laptev Sea biota. The expeditions sampled about 100 biological stations, and the collections were mainly being quantitative. In 1994, these investigations have been continued at 22 stations during an expedition with RV "Prof. Multanovsky" (Fig. 2).

Publications of the scientific results of biological research in the Laptev Sea are relatively scarce. Until 1990, data were published on plankton (Linko 1913; Virketis 1932; Yashnov 1940, 1946), on benthos of the Lena River estuary and the New Siberian shoals (Popov 1932; Derjugin 1932; Gorbunov 1939, 1941, 1946), on marine fish (Andriashev 1939, 1948), on relationship of some fish species with distribution of zooplankton (Lutsik et al. 1981), and on the complexes of benthic foraminifera (Tamanova 1970, Lukina 1978) and meiobenthos (Sheremetevsky 1977). In 1990, the Zoological Institute published a collection of articles entitled "Ecosystems of the New Siberian Shoals and fauna of the Laptev Sea and Adjacent Waters" (Golikov 1990), summarizing the results of the investigations in the previous years. In the past few years, Gukov (1989, 1991, 1992) presented a number of articles on the distribution of species assemblages (called biocoenoses in the following) in the southern parts of the Laptev Sea.

These publications presented data on biota mainly of the south-eastern and eastern regions of the Laptev Sea. The recently published preliminary results of the investigations conducted since 1993 (Petryashov 1993, Sirenko 1993, Rachor et al. 1994, Sirenko and Piepenburg 1994, Petryashov et al. 1994) may be regarded as the first stage of the large scale research program of the whole Laptev Sea.

Bottom biocoenoses of the Laptev Sea

Based on the quantitative collections available, 29 biocoenoses were distinguished in the Laptev Sea (Golikov et al. 1990; Gukov 1989, 1991, 1992; Petryashov et al. 1994). The greatest mosaicity with 19 of 29 biocoenoses was found in the shallow coastal parts at depths of 10-15 m.

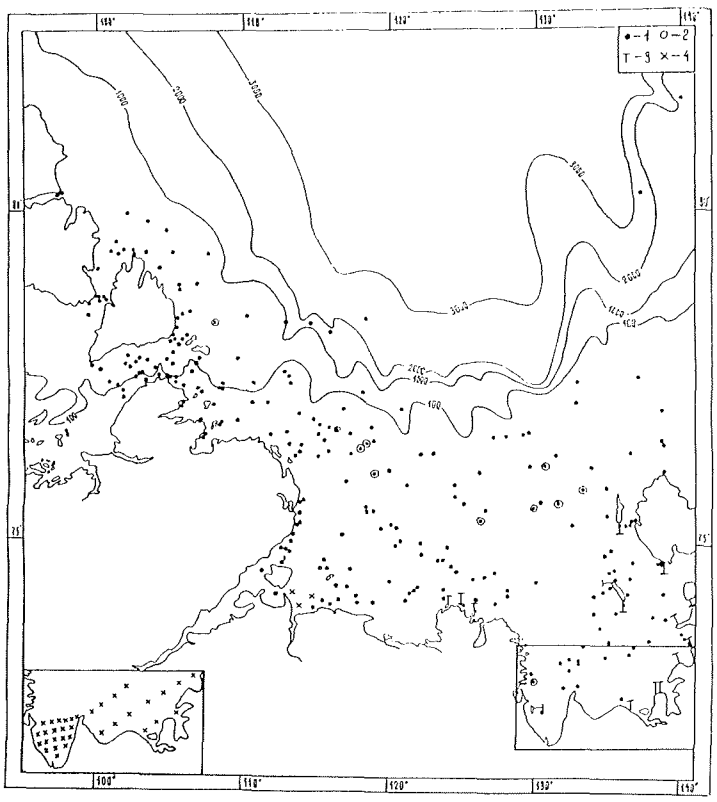

Fig.1: Location of biological stations in the Laptev Sea before 1993: 1 - biological stations; 2 - quantitative biological stations; 3 - diving sections of the Zoological Institute (RAS) in 1973 (several stations per section); 4 - biological stations of the Tiksi Hydrometeorological Service and Environmental Control in 1989-1990.

From the lower intertidal zone down to depths of 1-2 m, due to ice scouring during winter, either seasonal biocoenoses, such as the biocoenosis of *Gammarus setosus* on stony ground, or a very poor biocoenosis of polychaetes (with *Scoloplos armiger* and *Terebellides stroemi*) on muddy bottoms with very low biomasses of 2-0.4 g m^{-2} were found in summer (Fig.3). Biocoenoses of *Portlandia aestuariorum*, *Cyrtodaria kurriana*, *Rhizomolgula globularis* and *Yoldiella intermedia* (with an average biomass of 28-87 g m^{-2}) were distributed in the most brackish parts of the studa area: in Anabarsky Bay, the area of the Lena River delta, the Bay Buor-Haya, the Jansky Gulf and near Lyakhovskie Islands at depths of 1-2 m to 8-11 m on sandy and muddy grounds. At depths of 5-10 to 20-28 m, on similar grounds in areas where a strong influence of river runoff is still observed, biocoenoses of *Portlandia siliqua*, *Saduria sibirica* & *S. sabini* and *Tridonta borealis* & *Nicania montagui* & *P. siliqua* (biomass 21-168 g m^{-2}) were found mostly in the south-eastern part (Fig. 4).

Until recently, the macrobenthos on stony grounds in the Laptev Sea (depths > 2 m) has only been studied in the region of the New Siberian Islands (Golikov et al. 1990). At depths of 3-9 m, biocoenoses of *Phyllophora truncata* & *Laminaria*

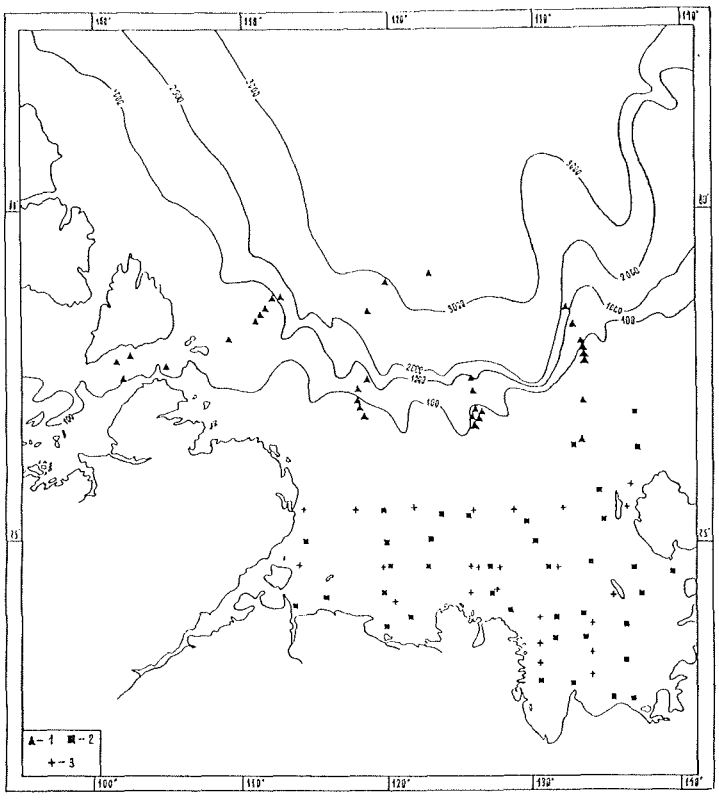

Fig.2. Location of biological stations in the Laptev Sea in 1993 and 1994: 1 - German ice-breaker RV"Polarstern", 1993; 2 - RV "Ivan Kireev", 1993; 3 - RV "Professor Multanovsky", 1994.

solidungula & Spongia (Stolbovoi Island, Belkovskii Island, average biomass 241 g m^{-2}) and *Laphoeina maxima* (Kotelnyi Island, average biomass 110 g m^{-2}) have been described. At greater depths (12-15 to 22 m), the following biocoenoses occur off Stolbovoi Island: *Balanus crenatus* & *Suberites domuncula* & *Eucratea loricata*, *Musculus corrugatus* & *Suberites domuncula* & *Phyllophora truncata* & *Alcyonidium gelatinosum*, and again *Suberites domuncula* & *Haliclona gracilis* also (with relatively high biomass: 136-138 g m^{-2}). Only a biocoenosis with *Saduria sibirica* & *Portlandia siliqua* & *Haliclona gracilis* & *Astarte crenata* & *Suberites domuncula* at the same depths off Belkovskii Island had a considerably lower biomass (on average 28 g m^{-2})on sandy-mud grounds with stones.

In the open waters of the north-eastern and south-western Laptev Sea, at depths of 22-45 m on muddy grounds, a biocoenosis dominated by *Leionucula bellotii* existed with an average biomass of 111-188 g m^{-2}. In the central and western regions which are not influenced by the fluvial freshwater runoff, a biocenosis of *Tridonta borealis* with subdominant polychaetes, bivalves and brittle stars (60-260 g m^{-2}) were found on mud-sand, mud and clay grounds at depths of 18-42 m.

In the northern Laptev Sea, at depths of 30-60 m on the eastern and north-western transects sampled by "Polarstern" in 1993, the brittle star *Ophiocten sericeum* is the dominant species; Polynoidae gen. sp., *Saduria sabini*, and *Myriotrochus rinkii*

were subdominant in the eastern part, whereas *Onuphis conchylega* and Bryozoa gen. sp. were subdominant in the north-western part (Fig. 5). There is a broad belt between 60 and 700 m depths inhabited by a brittle star biocoenosis (*Ophiocten sericeum* & *Ophiacantha bidentata* & *Ophiopleura borealis*) with subdominant polychaetes, molluscs, sponges, alcyonarians, holothurians, and isopods. Further offshore, at depths of 700-800 to 2000-2500 m, a biocenosis dominated by polychaetes Maldanidae gen. sp. & *Spiochaetopterus* sp. forms another belt. The subdominant group includes brittle stars, sponges, and holothurians. In greater depths down to approximately 3000 m, a biocoenosis dominated by the deep-water Arctic holothurians *Kolga hyalina* and *Elpidia glacialis*, the sea urchin *Pourtalesia jeffreysi*, as well as several polychaetes, amphipods, sponges and molluscs was found.

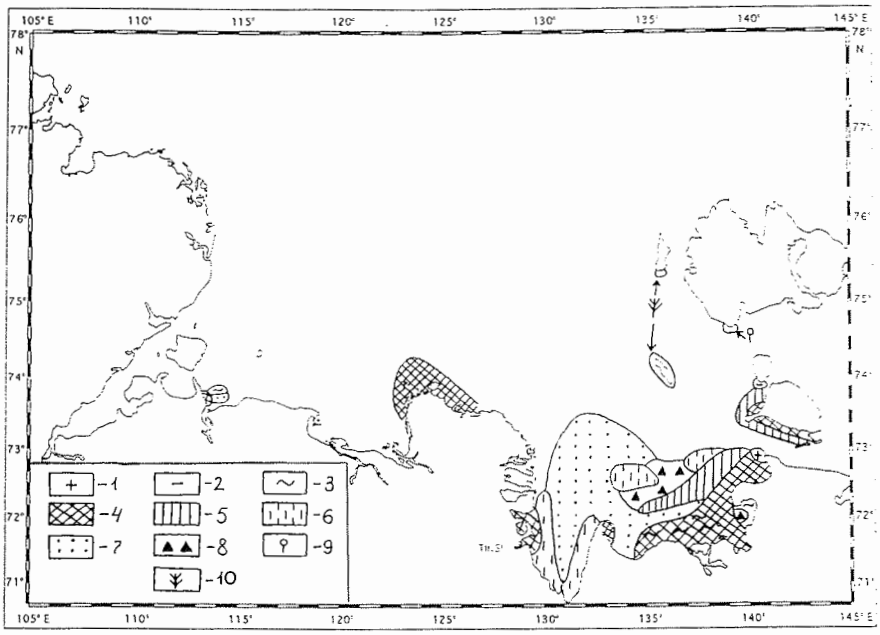

Fig.3. Distribution of bottom biocoenoses in the Laptev Sea at depths of 0 to 10-15 m: 1 - *Gammarus setosus*; 2 - *Scoloplos armiger* & *Terebellides stroemi*; 3 - *Cyrtodaria kurriana*; 4 - *Portlandia aestuariorum*; 5 - *Rhizomolgula globularis*; 6 - *Yoldiella intermedia*; 7 - *Portlandia siliqua*; 8 - *Tridonta borealis* & *Nicania montagui* & *Portlandia siliqua*; 9 - *Laphoeina maxima*; 10 - *Phyllophora truncata* & *Laminaria solidungula* & *Phakellia cribrosa* & *Haliclona gracilis* & *Suberites domuncula*.

The ecological-faunistic zonation

Based on the distribution of indicator species (out of 126 species of Bivalvia, Gastropoda, Malacostraca, and Echinodermata) and the faunistic composition of different regions, the Laptev Sea south of 76-77° N has been divided into two ecological-faunistic districts (Petryashov and Novozhilov, in press) (Fig.6, 7; Table 1): Estuarine-Arctic and Marine-Arctic. Both districts have their analogies or prolongations in other Siberian Arctic seas.

The Estuarine-Arctic district is usually comprised by small areas near river mouths. In the Laptev Sea, to this district belong the regions near the south-western coast of Lyakhovskie Islands, in the Anabarsky Gulf and, possibly, in the uninvestigated

Khatanga Bay. The largest part of the Estuarine-Arctic district, and probably its most integral area, extends as a thin belt along the coast from the Jansky Gulf to the Lena River delta and, possibly, to the mouth of the Olenek River. Bottom water salinities in the summer range between 5-8 to 16-18. The indicator species of the Estuarine-Arctic district are the molluscs *Portlandia aestuariorum* and*Cyrtodaria kurriana* as well as the crustaceans *Saduria entomon glacialis* and *Mysis relicta*. Echinoderms are absent. The macrobenthic fauna is more homogenous than that of the Marine-Arctic district (Jaccard index (Ij): 50-55.2%, Chekanovsky-Sörensen index (Ich: 53.3-71.1%, Shimkevich-Simpson index (Ish): 58.6-100 %), and it differs notably from the offshore benthos.

Table 1: Macrobenthos of the Laptev Sea: The locations of areas D1-D28 are shown in Fig.6. Underscored values in the main diagonal are numbers of species in every region. Faunistic similarities between stations, measured by the Chekanovsky-Sörensen index (below the main diagonal), and Degree of Inclusion from Less Diverse to More Diverse Fauna (%), measured by the Shimkevich-Simpson index (above the main diagonal).

	D1	D2	D3	D4	D5	D6	D7	D8	D9	D10	D11	D12	D13	D14	D15	D16	D17	D18	D19	D20	D21	D22	D23	D24	D25	D26	D27	D28
D1	29	67	82	92	56	69	100	56	31	83	69	57	45	69	42	40	7	25	14	28	32	52	27	22	7	23	30	11
D2	39	12	55	42	58	58	33	33	8	25	50	42	75	58	58	50	25	8	42	58	58	67	50	33	17	42	50	17
D3	45	52	11	36	64	73	36	73	9	46	73	55	82	91	82	64	9	27	36	64	73	91	64	64	18	36	55	9
D4	57	40	33	13	39	39	69	31	8	42	69	31	46	92	39	23	0	8	23	31	31	46	38	23	15	8	23	8
D5	40	50	52	35	16	39	31	38	15	17	56	50	88	75	69	38	20	25	38	50	50	94	50	38	25	38	31	13
D6	43	56	67	39	35	13	46	62	23	42	69	54	69	77	54	62	8	25	31	62	54	77	39	46	15	31	62	8
D7	71	29	30	62	31	41	16	25	15	67	100	29	38	75	25	25	0	8	13	25	19	50	19	25	6	6	19	19
D8	40	29	59	28	38	55	25	16	39	25	38	50	63	56	56	63	20	33	31	56	56	69	44	38	19	25	44	38
D9	19	8	8	8	14	23	14	35	13	17	46	15	39	39	31	54	39	17	54	46	39	54	46	39	31	15	46	69
D10	49	25	44	40	14	40	62	21	16	12	100	25	58	75	33	50	8	8	17	42	42	42	50	50	17	8	17	17
D11	66	27	37	40	38	40	67	25	27	55	32	43	50	59	58	60	40	33	31	34	32	56	59	44	32	41	50	33
D12	37	39	48	30	47	52	27	47	15	23	26	14	50	71	57	50	14	17	21	71	64	86	36	43	14	36	57	29
D13	39	32	38	24	53	36	23	38	20	29	46	28	37	48	79	50	33	42	30	46	39	60	68	44	32	27	50	33
D14	69	34	50	57	53	48	53	40	24	43	56	47	42	29	53	45	13	33	14	41	32	62	41	30	11	23	35	19
D15	33	45	60	31	63	44	23	51	25	26	43	49	54	42	19	47	27	42	37	63	53	79	58	47	32	37	42	32
D16	33	38	45	18	33	49	22	56	42	38	46	41	35	37	46	20	33	33	40	80	65	65	55	45	30	30	50	45
D17	5	22	8	0	19	7	0	19	36	7	26	14	19	9	24	29	15	8	73	53	53	47	40	47	47	40	53	87
D18	15	8	26	8	21	24	7	29	16	8	18	15	20	20	32	25	7	12	50	67	33	50	33	17	33	25	17	25
D19	12	20	16	12	22	15	9	18	27	8	28	11	29	12	24	27	41	24	39	49	54	31	46	59	71	50	50	59
D20	21	24	25	14	26	27	13	35	20	17	28	33	41	32	37	57	26	28	45	46	68	43	64	56	46	41	60	56
D21	32	35	41	20	36	31	14	41	24	25	30	43	34	32	43	54	37	20	45	51	28	54	64	56	39	50	55	41
D22	44	31	39	23	54	38	29	39	26	19	50	44	57	52	51	43	26	23	30	40	44	40	55	52	32	46	65	37
D23	24	35	42	29	42	29	16	37	34	35	48	28	51	35	54	52	32	24	33	41	56	39	22	64	55	36	40	41
D24	21	21	37	15	28	30	19	28	25	31	41	29	38	29	39	38	33	10	49	41	55	42	57	27	56	50	45	33
D25	7	10	10	10	18	10	5	14	20	10	30	10	28	11	26	25	33	20	60	35	39	27	48	55	28	46	45	41
D26	20	29	24	6	32	23	5	21	11	6	33	28	20	20	34	29	32	18	36	27	44	32	36	45	40	22	45	36
D27	25	38	39	18	28	49	17	39	36	13	39	47	35	29	41	50	46	13	34	36	46	43	38	38	38	43	20	45
D28	11	10	5	5	9	5	14	28	45	10	31	20	28	18	26	38	62	15	49	41	40	30	37	33	40	33	38	27

Note: Underscored numbers are numbers of species in every regions.

The Marine-Arctic district comprises three sections:

The Polyhaline-Arctic section is most extensive in the eastern Laptev Sea, between the Buor-Haya Bay, the Yansky Gulf and the Strait of Zarja and Stolbovoi Island. It extend to 74° 30' N at 131°-136° E; to the west, the width of the section becomes abruptly smaller and includes the areas around the delta of the Lena

River and part of the Olenek Gulf. This section will certainly be found also in Anabarsky and Khatanga Bay, but these regions have not been investigated yet. In this section, the species which are characteristic of the river plume zone (*Saduria sibirica* and *Portlandia siliqua*) are dominant or subdominant species. Among the echinoderms, only three species are noted here (*Leptasterias groenlandica, Urasterias linckii, Ophiocten sericeum*). Summer bottom water salinities range from 16-18 to 30.

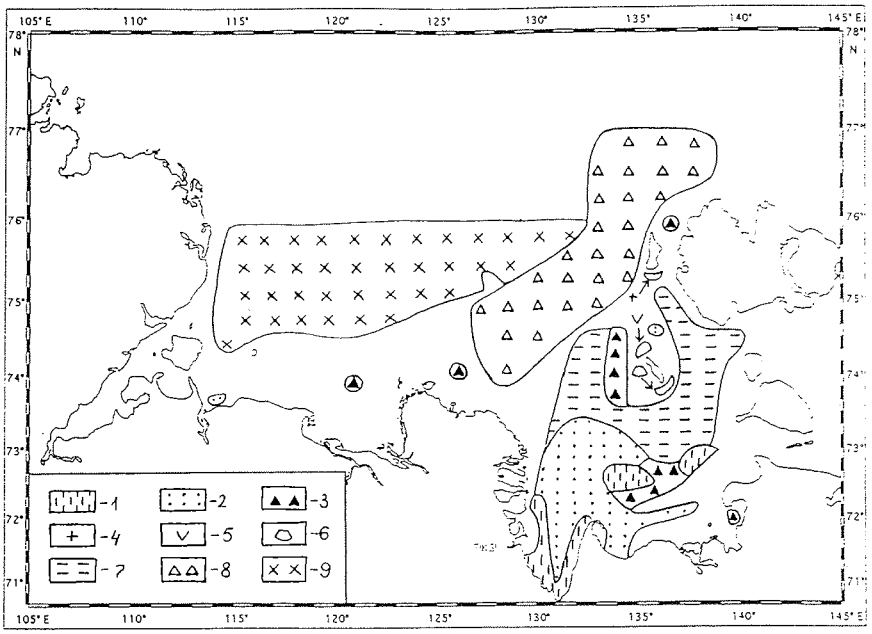

Fig.4. Distribution of bottom biocoenoses in the Laptev Sea at depths from 5-10 to 50 m: 1 - *Yoldiella intermedia*; 2 - *Portlandia siliqua*; 3 - *Tridonta borealis* & *Nicania montagui* & *Portlandia siliqua*; 4 - *Saduria sibirica* & *Portlandia siliqua* & *Haliclona gracilis* & *Astarte crenata* & *Suberites domuncula*; 5 - *Musculus corrugatus* & *Suberites domuncula* & *Haliclona gracilis* & *Phyllophora truncata* & *Alcyonidium gelatinosum*; 6 - *Balanus crenatus* & *Suberites domuncula* & *Eucratea loricata*; 7 - *Saduria sibirica* & *S. sabini*; 8 - *Leionucula bellotii*; 9 - *Tridonta borealis*.

2. The Poly-Euhaline-Arctic section has also its maximal extension in the eastern Laptev Sea, reaching 76°30' N in the north-east. Further to the west, the northern boundary of this section goes in south-western direction, nearly approaching the coast. It forms some projections to the north, corresponding to bottom depressions, along which a principal outflow of most of the transformed waters of the river runoff occurs. The above-mentioned species characteristic of the river-plume zone are not dominant in this section. The echinoderm fauna consists of 13 species. I_{ch} is 50-75%, I_{sh} is 50-65%. Summer bottom salinities are about 30-32. Transformed river runoff waters are always present, at least in the surface layers.

3. The Euhaline-Arctic section is situated in the northern Laptev Sea. In its fauna, there are no indicator species of river runoff water. Echinoderms (more than 40 species) are numerous, some of them often being dominant or subdominant. I_{ch} values range between 51.4-61.9%, I_{sh} between 50-86.7%. Summer bottom salinities are usually higher than 32. Transformed river waters do not influence the hydrography.

The proposed scheme of the biogeographic distribution will certainly be refined in the future, especially after obtaining new data from the western Laptev Sea.

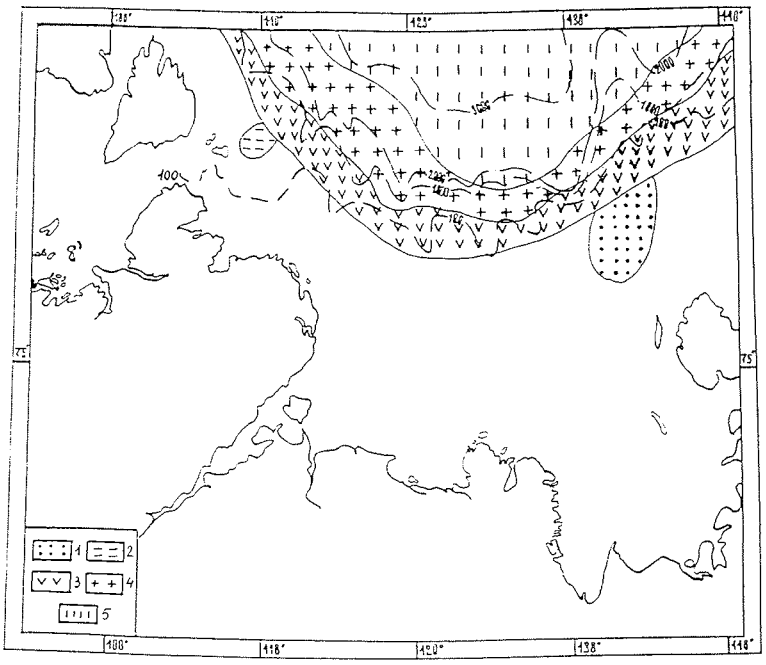

Fig.5. Distribution of bottom biocoenoses in the Laptev Sea at depths from 30-60 to 3800 m: 1 - *Ophiocten sericeum* & Polychaeta gen. sp. & *Saduria sabini* & *Myriotrochus rinkii*; 2 - *Ophiocten sericeum* & *Onuphis conchylega* & Bryozoa gen.sp.; 3 - *Ophiocten sericeum* & *Ophiacantha bidentata* & *Ophiopleura borealis*; 4 - Maldanidae gen. sp. & *Spiochaetopterus* sp.; 5 - *Kolga hyalina* & *Elpidia glacialis* & *Pourtalesia jeffreysi*.

Hydrothermal vents

One of the most interesting biological samples collected during the "Polarstern" cruise in 1993 was taken by an Agassiz trawl at station 50 in the central Laptev Sea at a depth of about 2000 m. The content of this trawl catch was notably different from the samples obtained at adjacent stations.

First, the muddy ground was characterized by a higher content of sulfuric hydrogen, by core concretions and unusual conglomerates of quaint shape not met at any other station.

Second, the bottom fauna was different in terms of both species composition and distribution on the substrate. The benthos was distinctly poorer than even that at station 54, loctated 1000 m deeper. All larger animals presumably inhabited the sediment surface, and no infauna characteristic of the soft grounds at other stations were found.

Third, typical forms of a hydrothermal fauna (bivalves of the family Vesicomyidae) were present in asubfossil condition. A preliminary examination of the shells by Dr. Ya. I. Starobogatov, St. Petersburg, showed that they belong to a new species of the genus *Archivesica* (Fig.8).

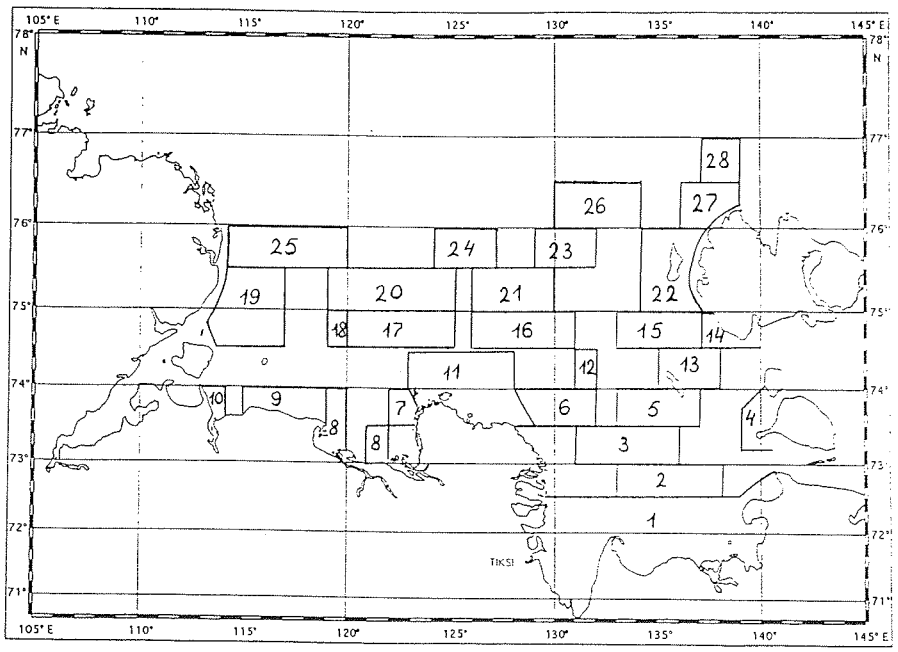

Fig.6. Map of the areas mentioned in the ecological-faunistic analysis (Tab.1).

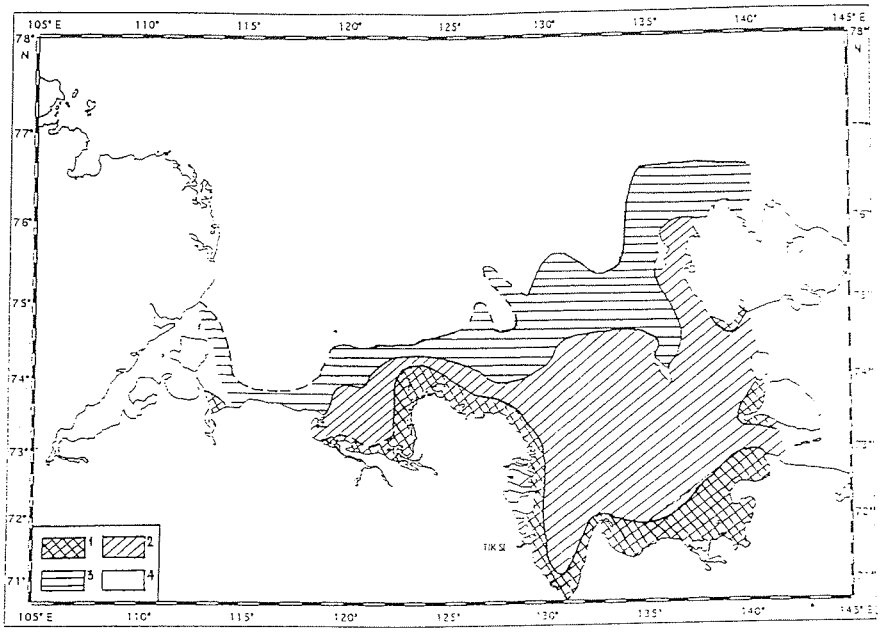

Fig.7. Ecological-faunistic zonation of the bottom fauna of the Laptev Sea: 1 - Estuarine-Arctic district; 2-4 - Marine-Arctic district: 2 - Polyhaline-Arctic section; 3 - Poly-Euhaline-Arctic section; 4 - Euhaline-Arctic section.

Fig.8. *Archivesica* sp. collected in the northern Laptev Sea.

All this evidence suggest that a spot with hydrothermal fauna could have existed in the area discussed. Accordingly, it may be possible to discover active hydrothermal vents in the investigated region of the northern Laptev Sea, as station 50 is situated at a place where the Gakkel Ridge meets with the continental slope. The Gakkel Ridge is one end of a gigantic middle-oceanic ridge encircling nearly the entire globe. It begins in the Laptev Sea, passes through the central parts of the Arctic Ocean, the entire Atlantic, southern part of the Indian Ocean, crosses the southern part of the Pacific Ocean diagonally and ends up in the Gulf of California. There, hydrothermal vents have been found with their characteristic fauna with molluscs of the genus *Archivesica* very similar to those found by us in the Laptev Sea.

The descriptive stage of the biological studies of the Laptev Sea has not yet been completed. Our knowledge on species composition and distribution of benthos and plankton for the coastal regions of the western Laptev Sea and for the entire area at depths of 50-200 m is still poorly known.

References

Andriashev, A. P., 1939. New data on ecology and distribution of fishes in the Laptev Sea . Dokl. AN SSSR, 25(7): 728-731. (In Russian).

Andriashev, A. P., 1948. To the study of fishes of the Laptev Sea (Based on material of expeditions on ice-breakers "Malygin" and "Sedov" in the summer 1973). Proc. Zool. Inst. AN SSSR. 7: 76-100. (In Russian).

Derjugin, K. M., 1932. Benthos of the Lena River estuary. Issled. morei SSSR, L. 15: 63-66. (In Russian).

Golikov, A. N., 1990. Ecosystems of the New Siberian shoals and the fauna of the Laptev Sea and adjacent waters. Explorations of the fauna of the seas 37(45): 1-463. (In Russian).

Golikov, A. N., Scarlato, O. A., Averincev, V. G., Menshutkina, T. V., Novikov, O. K., Sheremetevsky, A. M., 1990. Ecosystems of the New Siberian shoals, their distribution and functioning. in: Golikov, A. N (Ed.): Ecosystem of the New Siberian shoals and the fauna of the Laptev Sea and adjacent waters. Explorations of the fauna of the seas. 37(45): 4-79. (In Russian).

Gorbunov, G. P., 1939. Bottom population of the Soviet Arctic. Problemy Arktiki, 7-8: 89-96. (In Russian).

Gorbunov, G. P., 1941. Bivalve mollusc *Portlandia arctica* (Gray), as an index of distribution of continental waters in Siberian seas. Problemy Arktiki, 11: 46-55. (In Russian).

Gorbunov, G. P., 1946. Bottom population of New Siberian shoals and central part of the Arctic Ocean. Tr. dreif. exp. Glavsevmorputi na "G. Sedov" 1937-1940. M. L. 3: 30-138. (In Russian).

Gukov, A. Yu., 1989. Bottom biocoenoses of the Buor-Haya Bay (Laptev Sea). Okeanologiya. 29(2): 316-317. (In Russian).

Gukov, A. Yu., 1991. On the bottom fauna of the Yansky Bay of the Laptev Sea. Okeanologiya, 31(3): 454-456. (In Russian).

Gukov, A. Yu., 1992. To the study of the Anabar Bay of the Laptev Sea. Okeanologiya, 32(3): 506-509. (In Russian).

Linko, A. K., 1913. Zooplankton of the Arctic Ocean from the collections of the Russian Polar expedition 1900-1903. Zap. Imp. Acad. Nauk. S. Pb, 29(4): 1-54. (In Russian).

Lukina, T. G., 1978. Foraminifera of the New Siberian Shoals. II. Vsesoyuzn. konf. po biologii shelfa (All Union conference on biology of the shelf: Abstracts of communications). P. 2. Kiev: 66-67. (In Russian).

Lutsik, A. I., Silina, N. I., Lutsik, N. K., 1981. To the fauna of zooplankton and fishes of the south-eastern part of the Laptev Sea. Okeanologiya, 21(2): 370-374. (In Russian).

Petryashov, V. V., 1993. Marine biological studies. Marine interdisciplinary expedition to the Laptev Sea on board RV "Ivan Kireev" in August-September 1993. Part 2.9. Materials of expedition studies. A preliminary report on expeditions to the Taimir Peninsula and Laptev Sea in the summer 1993 on RV "Ivan Kireev" and ice-breaker RV "Polarstern" according to the program of Russian-German cooperation. S.Pb.: 117-124. (In Russian).

Petryashov, V. V., Sirenko, B. I., Rachor, E., Hinz, K., 1994. Distribution of macro-benthos in the Laptev Sea from materials of the expeditions of RV"Ivan Kireev" and ice-breaker RV "Polarstern" in 1993. Scientific results of the expedition LAPEX-93. S.Pb..: 277-288. (In Russian).

Petryashov, V. V., Novozhilov, A. V., (in press). The influence of the hydrological regime on the distribution of macrobenthos in the Laptev Sea. (In Russian).

Popov, A. M., 1932. A hydrobiological review of the Laptev Sea. Issled. fauny morei SSSR, L. 15: 189-229. (In Russian).

Rachor, E., Hinz, K., Sirenko, B. I., 1994. Biological investigations. 7.4.2. Macrofauna. In: Rachor, E. (Ed.): Die Expedition ARCTIC '93: Der Fahrtabschnitt ARK - IX/4 mit FS "Polarstern" 1993. Ber. Polarforsch. 149: 97-106.

Sheremetevsky, A. M., 1977. Meiobenthos in the intertidal zone of the Laptev Sea and the New Siberian Islands. Gidrobiol. zhurn. 13(1): 63-70. (In Russian).

Sirenko, B. I., 1993. Investigation of composition and distribution of the benthos in the northern Laptev Sea. Materials of expedition studies. A preliminary report on expeditions to the Taimir Peninsula and Laptev Sea in the summer 1993 on RV "Ivan Kireev" and ice-breaker RV "Polarstern" according to the program of Russian-German cooperation. S.Pb..: 238-251.

Sirenko, B. I., Piepenburg, D., 1994. Current knowledge on biodiversity and benthic zonation patterns of Eurasian Arctic shelf seas, with special reference to the Laptev Sea. in: Kassens, H. (Ed.): Russian-German Cooperation in the Siberian Shelf Seas: Geo-System Laptev Sea. Ber. Polarforsch. 144: 69-77.

Tamanova, S. V., 1970. Species composition of recent Foraminifera as an indicator of the hydrological regime of the Arctic seas. Severnyi Ledovityi okean i ego poberezhye v kainozoe, L.: 199-203. (In Russian).

Virketis, M. A., 1932. Some data on zooplankton of south-eastern part of the Laptev Sea. Issled. morei SSSR, 15: 105-125. (In Russian).

Yashnov, V. A., 1940. Plankton productivity of the northern seas the USSR.- M.: 1-35. (In Russian).

Yashnov, V. A., 1946. Distribution of autochthonous pelagic fauna of the Arctic. Bull. MOIP. Otd. biol., 51(6): 40-50. (In Russian).

FISH CAUGHT IN THE LAPTEV SEA DURING THE CRUISE OF RV "POLARSTERN" IN 1993

N. V. Chernova and A. V. Neyelov
Zoological Institute, Russian Academy of Sciences, St. Petersburg, Russia

Abstract

This paper presents a list of marine fish species caught during the cruise of RV "Polarstern" to the Laptev Sea in 1993. In total, 34 species of 21 genera and 6 orders were identified. 12 species were found for the first time in the Laptev Sea, 2 additional species had been listed as questionably for the Laptev Sea before this study. Thus, the list of fish species proven to occur in the Laptev Sea has been extended for about one fourth, and and the number of marine species has been doubled.

Introduction

The fish fauna of the Laptev Sea had been studied only insufficiently. Before 1993, merely 46 fish species were known from this region (Andriashev and Chernova 1994). Six of these species were questionably, and 10 of them were anadromous species, such as the Pacific salmon species, or semi-anadromous species, such as the Siberian sturgeon as well as the various charr and whitefish species (Berg 1949; Andriashev 1948, 1954; Kirillov 1972). Thus, only about 30 marine fish species were reported to occur in the Laptev Sea. Undoubtedly, this number was underestimating the true fish diversity. Investigations of fish and their distribution patterns in the Laptev Sea belonged to the first stage of a faunistic study.

The reasons of the poor knowledge are the remoteness, harsh climate, and heavy ice conditions of the Laptev Sea which make the area barely accessible for marine investigations. Therefore, the expedition of the German research ice-breaker "Polarstern" to the Laptev Sea in 1993 provided a rare opportunity to enrich our knowledge of the ichthyofauna of the Laptev Sea. Preliminary results of the analyses of the fish collections from the "Polarstern" cruise have been published by Neyelov and Chernova (1994) during the Russian-German workshop in St.Petersburg in November 1994. In this paper, we give the complete results of this fish study.

Material and Methods

This report is based on a small fish collection, received by the Zoological Institute (St. Petersburg) from the cruise of RV "Polarstern" to the Laptev Sea in 1993. Fish specimens were collected from Agassiz trawl catches carried out at 17 stations (Table 1).

Table 1: Agassiz trawl stations during the cruise of RV "Polarstern" to the Laptev Sea in 1993.

Station #	Date	Latitude N	Longitude E	Depth m	Temperature °C	Salinity
29	27.08.93	77°40.60-77°40.53	102°07.3-102°05.13	120	-1.05	34.24
31	01.09.93	76°29.83-76°29.53	133°10.29-133°11.29	39	-0.85	31.97

Table 1: Continue

Station #	Date	Latitude N	Longitude E	Depth m	Temperature °C	Salinity
32	02.09.93	78°42.68-78°42.70	132°33.8-132°38.08	3012-3028	-	-
35	04.09.93	78°23.4	133°09.5	2151-1934	-0.76	34.86
38	05.09.93	78°10.58-78°10.70	133°25.26-133°26.06	1038-1039	0.03	34.81
39	05.09.93	78°06.02-78°06.03	133°32.27-133°32.93	526-514	0.68	34.81
40	06.09.93	78° 04.56-78°04.52	133°34.9-133°33.77	231-233	-	-
41	06.09.93	77°54.83-77°54.67	133°34.37-133°35.39	72-71	-1.35	34.86
43	06.09.93	77°24.46-77°24.32	133°32.96-133°23.68	54	-1.61	33.03
44	07.09.93	77°02.32-77°02.63	126°25.30-126°25.01	96	-	-
47	09.09.93	77°11.67-77°11.65	126°19.11-126°20.41	1006-1079	0.13	34.82
48	09.09.93	77°07.83-77° 07.06	126°25.04-126°24.33	556-530	0.87	34.81
49	09.09.93	77°04.07-77°04.07	126°10.07-126°08.08	170-280	0.49	34.66
50	10.09.93	77°41.43-77°41.10	125°55.09-125°54.16	1992-1993	-0.81	34.87
54	13.09.93	79°11.33-79°11.81	119°56.37-119°56.22	3076-3081	-0.76	34.88
64	18.09.93	77°14.72-77°14.41	118°30.92-118°32.21	191-181	-0.44	34.54
67	20.09.93	78°15.32-78°15.56	109°14.58-109°15.53	51	-1.22	34.29
68	20.09.93	78°28.57-78°28.05	110°46.92-110°46.00	101	-	-

Results and Discussion

At least 34 fish species of 21 genera, 10 families and 6 orders were identified.

Order I. Rajiformes

Fam. 1. Rajidae

1. *Raja hyperborea* (Collett, 1879)

- St. 39 (1 adult female, L ca. 1 m), 47 (2 subadults, L ca. 60 cm, ca. 35 cm).

Order II. Myctophiformes

Fam. 2. Myctophidae

2. *Benthosema glaciale* (Reinhardt, 1837)

- 39 (1), 49 (1).

Order III. Gadiformes

Fam. 3. Gadidae

3. *Arctogadus glacialis* (Peters, 1874)
   - 39 (1), 41 (3).
4. *Boreogadus saida* (Lepechin, 1774)
   - 29 (3), 31 (5), 40 (2), 43 (4), 44 (2), 49 (10), 67 (1).

Order IV. Scorpaeniformes

Fam. 4. Cottidae

5. *Artediellus atlanticus* (Jordan et Evermann, 1898)
   - 49 (10).
6. *Gymnocanthus tricuspis* (Reinhardt, 1831)
   - 31 (6).
7. *Icelus bicornis* (Reinhardt, 1840)
   - 29 (1), 35 (1), 44 (6), 67 (15), 68 (10).
8. *Icelus spatula* (Gilbert et Burke, 1912)
   - 31 (2).
9. *Triglops nybelini* (Jensen, 1944)
   - 40 (29), 43 (8), 44 (6), 49 (10), 64 (4), 68 (4).

Fam. 5. Cottunculidae

10. *Cottunculus sadko* (Essipov, 1937)
    - 39 (1), 48 (1).

Fam. 6. Agonidae

11. *Leptagonus decagonus* (Schneider, 1801)
    - 49 (8), 50 (1), 64 (1).
12. *Ulcina olriki* (Lutken, 1876)
    - 31 (1).

Fam. 7. Cyclopteridae

13. *Cyclopteropsis macalpini* (Fowler, 1914)
    - 67 (5), 68 (1).

Fam. 8. Liparidae

14. *Liparis gibbus* (Bean, 1881)
    - 41 (2), 44 (3)
15. *Liparis fabricii* (Kroyer, 1847)
    - 31 (2), 40 (1), 41 (6), 43 (19), 44 (19), 67 (14), 68 (1).
16. *Careproctus* sp.
    - 29 (1), 35 (2), 38 (1), 39 (3), 41 (2), 43 (1), 48 (1), 49 (4), 64 (1).
17. *Paraliparis bathybius* (Collett, 1879)
    - 50 (4).
18. *Rhodichthys regina* (Collett, 1879)
    - 50 (5).

Order V. Perciformes

Fam. 9. Zoarcidae

19. *Gymnelus* sp.
    - 31 (2), 44 (1).
20. *Lycodes eudipleurostictus* (Jensen, 1901)

- 40 (1), 43 (1), 44 (1).

21. *L. frigidus* (Collett, 1880)
    - 32 (4), 39 (2), 50 (4).
22. *L. polaris* (Sabine, 1819)
    - 41 (1).
23. *L. pallidus* (Collett, 1878)
    - 29 (8), 35 (2), 40 (5), 44 (4), 49 (3), 68 (1).
24. *L. reticulatus* (?) (Reinhardt, 1835)
    - 29 (1), 43 (1).
25. *L. rossii* (Malmgren, 1864)
    - 29 (2), 44 (1).
26. *L. sagittarius* (McAllister, 1975)
    - 29 (1),35 (1), 39 (1), 40 (1), 47 (3), 49 (2).
27. *Lycodes nigricans* (Jensen, 1952)
    - 38 (12), 39 (2), 40 (4), 44 (2), 47 (3), 48 (1), 49 (1).
28. *L. adolfi* (Nielsen et Fossa, 1993)
    - 38 (30), 47 (9), 49 (4).
29. *Lycodes* sp. 1
    - 50 (8).
30. *Lycodes* sp. 2
    - 49 (2).
31. *Lycodes* sp. (juv.)
    - 31 (1).
32. *Lycodonus flagellicauda* (Jensen, 1901)
    - 47 (1), 48 (1).
33. *Lycenchelys cf. platyrhinus*
    - 39 (1), 50 (5), 54 (1).

Order VI. Pleuronectiformes

Fam. 10. Pleuronectidae

34. *Reinhardtius hippoglossoides* (Walbaum, 1792)
    - 38 (1 adult, L ca. 64 cm).

12 species have been found for the first time in the Laptev Sea (*R. hyperborea, B. glaciale, A. glacialis , C. macalpini, P. bathybius, L. rossii, L. sagittarius, L. nigricans, A. adolfi, L. flagellicauda, Lycenchelys* cf. *platyrhinus, R. hippoglossoides*) . The catch of North-Atlantic species such as the darkbelly ray, the black halibut and Polar *Paraliparis* were not unexpected, as they were known to occur in the more eastern parts of the Polar basin from catches carried out from the drifting ice-camp "North Pole 22" in the East-Siberian Sea (Tsynovsky 1980 a, b).

The Arctic species *L. rossii* was known before from the Kara Sea. One of the most interesting results is the occurrence of the Northern Lanternfish, *B. glaciale* . This small mesopelagic fish is considered as an indicator of Atlantic Water. It was recorded in the Arctic north of Spitsbergen (Neyelov and Chernova 1991), near Franz Joseph Land (Borkin 1986) and near Novaya Zemlya (Borkin and Shevelev 1980). The occurrence of *B.glaciale* so far to the east is reported for the first time. As this species is regarded to spawn in the temperate North Atlantic only, the whole region along the continental slopes of the polar basins might be considered as an

area of sterile expatriation. The same interpretation seems to hold true also for the Black Halibut.

L. flagellicauda was known from cold depth of the Norwegian and Greenland seas north of 80° N near Spitsbergen. The record in the Laptev Sea greatly enlarged the known area of its distribution to the east. This fish occurs probably in all parts of the Nansen Basin from the northern Greenland Sea eastward up to the Laptev Sea or possibly even more to the east.

A. glacialis is a poorly studied cod species, known before from Greenland waters and the East Siberian Sea (Andriashev et al. 1980). This species, like the other cryopelagic cod species *B. saida*, is assumed to occur in the high Arctic (80°-88° N) under pack ice, forming occasionally quite large stocks.

Some other fishes were known before by only a few specimens. The rare and poorly studied *C. macalpini* was described from northwestern Greenland and the central Barents Sea. It is also quite peculiar that only 2 adult specimens belonging to the genus *Cyclopteropsis* were known from Eurasian northern seas. The second species of this genus, *C. jordani* , had been described by only one specimen from the Kara Sea. The catch of six adult specimens of *C. macalpini* will allow to improve the existing description of this genus and species.

Two recently described *Lycodes* species were found: *L. sagittarius*, known from the Beaufort Sea (McAllister 1975) and the Kara Sea (with only 2 specimens!), as well as *L. adolfi*, described from East and West Greenland (Nielsen and Fossa 1993). Some other *Lycodes* specimens seemed to be identical with *L. nigricans* Jensen, 1952.

Specimens of *Lycenchelys* have been identified provisionally as *L. platyrhinus*. Only a single specimen of this species had been caught before between Iceland and Jan Mayen at a depth of 1848 m. The systematic position of this species is unclear. Some features suggest to put it in the genus *Lycenchelys*, but it differs significantly from by the absence of scales and some other important characters, revealing a transition to the genus *Lycodes* (Andriashev 1954; Anderson 1994). This species (1 specimen from St. 54) was caught at a depth 3076-3081 m - being the maximum depth in the polar basins from which a fish has been reported. Two species, *L. eudipoleurostictus* and *C. macalpini* , were listed before as questionably for the Laptev Sea (Andriashev 1954). The rare species *C. sadko* was known by only 4 specimens from the northwestern Kara Sea and one young, questionably identified specimen from the Laptev Sea (Andriashev 1954).

Two forms of *Lycodes* are very probably new to science. Fish of the genus *Careproctus* are not studied entirely yet, as they are mainly young. It is clear, however, that there are several species, including new one.

Thus, the small fish collection received by the 1993 expedition of RV "Polarstern" to the Laptev Sea is of great interest. The list of fish species known from the Laptev Sea comprises 58-60 species now, being extended for about one fourth. The number of marine fish species known from the Laptev Sea has even been doubled.

Acknowledgements

The authors are greatly thankful to the chief scientist of the "Polarstern" cruise Prof. Dr. D. Fütterer (Bremerhaven), to the head of the benthos group Dr. E. Rachor (Bremerhaven) and to Dr. B. I. Sirenko, the head of the Laboratory of Marine Research of the Zoological Institute RAS in St.Petersburg for fish sampling. The other part of fish received from this cruise was placed in the Institute of Polar Ecology (Kiel). We are thankful to the director of the Institute, Prof. Dr. M. Spindler,

and to Dipl.-Biol. Katja Hinz for making this collection available to us. This study was supported by RFFI, Grant # 62297.

References

Anderson, M. E., 1994. Systematics and osteology of the Zoarcidae (Teleostei: Perciformes). Ichthyological Bull. J.L.B. Smith. Institute of Ichthyology, 60: 1-120.

Andriashev, A. P., 1948. K poznaniyu ryb morya Laptevykh (To the knowledge of the fishes of the Laptev Sea). Trudy Zool. Inst. AN SSSR 7: 76-100. (In Russian).

Andriashev, A. P., 1954. Ryby severnykh morei SSSR (Fishes of the northern seas of the U.S.S.R.). Opredelitely po faune SSSR 53. Moskwa-Leningrad, Izdat. Akad. Nauk SSSR, 556 pp. (In Russian).

Andriashev, A. P., Chernova, N. V., 1994. An annotated list of fish-like vertebrates and fishes of the Arctic Seas and adjacent waters. J. Ichthyology 34(4): 435-456. (In Russian).

Andriashev, A. P., Mukhomediarov, B. F., Pavstiks, E. A., 1980. On mass aggregations of cryopelagic cod, *Boreogadus saida* and *Arctogadus glacialis*, in the circumpolar regions of the Arctic. In: Vinogradov, M. E., Mel'nikov, I. A. (Eds.): Biology of the Central Arctic Basin. Moskva, Nauka, pp. 196-211. (In Russian).

Berg, L. S., 1948, 1949. Ryby presnykh vod SSSR i sopredel'nykh stran. T. 1-3. (Fishes of the fresh water of the USSR and adjacent countries). 4 ed., 1. Opredeliteli po faune SSSR 27, 29, 30. 1381 pp. (In Russian).

Borkin, I. V., 1986. Record of northern lanternfish near Franz Josef Land. J. Mar. Biol. (Vladivostok) 3: 63-64. (In Russian).

Borkin, I. V., Shevelev, M. S., 1980. Northern lanternfish, *Benthosema glaciale* Reinhardt (Myctophiformes, Myctophidae), near Novaya Zemlya. J. Ichthyology 20(2): 345- 346. (In Russian).

Jensen, A. S., 1952. Recent finds of Lycodinae in Greenland waters. Meddr. om Grønland 142(7): 1-28.

Kirillov, F. N., 1972. Ryby Jakutii (Fishes of Jakutija). Moskwa. Izdat. Nauka. p. 359. (In Russian).

McAllister, D. E., 1975. A new species of Arctic eelpout, *Lycodes sagittarius*, from the Beaufort Sea, Alaska, and the Kara Sea, USSR (Pisces, Zoarcidae). Nat. Mus. Canada. Publ. Oceanography 9: 1-16.

Neyelov, A. V., Chernova, N. V., 1992. Taxonomy and zoogeography of fishes caught around Spitsbergen. Ber. Polarforsch. 115: 105-106.

Neyelov, A. V., Chernova, N. V., 1994. A preliminary check-list of fishes collected in the Laptev Sea during the expedition of the icebreaker "Polarstern" in 1993. In: Nauchnye resultaty expedicii LAPEKS-93 (Scientific results of the expedition LAPEX-93). St. Petersburg, Gidrometeoizdat, pp. 272-276. (In Russian, with English summary).

Nielsen, J. G., Fossa, S. A., 1993. *Lycodes adolfi*, a new species of eelpout (Zoarcidae) from Greenland. Cybium 17(1): 39-44.

Tsynovsky. V. D., 1980a. Fishes collected on drift station "North Pole 22" in the winters of 1978-79 and 1979-80. In: Parin, N. N. (Ed.): Fishes of the open Ocean. Moscow, P.P. Shirshov Inst. Oceanology, pp. 110-112. (In Russian).

Tsynovsky, V. D., 1980b. On the ichthyofauna of a deep-sea valley of the Central Arctic Basin. In: Vinogradov, M. E., Mel'nikov, I. A. (Eds.): Biology of the Central Arctic Basins. Moskva, Nauka, pp. 214-218. (In Russian).

HYDROBIOLOGICAL RESEARCH IN THE LENA POLYNYA

A. Yu. Gukov
Hydrometeorological Department, Tiksi, Yakutia

There is only few information available on the hydrobiological regime of the Lena polynya (Kolchak 1906, 1909; Kupetzki 1958; Gukov 1994). From 1985 until 1993, the Hydrometeorological Department of Tiksi compiled annual data about the distribution and abundance of bacterioplankton, phytoplankton, zooplankton and zoobenthos at two stations in its western part, north of the Oleneksky Bay between 74°25' and 73°50'N. The average water depth was 22.5 m at st. A and 26.2 m at st. B.

The pilot-ship "Brize" was used for summer sampling; winter samples were collected through sea ice holes. The bacterio- and phytoplankton samples were taken in surface and bottom layers. The water was filtered through membrane filters. Both quantitative and qualitative samples were selected. All samples were fixed by formalin. The zooplankton samples were collected by means of a Juday net with a N49 mesh size. The bottom fauna was sampled by means of a Petersen grab (0.025 m^2). The sediment was removed and washed through a series of screens; the smallest mesh was 1.5 mm. Samples of zooplankton and zoobenthos were preserved in 4 % buffered formalin.

In April 1991, the Lena polynya covered nearly 20,000 km^2. The mean annual air temperature was approximately -22 °C, varying between -53 °C and 28 °C. The mean annual water temperature was about 1.2 °C. The Lena river transports high amounts of fresh water and sediments into the polynya. The salinities varied, however, only slightly at the two stations, typically ranging from about 21.7 in August (coinciding with maximum water temperatures) to 32.4 in March. The sea floor consisted predominantely of grey silt (st. A) and of yellow silt in the eastern part of the polynya (st. B). Oxygen concentrations were always higher than 9.0 ml l^{-1}; pH values ranged from 7.75 to 7.90.

The abundance of microorganisms was 1.8 10^6 kl ml^{-1} (with a maximum in the surface layer in September), the bacterial biomass 1.8 mg ml^{-1}. The saprophyte numbers were 25 kl ml^{-1} on average in winter, in summer they raised to 0.25 10^6 kl ml^{-1}. The numbers of petroleum-oxydic bacterias varied between 18 kl ml^{-1} in March and 0.25 10^6 kl ml^{-1} in September.

The phytoplankton of the Lena polynya was represented by 58 algal taxa. Diatoms predominated in terms of abundance (83%), followed by Chlorophyta (11%) and Flagellata (6%). In winter, phytoplankton consisited primarily of diatoms (*Melosira granulata*, *Chaetoceros wighami*, *Diatoma elongatum*, *Thalassiosira baltica*, *Fragillaria oceanica*). Their average numbers amounted to 40 kl ml^{-1}, average biomass to 0.014 mg l^{-1}. Total abundance and biomass of phytoplankton was 100 kl ml^{-1} and 0.044 mg l^{-1}, respectively. In autumn, the phytoplankton assemblages comprised diatoms, chlorophytes, cyanophytes, and flagellates. Diatom algae dominated. Total abundances of phytoplankton were 1.6 10^6 kl ml^{-1}, total biomass 4.0 mg l^{-1}. The composition and number of species, the seasonal dynamics of abundances and biomass, and the composition of dominant complexes varied among years. However, diatoms found constantly optimum conditions for their development and were dominant in terms of abundances, with the peak of development in September (on average 1.2 10^6 kl l^{-1} and 2.4 mg l^{-1}).

In the Lena polynya, the zooplankton species composition was affected by the interaction of coastal brackish waters with cold and more saline Arctic waters.

Generally, marine species were dominant in terms of species numbers, while brackish water organisms dominated in abundances and biomass. A total of 28 species were caught. Zooplankton biomass ranged from 3.9 to 64 mg m^{-3} at st. A and from 6.6 to 39 mg m^{-3} at st. B. The average abundance and biomass were 230 ind m^{-3} and 36.4 mg m^{-3}, respectively. In winter, marine copepods dominated: *Pseudocalanus elongatus* (accounting for about 50 % of zooplankton biomass) and *Calanus glacialis*. In March, the faunistic composition varied little, while the quantitative composition was greater. In June, the development of certain forms had begun, copepodits and nauplii were abundant. Of copepods and cladocerans *Drepanopus bungei* were predominant. In August-September, copepods were most abundant (*Drepanopus bungei, Derjuginia tolli, Calanus finmarchicus, Limnocalanus grimaldii*). Maximum zooplankton abundances occurred in in autumn.

The zoobenthos was characterized by relatively high abundances, biomass and species diversity (Gukov 1994). The fauna is mainly composed of molluscs, amphipods, and polychaetes. In total, 34 macrobenthic species were found, mostly wide spread eurybiont boreal-Arctic and brackish water species. The highest numbers of species were found at a temperature of -1.5 °C and a salinity of 24. With regard to biomass, *Tridonta borealis*, *Eucratia loricata*, *Suberites domuncula* were the most important species. The bottom biocenosis was functioning in the Arctic surface water. The *Tridonta* biocoenosis accounted for 22% of biomass and about 30 % of the diversity (abundance 18,400 ind m^{-2}, biomass 61.4-115.4 g m^{-2}).

References

Gukov, A. Yu., 1994. Bottom fauna in the area of the Lena polynya. Scientific results of the expedition LAPEX-93. S-Pb. Gidrometeoizdat: 311-318. (in Russian)

Kolchak, A. V., 1906. Last expedition on the Benetta island, provided by Academy of Sciences for searching of Baron Toll. News of Russian Geographical Society, 42: 467-519. (in Russian)

Kolchak, A. V., 1909. Ice of the Kara and Siberian seas. Scientific results of the Russian Polar Expedition 1900-1903, Vol.1: 1-32. (in Russian)

Kupetzki, V. P., 1909. Stationary polynyas in the freezing seas. Vectnik of Leningrad University, 12(2): 1-177. (in Russian)

TROPHIC STRUCTURE OF THE BENTHOS OF THE LENA POLYNYA

A. Yu. Gukov
Hydrometeorological Department, Tiksi, Yakutia

From 1985 to 1993, the bottom fauna in the Lena polynya was annually sampled by means of a Petersen grab (0.025 m^2) at four stations. The pilotship "Brize" was used for sampling in summer (August-September), winter samples were taken through sea ice holes. The bottom samples were washed through a series of screens, the smallest mesh was 1.5 mm. Sieve residues were preserved in 4% buffered formalin.

The trophic structure of each station was divided into four feeding categories: suspension feeders, deposit feeders, predators and scavengers. Since the species are distributed along a continuum of feeding types and many organisms utilize several feeding modes, it is often difficult to place a species in a specific category. The bivalve *Thyasira gouldi*, for example, is generally regarded as a deposit feeder, but may also utilize suspended particles (Stanley, 1970). However, since these molluscs probably obtain most of their nutritional requirements from the sediment, we classified them as deposit feeders. The percentage of individuals belonging to each feeding category was calculated for each station.

Overall, the change in the faunal composition, i.e. the increase in diversity, corresponded to the increasing amount of silt and sand in the sediment, indicating that sediment grain size was a major factor for species distribution. The major discontiniuties in the faunal distributions were related to changes in grain size which in turn were controlled by the depositions of predominantly terrigenous fine sediments, mainly originating from river runoff. The grain size distribution ranged from silts prevailing in the western part of the polynya to sand in the middle and eastern part.

At St.1 (60 km north of Terpjai-Tumsa Cape), the sediment consisted of 70.25% silt, 29.5% clay and 0.25% sand and was, thus, intermediate in terms of median grain size.The bottom fauna at St.1 was dominated by deposit feeders, such as the polychaetes *Amphicteis sundevalli*, *Ampharete vega*, *Terebellides stroemi*, *Maldane sarsi*, and the molluscs *Thyasira gouldi* and *Portlandia siliqua*. *P.siliqua* was the dominant species. The abundance proportion of deposit feeders amounted to 59% in winter and decreases to 52% in summer, whereas the abundance shares of suspension feeders decreased from 30.2% in summer to 18.2% in winter (Table 1). The comparatively low abundances of suspension feeders on muddy sediments was noted by many investigators (Davis, 1925; Thorson, 1957; Sanders, 1958). The most important species of this feeding class were the sponges *Suberites domuncula*, *Phacellia cribrosa*, the molluscs *Serripes groenlandica* and *Mya truncata*, and the priapulid *Halicryptus spinulosus*.

Table 1: Percentages of sediment grain sizes and feeding categories in the Lena polynya. DF: deposit feeders; SF: suspension feeders; P: predators; S: scavengers.

Station	Sediment %				Feeding type (winter) %				Feeding type (summer) %			
	gravel	sand	silt	clay	SF	DF	P	S	SF	DF	P	S
1	-	0.25	70.25	29.5	18.2	59.0	12.8	10.0	30.2	52.0	10.0	7.8
2	3.25	42.8	31.2	22.75	31.2	32.6	16.0	20.2	28.4	33.8	15.6	22.2
3	0.05	39.05	36.2	24.7	31.2	42.6	11.0	15.2	27.4	43.0	14.0	15.6
4	5.2	36.0	31.4	27.4	41.2	28.2	21.8	10.8	37.5	23.6	15.9	23.0

The fauna at st.2 was dominated by deposit feeders. Their abundance percentages varied between winter and summer from 32.6 to 33.8 %. In summer, the dominant deposit feeders were *Portlandia siliqua*, *Yoldiella intermedia*, *Thyasira gouldi* (Bivalvia), *Aceroides latipes latipes* (Amphipoda), and *Diastylis sulcata* and *Brachydiastylis resima* (Cumacea). In winter, the community is dominated by the suspension feeding bivalves *Tridonta borealis*, *Nicania montagui* and*Lyonsia arenosa*, the amphipods *Ampelisca eschrichti* and *Haploops sibirica*, and the polychaete *Nereis zonata*. The most common predators were polychaetes, primarily *Nereis zonata*, and the gastropods *Lunatia pallidus*, *Obesotoma gigantea*, and *Propebella exarata*. Besides the polychaete *Harmothoe imbricata*., crustaceans were the most abundant scavengers: *Haploops sibirica*, *Saduria entomon*, *S.sabini*.

Bivalves were important components of the bottom biocenosis of this area. The largest specimens of *Tridonta borealis* were 27 mm in height and 36 mm length. 59% of the individuals with a shell length of less than 23.2 mm were in a prereproductive age. The oldest clam examined was 7 years old and 36 mm long. The numbers of comparatively large, old individuals were low (41%).

The bottom fauna at st.3 (50 km north-west of Dunay Islands) was also dominated by deposit feeders, such as the polychaetes *Ampharete vega*, *Terebellides stroemi*, *Travisia forbesi*, and *Maldane sarsi*, the bivalves *Thyasira gouldi* and *Portlandia siliqua*, as well as the cumacean *Diastylis sulcata*. Among the organisms found in this station were the suspension feeders *Polymastia mammillaris* and *Phacellia cribrosa* (Spongia), *Pandora glacialis* and *Lyonsia arenosa* (Bivalvia), *Haploops sibirica* and *Ampelisca eschrichti* (Amphipoda). The motile suspension feeding bivalve *Tridonta borealis* was numerically dominant in summer. Specimens of *T. borealis* taken on this station were small in size (15 mm at maximum). Most abundant predatory species were the gastropod *Cryptonatica clausa* and the polychaete *Nephtys longosetosa*. Seasonal examinations of the bottom fauna demonstrated a maximum abundance of predators in summer. The abundances of scavengers were relatively high throughout the year (mean 15.4 %).

At st.4 (130 km north-east of the Lena Delta area), bryozoans (*Alcyonidium disciforme*, *Eucratea loricata*, *Escharerella ventricosa*), hydroids (*Tubularia indivisa*), sponges (*Suberites domuncula*, *Phacellia cribrosa*, *Haliclona gracilis*), tunicates (*Rhizomolgula globularis*) and other organisms were found which require a solid substrate for attachment. The abundance of suspension feeders varied between winter and summer from 41.2 to 37.5%. For this feeding category, we found the molluscs *Musculus corrugatus* and *M.laevigatus*. The deposit feeders *Ampharete vega*, *Terebellides stroemi* (Polychaeta), *Priapulus caudatus*, *Halicryptus spinulosus* (Priapulida) were numerous in winter (up to 28.2 %) and in summer (up to 23.6 %). Most common predators were the gastropods *Acrybia islandica*, *Cylichna occulta* and *Retusa pertenuis*, as well as the polychaete *Nereis zonata*. Scavengers were rare in winter (10.8 %), but in summer their abundances increased (23 %).

Comparing all stations, the percentage of suspension feeders was relatively low at st.1 (18 %), increased at st.2 and 3 (31 %), and was highest at st.4 (41.2 %). The ratio of deposit feeders to suspension feeders decreased slightly at st.1-3 while the fauna at st.4 was dominated by suspension feeders. The percentage of deposit feeders was highest at st.1 (59 %), lowest at st.4 (28.2%). The percentage of predators was highest at st.2 (16 %), lowest at st.1 (12 %) in the weastern part of the polynya. The abundances of scavengers were low at all stations of the polynya (7.8 - 23 %). The coarser sediments of st.4 housed a greater percentage of small scavengers than the finer sediments in the western part (st.1).

Sessile organisms represented less than 30% of the fauna, except at st.4 where about 40% of the fauna was sessile. The low abundances of sessile organisms in areas with terrigenous deposits may be partly due to low concentrations of organic material in the sediment.

References

Davis, F. M., 1925. Quantitative studies in the fauna of the sea bottom of the southern North Sea. Fish. Invest. (Ser.II) 8: 1-50.

Sanders, H. L., 1958. Benthic studies in Buzzards Bay. Animal Sediment relationships. Limnol. Oceanogr. 3: 245-258.

Stanley, S. M., 1970. Relation of shell form to life habits of the Bivalvia (Mollusca). Geol. Soc. Am. 125: 1-296.

Thorson, G., 1957. Bottom communities. In: Hedgepeth, J.W. (Ed.): Treatise on Marine Ecology and Paleoecology, Vol.I, pp. 461-534.

THE ENVIRONMENTAL HISTORY OF THE LAPTEV SEA

HOLOCENE CLIMATIC, VEGETATION AND POLLEN DATA OF SIBERIA ADJACENT TO THE LAPTEV SEA

O. D. Naidina
Institute of the Lithosphere, Russian Academy of Sciences, Moscow, Russia

The present text and graphs represent a short review of published data concerning the Holocene paleogeography of the northern part of Siberia adjacent to the Laptev Sea. This part extends from Tajmyr peninsula in the west to the Indigirka mouth in the east and embraces the northern territories of Krasnoyarskiy kray and Republic Yakutiya - Sakha (Fig. 1).

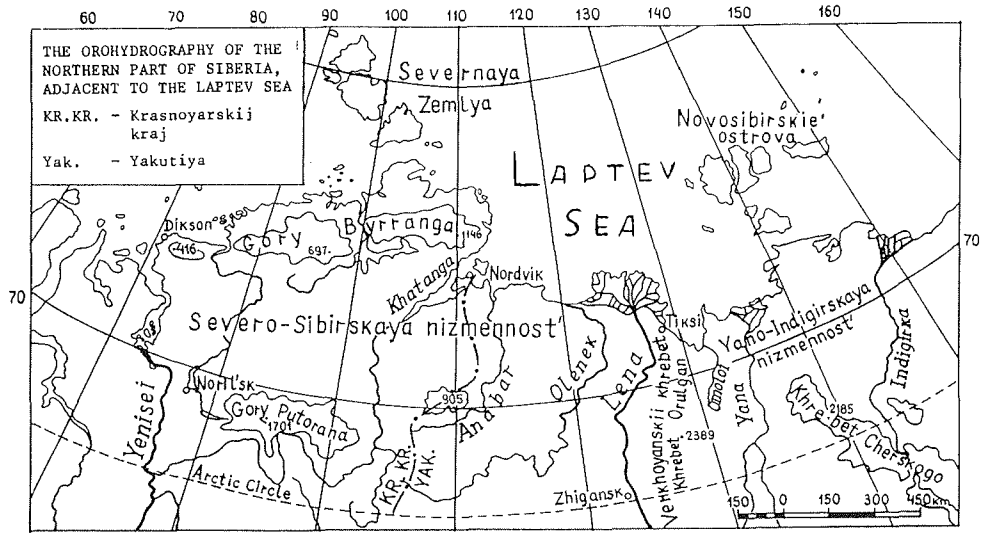

Fig. 1: The orohydrography of Northern Siberia adjacent to the Laptev Sea.

The reviewed part of Siberia belongs to the tundra and forest-tundra zones. The forestless landscapes were dominated here also in the Holocene (Fig. 1, 2, 4, 7; Tab. 1)

Regional peculiarity

A noTab. 1, and important feature of this subarctic region is the existence of the perennial frozen grounds. With this regional peculiarity is connected the development of three specific thermocarstic forms of the tundra-relief.

The first one are so-called b a j d z h a r a k h s (Yakut word). There are peat-bog elongated hillocks, having height up to 3-4 m and lengh up to15-20 m. Bajdzarakhs contain remains of trees such as larch, spruce, willow and others.

The second form of the tundra-relief is a l a s (Yakut word). Alases are patelliform depressions a few kilometres in diameter. Small flat bottomed lakes occupy some of the largest alases. Most of the part of vast alas-plains were formed 12 000-13 000 years ago in the Allerød period (Kaplina, Lozhkin, 1979).

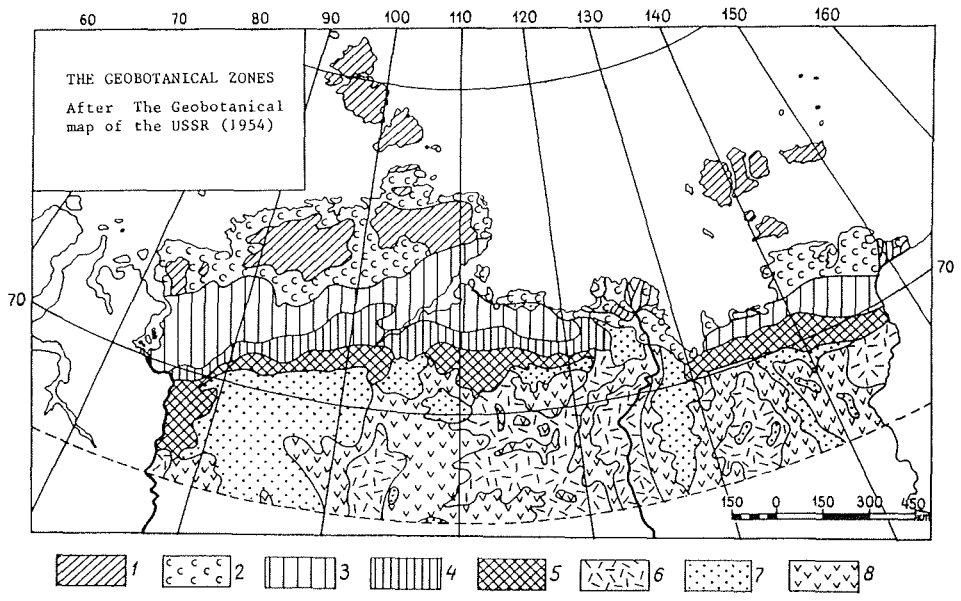

Fig. 2: The geobotanical zones.

1 - Arctic deserts and glaciers, 2 - arctic tundras, 3 - typical tundras, 4 - shrubs and tussockes tundras, 5 - forest-tundras, 6 - northern taigas, 7 - mountain tundras and shrubs of the Alpine taiga regions, 8 - mountain forest-tundras of the northern taigs regions.

The third typical form of tundra-relief are so-called edomas, or b u l g u n y a k h s (Yakut word) - no great assymetric hills, 20-30 m high. The hills are built up of ice-containing deposits formed in Late Pleistocene during the Sartan glaciation. Bulgunyakhs are mainly located in closed flat depresssions and in river deltas. For example, on the delta plain of Lena there are about 150-200 such hills (Northern Yakutiya, 1962, p. 78) forming a peculiar kind of hilly tundra (Mel'kheev, 1958).

Interpretation of pollen data

It is known that the formation of the vegetation cover was directly related to the climate. Plants are the most sTab. 1, and reliable indicator of changing temperature and humidity. Palynologists established that the composition of a spore and pollen assemblage does indeed correspond to the nature of the vegetation in the study area.

The most parts of the reviewed Holocene sections are located in the lower courses of rivers Lena, Yana and Indigirka (Fig 3).

According to pollen diagram of alas in the Lower Yana three major stages of Holocene vegetation and climatic conditions can be distinguished (Fig.9).

I Stage (interval 2,9-6 m) - shrubs-moss tundra and cooling

II Stage (interval 1-2,9m) - larch-birch-spruce forest-tundra

III Stage (interval 0-1 m) - forestless landscape and cooling

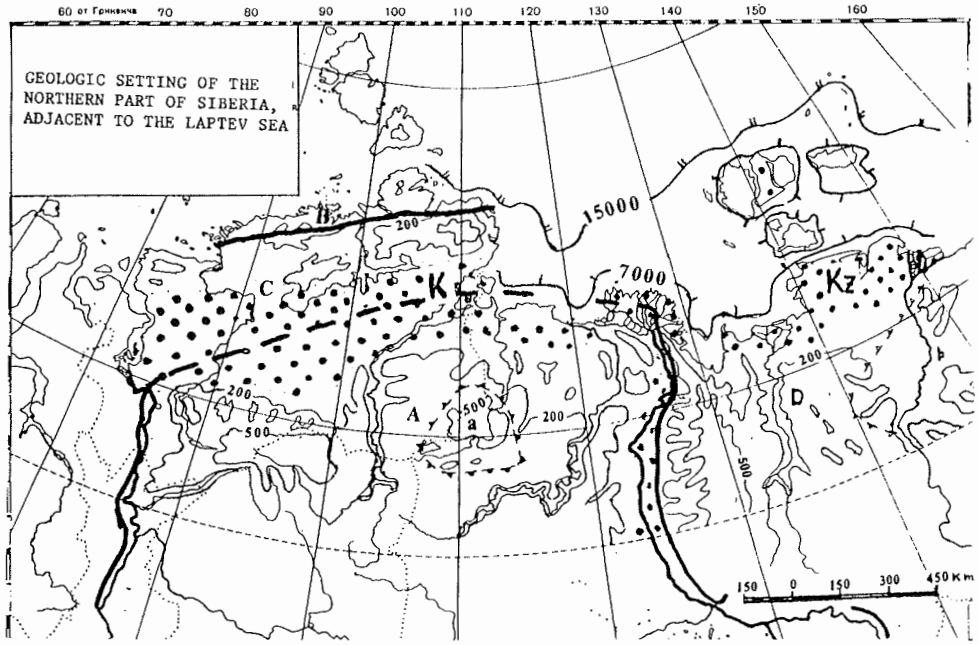

Fig. 3: Geologic setting of the northern part of Siberia adjacent to the Laptev Sea. A - Siberian Precambrian platform. B - Late Proterozoic folded belt. C - Hercynids. D - Early Mezosoide. a - Anabar Massif, b - Kolyma Massif. Distribution of Cretaceous (K) and Cenozoic (Kz) sediments. Position of the Laptev Sea shore-line 7000 and 15000 years ago (After V.S. Zarkhidze et al., 1984). 200 - Modern relief, contour lines (mm).

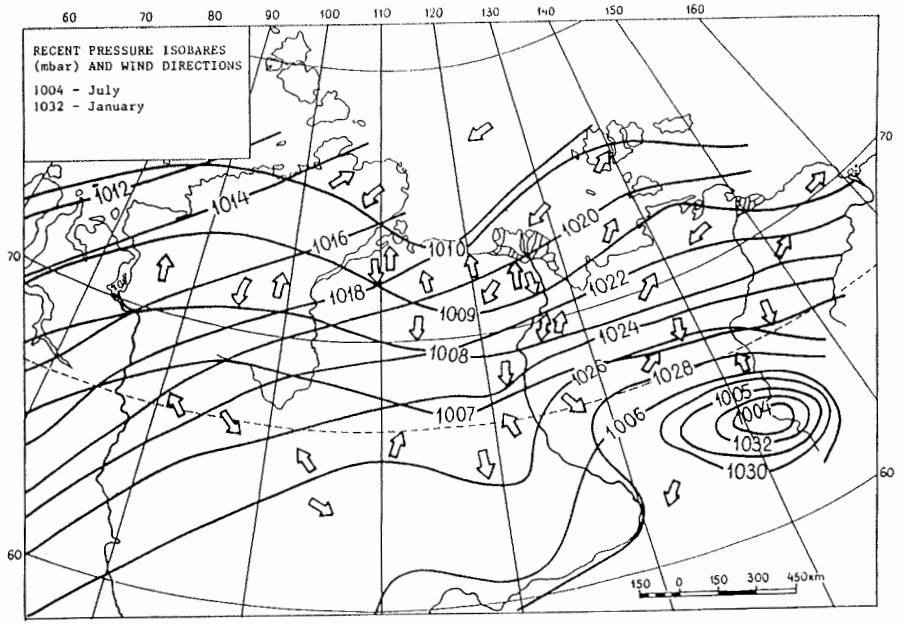

Fig. 4: Recent pressure isobars and wind directions. After "The Climatic Atlas of the USSR", 1960.

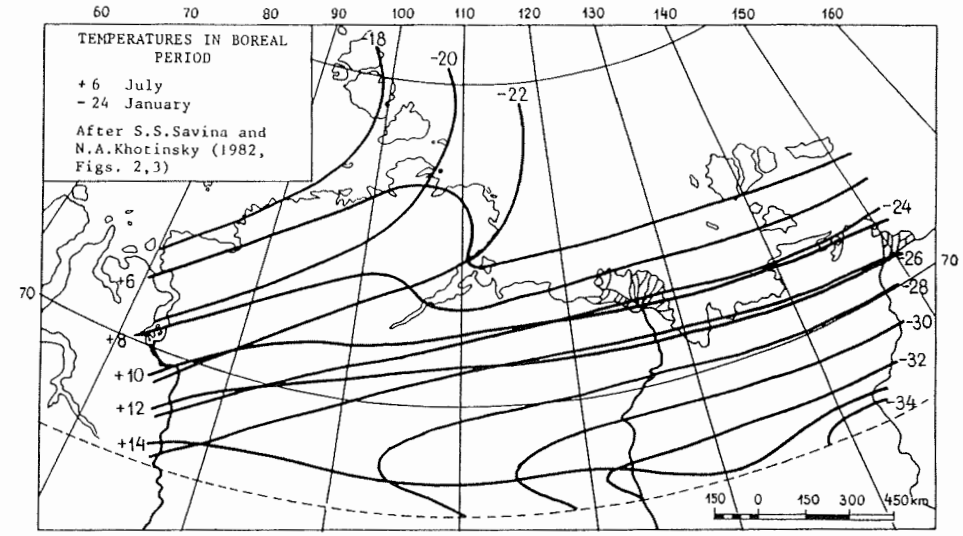

Fig. 5: Temperatures in the boreal period.

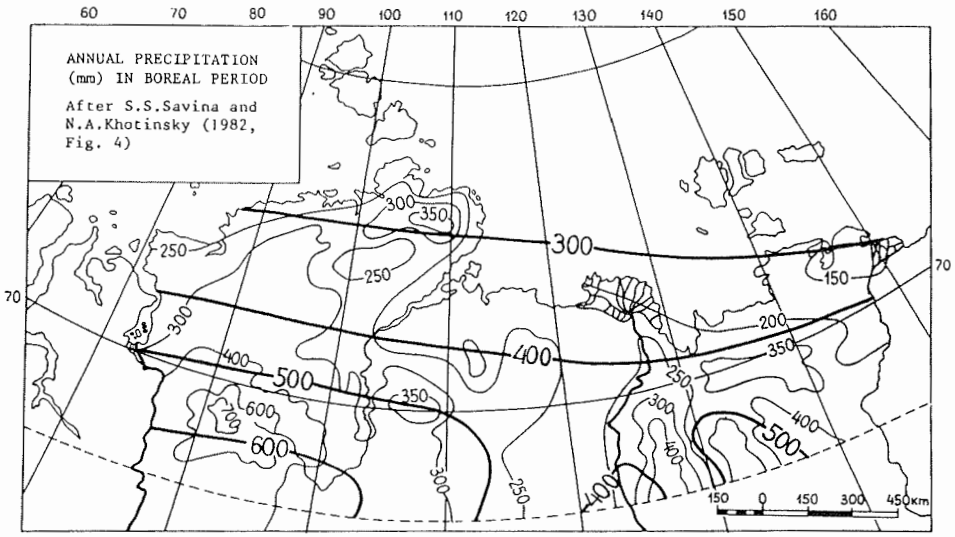

Fig. 6: Annual precipitation in the boreal period.

According to radiocarbon data 4 730-120 the cooling of stage III coincided with the beginning of the Subboreal period (Khotinsky,1977).

In the Yana-Indigirka lowland the Holocene onset was characterized by general rising of the territory to 100 m. In the places of wash-out of the ice deposits large thermocarstic depressions (alases) were formed.

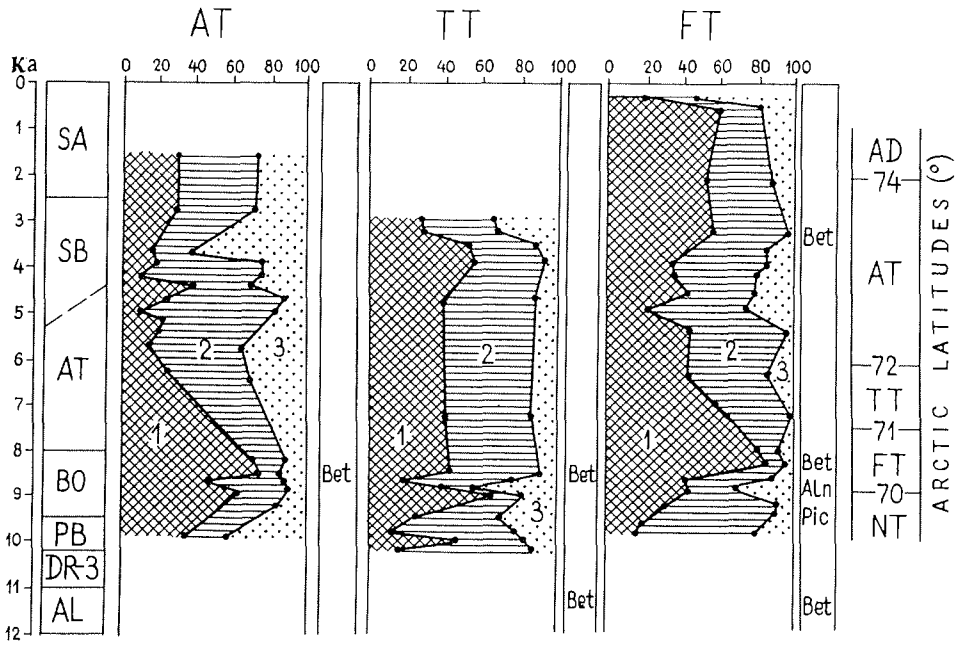

Fig. 7: The evolution of vegetation at coastal lowlands of Yakutiya between Lena and Kolyma during Holocene. After T.N. Kaplina and A.V. Lozhkin, 1982.

Recent tundras zones: AD - Arctic desert; AT - Arctic tundra; TT - Typical tundra; FT - Forest-tundra; NT - Northern taiga. Pollen and spores (%): 1 - pollen of trees and shrubs, 2 - pollen of herbs, 3 - spores. Remains of trees: Bet - stems of birch, Aln - woods of alder, Pic - woods of spruce.

After N.O.Rybakova (1981) the lower part of the sequence of alas deposits located on the left bank of Khroma River is characterized by a predominance of herbaceous pollen (56-88%). The arboreal pollen only belong to Alnaster and Betula sect. Nanae. In the upper part of the section the contents of arboreal pollen increased. Pollen of Betula sect. Nanae and Alnaster with Betula sect. Albae, Salix and rare pollen grains of Pinus sect. Cembrae comprise 50-65%. Pollen spectra point out the spreading of tundra vegetation here -Artemisia, Gramineae, Compositae, Ericaceae, etc. Only in the period of the Holocene climatic optimum the tree vegetation spreads again. According to the available palynological material typical tundra vegetation was formed at the end of the Middle - the beginning of the Late Pleistocene.

Holocene pollen diagrams from the deposits of alas and terrace in Kolyma lowland are shown on Fig. 10.

Data on the climate of vegetational period during the deposition of "ice" complex in Kolyma lowland were received by S.V.Kiselev, S.F.Kolesnikov and N.O.Rybakova (1987). On the basis of the complex analysis of contents and paleontological characters of Edoma deposits the conclusion is proposed that sediment formation of the "ice" complex took place in drier environments than today. Together with moss and grass tundra the cryoxerotic tundra-steppes occurred.

Tab. 1: Pollen Data: evolution of the vegetation and climatic conditions at coastal lowland of northern Yakutija. After N.A. Khotinsky, 1977; T.N. Kaplina and A.V. Lozhkin, 1982; S.S. Savina and N.A. Khotinsky, 1982; N.A. Khotinsky and S.S. Savina, 1985.

	ARCTIC TUNDRA					TYPICAL TUNDRA					FOREST - TUNDRA				
Periods	Pollen zones	Vegetation	T_I °C	T_{VII} °C	H mm/ year	Pollen zones	Vegetation	T_I °C	T_{VII} °C	H mm/ year	Pollen zones	Vegetation	T_I °C	T_{VII} °C	H mm/ year
RC	Gramineae, Bryales	Tundra with mosses and cereals	-36	4	250	Betula sect. Nanae, Alnaster, Ericaceae, Bryales	Tundra with shrubses birch, alder and ericaceae	-36	6	250	Larix, Betula sect. Albae, Betula exilis	Forest tundra with larch and birch	-31	10	350
SA	Betula sect. Nanae, Gramineae, Cyperaceae, Bryales	Tundra with mosses, cereals and carex	-30	<10	300	Betula sect. Nanae, Alnaster, Pinus pumila, Cyperaceae, Sphagnales	Tundra with shrubses birch and cedar	-34	10	300	Betula sect. Nanae - sect. Fruticosae, Alnaster, Ericaceae, Sphagnales	Forest - tundra with birch and ericaceae and peatbog	-38	10	300
SB	Betula sect. Nanae, Gramineae, Cyperaceae, Bryales	Tundra with mosses and cereals	-34	6	300	Betula sect. Nanae - sect. Fruticosae, Alnaster, Ericaceae, Valerianaceae	Tundra with shrubses birch and ericaceae	<-38	10	300	Larix, Betula sect. Albae - sect. Fruticosae, Alnaster, Gramineae, Cyperaceae	Forest - tundra with larch	-38	>10	300
AT	Betula sect. Nanae, Cyperaceae, Bryales	Tundra with mosses and carex	>-30	<10	300	Betula sect. Albae - sect. Fruticosae, Alnaster, Cyperaceae, Sphagnales	Forest - tundra with birch	-30	10	400	Betula sect. Albae - sect. Fruticosae, Alnaster, Umbelliferae	Forest with birch	-34	12	<400
BO	Betula sect. Nanae, Alnaster, Ericaceae	Tundra with shrubses alder and ericaceae													
PB	Betula sect. Nanae, Artemisia, Bryales	Tundra with shrubses birch and mosses				Betula sect. Nanae, Cyperaceae, Compositae, Bryales	Tundra with shrubses birch and carex				Salix, Chenopodiaceae, Compositae, Artemisia, Caryophyllaceae, Bryales	Tundra with many herbs			

RC - Recent time, T_I - January temperature, T_{VII} - July temperature, H - precipitation.

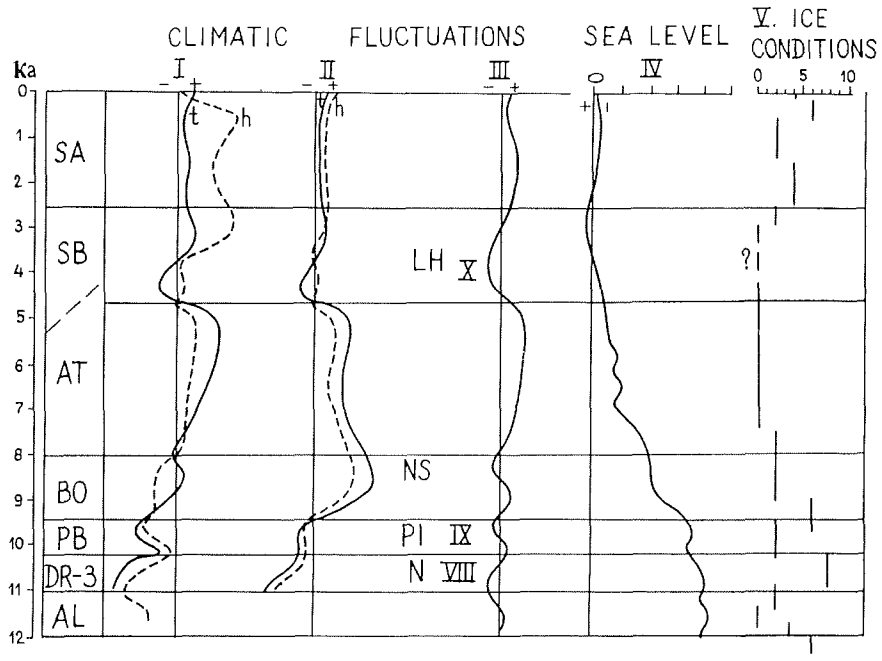

Fig.8: Some climatic features of Northern Eurasia. Climatic fluctuations (after N.A. Khotinsky, 1977). I - Russian Plane; II - Siberia; t - temperature, h - humidity; III -The Enisei, Verkhoyanskii khrebet (after N.N. Kind, 1974); N - Norilsk stage of Sartan glaciation; Coolings: PI - Pit-Igarka, NS - Novo-Sanczugovskoe; LH - Late Holocene; YIII-X - Mountain glaciers, Verkhoyanskii khrebet; Sea level; IY - Sea level changes (after N.-A. Mörner, 1969); Ice conditions; Y - Sea ice forces by the ten stages scale (after P.M. Borisov, 1970)

Evolution of vegetation and its correlation with climatic changes

Radiocarbon and palynological data enabled to precise the Holocene history of the vegetational evolution at coastal lowlands of Yakutiya are published by T.N.Kaplina and A.V.Lozhkin (1982) (Fig.7; Tab. 1).

Palynological analysis shows that the first epoch of significant Post Pleistocene warming in the North of Yakutiya was in Allerød. At this time at coastal lowlands the distribution of tree and shrub vegetation begins. The presence of birchstem remains in Allerød deposits shows that the climatic conditions were milder than recent. Towards the end of Preboreal period cooling and a spreading of tundra vegetation took place. The treeless landscapes developed.

The second significant warming episode coincided approximately with the middle of the Boreal period with its optimum 8500 years ago. In deposits accumulated during this climatic optimum on the Kotel'nyy Island (the largest island of the Novosibirskiy archipelago) the stems of birches and woods of alder were discovered. The palynological data also generally confirm the conclusion that the Holocene climatic optimum in Northern Yakutiya belong to the middle of the Boreal period. Due to climatical cooling at the end of the Atlantic period geobotanical zones acquired recent aspects. A warming trend is present in the Subboreal period (about 3500 years ago). This is demonstrated by remains of tree-birches in the Subboreal deposits.

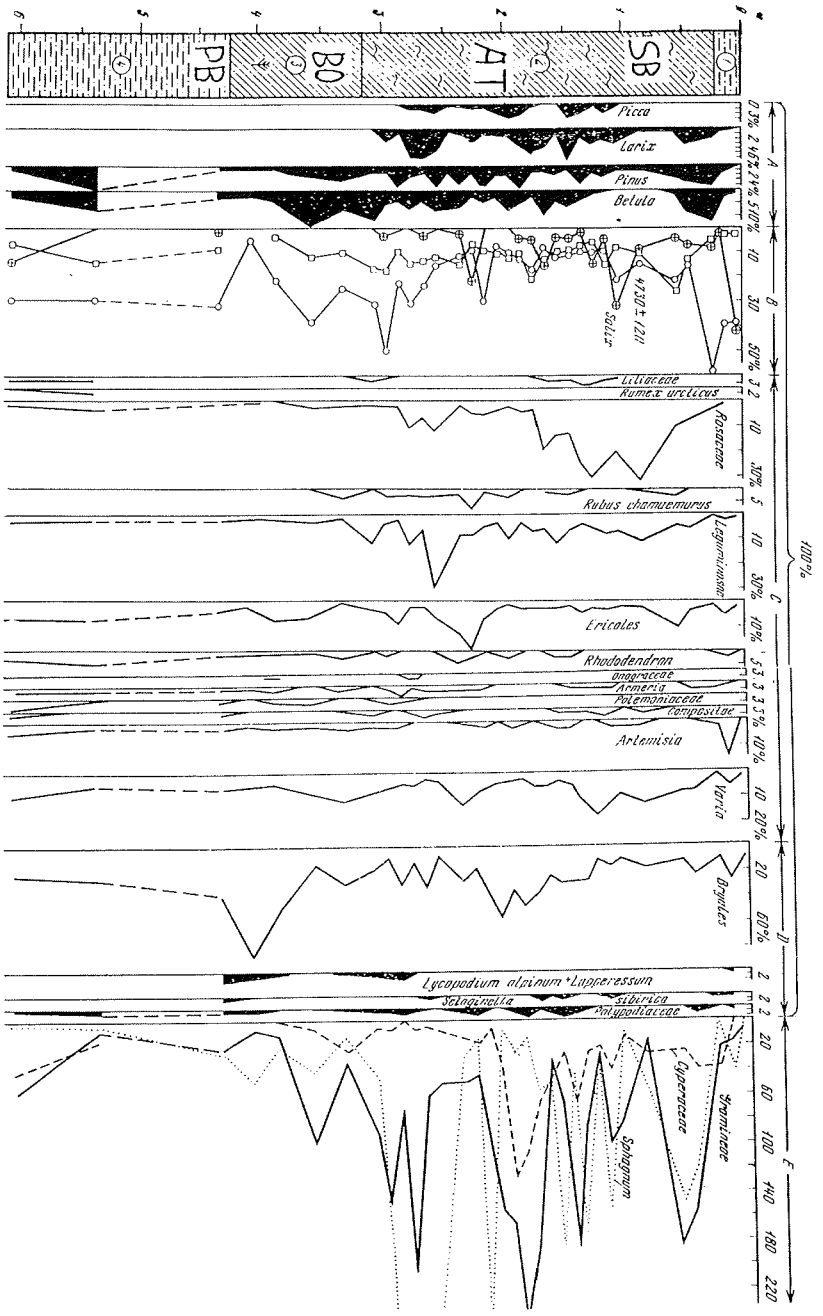

Fig.9: Holocene pollen and spores diagram of alas peat in the Lower Yana. After N.A. Khotinsky, 1977. A - tree pollen, B - shrub pollen, C - herbs and small shrub pollen, D - spores, E - pollen of Cereal, Carex and spores of Sphagnum.

In comparing the characteristics of the development of vegetation and spore and pollen associations, it should be noted that at the beginning of the Holocene the content of the pollen spectra in these deposits shows the existence of forestless tundra, but only in the period of the Holocene climatic optimum of Holocene the tree vegetation spreads again (Fig.7; Tab. 1).

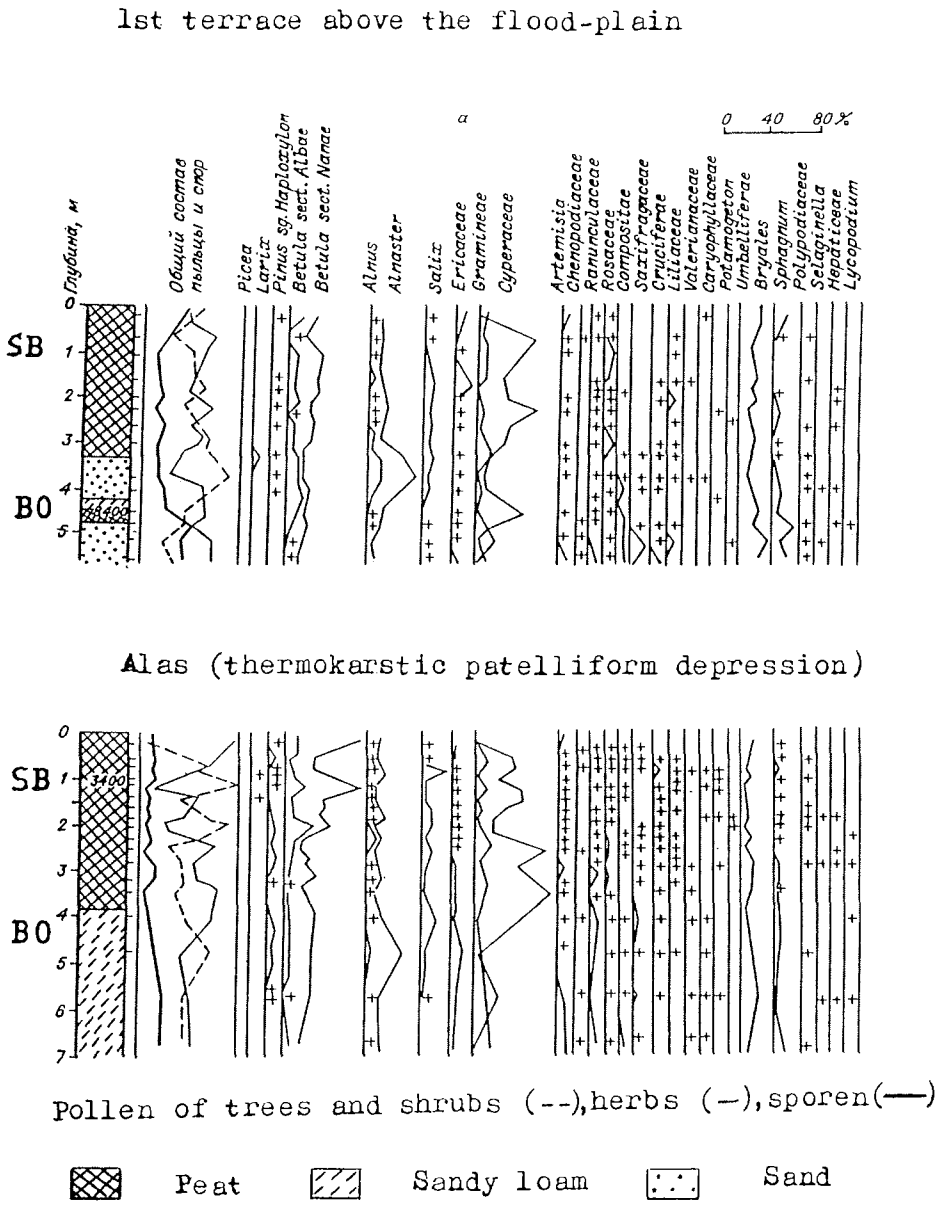

Fig.10: Holocene pollen and spores diagrams. NW part of Kolyma Lowland in lower course of Alaseya river. After N.O.Rybakova, 1989.

Climatic fluctuations are correlated with the Holocene periods by Blitt-Sernander (Kind, 1974; Khotinsky, 1977).

Radiocarbon data and palynological analysis enabled to precise the absolute chronology of the Holocene in Siberia. After N.V.Kind (1969, 1974) the recession of the Noril'sk Stage of the Sartan Glaciation in the Northern Yenisey area was in progress about 10700 year ago; therefore it corresponds to the Salpausselka and Late Dryas of Europe and Valders Stage of North America. The climatic change at the Pleistocene-Holocene boundary occured about 10500 years. During the Early Holocene a cold spell (about 9700-9500 years) is indicated. The well pronounced Postglacial warm period falls in the time interval from 8700 to 4500 years.

Comparison of Siberian chronological data with those of other continents confirms synchronous rhythms of climatic fluctuations during the Late Quaternary practically for the whole Northern Hemisphere. According to the available published radiocarbon data (Kind, 1974; Tab. 1, 17,p.136) the first Holocene warming was noted from 10300 to 9800 years. About 9800 to 9300 years was marked Pit-Igarka cooling, from 9300 to 8300 years was warming, then about 8300-7900 years Novo-Sanczugovskoe cooling. Optimum falls in the time interval from 7 900 to 4 500 years. Late Holocene cooling was indicated about 4 500 to 3 000 years. Mountain glaciers of Verkhoyanskiy range were marked in Dryas-3, Preboreal and Subboreal periods (Fig.8).

Global paleoclimatic reconstructions on the basis of statistical comparisons between recent pollen spectra and recent climatic conditions have been made by V.A. Klimanov (1994) (Fig. 11-13).

Temperatures, annual precipitation, anticyclones and ways of cyclones in Boreal, Atlantic and Subboreal periods are shown on paleoclimatic maps of former USSR territory (Fig. 5,6,14,15-23).

References

Averina U.M., Agapitov V.G., Doronina N.A., Zhadriuskaya N.G., Kruchinin Ya.A., Rutilevsky G.L., Sisko R.K., Semenov I.V., 1962. Northern Yakutiya. (In Russian), Trudy Arkticheskogo i Antarkticheskogo Instituta, 236. Morskoj transport, Leningrad, 280 p.

Borisov P.M., 1970. Experiment of reconstruction of the glacial cover of Polar basin in the Late- and Postglacial time. In: Arctic Ocean and its sea coasts in Cainozoj. (In Russian), Gidrometeoizdat, Leningrad, p. 61-70.

Kaplina T.N. and Lozhkin A.V., 1979. The age of alasc deposits at coastal lowlands of Yakutiya. (In Russian), Izvestiya AN SSSR, Geology, 2: 69-76.

Kaplina T.N. and Lozhkin A.V., 1982. History of the vegetation evolution at coastal lowlands of Yakutiya during the Holocene.In: Evolution of the environment at the USSR territory during Late Pleistocene and Holocene. (In Russian), Nauka, Moscow, p. 207-220.

Kind N.V., 1969. Late- and Postglacial of Siberia: Radiocarbon Chronology. In: Holocene. (In Russian), Nauka, Moscow, p.195-201.

Kind N.V., 1974. Late Quaternary Geochronology according to isotopes data. (In Russian), Transactions, 257. Nauka, Moscow, 255 p.

Kiselev S.V., Kolesnikov S.F., Rybakova N.O., 1987. On the climate of vegetational period during the deposition of "ice" complex in Omolon River. (In Russian), Bulletin Moskovskogo Obshchestva Ispytatelej Prirody, Geologiya, 62(1): 113-119.

MAXIMUM OF COOLING IN LATE DRYAS (10 500 years ago)

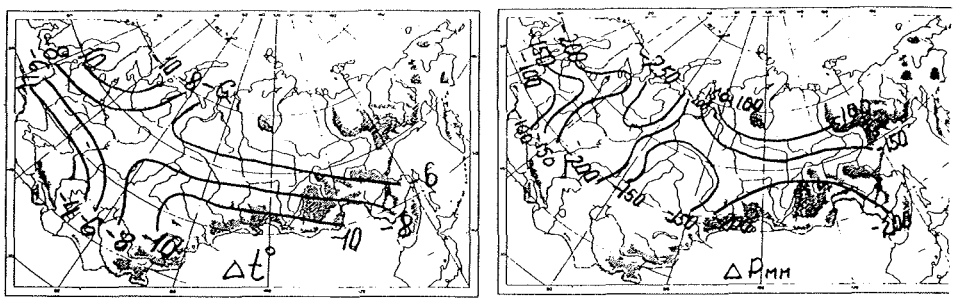

TERMAL MAXIMUM IN BOREAL PERIOD (8 500)

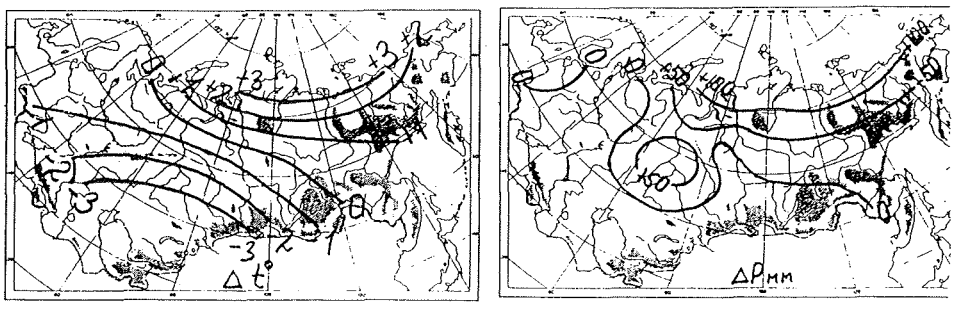

Fig. 11: The deviation of average annual temperatures (Δt°) and precipitation (Δ mm) from their recent values in Northern Siberia. After V.A. Klimanov, 1994.

Lavrenko E.M. and Sochava V.B. (editors), 1954. The Geobotanical map of the USSR. (In Russian), AN SSSR, Moscow-Leningrad, t.1.

Khotinsky N.A., 1977. Holocene of the Northern Eurasia (In Russian), Nauka, Moscow, 200 p.

Khotinsky N.A. and Savina S.S., 1985. Paleoclimatic scheme of the territory of the USSR in Boreal, Atlantic and Subboreal periods of Holocene. (In Russian), Izvestiya AN SSSR, Geography, 4: 18-34.

Klimanov V.A., 1994. The features of the changing climate of the Northern Eurasia in Postglacial and Holocene. (In Russian), Bulletin Moskovskogo Obshchestva Ispytatelej Prirody, Geology, 69(1): 12-20.

Mel'kheev M.N., 1958. The local geographical terms of Eastern Siberia. (In Russian), Trudy Irkutskogo Universiteta , Geography, 24(1): 5-12.

Mörner N.A., 1969. Eustatic and climatic changes during last 15 000 years. Geol. Mijnbouw, 48(4): 389-399.

Rybakova N.O., 1981. The main features of change of the vegetation in the southern part of the Yano-Indigirka depression during the Neogen-Pleistocene. IY Int. Palynol. Conf. Lucknow (1976-77), 3: 322-324.

ATLANTIC OPTIMUM (5 500)

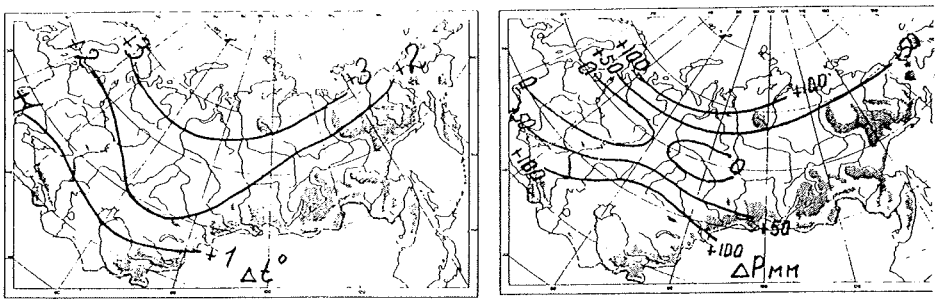

MAXIMUM OF SUBBOREAL WARMING (3 500)

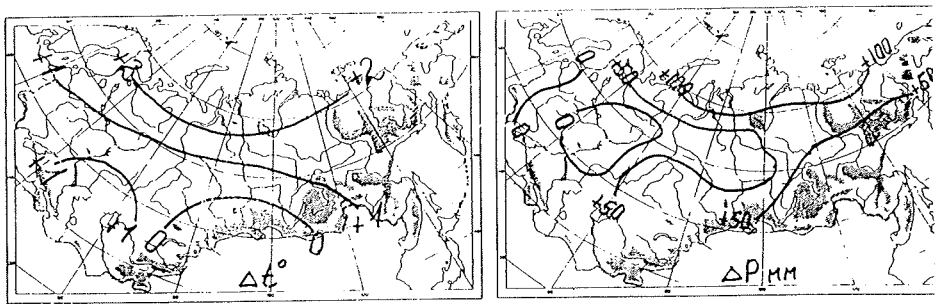

MAXIMUM OF SUBATLANTIC WARMING (1 000)

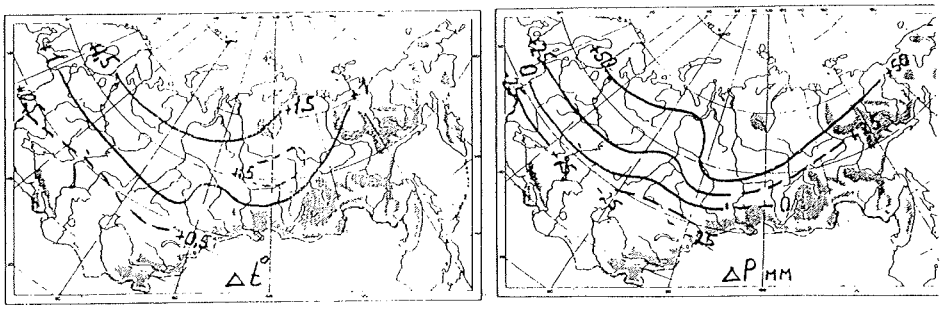

Fig. 12: Continuation of Figure 11.

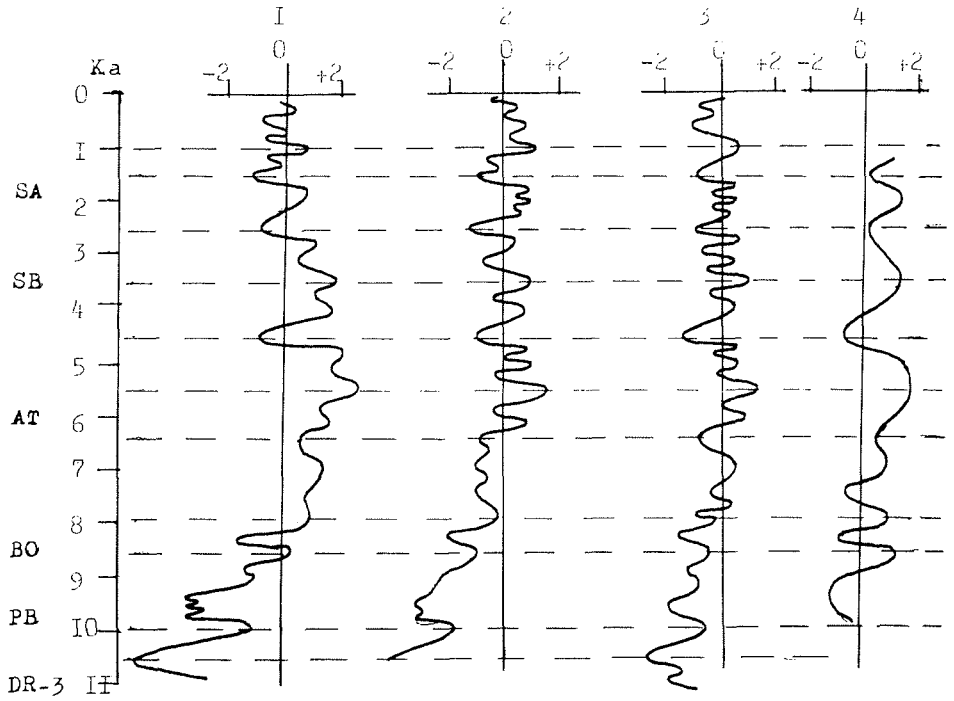

Fig. 13: The deviations from their recent values of July temperatures in Holocene periods of some regions of the Northern Eurasia. After V.A. Klimanov, 1994. 1 - Kareliya (63°N, 34°E), 2 - Centre of the Western Siberia (61°N, 78° E), 3 - Central Yakutiya (63°N, 125°E), 4 - Penzhinskaya Guba (63°N, 165°E)

Rybakova N.O., 1989. Changes in vegetation cover and climate in the Kolyma lowland in Late Quaternary time. In: Pleistocene of Siberia. Stratigraphy and interregional correlations. (In Russian), Nauka, Novosibirsk. Trudy Instituta geologii i geophyziki, 657: 137-142.

Savina S.S. and Khotinsky N.A., 1982. Zonal method of the Holocene paleoclimates reconstruction. In: Evolution of the environment at the USSR territory during Late Plestocene and Holocene. (In Russian), Nauka, Moscow, p. 231-244.

The Climatic Atlas of the USSR , 1960. (In Russian), Moscow, t.1.

Zarkhidze V.S., Solov'ev V.A., Baranovskaya O.F., Slobodin V.Ya., 1984. Conditions of the accumulation of Pliocene and Quaternary deposits on the islands and offshore regions of Soviet Arctic. In: Age and genesis of the overdeepening in offshore regions and history of river valleys. (In Russian), Nauka, Moscow, p. 29-37.

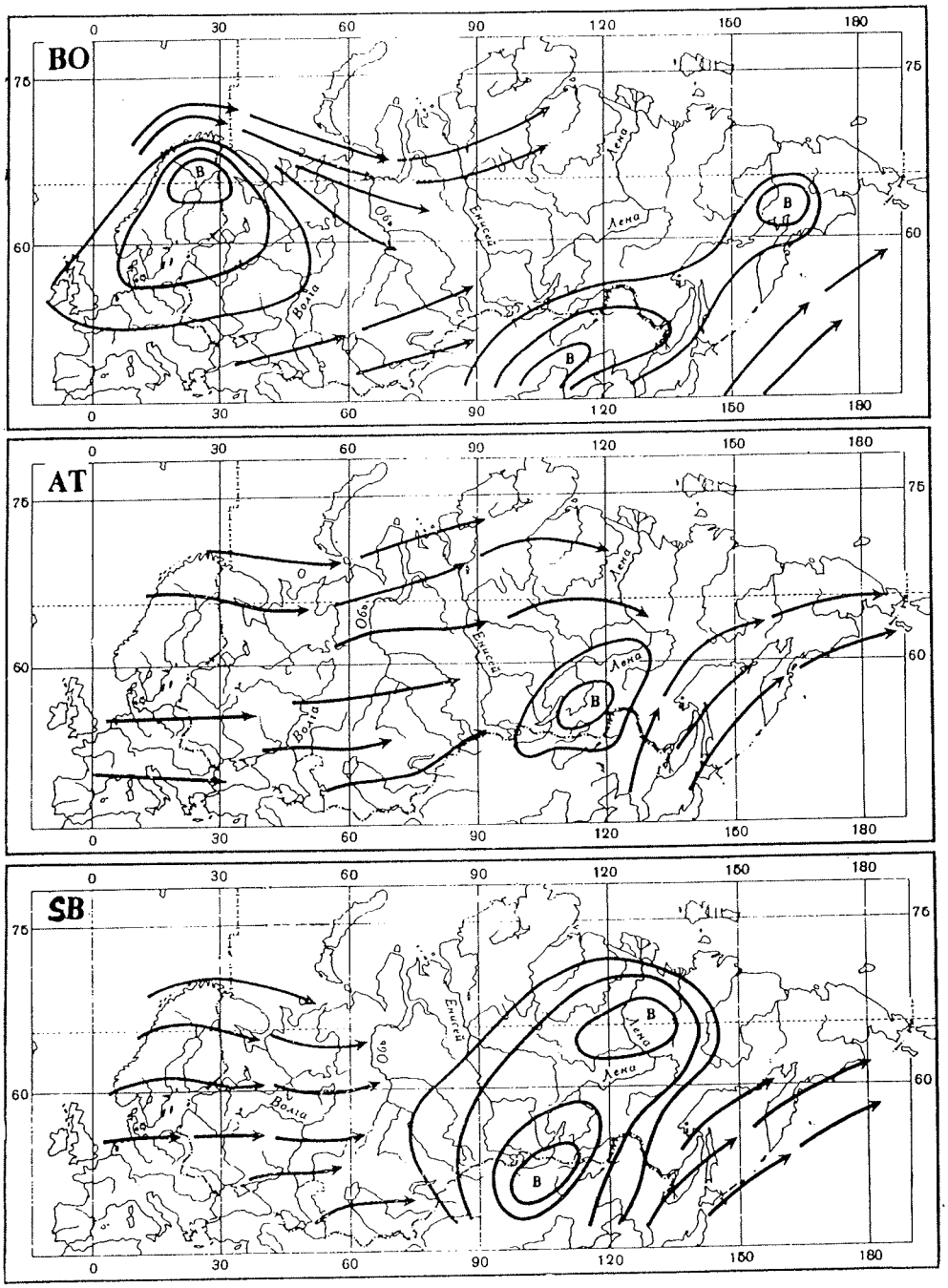

Fig. 14: Anticyclones (B) and ways of cyclones in the Northern Eurasia. After N.A. Khotinsky, 1977 (Fig. 50). Holocene termal maxima: BO -Boreal (8 300 - 8 900), AT - Atlantic (5 000- 6 000), SB - Subboreal (3 400 - 4 200).

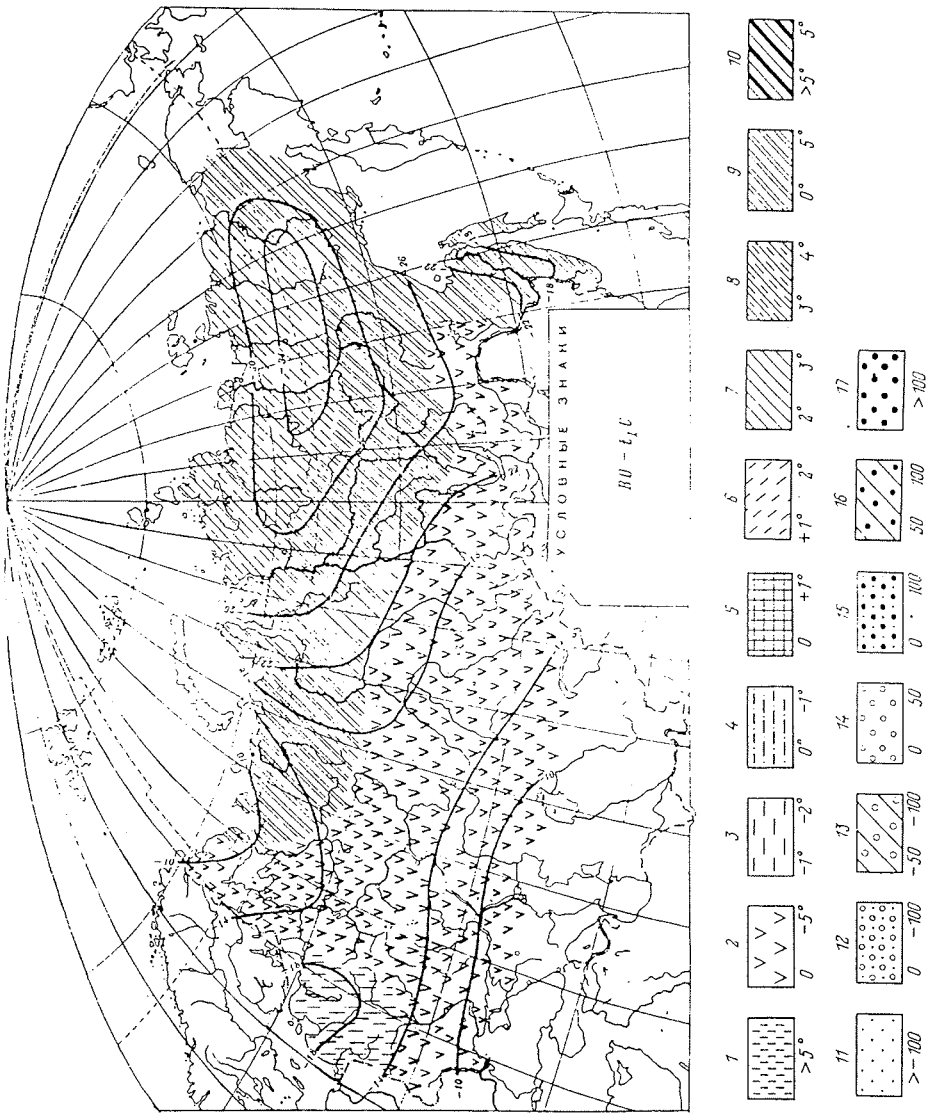

Fig. 15: Map of January temperature and anomalies of temperature in the boreal period. After N.A. Khotinsky and S.S. Savina, 1985. Symbols used in this and subsequent maps. Regions of negative and positive anomalies of temperatures for different Holocene periods in comparison with their recent values (t C):1-more-5, 2 - from 0 to 5, 3 - from - 1 to -2, 4 - from 0 to -1, 5 - from o to -1, 6 - from -1 to -2, 7 - from - 2 to 3, 8 - from -3 to 4, 9 - from 0 to -5, 10 - more -5. Regions of negative and positive anomalies of annual precipitation for different Holocene periods in comparison with recent values (H mm/year): 11 - more - 100, 12 - from 0 to -100,13 - from -50 to -100, 14 - from 0 to 50, 15 - from 0 to -100, 16 - from -50 to -100, 17 - more -100. I - January, VII - July; Holocene periods: BO - Boreal, AT - Atlantic, SB - Subboreal.

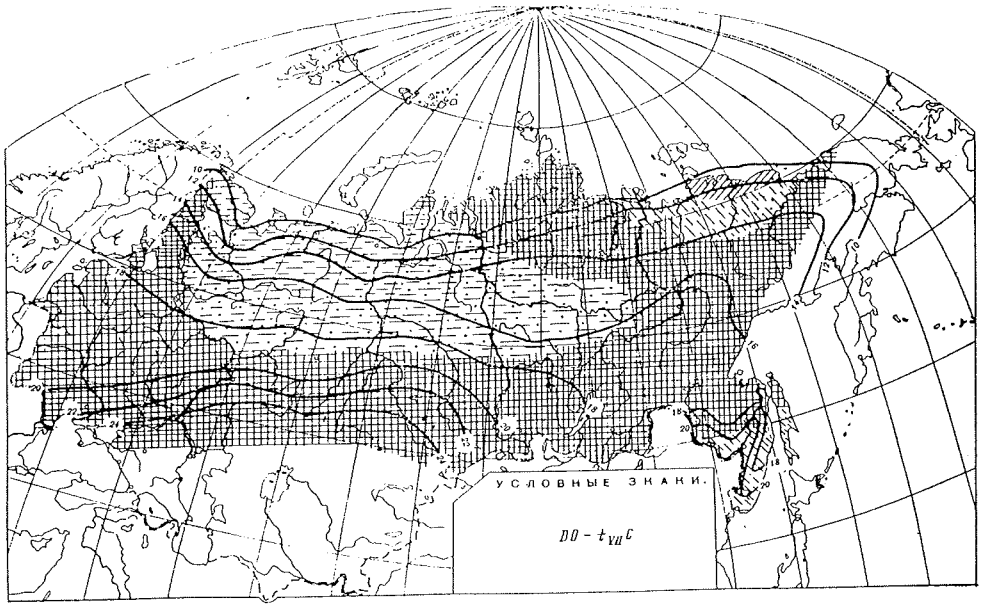

Fig. 16: Map of July temperature and anomalies of temperature in the boreal period.

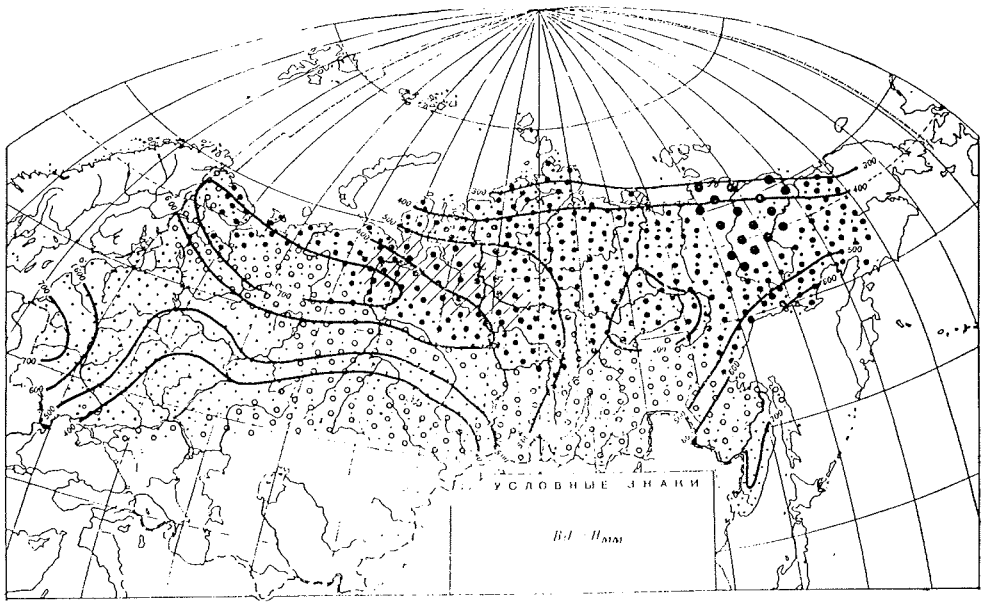

Fig. 17: Map of annual precipitation and anomalies of precipitation in the boreal period.

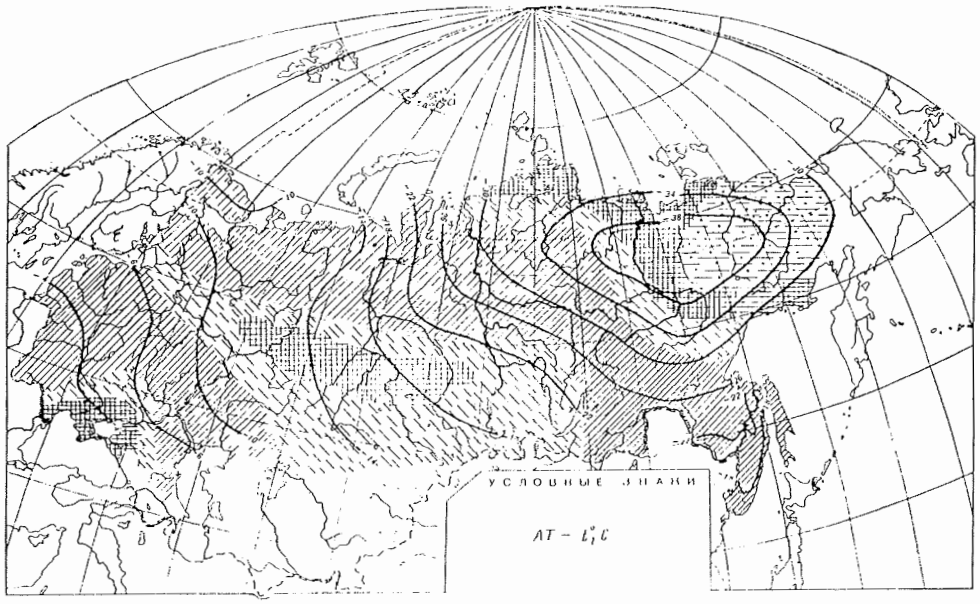

Fig. 18: Map of January temperature and anomalies of temperature in Atlantic period.

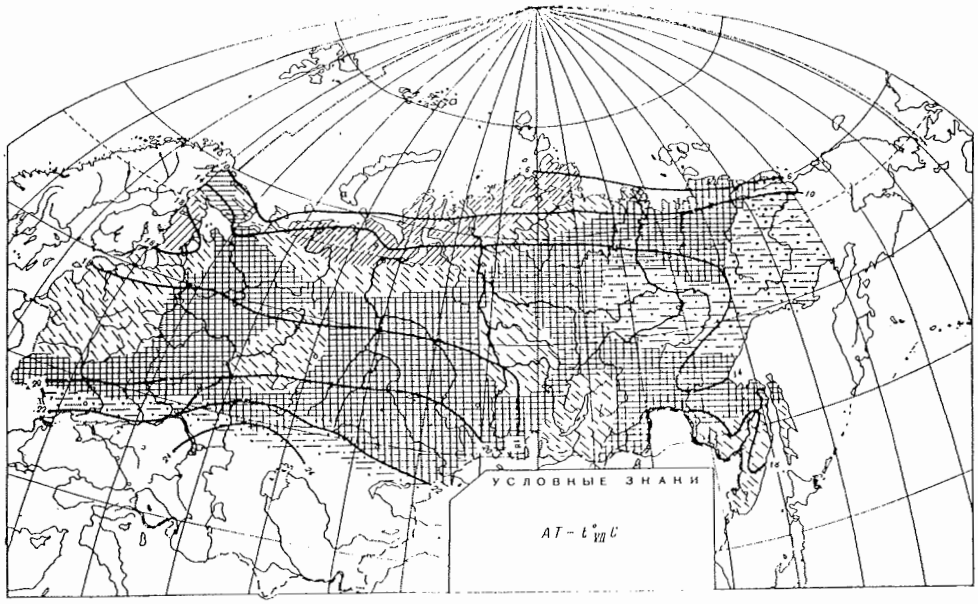

Fig. 19: Map of July temperature and anomalies of temperature in Atlantic period.

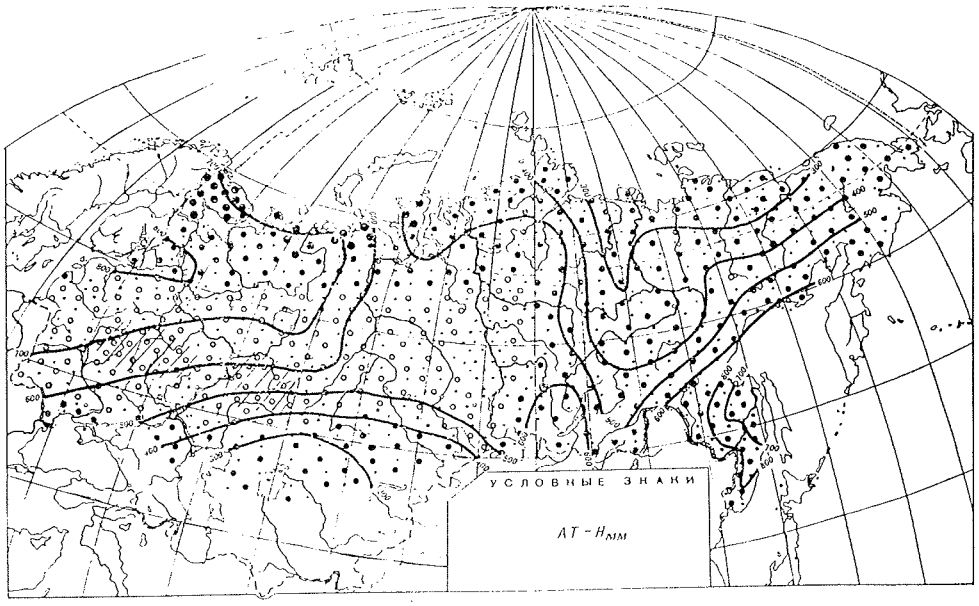

Fig. 20: Map of annual precipitation and anomalies of precipitation in Atlantic period.

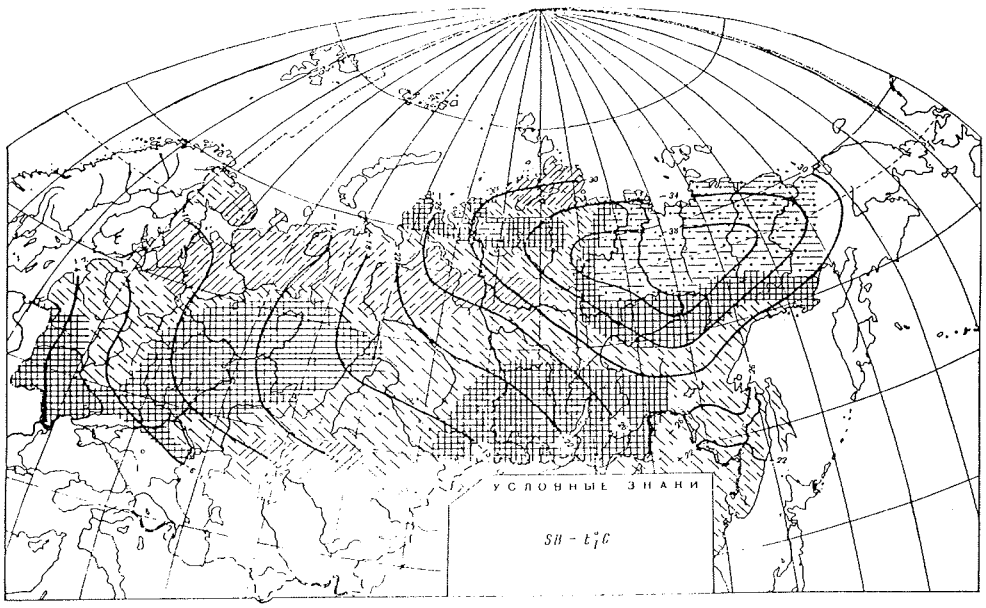

Fig. 21: Map of January temperature and anomalies of temperature in Subboreal period.

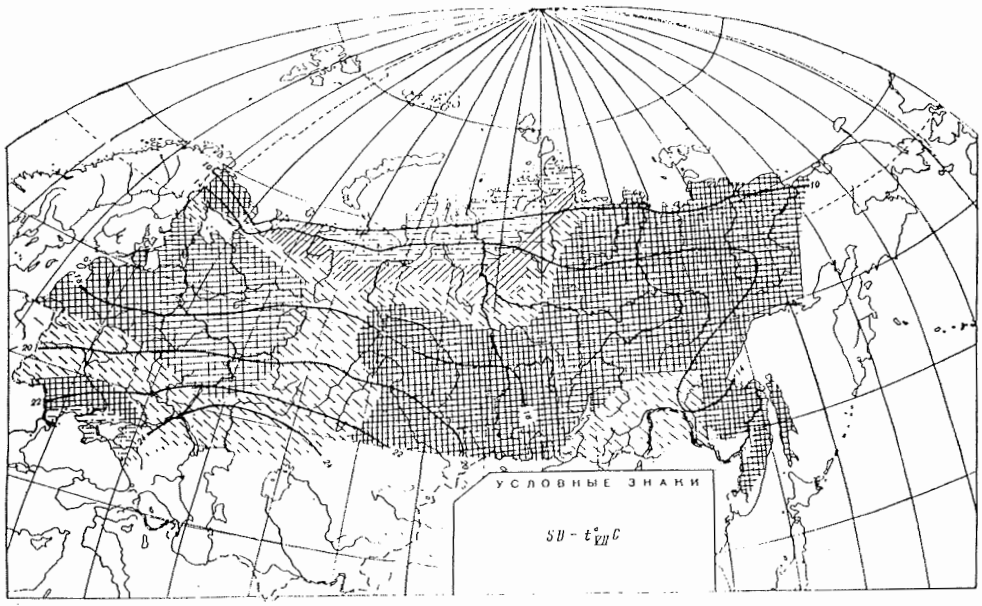

Fig. 22: Map of July temperature and anomalies of temperature in Subboreal period.

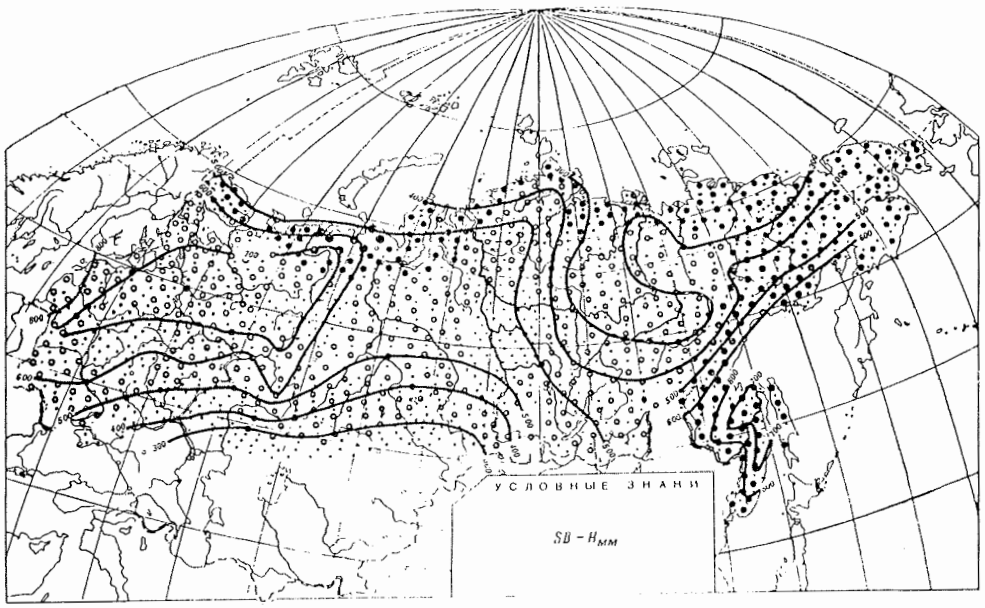

Fig. 23: Map of annual precipitation and anomalies of precipitation in Subboreal period.

PALEOGEOGRAPHICAL STUDIES OF PERMAFROST IN THE EASTERN TAYMYR LOWLAND

C. Siegert°, S.F. Khrutsky* and A. Yu. Derevyagin*

° Alfred-Wegener-Institut für Polar- und Meeresforschung, Forschungsstelle Potsdam, Germany

* Moscow State University, Department of Geocryology, Moscow, Russia

Introduction

The late Pleistocene development of the landscapes in the Taymyr region, especially with regards to the extent of the last glaciation, remains uncleare (Velichko, 1993). Recently, the role of marine transgression in the late Quaternary has also been discussed (Bolshiyanov, 1994). Permafrost investigations can yield an important contribution to a clarification of these problems.

This paper deals with the preliminary results of initial field studies in the tundra of the Labaz Lake area carried out during summer 1994 in the framework of the joint German-Russian Taymyr-Expedition.

The Labaz Lake area is located in eastern part of the Taymyr lowland tundra. It is assumed that the Labaz and several neighbouring lakes are relicts of a huge glaciolacustine basin, formed in the Zyryansk (Early Weichselian) glacial period (Kind & Leonov, 1982). During the Karginsk (Middle Weichselian) marine transgression, the Labaz area kept its continental conditions. Apparently this territory was not glacier-covered during the Sartan (Late Weichselian) period (Baulin & Danilova, 1984; Velichko, 1993). At the termination of the Pleistocene and during Holocene landscape forming processes developed here under permafrost conditions.

Material and methods

The paleogeographical studies have been carried out in the coastal zone of the Labaz Lake drainage area using outcrops and core drilling. The field research of ancient permafrost has been based on the frozen-ground facial analysis (ground ice stratigraphy). Combined with radiocarbon dating, paleontological, sedimentological, mineralogical and geochemical methods, these investigations should ecludate the relationship between climate change and the development of permafrost landscapes.

Observation of recent cryogenic processes (thermokarst, thermoerosion, solifluction, permafrost formation) in the lakeshore of Labaz Lake and other local sedimentation basins will estimate their infuence on transport and accumulation of sedimentary material under the stated geomorphological and geocryological conditions. These observations will serve as a basis for the paleogeographical interpretation of the cryolithological structure of the region's Late Quaternary permafrost profiles and those of bordering lowland areas surrounding the Laptev Sea.

Preliminary results

Cryolithological Study of ancient permafrost profiles

Results obtained in field work show that alluvial and lacustrine swamp processes dominated during the end of late Pleistocene and Holocene. Primarily ice-rich permafrosts with ice contents of 60-80 % (by volume) and higher were formed.

Numerous cycles of sediment accumulation were discerned within the various late Quaternary permafrost complexes of the Labaz basin. They began with the deposition of deep subaquatic sediments and ended with littoral, peat and swamp sediments. The former were transformed into permafrost without the direct influence of cryogenic processes through epigenetic freezing (i.e. after the action of early diagenetic processes). The epigenetic frozen sediments are evidenced through typical coarsely streaked, lattice-like cryogenic textures. The latter shallow water sediments made the transition to permafrost syngenetically, evidenced by characteristic bound, lens-shaped cryogenic textures and ice wedges. Polygonal ice-wedge systems penetrate the Holocene deposits to depths of up to 3-5 m, and the Pleistocene deposits by up to 10-15 m.

For the first time in the Taymyr lowland plain it was possible to prove the existence of thick polygonal ice-wedge systems in the deposits, which probable correlate with the Zyryansk glacial period. The deposits of this Zyryansk 'ice complex' contain almost no organic material but have increased amounts of coarse-grained, clastic materials (gravel, pebbles). The sediment lying between the ice wedges is enriched with segregated ice of different order of magnitudes. These facts support the conclusion that temperatures at the time of the permafrost horizon's formation were very low. Such cold and humid climatic conditions are characteristic for periglacial zones of the arctic desert.

The second cryolithogenic complex consisting of lacustrine and alluvial sediments correlate to the Karginsk period (^{14}C ages between 43.900 and > 47.000 years B.P.). Although similar sediments in their cryolithogenic formation, they contain much less ice. The size of the ice-wedge polygons is smaller. The clearly layered, sandy-silty sediments are composed of many horizons, in addition to containing humus or allochthonic organic material. These facts suggest more favourable conditions for vegetation and a pronounced seasonal cycle during sedimentation.

The lacustrine and alluvial sediments which have been formed in the Holocene contain a lot of plant remains including tree trunks (Larix). Peat beds take up the top of the Holocene deposits. ^{14}C-datings suggest the beginning of widespride peat accumulation between 9200 and 8760 radiocarbon years B.P. The environmental development during warmer periods (Karginsk period, Holocene) was subject to observable variations. Evidence exists for changes between warming and cooling phases within a spectrum of mean annual temperatures that varied between - 10 and -15 °C.

Pollen analysis

Deposits attributed to the end of the last glacial period are characterized by Xerophyten (Artemisia, Cereals) dominated grass pollen complex. The existence of open grasslands ('tundra steppes') under continental cold climate conditions is thus inferred.

The range of pollens found in the more recent deposits show that a distinct warming period with increasing precipitation began earlier than 9200 radiocarbon years B.P. in the Labaz Lake area, as in the entire North-Siberian lowland. The landscape was dominated by lakes and swamps, and where conditions were favourable peat formation began. The contribution of mosses and various grass communities to the vegetation increased, as did the distribution of trees and shrubs. The lake-swamp-tundra landscape reached its maximum development in the first half of the Holocene. The pollen spectrum during this period showed the widest distribution of trees (Larix, Betula sect. Albae) and shrubs. Increased peat accumulation and soil formation can be seen. The pollen spectrum of the second

half of the Holocene suggests a cooling phase. Trees died out, shrubs decreased in number and distribution and moss became a larger component of the vegetation.

Recent Geocryological and Sedimentary Processes

Because the very ice rich late Quaternary deposits in the Labaz Lake area are situated near the ground surface, the development of thermokarst, thermoerosion and solifluction features is favoured. Seasonal and perennial snow fields play an important role for weathering and sediment transport. It is estimated that through these processes about 500 m^3 of material (clay, silt, sand, pebbles and till, as well as organic material) was transported from the 12 km long north shore into the lake over a two month period (July-August 1994).

The rivers flowing into the Labaz drain an area with a very plain relief. Abundant lakes and swamps moderate the output of the rivers. In winter the rivers freeze down to the riverbed and isolate the Labaz. The predominantly 100 % plant cover protects the lake basin from erosion, with the exception of the lakeshore areas, and results in a low fluvial contribution of suspended sediments to the lake. The sediment accumulation on slopes, valley floors and in shallow water areas is accompanied by syngenetic freezing. The weakly indented relief and shallow seasonally ground thawing (0.4-0.5 m) leads quickly to saturated ground conditions in the Labaz catchment area. Newly formed permafrost is evidenced by a high ice content. Polygon ice wedges at various stages of formation are widely distributed over the catchment area. Temperatures of the permafrost at depths of 4-5 m are 8.5-9.4 °C. The low temperature of the permafrost limits the existence of perennially thawed ground (taliks), which could only be expected beneath deeper water bodies.

Perspectives for future work

The results of initial permafrost studies suggest a non-glaciated environment in the Labaz Lake area during the Sartan glacial period. Thick and very ice-rich syngenetical perennially frozen sediments were formed since the Karginsk period. These sediments are more or less influenced by soil formation processes. The existence of a continental climate can be assumed. The Labaz Lake area is thus highly suitable for environmental history reconstruction through permafrost studies.

Of major interest is a study of modern cryogenic processes in the lowland tundra landscapes in regard to the character of hydrothermic conditions of the active layer, vegetation and soil cover. Results of that kind of investigations are necessary to understand the influence of changing climate conditions on the landscape of subarctic flate regions.

References

Baulin, V.V and Danilova, N.S., 1984. Dynamics of Late Quaternary permafrost in Siberia. In: A.A. Velichko (ed.). Late Quaternary Environments of the Soviet Union. Longman Group Ltd, London, pp. 69-78

Bolshiyanov, D.Yu., 1994. New data on marine deposits of the Taimyr peninsula. In: L.A. Timokhov (ed.). Scientific results of the expedition 'Laptev Sea-93'. 'Hydrometeoizdat', St. Petersburg, pp. 237- 246. (in Russian)

Kind, N.V. and Leonov, B.N. (eds.), 1982. The Antropogene of the Taimyr Peninsula. 'Nauka', Moscow, 184 pp. (in Russian)

Velichko, A.A. (ed.), 1993. Evolution of Landscapes and Climates of the Northern Eurasia. Late Pleistocene-Holocene; Elements of Prognosis. I. Regional Paleogeography. 'Nauka', Moscow, 102 pp. (in Russian)

STUDYING SEASONAL WATER AND SOLUTE MOVEMENT IN THE ACTIVE LAYER IN A CONTINUOUS PERMAFROST SETTING - PRELIMINARY RESULTS FROM SIBERIA

J. Boike*, W.K.P. van Loon°, C. Kopsch* and H. W. Hubberten*

* Alfred-Wegener-Institut für Polar- und Meeresforschung, Forschungsstelle Potsdam, Germany

° Department of Agricultural Engineering and Physics, University of Wageningen, The Netherlands

Introduction

This research is part of a German-Russian research project initiated in early 1993 between the Alfred Wegener Institute (AWI), Germany and the Arctic and Antarctic Research Institute (AARI), Russia.

The paper reports preliminary results from field work carried out from July 20 to August 30, 1994 in the Levinson-Lessing catchment, Taymyr Peninsula, Siberia. This area is the northernmost continental area of the circumpolar Arctic (Figure 1). Levinson-Lessing lake is situated approximately 50 km west of Taymyr lake in the Byrranga mountain range (Figure 1). A varying topography and arctic tundra vegetation enable a study of transport processes under different geological and geomorphological conditions.

In continuous permafrost areas, the transport of water and solutes in the active layer is dependent on the seasonally thawing and freezing cycle. This study investigates seasonal flowpaths in the saturated (phreatic) and unsaturated (vadose) zone of the active layer using physical and isotope methods for the determination of water masses, sources, mixing rates and residence times.

Objectives

The main objectives of this paper are:

- to evaluate the use of Time Domain Reflectometry (TDR) for calculating soil volumetric water content and bulk electrical conductivity (BEC) in arctic field soils and
- to present preliminary results on solute and water transport from this year's field season

Field Work 1994 - Methods

Three slopes with a sum of 16 sites were instrumented during the summer in the Levinson-Lessing lake catchment (Figure 2). At each site, triple wire TDR probes, PT 100 temperature probes, wells, piezometers and suction lysimeters were installed (Figure 2). The TDR probes used in this study consist of three parallel steel rods (diameter 0.5 cm) with a length of 25 cm, separated by 3 cm and connected to a 50Ω cable. TDR readings were recorded in the field using a Tektronix 1502 B cable tester, a portable laptop and the program of Heimovaara and de Water (1993). Two different approaches for the calculation of volumetric water content from the soil dielectric number were applied: 1. the third-order polynomial relationship after Topp (1980) and 2. the composite dielectric approach after Roth (1990). These results are compared to the water content obtained gravimetrically in the field at 7 different sites.

The following parameters were measured daily at the sites on transects 1 to 3: volumetric moisture content and bulk electrical conductivity using TDR, water level

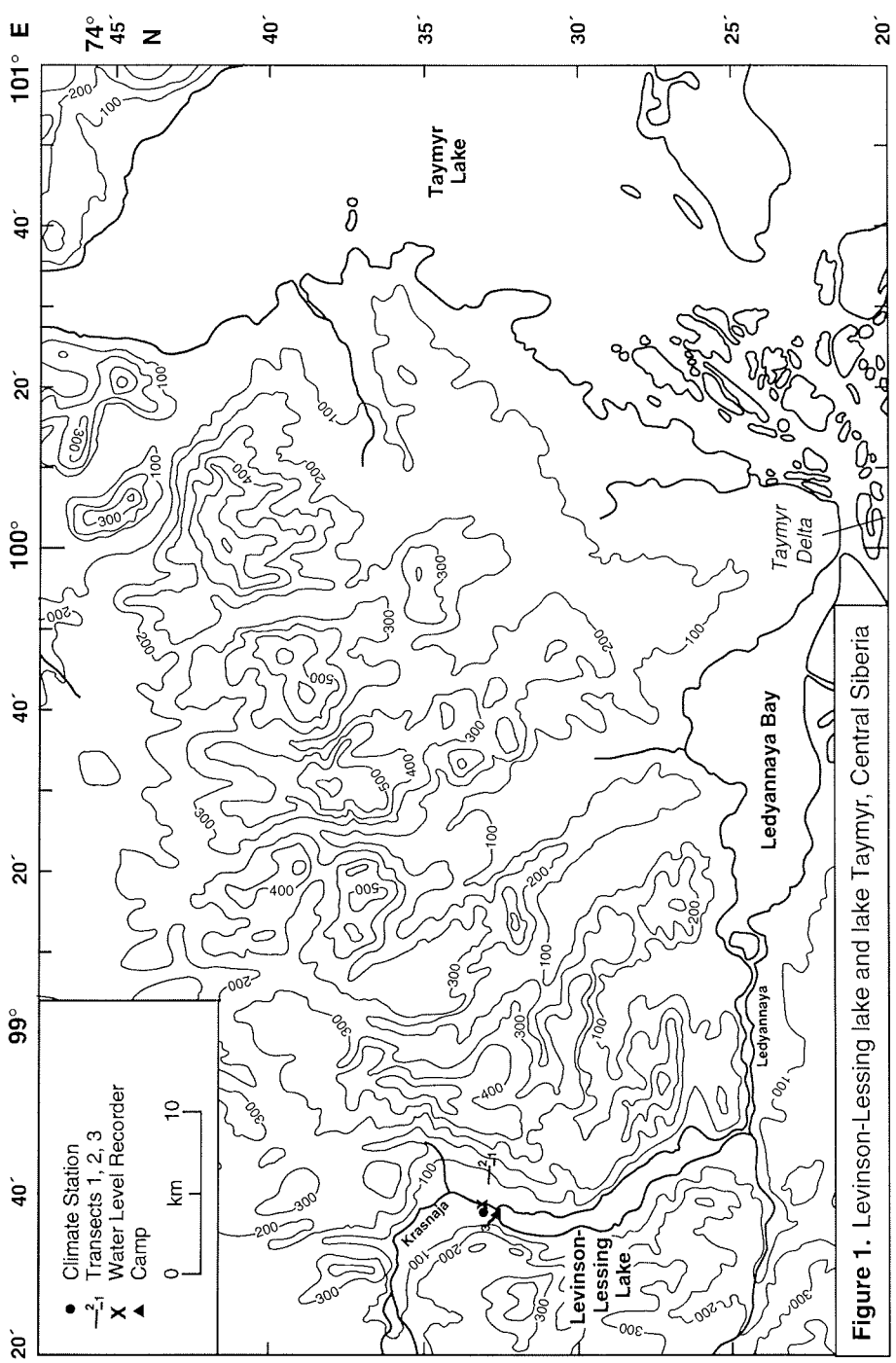

Figure 1. Levinson-Lessing lake and lake Taymyr, Central Siberia

Fig. 1: Levinson-Lessing Lake and Lake Taymyr, Central Siberia

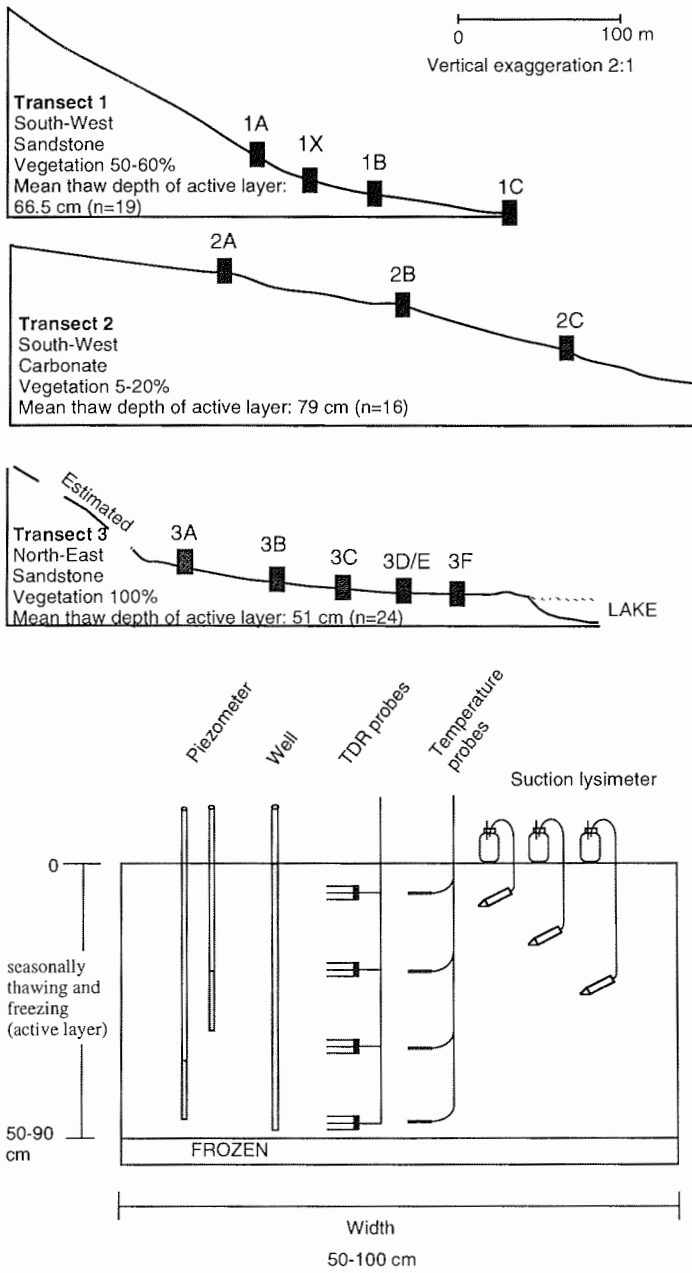

Fig. 2. Cross section of transects and schema of instrumented soil pit

in wells and piezometers, electrical conductivity and pH of ground, soil water and precipitation. Samples for isotope ($\partial^{18}O$, ∂D) analysis were taken at least every second day.

Results

A. Testing the TDR method

Figure 3 compares the results of gravimetric water content measurements with calculations based on TDR measurements at 7 sites; these sites represent typical surficial materials in this area (Table 1). All soils at all sites are mostly coarse grained (> 2 mm); only site 2D located at the base of the slope has a higher percentage of material finer than sand (< 2 mm).

Tab. 1. Soil physical characteristics on transect 2

site	depth range [cm]	grain size [% weight]		bulk density [g/cm^3]	saturated K* [cm/sec]	porosity +
		> 2 mm	< 2 mm			
1A	-	80.7	19.3	1.3	-	-
1B	59-49 29-28	67.4	32.6	1.4	$1.3 * 10^{-6}$ $5.0 * 10^{-3}$	0.4
1C	55-45 28-18	41.9	58.1	1.6	$2.1 * 10^{-5}$ $5.8 * 10^{-6}$	0.41
2A	-	64.6	35.4	1.9	-	0.29
2B	65-55 26-16	36.9 63.8	63.1 36.2	2.1	$2.4 * 10^{-6}$ $8.8 * 10^{-4}$	0.32
2C	78-68 39-29	43.6	56.4	1.6	$5.6 * 10^{-6}$ $1.2 * 10^{-4}$	0.33
2D	35-25 19-9	3.5	96.5	1.4	$8.3 * 10^{-4}$ $1.9 * 10^{-3}$	0.44

* measured using bail tests
\+ derived using TDR probes under saturation

Water contents calculated with the equations of Roth and Topp are close to the gravimetrically determined measurements (Figure 3). However, the dielectric approach of Roth yields a higher correlation coefficient between the gravimetrically determined and calculated water content (r^2Roth= 0.77; r^2Topp= 0.67 ; n=9).

B. Relationship between BEC and saturated soil water electrical conductivity

The relationship between BEC (calculated after Heimovaara and de Water, 1993) and the soil water electrical conductivity (EC) at all saturated sites from transects 1, 2 and 3 is shown in Figure 4. The three transects plot in three different groups due to differences in soil water EC; sites on transect 2 have the highest and widest range in soil water EC, sites on transect 3 have the lowest soil water EC.

There is no linear relationship between BEC and soil water EC for the set of all sites as it was found by Dasberg and Dalton (1985). However, a relationship exists between BEC and soil water EC within transects and for each transect site,

allowing BEC to be calibrated for each transect. For even better agreement, site specific (EC with depth) calibration must be undertaken.

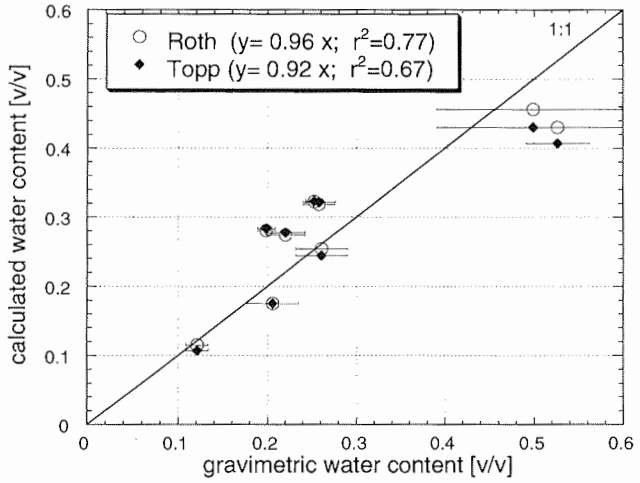

Fig. 3: Comparison between volumetric water content measured gravimetrically and calculated using TDR

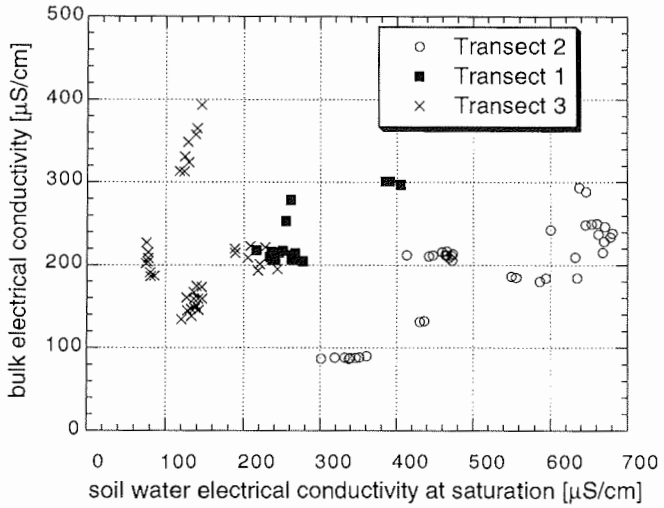

Fig. 4: Comparison between BEC calculated from TDR measurements and soil water electrical conductivity

C. The application of TDR for studying water movement

As an example, the seasonal changes in volumetric water content and groundwater table are presented for sites 2A, 2B, 2C and 2D on transect 2 (Figure

5). Generally, site 2A at the top of the slope is the dryest site and site 2D on the slope base is the wettest site. At both sites, there are only small seasonal changes in water content and groundwater level. In comparison, the upper soil layers at sites 2B (at 17 cm depth) and 2C (at 30 cm depth) undergo dramatic increase in water content and groundwater level as a result of the rainfall event (88 mm total) starting on August 17 (Figure 4). Interestingly, no site shows response in water content to earlier lower intensity rainfall events (e.g. August 15; 9 mm). Generally, the base of the slope (site 2D) is the wettest due to a larger (groundwater) contribution area and smaller water storage capacity (limited by the depth of unfrozen ground). In addition, site 2D has the largest percentage of material finer than sand (< 2 mm) and highest porosity (Table 1).

D. Sources of active layer water

Figure 6 displays $\partial^{18}O$ versus ∂ D for precipitation, groundwater, soil water and frozen ground relative to the Global Meteoric Water Line (GMWL). Data plot within a small range close to the Global Meteoric Water Line (GMWL) which suggests only small evidence of evaporative effects. The sources of active layer soil and groundwaters could be precipitation and melting of frozen ground. Further isotopic analysis on a larger data set currently underway will yield more information on water sources and flowpaths.

Conclusions

The TDR method is a promising *in situ* technique for studying water and solute movement in the active layer at this particular study site. The following preliminary conclusions can be made:

1. Generally, the use of TDR to determine soil water volumetric content yields good results whereby Roth's equation provides closer agreement with the gravimetric method. However, one should keep in mind that the data calculated with the TDR method should be treated as relative (not absolute) measurements of soil water content.

2. The TDR method for calculation of BEC shows promising results when calibrated site specifically.

3. High occurrence of rainfall events with low intensities are typical for this area. These data suggest that this type of rainfall is responsible for the maintenance of the moisture level of the ground. The different responses at the four sites on transect 2 to the rainfall event on August 17 suggest complex hydraulic properties of the active layer. Analysis of physical characteristics of the active layer (grain size, pF curves) are currently underway.

Future Work 1995

Field work is planned to start in May 1995 and continue until October 1995 to obtain data for one complete cycle of the active layer (thawing, maximum thaw depth, re-freezing). The following processes will be monitored from spring (May) to fall (October):

- infiltration and interaction of snowmelt water with the frozen ground during springmelt
- effects of the seasonal thawing on ion and water migration
- effects of active layer re-freezing on moisture and ion distribution

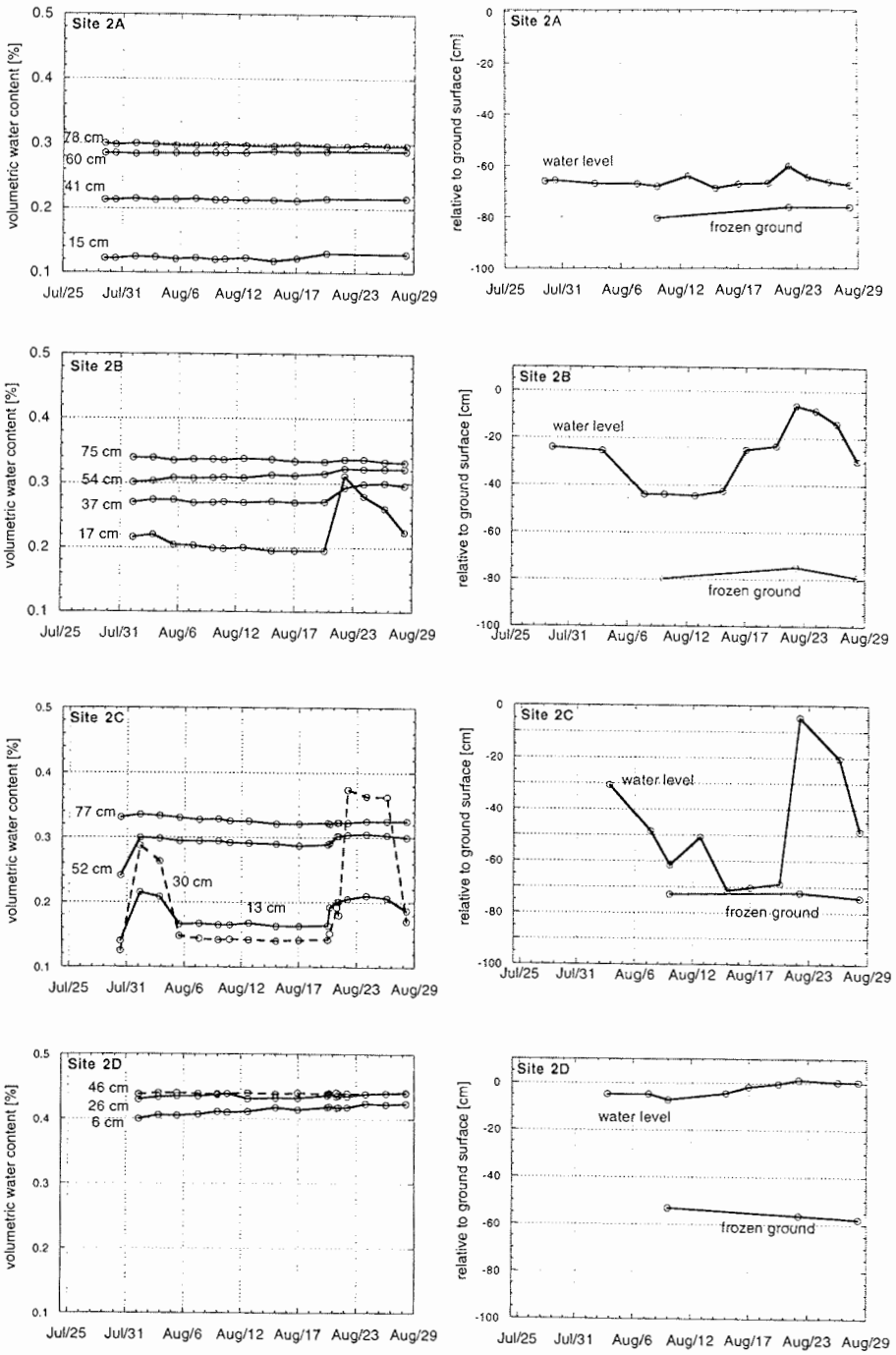

Fig. 5: Seasonal changes in volumetric water content and groundwater level at sites 2A, 2B, 2C and 2D on transect 2

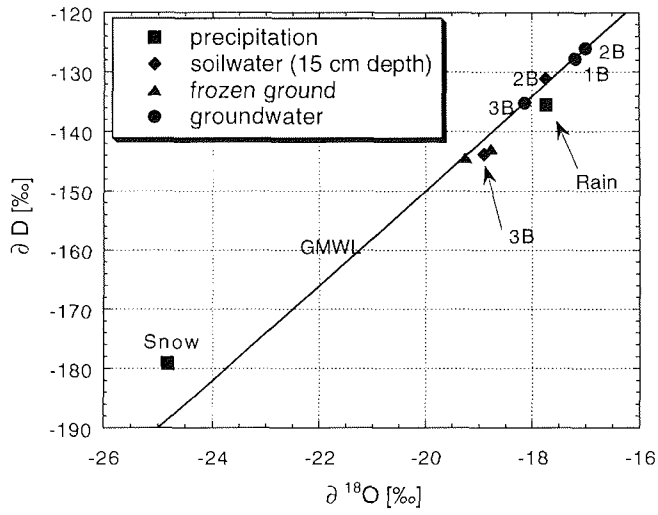

Fig. 6: Plot of $\partial^{18}O$ versus ∂ D for different waters from the Levinson-Lessing lake catchment

Literature

Dasberg, S. and F.N. Dalton (1985). Time Domain Reflectometry field measurements of soil water content and electrical conductivity. *Soil Sci. Soc. Am. J.* 49, pp. 293-297.

Heimovaara, T.J. and E. de Water (1993). A computer controlled TDR system for measuring water content and bulk electrical conductivity. Report # 41 (s. revised edition). Laboratory of Physical Geography and Soil Science, University of Amsterdam, 27 pp.

Roth, K., Schulin, R., Flühler, H. and W. Attinger (1990). Calibration of Time Domain Reflectometry for water content measurement using a composite dielectric approach. *Water Resources Research* 26(10), pp. 2267-2273.

Topp, G.C., Davis, J.L. and A.P. Annan (1980). Electromagnetic determination of soil water content: Measurements in coaxial transmission lines. *Water Resources Research* 16(3), pp. 574-582.

Acknowledgements

The following persons made this expedition to Siberia successful and unique: D. Bolshiyanov, M. Anisimova, M. Zhurbenko, P.P Overduin, D. Gintz. Their help in the field and data preparation is greatly acknowledged. Research is supported by the AGU in the form of a Horton Research Grant to J.Boike.

NATURAL AND TECHNOGENIC WATER AND SEDIMENT SUPPLY TO THE LAPTEV SEA

A. M. Alabyan, R. S. Chalov, V. N. Korotaev, A. Yu. Sidorchuk, A. A. Zaitsev
Moscow State University, Moscow, Russia

The water masses and sediments of the Laptev Sea are mainly formed by the yield of the Lena, the Yana, the Omoloi, the Khatanga and the Anabar River, draining a terrain area of 3.6 10^6 km^2. This vast territory encompasses three main tectonic regions of East Siberia: the Siberian Platform, the Baikalskaya and the Verkhoyano-Kolymskaya folding zones. Relief features and lithological composition of these areas are extremely various. The Siberian Platform comprises mainly plateaus and plains, formed by a complex of Triassic volcanic rocks (Puttorana Plateau and Oleneksko-Viluiskoe Table-Land), Arkhey and Proterozoic crystalline and metamorphic rocks as well as terrigenous limestone sediments (Anabarskoe Table-Land and Prilenskoe Plateau). The ranges and mountains of the Baikalskaya folding area are formed by gneiss, schist, quartzite and marblized limestone of the Proterozoic. The mountain and range systems of the Verkhoyano-Kolymskaya folding area are constituted by Permian and Carbon terrigenous sediments as well as volcanic rocks and granitoid of Triassic and Jurassic.

The neotectonic regime of this territory is relatively calm, except for the Puttorano Plateau and the Aldanskiy Shield where uplifting was followed by concentric and radial fracture system formation. The recent hydrographic network and water regime is controlled by neotectonic movements. Groundwater supply of the rivers from numerous fractures and geological structures control the migration of groundwater from one river system to another. Neotectonic processes indirectly influence the river yield through relief, lithology of river sediments, and permafrost conditions in valleys and watersheds. High variability of channel sediment thickness leads to a complicated interaction between channel and underchannel water flows, especially in small rivers.

Regular measurements of water and sediment discharge were carried out in this region during 1925-1935. Nowadays, there are 340 stations, randomly distributed over the vast area. The upper and middle reaches of the Lena and the Yana are relatively well studied, the hydrological data sets span 30-40 years.

The Research Laboratory of Soil Erosion and Channel Processes of the Geographical Faculty of Moscow State University has investigated hydrological and geomorphologic features of the basins, channels, confluences and deltas of the Vilui, the Aldan, the Kirenga, the Vitim, the Lena, the Omoloi and the Yana River. During 1969-1994, the depths and sediment distribution of ong sections of these rivers were mapped, and detailed geomorphologic and hydrological analyses of river channels and delta plains were conducted. All these data may be considered as a basis for calculations of water and sediment transport from Siberian rivers to the Laptev Sea and further to the Polar Basin.

Each year, the Siberian rivers discharge about 700 km^3 of water and about 27 10^6 tons of sediments to the Laptev Sea. Most important are Lena, Yana and Omoloi with a total of 552 km^3 of water and 24 10^6 tons of sediments (Fig.1). High water discharge happens in warm seasons (75-95% of yield), in relatively low regions in spring (up to 70-90%), in mountain areas in summer. The water regime reflects the type of river feeding: In snow-fed rivers, a single high flood takes place (East-Siberian Type)., whereas rain-fed rivers are characterized by a number of short high water periods in summer and autumn (Far East Type). The share of groundwater-fed rivers in the permafrost zone do usually not exceed 1-2%.

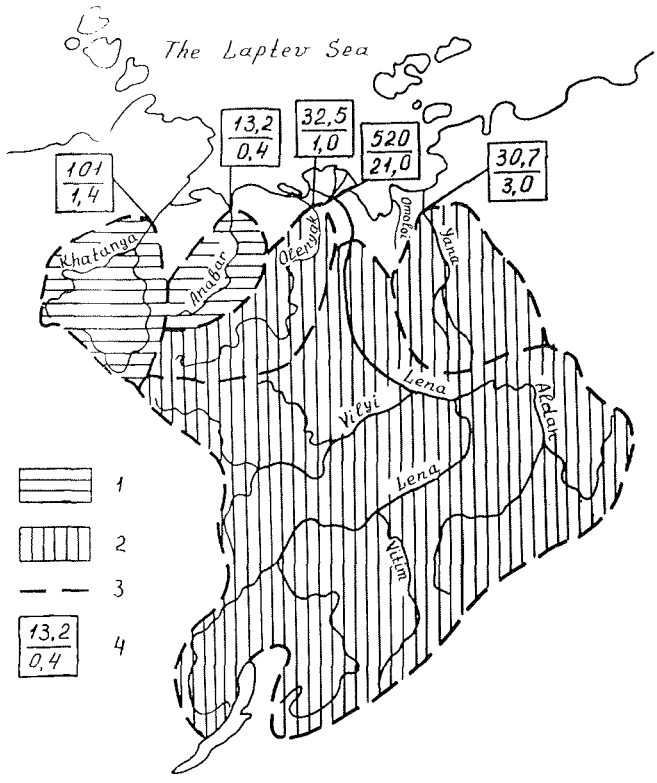

Fig. 1: Water and sediment supply to the Laptev Sea.

1 - region with a specific sediment discharge of 5-25 tons km^{-2}

2 - region with a specific sediment discharge of 25-100 tons km^{-2}

3 - boundaries of basins

4 - mean annual parameters in upper margin of deltas (water discharge in $km^3\ yr^{-1}$, sediment yield in 10^6 tons yr^{-1}).

The River Lena

The Lena River is 4,400 km long, its basin area covers 2.49 10^6 km^2, and its annual water volume amounts to 520 km^3. According to water supply volume and hydrological regime, the Lena can be subdivided into 3 main sections: the Upper Lena (above the junction with the Vitim River), the Middle Lena (from the Vitim to the Aldan River), and the Lower Lena (below the confluence with the Aldan). The Aldan River is the greatest tributary of the Lena River, supplying 35% of the Lena yield to the Laptev Sea. The second significant tributary of the Lena - the Vilui River - usually supplies not more than 10%.

Because the Lena River drains an area with different climatic and landscape conditions, the variability in the annual water flow is very low. The coefficient of the annual water discharge variation for the Kusur station (145 km above the Lena delta) is Cv=0.12, being the smallest of all Yakutian rivers. About 50% of the water of the lower Lena River is formed by snow melting, 35% by rain and 15% by underground water. This feeding regime is responsible for a high spring flood,

frequent water level rising after rains in summer and autumn, and very low water in winter. Because of the great river length, seasonal hydrological processes are prolonged. For instance, in the Upper Lena maximum water discharge occurs in April, in the middle Lena in May, and in the lower Lena in June (Fig. 2).

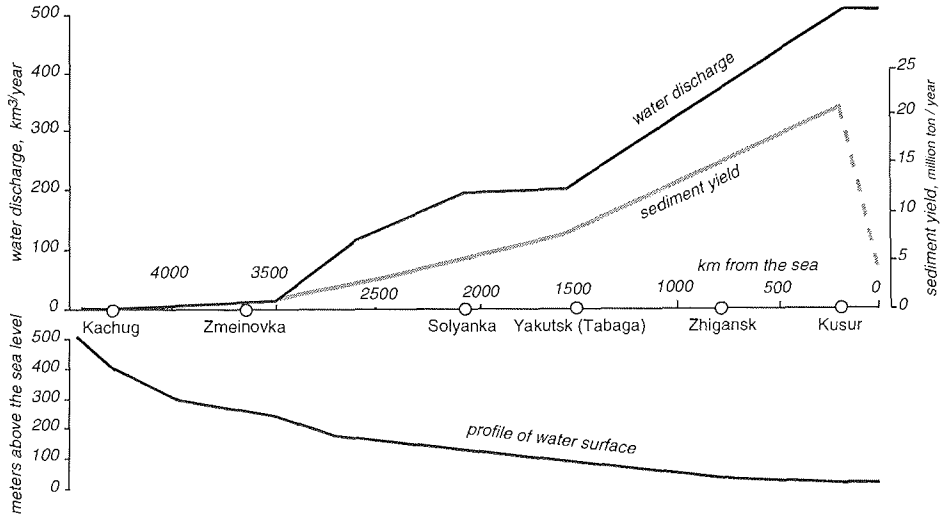

Fig. 2: Change of water discharge and sediment yield along the Lena River.

During a year, the concentrations of suspended sediment range from 25 to 40 g m^{-3} along the river. Because there is no spatial trend, sediment discharge is well correlated with water discharge (from 0.1 10^6 tons suspended sediment at Kachug to 9.9 10^6 tons at Tabaga and 21 10^6 tons at Kusur). The seasonal variability of sediment load is very pronounced. At the middle reach (Tabaga), sediment concentration reaches 60-80 g m^{-3} during the spring flood and decreases to ≤ 5 g m^{-3} in winter. With the summer rain floods, the turbidity increases only to 20 to30 g m^{-3}, i.e. most of the sediment discharge of the Lena takes place with the spring floods.

At Kusur, the mean annual water discharge is 16,500 m^3 s^{-1}, the mean annual sediment discharge 680 kg s^{-1}, and the mean annual sediment concentration 40 g m^{-3}. The corresponding maximum values are 20,000 m^3 s^{-1}, 1,300 kg s^{-1} and 66 g m^{-3}, respectively. The section between Kusur and Tit-Ary Island at the beginning of the Lena delta ('Lena's Pipe') do not have any significant tributaries.

The hydrological regime in the Lena delta is characterized by a gradual transition from pure river conditions to a delta regime (Korotaev 1984). The height of the flood wave decreases 2.5 times by the channel length, and water and sediment yields are partitioned among the delta branches in dependence of their morphological properties. According to data of from the gauge station Stolb Island, the eastern main delta branch (Bykovskaya Channel) receives 25% of the annual water discharge, the upper reaches of the Trofimovskaya Channel 61%, the Tumatskaya Channel 7%, and the western main branch (Olenekskaya Channel) 7%. During the last years, the shares of theTrofimovskaya and Tumatskaya

Channels have increased, while the share of the Olenekskaya Channel decreased and that of the Bykovskaya Channel remained constant.

The transformation of the water and sediment yield along the delta branches is also important for the understanding of the sediment transport to the Laptev Sea (Korotaev et al. 1990). In the eastern and central main delta branches (Bykovskaya and Trofimovskaya Channel), water discharge gradually decreases along the main channels. Only about 30% of their initial discharges reaches the sea through the main channels. The main water volume disseminates into second order arms and transverse distributaries. In the upper 40 km of the Bykovskaya Channel, up to 40% of the water flows into its western branches (Kuruyollakh and Byrdaktaakh). In its lower reaches, the Bukovskaya channel looses not more than 27% of water, with 10% flowing through the eastern channels (Gerasimova and Sinitsina) into the Neyolova Bay. The total sediment yield of the Bykovskaya Channel amounts to 1.0 - 1.3 10^6 tons.

The topographical structure of the Trofimovskaya Channel is very complicated and comprises several distinct regional delta systems. Therefore, the change of the water discharge along this channel is quite pronounced. At about 25 km downstream after splitting from the Sargakhskaya Channel, 41% of its initial water discharge is transported through the main channel, but only 7-8% eventually reaches the mouth of the Trofimovskaya Channel. Most of the water flows westwardly to the Baarchakh (22%), Malaya Trofimovskaya (12%) and Davida Channel (12%). The annual sediment transport through the Trofimovskaya Channel system does not exceed 0.4-0.8 10^6 tons.

The water discharge dynamics of the western main delta branch, the 145 km long Olenekskaya Channel, is characterized by a different regime. Its water discharge does not change significantly along the channel. Only 60 km above its mouth, the Olenekskaya Channel is divided into two branches. The western one (Angargamskaya) takes 53% of water. The main channel increases its share from 47% to 75% (compared to the initial discharge at the head of the branch), due to additional water supply from the Ardynskaya Channel. The bulk of this water volume reaches the mouth of the Olenekskaya Channel, and only 10% of its initial discharge flows into second order arms. The annual sediment transport through the Olenekskaya Channel ranges from 0.7 to 1.1 10^6 tons.

Overall, only 2.1-3.5 10^6 tons (10-17%) of a total of 21 10^6 tons of suspended sediment load coming into the subdelta section (at Kusur) reach the Laptev Sea , and the bulk of the sediment accumulates in the vast delta plain.

The River Yana

The Yana River is 1,170 km long and drains an area of 238,000 km^2. The river headwaters are in the Verkhoyansk Ridge at the confluence of the Dulgalakh and Sartang River. The Yana has 12,000 tributaries, with 21 being longer than 100 km. The Yana River flow regime is of East Siberian type, i.e. most of the water flow (up to 99%) occurs during June - September in several flood waves (up to 10) due to spring snow melt and summer rains. The maximum measured discharge is 12,400 $m^3\ s^{-1}$ during spring melt and 13,000 $m^3\ s^{-1}$ during summer rains at the Dzhangy station at the lower section of the river, 381 km from the mouth. The mean winter discharge near Dzhangy was only 13 $m^3\ s^{-1}$ during October-May. On average, the river channel is frozen to bottom once in four years. The mean annual water discharge at Dzhangy station was 928 $m^3\ s^{-1}$ (= 27.2 $km^3\ yr^{-1}$) during 1938-1988.

The suspended sediment supply is also concentrated in the warm season (with up to 99.2%). The mean annual sediment load is 3.9 10^6 tons at Dzhangy station, mean annual sediment discharge 120 kg s^{-1} and mean sediment concentration 130

g m^{-3} . The maximum daily sediment discharge can be higher than 5,000 kg s^{-1} with a maximum sediment concentration of up to 1,100 g m^{-3} . In some years, the principal sediment transport can happen during the spring melt period, in others during the summer floods.

Within the Yana delta, the transformation of the water and sediment flow reflects the delta channels hydraulics and geomorphologic patterns (Babitch et al. 1992). The delta is formed by two main branches (Main Channel and Right Channel) and 6 additional branches, which are not connected with each other by transverse distributors. These branches can be divided to three main groups: Western (Ilyin Shar, Taryngnaakh branches and Right Channel), Central (Main Channel , Kamelek and Durganova branches), and Eastern (Kochevaya and Samandon branches). During the low-water period, 34% of the water flow is partitioned to the western, 57% to the central and 9% to the eastern group. During the floods, 35% of the water flow is distributed to the western, 43% to the central and 22% to the eastern branches. The partitioning of suspended sediments is significantly different. During the low water period, 18% of the sediment load goes to the western, 81% to the central and 1% to the eastern group, while during the flood period, 49% is distributed to the western, 46% to the central and 5% to the eastern group.

The western branches of the Yana delta tend to silt because of the relative increase of sediment supply and relative decrease of water flow from low to high water. The eastern branches are characterized by a trend to activation, due to the low relative increase sediment supply and high relative increase of water flow from low to high water. The central branches do not show any clear trend, because the relative increase of sediment supply from low to high water is favorable for siltation, but the relative increase of water flow at the same time is favorable for channel activation. The sediment budget measurements along the Main Channel showed that there is an exchange of sediments within the channel: sandy particles are accumilated on the riffles, and silt is eroded from the banks. The volume of suspended sediments is the same at the head and at the mouth of the branch but the composition is different: the sediments at the head are coarser that at the mouth. The annual sediment load at the mouth of the Main Channel is 0.5-1.0 10^6 tons for a low-water year and 1.5 -2.0 10^6tons for a high-water year.

Technogenic sediment supply

The human influence on the sediment yield of the Lena River system primarily derives from the mining industry. Gold mining enterprises explore alluvial placers along small tributaries of the Lena, the Vitim and the Aldan River. Their activities lead to additional sediment input to the water and change its chemical composition. This impact is particularly evident in the Vilui River where intensive brine drawings from kimberlit quarries take place. These pollutants move directly to the upper reaches of the Markha River, the Markoka River and other tributaries of the Vilui River.

It is very difficult to determine the natural background turbidity because systematic monitoring of sediment load had begun only at the same time or later than mining works. In tributaries of the Vitim River, for instance, the gold exploration started at the end of ninetieth century, and the regular monitoring of sediment load was organized not before the 1930ies. In the Aldan River basin, however, mining activities and sediment load measurements started at the same time (in the 1930ies), and here a significant increase of the suspended sediment load due to human impact can be distinguished: While in June 1938 the mean water discharge was 17,100 m^{-3} s^{-1} and the mean sediment discharge 200 kg s^{-1}, the sediment load in June 1984 was two times higher (420 kg s^{-1}) at approximately the same water

discharge (17,700 m^{-3} s^{-1}). The increase of sediment load is even more conspicuous during the low-water period. In September of 1938, the mean sediment load was 42 kg s^{-1} at a mean water discharge 7,480 m^{-3} s^{-1}. In September of 1984, the mean water discharge has not changed, but the sediment load was almost four times higher (160 kg s^{-1}).

Most of the sediments in the Aldan and Vitim Rivers is transported as suspended load, the bed load is not significant. The bottom sediments consist mainly of gravel, cobbles and boulders, being suspended only during the main floods. The technogenic sediments, however, consist mainly of very fine particles and colloids which can be transported over the long distances to the river delta and to the Laptev Sea shelf.

Another source of technogenic sediment supply is the regular channel dredging of the Lena River and its main tributaries for navigation improvement (Zaitsev and Chalow 1989). Dredging resuspends thin particles and activates bottom load movements. The same effect has the mining of channel alluvium for construction purposes. For example, near Yakutsk the volume of channel dredging amounted to 4 10^6 tons of sediments per year, and 2 10^6 tons were removed from the channel. This is comparable to the sediment supply to this reach of the river channel (about 8 10^6 tons).

At the northern part of the Yana-Omoloy interfluve, the Kular mining field is situated. The mine exploitation (underground and open) led to a significant relief transformation. The mechanical removing of huge masses of fine frozen deposits and the land cover destruction caused intensively accelerated erosion processes, such as thaw flows of the active layer of artificial steep slopes, sheet erosion of thaw sediments with very low cohesion, thermogullies formation, and bank erosion in the artificial water channels. Despite the building of hydrotechnical constructions (dams, settling basins), the accelerated erosion resulted in additional sediments being delivered to the creeks (right tributaries of the lower Omoloy River and left tributaries of the lower Yana River). The specific sediment yield of the most erodible catchments is higher than 20,000 tons km^{-1} yr^{-1}. These sediment formation coincided with relatively small open areas at the upper part of catchments. The suspended sediment concentration is up to 500-700 kg m^{-3} at the upper reaches of creeks and up to 13 - 15 kg m^{-3} at the lower reaches. This high sediment load transforms channel and floodplain alluvium composition and channel morphology. During a flood, up to 40% of the sediment supply from a mining area can be deposited on the alternating bars and floodplain. Channel form migrations led to removing of fine sediments from the channel alluvium, and only 2 - 3 % of the technogenic fine sediment supply remain in bars (on average during 20 years). The floodplain alluvium composition near the channels became coarser and more silty.

The whole technogenic sediment yield from the mining areas to the Yana delta can be 1.0 10^6 tons in average years and up to 2.4 10^6 tons in high-water years (Alekseevskiy and Sidorchuk 1992). This represents 25-50% of the natural sediment supply in the Yana River basin. These sediment rates change significantly the delta formation processes in the Yana delta and increase the natural tencency of the western Yana delta branches for siltation. In the Ilyin Shar branch, which is directly contaminated by technogenic sediments, the point bars are composed from very fine silt. The technogenic sediment supply to the Omoloy River mouth is 1.0 and 3.0 10^6 tons yr^{-1} in average and high-water years, respectively. This is 200-600% of the natural sediment load in the river. The sediment concentration in the Omoloy River reaches to 0.7 kg m^{-3} during the flood period. For comparison, the natural suspended sediment concentrations in the river were 0.05 -0.15 kg m^{-3}. In the mouths of the main tributaries of the Omoloy, which

are affected by mining activities, the sediment concentrations amount to 2.4 - 5.3 kg m^{-3}, and in the mouths of minor streams they are up to 13-15 kg m^{-3}. The maximum values of the specific sediment yield are higher than on the Loess plateaus in China. Most of thesediments is delivered to the Laptev Sea shelf. The plume of turbid water at the mouth of the Omoloy River is clearly discernible on satellite images. The calculation of the sediment distribution in Laptev Sea shelf waters showed that during the flood period the concentration of technogenic sediments can be 10-25 mg m^{-3} at the Lena delta front.

References

Alekseevskiy, N. I., Sidorchuk, A. Yu., 1992. The accelerated erosion in the landscapes, changed by mining works: a case study of the Yana River and the Omoloy River basins. In: Chalov, R. S. (ed.). The ecological problems of soil erosion and channel processes. Moscow Univ. Publ. House, Moscow, pp. 187-198. (in Russian)

Babitch, D. B., Zaets, G. M., Korotaev, V. N., Mikhailov, V. N., 1992. Hydromorphological processes in the mouth area of the Yana River, their natural and technogenic variability. In: Chalov, R. S. (ed.). The ecological problems of soil erosion and channel processes. Moscow Univ. Publ. House, Moscow, pp. 187-198. (in Russian)

Korotaev, V. N., 1984. Formation of a hydrographical network of the Lena Delta. Vestnik Moskovskogo Universiteta 6: 39-44.

Korotaev, V. N., Mikhailov, V. N., Babitch, D. B., Zaets, G. M., Bogomolov, A. L., 1990. Hydromorphological processes, dynamics of hydrographic network, and channel deformations in the delta of the Lena River. In: Chalov, R. S. (ed.). The ecological problems of soil erosion and channel processes. Moscow Univ. Publ. House, Moscow, pp. 187-198. (in Russian)

Zaitsev, A. A., Chalov, R. S., 1989. Channel processes and channel management in the Lena River at Yakutsk City. Wodnye Resursy 5: 75-80. (in Russian)

GEOCHEMISTRY OF LENA RIVER SUSPENDED LOAD AND SEDIMENTS - PRELIMINARY RESULTS OF THE EXPEDITION IN JULY/AUGUST 1994

V. Rachold

Alfred-Wegener-Institut für Polar- und Meeresforschung, Forschungsstelle Potsdam, Germany

Introduction

The Laptev Sea shelf is thought to be the main source area of sediment material included into sea ice and transported to the Arctic Ocean via the Transpolar Drift (Dethleff et al. 1993, Kassens & Karpiy 1994 and Kassens et al. 1994). For this reason the characterisation and quantification of material supplied to this shelf areas by the Siberian rivers, its transport to the deep Arctic basin and its variations between glacial and interglacial stages reveal important information on the paleoclimate of the Eurasien continent and the history of circulation patterns in the Arctic Ocean.

The scientific cooperation between the Alfred Wegener Institute, Research Department Potsdam and the Moscow State University, Geographical Faculty is devoted to the investigation of sediment transport of the Lena, Yana, Khatanga, Olenyok, Anabar and the Omoloy River to the Laptev Sea. Research objectives of this study are to

- quantify and to qualify the recent sediment transport of this rivers to the Laptev Sea,
- document variations in the geological past,
- distinguish between material transported by different rivers by chemical and mineralogical characteristics related to the geology of their source areas and to identify riverine material in the marine environment.

The working group of AWI concentrates on the chemical and mineralogical composition of river sediments and suspended material. The investigations include

- mineralogy of the sediments, especially heavy mineral composition,
- inorganic geochemistry of the suspended load and the bulk sediment,
- chemical signatures of mineral phases,
- isotopic composition ($\delta^{13}C$ and $\delta^{15}N$) of the organic material
- dating of sediments with ^{14}C-method.

The results will be combined with

- hydrological, geomorphological and sedimentological data of these rivers studied by the Moscow State University, Geographical Faculty
- mineralogical/geochemical data of Laptev Sea sediments.

A first expedition to the Lena River organised by the Moscow State University in cooperation with the AWI Potsdam took place in July/August 1994. Two participants from AWI and one from Moscow State University joint the expedition on the RV "Prof. Makkaveev". Samples of water, sediments and suspended material were taken along the course from Yakutsk to the Lena Delta and back to Yakutsk (Fig. 1).

This study reports the first results on the geochemistry of the suspended material.

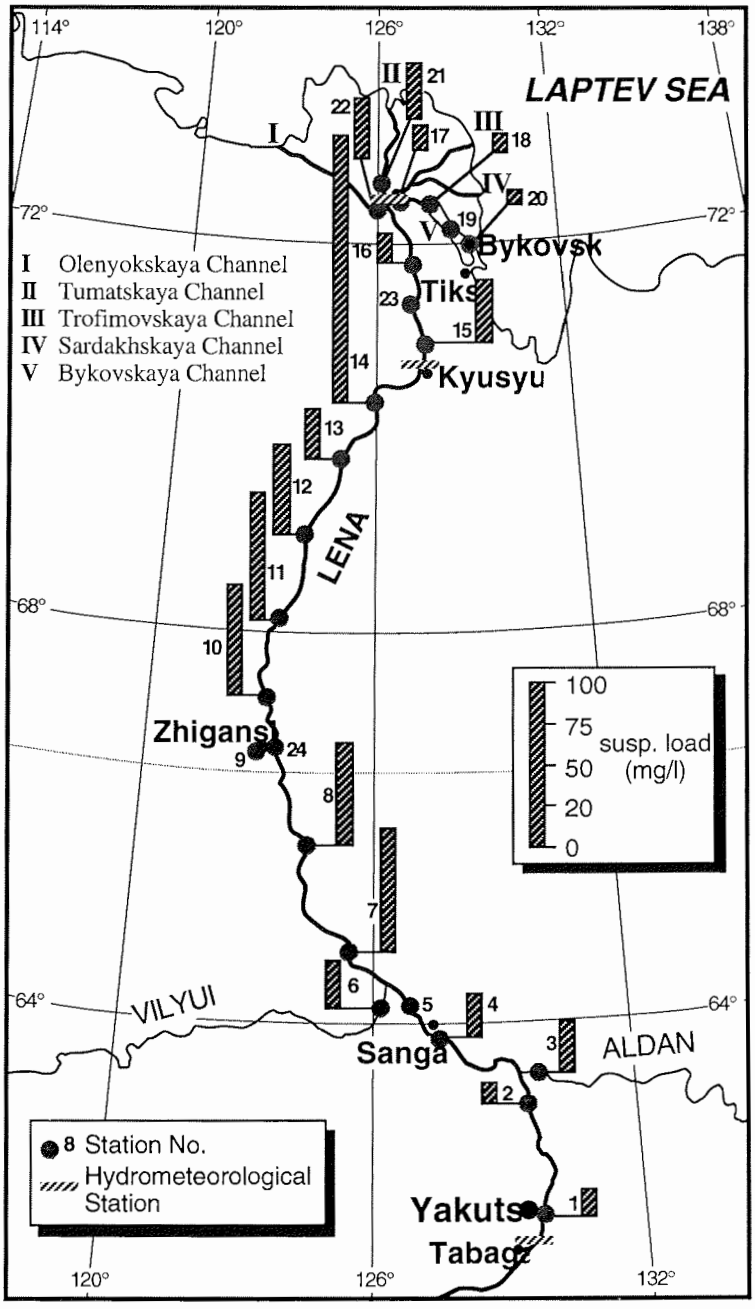

Fig. 1: Location map of the expedition to the Lena River in July/August 1994 showing sampling stations and suspended sediment load.

Sampling

The sampling equipment was reduced to a minimum since the complete material had to be transported by aeroplane in the personal luggage. Therefore sampling instruments available onboard RV "Prof. Makkaveev" were applied.

Surface sediments were obtained by a simple pail because box corer and piston corer installed onboard "Prof. Makkaveev" did not work satisfactorily in the strong current of the Lena River.

Integrated water samples (from the surface to the bottom) were obtained by a 1 l bottle placed inside of a 50 kg weight operating by a small manual winch system. Suspended material was obtained by vacuum filtration of river water. The filtered volume varied between 500 and 1500 ml depending on sediment load. Two different types of filters were used at each station: acetate filters for inorganic and glass fibre filters for organic analyses. The suspended sediment load was calculated from the weight difference between the pure cellulose acetate filters and the sediment loaded filters after freeze drying. For detailed informations about sampling and locations the reader is referred to Rachold et al. 1995.

Geochemical Methods

Acid digestions of the complete cellulose acetate filters including the suspended material were performed in PTFE containers. The filters and the organic material decompose in concentrated HNO_3, the remaining sediment breaks up in a combination of concentrated $HClO_4$ and HF. To avoid contamination, only ultrapure acids were used. The acids were evaporated to dryness on a hotplate, the residues redissolved in concentrated HNO_3 and made up to a final volume of 25 or 50 ml depending on sediment load. Major and minor element concentrations were analysed in the solution by ICP Atomic Emission Spectroscopy.

Preliminary Results

Sediment load varies between 10 mg/l and more than 100 mg/l, with high values between Zhigansk and Kyusyur and low values near Yakutsk and in the delta (Fig.1). The average sediment load of approximately 40 mg/l is in good agreement with data of the hydrometeorological stations (Leningrad Hydrometeorological Service 1987).

Geochemistry of the suspended material

To compensate for different amounts of organic material diluting the mineral fraction, Aluminium normalisation was applied. Aluminium is a conservative element and exclusively bound to the mineral component. Therefore the normalised concentrations are independent of the content of organic material.

Histograms of some normalised major and minor element concentrations are presented in Fig. 2 a and 2 b, respectively. Samples plotted here were taken along the 1700 km way from Yakutsk to the delta. Data of typical granitic and basaltic rocks (Mason & Moore 1985) as well as the values of average shale (Wedepohl 1971 & 1991) are displayed for comparison.

The composition of Lena suspended load is surprisingly homogenous, very similar to that of average shale for most of the major elements. The average shale is formed from weathering products of crustal rocks and therefore reflects the composition of the upper continental crust. Since the Lena River drains a large area, the composition of the suspended sediment represents an average of the rocks in the area, that is comparable to the upper crust composition.

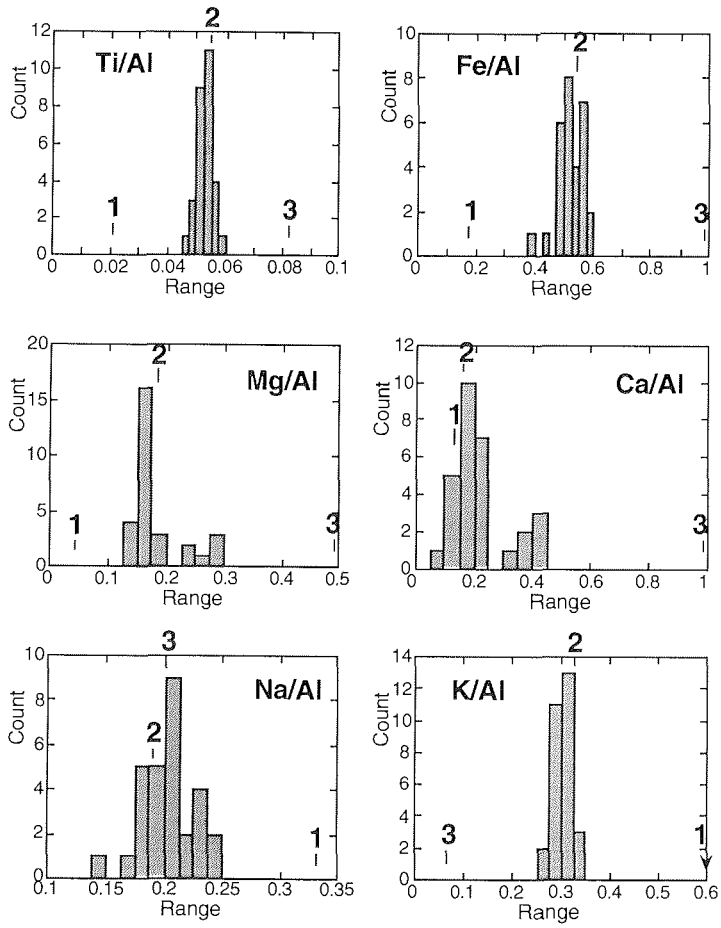

Fig. 2 a: Histograms of Al-normalised major element concentrations (weight ratios) of Lena suspended load. Values of granite (1), average shale (2) and basalt (3) are shown for comparison.

The trace elements show a similar behaviour. However, some differences are obvious: very high Zn values cannot be explained at the moment.

A more detailed study of the geochemical data exhibits some regional variations in the suspended load composition. Ti/Al, Fe/Al, Ca/Al, and Mn/Al ratios of the suspended sediment sampled between Yakutsk (0 km) and Cape Bykovsky (distance from Yakutsk is approximately 1700 km) are shown in Fig. 3 a and 3 b.

The values analysed in the mouth areas of the Vilyui and the Aldan River are also displayed.

Material of the Vilyui River can be distinguished very clearly, whereas the Ti/Al and Fe/Al ratios of the Aldan River are very similar to that of the Lena River. The same situation occurs for Mn/Al and Ca/Al ratios.

Furthermore higher Ca/Al ratios are observable in the area of Yakutsk, where carbonates are present.

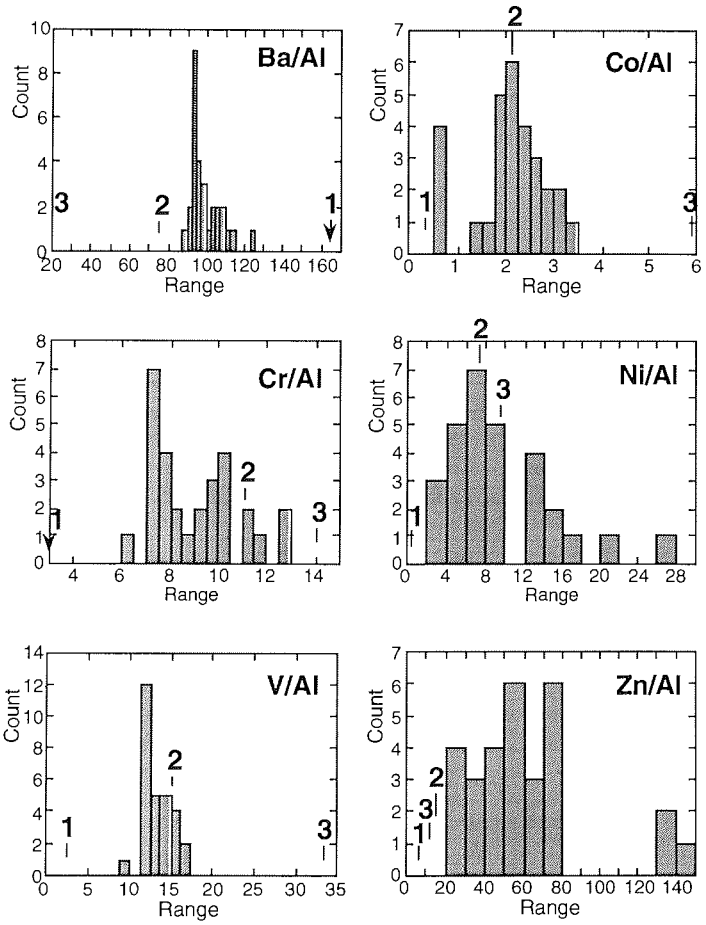

Fig. 2 b: Histograms of Al-normalised minor element concentrations (weight ratios • 10^4) of Lena suspended load. Values of granite (1), average shale (2) and basalt (3) are shown for comparison.

Conclusions

The preliminary results of this study indicate that the geochemistry of the Lena River suspended material obviously reflects the geology of the source area. Since the Lena Rivers drains a large basin, the composition of the suspended load is very similar to that of average shale representing the upper continental crust. Furthermore small variations related to the regional geology are also seen.

However, the bulk geochemistry of the river suspended load and bottom sediments will probably not enable the identification of material transported by different rivers in the marine realm. For this reason future investigations have to include more specific analyses, i.e. chemical composition of mineral phases and isotope studies.

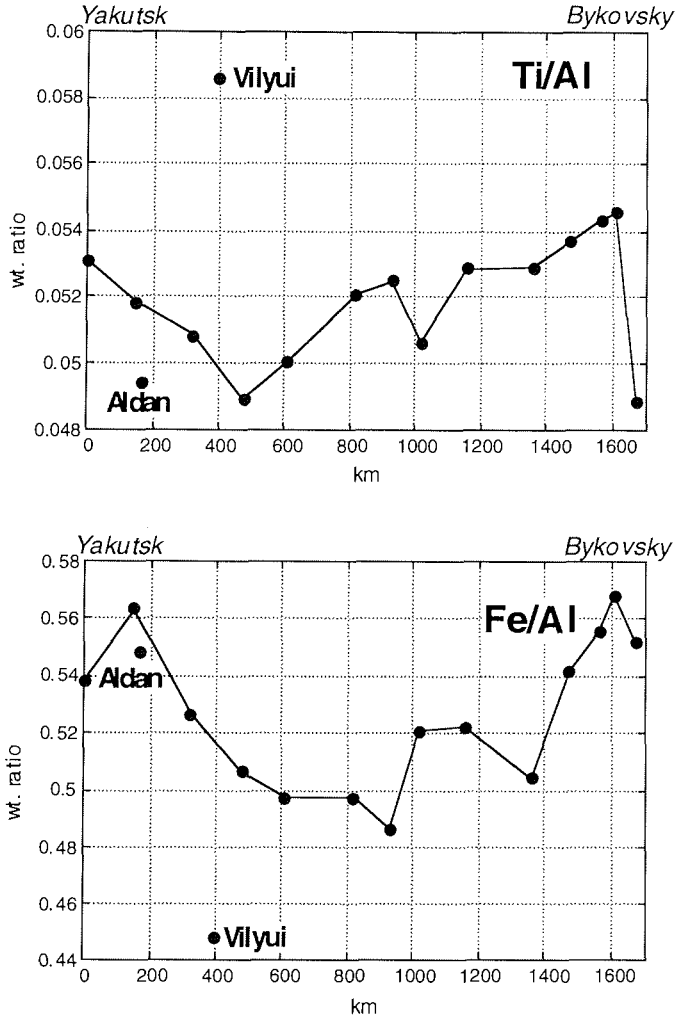

Fig. 3 a: Ti/Al and Fe/Al ratios of Lena suspended load including the mouth areas of the Aldan and the Vilyui River. The graph displays values analysed at stations from Yakutsk to Cape Bykovsky in the Lena Delta.

Future Work

The analytical work will be continued during winter. The investigations will concentrate on the geochemistry of the bulk bottom sediment and specific minerals as well as on stable isotope studies of the organic material.

In the next summer a second expedition to Yakutia will be carried out (Fig. 4). It will include sampling on the upper Lena River south of Yakutsk and between Yakutsk and the delta again. An attempt to reach the Olenyok throughout the Olenyokskaya Channel will be made. The second leg will focus on sampling in the Yana River between Niszneyansk in the delta and Verkhoyansk.

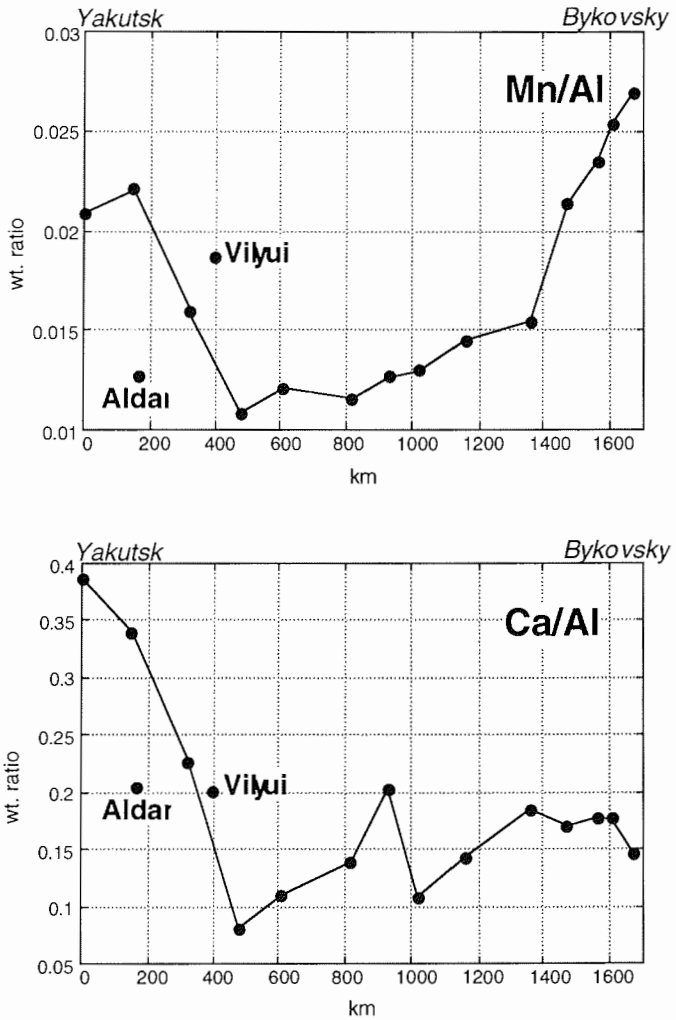

Fig. 3 b: Ca/Al and Mn/Al ratios of Lena suspended load including the mouth areas of the Aldan and the Vilyui River. The graph displays values analysed at stations from Yakutsk to Cape Bykovsky in the Lena Delta.

References

Dethleff, D., Nürnberg, D., Reimnitz, E., Saarso, M. & Savchenko, Y.P., 1993. East Siberian Arctic Region Expedition '92: The Laptev Sea - Its significance for Arctic sea-ice formation and transpolar sediment flux. Rep. Polar Research 120, 1-44

Kassens, H. & Karpiy, V., 1994. Russian-German cooperation: the Transdrift 1 Expedition to the Laptev Sea. Rep. Polar Research 151

Kassens, H., Hubberten, H.-W., Pryamikov, S.M., Stein, R., 1994. Russian-German cooperation in the Siberian shelf seas: Geo-System Laptev Sea. Rep. Polar Research 144

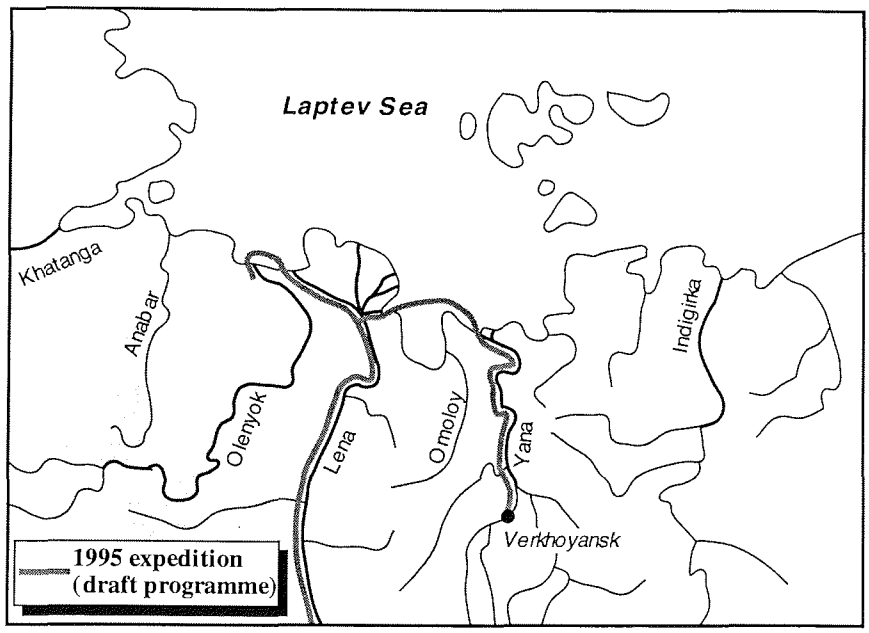

Fig. 4: Draft programme of the next expedition to the Siberian rivers planned in 1995.

Leningrad Hydrometeorological service, 1987. Data about regime and resources of surface water in the USSR, Part 1. Volume 16: Middle and lower Lena basin (in Russian)

Mason, B., Moore, C.B., 1985. Grundzüge der Geochemie. Enke Verlag, Stuttgart, 340 pp.

Rachold, V., Hermel, J., Korotaev, V.N., 1995. Expedition to the Lena River July/August 1994. Rep. Polar Research (in prep.)

Wedepohl, K.H., 1971. Environmental influences on the chemical composition of shales and clays. In: Ahrens, L.H., Press, F., Runcorn, S.K. & Urey, H.C. (Eds.): Physics and Chemistry of the Earth, Vol. 8. Pergamon, Oxford, 305-333

Wedepohl, K.H., 1991. The composition of the upper earth´s crust and the natural cycles of selected metals. Metals in natural raw materials. Natural resources. In: Merian, E. (Eds.): Metals and their compounds in the environment. VCH-Verlagsgesellschaft, Weinheim, 3-17

SEDIMENT REWORKING BY ICE GOUGING IN THE WESTERN LAPTEV SEA

F. Lindemann*, H. Kassens* and E. Reimnitz°

* GEOMAR Forschungszentrum für marine Geowissenschaften, Kiel, Germany

° United States Department of the Interior, Geological Survey, Menlo Park, USA

An important geological factor for sediment reworking on Arctic shelves is through the contact of ice and sea floor. Furrows, or ice gouges, are the most prominent features of these interactions at the sea floor. These ice gouges are a well known and often described phenomenon, e.g. in the Beaufort Sea, where they are influencing sediment distribution patterns (Rearic et al. 1990). For the first time we are able to show recent ice gouges in the Laptev Sea. During the Expedition TRANSDRIFT I (July-September 1993) aboard RV IVAN KIREEV, side scan sonar surveys over thirteen transects (more than 170 km) were carried out in order to gain a closer insight into the small scale topography of the Laptev Sea. Surveys between 10 and 35 metres water depth yielded best results. Shallower areas were restricted due to the ships draught. In this paper we presented the results of analysing the side scan sonar transects IK93 Sc-2, Sc-3 and Sc-10 (Fig. 1).

Method

Geologists are primarily interested in the effect ice gouging has on the seabed rather than in the tools that caused the gouging, we therefore consider each seabed incision as a separate gouge even when several parallel gouges may have been caused by the same ice movement event or even the multiple tools of a single ice keel (Rearic et al. 1981). High gouge densities are associated with wide, shallow "multiplet" gouging events, where long sections of pressure-ridge keels raked the bottom (Barnes & Rearic 1985).

The side scan records were split into 1 km segments by using GPS navigational data. The gouges in each 1 km segment were counted and measured as striking linears against the ships track. After that, we computed these data into data corrected to true north. To allow a correlation to US data from the Beaufort Sea (e.g. Rearic, Barnes & Reimnitz 1981, Barnes & Rearic 1985), we decided to present total gouges, single gouges and multiple gouges, and not events. Following the usage of Barnes & Rearic (1985), we defined each parameter as follows:

1. Multiple gouges - Gouges generated by a tool with 2 or more indenters leaving one or more adjoining furrows on the sea floor.
2. Single gouges - Gouges generated by a single tool indenting the bottom leaving a single furrow.
3. Total gouges - Total number of sea floor furrows observed in a segment. Each furrow in a multiple gouge is counted separately.

Results and Discussion

The data corrected to true north, show no preferred or dominant orientation along the transects we are presenting here. This contrasts with the Beaufort Sea, where dominant trends generally are parallel to the coast and isobaths.

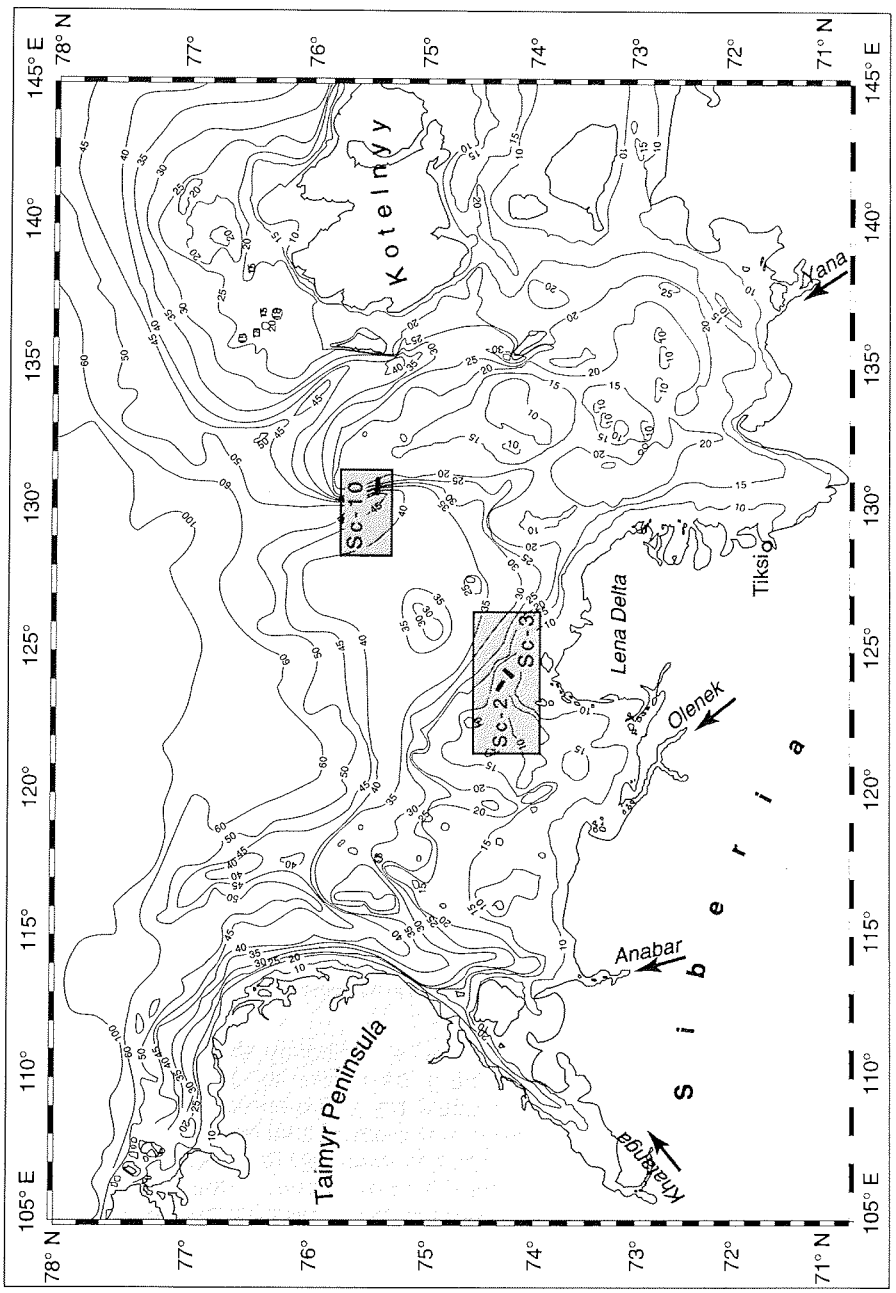

Fig. 1: Bathymetric map showing the locations of three side scan sonar transects presented in this paper.

In the western Laptev Sea NW of the Lena Delta, ice gouges are strongly tied to water depth, increasing in numbers with decreasing depth. The records of transects IK93 Sc-2 and Sc-3 show a correlation of total gouges vs. water depth of r= 0.81 (Fig. 2 and 3).

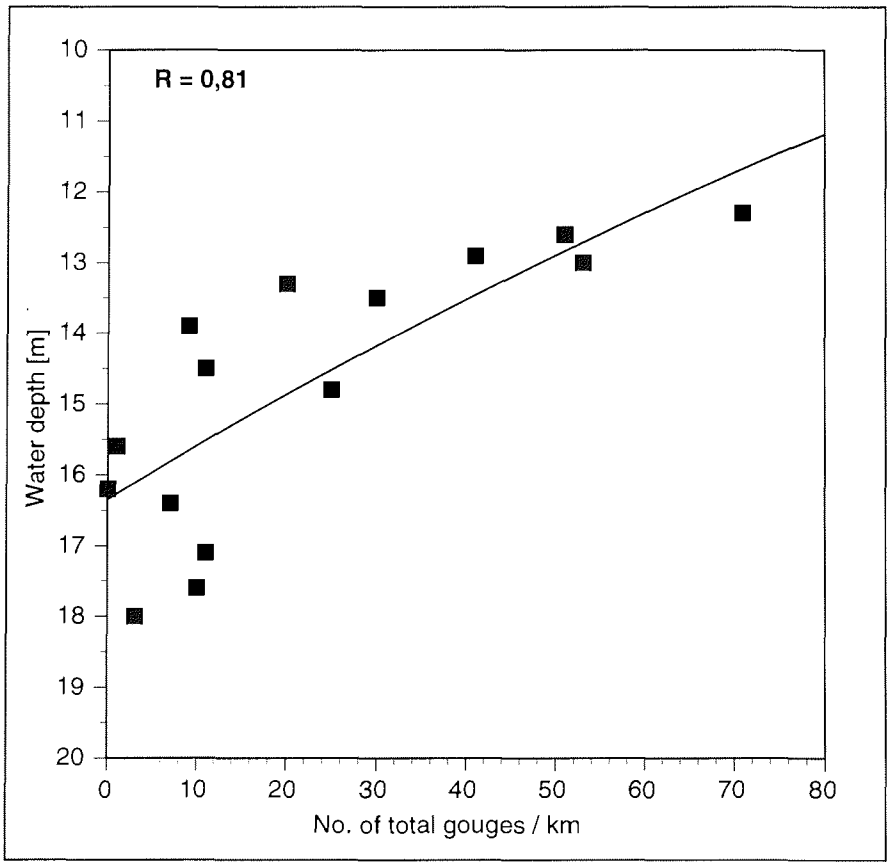

Fig. 2: Correlation between ice gouges vs. water depth in the western Laptev Sea.

Transect IK93 Sc-10 at the western flank of Stolbovoy shoal gives evidence for the predominant drift direction of floating ice before its grounding, and for ice draught. At this transect, ice gouges could be documented down to 42 m water depth. Furthermore, the records show a maximum of total gouges in the upper part. Remarkable is that the number of ice gouges decrease to the very top of the shoal flank (Fig. 4). Therefore, the ice must be driven by west-east directed forces such as currents or wind and the dominant draught of the floating ice seems to be between 28 and 23 m water depth.

The results show, that at the western flank of Stolbovoy shoal, grounded ice considerably influences sediment distribution patterns by reworking between 23 and 28 m water depth (Fig. 4).

Possible source areas for deep draught ice grounding in the Laptev Sea west of Stolbovoy shoal are (i) Severnaya Zemlya NW of the Laptev Sea and (ii) the

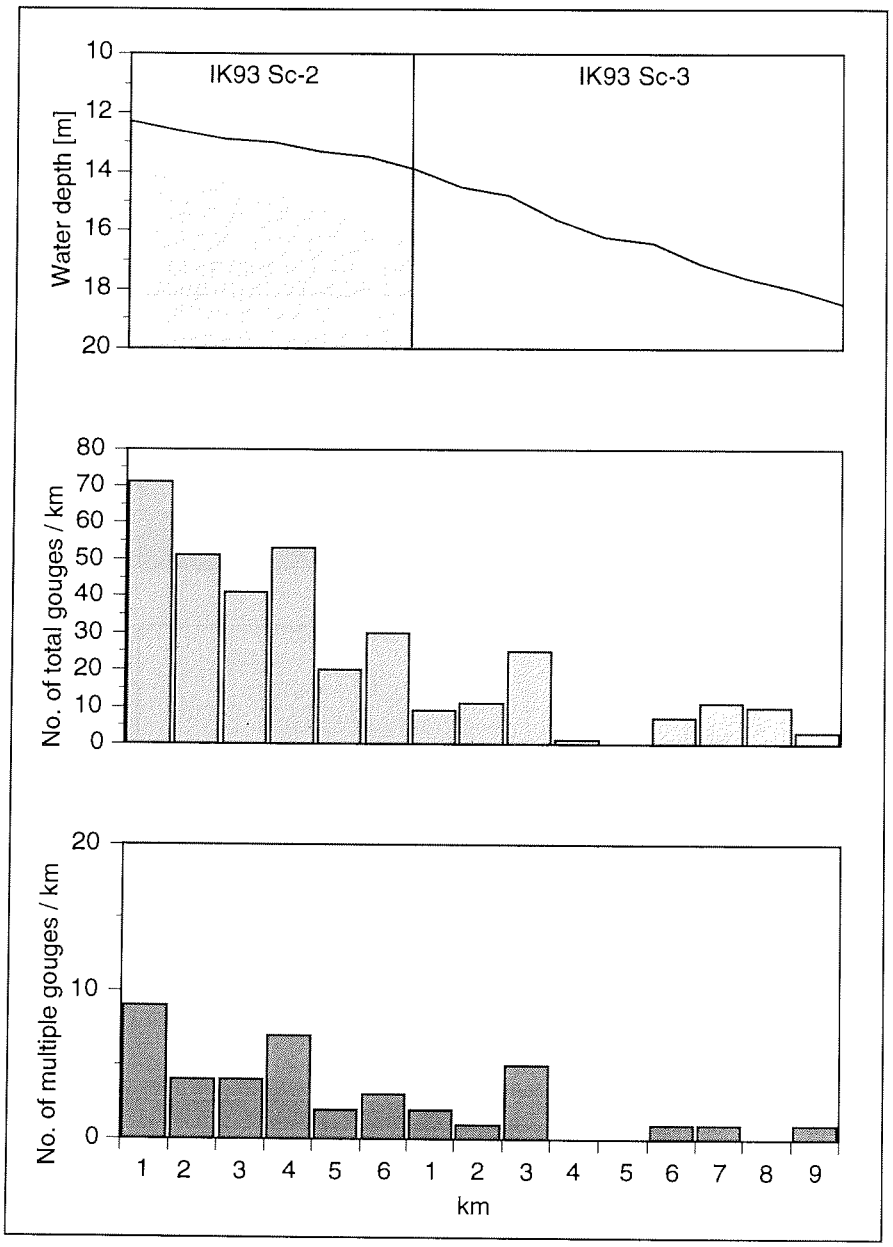

Fig. 3: Ice gouges distribution along side scan sonar transects IK93 Sc-2 and Sc-3.

Taimyr Massif east of Taimyr Peninsula. Along these coasts, icebergs, bergy bits and/or ice-pressure ridges are carried by current into the Laptev Sea were they run aground and thus reworking the sediment.

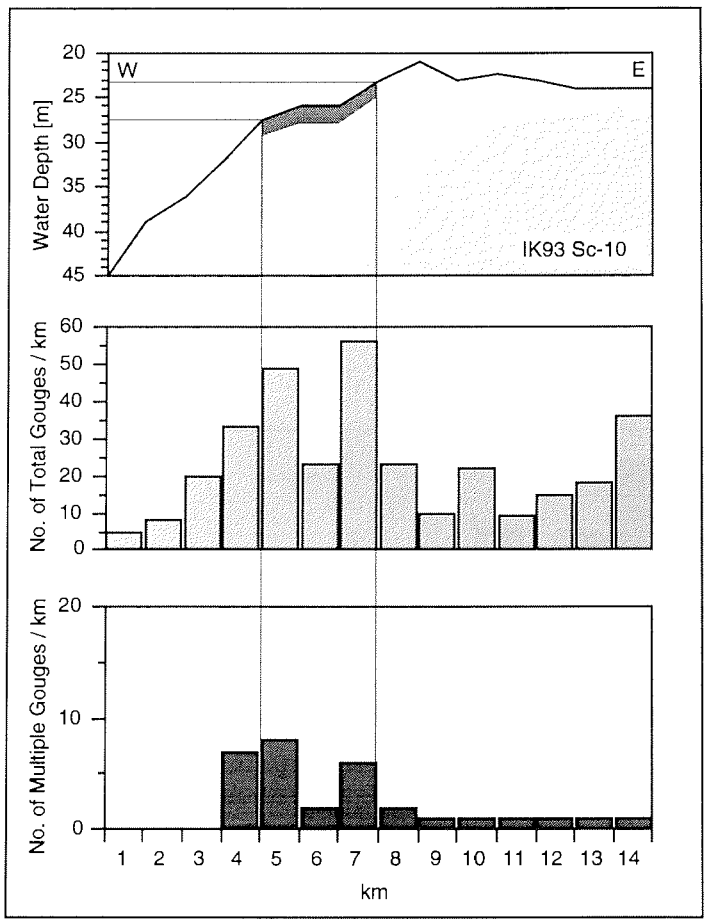

Fig. 4: Ice gouge distribution along side scan sonar transect IK93 Sc-10.

Conclusions

1. In the western Laptev Sea NW of the Lena Delta, ice gouges are strongly tied to water depth.
2. Ice gouges could be documented down to 42 m water depth.
3. At the western flank of Stolbovoy shoal, the dominant draught of the floating ice seems to be between 28 and 23 m water depth.
4. Grounded ice considerably influences sediment distribution patterns by re-working.

References

Barnes, P.W., Rearic, D.M., 1985. Rates of sediment disruption by sea ice as determined from characteristics of dated ice gouges created since 1975 on the inner shelf of the Beaufort Sea. Open-File Report, 85-473, United States Geological Survey.

Rearic, D.M., Barnes, P.W., Reimnitz, E., 1981. Ice-gouge Data, Beaufort Sea, Alaska, 1972-1980. Open-File Report, 81-950, United States Geological Survey.

Rearic, D.M., Barnes, P.W., Reimnitz, E., 1990. Bulldozing and resuspension of shallow-shelf sediment by ice keels: implications for Arctic sediment transport trajectories. Mar. Geol., 91: 133-147.

PRODUCTIVITY PROXIES: ORGANIC CARBON AND BIOGENIC OPAL IN SURFACE SEDIMENTS FROM THE LAPTEV SEA SHELF AND THE ADJACENT CONTINENTAL SLOPE

R. Stein and D. Nürnberg
Alfred-Wegener-Institut für Polar- und Meeresforschung Bremerhaven, Germany

Abstract

In order to understand modern processes controlling organic carbon deposition (i.e., primary productivity vs. terrigenous supply), surface sediments from the Laptev Sea shelf and its adjacent continental margin were investigated for their content and composition of organic carbon and biogenic opal.

Total organic carbon (TOC) values vary between 0.3 and 2.3 %. In general, areas of high TOC concentrations coincide with low hydrogen index (HI) values and high carbon/nitrogen (C/N) ratios indicating dominant proportions of terrigenous organic matter. Maximum organic carbon enrichment off the eastern Lena Delta is mainly controlled by a significant fluvial supply of terrigenous organic matter.

Opal concentrations within Laptev Sea shelf and continental slope sediments range from undetectable to ca. 6%, with high values typical for the eastern inner Laptev Sea shelf between the New Siberian Islands, the Lena Delta, and the mainland. An enhanced biological activity in the surface layer caused by high fluvial nutrient supply (dissolved silica) is reflected in the bottom sediments east of the Lena Delta with relatively high sedimentary opal concentrations of 3-6%. A second distinct opal maximum, which coincides with a significantly increased content of marine organic matter and elevated portions of biogenic barium, is observed in upper continental slope sediments in 500 - 1000 m water depth, probably related to phytoplankton blooms at the ice edge.

Introduction

The Arctic Ocean and its marginal seas are key areas for understanding the global climate system and its change through time (ARCSS Workshop Steering Committee, 1990; NAD Science Committee, 1992). The permanent Arctic sea-ice cover with its strong seasonal variations especially in the marginal zones strongly influences the earth's albedo, the marine ecosystem, and the oceanic circulation, which are all major mechanisms affecting the global climate. Despite the importance of the Arctic Ocean for the global climate system, its exploration remained relatively small up to now. Especially, the knowledge on spatial and temporal changes in marine productivity is still insufficient, though the global importance of the Arctic shelves for organic carbon storage is apparent.

In relation to the world's ocean, the Arctic Ocean is rather low-productive due to the permanent ice-cover (Subba Roa & Platt, 1984), however, regional differences occur. In marginal seas (such as the Laptev Sea) characterized by an increased fluvial nutrient supply, near ice edges, and at local/regional upwelling cells significantly raised primary production rates are expected. The mapping of sedimentological, geochemical and biological proxies reflecting surface water productivity in seafloor deposits, and the subsequent comparison to recent oceanographic and biological parameters will allow to decipher processes most important for primary production in the Arctic Ocean. In addition to marine organic carbon produced in the water column, the Lena River may supply major amounts of terrigenous organic matter into the Laptev Sea (Martin et al., 1993).

This study focusses on the identification of geochemical parameters reflecting marine productivity in the Laptev Sea shelf and slope. We attempt (i) to determine the amount of organic carbon, (ii) to characterize the mechanisms controlling organic carbon deposition (i.e., surface-water productivity vs. terrigenous input), (iii) to describe biogenic opal distribution patterns. First results of the investigation of surface sediments include total organic carbon contents, hydrogen index (HI) values, and carbon/nitrogen (C/N) ratios as well as biogenic opal data, as further proxy for primary productivity.

Methods

During RV *Polarstern* Cruise ARCTIC'93 (ARK-IX/4; Fütterer, 1994) and RV *Ivan Kireyey* Cruise Transdrift I (Kassens and Karpiy, 1994), surface sediments and long cores were recovered from the Laptev Sea shelf and slope (Fig. 1).

Total carbon, total nitrogen, and organic carbon contents were determined on both ground bulk samples and HCl-treated carbonate-free samples, using a HERAEUS CHN analyser. Carbonate contents were calculated as:

*(total carbon - total organic carbon) * 8.333.*

Rock-Eval pyrolysis was performed according to the method described by Espitalié et al. (1977). To obtain a preliminary estimation on the composition of the organic matter, hydrogen index (HI) values from Rock-Eval-pyrolysis and C/N ratios were determined. In immature sediments, hydrogen indices < 100 mgHC/gC are typical of terrigenous organic matter (kerogen type III), hydrogen indices of 300 to 800 mgHC/gC are typical of marine organic matter (kerogen types I and II) (e.g., Tissot and Welte, 1984). C/N ratios of marine organic matter are around 6, whereas terrigenous organic matter reveals C/N ratios of > 15 (e.g., Bordowskiy, 1965; Hedges et al. 1986). Furthermore, the temperature of maximum pyrolysis yield (T_{max}) is indicative for the stage of maturity of the organic matter. T_{max} values > 435°C suggest the presence of more mature reworked organic matter (Espitalié et al. (1977).

Biogenic silica (opal) in sediments was determined by applying an automated leaching method according to DeMaster (1981) and Müller and Schneider (1993). The opaline material was extracted from the dry and ground bulk sediment by concentrated NaOH (1M) at ca. 82 °C in a stainless vessel under constant stirring. The leaching solution was continously analyzed for dissolved silicon by molybdate-blue spectrophotometry. The corresponding absorbance versus time plot was subsequently assessed according to the extrapolation procedure of DeMaster (1981).

The calibration of the autoanalyzer is done by running silicon standard solutions. The reproducibility of about 0.5% was tested by running replicate measurements of samples and silicon standards.

Results

Amount and composition of organic carbon

Total organic carbon (TOC) values vary between 0.3 and 2.3 % (Fig. 2). Maximum TOC values occur in the vicinity of the eastern Lena Delta, off the Kotuy river mouth, southwest of the New Siberian Islands, and in the central part of the lower Laptev Sea continental slope. Areas of high TOC concentrations commonly correspond to low HI values (< 100 mgHC/gC) and high C/N ratios (> 7) indicating the dominance of terrigenous organic matter (Figs. 3 and 4). In the central part of

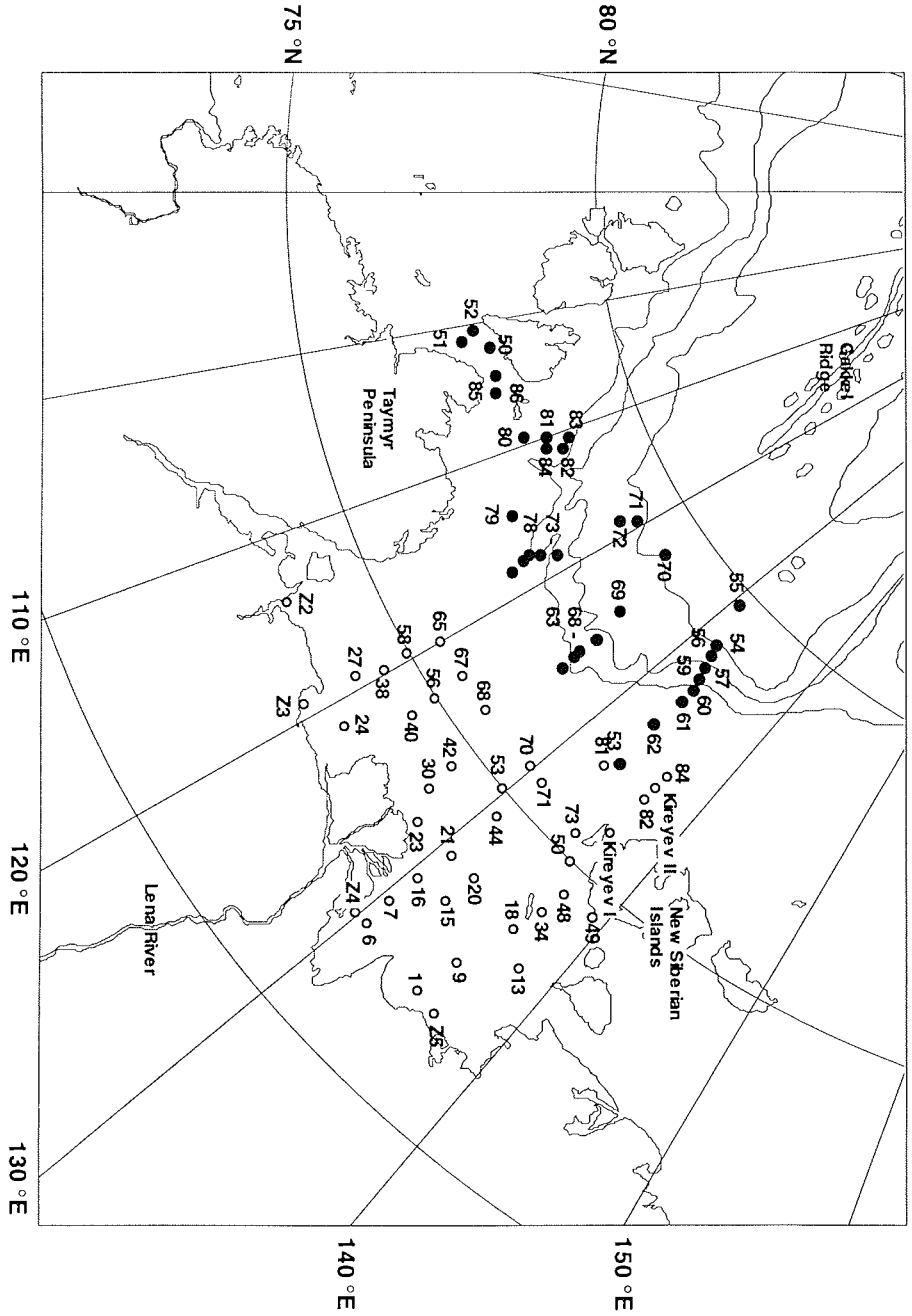

Fig. 1: Position of surface sediments taken during the 1993 RV *Polarstern* and RV *Kireev* cruises. Black dots indicate *Polarstern* samples (50 = PS2450, 51 = PS2451, etc.), open circles indicate *Kireev* samples (1 = IK9301, 6 = IK9306, etc.).

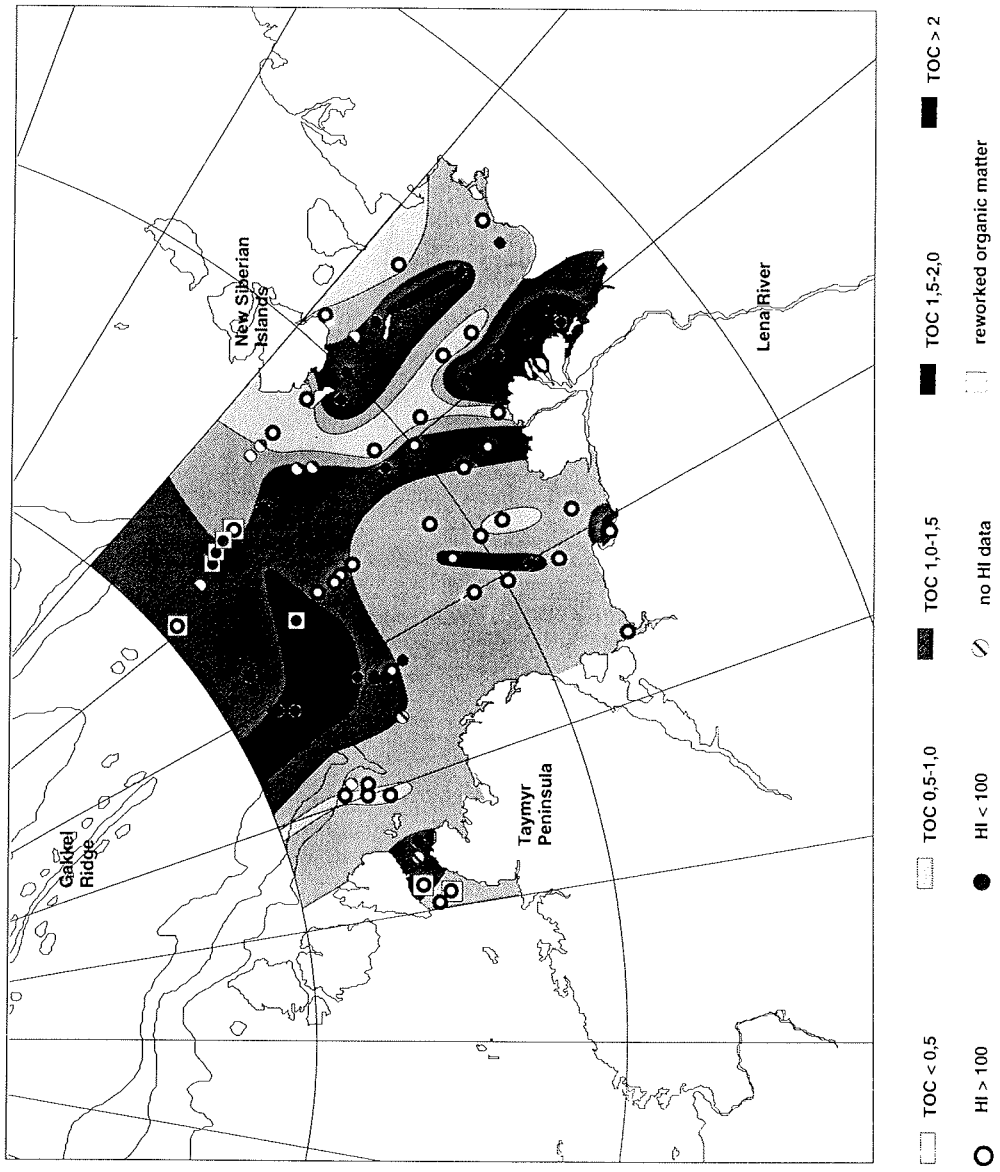

Fig. 2: Distribution map of total organic carbon content in Laptev Sea surface sediments. Open circles indicate samples with hydrogen indices > 100 mgHC/gC, black dots indicate hydrogen indices < 100 mgHC/gC. Open squares mark samples with Tmax values > 435°C, indicative for reworked organic matter (for details of Rock-Eval data see Stein, 1995).

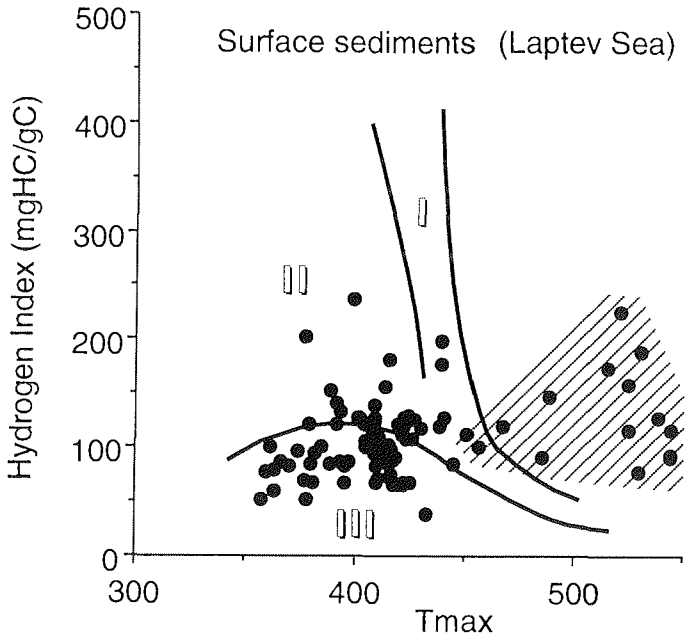

Fig. 3: Diagram of hydrogen index vs. T_{max} values. Roman numbers indicate kerogen types (fields I and II = marine organic carbon; field III = terrigenous organic carbon). Samples with T_{max} values >> 435°C (hatched area) suggest the presence of significant amounts of more mature reworked organic carbon (cf., Tissot and Welte, 1984).

the Laptev Sea and along the upper continental slope, in contrast, the hydrogen indices reach values > 100 mgHC/gC suggesting the presence of significant concentrations of marine organic matter. At the eastern most continental slope, increased temperatures of maximum pyrolysis yield (T_{max} values > 435°C) presumably indicate that most of the organic carbon is reworked (Fig. 4).

Biogenic silica (opal) in surface sediments

Opal concentrations within Laptev Sea shelf and continental slope sediments range from undetectable to ca. 6% (Fig. 5). The eastern inner Laptev Sea shelf between the New Siberian Islands, the Lena Delta and the mainland exhibits opal concentrations > 3%. North and west of this area, opal concentrations diminish to 0-2% being characteristic for the inner western Laptev Sea shelf. The outer shelf and continental slope areas as well as the Strait of Vilkitzky, which are permanently influenced by sea ice, exhibit medium concentrations of 2-3%. In the direct vicinity of the summer '93 ice edge, opal concentrations are enhanced to 3-5% (Stations PS2458, PS2459, and PS2466) in upper slope sediments.

Discussion

Proxies for primary productivity

The mapping of geochemical and biological proxies reflecting the surface-water

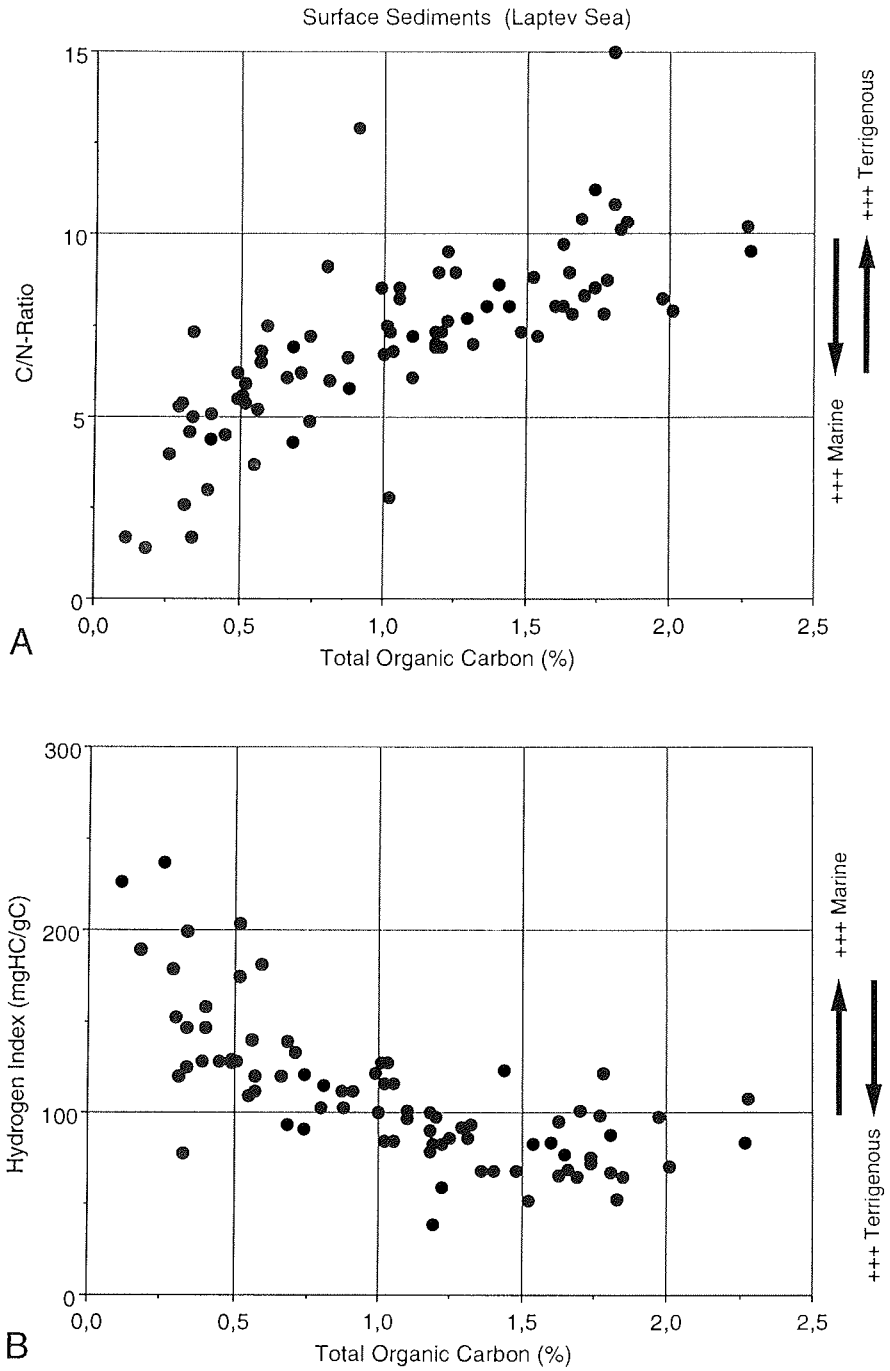

Fig. 4: A. Total organic carbon contents vs. C/N ratios; B. Total organic carbon contents vs. hydrogen index values. Highest TOC values correspond to low hydrogen index values and high C/N ratios, respectively, indicating an increased presence of terrigenous organic matter.

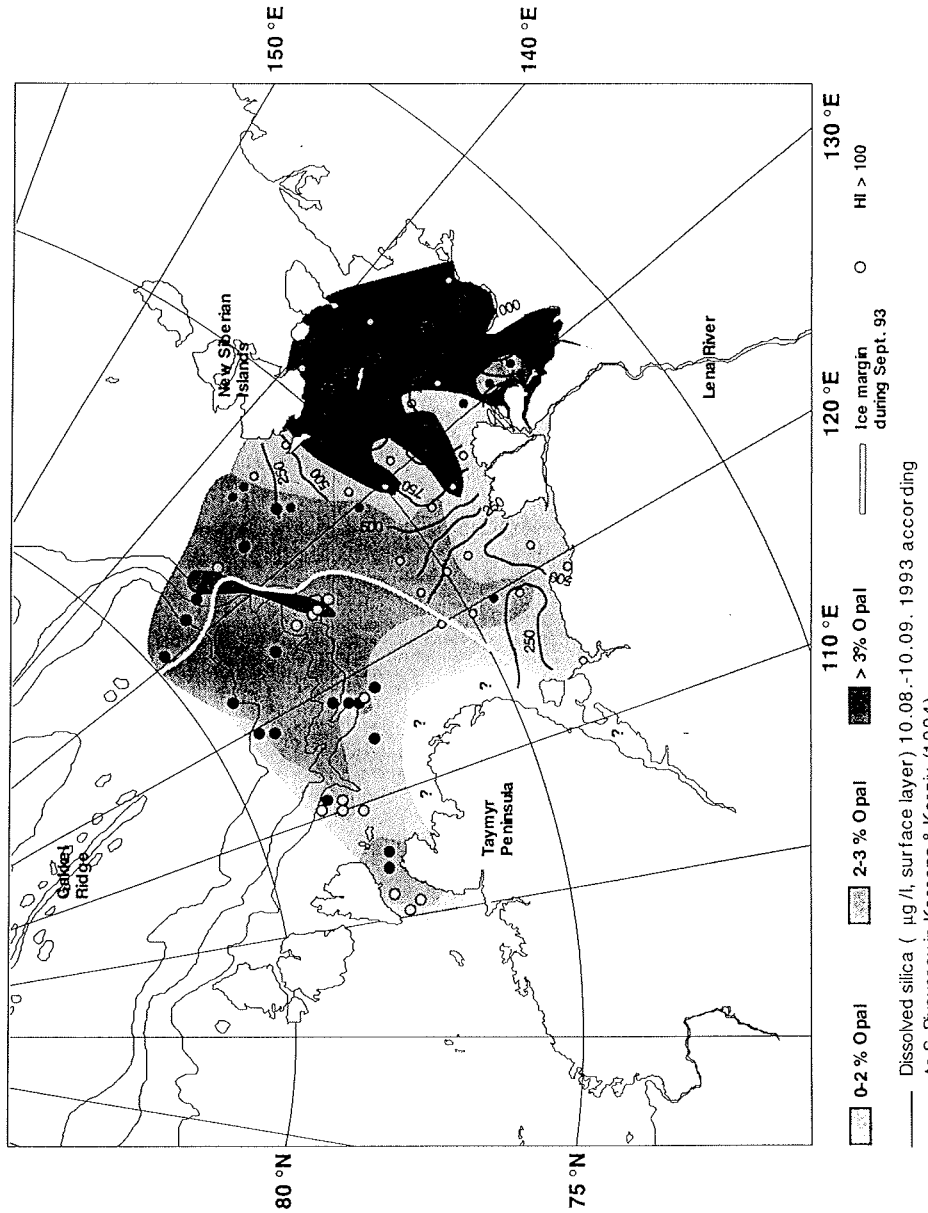

Fig. 5: Distribution map of biogenic opal in surface sediments. Open circles indicate samples with hydrogen index values > 100mgHC/gC (cf. Figure 2); dissolved silica values in surface waters from S. Pivovarov (in Kassens and Karpiy, 1994).

productivity in surface sediments, and the subsequent comparison to recent oceanographic and biological parameters will allow to decipher processes most important for the primary productivity in the Arctic Ocean.

The marine organic carbon flux is mainly controlled by primary productivity and sedimentation rate (e.g., Müller and Suess, 1979; Berger et al., 1989; Stein, 1991). High productivity environments such as upwelling areas with values of > 250 $gC/m^2/y$ are characterized by flux rates of > 1 $gC/cm^2/ky$, whereas open-ocean environments with productivity values of about 50 $gC/m^2/y$ display flux rates of about 0.005 gC/cm2/ky (Stein, 1991 and further references therein). At the ice edge, primary productivity values may also be significantly increased (e.g., Sakshaug and Holm-Hansen, 1984; Nelson et al., 1989). Thus, increased accumulation of marine organic matter may indicate enhanced primary productivity.

Biogenic opal is also commonly used as a proxy for surface water productivity (e.g. Mortlock and Froelich, 1989). The presence of siliceous sponge spicules, however, may significantly falsify the opal concentrations erroneously indicating an enhanced surface water productivity. Visual and microscopic investigations of the Laptev Sea surface sediments reveal that benthic siliceous sponges are of minor importance in the Laptev Sea (Fütterer, 1994). At only 7 sites, solitaire sponges were observed. The opal concentrations therefore, are exclusively related to the presence of siliceous plankton.

Because factors controlling the opal concentration in sedimentary deposits comprise surface water productivity, regional variations in solubility, dissolution kinetics of opal raining to the seafloor and finally, preservation within the sediments (Archer et al., 1993), the interpretation of downcore opal concentrations in terms of changes in opal production can only be done with great caution. However, high accumulation rates generally favor an enhanced opal preservation in the sediments (e.g., Bohrmann, 1986).

The sedimentary environment of the Laptev Sea shelf is characterized by comparatively high bulk sedimentation rates of about 50 cm/1000yrs (Nürnberg et al., in press). These rates correspond to ca. 40 cm/1000 yrs calculated from a radiometrically dated sediment core from the Laptev Sea shelf edge (Kassens, pers. comm.), which is presumably caused by a strong lateral transport of debris on the shelf in off-shore direction, decreases successively downslope as indicated by wedging-out of undisturbed sediment layers, slumps, and fan deposits on the lower slope (Nürnberg et al., in press). In such an enviroment, the preservation of opal is expected to largely exceed dissolution and therefore, allowing productivity reconstructions even from downcore opal records.

River discharge controlling the primary productivity and the flux of terrigenous organic matter

The Lena river run-off is of considerable importance for the hydrochemical and depositional structure in the Laptev Sea. The large brackish surface plume extends up to 200 miles or more northward (Létolle et al., 1993). Thereby, approximately 84% of the total outflow is directed to the east and northeast. According to Pivovarov (in Kassens and Karpiy, 1994), the influence of freshwater supply to the Laptev Sea is reflected in the distribution pattern of dissolved silica in the surface water layer (ca. 5-10 m water depth). Maximum concentrations of about 1400 µg/l were observed near the eastern side of the Lena river mouth during summer 1993, indicating a predominant outflow to the east (Fig. 5). Concentrations gradually decrease with increasing distance from the delta. The Lena river, thus, serves as the major source of dissolved silica in the Laptev Sea (Sidorov, 1993). The fact that i) diatoms represent more than 95% of the total biomass near the mouth of the Lena

river (Sidorov, 1993) and ii) bottom waters are always enriched in dissolved silica (Létolle et al., 1993) most probably indicate that the surface depletion results from biological uptake. An enhanced biological activity in the surface layer is definitely reflected in the bottom sediments east of the Lena Delta with relatively high sedimentary opal concentrations of 3-6% (Fig. 5). The diminishing dissolved silica concentrations to the north and to the west result in correspondingly low opal concentrations in the bottom sediments.

The distinct organic carbon enrichment off the eastern Lena Delta is mainly controlled by increased supply of terrigenous organic matter as indicated by low hydrogen index values and high C/N ratios. This terrigenous signal probably superimposes the expected marine organic carbon (high-productivity) signal. Detailed biomarker data from these sediments will help to identify the productivity signal controlled by fluvial nutrient supply (Fahl and Stein, in prep.).

Ice-edge effects controlling primary productivity

A distinct opal maximum of about 3-5% is observed in upper continental slope sediments in 500 - 1000 m water depth (Stations PS2458, PS2459, and PS2466). At the same stations, hydrogen indices are > 100 mgHC/gC suggesting some increased amounts of marine organic matter (Fig. 5). These sites are situated directly below the ice edge, which is relatively stable during summer over years as inferred from satellite imagery (H. Eicken, pers. com. 1995). Surface waters overlying these sites showed drastically enhanced chlorophyll A and phaeopigment concentrations during summer 1993, whereas nutrients (NO_3, PO_4) are significantly depleted (Boetius and Nöthig, in prep.) indicating a plankton bloom at the ice edge. Due to the relatively stable position of the ice edge during summer, repeated plankton blooms are apparently providing enough biogenic silica and marine organic matter to be reflected in the surface sediments.

Biogenic barium as an alternative proxy for marine surface water productivity (Stroobants et al., 1991; Dehairs et al, 1992; Dymond and others, 1992; Gingele and Dahmke, 1994; Nürnberg, 1995) is also enhanced in these surface sediments. Applying a detrital Ba/Al ratio of 0.0065 (Wedepohl, 1991) for the calculation of biogenic barium (Dymond et al, 1992), concentrations increase to about 300 ppm, representing the highest Babio occurrences in the Laptev Sea area at all (Nürnberg et al., in prep.). The covariance between opal and biogenic barium in addition to the resemblance of these parameters to the HI indices thus, indicates i) the reflectance of plankton blooms in the seafloor deposits by geochemical proxies and ii) the relatively permanent summer position of the ice edge. Mapping these parameters should subsequently allow the spatial and temporal reconstruction of the changing ice edge position.

Acknowledgements

We thank Martina Siebold and Michael Seebeck for technical assistence. The financial support by the Ministry for Education, Science, Research, and Technology (BMBF) is gratefully acknowledged.

References

Archer, D., Lyle, M., Rodgers, K., and Froelich, P., 1993. What controls opal preservation in tropical deep-sea sediments? Paleoceanography, 8/1: 7-21.

ARCSS Workshop Steering Committee, 1990. Arctic System Science: Ocean-Atmosphere-Ice Interactions. Lake Arrowhead Workshop Report, JOI Inc., Washington DC, 132 pp.

Berger, W.H., Smetacek, V., and Wefer, G., 1989. Productivity of the Ocean: Past and Present. Life Sciences Research Report, Vol. 44, Wiley & Sons, New York, 471p.

Bohrmann, G., 1986. Accumulation of biogenic silica and opal dissolution in upper Quaternary Skagerrak sediments. Geo-Marine Letters, 6: 165-172.

Bordowskiy, O.K., 1965. Sources of organic matter in marine basins. Mar. Geol., 3, p. 5-31.

Dehairs, F., Baeyens, W., and Goeyens, L., 1992. Accumulation of suspended barite at mesopelagic depths and export production in the Southern Ocean. Science, 258: 1332-1335.

DeMaster, D.J., 1981. The supply and accumulation of silica in the marine environment. Geochim. Cosmochim. Acta, 45: 1715-1732.

Dymond, J., Suess, E., and Lyle, M., 1992. Barium in deep sea sediment: A geochemical indicator of paleoproductivity. Paleoceanogr., 7 (2. 163-181.

Espitalié, J., Laporte, J.L., Madec, M., Marquis, F., Leplat, P., Paulet, J., and Boutefeu, A., 1977. Méthode rapide de characterisation des roches-mere, de leur potential petrolier et de leur degre d´évolution. Rev. Inst. Tranc. Petrol., 32, p. 23-42.

Fütterer, D.K. (ed.), 1994: The Expedition ARCTIC´93 Leg ARK IX/4 of RV "Polarstern" 1993. Ber. Polarforsch., 149/94, 244 pp.

Gingele, F., and Dahmke, A., 1994. Discrete barite particles and barium as tracers of paleoproductivity in South Atlantic sediments. Paleoceanogr., 9 (1. 151-168.

Kassens, H., and Karpiy, V.Y., 1994. Russian-German Cooperation: The Transdrift I Expedition to the Laptev Sea. Ber. Polarforsch., 151/94, 168 pp.

Létolle, R., Martin, J.M., Thomas, A.J., Gordeev, V.V., Gusarova, S., and Sidorov, I.S., 1993. 18O abundance and dissolved silica in the Lena delta and Laptev Sea (Russia). Marine Chemistry, 43: 47-64.

Martin, J.M., Guan, D.M., Elbaz-Poulichet, F., Thomas, A.J., and Gordeev, V.V., 1993. Preliminary assessment of the distributions of some trace elements (As, Cd, Cu, Fe, Ni, Pb and Zn) in a pristine aquatic environment: the Lena River estuary (Russia). Marine Chemistry, Vol. 43, 185-199.

Mortlock, M.A., and Froelich, P.N., 1989. A simple method for the rapid determination of biogenic opal in pelagic marine sediments. Deep-Sea Research, 36:1415-1426.

Müller, P.J. and Suess, E., 1979. Productivity, sedimentation rate, and sedimentary organic matter in the oceans. I.- Organic matter preservation. Deep-Sea Res., Vol. 26, p. 1347-1362.

Müller, P.J., and Schneider, R., 1993. An automated leaching method for the determination of opal in sediments and particulate matter. Deep-Sea Research I, 40/3: 425-444.

NAD Science Committee, 1992. The Arctic ocean record: Key to global Change (Initial Science Plan of the Nansen Arctic Drilling Program). Polarforschung, 61, 1-102.

Nelson, D.M., Smith, W.O., Muench, R.D., Gordon, L.I., Sullivan, C.W., and Husby, D.M., 1989. Particulate matter and nutrient distribution in the ice-edge zone of the Weddell Sea: relationship to hydrography during late summer. Deep-Sea Res., Vol. 36, p. 191-209.

Nürnberg, C.C., 1995. Bariumfluß und Sedimentation im südlichen Südatlantik - Hinweise auf Produktivitätsänderungen im Quartär. Unpubl. Ph.D. thesis, Univ.

of Kiel.

Nürnberg, D., Fütterer, D.K., Niessen, F., Nørgaard-Petersen, N., Schubert, C.J., Spielhagen, R.F., and Wahsner, M., submitted. The depositional environment of the Laptev Sea continental slope. Polar Research.

Nürnberg, D., Schubert, C.J., and Stein, R., in prep. Biogenic barium and opal in Arctic Ocean sediments - Do they reflect paleoproductivity? Earth Planetary Science Letters.

Sakshaug, E. and Holm-Hansen, O., 1984. Factors Governing Pelagic Production in Polar Oceans. In: Holm-Hansen, O., et al. (Eds.), Marine Phytoplankton and Productivity, Lect. Notes Coast. Est. Studies, Vol. 8, p. 1-17.

Sidorov, I.S., 1993. Dissolved silica in the coastal waters of the Laptev Sea. in preparation.

Stein, R., 1991. Accumulation of organic carbon in marine sediments : Lecture Notes in Earth Sciences 34. Springer, Heidelberg, 217 pp.

Stein, R., 1995. Organic carbon in surface sediments from the eastern central Arctic Ocean and the Eurasian Continental Margin: Sources and pathways. In: Surface-sediment composition and sedimentary processes in the central Arctic Ocean and along the Eurasian Continental Margin (Eds. R. Stein, G. Ivanov, and M. Levitan), Reports on Polar Research, subm.

Stroobants, N., Dehairs, F., Goeyens, L., Vanderheijden, N., and Van Grieken, R., 1991. Barite formation in the Southern Ocean water column. Mar. Chem., 35: 411-421.

Subba Rao, D.V. and Platt, T., 1984. Primary Production of Arctic Waters. Polar Biol., 3, p. 191-201.

Tissot, B.P. and Welte, D.H., 1984. Petroleum Formation and Occurrence. Springer Verlag Heidelberg, 699 p..

Wedepohl, K.H., 1991. The composition of the upper earth`s crust in the natural cycles of selected metals. - Metals in natural raw materials. In: Merian, E. (ed.), Metals and their compounds in the environment. VCH Verlagsgesellschaft, Weinheim.

TRANSPORT AND DISTRIBUTION OF TRACE ELEMENTS IN THE LAPTEV SEA: FIRST RESULTS OF THE TRANSDRIFT EXPEDITIONS

J. A. Hölemann°, M. Schirmacher*, A. Prange* and TRANSDRIFT Shipboard Scientific Party

° GEOMAR Forschungszentrum für marine Geowissenschaften, Kiel, Germany

* GKSS Forschungszentrum Geesthacht, Germany

Introduction

The large Siberian river systems carry huge amounts of dissolved and particulate trace elements to the Siberian shelf seas and the Arctic Ocean. Up to now only little is known about the biogeochemical cycling of these elements in the Arctic shelf seas.

Weathering, erosion and anthropogenic input are the major sources of particulate and dissolved trace elements entering the Laptev Sea with the fresh water outflow of the Lena, Khatanga, Yana and other rivers. Beside these point sources, the diffuse input via atmospheric transport, the influence of pore water diffusion into the water column and the admixture of ocean water masses control the trace element distribution in the waters of the Laptev Sea. If looking at the pathways and depositional sites of trace elements including heavy metals within the Arctic shelf seas, a specific feature of these regions has to be taken into account. What is so special about these regions is the complex geochemical processes during the formation of new ice wich are for the most part unknown. Within the frame of the project "System Laptev See" it is planned to study the sources, pathways and sinks of trace elements during different seasons. The focus will be the study of processes leading to the incorporation of trace elements into ice and the enrichment/depletion of trace elements in the water column during sea ice formation. These investigations give a key for the interpretation of geochemical tracers in the water masses and pack ice of the Arctic Ocean. Nevertheless, the base for these ice related studies are detailed investigations of the trace element cycling in the ice free season in the Laptev Sea.

During the summer/early autumn expeditions TRANSDRIFT I and II there were collected sediment, suspended matter and water samples for trace and major element analysis at more than 50 stations covering almost every region in the Laptev Sea. Detailed sampling was carried out near the river mouthes of the Khatanga, Anabar, Olenek, Yana and especially the Lena (TRANSDRIFT II). Here we will present the first, preliminary results of a work still in progress.

Material and Methods

Sediment samples (upper 2 cm), suspended matter and water samples were taken for the analysis of their major and trace element composition. During TRANSDRIFT II, additional suspended particulate matter samples were taken at about 50 sites in order to the determination of suspended particulate matter concentration (SPM), particulate organic carbon (POC). These analyses will be completed by scanning electron microscopy (SEM) observations combined with electron dispersive analysis of X-rays (EDAX). This sampling programme was complemented by 30 water samples taken near the mouth of the river Lena for the analysis of dissolved organic carbon (DOC).

At all sampling locations water samples were taken 2m below sea surface and 5m above the ground. Surface sediment samples were taken from the undisturbed

upper two centimeters of sediment from a spade box core. To reduce grain size effects in the sediment samples, only the fraction smaller than 20 µm was analysed.

Water samples for trace element analysis were taken using Teflon water samplers (Hydro-Bios) with 2l pre-cleaned polyehylene (surface sample) and two 0.5l pre-cleaned teflon bottles (bottom sample) hung on a plastic coated hydrowire. Sampling was carried out from the bow of the research vessel. Sea water was filtered through acid pre-treated 0,45µm Nuclepore filters to collect particulate matter. For that purpose, a pressure filtration (Nitrogen 5.0) in a transportable clean room laboratory (clean bench) was used. Filters were stored frozen for subsequent analysis while the filtrate was acidified.

Final analysis was performed at the Research Center Geesthacht including salt-matrix seperation and pre-concentration of the water samples followed by analysis with Total Reflection X-Ray Fluorescence (TXRF). Measurements using Atomic Absorption Spectroscopy (AAS) and Inductively Coupled Plasma Mass Spectrometrie (ICP-MS) complete these investigations. Elements measured in sea water include V, Mn, Fe, Ni, Cu, Zn, Se, Mo, Cd, U and Pb. In the sediments (< 20 µm fraction) and the suspended particulate matter, about 30 elements including the REE can be measured.

SPM, POC measurements and scanning electron microscopy in combination with EDAX was carried out at GEOMAR in Kiel. Determination of DOC was performed by A. Reimers at the Institute of Biogeochemistry and Marine Chemistry in Hamburg.

Concentration of Suspended Matter

A great number of trace elements are highly reactive and have a strong affinity for association with fine grained particles. The movement of these reactive elements, their removal from the water, and their accumulation in the sediment are thus governed to a great extent by sedimentary processes. The dynamics of fine-grained particles in coastal marine environments are extremly complex especially in estuarine zones where fresh water mixes with sea water.

During the Transdrift II Expedition samples of suspended particulate matter (SPM) were taken at 47 locations 2m below sea surface and 5m above the seafloor. The distribution pattern of SPM in the eastern Laptev Sea is given in Figures 1 and 2. The most important source of SPM in the surface and bottom water in this region is the fluvial input through the different branches of the Lena river delta. Highest fresh water discharge (57% of total discharge) was recorded at the Trofimovskaya branch at the north eastern part of the Lena delta (Létolle et al. 1993). The Bykovskaya branch (27%) north of Tiksi and the Tumatskaya branch (9%) in the northern part of the delta are also important outlets of the Lena. Concentration of SPM near the mouthes of these branches runs to maximum values of 9 mg/l in surface and 13 mg/l in bottom water (20 nautical miles east of the Trofimovskaya outlet). Nevertheless, the Tumatskaya branch is only of minor importance concerning the water discharge. It appears to be a major source for the input of suspended matter. A characteristic feature is a SPM maximum in the bottom water that can be followed north as far as 75° N (Fig. 2). This area of higher SPM loads in bottom and also in surface water branches into in two different maxima. This correlates with the salinity and silica distribution pattern in this area indicating a split of the fresh water outflow into to seperate branches (Pivovarov, this volume) caused by a shoal north of the delta. Areas of high SPM concentration in the surface water find their exact counterpartalso in the more saline bottom waters. Earlyer studies underline the imortance of the strong halocline as a barrier for suspended particles settling out from freshwater. Our data point to a less

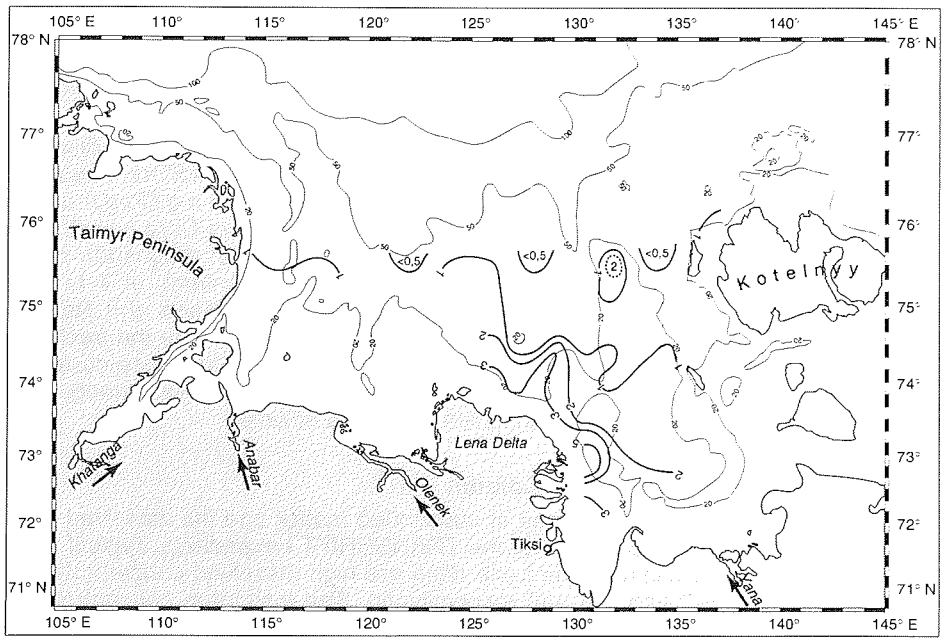

Fig.1: Suspended particulate material (SPM, mg/l) 2 m below sea surface, TRANSDRIFT II - September 1994.

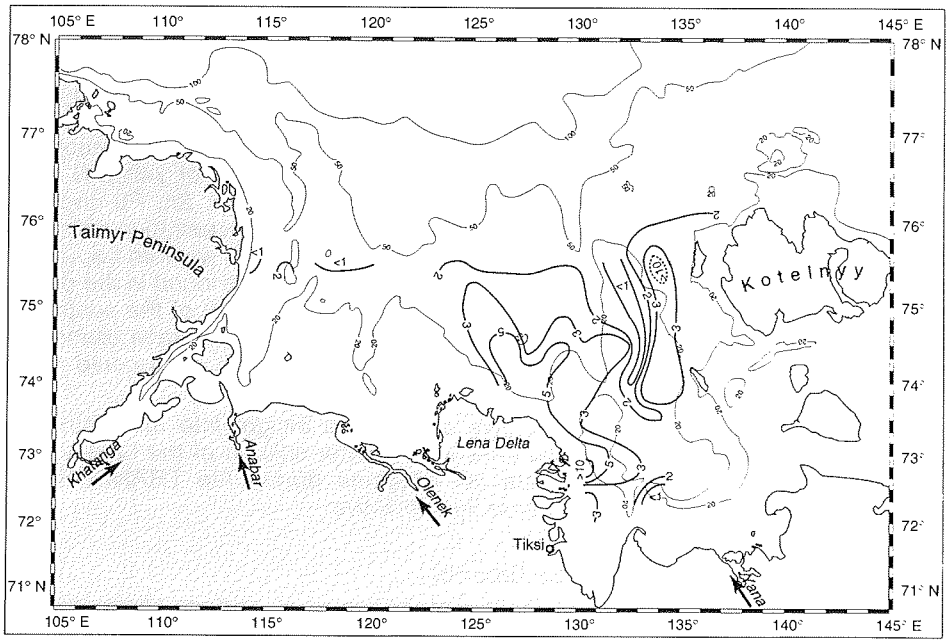

Fig. 2: Suspended particulate material (SPM, mg/l) 5 m above seafloor, TRANSDRIFT II - SEPTEMBER 1994.

significant influence of the strong halocline on the sedimentation of lithogenic particles. This is also supported by hydro-optical studies wich did not show turbidity maxima near the halocline caused by lithogenic particles (Anoshkin et al., this volume). Only the increase of in-situ fluorescence points to a higher concentration of phytoplankton near the halocline (Anoshkin et al., this volume).

The distribution patterns of particulate organic carbon (POC) and dissolved organic carbon (DOC) show uniform values in water bodys with different salinities. Typical for surface water are POC concentrations between 0,15 mg Corg./l and 0,2 mg Corg./l. Bottom water values are only slightly lower (0,1 mg Corg./l to 0,15 mg Corg./l). The pool of dissolved organic carbon is one order of magnitude higher. The south-eastern Laptev Sea is charakterized by DOC contents of 4 to 5 mg Corg./l in surface and 2 mg Corg./l in bottom waters (Hölemann and Reimers, unpubl. data). These high concentrations are directly connected with the freshwater input of the Lena. Furthermore, the hydro-optical studies show the close correlation between fresh water input and high amounts of dissolved organic substances in the surface waters of the Laptev Sea (Anoshkin et al., this volume).

Trace Elements in the Water Column

Until now, trace element analyses of suspended matter and the dissolved phase of surface water are only available for the TRANSDRIFT I expedition. Typical for the low salinity surface water near the Lena delta are high dissolved concentrations of Fe and Mn (> 60 µg/l and > 8 µg/l respectilvely). The maximum concentration of dissolved Fe (> 150 µg/l) was found near the mouth of the river Yana. Higher concentrations of dissolved Ni, Cu, and Zn are also directly connected with the fresh water discharge of the rivers. In contrast, elements like U and Mo and Cd show highest concentrations in more saline surface waters. A well studied phenomena is, for example, the very close correlation between salinity and Mo.

First results indicate that no significant exchange processes between trace elements in the dissolved and particulate phase can be found in the mixing zone of river and sea water. This coincides with earlier investigations by J.M. Martin et al. (1993). Apparently, Fe and Mn are only slowly transfered from the dissolved to the particulate phase. This could be one of the reasons why maximum concentration of Fe and Mn in suspended matter were found mainly north of 74°30´N in the northern part of the Laptev Sea. Highest concentrations of Ni, Zn, Pb and Cr in SPM were also usually found in the northern Laptev Sea. Concentration maxima in the coastal zone were recorded for Cu and As. The SPM in the western Laptev Sea is characterized by higher V contents (> 140 mg/kg) than those found in the eastern part (around 120 mg/kg). High contents of Ti and K are typical of the suspended matter near all major river mouthes. The overall concentration of trace elements is closed to natural background values. A strong anthropogenic input could not be observed in the so far analyzed samples.

The results presented here can give only a first insight into the distribution patterns and pathways of trace elements in the water column of the Laptev Sea. The interpretation of the large data set obtained during the TRANSDRIFT II expedition will be a further step towards this objective.

Trace Elements in Surface Sediments

The evaluation of the trace element composition of 40 surface sediments from different areas of the Laptev Sea and the review of already published data (Van Dalen & Nolting, 1992; Yakolev, this volume) points to three factors mainly influencing the concentration and distribution of different trace elements in the

uppermost sediment section: 1) The discharge of particle associated trace elements by the major river systems. 2) Suboxic conditions established very near to the water-sediment interface in most of the analyzed cores. 3) The sediment reworking by ice in the more shallow parts of the Laptev Sea (Lindemann & Kassens, this volume).

Maxima in the concentration of Zn (> 110 µg/g), Ni (> 50 µg/g) and Mn (> 1000 µg/g) are typical for surface sediment within the old, deep river valleys on the shelf. According to results of the sedimentological investigations these troughs (Lindemann, 1994) are the depositional centers for fine-grained sediments of fluvial discharge.

Suboxic to anoxic porewater conditions close to the sediment/water interface can be found in most parts of the Laptev Sea especially in the river valleys (van Dalen & Nolting, 1992; Kassens et al., 1994). In winter, most parts of the south eastern Laptev Sea are covered by fast ice. During this season anoxic conditions with presence of H_2S in the water column are characteristic for the Buor Khaya Bay east of the Lena delta (Pivovarov, this volume). This leads to an accumulation of elements like Fe, Mn, V, As, Ni, Co and Mo in the uppermost oxic sediment layer and probably also to a diffusion of Mn and other elements into the water column. As evidence for this process,authigenic iron/manganese crusts covering worm tubes, bivalve shells and dropstones could be found in some river valleys, but first and foremost in the northern Laptev Sea (north of 74°30´N) (Kassens et al, 1994; Yakolev, this volume). The trace element analysis of these crusts shows an up to tenfold enrichment of Fe, Mn, As, Co, Mo, V, Ni, Cu and sometimes Cd, compared to the surrounding sediment. Elements like Pb and Zn are not effected. Most typical for these crusts are As contents up to 500 µg/g. Several reasons have to be considered if one tries to explain why these crusts are mainly found in the northern, more deep parts of the Laptev Sea shelf. One important reason is probably the strong sediment reworking by ice in the shallow parts of the Laptev Sea. Ice keels may even bring deeper anoxic sediments to the oxic surface. Strong resuspension and the oxidation of metal sulfides connected with a strong increase of metals in the dissolved form would be the effect of this "bulldozing". Enrichment of Fe and especially Mn in the oxic surface sediments due to pore water diffusion and the subsequent resuspension of Mn-enriched fine-grained surface sediments was first proposed by Nolting et al. (in press) based on results of the SPASIBA expeditions. This is confirmed by Mn concentrations in SPM of more than 5000 µg/g and Fe concentrations in excess of 5% are commonly found, and the ratio of Mn to Fe increases in the northward direction. Comigration of As and V with Mn and Fe leads also to a high enrichment of these elements in the crusts.

Acknowledgements

The authors would like to thank Stephanie Schultz and Christopher Strobl for sampling support during the TRANSDRIFT II Expedition. We are grateful to Andreas Reimer for the DOC analysis. The BMBF is acknowledged for the financial support (grant no. 525-4003-0G0517A).

References

Martin, J. M., D. M. Guan, F. Elbaz-Poulichet, A. J. Thomas & V. V. Gordeev, 1993. Preliminary assessment of the distributions of some trace elements (As, Cd, Cu, Fe, Ni, Pb and Zn) in a pristine aquatic environment: the Lena River estuary (Russia). - Mar. Chem. 43, : 185-199.

van Dalen, M. & R. F. Nolting, 1992. Spoor- en hoofdelementen in sediment en

poriewater van het Lena-esuarium en den Laptevzee. NIOZ Data-Report 1992-5: 1-79

Kassens, H., V. Karpiy & Shipboard Scientific Party, 1994. Cruise report of the Expedition TRANSDRIFT I in the Laptev-Sea. - Ber. Polarforsch., 151: 1-168.

Letolle, R., J. M. Martin, A. J. Thomas, V. V. Gordeev, S. Gusarova & I. S. Sidorov, 1993. 18-O abundance and dissolved silicate in the Lena delta and Laptev Sea (Russia). Mar. Chem., 43: 47-64.

Nolting, R. F., M. van Dalen & W. Helder, in press. Trace and major elements in pore waters of the Lena delta and Laptev Sea. Mar. Chem.

MINERALOGICAL AND SEDIMENTOLOGICAL CHARACTERIZATION OF SURFACE SEDIMENTS FROM THE LAPTEV SEA

M. Wahsner
Alfred-Wegener-Institut für Polar- und Meeresforschung, Bremerhaven, Germany

Abstract

Sedimentation in the Eurasian part of the Arctic Ocean is characterized by high input of terrigenous material derived from the surrounded land masses and supplied by big river systems. Because of the permanent ice cover, productivity is relatively low in comparison to other ocean regions. Only along ice edges and in the areas, which are ice free during summer months, sometimes higher productivities occur. Therefore, the sediments in the Arctic Ocean mainly show a terrigenous composition, and biogenic particles only occur in minor amounts. This means, that mineralogical investigations on these sediments are very useful and necessary to characterize the sedimentary processes, the terrigenous supply and the composition of sediments and to identify different provinces and source areas of the terrigenous material. The investigations discussed in this article are closely connected to mineralogical investigations of surface sediments from the inner shelf (GEOMAR, Kiel; Uni Freiberg) and from bottom sediments and suspension material of the Lena River (AWI, Potsdam).

The clay-mineral distribution in the Laptev Sea reflects the supply from different source areas. In the western part exists a stronger input from the Kara Sea and and from the Khatanga River. The eastern part is more influenced from the East Siberian Sea and from the Lena River. The distribution of the clay particles depends on bottom morphological features of the shelf, characterized by ancient river channels and very shallow plateaus, and follows oceanographic conditions in the water column and on the sea surface. The influence of sea-ice and ice-berg transport on sedimentation processes is reflected in the grain-size distribution of the surface sediments. Because of the changing ice cover, it is necessary to distinguish between winter and summer conditions, and, looking into the past, between strong oceanographic variations during glacial and interglacial times on this shallow Laptev Sea shelf.

Introduction

The Eurasian part of the Arctic Ocean is surrounded by broad and shallow shelf seas which are supplied with a high amount of fresh water and fluviatil sediment material by various large Russian river systems. The sediment supply from the Eurasian continent to the marine system and its transfer from the shelf to the deep sea is one main argument for the investigations concerning the terrigenous sediment supply to the ocean. Controlling factors for particle supply, transportation, and accumulation are the amount of river discharge, the sea-ice distribution, ice-berg occurence, ocean currents, downslope gravitational transport, and, of minor importance, the aolian supply.

The sedimentary Environment of the Laptev Sea

The Laptev Sea is one of five marginal seas bordering the Eurasian part of the Arctic Ocean (Fig. 1). It is a very shallow shelf sea with water depths between 15 and 200 m and a mean depth of 53m (Timokhov 1994). There are 5 major river system which flow into the Laptev Sea, with the Lena River as the biggest one (Fig. 1).

The river outflow of the Lena amounts to 520 km³/year (Aagaard & Carmack, 1989) and the annual discharge of suspended matter reaches 17.6*10⁶ tons (Martin et al., 1993).

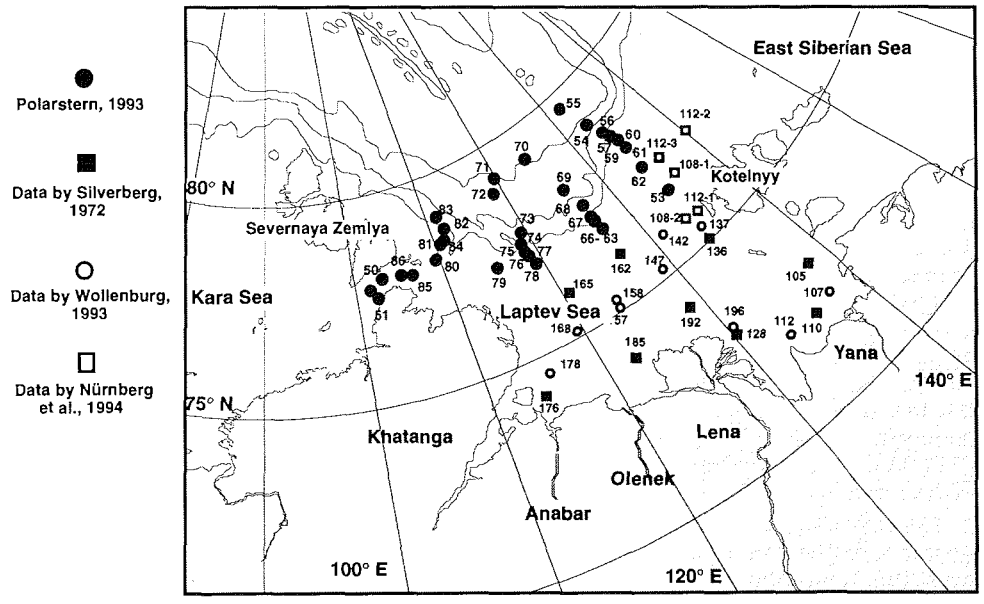

Fig. 1: Station map of surface sediments from the Laptev Sea, discussed in this paper

The Laptev Sea, situated between the Kara Sea to the west and the East Siberian Sea to the east, is of great importance for the sediment transport into the deep Arctic Ocean. During the formation of sea ice on the shallow shelf, sediment particles are incorporated and, therefore, during its drift through the Arctic Ocean towards the Fram Strait (Kubisch, 1992; Wollenburg, 1993; Nürnberg et al., 1994), the sea ice is one important transport medium to bring shelf sediment particles into the deep sea. Furthermore, the Laptev Sea slope is directly connected to the deep Amundsen and Nansen basins and the way from the river mouths to the shelf/slope border is only about 500 km long. This is much more shorter compared for example to the Kara Sea, where the shelf is longer and deeper (the mean water depth is 111m, Timokhov 1994) and where more sediment material is accumulated on the shelf bottom in the area of broad deltas in front of the rivers Yenisey and Ob.

This study focusses on the characterization of the clay-mineral composition of surface sediments along the outer shelf and the continental slope to the deep basin. The results are completed with some literature data from the inner shelf region (Wollenburg et al., 1993; Silverberg 1972, Nürnberg et al., 1994).

Methods

35 surface samples, taken with a giant box corer (GKG) from the Laptev Sea shelf and continental slope (Fütterer 1994) were analyzed for grain-size distributions and clay minerals. For disaggregation and removal of organic carbon, each sample was shaked in a 5% hydrogenic peroxide solution for about 24 hours.

After wet sieving of the sand fraction (> 63μm) silt and clay was seperated by the Atterberg settling method. Sodium pyrophosphate (1%) was used to avoid coagulation of clay particles and the clay fraction (> 2μm) was treated with $MgCl_2$ to provide a unique cation charging. Free ions were removed by centrifuging the clay at least two times.

The dried clay fraction was carefully grinded in an agate mortar. For measuring the clay texture preparations were carried out by vakuum filtration. To support quantitative measurements an internal standard of 1ml of 0.4% molybdenite suspension was added to 40 mg of clay during resuspension of the sample. This suspension was sucked onto a membran filter by vakuum filtration. After drying, the clay cakes were transfered onto aluminium platelets. This preparation technique (see Ehrmann et al., 1992) leads to highly texturated , low particle-size segregated clay films with a thickness of about 50 to 100μm (10mg/cm², see Petschik et al., in prep.)

All samples were measured with a Philips PW 1820 goniometer, using CoKα radiation, equipped with a theta-circle-integrated automatic divergence slit, a graphite monochromator, and an automatic sample changer. At first, "air-dried" samples were measured by a step scan with 2 seconds counting for each angle between 1-18°2θ with a step size of 0.02°. After vaporisation with ethyleneglycol at 50° C for at least 1 day, samples were measured between 2-40° 2θ with the same step size. In addition, the area between 28 and 30.5° 2θ was measured with steps of 0.005° to seperate the (002) peak of kaoline minerals from the (004) reflections of chlorite minerals.

For the semi-quantitative calculations the relative clay mineral content (rel%) of smectite, illite, kaolinite, and chlorite were determined using the integrated peak areas of their basal reflections, weightened by empirically estimated factors after Biscays (1965). For smectite the 17Å line, after removal of the chlorite 14Å line, and for illite the 10Å peak was used for the calculations. Kaolinite at 3.57Å - 3.58Å and chlorite at 3.53Å - 3.54Å were identified from the slow scan, by their intensity ratios The share of the respective mineral was transformed to the 7Å peak of both minerals, following Biscaye (1965).

Results

Grain sizes

The grain-size distribution of the surface sediments plotted in a triangular diagram (Fig.2) shows two main groups, one of silty clay or clayey silt and the other of clayey silty sand or sandy clayey silt. Very coarse sediments occur within the Vilkitsky Strait and in front of its eastern entrance in the Laptev Sea. The sand content show a wide range and varies between 2 and 80%. Some locally sand-rich sediments are also observed in some stations along the slope and in front of river mouths (Anabar, Yana, see Fig. 3a).

In general, the sediments in the western Laptev Sea are more sandy than in the eastern part. The silt concentration varies between 10 and 60% and the lowest values occur in the more western part along the continental slope (Fig. 3b). The clay content varies between 6 and 70% and highest values (>50%) occur along the slope to the deep sea (Fig. 3c). The clay content in the investigated samples from the outer shelf and the continental slope show a high positive correlation to the organic carbon content (Stein & Nürnberg, this volume).

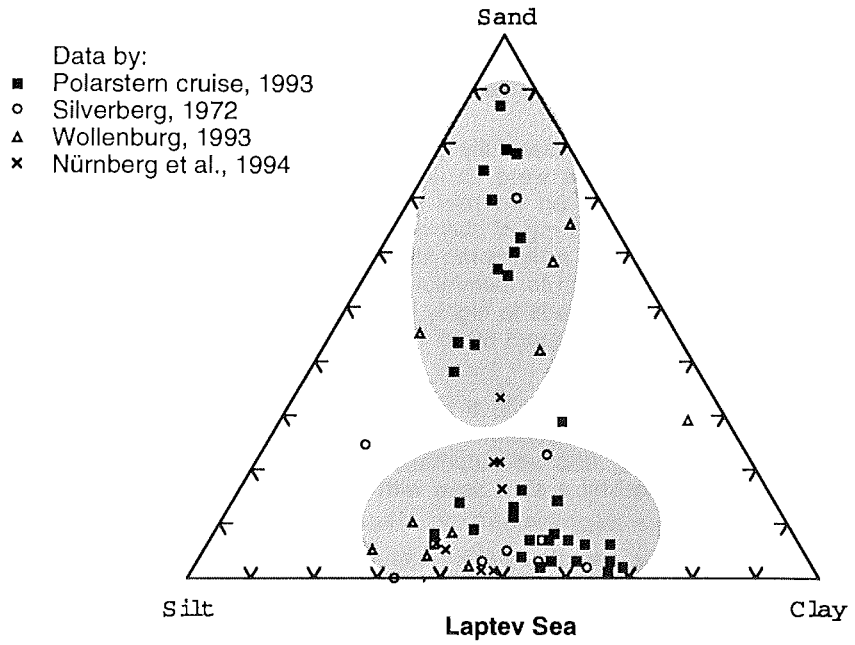

Fig. 2: Sand, silt, clay distribution of surface sediments plotted in a triangular diagram

Clay minerals

Illite is the main clay mineral in the investigated sediments with concentrations between 30 and 50%. Highest values occur in the eastern Laptev Sea, where values up to 60% were reached on the inner shelf east of the Lena River (Fig. 4a; Silverberg, 1972).

In contrast to this, smectite shows an enrichment in the western Laptev Sea with values up to 40%. There is a slight decrease of smectite to the deep sea and to the eastern part of the Laptev Sea (Fig. 4b). Kaolinite concentrations are relatively low (10-15%) and show no significant variations in the investigated sediments. Chlorite also show no strong concentration changes. Slightly higher values were measured along the deeper continental slope (Fig. 4c). Because of probable different calculation methods for kaolinite and chlorite the ratio of smectite to kaolinite+chlorite is plotted in Fig. 4d. The triangular diagram in Fig. 5 reflects the relatively large variation of smectite and illite concentrations in contrast to the nearly constant kaolinite+chlorite content in surface samples from the Laptev Sea.

Discussion

As different investigations on clay minerals in the Arctic have already shown (Clark et al., 1989; Dalrymple & Maass, 1987; Darby et al., 1989; Nürnberg et al., in press), the clay fraction mineralogy can be a valuable indicator of sediment sources and transport pathways. This is of special importance in polar and subpolar regions, where physical weathering processes dominate and chemical and diagenetic alteration are negligible. In general, the clay mineralogy of Arctic Ocean sediments reflects the source mineralogies of the landmasses and shelf areas

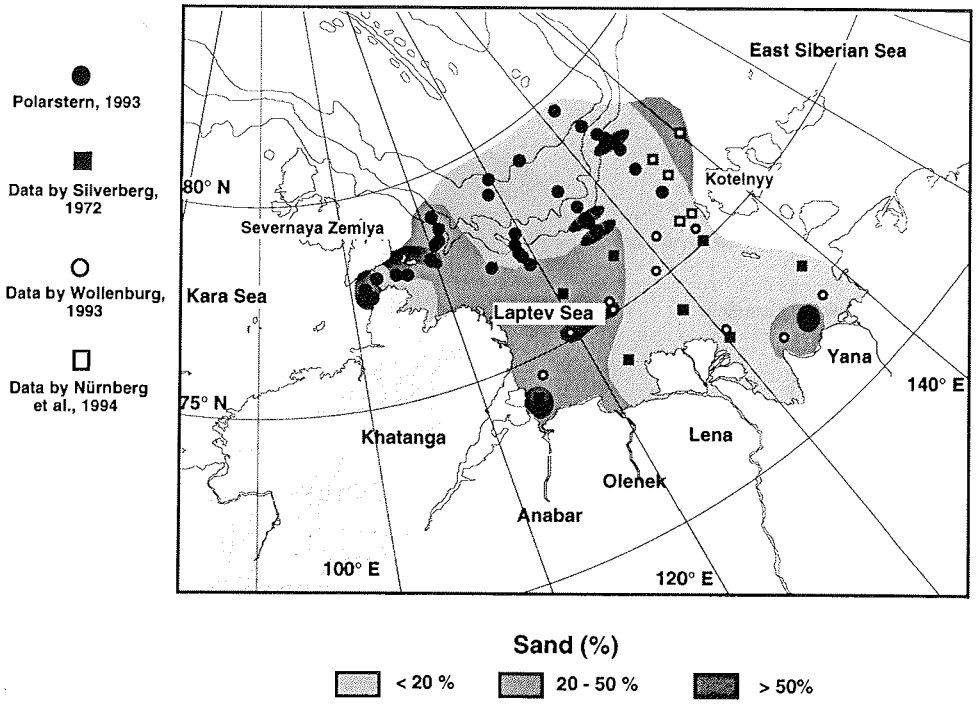

Fig. 3a: Distribution map of sand (weight%)

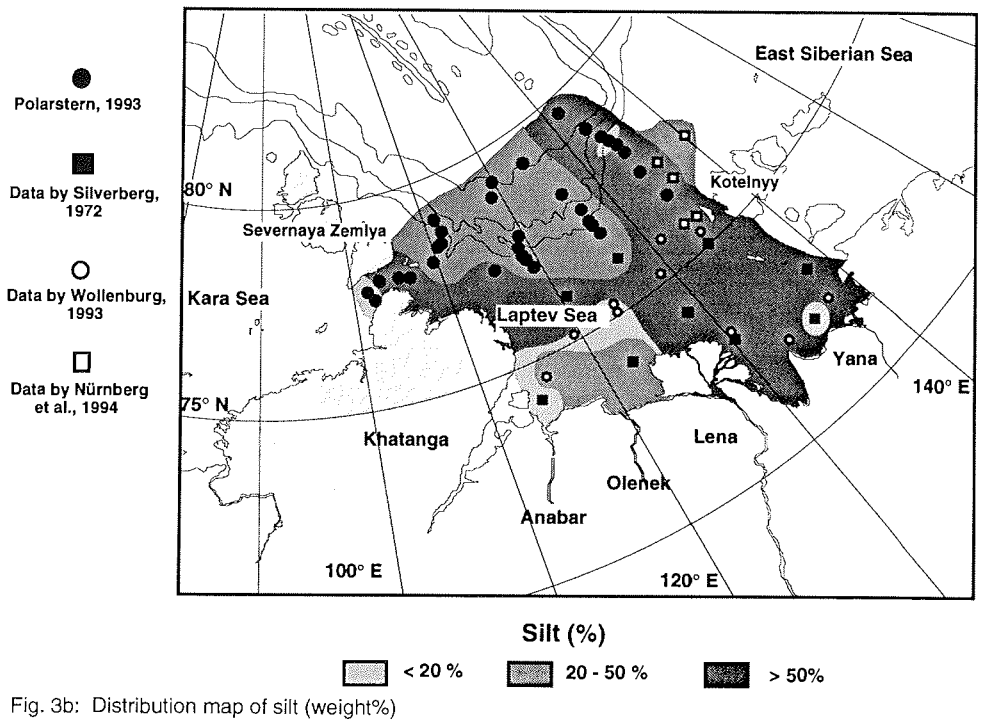

Fig. 3b: Distribution map of silt (weight%)

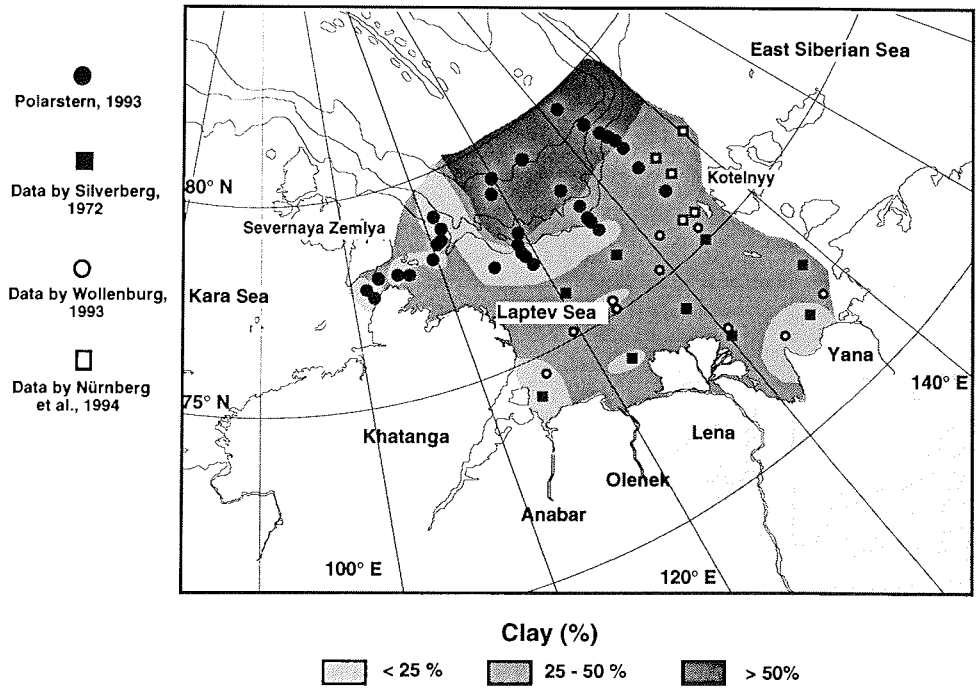

Fig. 3c: Distribution map of clay (weight%)

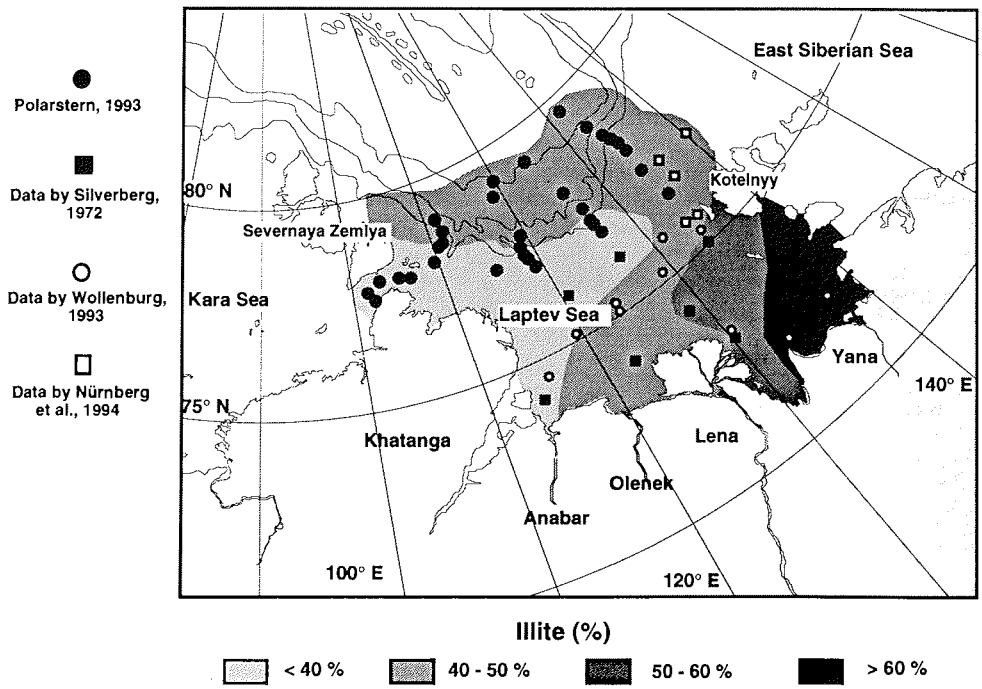

Fig. 4a: Distribution map of illite (rel%)

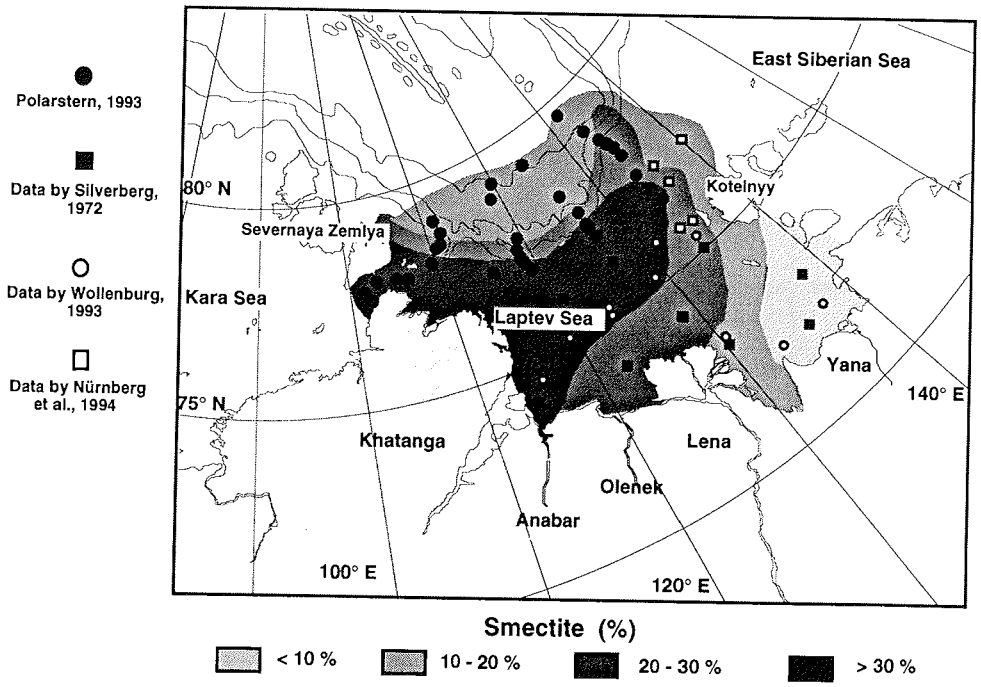

Fig. 4b: Distribution map of smectite (rel%)

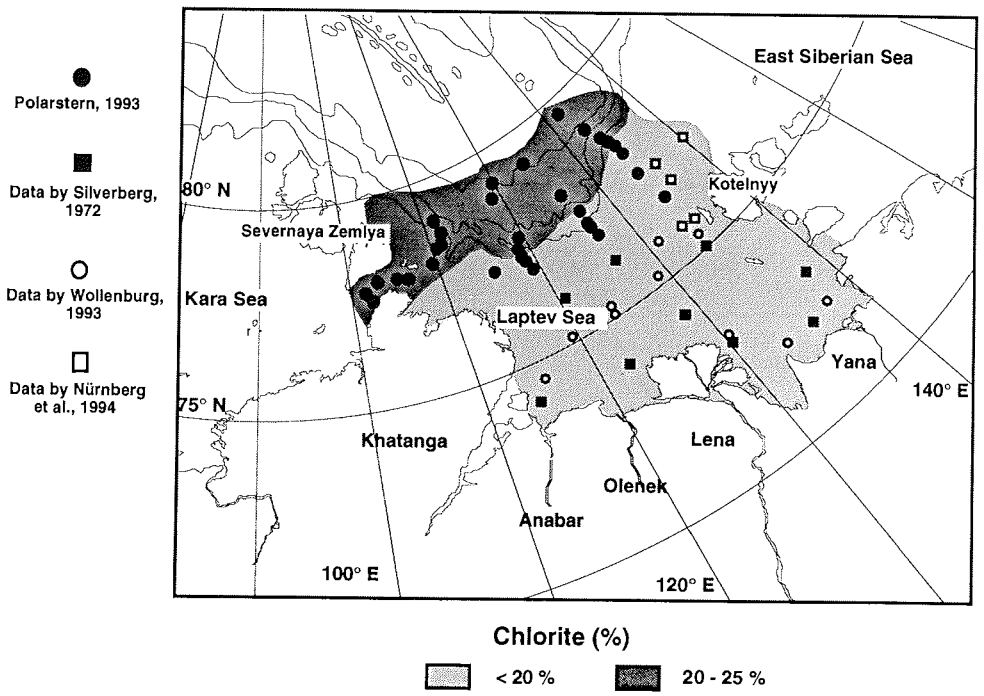

Fig. 4c: Distribution map of chlorite (rel%)

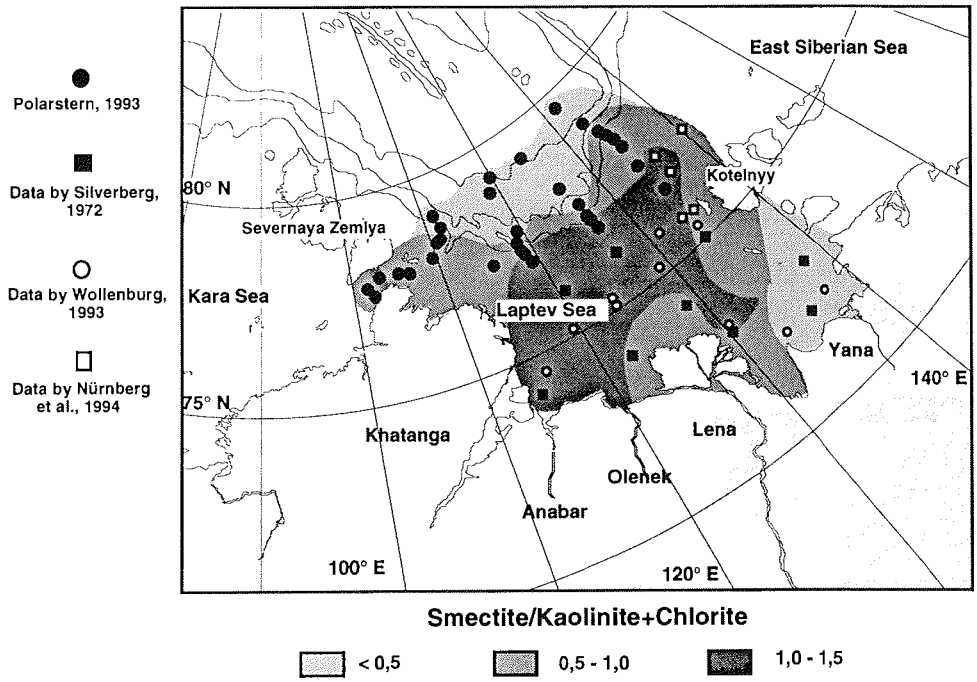

Fig. 4d: Distribution map of the ratio smectite/chlorite+kaolinite

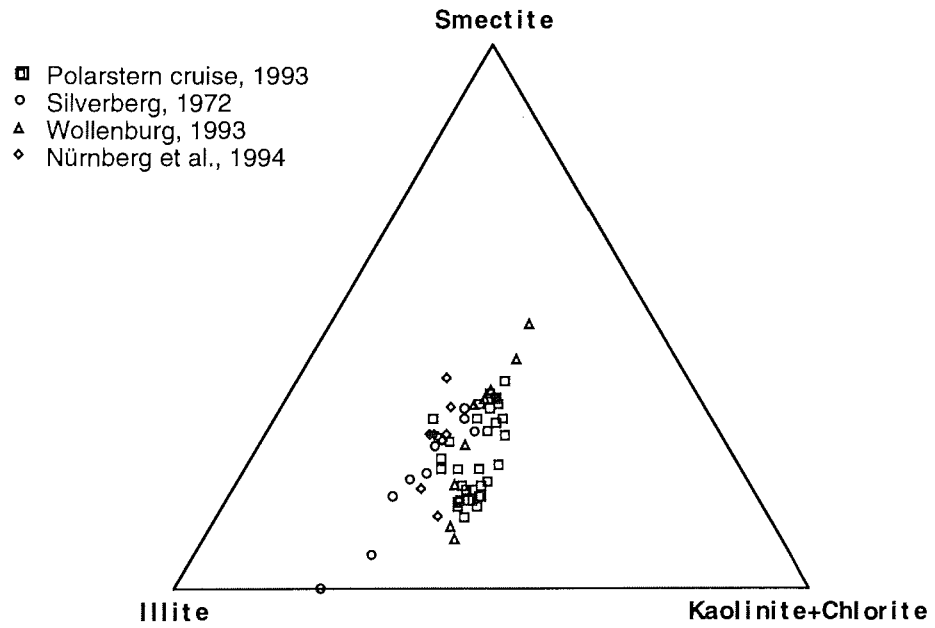

Fig. 5: Triangular plot of smectite, illite and kaolinite+chlorite of surface sediments in the Laptev Sea

surrounding the central Arctic Ocean basins (Darby et al., 1989). Therefore, it is necessary to investigate the clay composition of the shelf sediments to understand the supply and transport mechnisms of the sediments into the deep ocean and to interpretate mineralogical changes within the sediment cores (Elverhoi et al., 1989; Elverhoi et al., 1995).

The grain-size distributions of the Laptev Sea show a different pattern and a different mechanical differentiation as it normally exists on shelf areas in none polar ocean areas. Sediment distribution in the Laptev Sea is strongly influenced by the sea ice and its seasonal changes and, mainly in the western part, by the occurence of ice bergs. Both are transport media, which release particles by melting and this means, that the particles on the sea floor do not show a clear dependence from water depth and distance from the coast (Yashin & Kosheleva, this volume). This is reflected by the more coarse grained sediments in the north western part of the Laptev Sea, where intensive ice-berg transport occurs, and by some locally sand-rich surface sediments along the slope.

The investigation of the Laptev Sea sediment was carried out within the frame of intensive clay mineral analyses from different shelf areas and the deep sea in the Eurasian part of the Arctic Ocean (Wahsner et al. 1995). The data show, that the Laptev Sea, besides the Kara Sea with up to 70% smectite in the surface sediments (Wahsner & Shelekova, 1994), is another important source area for this clay mineral.

These high smectite values on the shelf of the Kara Sea result from the supply of the big rivers Ob and Yenisey. Both river systems drain huge sheet basalt complexes in the Siberian hinterland, where erosion and weathering of the basalt leads to the formation of smectite. The slighter lower, but in comparison to other Arctic regions, still relatively high values of up to 40% smectite, in the western part of the Laptev Sea show, that there is sediment transport from the Kara Sea through the Vilkitsky Strait into the western Laptev Sea. This higher smectite concentration in the western Laptev Sea has already been described in Stein & Korolev, 1994. In addition, the river Khatanga also drains parts of the sheet basalt complex and therefore transports a higher smectite content to the shelf. The eastern Laptev Sea is more influenced by the East Siberian Sea, where smectite only occur in minor concentrations (<10), because the erosion and weathering of more cristalline rocks supplies mainly illite to the shelf.

Recent investigations from Pfirman et al., (in press) have shown, that clay minerals in surface sediments from different shelf areas and sediments from sea ice supports very well the transport pathways of the sea ice within the Transpolar Drift. The reconstructed backwards trajectories identify the Laptev Sea as the main source for the sediment-laden ice in the Eurasian Arctic with smectite concentrations in the sea ice varying between 10 and 40%. On the other hand, ice with very high smectite concentrations (up to 60%) from the southern part of the Siberian branch of the Transpolar Drift was tracked back to the Kara Sea, just east and north of the Yenisey River discharge and ice with the lowest smectite content was traced back to the East Siberian Sea (Pfirman et al., in press) .

A next step for the future is now to transfer the recent situation of sedimentary processes in the Eurasian Arctic, characterized by the investigation of surface sediments from different shelf and deep-sea areas, into the past system, by intensive mineralogical investigations of sediment cores.

References

Aagaard, K. and Carmack, E.C., 1989. The role of sea ice and other fresh water in the Arctic circulation. Journ. Geophys. Res., 94, C10: 14485-14498.

Biscaye, P. E., 1965. Mineralogy and sedimentation of recent deep-sea clays in the Atlantic Ocean and adjacent seas and oceans. Geol. Soc. Amer. Bull., 76 : 803-832.

Clark, D.L., Whitman, R.R., Morgan, K.A., and Mackay, S.D., 1980. Stratigraphy and glacio-marine sediments of the Amerasian Basin, central Arctic Ocean. Geol. Soc. Amer., Spec. Paper, 181.

Dalrymple, R.W. and Maass, O.C., 1987: Clay mineralogy of late Cenozoic sediments in the CESAR cores, Alpha Ridge, central Arctic Ocean. Can. Journ. Earth Sci., 24: 1562 - 1569.

Darby, D. A., Naidu, A. S., Mowatt, T. C. and Jones, G., 1989. Sediment composition and sedimentary processes in the Arctic Ocean. In: Herman, Y. (Ed.), The Arctic Seas - Climatology, Oceanography, Geology, and Biology. New York (van Nostrand Reinhold): 657-720.

Ehrmann, W.E., Melles, M., Kuhn, G., Grobe, H., 1992. Significance of clay minerals assemblages in the Antarctic Ocean. Marine Geology 107, 249-273.

Elverhøi, A., Andersen, E. S., Dokken, T., D., H., Spielhagen, R., Svendsen, J. I., Sørflaten, M., Rørnes, A., Hald, M. and Forsberg, C. F., 1995. The growth and decay of the Late Wechselian Ice Sheet in western Svalbard and adjacent areas based on provenance studies of marine sediments. Quaternary Research, in press.

Elverhoi, A., Pfirman, S. L., Solheim, A. and Larssen, B. B., 1989. Glaciomarine sedimentation in epicontinental seas exemplified by the Northern Barents Sea. Mar. Geol., 85 : 225-250.

Fütterer, D. K., 1994: The Expedition Arctic `93 of RV "Polarstern" in 1993. Berichte zur Polarforschung , 149, Bremerhaven (Alfred Wegener Institute for Polar and Marine Research, AWI).

Kubisch, M., 1992. Die Eisdrift im Arktischen Ozean während der letzten 250.000 Jahre. Kiel. GEOMAR report, 16.

Martin, J.M., Guan, D.M., Elbaz-Poulichet, F., Thomas, A.J., and Gordeev, V.V., 1993. Preliminary assessment of the distributions of some trace elements (As, Cd, Cu, Fe, Ni, Pb, and Zn) in a pristine aquatic environment: the Lena River estuary (Russia). Marine Chemistry, 43: 185-199.

Nürnberg, D., Wollenburg, I., Dethleff, D., Eicken, H., Kassens, H., Letzig, T., Reimnitz, E. and Thiede, J., 1994a. Sediments in Arctic sea ice: Implications for entrainment, transport and release. In: Thiede, J., Vorren, T. O. and Spielhagen, R. F. (Eds.), Marine Geology. 119: 185-214.

Nürnberg, D., Levitan, M. A., Pavlidis, J. A. and Shelekhova, E. S., 1995. Distribution of clay minerals in surface sediments from the eastern Barents and southwestern Kara seas. Geol. Rund. 84, (in press).

Petschik, R., Kuhn, G., and Gingele, F. (in prep): Clay mineral distribution in surface sediments of the South Atantic: sources, transport, and relation to the oceanography. in prep for Marine Geology.

Pfirman, S.L., Colony, R., Nürnberg, D., Eicken H., (in press). Reconstructing the origin and trajectory of drifting Arctic sea ice.

Silverberg, N., 1972: Sedimentology of the surface sediments of the east Siberian and Laptev Seas. PhD thesis, University of Washington.

Stein, R. and Korolev, S., 1994. Shelf-to-basin sediment transport in the eastern Arctic Ocean. In: Kassens, H. and Karpiy, V. Y. (Eds.), Russian-German cooperation in the Sibirian shelf seas: Geo-system Laptev-Sea. Berichte zur Polarforschung., 151: 87-100.

Stein, R., Grobe, H. and Wahsner, M., 1994a. Organic carbon, carbonate, and clay mineral distributions in eastern central Arctic Ocean surface sediments. In: Thiede, J., Vorren, T. O. and Spielhagen, R. F. (Eds.), Marine Geology, 119: 269-285.

Timokhov, L.A., 1994. Regional characteristics of the Laptev and the East Siberian seas: climate, topography, ice phases, thermohaline regime, circulation.- Berichte zur Polarforschung 144, Bremerhaven (Alfred-Wegener Institut).

Wahsner, M. & Shelekova, E.S. 1994. Clay-mineral distribution in Arctic deep sea and shelf surface sediments. Greifswalder geologische Beiträge, A829: 234 (abstract).

Wahsner, M., Stein. R. and Vogt, C., 1995. The recent eastern Arctic Ocean sedimentary environment and its change during the Late Quaternary.- Terra Nostra 1/95, Schriften der Alfred-Wegener-Stiftung, S. 48, (abstract, Bremen Februar 1995).

Wollenburg, I., 1993. Sedimenttransport durch das arktische Meereis: Die rezente lithogene und biogene Materialfracht. Berichte zur Polarforschung., 127. Bremerhaven (Alfred-Wegener-Institut).

Yashin, D.S. & Kosheleva, V.A. (this volume). Holocene sediments of the Russian east-Arctic seas.

THE SEDIMENTARY ENVIRONMENT OF THE LAPTEV SEA: PRELIMINARY RESULTS OF THE TRANSDRIFT II EXPEDITION

J. Dehn°, H. Kassens* and TRANSDRIFT II Shipboard Scientific Party

° Geological Survey of Japan, Sapporo, Japan

* GEOMAR Forschungszentrum für marine Geowissenschaften, Kiel, Germany

Abstract

One of the objectives of the TRANSDRIFT II expedition to the Laptev Sea during summer of 1994 was to identify transport paths and depositional center of river discharge in order to quantify the runoff patterns of North Siberian rivers through time and space. During the expedition a sedimentological working program was conducted on a total of 16 stations on the shelf area.

The modern sedimentary regime of the Laptev Sea is characterized by Holocene normal consolidated fine-grained near surface sediments. Ongoing sedimentological studies indicate that sediments from the eastern Laptev Sea differ from those in the west in grain-size, composition and density. Five facies have been identified on the basis of these changes by smear slide analyses. The eastern-most site (PM9462) in the Yana Valley exhibits clayey surface sediments (0-5 cm, facies 1) overlying a silty to clayey unit (facies 2) ending on a sandy layer (430 cm, facies 3). This is also observed in the Lena Valleys of the central Laptev Sea (sites PM9463 & PM9442). In these sites a new unit (facies 4) rich in clay (>70 %) is present between facies 1 and 2. This unit is absent in the Anabar-Khatanga Valley to the west (sites (PM9494 & PM9499) where the older (> 1.2 m depth) sediments are rich (ca. 20%) in organic material, and make up facies 5. These changes are indicators of changing environments through time, particularly, (1) different sediment sources for the Laptev Sea, (2) different water masses, and (3) changing depositional environments, particularly from active delta to estuary and shallow marine. The basal sandy sediments in the central and eastern regions mark the active Lena Delta, now submerged. The terrigenous, organic rich sediments to the west are indicators of either a change in the course of the Khantanga or Anabar rivers, or in the temporal position of the tree line.

Introduction

Most recent investigations in the Arctic Ocean have stressed the importance of the broad Siberian shelves for shelf-to-basin sediment transport processes, in particular for the formation of 'dirty' sea ice. Above all, the Laptev Sea, which belongs to the world's largest and shallowest shelf areas, acts as an important source area for fine-grained sediments being transported to the deep Arctic Ocean (e.g. Wollenburg, 1993, Nuernberg et al., 1994). The Laptev Sea is a shallow shelf sea north of East Siberia between the Taymyr Peninsula and the New Siberian Islands (Figure 1). Whereas the transport of sediments in the Laptev Sea is related to (i) specific ice formation processes, such as anchor ice or suspension freezing, as well as to (ii) hydrological and geomorphological phenomena, such as currents or transport of suspended particulate matter. As a result, even short-term climatic fluctuations will have a significant impact on the cross-shelf sediment transport. An important feature of the depositional environment of the Laptev Sea is river run-off of the large Siberian river systems, such as the Rivers Yana, Lena, Olenek, Anabar and Khatanga (Figure 1), which have a drainage basin of 3,6 million km^2 and contain numerous industrial sites (Alabyan et al., this volume). With an average river discharge of 552 km^3/year (Alabyan et al., this volume), the Lena River is the

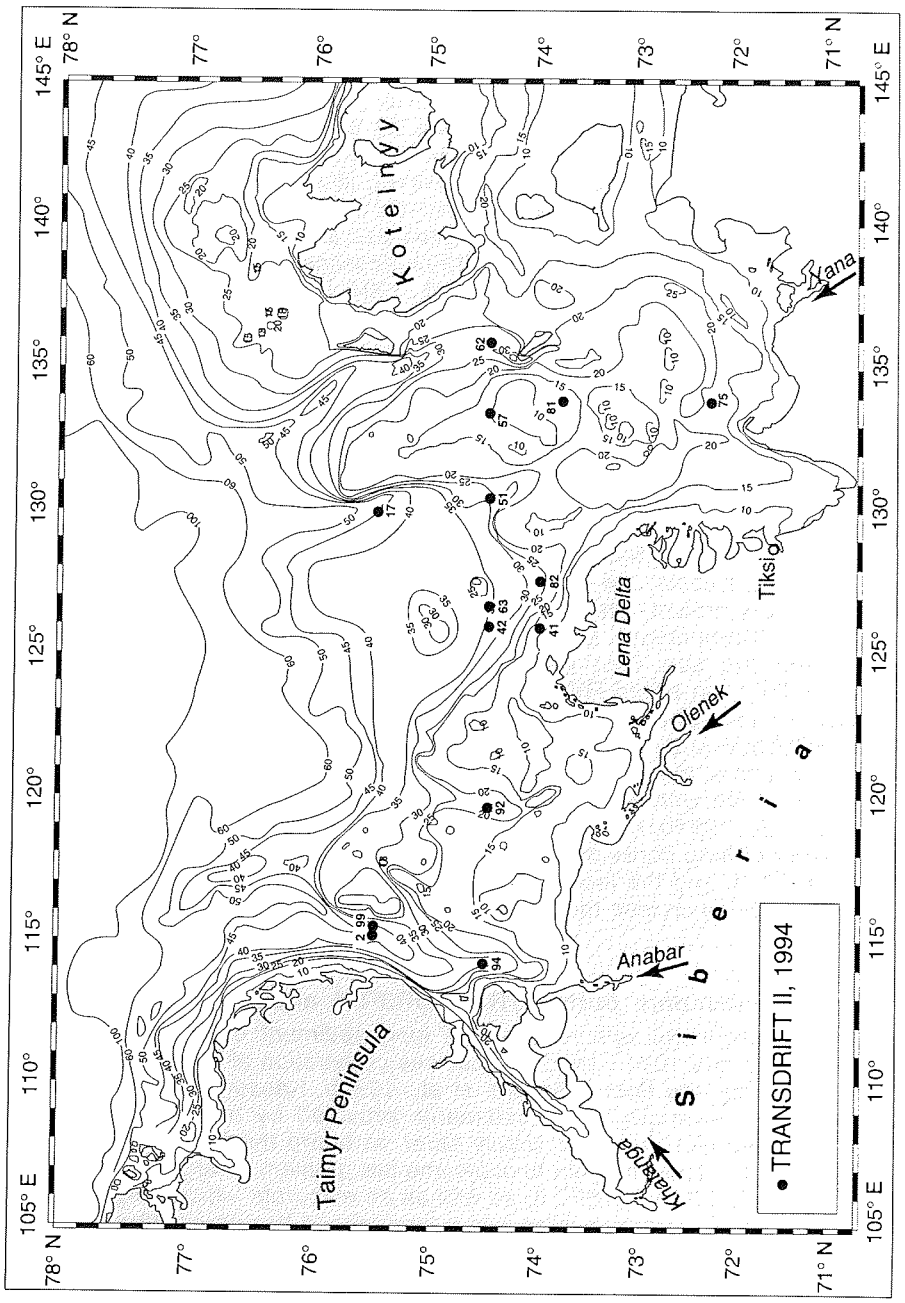

Figure 1. Location map of the Laptev Sea. The circles denote sampling sites for the TRANSDRIFT I and II expeditions. Filled circles indicate locations where bottom sediments were recovered. The other symbols mark the sites of the early Northwind expedition.

second largest river discharging to the Arctic Ocean and the eighth largest of the world (Gordeyev and Sidorov, 1993). The Lena run-off accounts for more than 70% of the overall inflow of riverine waters into the Laptev Sea. On its way through swampy lowlands, the river accumulates a high dissolved organic load and loses the suspended sediment load. The Lena River annual discharge of total organic carbon is 5,0 million tons, which is about 30 % of the overall organic carbon transport to the Arctic Ocean (Romankevich and Artemyev, 1985). This is by far the highest discharge of all Arctic rivers. However, little is known in detail about the relationship between morphology, river run-off and discharge, erosion, sediment transport and sea ice formation in the Laptev Sea area (e.g. Holmes and Creager, 1974; Dethleff et al., 1993; Martin et al., 1993; Kassens et al., 1994a; Kassens et al., 1994b; Kassens et al., 1994c; Reimnitz et al., 1994; Dethleff, 1995).

Importance of studies here

In 1994 a major multidisciplinary research program 'Laptev Sea System' was designed between Russia and Germany to understand the Arctic environment and its significance for the global climate. Ongoing bilateral research activities in the scope of the 'Laptev Sea System' include land and marine expeditions to the Laptev Sea area during different seasons of the year, workshops, as well as the exchange of scientists. The GEOMAR Research Center for Marine Geosciences in Kiel, Germany, and the State Research Center for Arctic and Antarctic Research in St. Petersburg, Russia, are jointly responsible for organizing and coordinating the multidisciplinary project, which is funded by the Russian and German Ministries of Science and Technology. Comprehensive studies of the atmosphere, the water column and the sea floor were carried out already during the expeditions TRANSDRIFT I, on board RV IVAN KIREYEV (August to October in1993) in the scope of the pilot phase, and TRANSDRIFT II, on board the RV PROFESSOR MULTANOVSKY (July to October in 1994). The remote location, seasonal ice cover (9 months of the year) and harsh conditions make working in the Laptev Sea problematic. Nevertheless, TRANSDRIFT I recovered sediments at 47 sites (Kassens et al., 1994b; Kassens et al., 1994c). The shallow permafrost level made the recovery of long cores difficult. This particular problem was overcome during TRANSDRIFT II, and the first long cores (up to 5m) were recovered in the Laptev Sea. Both of these cruises recovered key data for the understanding of the Laptev Sea System.

Challenges overcome during TRANSDRIFT I and II

Technical problems with recovery of long sediment cores arose during the cruises in 1993 and 1994. The foremost was penetration of the permafrost level at 12 cm below the sea floor (Kassens et al., 1994b, Kassens et al., 1994c). The increased yield strength of the sediments provided by the ice was enough to withstand penetration from the gravity corer on board the IVAN KIREYEV during TRANSDRIFT I (1 ton). In order to overcome this problem, a larger weight (2,5 tons) was used during TRANSDRIFT II, as well as an elaborate vibrocoring device. The surface sediments were recovered with a large spade box corer (50 x 50 x 60 cm). Each device had its own sampling scheme. For each box core, samples were taken for immediate study, as well as two archive liners. Surface samples were taken for biogenic study and clay mineralogy. A profile was taken whenever possible for later X-ray to define the fine sturctures in the sediments. The sediment was described on deck, immediately after recovery, often in inclement conditions. Samples were then taken and prepared at the earliest opportunity. Macroscopic description of the sediments was primarily concerned with color, structure, and

macroscopic components which would not appear in a smear slide, such as drop stones and large organisms. A Minolta CM 2002 scanner was used to classify the colors on board, thus eliminating bias due to conditions or lighting. The sediments were scanned immediately after recovery to ensure accurate color readings. The color readings were not taken at a regular intervals since small variations in the color of the surface can seriously effect the results. A flecked or speckled core often gave erroneous results based on how many specks were present in the scanning field. Thus a qualitative effort was given to choose an area which had the most homogenous and representative color of the core. On board smear slides were made in order to better classify the sediments. Smear slides were taken where there was an obvious change in the sediments, where a minor lithology was present, or every meter when the sediment appeared homogeneous. On the basis of other shipboard analyses, smear slides were sometimes taken later as a control of these results. Each slide was examined in detail at a minimum a three spots radially from the center of the slide to help eliminate the error caused by sorting and cohesion of the sample during preparation. At each spot the percent of each mineral type was estimated using scatter charts. The results of each location are then averaged to yield a value for the entire sample. The name of the sediment is based on these analyses. The nomenclature used varies from that of the Ocean Drilling Program for terrigenous sediments, but more closely resembles the naming convention for biogenic sediments. The name is based entirely on the composition of the sediments, the grain size is noted independently. This provides a more accurate name as well as a better basis of comparison to biogenic sediments, allowing separate comparison of composition and grain size. The macroscopic descriptions were annoted with the proper sediment name after the smear slide analysis was complete for each sample.

Initial results of the sedimentological study

Based on the smear slides made during and after TRANSDRIFT II and macroscopic sediment descriptions, the sediments were classified into 5 facies. The results are summarized in Figure 2.

The surface sediments of the Laptev Sea (Facies 1) are very dark gray or olive gray clay to silty clay, with various clays as their main component (15 to 75%). Secondary components are primarily quartz (50% or less) and chlorite (<25%). Facies 1 generally exhibits a large variety of minor components, dominated by opaque minerals. This opaque material can be found ringing the dropstones found on the ocean floor, and is a magnesium/manganese/iron oxide precipitate. Site PM94 92 differs from the others since quartz dominates clay, and the overall grain size increases to sand. This is probably due to the location of the site, in the Olenek valley, a place where finer material would be absent due to higher current speeds. Despite its grain size, this sediment here resembles Facies 1 in its diversity of minor components, dominated by opaque minerals. Facies 1 ranges in thickness from 30 to 80 cm. At Sites PM9441-4, PM9451-7, PM9457-5 tourmaline needles were observed in rounded quartz grains. All of these Sites are located off the Lena Delta (Figure 1) and suggest a highly evolved igneous province as the source area for the sediments.

Facies 2 is a silty unit, composed primarily of rounded to sub-rounded quartz grains (40-90%). The sediments range in color from dark gray with black mm-size flecks to dark greenish gray with cm size darker mottles. Secondary components are alternately clay or potassium feldspars. The feldspar grains exhibit clear pericline twinning, suggesting that they are microcline. In the western Laptev sea this sediment become increasingly rich in organic debris (up to 20%). The source

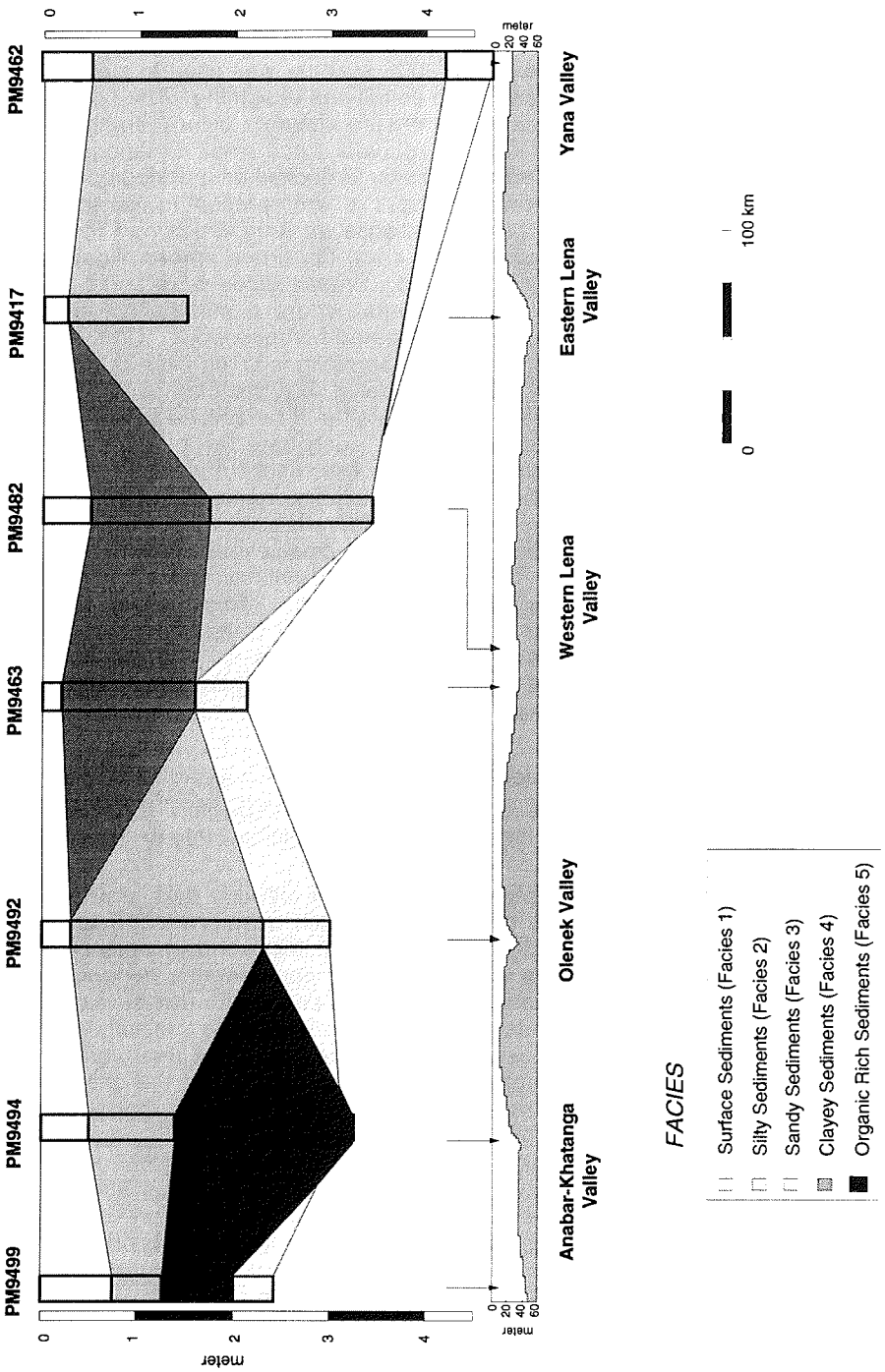

Figure 2. Summary of the sediments recovered in the Laptev sea during TRANSDRIFT II. Maximum penetration was achieved at Site PM9462. Five facies are seen noted on the basis of composition and grain size.

area for this material seems to be the Anabar and Khatanga Rivers. Facies 2 ranges from 50 to 350 cm in thickness. The general trend indicates a thickening to the eastern Laptev Sea. This sediment is present every where except at Site PM9463, in the western Lena Valley. Here a finer grained sediment is present. This unit more resembles Facies 1, though if indeed the same unit, there is an assymetrical distribution of this sediment or higher sedimentation rates in the western Lena Valley and on the topographic high between the eastern and western Lena valleys north of the delta. For now, this unit is designated Facies 4.

Facies 3 is a coarser unit of primarily brown to very dark brown silty to sandy sediments. It is also pervasive though absent at site PM9417 (due to very shallow penetration) and PM9482. Quartz is the primary component and exceeds 75% in all recovered cores. A secondary clay component is as high as 20%, but usually is present only as a minor component. The thickness of this unit is unknown since it represents the maximum penetration at all sites where it was recovered.

Facies 4, as described above, closely resembles Facies 1. It is a dark greenish gray silty clay. The primary difference is a depletion in opaque material and minor components relative to Facies 1. For the purposes of the discussion we shall separate these two units.

Facies 5 is an organic rich very dark gray sandy silt present only in the western Laptev Sea (Figure 3). The organic material, composed primarily of mm size wood fragments, reaches a maximum of 20% at Site PM9494-4. The entire facies is nearly black, and issued a sulphurous odor. The organic material was often concentrated in layers ca. 1 cm in thickness. These layers were an area of structural weakness in the cores, and the core at Site PM9494-4 broke off on one such layer. This unit had a minimum thickness of 75 cm at Site PM9499, the thickness at Site PM9494-4 is unknown. Crystalline nodules were present in Facies 5. These nodules reached a maximum length of 8 cm, and were generally less than 5 cm in diameter. The nodules are composed of clusters of up to 6 mm long monoclinic orange crystals. The crystals rapidly turned to a white ($CaCO_3$) powder when heated. These hydrated calcium carbonates have a low relief (ca. 1.55). This mineral was thought to be ikaite, the predecessor of the pseudomorph glendonite, which has been previously discovered in the Antarctic deep-sea sediments in 1950 m water depth (Suess et al., 1982). Ongoing crystallographical (e.g. deep temperature x-ray diffraction and differential thermal analysis) and isotopical (∂O, ∂C) studies will determine if this is a new mineral and/or a new paleoceanographic indicator (or tool) for extreme environments such as the Laptev Sea.

Discussion

These studies in the Laptev Sea provide an important clue to the present environmental system. We can use an understanding of the past to give us better indications of what to expect in the present Laptev Sea System. Gradual changes can be interpreted, and their causes determined. In general, the sediments of the eastern Laptev Sea differ from those of the west. In addition, the sediments show a significant change through time. These changes reflect changing environments not only in the Laptev Sea, but in the source regions of the sediments. The western Laptev Sea seems richer in organic sediments than the east. This comes intially as a surprise since the dissolved organic carbon value is so high in the Lena River (eastern Laptev Sea). One explanation for this may be a nearer source region for the organic material in the western Laptev Sea. The material is largely whole, leaf fragments and wood chips are common. The material has not been dissolved or altered by long transport distances.

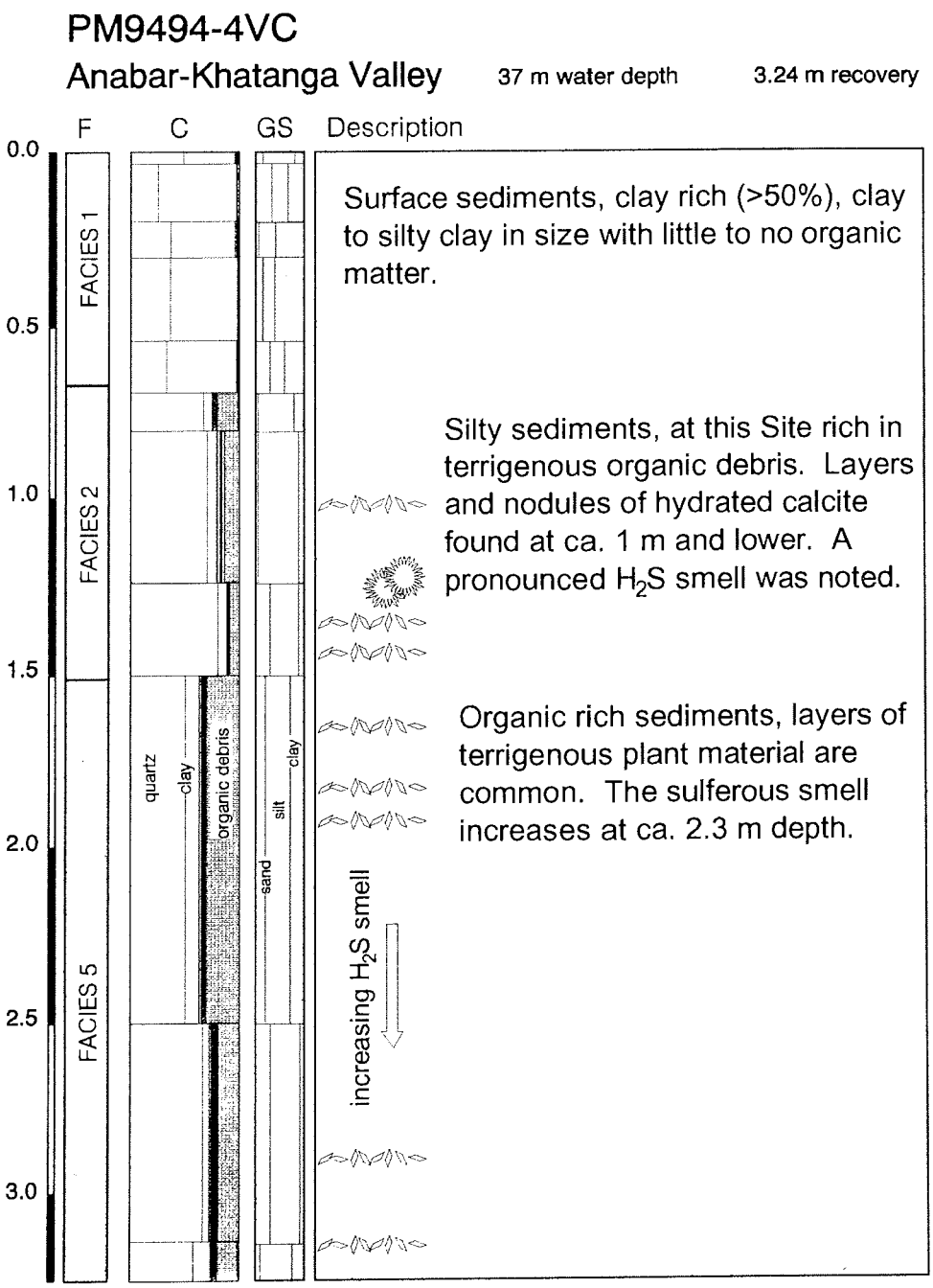

Figure 3. Description of sediment core PM9494-4VC taken during the TRANDRIFT II expedition to the Laptev Sea.

The central Laptev Sea is dominated by the fine grained sediments. This may be the result of the source for this region, presumably the Lena Delta, or by a higher sedimentation rate for these sediments at this location. A decrease in flux from the northern Lena Delta would favor a lower energy depositional regime, and deposit clay sized material as seen on the topographic high between the Lena valleys north of the delta. The eastern Laptev Sea has a larger component of silty sediments, perhaps again either a result of a depositional regime favoring these sediments, and/or a higher sedimentation rate. This distribution of sediments is characteristic for the river systems feeding the Latev Sea at these points. Present activity at the Lena Delta indicates that the largest influx of water takes place on its eastern side (Alabyan et al., this volume). The slightly higher energy regime favors the deposition of silty sediments, and might account for a potentially higher rate of deposition. The distribution of surface sediments (Figure 4) on the basis of their grain sizes supports the conculsions drawn from each individual site. A large area of coarse grained material is seen to the west of the Lena Delta. The contour turns sharply coastward as it passes to the north, suggesting a lower energy regime.

Categorizing the sediments through time is difficult since there is - up to now - no reliable high resolution age control on these young shelf sediments. However, the Laptev Sea surface sediments show normal to underconsolidated behaviour, that is physical-property profiles exhibit no evidence for desiccation, past erosional or seabed loading events. For instance, the porosity records show only little negative trend with depth, which indicates to high sediment accumulation rates. Summing-up our results the modern Laptev Sea is covered by marine sediments not older than the Holocene. For the purpose of comparison we will assume a relatively homogenous rate of deposition (intial studies show that the rate ranges from 30-100 cm/1000yr). As suggested above, the variations in thickness of some of the facies may be a result of changes in the rate of deposition. Regardless, each Site shows a distinct transition from coarse to fine grained sediments with time. This most certainly is a reflection of changing environment.

Conclusions

Studies of sediments in the Laptev Sea are key to the understanding of the evolution of the system with time. The recover of the first long cores in the Laptev sea has allowed us to see its development for the first time. The trends in such long-term systems help us to better evaluate the impact caused by industrialization as well as naturally occuring events. Understanding of the system enables us to quantify and mitigate the environmental effects caused by man.

Acknowledgements

The authors wish to thank the scientific, technical, and command crews of the RV Professor Multanovsky and the German Ministry of Sciences and Technology (BMBF grant No. 525-4003-0G0517A), as well as the staff of the Russian Antarctic and Arctic Research Institute and GEOMAR for their assistance before, during, and after the cruise.

References

Alabyan, A.M., Chalov, R.S., Korotaev,V.N., Sidorchuk, A.Yu., and Zaitsev, A.A., 1995. Natural and Technogenic Water and Sediment Supply to the Laptev Sea.- This volume.

Dethleff, D., Nuernberg, D., Reimnitz, E., Saarso, M. and Savchenko, Y.P., 1993. East Siberian Arctic Region Expedition '92: The Laptev Sea - Its significance for

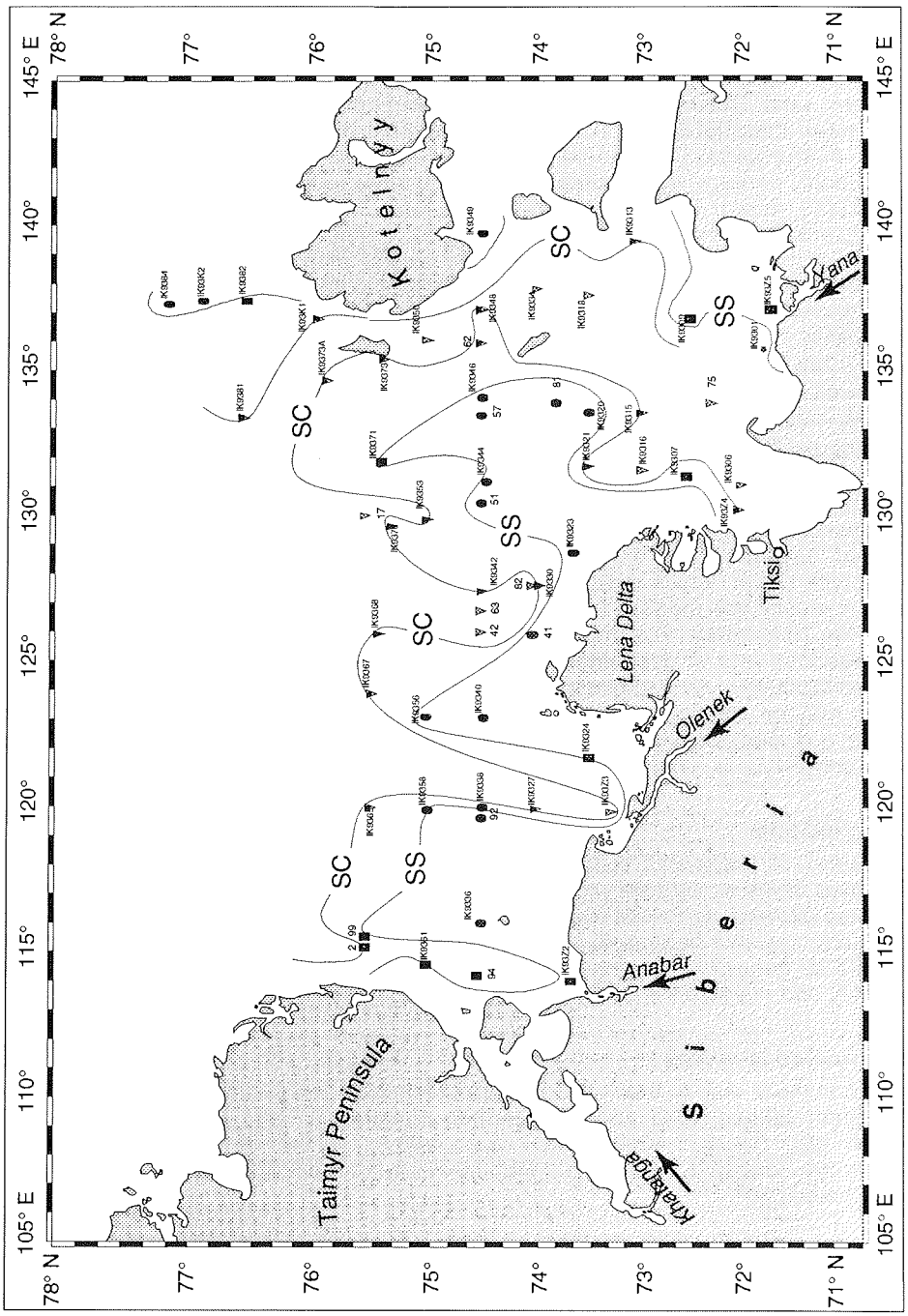

Figure 4. Grain size distribution map of surface sediments in the Laptev Sea. Circles are sand sized, squares are silt, and triangles are clay sized. The contours denote the boundaries between the regimes. SS is the sand-silt and SC is the sand-clay boundary.

Arctic sea-ice formation and transpolar sediment flux. Ber. Polarforsch. 120, p. 1-44.

Dethleff, D., 1995. Die Laptevsee - eine Schlüsselregion für den Fremstoffeintrag in das arktische Meereis. Unpubl. Doctoral Thesis, University of Kiel, 111 pp.

Gordeev, V.V. and Sidorov, I.S., 1993. Concentrations of major elements and their outflow into the Laptev Sea by the Lena River. Mar. Chem. 43, p. 33-45.

Holmes, M.L. and Creager, J.S., 1974. Holocene history of the Laptev Sea continental shelf. In: Y. Herman (ed.): Marine Geology and Oceanography of the Arctic Seas. Springer Verlag Berlin, p. 211-229.

Kassens, H., Hubberten, H.W., Priamikov, S. and Stein, R., 1994a. Russian-GermanCooperation in the Siberian Shelf Seas: Geosystem Laptev Sea. Ber. Polarforsch., 144, 133 pp.

Kassens, H., Karpiy, V. and the Shipboard Scientific Party, 1994b. Russian-GermanCooperation: The TRANSDRIFT I Expedition to the Laptev Sea. - Ber. Polarforsch., 151, 168 pp.

Kassens, H. and the TRANSDRIFT I Shipboard Scientific Party, 1994c. Along the Northern Sea Route into the Ice Factory of the Arctic Ocean. The Nansen Icebreaker, 6, p. 4-6.

Martin, J.M., Guan, D.M., Elbaz-Poulichet, F., Thomas, A.J. and Gordeev, V.V., 1993. Preliminary assessment of the distributions of some trace elements (As, Cd, Cu, Fe, Pb and Zn) in a pristine aquatic environment: the Lena River estuary (Russia). Mar. Chem. 43, p. 185-199.

Nuernberg, D., Wollenburg, I., Dethleff, D., Eiken, H., Kassens, H., Letzig, T., Reimnitz, E. and Thiede, J., 1994. Sediments in Arctic sea-ice: Implications for entrainment, transport and release. Mar. Geol., 119 (3-4), 185-214.

Reimnitz, E., Dethleff, D. and Nuernberg, D., 1994. Contrasts in Arctic shelf sea-ice regimes and some indications: Beaufort versus Laptev Sea. Mar. Geol., 119 (3/4), 215-226.

Romankevich, S. and Artemyev, F., 1985. Input of organic carbon into seas and oceans bordering the terretory of the Soviet Union. In 'Transport of carbon and minerals in major world rivers, Part 3' (ed. Degens, E.T.). Mitt. Geol.-Paläont. Inst. Univ. Hamburg, SCOPE/UNEP Sonderbd. 53, p. 66-75.

Suess, E., Balzer, W., Hesse, K.F., Müller, P.J., Ungerer, C.A. and Wefer, G., 1982. Calcium Carbonate Hexahydrate from Organic-Rich Sediments of the Antarctic Shelf: Precursors of Glendonites. Science, 216, 1128-1130.

Wollenburg, I., 1993. Sedimenttransport durch das arktische Meereis: Die rezente lithogene und biogene Materialfracht. Ber. Polarforsch. 127, p. 1-159.

SOME LITHOLOGICAL-GEOCHEMICAL FEATURES OF MODERN BOTTOM SEDIMENTS OF THE LAPTEV SEA SHELF

A. V. Yakovlev
VNIIOkeangeologia, St. Petersburg, Russia.

The Laptev Sea is a marginal basin of the Arctic Ocean. The average depth of the sea is about 533 m; the major part of the sea is a flat plain with depths of up to 50-60 m. In contrast to other Arctic basins, the Laptev Sea is marked by a number of specific features. The influence of warm atlantic and pacific waters is minimal here. The sea is characterized by a significant fresh-water discharge which controls a system of currents as well as the ice regime. The complex Russian-German expedition TRANSDRIFT-I aboard the hydrographic vessel "Ivan Kireyev" aimed to study the hydrological, sedimentological and other characteristics of the Laptev Sea; the author was a participant of this expedition (Yakovlev 1994).

During the cruise we sampled recent bottom sediments at 42 stations. The investigations were carried out according to the "Instruction of small-scale geological survey of the shelf" (Lopatin & Gurevich, 1990) and "Temporary methodic recommendations on the landscape-ecological mapping" (Gurevich & Kazakov 1989). Petersen and Van-Vin grabs and a box corer constructed in Germany were used for sampling bottom sediments. The author is very grateful to his German colleagues for technical assistance during the sampling. Analytical lithological-geochemical investigations were carried out in the laboratories of VNIIOkeangeologia in accordance to standard methods. This work deals with some lithological-geochemical features of recent bottom sediments of the Laptev Sea shelf.

One of the most significant processes in the Laptev Sea is the influence of river discharge. Zones of mixed fresh river water and marine water masses are specific areas of shelf sedimentation - so-called "marginal filters" (Lisitzyn 1994). They are characterized by significant processes of flocculation and coagulation of dissolved and suspended matter, the deposition of large amounts of suspension transported by river waters; these areas are practically transition zones between continent and ocean. The width of this zone in the Laptev Sea runs to several hundred kilometers, including practically the whole shelf. The main volume of river water is pushed to the eastern part of the sea, because the Lena River discharge is more than 70 % of the total fresh-water discharge.

Sandy and pelitic silts and sometimes fine-grained sands are the most widespread recent bottom sediments of the Laptev Sea (Gurevich 1986; Belov & Lapina 1961). We will consider the distribution of the fraction less than 0.001 mm, i.e. subcolloidal pelite. Its content in bottom sediments does not exceed 50%, but, nevertheless, this parameter requires special attention.

Fig. 1 shows that small areas of increased contents (more than 30%) of subcolloidal pelite are concentrated in zones of mixed waters of the Laptev and East Siberian Seas near the Dmitriy Laptev and the Sannikova Strait. The largest of these zones is located near the mouth of the Lena River. It is directed opposite the fresh water discharge. It is a part of the "marginal filter" (Lisitzyn 1994) affected by fresh river and sea water with low salinity. Coagulation of clay minerals, disappearence of fresh-water plankton, transformation of iron from dissolved form into suspension and especially sedimentation of a significant part of suspended matter to bottom sediments are the most remarkable processes here.

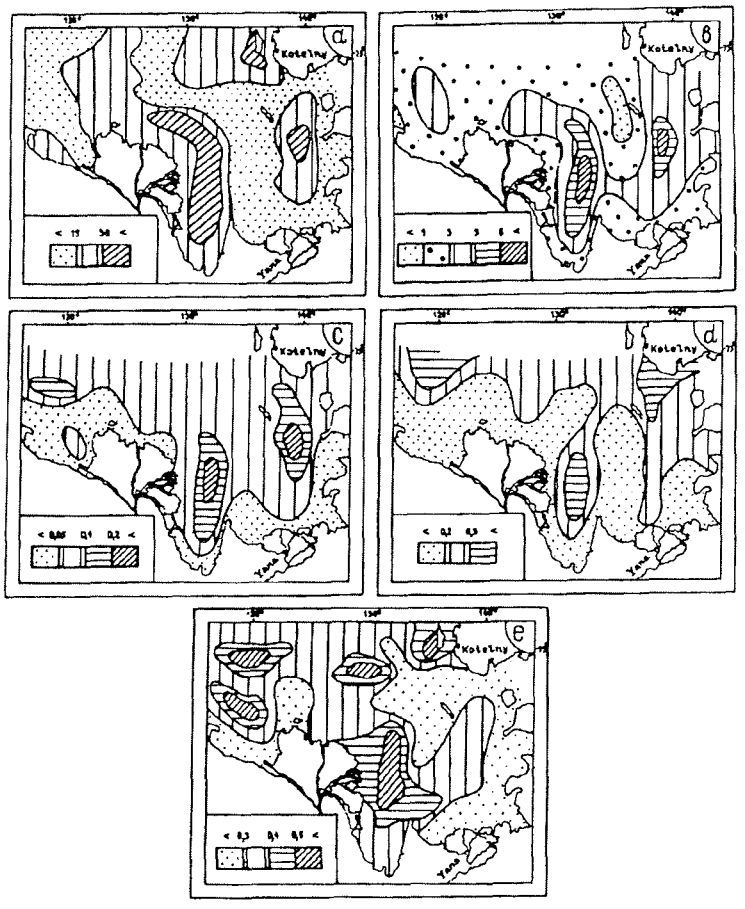

Fig. 1. Subcolloidal pelite (a), Fe_2O_3 (b), MnO (c), P_2O_5 (d), and amorphous SiO_2 (e) in recent bottom sediments of the south-eastern part of the Laptev Sea (mass %).

These data are illustrated by distribution schemes of mobile forms of Fe (counted to Fe_2O_3), Mn (MnO) and P (P_2O_5) in the surface layer of bottom sediments (chemical analyses of HCl-extract). The distribution of amorphous SiO_2 is more complicated as it is connected not only with fluvial discharge but also with microorganisms with opaline skeletons (radiolarias, diatoms).

Bottom sediments of the south-eastern Laptev Sea were examined by a quantitative spectral method to investigate the whole number of microelements. The concentrations of almost all microelements are generally near clarke concentration or less. Most interesting are the distributions of Cu, Sn, V and Sr (Tab. 1 and Fig. 2a).

The average content of Cu in bottom sediments of the south-eastern Laptev Sea is almost by two times higher (in several samples by six times higher) than the clarke concentration. In lithological types of deposits, Cu is distributed quite similarly, while increased concentrations are fixed in sands and pelites. Areas of maximal Cu contents are located near river mouths (Fig. 2a) and are obviously

Table 1: Contents of Cu, Sn, V and Sr in bottom sediments of the south-eastern Laptev Sea

Element	Content, mass %						Clarke in marine sediments (Vinogradov, 1967)
	minimal	maximal	average arithmetic				
			sands	silts	pelites	whole deposits	
Cu	0.0014	0.0190	0.0061	0.0044	0.0063	0.0050	0.0030
Sn	not detected	0.0030	0.0002	0.0003	0.0004	0.0003	0.0005
V	0.0010	0.0140	0.0037	0.0077	0.0094	0.0073	0.0080
Sr	0.030	0.096	0.056	0.076	0.076	0.071	0.010

Fig. 2. Elements in recent bottom sediments of the south-eastern part of the Laptev Sea (mass %): a - Cu; b - Sn; c - V; d - Sr.

connected with river discharge. It is known that Cu migrates in river waters as dissolved load and as a component of suspension (Vinogradov 1967). Cu transfers into bottom sediments as a component of metal-organic compounds by mixing of river and sea waters as well as by deposition of Cu-containing minerals and mineral associations. Increased contents of Cu in sands on one hand and in pelites on the other hand can be explained by these processes.

The average content of Sn in offshore bottom sediments is less than clarke concentration (Tab. 1, Fig. 2b). However, some samples show a content which is by 5-6 times higher (similarly to Cu). A wide area of increased Sn concentrations is located in the eastern part of the offshore area due to transport of Sn by river waters eroding rocks of the Sn-containing Yana-Indigirskaya province (Atlas of the Arctic,

1985). The averaged Sn content in deposits of the southern and eastern parts of the Laptev Sea shows that these contents are twice as high in the eastern part (0.0002 and 0.0004 % respectively).

Vanadium is found in bottom sediments of the south-eastern Laptev Sea in average quantities close to clarke concentrations. However, Tab. 1 shows that V concentrations increase while the grain size of sediments decreases. V contents are in pelites almost three times as high as in sands. Areas of maximal V concentrations are situated in the eastern part of the studied shelf (Fig. 2c). These areas are evidently connected with deposition under conditions of "marginal filters" of suspended organic matter sorbing V (Lisitzyn 1994) or coagulation of iron, which also pushes V to sediments (Belov & Lapina, 1961).

Sr concentrations are 5-7 times as high as clarke concentrations in all investigated lithological types of bottom sediments of the south-eastern Laptev Sea (Tab. 1, Fig. 2d). It is well known that Sr is present in many minerals and rocks as isomorphic admixture (sienites, granites, avgites, nefelines, potassium feldspars). Belov and Lapina (1961) consider that Sr is transported to recent sediments of Arctic seas by weathering of both sedimentary and igneous rocks and by disturbance of Sr-containing minerals. Increased Sr concentrations in sediments near the shore, i. e. comparatively not far away from their source areas, can obviously be explained by transportation of Sr-containing minerals over short distances.

Organic matter is an important factor in sedimentary environment. The presence of organic matter creates alkaline conditions during sedimentation. Fig. 3 shows that organic matter is transported to the Laptev Sea by fluvial discharge. The distribution scheme of organic carbon in sediments is compiled using the author's original data (Yakovlev & Petrova 1994), the data of Holmes (1967) as well as those of Kassens et al. (1994).

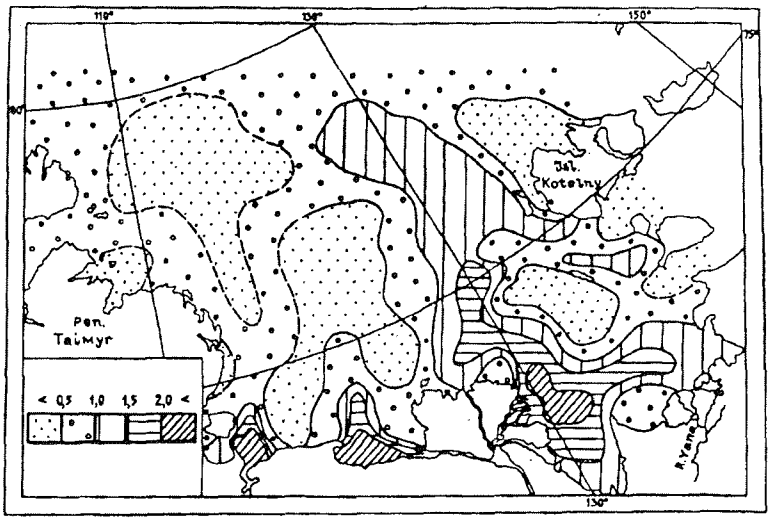

Fig. 3. Organic carbon in recent bottom sediments of the Laptev Sea (mass %).

Distribution schemes of dissolved SiO_2 and the salinity of the surface water layer sufficiently illustrate the penetration of river water into the Laptev Sea (Fig. 4a, 4b). These maps were kindly given by oceanographers of the AARI (Dmitrenko 1994). Accumulation of Fe, Mn, amorphous SiO_2 and other components in recent sediments is mainly found within an anomalous zone located in the near-mouth part of the Lena River the salinity of which ranges from 1-2 to 6-8, rarely 12 promille and the content of dissolved SiO_2 from 1500 to 1100-900 mkg/l.

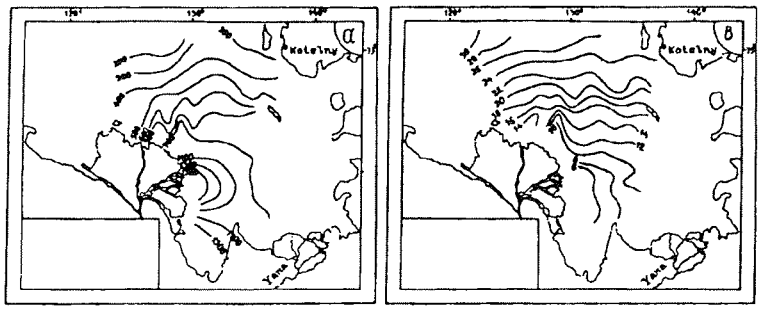

Fig. 4. Dissolved SiO_2 (a) and salinity (b) in the surface water layer of the south-eastern part of the Laptev Sea in summer 1994 (pers. comm. Dmitrenko, 1994).

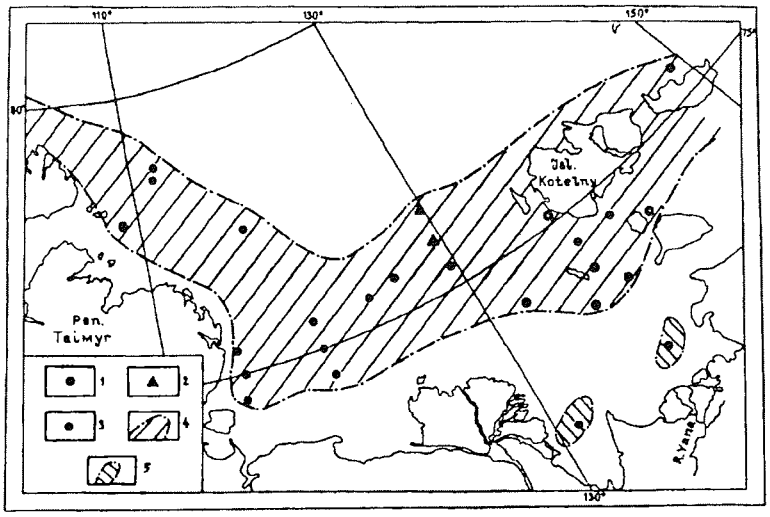

Fig. 5. Distribution of Fe-Mn nodules in the Laptev Sea: 1 - previous Russian research, 2 - after Holmes (1967), 3 - after Yakovlev (1994), 4 - transregional belt of authigenously formed Fe-Mn mineral, 5 - local areas with predominantly formed Fe-nodules near the mouths of major rivers.

Authigenous forming of Fe-Mn minerals is one of the remarkable features of sedimentation in the Laptev Sea. Locations of Fe-Mn nodules previously obtained by various scientists is shown in Fig. 5. Generally, one transregional belt of authigenously formed Fe-Mn nodules is marked on the Laptev Sea shelf. This belt of circumcontinental direction is located from the Vilkitsky Strait and adjoining parts of the Kara Sea (Gurevich & Yakovlev, 1993; Yakovlev at al., 1994) to Kotel'nyy Island and adjacent parts of the East Siberian Sea. Local areas, where predominantly Fe-nodules are formed, are also marked near the mouths of major rivers.

There are three morphological types of Fe-Mn nodules in the Laptev Sea (Fig. 6a, 6b, 6c). The first one is represented by tube-like nodules, genetically connected with Polychaeta tubes. The second type includes nodules formed on shells of the mollusk *Tridonta borealis*. The third type is represented by pancake-shaped nodules with nuclei consisting of pebbles of diverse roundness or without a core. The locations of these three types of nodules are shown in Fig. 7.

Generally this belt of Fe-Mn nodules is located within a zone of sea water mixed with river discharge. The northern boundary of the belt approximately corresponds to the "shelf-bathyal" boundary, and the southern boundary is located near the "river-sea" geochemical barrier.

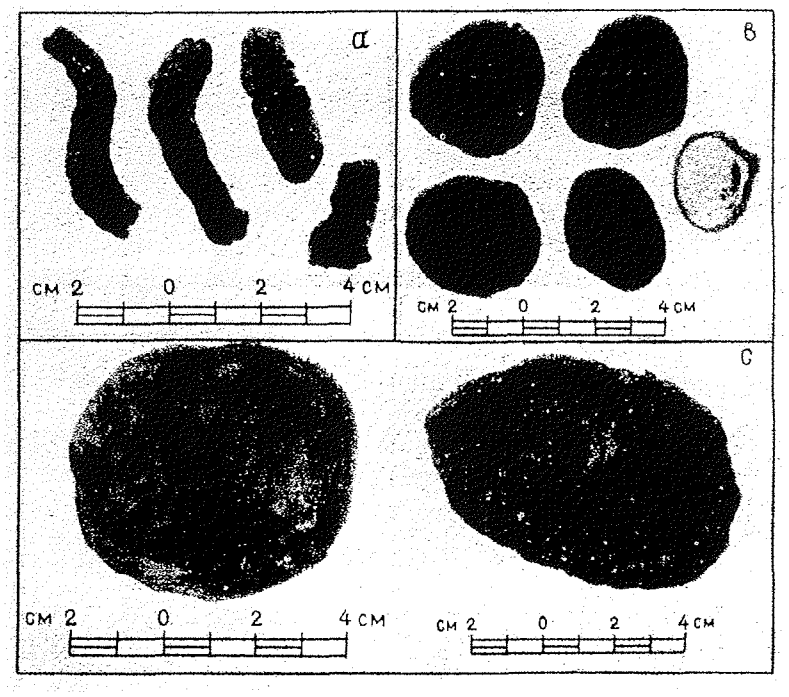

Fig. 6. Photos of the different morphological types of Fe-Mn nodules and crusts of the Laptev Sea: a - tube-like nodules, b - nodules formed on shells of the mollusk *Tridonta borealis*, c - pancake-shaped nodules with a pebble nucleus.

The distribution of coarse-grained terrigenous material (gravel, pebbles and small boulders) in recent bottom sediments of the Laptev Sea shelf is very interesting; it is shown in Fig. 8. Considering the small amount of coarse-grained

material at stations of bottom sampling we have compiled the scheme of its distribution based mainly on visual half-amount evaluations according to the data of the expeditions aboard R/V "Ivan Kireyev" and "Polarstern". The analysis of gravel and pebble distribution revealed that they are not common to offshore zones and mainly concentrated in near-shore areas and in straits. Their maximum amount

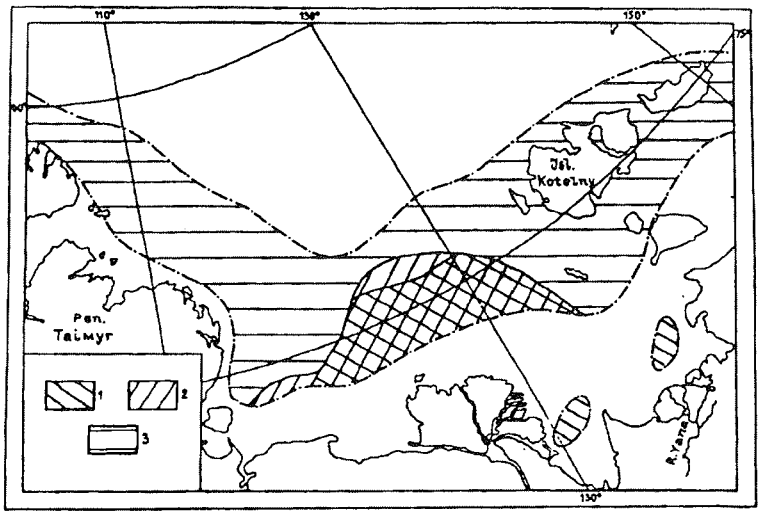

Fig. 7. Distribution of the different morphological types of Fe-Mn nodules on the bottom surface of the Laptev Sea: a - tube-like nodules, b - nodules formed at shells of mollusk *Tridonta borealis*, c - pancake-shaped nodules with a pebble nucleus.

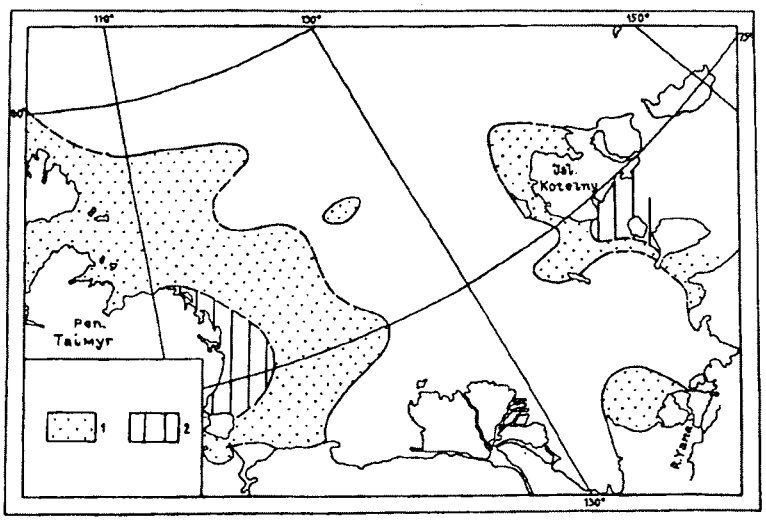

Fig. 8. Rate of occurences of coarse-grained fractions in recent bottom sediments of the Laptev Sea: 1 - single, 2 - rare.

is found in the south-western coastal part of the Laptev Sea due to floating ice during the melting of the Taimyr ice sheet. Generally, the role of stones transported by floating ice is not significant in the Laptev Sea and especially in its bathyal zone.

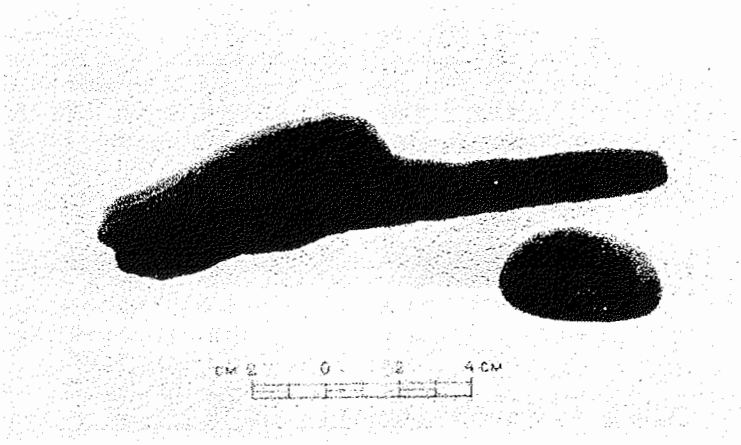

Fig. 9. Photo of wood fragments of recent bottom sediments of the Laptev Sea.

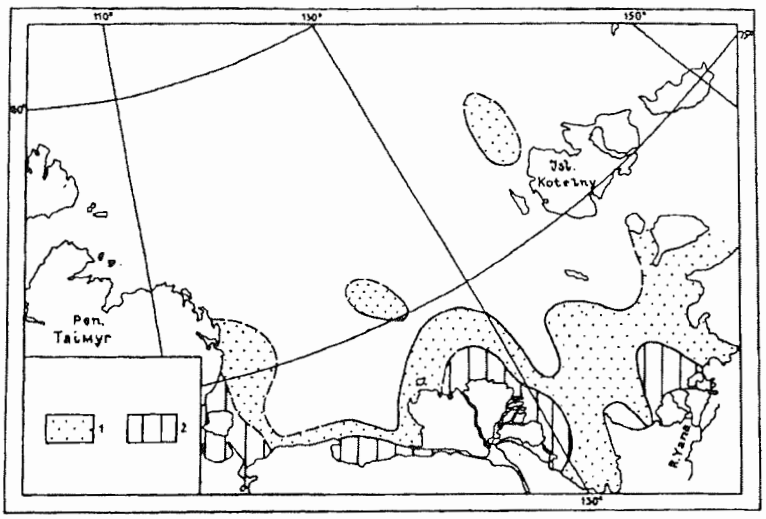

Fig.10. Rate of occurences of wood fragments of recent bottom sediments of the Laptev Sea: 1 - single, 2 - rare.

The presence of wood fragments in recent bottom sediments of the Laptev Sea shelf is also very interesting. These fragments are often up to 5-15 cm in size. They occasionally look like well rounded pebbles due to their long-lasting transportation by rivers (Fig. 9).

For compiling the distribution scheme of wood fragments in modern sediments (Fig. 10) we used own original data (visual half-amount evaluation of occurence of large wood fragments) as well as data of German colleagues about small wood fragments obtained by means of microscopic analyses of silt and sand fractions (Kassens 1994). Fig. 10 shows that the input of wood into bottom sediments is almost only due to river discharge. The drift of wood in the Laptev Sea is evidently connected with the distribution of river water. It is an indirect characteristic feature of the direction of prevailing currents (Fig. 11).

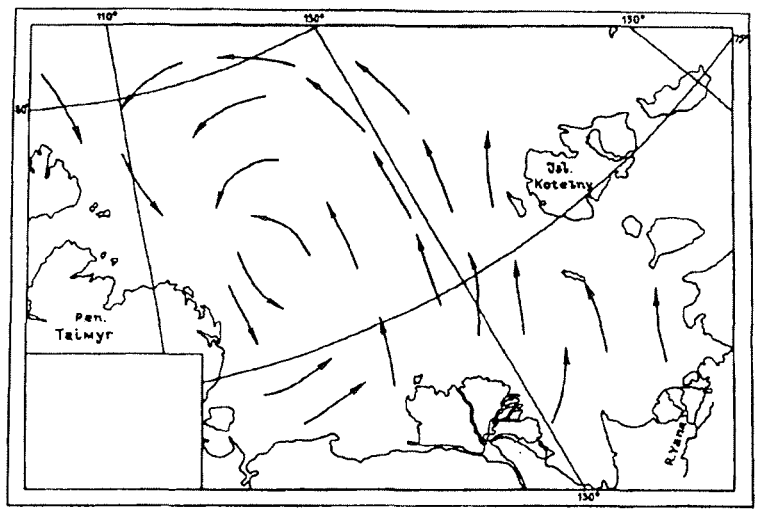

Fig.11. Predominant directions (arrows) of currents in the Laptev Sea in summer (Dobrovolskiy & Zalogin, 1965).

Conclusions

1) One of the results of the studies of modern sedimentation processes in the Laptev Sea is the evaluation of the distribution scale of river and low-salinity marine waters.
2) The analysis of distribution of coarse-grained material through the bottom surface proves that, in the Laptev Sea, floating ice is of comparatively minor importance for its transportation.
3) Lithological-geochemical studies of recent bottom sediments in the south-eastern part of the Laptev Sea permitted locating the sedimentation zone of the main volume of suspension transported by the Lena River waters.
4) The unified Laptev Sea belt of an authigenous forming of Fe-Mn nodules is established by the distribution of Fe-Mn nodules.

References

Atlas of the Arctic, 1985. GUGK (Geodesy and Map-making General Department) publ., Moscow, 204 p. (In Russian)

Belov, N. A., Lapina, N. N, 1961. Bottom sediments of the Arctic Basin. "Marine transport" publ., Leningrad, 150 p. (In Russian)

Dobrovolsky, A. D., Zalogin, B. S, 1965. Seas of USSR (nature and industry). "Idea" publ., Moscow, 351 p. (In Russian)

Gurevich, V. I., 1986. Methodic recommendations for grain-size classification of sediments. "Sevmorgeologia" publ., Leningrad, 18 p. (In Russian)

Gurevich, V. I., Kazakov, N. I., 1989. Preliminary methodic recommendations for landscape - ecological mapping during geological survey of the shelf. "Sevmorgeologia" publ., Leningrad, 41 p. (In Russian)

Gurevich, V. I., Yakovlev, A. V., 1993. Fe-Mn crusts and nodules of Kara Sea. - In: Co-containing Fe-Mn crusts of Pacific Ocean. "VNIIOkeangeologia" publ., St.Petersburg, p. 97-111. (In Russian)

Holmes, M. L., 1967. Late pleistocene and holocene history of the Laptev Sea. - University of Washington, 98 p.

Kassens, H., Karpiy, V. and the Shipboard Scientific Party, 1994. Russian-German Cooperation: The Transdrift I Expedition to the Laptev Sea. Ber. Polarforsch., 151, 168 pp.

Lisitzyn, A. P. Marginal filter of oceans. J. "Oceanology", v. 34, N 5, p. 735-747. (In Russian)

Lopatin, B. G., Gurevich, V. I., 1990. Instruction for organisation and carrying out of small-scale geological survey of the shell and compiling of the State Geological map of the USSR shelf with scale 1:1,000,000. "Sevmorgeologia" publ., Leningrad, 98 p. (In Russian)

Vinogradov, A. P., 1967. Introduction to the ocean geochemistry. "Science" publ., Moscow, 212 p. (In Russian)

Yakovlev, A. V., 1994. Ecological-Geochemical Studies. Ber. Polarforsch. 151: 77-80.

Yakovlev, A. V., Kassens, H., Fütterer, D., 1994. Nodule formations of the Laptev Sea shelf. In: Scientific results of LAPEX-93 expedition. "Hydrometeoizdat" publ., St.Petersburg, p. 227-236. (In Russian)

A STUDY OF THE CALCAREOUS MICROFAUNA FROM LAPTEV SEA SEDIMENTS

H. A. Bauch°, M. Kubisch-Popp°, T. M. Cronin*, B. Rossak and TRANSDRIFT I Shipboard Scientific Party

° GEOMAR Forschungszentrum für marine Geowissenschaften, Kiel, Germany

* United States Department of the Interior, Geological Survey, Reston, USA

Regional Hydrography and Physiography

Today, the Arctic Ocean is strongly influenced by waters from three main sources. Through Fram Strait and across the Barents and Kara seas high-salinty water enters the Eurasian basin of the Arctic Ocean within the upper 600 m of the water column (Hanzlick, 1983). To a much lesser degree Pacific water flows in via the Bering Strait. In contrast to these marine sources, the Arctic Ocean is also fed by a vast fluvial runoff, which in particular derives from large Siberian rivers such as Ob, Jenisey, and Lena. Even though the contribution of the total mass of this freshwater to the Arctic Ocean is relatively low in comparison to the other two sources, it is of major significance for the formation of sea ice on the shelves. Here, the lowering of the surface water salinity results in a distinct halocline. Especially during winter increased cooling and subsequent sea ice formation favours the release of very saline and dense brines (Aagaard and Carmack, 1989). This process is probably responsible for much of the water mass transformation within the Arctic Ocean circulation system.

A large part of Siberian shelves are rather shallow on the average (<50 m) whereas the continental slope exhibits a steep break at ~100 m water depth. The general topographic feature of the Laptev Sea (Fig. 1) is marked by a gently northward sloping plain which is cut by various subaquaeous gorges (Holmes and Creager, 1974). These canyon-like troughs are linked to the mouths of the major rivers e.g., Lena, which terminate in the Laptev Sea. The water from these rivers not only reduces the salinity at the surface, it also influences the temperature of the surface water during summer, which can reach 8-10°C or more (Baskakov et al., 1987). Further off the shelf, termperatures within the upper 100 m are - 1.8°C on the average. Below that depth the strong influence of Atlantic core water with temperatures of ~1.5°C is noted (Timokhov, 1994). This water reaches the Laptev Sea shelf via flowing along the continental slope of the Barents and Kara seas.

As with the surface water temperatures, the salinity is a reflection of the interactions between these marine and freshwater masses. Long-term Russian investigations show that the salinity varies, depending upon the vicinity to the river mouths, between 10-30‰ in the upper part. At greater depth, e.g. 30 m, salinities seem to be more constant with values averaging ~34‰ (Timokhov, 1994).

Material and Methods

The sediment material was gained during the Russian-German TRANSDRIFT I expedition of RV *Ivan Kireyev* to the Laptev Sea in 1993. Coring was carried out by applying box corer and kasten corer devices. A total of 48 surface samples were obtained, which broadly cover the area of the Laptev Sea shelf (Fig.1). These samples were examined by quantitative sand size fraction analyses and grain size measurements. Beside these surface samples, core IK 93 73-10 from the eastern Laptev Sea (75°20,8'N, 135°12,3'E) from a water depth of 47 m was selected for monitoring the temporal variabilities. Samples were taken at 5 cm intervals.

For studying the calcareous microfaunal components in the sediments all samples were freezed, dehydrated, then wet-sieved over 63 µm meshsize, and eventually dried. The simultaneous investigations of the spatial grain-size distribution gave evidence that surface sediments of the Laptev Sea are generally coarser than in the eastern part where silty clays dominate the surface pattern due to the large input of suspended matter by the Lena and Yana rivers (Lindemann, 1995). In addition, the eastern sediments were in particular dark in colour because of high organic contents. Therefore, most of these samples had to be treated with hydrogenperoxide (H_2O_2) to prevent the formation of aggregates during washing.

Since it was already realized during the early part of the sample processing that faunal constituents will remain rather low, the > 63µm size fraction was left unsplit in order to take into account every specimen for the qualitative determination down to species level. Later quantifications are expressed as specimens per weight dry bulk sediment.

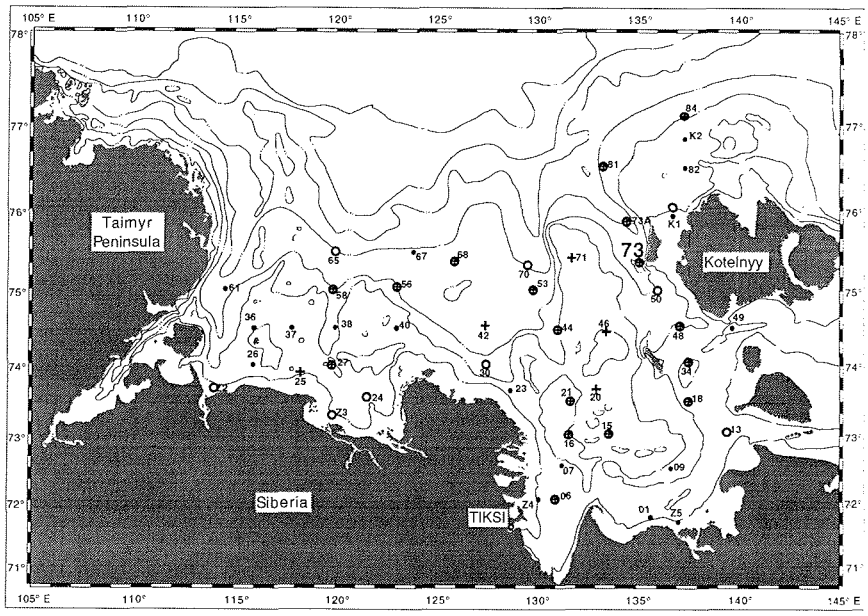

Fig.1: Laptev Sea Bathymetrie and the distribution of studied surface samples; the position of Core IK93 73-10 is also indicated (73).

Faunal Characteristics

The calcareous microfaunal assemblage in the Laptev Sea is mainly comprised of ostracods and benthic foraminifera. They exhibit a wide lateral distribution in the recent sediments (Fig. 1). Their low total number did not yet allow to recognized any pattern which could be linked to oceanographic characteristics. Nevertheless a relative high number of different species has been identified for both groups (Table 1); 33 species and genera of benthic foraminifera and 17 belonging to the ostracod assemblage respectively.

Tab.1: List of identified species and genera.

Benthic Forams	Ostracods	Planktic Forams
Ammotium cassis	*Actinocythereis dunelmensis*	*Globigerina bulloides*
Astaculus hyalacrulus	*Argilloecia spp.*	*Globigerinita glutinata*
Brizalina pseudopunctata	*Baffinicythere*	*Globoturborotalita tenella*
Buccella frigida	*Cluthia cluthae*	*Turborotalita clarkei*
Casidulina reniforme	*Cytheromorpha macchesneyi*	*Neogloboquadrina pachyderma* (d)
Cyclogyra involvens	*Cytheropteron arcuatum*	*Neogloboquadrina pachyderma* (s)
Dentalina frobisherensis	*Cytheropteron elaeni*	
Dentalina ittai	*Elofsonella concinna*	
Eggerella advena	*Heterocyprideis sorbyana*	
Elphidium bartletti	*Palmenalla limicola*	
E. excavatum f. *clavatum*	*Parcyprideis pseudopunctillata*	
E. incertum	*Polycope spp.*	
E. subarcticum	*Rabilimis septentrionalis*	
Elphi diella groenlandica	*Sarsicytheridea bradii*	
Epistominella mitis	*Sarsicytheridea macrolaminata*	
Fissurina sp.	*Sarsicytheridea punctillata*	
Globulina sp.	*Semicytherura complanata*	
Guttulina sp.		
Haynesina orbiculare		
Lagena gracillima		
Melonis barleeanum		
Miliolinella circularis		
M. subrotunda		
Nonion labradoricum		
Parafissurina himatiostoma		
Pyrgo williamsoni		
Reophax fusiformis		
Pseudopolymorphina sp.		
Recurvoides cf. *turbinatus*		
Saccammina atlantica		
Spiroplectammina biformis		
Stainforthia loeblichi		
Trifarina fluens		

Since the distribution of Arctic foraminifera is basically circumpolar only few species are governed by water depth (Löblich & Tappan, 1953). The most abundant foraminiferal forms, e.g. *Elphidium spp*, *Cassidulina reniforme* are opportunistic, tolerating low temperatures with at least winter sea ice cover and changing salinities. There are only low differences to the benthic foraminiferal assemblage in the Barents- and Kara seas were additionally some Atlantic forms occur (Polyak and Solheim, 1994). The benthic foraminiferal fauna in the Laptev Sea is dominated by infaunal or ubiquitous forms. They are also characteristic for a deltaic biotope (e.g., Vilks 1989; Steinsund et al. 1994).

The rare finds of agglutinated foraminifera, even in the surface and subsurface sediments, is a typical feature for sediments from the Eurasian Arctic shelf and probably results from desintegration during early diagenesis (Spiridonov et al. 1992) and/or the availability of suitable grain sizes.

As with the benthic foraminifera ostracods contained in Laptev Sea coretops (Table 1) are a very typical inner shelf Arctic Ocean assemblage that characterizes also the inner zone along the Alaskan and Canadian shelf (e.g. Cronin, 1989). Species such as *P. pseudopunctillata*, *Sarsicytheridea spp*, *H. sorbyana* and

Cluthia cluthae are the most typical representatives of this environment. Most of these species tolerate reduced salinities, in the case of Arctic shelves down to about 28-30 ppt, although several of these species also live at lower salinities in boreal regions. On most found specimens from the Laptev Sea appendages were still attached. This is good indication for a life assemblage demonstrating that these species do indeed live in this region and that the coretops represent youngest sediments.

Planktic foraminifera were not recognized in the studied surface samples. This is not much of a surprise for they are strictly speaking a pelagic group which is usually not encountered to that degree on shallow shelves. If they do occur their numbers are exceedingly low and sizes are small, which may indicate that transportation by surface currents is a likely potential mechanism, rather than that they actually represent an indigenous fauna.

All species listed in Table 1 have been identified from Core 93 73-10. Their composition nevertheless is rather unusual since some of these species do not occur in Arctic Ocean sediments. Indeed, they are not even representatives of subarctic regions such as the Norwegian-Greenland seas (e.g., Kellogg, 1984; Bauch, 1994). Whereas species such as *G. bulloides* and *G. glutinata* may invade the Laptev Sea via Atlantic derived waters across the Barents Sea or along the Eurasian continental margin, the presence of *G. tenella* and the minute species *T. clarkei* is not so easily explained.

Temporal Variability

The downcore faunal investgations of Core 93 73-10 indicate that both benthic groups, the foraminiferal and ostracodal assemblage, show a continuous record through time. Particularly the ostracods reveal the most significant changes (Fig. 2). This is in contrast to the planktic foraminifera which only exhibit two distinct levels, close to the surface and at a depth of about 70 cm. Especially the depth range between 70-80 cm stands out because the total number of benthic foraminifera and ostracods increases also. If this increase in raised numbers of the planktics is an indication for varying surface water masses i.e., stronger influence of marine water masses from outside the Arctic, then the question inevitably arises, where did they derived from? With our present data set we can only speculate on this matter, but it appears as if a solution has to do with variations in the output of freshwater from the large rivers into the Laptev Sea. Years with significant increase should result in a thicker freshwater lid which consequently would surpress circulation and favour sea ice formation. On the other hand Atlantic or Pacific water masses may be able to better penetrate the Laptev Sea region during times of reduced riverine outflow and in this way could cause a deposition of planktic foraminifera.

References:

Aagaard, K. and Carmack, E.C., 1989. The role of sea ice and other freshwater in the arctic circulation. J. Geophys. Res., 94: 14,485-14,498.

Baskakov, G., Borodachev, V., Dvorkin, Y., Mustafin, N. and Yanes, A., 1987. Hydrological and ice conditions of the shelf zone of the Arctic seas. In: Biological resources of the Arctic and the Antarctic. Nauka, pp. 15-48.

Bauch, H.A., 1994. *Beella megastoma* (Earland) in late Pleistocene Norwegian-Greenland Sea sediments: Stratigraphy and meltwater implication. J. Foram. Res., 24: 171-177.

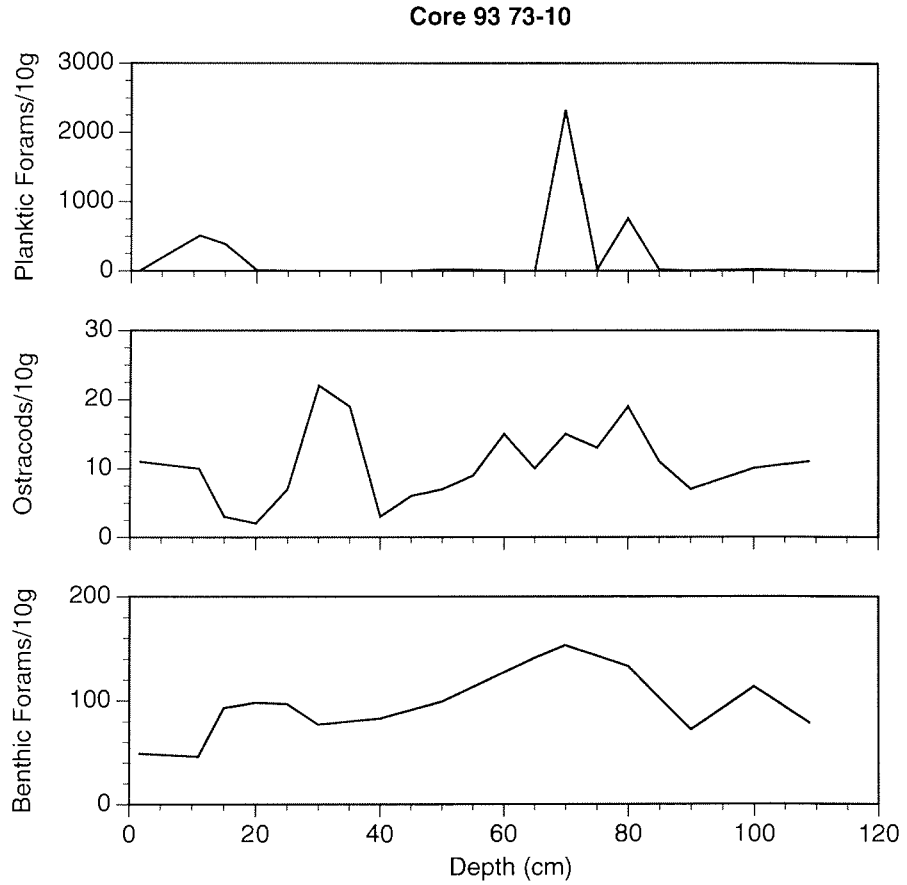

Fig. 2: Downcore variability of the calcareous microfauna from the eastern Laptev Sea.

Cronin, T.M., 1989. Paleozoogeography of post-glacial Ostracoda from north-eastern North America. In: Gadd, N.R. (ed.), Late Quaternary development of the Champlain Sea Basin: Geological Association of Canada Special Paper 35: 125-144.

Hanzlick, D., 1983. The West Spitsbergen Current: Transport, forcing and variability. PhD thesis, Univ. of Washington, p. 127

Holmes, M.L. and Creager, J.S., 1974. Holocene history of the Laptev Sea continental shelf. In: Y. Herman (ed.), Arctic Ocean sediments, microfauna, and climatic record in the Late Cenocoic Time: 211-229.

Kellogg, T.B., 1984. Paleoclimatic significance of subpolar foraminifera in high-latitude marine sediments. Canadian Journal of Earth Science, 21: 189-193.

Lindemann, F., 1995. Sonographische und sedimentologische Untersuchungen in der Laptevsee, sibirische Arktis. MSc thesis (unpubl.), p. 75.

Loeblich, A.R.J. and Tappan, H., 1953. Studies of Arctic Foraminifera. Smithsonian

Miscellaneous Collections, 121: 1-150.

Polyak, L. and Solheim, A., 1994. Late- and postglacial environments in the northern Barents Sea west of Franz Josef Land. Polar Res., 13: 197-207.

Spiridinov, M.A., Rybalko, A.Y. and Polyak, L.V., 1992. Late Quarternary stratigraphy and paleogeography of the eastern Barents Sea off central Novaya Zemlya.

Steinsund, P.I., Polyak, L., Hald, M., Mikhaylov, V. and Korsun, S., in press. Distribution of calcareous benthic foraminifera in recent sediments of the Barents and Kara Seas. J. Foram. Res.

Timokhov, L., 1994. Regional characteristics of the Laptev and East Siberian seas: climate, topography, ice phases, thermohaline regime, circulation. In: H. Kassens et al. (eds.) Russian-German cooperation in the Siberian shelf seas: Geo-system Laptev Sea. Berichte zur Polarforschung, 144: 15-31.

Vilks, G., 1969. Recent Foraminifera in the Canadian Arctic. Micropaleontology, 15: 36-60.

Distribution of Fe and Mn in pore waters and sediments of the Laptev Sea - Results of the expedition TRANSDRIFT I

C. Langner and TRANSDRIFT I Shipboard Scientific Party
Alfred-Wegener-Institut für Polar- und Meeresforschung, Forschungsstelle Potsdam, Germany

Introduction

This paper reports results of the Expedition TRANSDRIFT I carried out from August to September 1993 with the research vessel "Ivan Kireev" in the Laptev Sea.

The objectives are geochemical investigations of the distribution of Fe and Mn in pore waters and sediments in the shelf region of the Laptev Sea. The different geochemical behaviour of these elements affects their distribution in pore waters and sediments, which varies vertically as well as laterally. The distribution of Fe and Mn suggests an estuarine mixing as well as early diagenetic processes.

Sediment cores of two N-S profiles starting near the mouth of the Lena River (Bykowskaya Channel) and the Olenek River were investigated.

Working program and methods

From the cores, sediment samples for the extraction of pore waters were taken in fixed intervals: from 0 to 4 cm every centimetre, from 4 to10 cm every 2 cm, from 10 to 20 cm every 3 cm, from 20 to 30 cm every 5 cm, from 30 to 50 cm every 10 cm. Sediment pore waters were extracted on board ship with a centrifuge (15 - 20 min, 4500/min). The remaining solid phase was put into separate containers. Both sets of samples were stored at 4°C.

The concentrations of dissolved Fe and Mn were measured by ICP-Atomic Emission Spectroscopy. Sulfate was determined by Ion Chromatography and the major elements of the solid phase were analysed by XRF. The Fe-Mn concretions were investigated using REM/EDAX.

Results and discussion

The results of the investigations show distinct differences between the analyzed Laptev Sea sediments. The distribution of Fe and Mn in pore waters and solid phases are different as a consequence of bond type and geochemical behaviour. The distribution of these elements is influenced by geogenic detritus and by estuarine mixing and early diagenetic processes.

A. Distribution of Fe

The distribution of Fe in the solid phases is influenced by the sediments, which are transported to the Laptev Sea by rivers. The greatest part of Fe is bound on the clay minerals. Thus its distribution depends on the sedimentation processes. Two types of sedimentation are important: 1. sedimentation controlled by bathymetry and 2. sedimentation regionally controlled by the rivers. Within the deposition areas of the rivers in the Laptev Sea it is possible to characterize proximal and distal regions.

This strong differentiation within the N-S-profiles of Lena and Olenek is demon-

strated by the distribution of the maximum Fe-concentrations in pore waters (Fig.1). Fe-concentration decreases exponentially with increasing distance from the river mouths. This could be the result of agglomeration into flocs, where Fe is present as oxidhydrates.

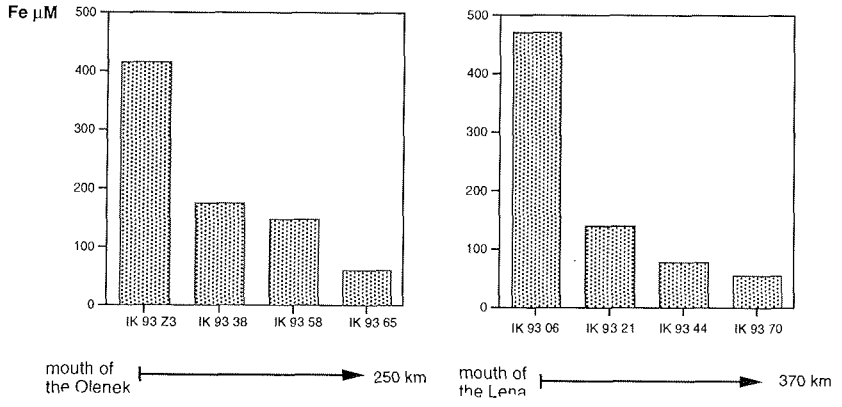

Fig. 1: Highest concentrations of dissolved Fe in pore waters of the Olenek- and Lena-profile.

A large volume of freshwater is supplied to the shelf region of the Laptev Sea by Siberian rivers, e.g. the Lena River and the Olenek River. During the mixing with saline water the dissolved Fe enters into a specific bond. Flocculation occurs. Iron is bound adsorptively on to the clay minerals or precipitates as oxidhydrates. Because of bond form in the sediments Fe can easily be mobilized during early diagenetic processes.

As a result of the flocculation the Fe concentration decreases in the mobilization horizon of the pore waters with increasing distance to the coast. It can be concluded that the highest Fe concentrations in the pore waters due to estuarine mixing processes.

B. Distribution of Mn

In contrast to Fe the distribution of Mn in the solid phases and pore waters of the sediments is predominantly influence by early diagenetic processes.

In the first centimetres of the sediment, dissolution of the Mn oxides occurs and thus the concentration of Mn in pore waters increases (Fig. 2). The highest concentration gradient of the Mn profiles is established under the sediment surface. This is caused by the mobilization of Mn in the suboxic layer, the upward migration of dissolved Mn and remobilization in the oxic layer. The concentrations in the solid phases at the surface exceed many times the average concentrations (Fig. 2). Mn is bound adsorptively at the surface of the clay minerals and / or is accumulated as oxides in crusted concretions at the sediment surface.

It is possible to distinguish geochemically oxic, suboxic and anoxic horizons in the sediment profiles. The characterization of the environments is mainly possible through the pore water profiles of dissolved Mn, Fe and sulfate and the distribution of MnO in the solid phases. It is assumed that the sediment cores are very similar in their diagenetic zonation (Fig. 3). The accumulation horizon of Mn at the sediment surface suggests a very small layer of an oxic environment, . The mobilization of Mn and Fe indicate suboxic environments. Because in most of the sediment cores no

reduction of sulfate could be found there is a rather larger suboxic horizon. In one core taken near the mouth of the Olenek the anoxic environment starts at a depth of 20 cm below under the sediment surface.

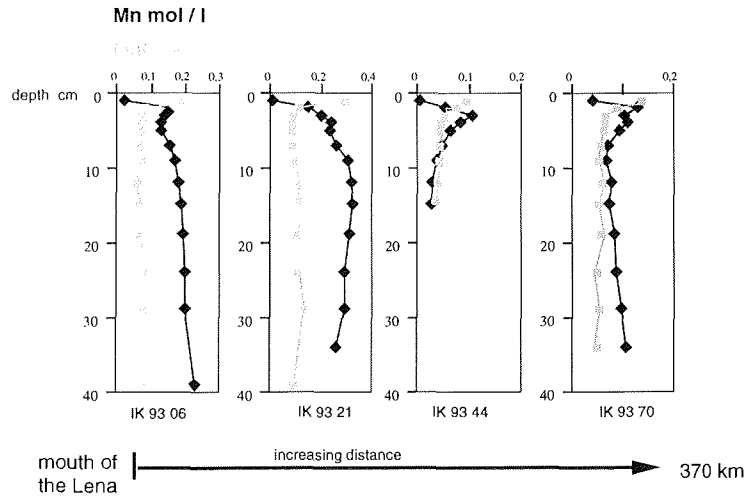

Fig. 2: Distribution of dissolved Mn in pore waters and MnO in solid phases. Lena-profile

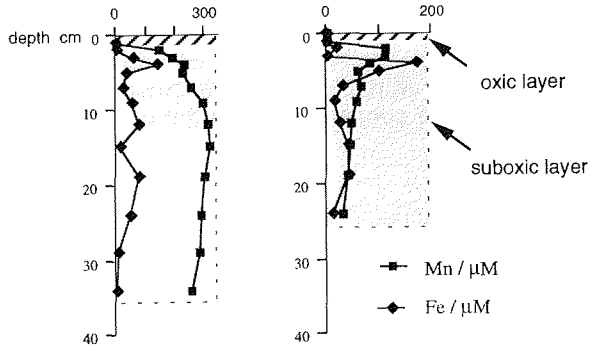

Fig. 3: Diagenetic zonation in the sediment cores and the different geochemical behaviour of dissolved Fe and Mn in pore waters of the sediments during early diagenetic processes.

C. Fe and Mn crusted shells

The analyses of Fe and Mn in crusted shells demonstrate that the major elements in these concretions are Si, Fe and Mn (> 5 %). Fe and Mn are present as oxides. Si is bound in quartz and silicates, which exist in the layers of the crusted shells. The analysis of crusted shells shows zonated Fe and Mn oxide precipitates (Fig. 4) on the sediment surface, which is a consequence of early diagenetic mobilization / remobilization and estuarine mixing processes.

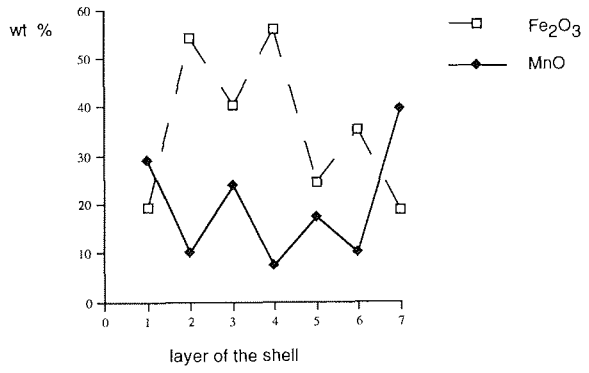

Fig. 4: Distribution of Fe_2O_3 and MnO in the layers of the crusted shell. The first layer is beginning outside of the shell and the last layer is located in the middle of the crossection of the shell.

HOLOCENE SEDIMENTS OF THE RUSSIAN EAST-ARCTIC SEAS

D. S. Yashin and V. A. Kosheleva
VNIIOkeangeologiya, St. Petersburg, Russia

Five lithological units can be discerned in late Pleistocene-Holocene, which correspond to respective climatic stages. Their paleontologic, mineralogic and geochemical features are considered. The present paper presents the lithostratigraphic and paleogeographic parameters of late Pleistocene-Holocene sediments. Features of the Holocene sedimentogenesis, typical of the polar regions, are considered as well.

Bottom sediments of the Laptev, East-Siberian and Chuckchi Seas have regularly been studied by AARI and NIIGA since the fifties. All the data obtained mainly on the surface sedimentary layer were processed by Yu.P. Semenov (1961, 1965). In 1976-1988, regular investigations of new quality were carried out by the geologists of VNIIOkeangeologiya O. V. Kirillov, O. N. Kuleshova and I. I. Rozhdestvenskaya. In this period, masses of 2-3 m long cores were gained. As a result, the stratigraphic range and the age of the sediments sampled could be extended. It was possible to begin studying their organic geochemical components. A great deal of diverse data obtained at both investigation stages was analyzed and integrated in a study conducted at VNIIOkeangeologiya (D.S.Yashin et al., 1990). However, investigations of these offshore areas are hitherto in its initial stage except for some local segments (1-2 stations each 1000 km^2). The East-Siberian Sea as well as the marginal shelf and the continental slope within the Laptev and Chuckchi Seas are the least studied.

A division of Holocene sediments into lithological types is based upon the classification of a dominant fraction, considering certain quantitative combinations of sand (1.0-0.1 mm), aleurite (0.1-0.01) and pelite (under 0.01 mm) fractions. Sediments containing more than 75% of one fraction are referred to sands, aleurites or clays, respectively. Mixed sediments (sands aleuritic, aleurites clayey etc.) contain 50-75% of the main fraction (begining the name of the sediment) and 25-50% of the other one.

At the end of Pleistocene development of the Arctic shelf the World ocean level considerably sank. The late Cenozoic Laptev-Chuckchi shelf consists of alluvial and lacustrine-alluvial sediments. The flat subdued relief is the sharpest contrast in the western region. The landscape was most probably close to the reglacial: dry cold and forestless areas prevailed. Deposits developed on the shelf are similar in their granulometric composition to those developed the in forests of northern Yakutiya and Chukotka. Their high density may be explained by the nature of the reglacial weathering.

The sediments which are the subject of the present investigation belong to the latest transgression beginning 12 thous years ago. This transgression was the start of a new hitherto unfinished cycle of the Arctic shelf development.

A typical feature of the Holocene sedimentogenesis at the East-Arctic shelf is that, independently of the distance from the shoreline, a stratum has formed (and is formed now) nearly throughout, which spreads over 3000 km and is built up mainly by aleurite and pelite fractions the ratio of which is virtually invariant through the section. Relatively coarse sediments (sand, aleurite-sand) are locally formed (Central-Laptev, Alaska shelves), mostly in the initial stages of the transgression.

In the section of cores in the Laptev and East-Siberian Seas, five units are discerned on the basis of their texture, colour and consistency. In one section they

are rarely recorded because of the wide development of intraformational erosion observed throughout the Holocene section. However, they are usually recognizable and comparable despite of the local distance of the sections.

The section is composed as follows (upward):

Unit V Sands, sands aleuritic and clayey, bluish-dark-grey, very dense (over 2.0 g/cm^3), dry. The lack of any inclusions is typical. The thickness is 0.6 m. A fine-lattice and thinly lamellar cryogenic structure of sediments, that points to their freezing, is occasionally observed.

Unit IV Sandy clays, sands aleuritic dark-grey, viscous, less dense (1.8-1.9 g/cm^3). Mollusk test inclusions, rare black spots, occasionally hydrosulphuric smell. The penetrated thickness is 0.8 m.

As supposed by O. F. Baranovskaya, the microfauna found in both units (Laptev Sea) shows that the composition of associations is extremely unstable. This is indicative of very disalted cold conditions (coastal or deltaic facies). The shallow-water Eurybionite *Ammotium cassis* (Parker) dominates in the lower unit. In the overlaying one the dominanting *Reophax curtus, Haykesina orbicularis, Eggerella advena* vary at a minor distance from each other. O. F. Baranovskaya is of the opinion that sedimentation has upward changed the units' section from alluvial-marine to marine-transgressive as judged from a combination of all paleontological parameters. A similar change took place at the Pleistocene-Holocene boundary.

Unit III Aleurites, aleurites sandy and clayey, clays aleuritic. The density gradually increases with increasing depth (down the section) from 1.6 g/cm^3 to 1.8 g/cm^3. A great deal of laminas, inclusions and attachments of black decomposed organics, causing the dark-grey colour of sediments, is a typical feature. Inclusions contain abundant fragments of mollusk tests and half-decomposed Polychaeta pipes. There is a well-defined contact with sediments of unit IV (different composition, colour, consistency). Sediments of this horizon are found in most of the cores and nearly throughout the shelf segments with a depth of more than 30 m. The maximum penetrated thickness is 1.6 m.

Unit II Aleurites, their sandy and clayey equivalents, at a depth of up to 15 m mostly sands. The colour varies from dark-grey in the basement to greenish-grey in the upper section. Sediments often show a cloddy structure, rare black spots are observed in the basement. The density is 1.4-1.6 g/cm^3. The horizon is developed by fragments. Dense sands of unit IV overlap at a depth of up to 15 m. A boundary between sediments of unit II and III is tentatively can be discerned from the abrupt reduction of black fine-dispersed product. The maximum thickness is 1.0 m.

Unit I Surface sediments are mostly composed of aleurite and overlap different Holocene horizons. They are of semi-fluid consistency. The thickness is 0.1-0.5 m.

According to O.F. Baranovskaya, the sediments of the Laptev Sea, which belong to the units I-III, contain a similar stable microfauna complex differing from the one of the units IV and V. The species *Eggerella advena* dominates with rare exception. The widely observed species *Protconella atlantica*, *Reophax curtus*, *Cunlata arctica*

etc. constitute complex sediments. Sediments of units I and II are characterized by the lack of plankton and deep-sea fauna. The microfauna complex in unit III is richer and more diverse. L. V. Polyak has marked the presence of the plankton *Neogloboquadrina pachyderma* and the exotic *Cassidulina teratis*, *Bulimina cullata* that suggests an inflow of Atlantic waters which was more intensive than it is at present. On the basis of the combined properties, the sediment formation of unit III may be referred to the Holocene climatic optimum.

The most entire Holocene section in the Chuckchi Sea is its central part of the Chuckchi basin. 4 diatom complexes are found here by Ye.I.Polyakova in the continuous 4 m long section of aleurite-clay sediments sampled in the southeastern Chuckchi basin. She correlates them (upward) with the Boreal, Atlantic, Subboreal and Subatlantic of the Holocene (Polyakova, 1984, 1988). The continuous sedimentation in the Chuckchi basin and a reflection of all the above-named climatic epochs of the Holocene in the section were also inferred by Kh.M.Saidova (1982) from microfauna. Holocene sediments of the Chuckchi basin are more than 4.6 m thick (non-penetrated foot).

Holocene sediments of the Alaska shelf in the Chuckchi Sea are sandy and aleurite-sandy containing dispersed gravel and fragments of broken shell. Their thickness varies from 0.6 to more than 2.4 m. The diatom complexes found by Ye.I.Polyakova as well as the gravel and pebble interbeds suggest a discontinuous sedimentation and the presence of gaps corresponding to various temporal intervals of the Holocene.

Hence, the complex analysis of organic remnants and structural features of the Holocene section indicates that the western (Laptev shelf) and the eastern (Chuckchi shelf) parts of the basin were noticeably dissimilar. In the former part, Holocene sediments were mostly formed in shallow water and are strongly influenced by continental waters, as it is proved by the lack of plankton and deep-sea fauna. Arctic species of the microfauna dominating in the complex indicate that the conditions were typical of the inner shelf of recent polar seas which showed insignificant variations as judged from the stability of the main parameters. Another typical feature is the great amount of cryophylic diatoms in sediments. This points to a high glaciation of the Laptev basin. The Chuckchi basin was formed in the Holocene as a marginal sea: it was deeper (up to 50 m), less influenced by the continent and had a periodical connection with the Pacific Ocean. Thus, deep-sea plankton and a far less content of fresh-water diatoms are found in the Holocene section.

The analysis of granulometric fractions in correlation with water depth carried out for the Laptev Sea provides information about peculiar features of the recent sedimentogenesis. The bathymetric control is clearly recorded merely for the pelite fraction except for its fine-dispersed component (less than 0.001 mm). Grains of the sand and aleurite fractions are always absolutely passive to the depth parameter. A sharp antipode of the sand fraction is not only the pelite but the fine-aleurite fraction (0.05-0.01 mm) as well. The coarse aleurite fraction (0.1-0.05 mm) behaves similarly to the sand one as as compared with the pelite fraction. However, there is no evidence of a positive interrelation between the sand and the coarse aleurite fractions.

As inferred from the above, after the fine and the coarse particles are separated near the coast, the major part of the coarse aleurite particles does not turn into suspension migrating then into the deep-sea part of the basin, but remains in the shallow water as the sand fraction does. They show an exclusively individual distribution within the shelf and are usually independent of the water depth. Hence, the analysis suggests that the processes of mechanical differentiation which are

responsible for sediment distribution in offshore areas of a humid zone are strongly smothered in the polar area. The significant part of terrigenous detritus arrives at the bottom because it melted out of ice. Therefore, the detritus distribution on the shelf depends neither on the basin's depth nor on the location relative to the shoreline.

Thus, Holocene formations of the East-Arctic seas are mostly presented by a stratum of corygenic sediments composed of aleurite and pelite fractions in different ratios. Their distribution curves are close to maximum contents in the vicinity of average values. The persistant composition of recent sediments on the major parts of the shelf is also indicated by average and median values for the aleurite (especially) and pelite fractions. The distribution curve of the sand fraction is radically different: the maximum content is sharply biased to ward minimum values, median and average statistics are accordingly very different.

Holocene sediments are of biogenic-terrigenic nature in the central Chuckchi Sea where a 'stagnant' zone is formed due to hydrodynamic features. Along with the terrigenous sedimentogenesis there is an intensive precipitation of silicic acid (up to 14% of SiO_2).

Fields of sand extend as a narrow band along the coast, cover shallow-water zones of the central Laptev shelf and the bottom in the vicinity of the Wrangel island and the Gerald bank where they are especially enriched by gravel-pebble products.

The mineral composition of the sediments is presented largely by quartz and feldspar. The latter prevails in the light fraction in most parts of the Laptev and East-Siberian Seas. Quartz dominates in sediments of the Chuckchi Sea and in coastal segments of the other seas. Poor quartz are rare and observed only in the vicinity of the Wrangel island. In the Chuckchi Sea and near the river mouths on the Laptev shelf, grey wackes are prominent. Their light fraction contains more than 25% of rock fragments.

References

Polyakova, Y. I., Vozovik, Yu.I., 1984. Some problems of the Chuckchi Sea development during the Holocene (from diatom complexes). In: Okeanologiya. V.XXIV. N 5, p. 789-793.

Polyakova, Y. I., 1988. Diatoms of the USSR Arctic seas and their role in investigation of bottom sediments. In: Okeanologiya. V.XXVIII. N 2, p. 286-292.

Saidova, Kh. M., 1982. The Holocene stratigraphy and paleogeography of the Chuckchi Sea and Bering Strait as inferred fromforami nifera. In: Problema geomorfologii, litologii i litodinamiki shelfa. Moscow: Nauka, p. 92-114.

Semenov, Yu. P., 1961. Formation conditions of bottom sediments in the Laptev Sea. In: Geologiya morya. V.I. Leningrad, p. 47-53.

Semenov, Yu. P., 1965. Some features of formation of bottom sedi ments in the East-Siberian and Chuckchi seas. In: Antropogeno vyi period v Arktike i Subarktike. Leningrad: NIIGA. V.143, p. 350-352.

STRUCTURAL PATTERN AND TECTONIC HISTORY OF THE LAPTEV SEA REGION

S. S. Drachev*, L. A. Savostin+ and I. E. Bruni°

* P. P. Shirshov Institute of Oceanology, Russian Academy of Sciences, Moscow, Russia

\+ Laboratory of Regional Geodynamics, Moscow, Russia

° State Research and Production Enterprise "Airgeology", Moscow, Russia

Introduction

The Laptev Sea is a part of the Eurasia Arctic margin between the Taimyr Peninsula and the Novosibirsk Islands (Fig. 1). It is the southern termination of the Nansen-Gakkel spreading ridge and thus the location of structural features resulting from a continental margin/spreading ridge intersection. It is a natural laboratory for addressing the processes of an initial breaking-up of the continents.

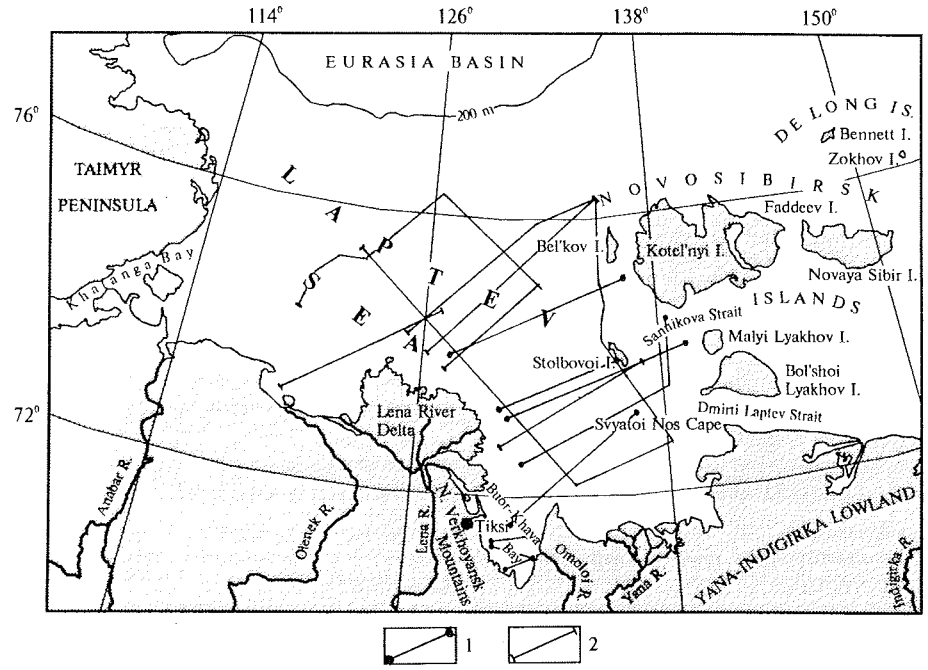

Fig. 1. Index map of the Laptev Sea Region and location of the multichannel seismic reflection profiles carried out by: 1 - LARGE (1989), 2 - MAGE (1986 and 1987).

The initial concept of the Gakkel Ridge propagation into the Laptev Sea Shelf was proposed by Grachev with co-authors at beginning of 1970's after the spreading nature of the Eurasia Basin's sea floor was established (Grachev et al., 1970). However, prior to the middle of 1980's the contours of the predicted shelf rift system could only be delineated by the bathymetric and a few gravity data (Grachev, 1982).

The present-day understanding of the Laptev Sea Shelf geology is based on the Russian multichannel seismic reflection data obtained by the MAGE (Marine Arctic Geologic Expedition, Murmansk) and the LARGE (Laboratory of Regional Geodynamics, Moscow) during 1986-1990. These data allowed delineation of the rift system structure and the seismic stratigraphic features of its sedimentary filling (Ivanova et al., 1990; Drachev and Savostin, 1994; Sekretov, 1993).

In this paper we will demonstrate what is now well-established concerning to the Laptev Sea Shelf geology and what remains to be solved. We are utilizing the data collected by the authors during several onshore and offshore expeditions to the Laptev Sea from 1985 to 1991. The available data of the MAGE's 1986-1987 seismic surveys were used also for preparation of the structural maps.

Tectonic setting of the Laptev Sea Shelf

From geologic point of view this region is characterized by two important features. On the one hand, it occupies an area where the Siberian Craton, Early Mesozoic Taimyr Fold Belt and Late Mesozoic Novosibirsk-Chukchi and Verkhoyansk-Kolyma fold belts join (Fig. 2). Tectonic history of this poorly known structural ensemble underlying the shelf sedimentary basin was very long and its structure was formed finally during a Late Mesozoic orogenic event. On the other hand, it is one of two places in the world where an active mid-oceanic ridge enters a continent. This Arctic termination (the Nansen-Gakkel Ridge) of the Mid-Atlantic Ridge System is the boundary of the North American and Eurasian lithospheric plates and is near the pole of plate rotation and thus the spreading rate is very low at less than 0.35 cm/yr. The spreading of oceanic lithosphere is creating a tensional force on the continental shelf. This process has caused the origin and development of the Cenozoic Laptev Sea Rift System (LSRS). The general concept of the Laptev Sea Shelf geology can be derived from consideration of the surrounding continental areas. These onshore data are the only base for an interpretation of the seismic survey results because there are no the offshore drill-holes.

Pre-Late Cretaceous basement

The basement of the shelf sedimentary basin is well-exposed within near-shore areas and western part of the Novosibirsk Islands. Practically everywhere it is composed of the Paleozoic and Mesozoic carbonate and terrigenous complexes of the ancient passive continental margins deformed by the folds and thrusts during the second half of the Cretaceous (Fig. 3).

The Upper Paleozoic to Jurassic Verkhoyansk clastic complex of up to 7-10 km thick forms the South Taimyr, Olenek (Lena-Taimyr), and Verkhoyansk folded zones. It is underlain by the Riphean-Middle Paleozoic carbonate and clastic-carbonate formations belonging to the marginal parts of the Siberian Craton and represents a sedimentary prism of the Siberian passive margin. This old passive margin probably extends northeastward up to the Stolbovoi and Malyi Lyakhov Islands where the Upper Jurassic to Lower Cretaceous clastic turbidites similar to the Verkhoyansk Complex are exposed (Ivanov et al., 1974). The Kotel'nyi and Bel'kov Islands belong to the Novosibirsk-Chukchi Fold Belt. They are characterized by practically uninterrupted sequence of the carbonate and terrigenous rocks from the Ordovician to the Upper Mesozoic with total thickness of 6-10 km (Kos'ko et al., 1990). The Upper Paleozoic and Lower Mesozoic complexes differ significantly from the coeval Verkhoyansk Complex. This may indicate that an area of these islands was not been connected with the Siberian continental margin at this time.

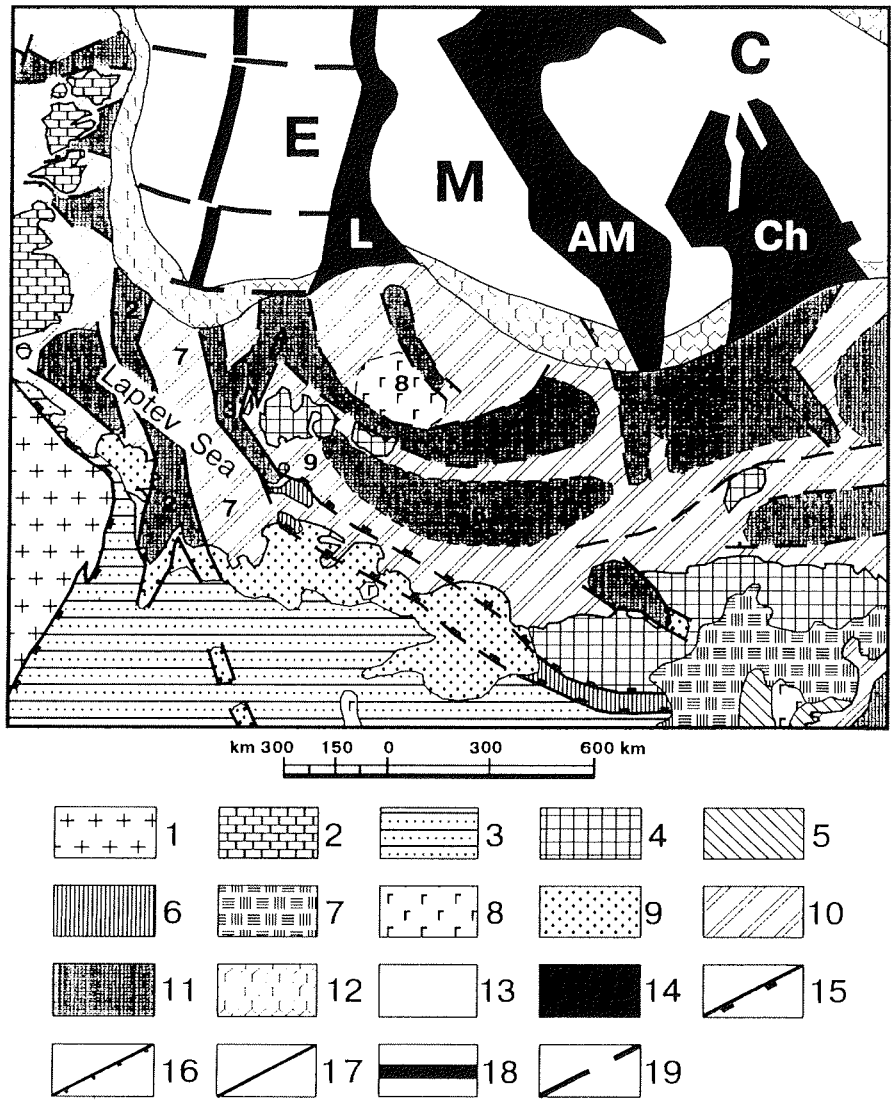

Fig. 2. Tectonic scheme of the Eastern Arctic Region. 1 - Siberian Craton; 2 - Early Mesozoic Taimyr Fold Belt; 3-4 - Late Mesozoic fold belts: 3 - Verkhoyansk-Kolyma, 4 - Novosibirsk-Chukchi; 5 - Koryak-Kamchatka Cenozoic fold belt; 6 - Late Mesozoic South Anyui-Lyakhov Suture; 7 - Cretaceous Okhotsk-Chukchi Volcanic Belt; 8 - Late Cretaceous to Eocene riftogeneous tholeiitic basalts; 9 - Cenozoic sedimentary cover and grabens on the land; 10 - uplifts and horsts within the shelves; 11 - shelf sedimentary basins; 12- continental slope; 13 - oceanic basins; 14 - intraoceanic ridges and uplifts; 15-19 - the main tectonic fracture zones (are dashed where inferred or uncertain): 15 - reverse faults and thrusts, 16 - normal faults, 17 - strike-slip faults, 18 - Nansen-Gakkel Spreading Ridge, 19 - transform faults. The letters and numbers are: E - Eurasia Oceanic Basin, M - Makarov Oceanic Basin, C - Canada Oceanic Basin, L - Lomonosov Ridge, AM - Alpha-Mendeleev Ridge, Ch - Chukchi Borderland, 1 - South Laptev Basin, 2 - Ust' Lena Rift, 3 - Bel'kov-Svyatoi Nos Rift, 4 - Anisinsk Basin, 5 - Novosibirsk Basin, 6 - Blagoveshchensk Basin, 7 - East Laptev Uplift, 8 - De Long Volcanic Uplift, 9 - uplift of the Novosibirsk Islands.

The South Anyui-Lyakhov Suture separates the Novosibirsk-Chukchi and Verkhoyansk-Kolyma fold belts (Fig. 2) (Natal'in and Parfenov, 1983). In part of the shelf area it comprises Svyatoi Nos Cape and Bol'shoi Lyakhov Island and is poorly expressed in geophysical data to the west. The suture is characterized by fragments of the Upper Paleozoic spreading ophiolites, the Upper Jurassic to Lower Cretaceous island arc volcanic rocks, as well as granodiorites and granites with isotopic age 110-90±5 Ma (Drachev and Savostin, 1993). The island arc and granitic complexes are an evidence of a collision in middle of Cretaceous.

The folds of the Taimyr Peninsula, Northern Verkhoyansk Ranges and New Siberian Islands are cut by shoreline and presumably continue into adjacent parts of the shelf. The Olenek Fold Zone traces along the shoreline extending to offshore at it's northern part (Fig. 3). Some investigators consider this zone as a marginal part of a shelf continuation of the Verkhoyansk Fold Belt which changes the strike in the Lena River Delta (Zonenshain and Natapov, 1989). According to the other point of view, the Olenek Zone is a narrow inverted aulacogen which separates the Siberian Craton from it's outermost part, the Laptev Sea Block, within western part of the shelf (Vinogradov, 1984).

Enisei-Khatanga Rift separates the Siberian Craton from the Taimyr Fold Belt (Fig. 3). The most eastern part of it occupies the Khatanga Bay and probably some ajacent area of the shelf. The rift is filled up by the Permian to Upper Cretaceous clastic marine, lagoonal and continental sediments. The total thickness of the rift filling varies from 2-3 km on the east to more than 9 km on the west.

Upper Cretaceous to Cenozoic sedimentary cover

Sequences of sedimentary cover are widespread within the Yana-Indigirka Lowland (Fig. 3) which is onshore continuation of the shelf sedimentary basin, as well the Lena River Delta, eastern part of Novosibirsk Islands, and several small grabens in North Verkhoyansk Mountains. Continental sediments predominant everywhere. Several sedimentary sequences bounded by regional unconformities have been established within the onshore Cenozoic key-sections (Fig. 4).

The Upper Cretaceous sequence outcrops on the Novaya Sibir Island is composed of Cenomanian and Touronian continental clays, silts, sands and lignites with the thickness of more than 300 m.

Paleocene to Lower Eocene sequence of continental sandy-argillaceous coal-bearing sediments occurs within the grabens of North Verkhoyansk Mountains and the Yana-Omoloi watershed area. They overlie the folded basement and have a thickness of several hundreds of meters. There are the thin caoline-hydromicaceous weathered crusts in many places within the mainland and on islands of the same age corresponding to regional peneplain conditions (Patyk-Khara and Laukhin, 1986; Kim, 1986).

The Middle to Upper Eocene sequence represents a major component of the sedimentary fill of the onshore grabens. It consists of continental and littoral (northern part of the Faddeev Island) argillaceous sediments containing abundant carbonized wooden material and lignite beds. The thickness of the sediments varies from several tens meters up to 1300 m (Mezhvilk, 1958).

The Oligocene to Lower Miocene sequence (several hundreds of meters thick) consists mostly of the sandy-argillaceous continental sediments which are characterized by numerous local stratigraphic unconformities and an increase of coarse grained material upward in the sections. These sediments were deposited during the Oligocene regression which is clearly identified throughout the East Arctic region (Patyk-Kara and Laukhin, 1986). Continental sedimentation was preserved in areas around Laptev Sea up to the end of Pliocene.

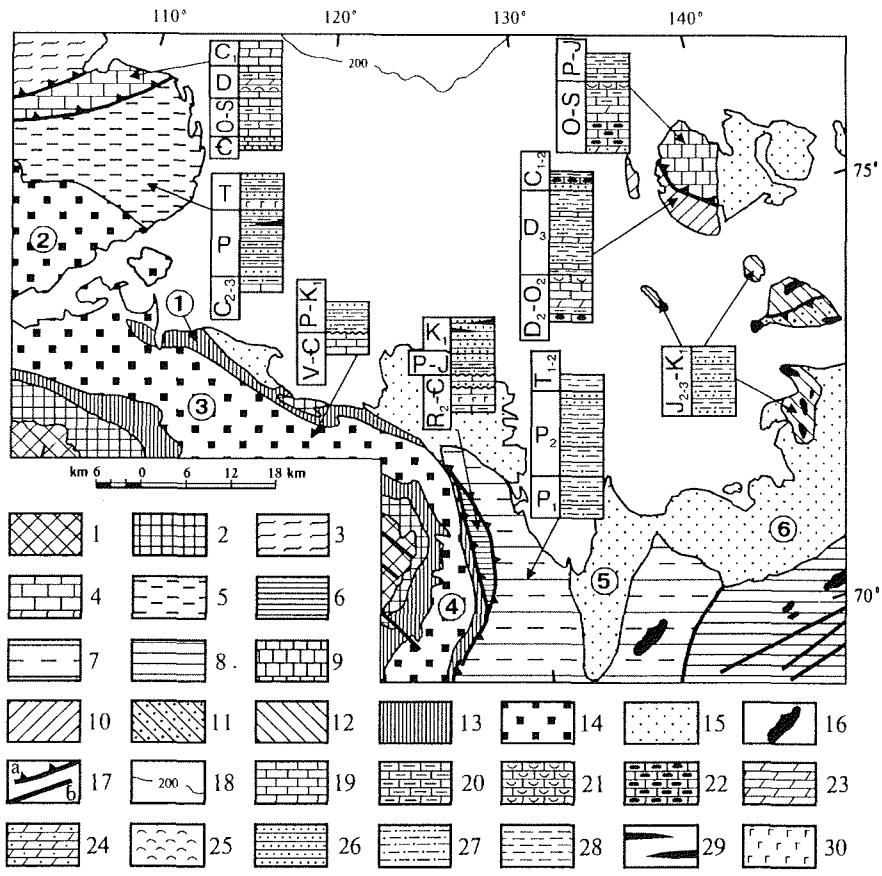

Fig. 3. Tectonic map of the Laptev Sea Rim (adapted from Okulitch et al., 1989). 1-2 - Siberian Craton: 1 - Riphean and Lower Paleozoic carbonates, 2 - Permian and Triassic clastic rocks; 3-5 - Early Mesozoic Taimyr Fold Belt: 3 - Kara Massif, 4 - North Byrranga Zone, 5 - South Taimyr Zone; 6-8 - Verkhoyansk-Kolyma Late Mesozoic Fold Belt: 6 - Tuora-Sis Zone (deformed cover of the Siberian Craton), 7 - Verkhoyansk Zone, 8 - Polousnyi Zone (Triassic and Jurassic clastic and volcano-clastic turbidites); 9-10 - Anzhu Structural Unit of the Novosibirsk-Chukchi Late Mesozoic Fold Belt: 9 - Kotel'nyi Zone, 10 - Bel'kov-Nerpalakh Zone; 11-12 - Lyakhov Late Mesozoic Suture: 11 - Upper Paleozoic clastic turbidites, metabasites and MORB-type ophiolitic rocks, 12 - Jurassic and Lower Cretaceous (?) terrigenous and volcano-clastic turbidites, island arc basalts and calc-alkaline lavas; 13-14 - Mesozoic depressions and foredeeps: 13 - Triassic and Jurassic sallow marine clastic sequence, 14 - Cretaceous marine to continental clastic sequence; 15 - Cenozoic sedimentary cover; 16 - granitic intrusions; 17-fractures (a - thrusts, b - strike-slip faults); 18 - bathymetric contour in meters; 19-30 - lithologic patterns (for the columns only): 19 - carbonate rocks (mainly limestones), 20 - clayey carbonates; 21 - bioclastic carbonates, 22 - limestone with nodules of chert, 23 - dolomites, 24 - sandy dolomites, 25 - gypsum and anhydrides, 26 - sandstone, 27 - siltstone, 28 - mudstone, 29 - brown coal; 30 - basalts. The numbers in the circles mark: 1 - Olenek Fold Zone, 2 - Enisei-Khatanga Rift, 3 - Lena-Anabar Depression, 4 - Pre-Verkhoyansk Foredeep, 5 - Omoloi Graben, 6 - Yana-Indigirka Depression (lowland).

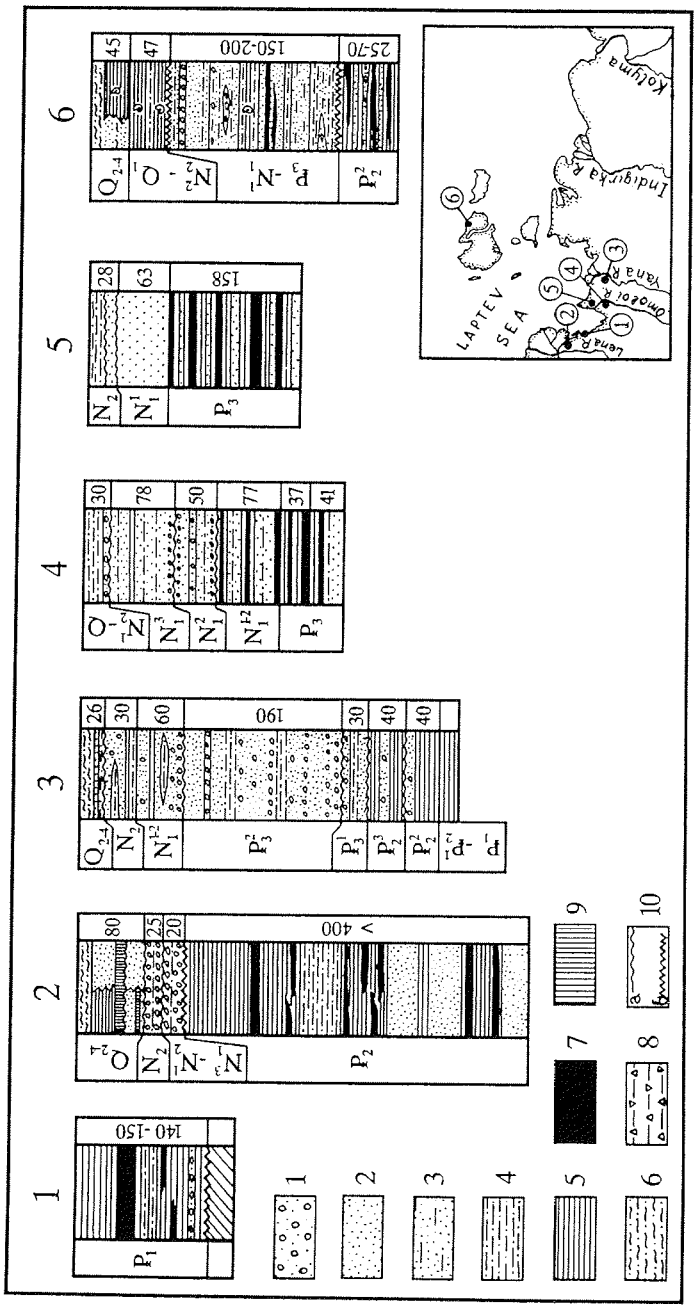

Fig. 4. Cenozoic stratigraphic-lithologic column of eastern Laptev Sea Region (from: Trufanov et al., 1979; Strepetova et al., 1981; Koval'skii, 1985; Grinenko et al., 1989). Location: 1, 2 - North Verkhoyansk Mountains (1 - Sogo Graben, 2 - Bykov Stream Graben), 3-5 - Yana-Omoloi watershed area (3 - Ust' Yana Graben, well-15; 4 - Omoloi Graben, well-103; 5 - Ortostan Uplift, well-213), 6 - Nerpichii Cape, northern Faddeev Island (see also map in the right lower corner). 1 - fine and coarse gravel; 2 - sand; 3 - loamy sand; 4 - silts and sandy silts; 5 - muds; 6 - loam; 7-brown coals; 8-weathered crust; 9-lenses of ice; 10-stratigraphic (a) angular (b) unconformities.

The Upper Miocene sequence up to 50-100 m of thickness has been described in grabens of North Verkhoyansk Mountains and northern part of the Cherskii Range. It is represented by interbedding of the continental sands and clays, containing abundant carbonized wooden material. Some tendency toward coarse grained material increasing upsection is noted there (Grinenko et al., 1989; Koval'skii, 1985).

The Pliocene sequence differs from the Upper Miocene one by a higher content of the coarse grained clastic material related to the rapidly elevating Cherskii Range within the mainland (Koval'skii, 1985). The thickness of the sediments reach several tens of meters.

The Upper Pliocene to Quaternary sequence forms a continuous horizontal cover of several ten to several hundred meters thick. The sections located onshore farther from the coast are composed by continental sediments only, while within the near-coastal areas and on the islands the marine and littoral sandy-loamy and loamy sediments predominant. The formation of this sequence was connected with a series of the transgressions. The first of them took place at end of the Pliocene and reached the areas of the present shoreline (Laukhin and Patyk-Kara, 1985; Patyk-Kara and Laukhin, 1986).

Plate tectonic framework

The evolution of the Arctic is connected with a creation and disintegration of the Laurasia supercontinent (Zonenshain et al., 1987). The latest stages of these tectonic processes took place in the East Arctic Region. Several terrane accretions to the Siberian continental margin at Mesozoic time with the following rifting of the Mesozoic tectonic collage produced by the spreading within deep water Arctic basins determined the main structural features of the heterogeneous basement and sedimentary cover of the shelf sedimentary basins. The history of the East Arctic fold belts was described in detail by Fujita (1978), Churkin (1981), Savostin with co-authors (1984b), Zonenshain and Natapov (1989) and others researchers. Here we will settle on a kinematics of the Eurasia Basin opening which caused a greatest effect on a development of the Laptev Sea Shelf (see also: Karasik, et al. (1983), Savostin and Karasik (1981), Savostin et al. (1984a), Savostin and Drachev (1988)).

The end of Late Cretaceous, Paleocene and Eocene were the time of the initial and most active rifting within Laptev Sea Shelf (Fig. 5, 56 Ma). The spreading rates in the Eurasia Basin reached a maximum value at 2 cm/year at the Eocene. During this time all of main structural features of the LSRS were formed. The development of the grabens was not accompanied by an arch growth that is reflected in a size composition of the synrift sediments.

At the Eocene-Oligocene boundary the change of the lithospheric plate movements took place (Fig. 5, 36 Ma). As a result the pole of North America/Eurasia plate rotation was shifted northward of the New Siberian Islands. This event led to compression within the Laptev Sea Region. In many places the Upper Cretaceous to Lower Miocene sediments are affected by thrust-fold dislocations. They are on the Novaya Sibir and Faddeev Islands, within the grabens of North Verkhoyansk Mountain and at some places of the Yana-Indigirka Lowland (Vinogradov, 1984; Savostin and Drachev, 1988; Grinenko and Imaev, 1989). Geological data indicate an Oligocene to Middle Miocene age for these dislocations. Within the Eurasia Basin the plate divergence continued, but with very low rate (0.2-0.3 cm/year).

From the Middle Miocene the Laptev Sea Shelf is affected gradually by an extension again (Fig. 5, 20 Ma). By the Late Miocene and Pliocene the rate of plate

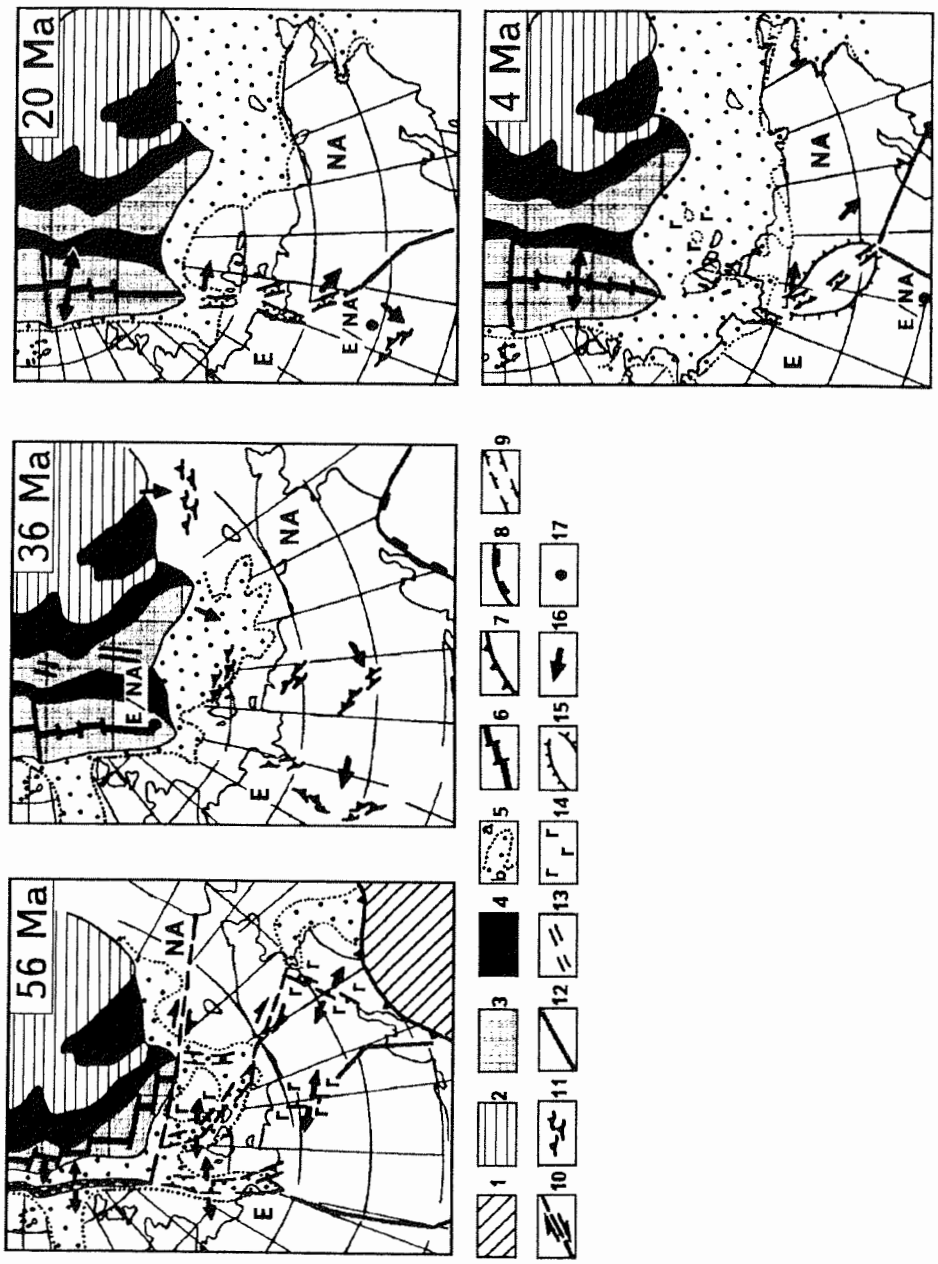

Fig. 5. Cenozoic plate tectonic reconstruction of the Eastern Arctic (Eurasia is fixed). 1 - Pacific Plate; 2 - Canada Late Mesozoic Oceanic Basin; 3 - Eurasia and Makarov oceanic basins; 4 - intra-oceanic ridges and uplifts; 5 - continental (a) and shallow seas (b); 6 - active spreading axis; 7 - subduction zone; 8 - obduction zone; 9 - continental rifts; 10 - transform and strike-slip faults; 11 - fold-and-thrust dislocations; 12 - boundaries of the lithospheric plates and microplates; 13 - spreading axis; 14 - continental riftogeneous basalts; 15 - Cherskii synrift arch; 16 - directions of North American Plate and microplates movements relative to the Eurasian Plate; 17 - Eurasian/North American plates rotation pole.

divergence within the Eurasia Basin increased up to 1.2-1.5 cm/yr. It was accompanied by faulting and significant subsidence within the shelf sedimentary basins. Within the continent the large Cherskii Arch complicated by Moma Rift was formed in the Pliocene (Fig. 5, 4 Ma). The compressional structures are unknown in this part of the sedimentary cover but extensional structures, mostly normal faults, are widespread here (Savostin and Drachev, 1988).

It was hypothesized earlier that the latest extension still is occurring (Zonenshain et al., 1978; Savostin et al., 1984a). Later it was established that the mechanisms of the Cherskii Range earthquakes are mainly dominated by sinistral strike-slip fault and reverse fault displacements (Parfenov et al., 1988; Imaev et al., 1990). Cook with co-authors (1986) based on the seismological data calculated the present-day Euler Pole of the Eurasian and North American plates to be near the Buor-Khaya Gulf coast.

Thus the plate kinematic data show that the LSRS developed under direct influence of the Eurasian/North American plates interaction. It means that the extension and compression phases, major transgressions and regressions, tectonic elevations were manifested simultaneously in the Laptev Sea Shelf and adjacent regions. Combining the stratigraphic and structural data on the Cenozoic key-sections with plate kinematic ones we can create a general geological background to interpret the seismic results (Fig. 6).

Seismostratigraphy and structure of the Laptev Sea Shelf

There are two large structural provinces within the Laptev Sea Shelf (Fig. 7). The central and eastern parts are occupied by the LSRS which is bounded by the New Siberian Islands Uplift from the east. The seismic data of the LARGE and MAGE (Fig. 1) characterize this structure in detail. The poorly studied West Laptev Province occupies within the western part of the shelf.

Laptev Sea Rift System

As it was mentioned above the LSRS was formed by destruction of the Late Mesozoic heterogeneous basement during the Eurasia Basin opening. A dynamically expressed reflector "A" is well-traced within the LSRS. It corresponds to a roof of the acoustic basement and divides the chaotic seismic record produced by the Pre-Late Cretaceous folded complexes from the more regular one characterized the sedimentary cover. Seven seismic stratigraphic complexes (SSC) bounded by the clear regional reflectors are distinguished within the rift system (Fig. 8).

The SSC-1 is a lowermost part of the rift sedimentary filling. This unit overlaps transgressively the eroded surface of the folded basement and is represented by a series of high amplitude reflections. The SSC-1 due to its dynamic expressiveness and reflective intensity is a marker which allows recognition the complete block structure of the LSRS.

The seismic records of the SSC-2 and SSC-5 could be characterized as "transparent" while the seismic wave fields of SSC-3 and SSC-4 have more contrast. The reflector "4" in a base of SSC-5 is one of the basic seismic markers. The typical feature of the SSC-2, SSC-3 and SSC-4 is a presence of wedge-shaped sedimentary bodies which probably correspond to the former Lena and Yana deltas. The SSC-6 and SSC-7 as distinct from the lower seismic stratigraphic units which are mostly within the grabens cover the whole area of the shelf. The regional reflector "B" in a bottom of the SSC-6 cuts out the block-like rift structure and is clearly distinguished as an erosional surface.

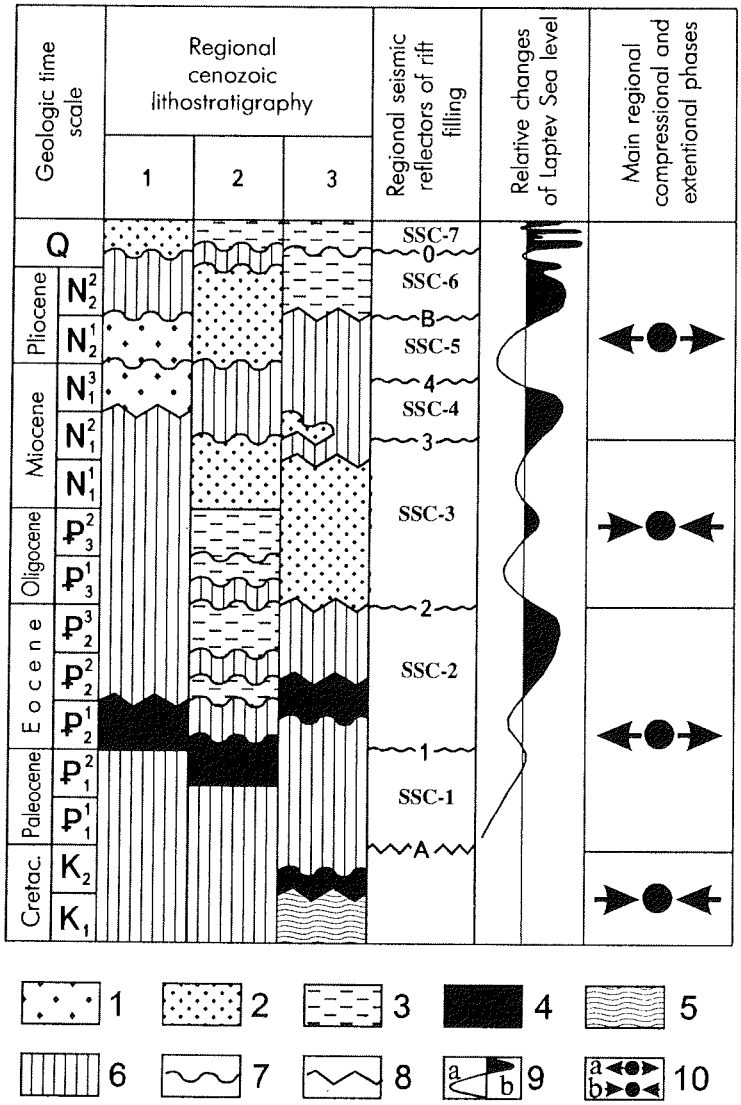

Fig. 6. General geologic scheme of the Laptev Sea Region. 1 - coarse sedimentary sequence (sand and gravel in mainly); 2 - fine sediment sequence (middle- and fine-grain sand and silt in mainly); 3 - muddy sediment sequence (clay and silt in mainly); 4 - coal-bearing sedimentary sequence; 5 - weathered crust; 6 - absent or not identified sediments; 7-8 - unconformities: 7 - stratigraphic, 8 - angular; 9 - curve of sea level oscillation (Alekseev et al., 1992): a - regression, b - transgression; 10 - tectonic stress conditions: a - extension, b - compression. SSC - seismic stratigraphic complex.

The stratigraphic setting of the described seismic stratigraphic units can be only assessed as preliminary. We have used for this purpose a general scheme of the Laptev Sea Shelf development derived from the regional geological, paleogeographic and plate kinematic data presented above (Fig. 6). These data allow us to make the supposition that the major unconformities within the shelf

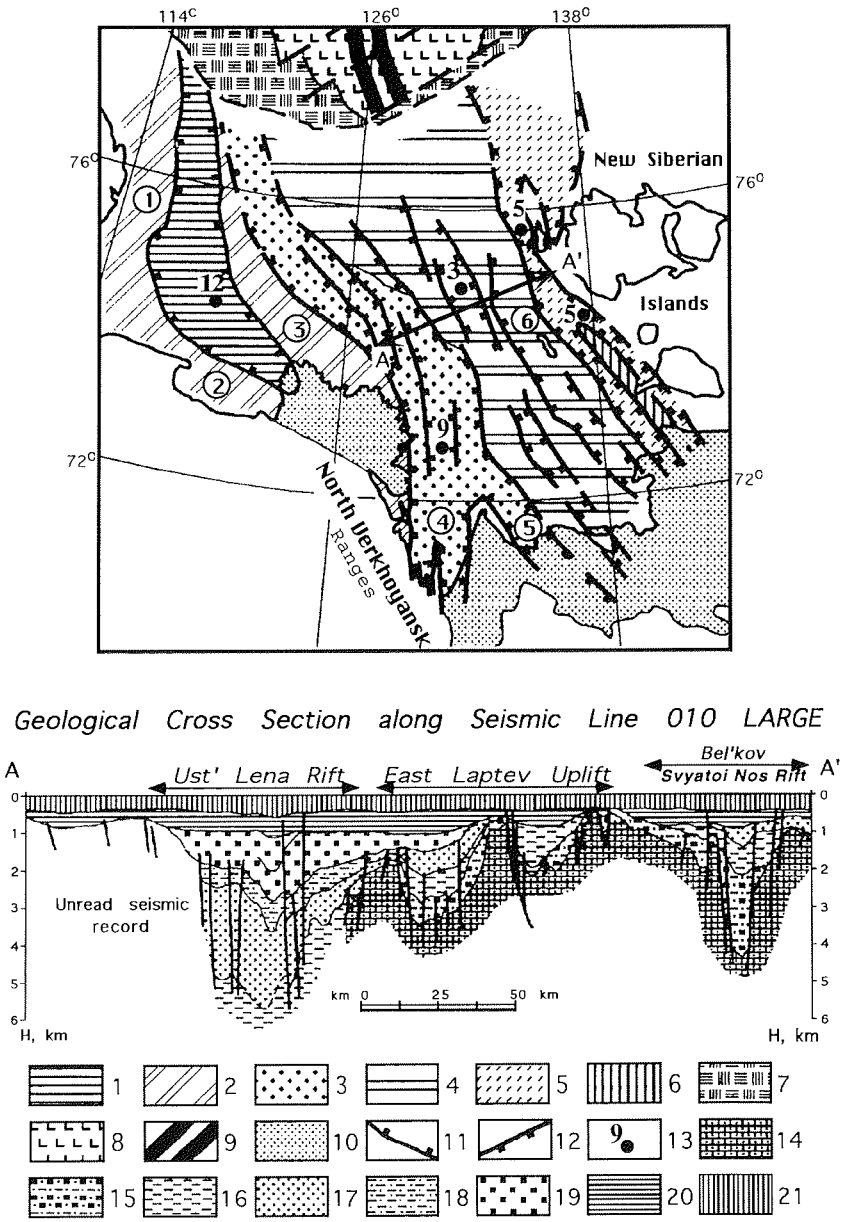

Fig. 7. Tectonic map and geological cross section showing the main tectonic elements of the Laptev Sea Shelf (prepared with use of the LARGE's and MAGE's seismic data).
1-2 - Western Laptev Pre-Cretaceous (?) structural province: 1 - West Laptev and South Laptev sedimentary basins, 2 - uplifts; 3-6 - Eastern Laptev Structural Province (Laptev Sea Cenozoic Rift System): 3 - Ust' Lena Rift, 4 - East Laptev Uplift, 5 - Bel'kov-Svyatoi Nos Rift, 6 - Kigilyakh Horst; 7-9 - Eurasia Oceanic Basin: 7 - continental slope, 8 - abyssal plain, 9 - Gakkel Spreading Rift Zone; 10 - Cenozoic sedimentary cover on the land; 11 - fracture and flexure zone bounded the West Laptev sedimentary basin; 12 - normal faults; 13 - maximum values of the sedimentary cover thickness for the each structure (in km); 14-21 - seismic stratigraphic complexes (for the cross section only): 14 - folded (acoustic) basement, 15 - SSC-1 (Upper

Fig. 7. Cretaceous-Paleogene), 16 - SSC-2 (Eocene), 17 - SSC-3 (Oligocene to Middle Miocene), 18 - SSC-4 (Middle-Upper Miocene), 19 - SSC-5 (Pliocene), 20 - SSC-6 (Upper Pliocene to Lower Quaternary), 21 - SSC-7 (Quaternary). The circled numbers are: 1 - Taimyr Uplift, 2 - Olenek Uplift, 3 - Trofimov Uplift, 4 - Omoloi Graben, 5 - Ust' Yana Graben, 6 - Stolbovoi Horst.

sedimentary cover correspond to the main stages of the Eurasia Basin opening and may be of the same age with the unconformities which are known onshore.

The stratigraphic position of the reflector "B" is determined with the most confidence. This reflector has a well expressed erosional character. The overlying SSC-6 was obviously formed during the first extensive transgression in the end of Pliocene. Therefore the part of the sedimentary cover located between the "A" and "B" reflectors is suggested to be of the Late Cretaceous to Pliocene age.

The SSC-1 locates in the lower part of the sedimentary cover and shows everywhere the pre-rift or quasi-rift character. It is very likely that it corresponds to the Late Cretaceous to Paleocene epoch of an initial continental rifting along the future Gakkel Ridge.

The clearly synrift SSC-2 corresponds to the well-defined Eocene stage of the rifting. Seismic reflector "2" which presents the top of SSC-2 may be correlated to an unconformity between Eocene and Oligocene well-expressed within onshore sections.

The SSC-4 and SSC-5 have several signs of synrift formation also. We suppose that an accumulation of these sequences was connected with the Late Miocene to Pliocene rift stage and that the seismic reflector "4" corresponds to the regression at the Miocene/Pliocene boundary. At the same time the SSC-3 located between these units does not demonstrate any features of synrift sedimentation and probably corresponds to the Oligocene - Early Miocene stage of the plate convergence.

According to the seismic stratigraphic characteristics the uppermost SSC-7 consists of the shallow-marine deposits. It was formed obviously during the Pleistocene transgressions. The seismic reflector "0" may corresponds to the Middle Pleistocene unconformity.

The LSRS consists of three main structural elements (Fig. 7). The East Laptev Uplift complicated by the small grabens is located within the central part of the rift system. This uplift is bordered by Bel'kov-Svyatoi Nos Rift from the east and Ust' Lena Rift from the west which strike from the coast up to the shelf edge.

The Ust' Lena Rift is a large structure with a 600 km length and a 50-70 km width. The continental crust here is most stretched and thickness of the sedimentary filling are maximum, probably more than 9 km. The rift sides are bounded by the listric normal faults which were formed during the initial rifting at the Late Cretaceous and were active over the Cenozoic. On the south the Ust' Lena Rift branches to the Ust' Yana and Omoloi grabens which continue on the land.

The sedimentary filling of the Ust' Lena Rift is represented by the Upper Cretaceous to Pliocene sediments. For the most part it is represented by the synrift SSC-1, SSC-2, SSC-4 and SSC-5. Thus the sedimentation within the rift took place throughout the LSRS evolution. The adjacent areas were affected by denudation during the regression stages and provided clastic material into a subsiding rift valley to form wedge-shaped sedimentary bodies along its marginal parts.

The East Laptev Uplift of 500 km length and width from 100 km on the south to 150-180 km on the north is characterized by complicated block relief of the folded

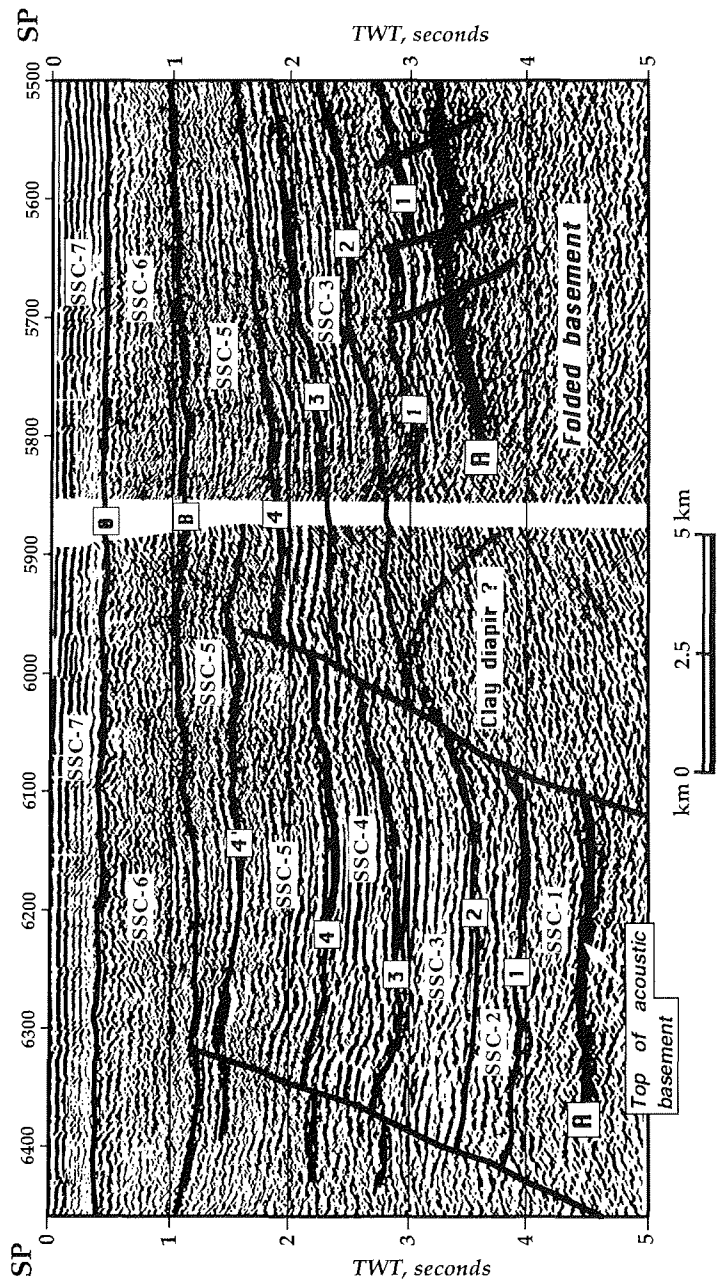

Fig. 8. Fragment of the seismic reflection record from the eastern side of Ust' Lena Rift (profile 006 LARGE). For the explanations see to the text.

basement surface. The grabens branch toward the southeast. Most uplifted Stolbovoi Horst occupies the eastern part of the East Laptev Uplift. There is a general rise of the folded basement surface and seismic reflecting horizons toward southeast.

The sedimentary cover of the East Laptev Uplift is composed mostly of the Upper Cretaceous to Lower Miocene and the Upper Pliocene to Quaternary deposits.

Their accumulation took place simultaneously with the displacements of basement blocks. All seismic stratigraphic units below the horizon "B" are disturbed by low-amplitude faults. Many of these faults were active up to the end of the Pliocene. The thickness of the sedimentary cover varies insignificantly although some increase of the thickness is noted in central parts of the grabens. An irregular erosion during the Late Miocene to Early Pliocene time exerted influence on the thickness variability. The Stolbovoi Horst where only the SSC-1 is present between the seismic reflectors "A" and "B" is most eroded.

The Bel'kov-Svyatoi Nos Rift extends 500 km from the southeast to the northwest along the proposed fault zone between the Novosibirsk-Chukchi and Verkhoyansk-Kolyma fold belts. A width of the rift varies from 10-15 km near Bel'kov Island to 50 km in the southern part where it branches into two grabens divided by Kigilyakh Horst (Fig. 7).

The age of the sedimentary filling of the Bel'kov-Svyatoi Nos Rift is most disputable because practically all of regional reflectors established within Ust' Lena Rift are pinch out on the Stolbovoi Horst which bounds the rift from the west. Probably it comprises the SSC-1, 2 and lower part of the SSC-3 (the Upper Cretaceous to Oligocene) up to 3.5-4 km thick. The thickness of the SSC-1 increases toward the central part of the grabens up to 2.2 km. At the same time we do not exclude an younger age of the sedimentary filling which can be represented by SSC-4 and 5 (Upper Miocene-Pliocene).

All structural elements of the LSRS except the Stolbovoi Horst are covered by the Upper Pliocene to Quaternary sediments (SSC-6 and 7) from several hundred meters to 1-1.2 km thick. A formation of this sedimentary cover may be considered as a result of two factors: a sea level rise and slowing-down of the rifting connected with youngest plate movement reorganization. However two linear zones of highest thickness of covered sequences coincide with the Bel'kov-Svyatoi Nos Rift. It probably indicates a local rift activity during the Late Pliocene and Pleistocene.

Western Laptev Structural Province

Structurally the western part of the shelf differs clearly from the LSRS. The depression with sedimentary thickness up to 7-12 km called South Laptev Basin (Ivanova et al., 1990; Sekretov, 1993) is located within the central part of the province. This depression is bounded by Trofimov, Taimyr and Olenek uplifts from the east, west and south, correspondingly (Fig. 7). The thickness of the sedimentary cover within the uplifts are 1-3 km. All these structural units are complicated by numerous fracture zones of both normal and reverse types. The higher thickness of the sedimentary cover and high seismic velocities reached 5.5-6.2 km/s within its lower part allow the suggestion that the age of the South Laptev Basin may be older than the Cretaceous.

Discussion

The new offshore multichannel seismic reflection results combined with the geological data from the adjacent parts of the land and islands have improved our understanding of the Laptev Sea Shelf geology significantly. At the same time several important questions are still open.

The most disputable point is a stratigraphic age of the sedimentary sequences derived from seismic data. There are two main points of view on the age and development of the major structures of the Laptev Sea Shelf. One of them is

presented in this paper. We have tried to support it by all the regional stratigraphic, paleogeographic and plate kinematic data presented above.

Another geological model of the Laptev Sea Shelf was proposed by the geophysicists of the MAGE (Ivanova et al., 1990; Sekretov, 1993; Alekseev et al., 1992). They distinguish the south to north trending Omoloi Rift which is the main structural element of the LSRS (Fig. 9). It stretches out from the Buor-Khaya Bay up to the southern edge of the Gakkel Ridge. The Omoloi Rift has the discordant position relative to other structural elements of the LSRS and crosses the Ust' Lena Rift near the Lena River Delta. This structure is suggested to have been formed along of fracture boundary between the Novosibirsk-Chukchi Fold Belt and the Laptev Block which is an outermost part of the Siberian Craton. According to these authors the Late Cretaceous to Cenozoic age of sedimentary cover is inherent for the East Laptev Uplift, Bel'kov-Svyatoi Nos Rift and eastern part of the Omoloi Rift only. The sharply increase of the sediment thickness within the axial part of the Omoloi Rift is considered as a consequence of an appearance of the older successions from Lower Cretaceous up to Riphean (Fig. 9 B). The Riphean to Mesozoic complexes are considered as a paraplatformian sedimentary cover of the Laptev Block which occupies the part of the Omoloi Rift and whole West Laptev Province. It seems to us that there are not any stringent evidence in favor of the existence of the Paleozoic to Upper Riphean successions within the Ust' Lena Rift sedimentary filling. For example the interval seismic velocities within lowermost part of this rift do not mainly exceed 5.0 km/s whereas the dense Lower Paleozoic-Upper Riphean carbonates penetrated by several onshore wells are characterized by the higher values of the interval velocities (between 5.7-6.9 km/s).

The existence of the Omoloi Rift as a direct continuation of the Gakkel Ridge spreading zone is questionable also. In first place it is not expressed in the seismic records to the north of 74° N (see cross section on Fig. 9). In the second place it seems to be unlikely that such continuation could continuously exists over whole Eurasia Basin opening. Some transform fault between southern termination of the Gakkel Ridge and the LSRS is required to explain the different values of a plate convergence within the oceanic Eurasia Basin and the shelf area where there is a stretched continental crust. Probably such fault could be formed along boundary between oceanic and continental crust at a continental slope area.

Now we have only a few data to discuss an origin of the West Laptev Structural Province. The thick sedimentary cover and higher seismic rates probably indicate its older than the LSRS origin and we cannot exclude an existence of the Archaean to Lower Proterozoic basement covered by Riphean to Lower Mesozoic platformian or quasi-platformian sedimentary successions.

Summary

The Laptev Sea Shelf is a key region for the reconstructions of the Late Mesozoic and Cenozoic history of the Arctic and study of the initial break-up of the continents. This area developed under influence of a spreading along Nansen-Gakkel Ridge during last 56 Ma. This process led to stretching a continental lithosphere within the shelf and to forming the Laptev Sea Rift System. The rift system consists of three main structural elements (from the west to the east): Ust' Lena Rift, East Laptev Uplift and Bel'kov-Svyatoi Nos Rift. The westward decreasing of the thickness of the rift sedimentary filling from 9-10 km to 4-5 km and simplification of the rift structure as well can indicate a rejuvenation of the rifts in this direction.

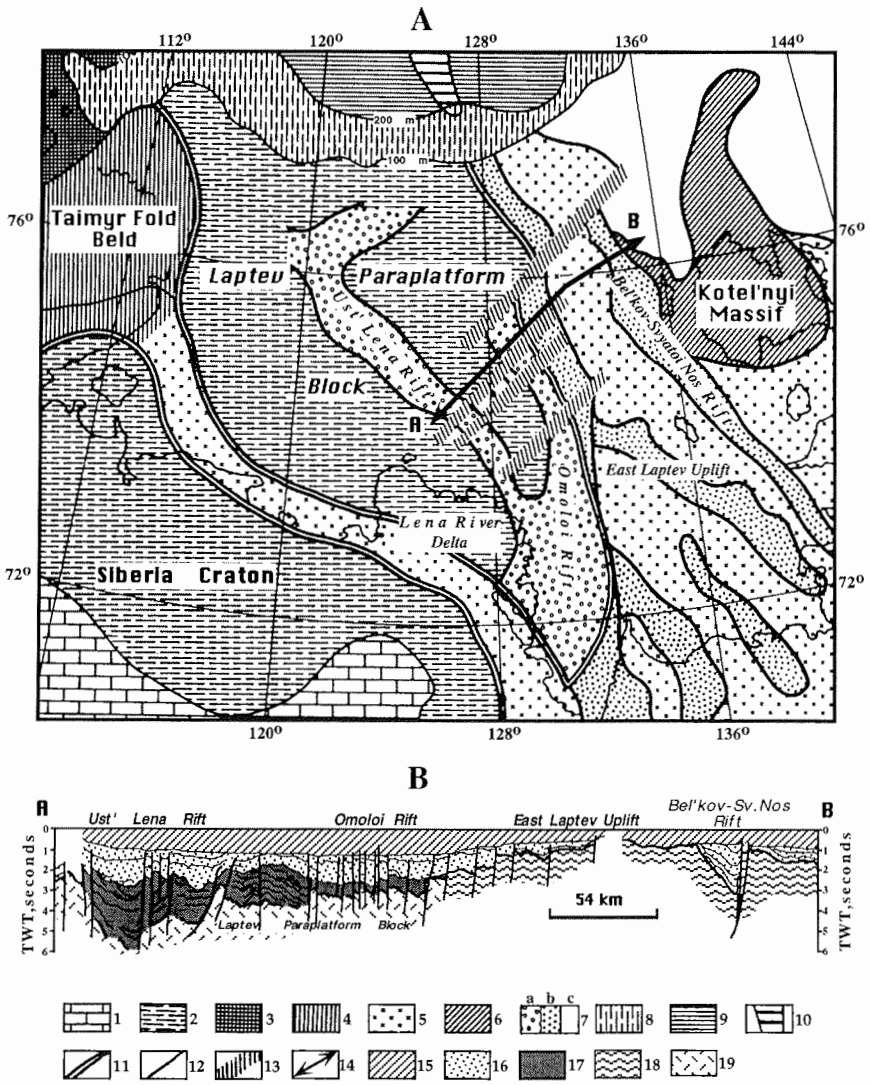

Fig. 9. Tectonic zonation of the Laptev Sea Shelf (Alekseev et al., 1992) (A) and geologic cross section along seismic profile 86705 MAGE (B). 1-2 - Siberian Craton: 1 - Epikarelian platform complex, 2 - Epikarelian paraplatform complex; 3-4 - Taimyr Fold Belt: 3 - Archaean-Middle Proterozoic granite-metamorphic complex, 4 - Early Kimmerian folded complex; 5 - Late Kimmerian folded complex of the Mesozoides of the USSR North-East; 6 - Median Massif; 7 - Late Cretaceous-Cenozoic grabens and depressions superimposed on: a) the paraplatform basement, b) Mesozoides of the USSR North-East, c) basement of unclear nature; 8-10 - Eurasia Oceanic Basin: 8 - continental slope, 9 - abyssal depression, 10 - rift zone of the Gakkel Ridge; 11-12 - structural boundaries: 11 - between platform elements and fold belts, 12 - between the others structures smaller order; 13 - strike slip faults; 14 - line of geologic cross section along seismic profile 86705 MAGE, 15-18 - main seismis stratigraphic complexes of the shelf sedimentary basin (on cross section only): 14 - Neogene-Quaternary post-rift complex, 15 - Late Cretaceous-Paleogene syn-rift complex, 16 - Riphean-Early Cretaceous paraplatform cover of the Laptev Block, 17 - folded basement of the Late Mesozoides, 18 - Archaean-Early Proterozoic crystaline basement.

In this paper we have mainly concentrated on consideration of several general geological and seicmic stratigraphic features of the Laptev Sea Shelf. The recent geodynamics of it is another important and at the same time poorly studied question. The uninterrupted cover of the Quaternary sediments is to be indicated a post-rift subsidence of the whole Laptev Sea Sedimentary Basin. However the present-day seismicity shows that the extension of the Laptev Sea lithosphere is still active (Fujita et al., 1990; Parfenov et al., 1988). The present geodynamics of the region can probably be considered as a result of slowing-down of the rifting near North America/Eurasia pole of lithospheric plate rotation (Cook et al., 1986). An alternation of the extension, compression and quiet tectonic periods may presents an important geodynamic feature of the oceanic spreading ridge/continental margin intersection area.

Acknowledgments

This paper has been finished during the visit of one of the authors at the GEOMAR Research Center for Marine Geosciences in Kiel, Germany. We are grateful to Prof. J. Thiede and Dr. H. Kassens who generously provided this possibility. Many aspects of the geology of the East Arctic Region have been discussed with Dr. L. Johnson and we thank him for the constructive comments. This work was in part supported by International Science Foundation (grant number M5U000), the German Ministry for Science and Technology, (grant number 525 4003 03 G 0517 A) and Executive Committee of the Nansen Arctic Drilling Program.

References

Alekseev, M.N., Arkhangelov, A.A., Ivanova, N.M., et al., 1992. Laptev and East Siberian Seas. Cenozoic. In: Palaeogeographic Atlas of the Shelf Regions of the Eurasia for the Mesozoic and Cenozoic. Vol. 1. By the Robertson Group plc, UK, and Geological Institute, Academy of the Sciences, USSR, pp.1-14 - 1-33.

Churkin, M., Jr. and Trexler, J.H., Jr., 1981. Continental plates and accreted oceanic terranes in the Arctic. In: A.E.M. Nairn, M. Churkin, Jr. and F.G. Stehli (Editors), The Ocean Basins and Margins. Vol. 5, The Arctic Ocean. Plenum Press, New York and London, pp. 1-20.

Cook, D.B., Fujita, K. and McMullen, C.A., 1986. Present-day plate interactions in northeast Asia: North American, Eurasian, and Okhotsk plates. In: G.L. Jonhson and K. Kaminuma (Editors), Polar Geophysics. J. Geodyn., 6: 33-51.

Drachev, S.S. and Savostin, L.A., 1993. Ophiolites of the Bol'shoi Lyakhov Island (Novosibirsk Islands). Geotektonika, 6: 33-51 (in Russian).

Drachev, S.S. and Savostin, L.A., 1994. Structure and plate tectonics of the Laptev Sea Shelf: drilling of the geological record. In: H. Kassens, H.W. Hubberten, S. Pryamikov and R. Stein (Editors), Reports on Polar Research. V. 144. Alfred Wegener Institute for Polar and Marine Research, Bremerhaven, Germany, pp. 115-117.

Fujita, K., 1978. Pre-Cenozoic tectonic evolution of northeast Siberia. Journal of Geology, 86: 159-172.

Fujita, K., Cook, D.B., Hasegava, H., Forsyth, D. and Wetmiller, R., 1990. Seismicity and focal mechanisms of the Arctic region and the North American plate boundary in Asia. In: Arthur Grantz, L. Johnson and J.F. Sweeney (Editors), The Geology of North America. Vol. L., The Arctic Ocean region. The Geological Society of America, pp. 79-100.

Grachev, A.F., 1982. Geodynamics of the transitional zone from the Moma rift to the

Gakkel ridge. In: J.S. Watkins and C.L. Drake (Editors), Studies in Continental Margin Geology. Am. Assoc. Pet. Geol. Mem., 34: 103-113.

Grachev, A.F., Demenitskaya, R.M. and Karasik, A.M., 1970. Mid Arctic Ridge and their continental continuation. Geomorphologiya, 1: 42-45 (in Russian).

Grinenko, O.V. and Imaev, V.S., 1989. Cenozoic thrusts of the northern part of the Kharaulakh Ridge. Geologiya and Geophizika, 5: 121-123 (in Russian).

Grinenko, O.V., Zharikova, L.P., Fradkina, A.F. and etc., 1989. Paleogene and Neogene of North-East of the USSR. Scientific Center of Siberian Department of Academy of Sciences of USSR, Yakutsk, 184 pp (in Russian).

Karasik, A.M., Savostin, L.A. and Zonenshain, L.P., 1983. Parameters of the lithospheric plate movements within Eurasia Basin of North Polar Ocean. Dokl. Acad. Nauk SSSR, Earth Sci. Sect., 273: 1191-1196 (in Russian).

Kim, B.I., 1986. Cenozoic history of the development of the East Arctic shelves and paleoshelves. In: B.K. Egiazarov and Y.B. Kazmin (Editors), Cenozoic history of the shelf and islands of the Soviet Arctic. Sevmorgeologiya, Leningrad, pp. 105-119 (in Russian).

Koval'skii, V.V. (Edritor), 1985. Structure and Evolution of the Earth Crust of the Yakutiya. Nauka, Moskva, 248 pp (in Russian).

Kos'ko, M.K., Lopatin, B.G. and Ganelin, V.G., 1990. Major geological features of the islands of the East Siberian and Chukchi Seas and the northern coast of Chukotka. Marine Geology, 93: 349-367.

Imaev, V.S., Imaeva, L.P. and Koz'min, B.M., 1990. Active faults and seismic tectonics of the North-eastern Yakutia. Scientific Center of Siberian Department of Acad. of Sci. of USSR, Yakutsk, 140 pp (in Russian).

Ivanov, V.V., Ivanov, B.A. and Pokhialaynen, V.P., 1974. New data on the geology of Stolbovoi Island, New Siberian Archipelago. Dokl. Acad. Nauk SSSR, Earth Sci. Sect., 216: 74-75 (in Russian).

Ivanova, N.M., Sekretov, S.B. and Shkarubo, S.N., 1990. Geological structure of the Laptev Sea shelf according to seismic studies. Oceanology, 29: 600-604.

Laukhin, S.A. and Patyk-Kara, N.G., 1985. About extension of the Paleogene transgressions on north of the Yakutia. Dokl. Acad. Nauk SSSR, Earth Sci. Sect., 280: 1197-1201 (in Russian).

Mezhvilk, A.A, 1958. Geologic development history of north Kharaulakh. Izv. Acad. Nauk SSSR, Ser. Geol., 23: 68-74 (in Russian).

Natal'in, B.A. and Parfenov, L.M., 1983. Accretional and collisional eugeosynclinal folded systems of the northwestern Pacific rim. In: M. Hashimoto and S. Ueda (Editors), Accretion tectonics in the Circum-Pacific regions. Terra Scientific, Tokyo, pp. 59-68.

Okulitch, A.V., Lopatin, B.G. and Jackson, H.R., 1989. Circumpolar Geological Map of the Arctic. Geological Survey of Canada, Map 1765 A, Scale 1:6 000 000.

Parfenov, L.M., Koz'min, B.M., Grinenko, O.V., Imaev, V.S. and Imaeva, L.P., 1988. Geodynamics of the Chersky seismic belt. J. Geodyn., 9: 15-37.

Patyk-Khara, N.G. and Laukhin, S.A., 1986. Cenozoic evolution of the Arctic coastal relief of North-Eastern Asia. Sovetskaya Geologiya, 1: 75-84 (in Russian).

Savostin, L.A. and Karasik, A.M., 1981. Recent plate tectonics of the Arctic basin and of Northeastern Asia. Tectonophysics, 74: 111-145.

Savostin, L.A., Karasik, A.M. and Zonenshain, L.P., 1984a. The history of the opening of the Eurasia basin in the Arctic. Trans. USSR Acad. Sci., Earth Sci. Sect., 275: 79-83.

Savostin, L.A., Natapov, L.M. and Stavsky, A.P., 1984b. Mesozoic paleogeodynamics and paleogeography of the Arctic region. In: Arctic geology. Reports. V. 4. 27th International Geological Congress (Moscow). Nauka, Moskva, pp. 217-237.

Savostin, L.A. and Drachev, S.S., 1988. The Cenozoic compression in Novosibirsk Islands Region and its relationship with Eurasia basin opening. Oceanology, 28: 775-782 (in Russian).

Sekretov, S.B., 1993. The geological structure of Laptev Sea Shelf on seismic reflection data. Ph.D. thesis, Institut "Vniiokeangeologia", St. Petersburg, 19 pp (in Russian).

Strepetova, Z.V., Laukhin S.A., Ryzhov, B.V. and Dubinchik, A.N., 1981. Cenozoic key-section on Yana-Omoloi watershed area. Izvestiya Acad. Nauk SSSR, Ser. Geol., 7: 48-63 (in Russian).

Trufanov, G.V., Belousov, K.N. and Vakulenko, A.S., 1979. The data on stratigraphy of Cenozoic deposits of Novosibirsk Archipelago. In: Continental Tertiary sequences of North-Eastern Asia. Nauka, Novosibirsk, pp. 30-40 (in Russian).

Vinogradov, V.A., 1984. Laptev Sea. In: I.S. Gramberg and Y.E. Pogrebitskii (Editors), Geologic Structure of the USSR and its Relationship to the Distribution of Mineral Resources. V. 9, Seas of the Soviet Arctic. Nedra, Leningrad, pp. 51-60 (in Russian).

Zonenshain, L.P., Natapov, L.M., Savostin, L.A. and Stavsky, A.P., 1978. Recent plate tectonics of the northeastern Asia in connection with the opening of North Atlantic and the Arctic Ocean basins. Oceanology, 18: 550-555.

Zonenshain, L.P., Kuz'min, M.I. and Natapov, L.M., 1987. Phanerozoic palinspastic reconstructions of the USSR. Geotektonika, 6: 3-19 (in Russian).

Zonenshain, L.P. and Natapov, L.M., 1989. Tectonic History of the Arctic Region from the Ordovician through the Cretaceous. In: Y. Herman (Editors), The Arctic Seas: Climatology, Oceanography, Geology and Biology. Van Nostrand Reinhold, New York, pp. 829-862.

MARINE GEOPHYSICAL INVESTIGATIONS IN THE LAPTEV SEA AND THE WESTERN PART OF THE EAST SIBERIAN SEA

H. A. Roeser, M. Block, K. Hinz and C. Reichert
Bundesanstalt für Geowissenschaften und Rohstoffe, Hannover, Germany

Introduction

Since more than 20 years the Federal Institute for Geosciences and Natural Resources (BGR) has carried out geophysical investigations in Arctic and Antarctic regions. Already in the seventies BGR worked out exploration concepts for the area of the Laptev Sea shelf on behalf of the former German-USSR Economic Commission. However, at that time none of the projects could be realized.

After the radical political changes BGR took the opportunity to carry out 2D-reflection seismic surveys in co-operation with Sevmorneftegeofizika (SMNG), Murmansk, in the eastern part of the Laptev Sea shelf and in the western part of the East Siberian Sea.

The Laptev Sea is of great geoscientific importance because of its unique plate tectonic situation. Since the breakup of Gondwanaland about 200 Ma ago Europe and Africa to the east and North and South America to the west are moving apart with velocities of some cm/y . According to the plate tectonic framework the Eurasia Basin in the Arctic Ocean is the northward continuation of the Atlantic Ocean. In the prolongation of the Eurasia Basin towards the Asian continent the Laptev Sea is situated. On the present Earth, the Laptev Sea is the most interesting example of a rift axis propagating into a continuous crustal plate.

According to the observed magnetic anomalies (Fig.1) the Eurasian Basin formed by sea-floor spreading since about 55 Ma (Kristoffersen, 1990). The total spreading rates vary between 1.3 cm/year near Svalbard and 0.7 cm/year off the Laptev Shelf. The age of the oldest oceanic crust in the easternmost 500 km of the basin cannot be derived from the magnetic anomalies because the lineations are not sufficiently pronounced. Instead the area of the oldest oceanic crust is characterized here by wide negative magnetic anomalies. The adjacent continental crust shows partly wide positive anomalies. These are due to the higher overall magnetization of continental crust. The different character of the anomalies indicates that regular sea-floor spreading will not propagate any more.

The pole of rotation lies in northern East Siberia. The formation of oceanic crust ends about 1500 km away from the pole of rotation. In the northernmost Laptev Sea we would expect crustal extension by about 300 km and in its southern part, which is about 400 km nearer to the pole of rotation, still more than 200 km (Fig.1). This has generated a complex system of geological horsts and sedimentary troughs in the Laptev Sea. According to findings from onshore, the troughs may have a high hydrocarbon potential.

The extension determined from the horst and graben structures in the Laptev Sea (Vinogradov, 1984) is much too small. Therefore extensional features outside the Laptev Sea must contribute to the extension. The crustal thickness of about 30 km (Kogan, 1974) for the area southwestward of the Lena delta is not indicative of widespread crustal thinning and extension. A much more likely candidate is the New Siberian Basin east and northeast of the New Siberian Islands. In view of the ice conditions we have concentrated our work on this basin and its surroundings in 1993.

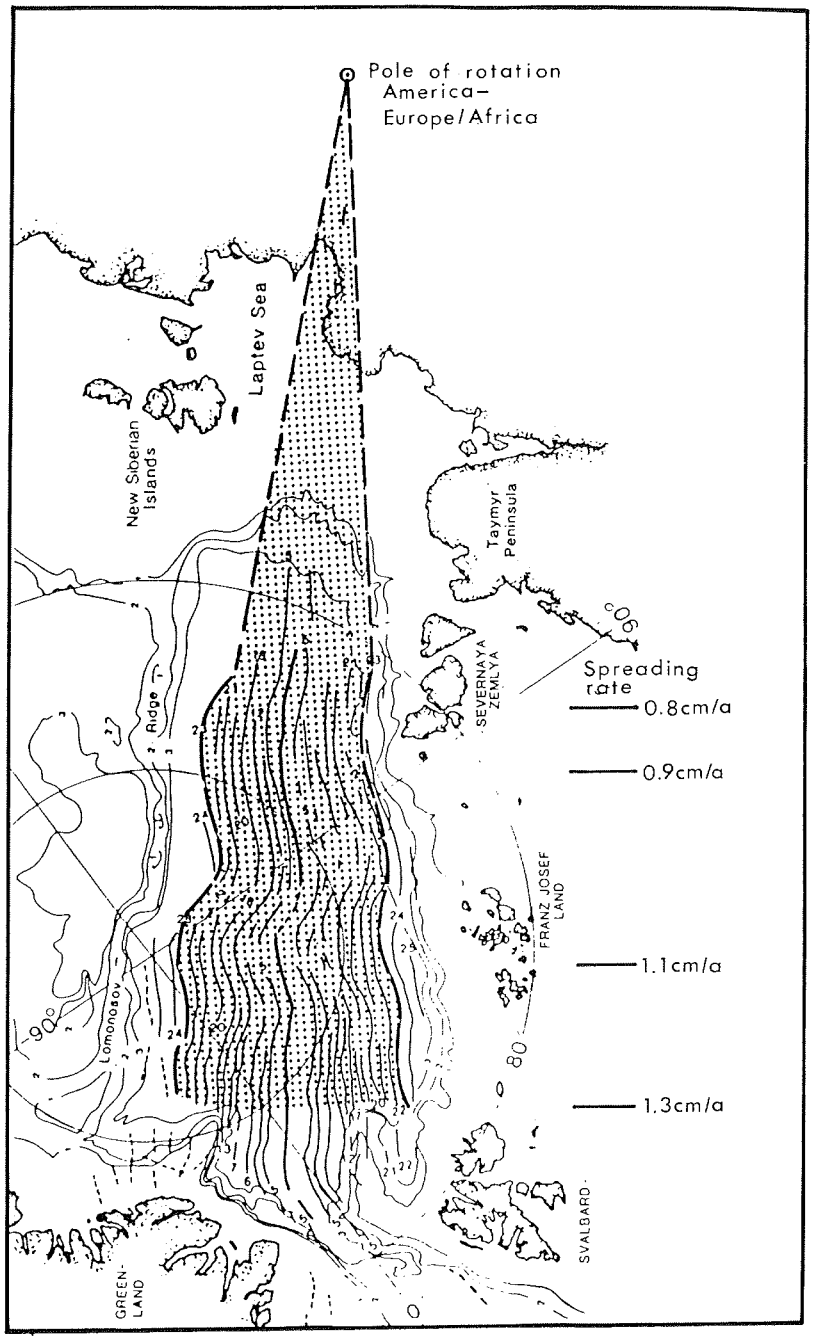

Fig. 1: Magnetic lineations in the Eurasia Basin (after Kristoffersen, 1990) and the extrapolated crustal extension up to the pole of rotation during the last 55 mill. years.

Geophysical data

SMNG and SE MAGE (State Enterprise Marine Arctic Geological Expeditions), Murmansk, have measured an extensive grid of reflection seismic profiles on the Laptev Sea shelf mainly south of 76°N. In addition SE MAGE succeeded in shooting some lines across the slope of the Laptev Sea up to nearly 80°N. These lines probably cross the Arctic Mid Ocean Ridge of the Eurasia Basin near its contact to the continental crust of the Laptev Sea. Two lines of SE MAGE run from the shelf of the East Siberian Sea into the Makarov Basin. In 1989, the eight seismic profiles with a total length of about 1,700 km were also carried out by LARGE (Laboratory of Regional Geodynamics, Moscow) in the eastern part of the Laptev Sea. On the basis of these reflection seismic data Drachev (1994) proposed seven sites for the Nansen Arctic Drilling Program on the Laptev Sea shelf between Kotel'nyi I. and the Lena River delta.

During two cruises in September 1993 and in September 1994 BGR surveyed in co-operation with SMNG multichannel reflection seismic lines with a total length of more than 7000 km (Fig.2).

The first cruise was carried out with the Russian research vessel AKADEMIK LAZAREV. We used a linear airgun array and a 2400 m long analog streamer. A grid of multichannel reflection seismic lines with a total length of about 3200 km was acquired during the first cruise in 1993. The most of these profiles cover the area of the New Siberian Basin north of Kotel'nyi I. and Novaya Sibir' I. where they have a distance of 20 nm from each other.

The second cruise was carried out with the Russian research vessel AKADEMIK NEMCHINOV equipped with a sleeve gun array and a 3,000 m long streamer.

Structural zones

In the following some preliminary results of our investigations with the research vessel AKADEMIK LAZAREV (1993) are presented and discussed.

On board of the vessel we were able to carry out a first preliminary interpretation of the single-trace monitor records. Figure 3 shows interpreted sections of the reflection seismic lines BGR93-003 and BGR93-012 . A structural map based on the compilation of Grantz et al. (1990) and on our own interpretation of all the new seismic monitor records is shown in Figure 4 . The following structural zones were observed from east to west:

The DeLong Island flood basalt province is the easternmost structural zone in the area of our investigation with AKADEMIK LAZAREV. Paleozoic and Cretaceous sediments are covered by shallow lava flow series (Okulitch et al.,1989; Fujita & Cook, 1990). Two lava flow units were mapped on Bennett Island (Fujita & Cook, 1990). The lower one is about 60 m and the upper one about 300 m thick. Fujita & Cook (1990) assume that these basaltic flow units are extruded in Cenozoic time. But they do not exclude an age of Early Cretaceous for this volcanic activity.

On some locations of this structural zone folded layers and fault blocks can be observed under the basaltic cover.

The New Siberian Basin follows to the west of the flow basalt province. A distinct normal fault facing southwestward separates the two structural zones. According to Grantz et al. (1990) this huge basin extends from the northwestern area of the East Siberian Sea between Novaya Sibir' I. and Bennett I. onto the shelf north of the New Siberian Isl. and is filled with Paleozoic to Cenozoic sediments.

The 70 km wide New Siberian Basin was covered by our reflection seismic profiles on a length of 300 km . In the north of the New Siberian Is. the boundaries of the New Siberian Basin given by Grantz et al. (1990) disagree with our reflection

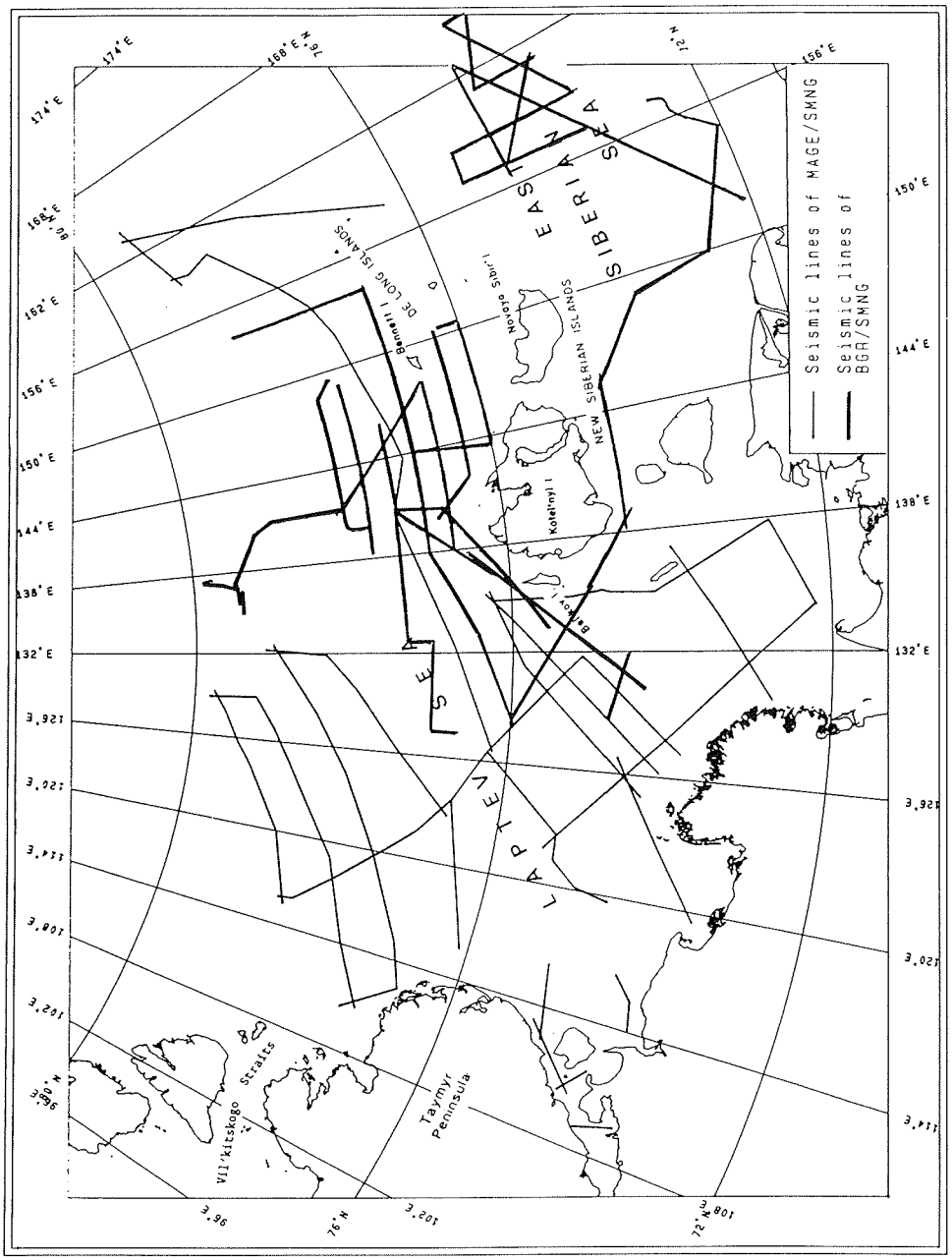

Fig. 2: The Laptev Sea and the western part of the East Siberian Sea with the surveyed reflection seismic lines.

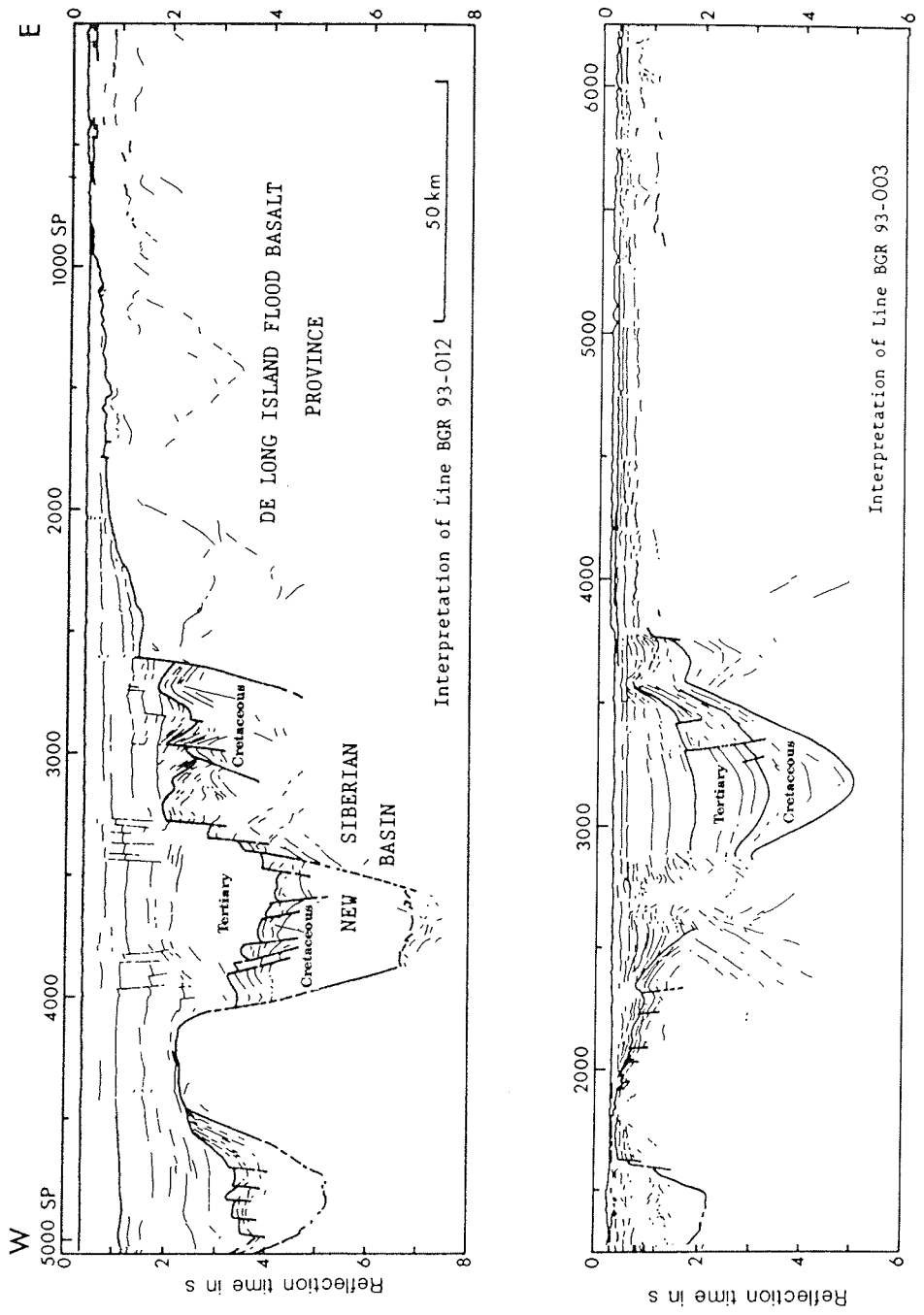

Fig. 3: Interpretation of the reflection seismic lines BGR93-012 and BGR93-003.

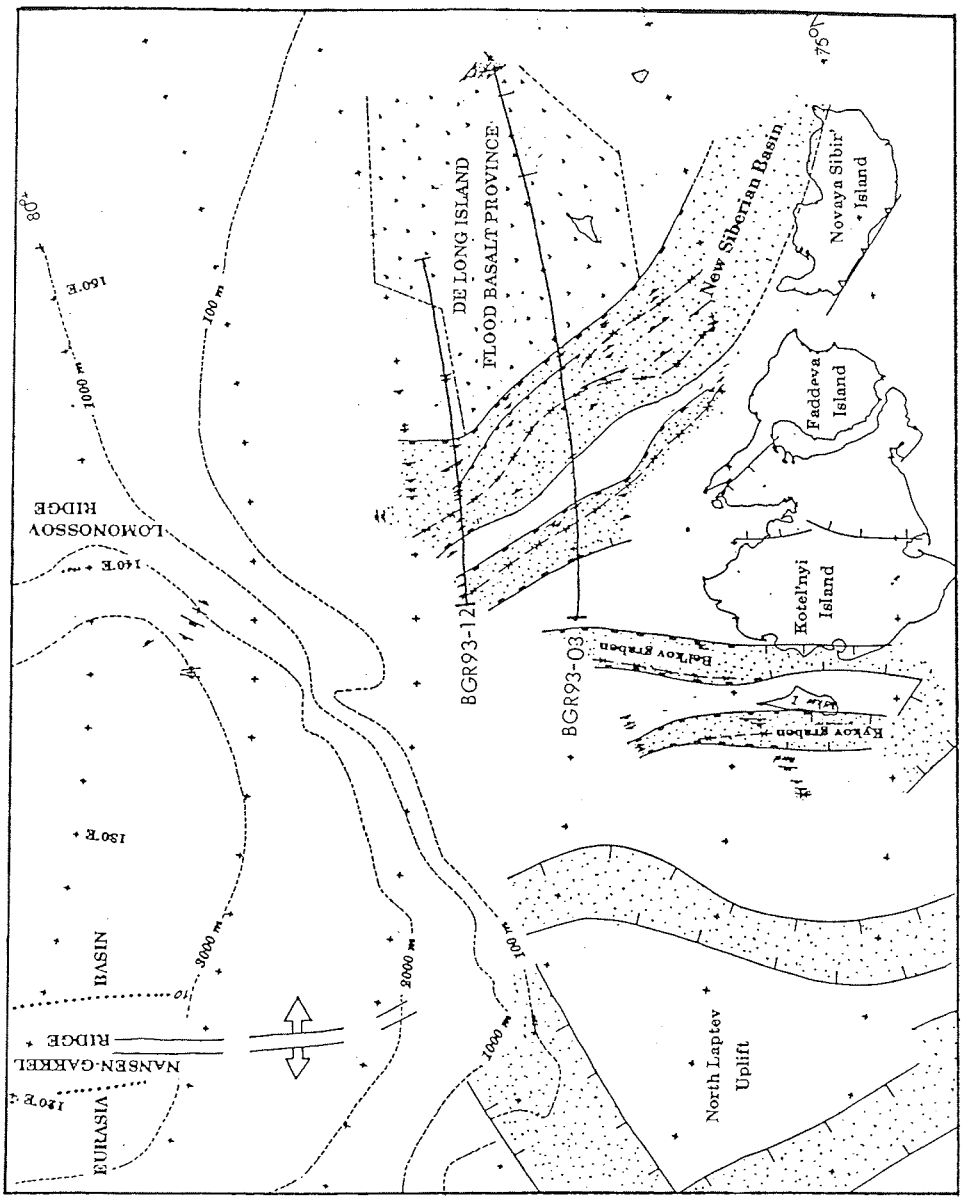

Fig. 4: Structural map of the area of investigation with AKADEMIK LAZAREV.

seismic lines. On line BGR 93-003 the deepest part of the New Siberian Basin is located outside of the basin area of Grantz et al. (1990).

Because of the ice conditions we were not able to survey the northwestern extension of the basin. Therefore it is not clear whether the New Siberian Basin extends up to the shelf edge and probably beyond it.

With the exception of line BGR 93-012 an accurate western boundary of the New Siberian Basin is difficult to define.

After our interpretation the New Siberian Basin belongs to the rift-graben system of the Laptev-Sea shelf which is caused by the opening of the Eurasian Basin. A ridge 10 km to 35 km wide bounds the New Siberian Basin in the west. The ridge is intensively folded and thrusted indicating a compressional event. On Faddeya I. and on Novaya Sibir' I. the Novosibirsk Complex is exposed (Fujita & Cook, 1990) consisting of Late Cretaceous to Eocene extensively folded and overthrusted layers. We assume that the Novosibirsk Complex continues to the north up to the intensively folded ridge.

North of Kotel'nyi I., we have detected a 35 km wide graben which was not mapped by Grantz et al. (1990). The graben lies west of the ridge described before and is bounded on both flanks by steep normal faults. The thickness of the Cenezoic sedimentary infill is increasing to the north.

The Bel'kov graben and the Kykov graben were crossed by our lines BGR 93-002 and BGR 93-025. Both grabens are already mapped by Grantz et al. (1990). The Bel'kov graben runs along the Zarya Strait between Bel'kov I. and Kotel'nyi I. and extends northwards. The Kykov graben is situated in the west of Bel'kov I. Normal faults are observed at the flanks of the two grabens, which are filled by more than 3 km thick Cenozoic deposits. Beneath the tertiary infill we expect Cretaceous sediments.

The two cross-sections of Figure 3 run across the De Long Island Flood Basalt Province, the New Siberian Basin, the intensively thrusted ridge at the western boundary of the New Siberian Basin, and end in the basin north of Kotel'nyi I.

In the area of our investigation the most striking structure is the New Siberian Basin. The greatest thickness of Cenozoic sediments is existing in the north of this graben, where more than 4300 m (3.5 s twt) were deposited. The thickness decreases rapidly southeastward. In the south an area with a Cenozoic sedimentary thickness of less than about 1700 m (1.5 s twt) is situated in the centre of the basin. Our southernmost line crosses two outcrops of the assumed base of the Tertiary sediments. A lot of normal faults are caused by still active subsidence of the basin.

These Cenozoic sediments are resting probably on Cretaceous deposits. Beneath we assume sediments of Mesozoic and even Paleozoic age. The boundary between Tertiary and Cretaceous sediments is characterized by many normal faults with partly big offsets probably caused by the opening of the Eurasia Basin.

Discussion and conclusions

North of the New Siberian Is. the New Siberian Basin is now covered by a relatively dense grid of seismic lines with a profile spacing of 20 nm. An additional line runs from the shelf of the Laptev Sea into the abyssal plain of the Eurasian Basin reaching nearly 80°N.

We can separate our area of investigation with AKADEMIK LAZAREV into the following structural zones:

- The De-Long Island Flood Basalt Province is the easternmost structural zone of our survey area. Paleozoic and Cretaceous sediments are covered there by Cenozoic lava flow units.
- The New Siberian Basin follows in the southwest. This huge graben about 70 km wide was surveyed during our cruise along about 300 km. The basin is probably filled with Cenozoic sediments which are in the north more than 4500 m thick. We assume that Mesozoic to Paleozoic sediments are deposited beneath. The assumed boundary between Tertiary and Cretaceous deposits is intensively faulted. Numerous normal faults indicate active depression. After our interpretation the New Siberian Basin belongs to the graben system of the Laptev Sea shelf.
- An intensively folded and thrusted ridge is located along the western boundary of the New Siberian Basin which probably was formed by compression during wrenching.
- A new graben was found by our reflection seismic measurements north of Kotel'nyi I.
- Bel'kov Graben and Kykov Graben were modified in the north. Both grabens are filled with more than 3 km of Cenozoic sediments. Beneath we expect Cretaceous deposits.

The New Siberian Basin as well as the other troughs in our survey area may have a high hydrocarbon potential and could be interesting for oil and gas exploration . However, the extension which is still active, may have a negative effect on the accumulation of hydrocarbons.

Fujita et al. (1990) published a map of the earthquake epicenters for the Laptev Sea and its surroundings. The earthquake information should not be overestimated because they cover only a fairly short time interval. Nevertheless, some conclusions seem justified.

The focal mechanisms show mainly normal faulting with a slight strike-slip component. South of 76°N the tectonically active area widens. However, only very few earthquakes are observed east of 136°E, and these fall mainly into the basins which we have mapped. Therefore we conclude that the basins which we have found together with those which were already known in the Laptev Sea make up the whole presently tectonically active area. There are no indications for the existence of an active E-W striking transform fault at the boundary between the Eurasia Basin and the shelf of the Laptev Sea/East Siberian Sea.

One can determine the widths of the observed basins and sum them up in E-W direction. This number is an upper limit for the actually observed crustal extension on the Laptev Shelf. In Figure 5 this total width is compared with the extension predicted by the amount of oceanic crust produced during the last 55 mill. years in the North Atlantic and the Eurasian Basin. Although the definition of the basins is somewhat arbitrary, it is very clear that the total width of the basins including the newly detected ones is only 200 - 300 km. Thus its size and also its latitude dependence equal fairly well to that predicted by the plate tectonic model for the last 55 mill. years.

This is a surprising result, because the amount by which the distance between the flanks of a basin has increased during the development of the basin, is usually much less than the width of the basin. Moreover, the basins on the Laptev shelf have formed partly already before the Tertiary. The insufficient total width of the basins is a problem for which we presently do not see a solution.

Following a model of Fujita et al. (1990) and the considerations of Lister et al. (1986) we tend to the assumption that some kind of delamination model is realized here (Fig.6). The New Siberian Basin is deeper than the other ones. One can

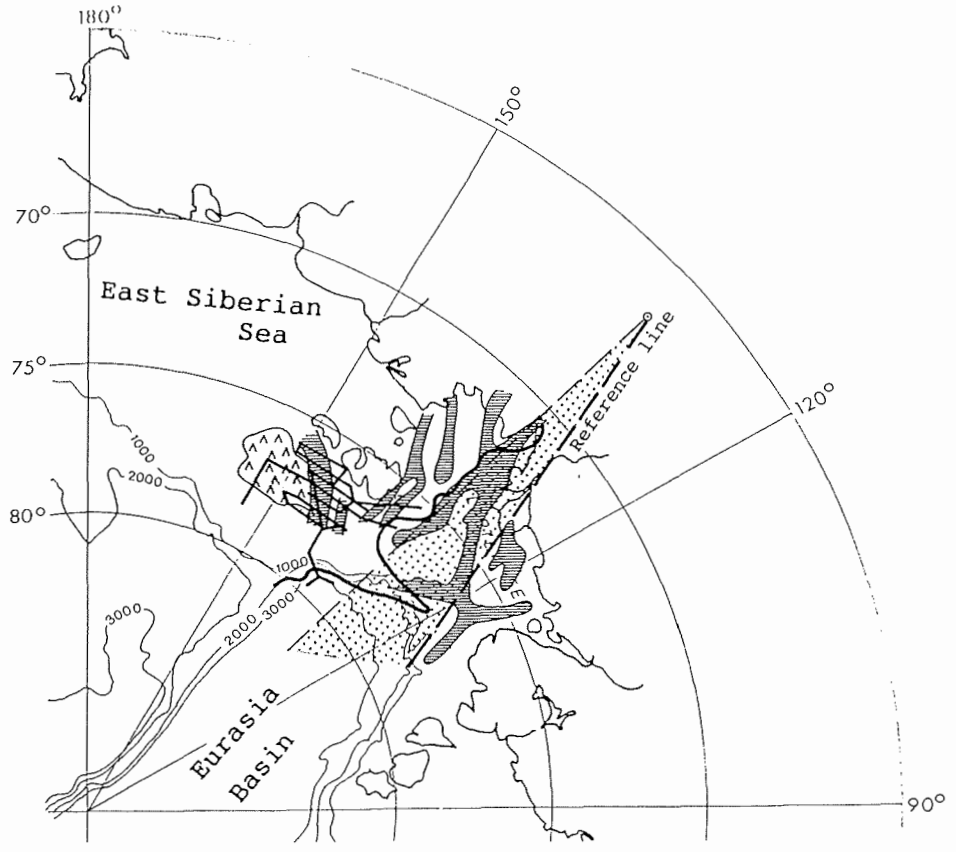

Fig. 5: Comparison of the expected crustal extension on the Laptev shelf with the total basin widths. The lines north of the New Siberian Islands are the seismic profiles of the cruise in 1993. Hachured: observed sedimentary basins, ticks: volcanic rocks exposed at the seafloor, dotted: expected crustal extension by extrapolation of the amount of oceanic crust generated in the Eurasia Basin during the last 55 mill. years, heavy line: widths of all basins summed up relative to the reference line.

speculate that here the lower crust and the uppermost mantle subsided into such a depth that partial melt occurred. The ascending magma caused the De Long Island flood basalt province. We do not think that in future seafloor spreading will propagate into the Laptev Sea. Already in the easternmost 200 km of the Eurasian Basin the magnetic lineations which are so characteristic for seafloor spreading, do not exist anymore. Instead we see two wide magnetic anomalies. Presumably the dike injection zone is here already much too wide for seafloor spreading in sensu strictu. It is very important, however, that during the POLARSTERN cruise ARK-IX/4 at station 27/050 (77°42'N, 125°55'E) hydrothermally influenced fauna was observed (Fütterer et al., 1994, S. 105). This point lies remarkably good at the intersection of the prolongation of the axis of the Eurasian Basin with the 2000 m isobath off the Laptev shelf.

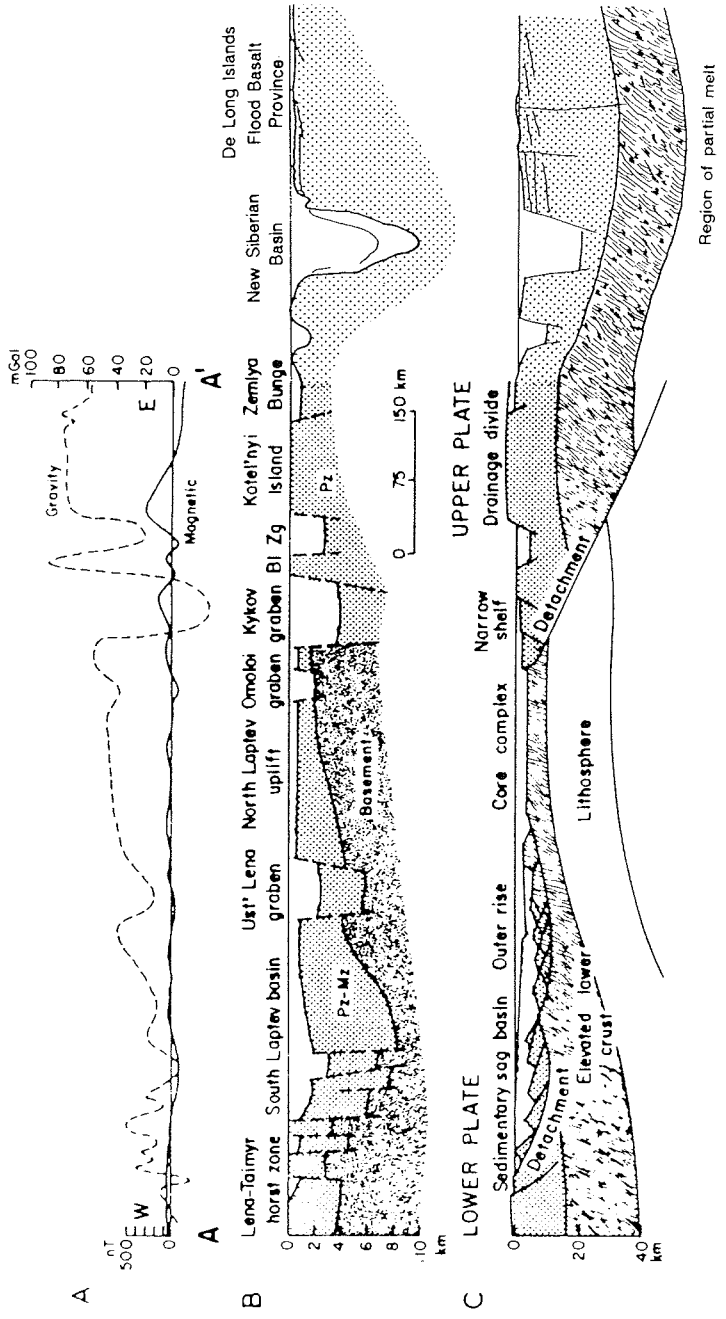

Fig. 6: Crustal section across the Laptev Sea from Fujita et. al. (1990); extended eastward to include the New Siberian Basin and the De Long Island flood basalt province; the flood basalt province lies above the inferred zone of partial melt.

On the Laptev shelf the crustal extension is distributed over several basins. The production of new surface (not new crust!) is not restricted to a well-defined ridge axis. Instead it occurs "diffusely" over several basins. From all these observations we conclude that seafloor spreading is impossible at total spreading rates below 0.7 cm/year. However, this number may depend also on the type of crust which is exposed to extension, and the amount of magma available. From the Red Sea we know that the process of spreading can vary in a wide range (Cochran & Martinez, 1988).

Although a great deal of work remains to be done to fully evaluate the seismic data acquired during the cruises in 1993 and 1994, we feel that our new results considerably improve the knowledge on the crustal architecture of the Laptev shelf area.

References

Cochran, J.R. & Martinez, F., 1988. Evidence from the northern Red Sea on the transition from continental to oceanic rifting.- Tectonophysics 153, 25-53.

Drachev, S.S., (1994): The Laptev Sea drilling plans.- Bericht, 49 S.

Fujita, K., Cambray, F.W. & Velbel, M.A., (1990): Tectonics of the Laptev Sea and Moma Rift systems, northeastern USSR.- Marine Geology 93, 95-118.

Fujita, K. & Cook, D.B., (1990): The Arctic continental margin of eastern Siberia.- In Grantz, A., Johnson, L. & Sweeney, J.F. (eds.): The Arctic Ocean region, The Geology of North America, v. L., 289-304.

Fütterer, D.K. (ed.), (1994): Die Expedition ARCTIC '93. Der Fahrtabschnitt ARK-IX/4 mit FS POLARSTERN 1993.- Berichte zur Polarforschung 149, 244 S.

Grantz, A., Johnson, L. & Sweeney, J.F., (eds.) (1990): The Arctic Ocean region, The Geology of North America, v. L.- GSA, 654 S.

Kogan, A.L., (1974): Staging seismic work of the CRWS-DSS method on oceanic ice on the shelves of Arctic seas (experimental work in the Laptev Sea).- Geofiz. Metody Razved Arkt. 9, 33-38.

Kristoffersen, Y., (1990): Eurasia Basin.- In Grantz, A., Johnson, L. & Sweeney, J.F. (eds.): The Arctic Ocean region, The Geology of North America, v. L., 365-378.

Lister, G.S., Etheridge, M.A. & Symonds, P.A., (1986): Detachment faulting and the evolution of passive continental margins.- Geology 14(3), 246-250.

Okulitch, A.V, Lopatin, B.G. & Jackson, H.R., (1989): Circumpolar geological map of the Arctic, Geological Survey of Canada, Map 1765A, scale 1 : 6 000 000.

Vinogradov, V.A., (1984): Laptev Sea.- In Gramberg, I.L. & Pogrebitskii, Y.E. (eds.): Geologic structure of the USSR and its relationship to the distribution of mineral resources.- Vol. 9, Seas of the Soviet Arctic, Nedra, Leningrad, 51-60.

THE AIM OF PLANNED GEOLOGICAL ON-SHORE INVESTIGATIONS ON THE NOVOSIBIRIAN ISLANDS WITHIN THE PROJECT "CORRELATION OF CIRCUM-ARCTIC ALPINE STRUCTURAL EVENTS" (CASE)

H.-J. Paech
Bundesanstalt für Geowissenschaften und Rohstoffe, Hannover, Germany

The Federal Institute for Geosciences and Natural Resources (BGR) plans an international joint German-Russian/Yakutian expedition to the Novosibirian Islands (CASE-3) for field observations of phenomena associated with Alpidic structural events (CASE = Correlation of Circum-Arctic Structural Events). These on-shore plans must be seen in connection with off-shore activities carried out 1993 (see ROESER present volume) and 1994. CASE-3 will be focussed on the continuation of adequate tectonical investigations on-shore in Spitsbergen (CASE-1) and North Greenland (CASE-2). Here, the objective has been the characterization of Alpidic compressive movements and the associated palaeogeothermal regime. The most important results can be summarized as follows: The movements during Alpidic structural events attained high intensity causing considerable tectonical shortening with formation of nappes in fold-and-thrust belts or narrow deformation strips, which have the same transport direction in Spitsbergen and Northern Greenland. The same vergency in both regions conflicts with an interpretation of simple transpression. On the base of palaeogeothermal data it can be concluded, that here the Alpidic events of Tertiary age occurred under hyperthermal conditions.

In general, in circum-Arctic regions compressive structures of Alpidic age are widespread. But hitherto no plausible explanation of the paradoxon could be found: centrifugal compression in peripheral regions versus coeval bilateral spreading in central parts of the Arctic Ocean. An interpretation of all these compressive structures as caused by transpression is impossible. For conclusive explanation more detailed geological observations are needed in further regions, including the Novosibirian Islands. In preparation of the CASE-3 expedition the literature data has been analyzed and a short history description of the study area will be given below.

The geotectonical history of the Novosibirian Islands and adjacent regions in Mesozoic and Cenozoic times is characterized by changing of compression versus dilatation. It will be outlined very roughly using the sketch maps in Figures 1a and 1b which are based on numerous literature data scattered in Soviet and in recent times in joint Russian/foreign publications.

Compressive processes of Jurassic age are known from the Taymyr Peninsula and the Verkhoyanski Khrebet where the main deformation continued in early Cretaceous time as known also from the Novosibirian Islands. In this period intrusion and extrusion of acid magma were typical. Furthermore, ophiolite-like magmatic associations occurred. Possibly in early Cretaceous time the rifting started evidenced in graben-like structures filled with coal-bearing sediments. No doubt exists on the rifting processes in late Cretaceous time which continued in the entire Cenozoic period. In that time, the alternating change of compression and extension is evident. It can not be explained by rotation of tectonical plates due to the wide distribution. Mostly, the Tertiary compression can be assigned to Palaeogene times. Within the continent, in the Moma Rift also Neogene sediments have been included. Here even Quaternary volcanism was present. Compressive structures are not confined to Tertiary sequences. Underlying units even of Carboniferous age were effected, too, and thrust onto Tertiary sequences. Hitherto

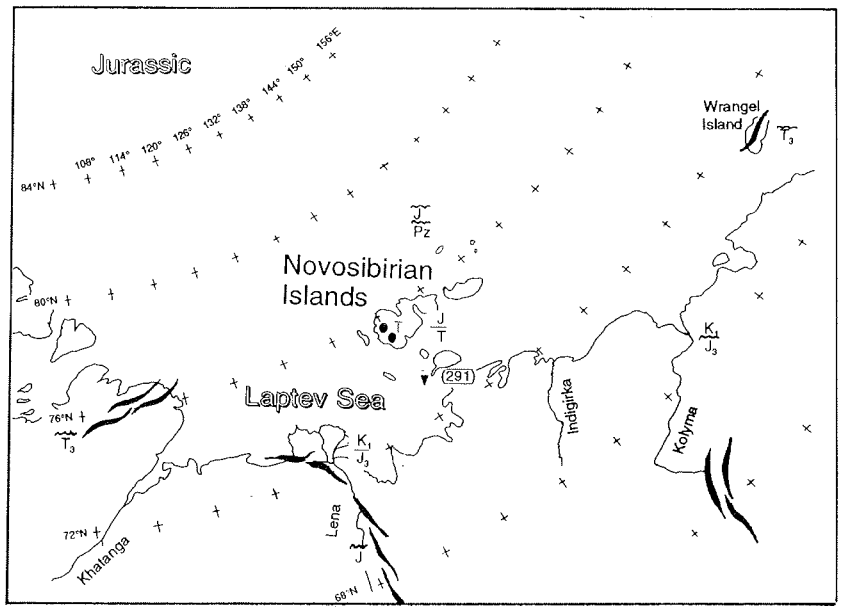

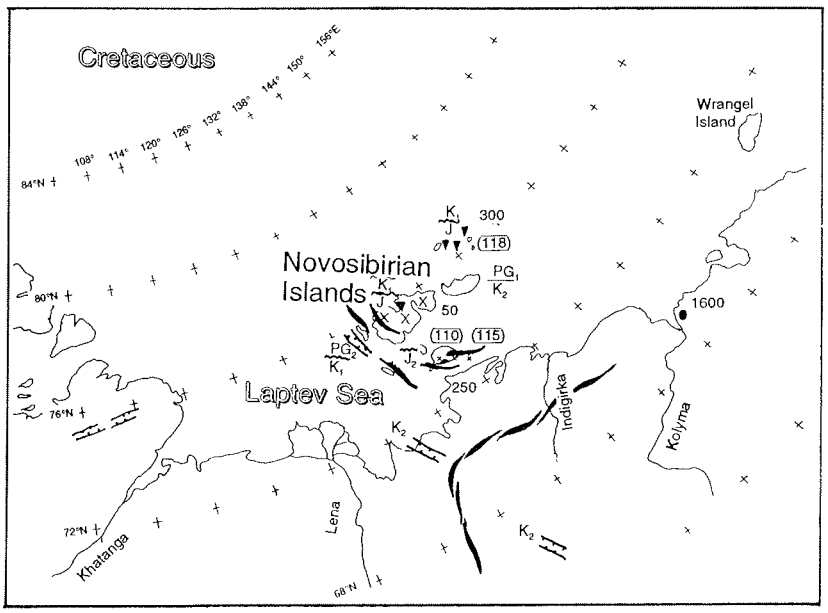

Fig.1a: Palaeotectonical sketch maps compiled on the basis of literature data mentioned selectively in the references. (Symbols: Pz - Palaeozoic, T - Triassic, K - Cretaceous, PG_1 - Paleocene, PG_2 - Eocene, N - Neogene, Q - Quaternary)

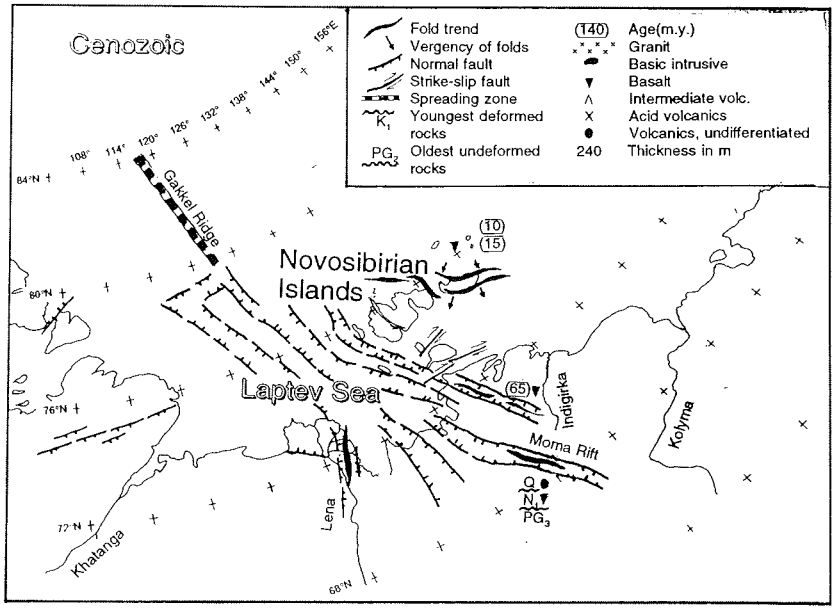

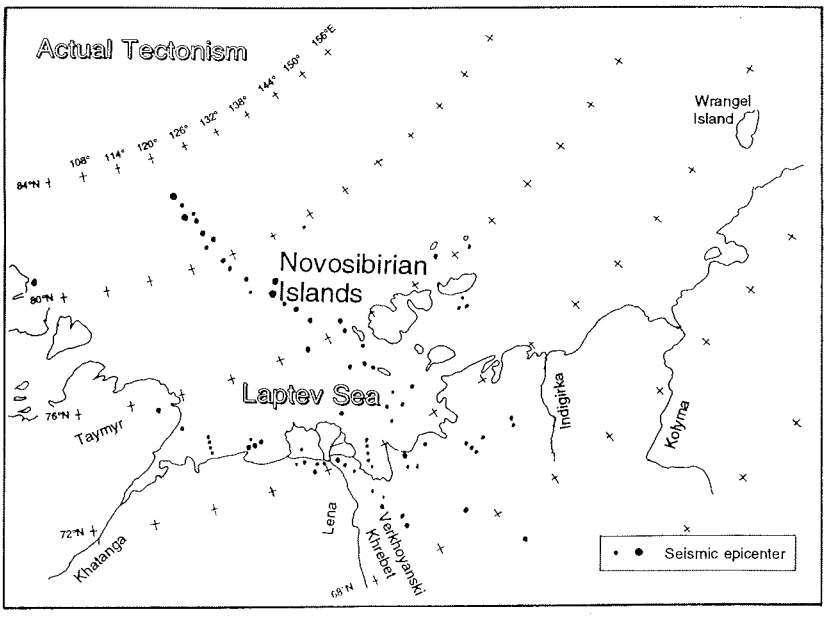

Fig.1b: Palaeotectonical sketch maps compiled on the basis of literature data mentioned selectively in the references. (Symbols: Pz - Palaeozoic, T - Triassic, K - Cretaceous, PG_1 - Paleocene, PG_2 - Eocene, N - Neogene, Q - Quaternary)

the appearance of compressive structures of Tertiary age is genetically not understandable. The actual tectonical regime is characterized by high seismicity which can be traced in two branches. One follows the Gakkel Ridge and continues onto the shelf of the Laptev Sea. The other can be traced along the Lena delta in NW direction. Within the continent the earthquakes are not confined to the graben structures but to the adjacent horsts.

The CASE-3 Expedition will be adressed to tectonical structures within the entire sedimentary pile effected by Alpidic deformations, particularly the Cenozoic sequences. It includes documentation of tectonical structures with respect to compressive but also to extensional deformations and their kinematical interpretation. Furthermore, the palaeogeothermal conditions will be characterized by coal rank and determination of illite crystallinity data.

References

- Used particularly for the compilation of the figure -

Avetisov, G. P. (1991): Gipocentriya i fokal'nye mekhanismy zemletryasenij del'ty r.Leny i ee obrambleniya. Vulkanologiya i seysmologiya, 6, 59-69, Moskva.

Bogdanovskiy, O. G.; Mineyev, S.D.; Assonov, S.S.; Silant'ev, S.A. et al. (1992): Magmatizm arkhipelaga De-Longa (Vostochnaya Arktika): geokhimiya izotopov i geokhronologiya. Geokhimiya 1992, 1, 47-56, Moskva.

Drachev, S. S.; Savostin, L.A. (1993): Ofiolity ostrova Bol'shogo Lyakhovskogo (Novosibirskie ostrova). Geotektonika 1993, No.3, 98-107, Moskva.

Fujita, K.; Cambray, F.W.; Velbel, M.A. (1990): Tectonics of the Laptev Sea and Moma rift system, northeastern USSR. Marine Geology, 93, 1/4, 96- 118, Amsterdam.

Grachev, A. F. (1982): Geodynamics of the transitional zone from the Moma rift to the Gakkel ridge. In: Watkins, J.S.; Drake, C.L. (eds.), Studies in Continental margin geology. Am. Ass. Petrol. Geol. Mem. 34, 103-113, Tulsa.

Gramberg, I. S.; Demenitskaya, R.M.; Sekretov, S.B. (1990): Sistema riftogennykh grabenov shel'fa morya Laptevykh kak nedostayushchnogo zvena riftovogo poyasa khrebta Gakkelya-Momskogo rifta. Dokl. Akad. Nauk, 311, 3, 689-694, Moskva.

Gramberg, I. S.; Pogrebitsky, Yu. E. (eds.) (1984): Morya sovetskoy Arktiki. In: Geologicheskoe stroenie SSSR i zakonomernosti razmeshcheniya poleznykh iskopaemykh, tom 9, 280 pp. Leningrad.

Gramberg, I. S.; Shulgina, N. I. (1992): Geologicheskaya istoriya Arktiki v mezozoe i kajnozoe. VNIIOkeangeologiya Kniga 1 117 pp, St. Petersburg.

Imaev, V. S.; Grinenko, O. V. (1989): Pozdnekaynozoyskie dadvigi, vzbrosy i skladchatye dislokacii Vostochnoy Yakutii. Dokl. AN SSSR 1989, 307, 2 413-417, Moskva.

Koz'min, B. M. (1986): Seismicheskie poyasa Yakutii i mekhanismy ochagov ikh zemltryasenii. Nauka, 126 pp, Moskva.

Lazurkin, D. V.(1992): More Laptevykh. In: Atlas paleogeograficheskikh kart shel'fy Evrazii v mezozoe i kajnozoe, Tom 1, S. Karty 1-1 to 1-25, 1:7.500.000 und 5.000.000, Moskva.

Mokshantsev, K. B. et al. (1975) Tektonika Jakutii. AN SSSR, Sib. Otd. 196 S., Novosibirsk.

Pogrebitsky, Yu. E. (1984): Svyaz' sovremennoy struktury s glubinnym stroeniem zemnoy kory. In: Gramberg, I. S.; Pogrebitsky, Yu. E. (eds.) Geologicheskoe

stroenie SSSR i zakonomernosti razmeshcheniy poleznykh iskopaemykh. Tom 9 Morya sovetskoy Arktiki. Nedra, 107-111, Leningrad.

Pol'kin, Y. A. (Ed.) (1992): Laptev, East Sibirian and Chuktchi Seas. In: Atlas paleogeograficheskikh kart shel'fy Evrazii v mezozoe i kajnozoe, Tom 1, S. Karty 1-1 to 1-25, 1:7.500.000 und 5.000.000, Moskva.

Savostin, L. A.; Drachev, S. S. (1988): Kaynozoyskoe szhatie v rayone Novosibirskich ostrovov i ego svyas' s raskrytiem evraziyskogo basseyna. Okeanologiya XXVII, vyp. 5, 775-782, Moskva.

Sekretov, S. B. (1992): Tectonics of Eurasian basin in the zone of its junction with Laptev Sea continental margin. Tezisy dokladov 10. mezhdonarodnoy shkoly morskoy geologii, tom 4, 114-115, Moskva.

Silant'yev, S. A.; Bogdanovskiy, O. G.; Savostin, L. A.; Kononkova, N. N. (1991): Petrologiya i petrokhimiya effuzivnykh porod i assotsiiruyushchikh s nimi ksenolitov (ostrova Zhokhova i Vil'kitskogo). Geokhimiya 1991, 2, 267-277, Moskva.

Trufanov, G. V.; Vakulenko, A. S. (1978): Eotsenovye uglenosnye otlozheniya na Novosibirskikh ostrovakh. Geologiya i geofizika Nr. 4, 135-137, Moskva.

Vinogradov, V. A. (1984): More Laptevykh. In: Gramberg, I. S.; Grebovitsky, Yu. E. (eds.): Geologicheskoje stroenie SSSR i zakonomernosti razmeshcheniya poleznykh iskopaemykh, Tom 9 Morya sovietskoy Arktiki, 50-60, Leningrad.

THE GEOLOGICAL STRUCTURE OF THE LAPTEV SHELF AND ADJACENT PARTS OF THE EURASIAN SUBBASIN (IN THE CONTEXT OF PLANNED DRILLING)

V. I. Kim and V. V. Verba
VNIIOkeangeologia, St. Petersburg, Russia

The Laptev Sea shelf is located on the Eurasian oceanic subbasin where the mid-oceanic Gakkel Ridge (complicated by a rift valley), the Nansen and the Amundsen basins join with structures of the Laptev plate. The solution of problems as the interconnection of these structures, the evolution of their geological and tectonic structure, the time of their origin, the influence of rifting processes on the shelf structure as well as the handling of many other questions closely depend on a right strategy of drilling planned both on the shelf and in deep-sea parts of the ocean. In connection with these questions let us briefly review the main geological results of investigations with the aim of determining the location of wells and the objectives which must be gained by testing drilling.

Tectonic zonation

By a classification of tectonic structures, the Laptev shelf is determined as marginal continental plate. Epikarelian complexes of the Siberian platform extend to the western and central parts of the Laptev shelf. The sedimentary cover is represented here by Riphean-Cenozoic formations. The eastern platform margin on the shelf is established by the results of multichannel seismic profiling (Ivanova et al.,1989) and is confined to the suture fault zone within the Omoloy graben. The extinct branch of the Verkhoyan-Kolyma fold system, developed in the coastal zone, has the character of an intraplatform.

The eastern part of the shelf consists of Late Cimmerian fold systems: the Verkhoyan-Kolyma and the Novosibirsk systems as well as the Rauchua-Oloi system dividing the former ones and wedging out (Rusakov et al.,1969). The first two systems can be characterized as a miogeosyncline, the third one as an eugeosincline. Besides, on the south-eastern shelf, the buried Berelyekh geoanticline divides the Verkhoyan-Kolyma and the Rauchua-Oloy systems. The sedimentary cover in this part of the shelf belongs to Upper Cretaceous formations, but the existence of Albian deposits within the negative structure cannot be ruled out.

The western part of the shelf and the adjacent coastal zone of north-eastern Taymyr are composed of a middle-Proterozoic granite-metamorphic complex and an Early Cimmerian fold over-geosyncline complex. Its distribution on the shelf is extremely insignificant and is controlled by the fault system confined to the western continental slope of the Eurasian subbasin. On the shelf, these complexes lie beneath Jurassic-Cenozoic sedimentary cover.

The structure and thickness of the sedimentary cover

The Laptev plate structures have a heterogeneous basement. The upper Cretaceous-Cenozoic structural complex, the formations of which occur universally, is common to the plate. The maximum thickness of the sedimentary cover in the western and central parts of the shelf amounts upt to 12 km (its Riphean-Lower Cretaceous part accounts for 4-7 km) and in the eastern up to 5.4-6.6 km. The structural map compiled for the sedimentary cover base indicates that its thickness

in the South-Laptev basin accounts for 12 km. In the Ust´-Lena and the Omoloy grabens (in the western part of the Buor-Haya Bay) it runs up to 11-12 km, while in the Central Laptev and the Trofimov height as well as in the Minin bar it accounts for 8.7 and 6 km, respectively (Ivanova et al., 1989).

It has been established than the Omoloy graben is the natural structural continuation of the Gakkel Ridge rift valley on the shelf (Kim, 1986). In the northern part of the shelf, it was formed at the junction of the Siberian platform and Mesozoic folds. In the central and southern parts it is superimposed both on platform and fold structures, whereas only in the extreme south it is completely superimposed on Mesozoic fold structures.

The structural maps compiled for the base of upper Cretaceous, Neogene and Pliocene deposits have revealed the relationship between the thickness distribution and the structure (grabens, uplifts, depressions) that testifies to the inherited character of the first-order structures development. Before the maps were compiled, a scheme of main reflectors and their correlation with known sections of the coastal and island surroundings had been prepared (Kim 1994).

The maximum thickness of Upper Cretaceous-Cenozoic deposits within the Laptev plate accounts for 6.6 km the maximum thickness of Upper Cretaceous deposits being 2 km, that of Cenozoic 4.6 km. The maximum thickness of Paleogene deposits is 2.6 km, of Miocene deposits 1.5 km, and of Pliocene-Quaternary deposits 1.3 km. According to data of high-resolution profiles, the thickness of the Quaternary deposits does not exceed 70-100 m.

In the Ust´-Lena graben, the thickness of Upper Cretaceous-Cenozoic deposits accounts for 5.4 km, in the Omoloy graben it is 4.5 - 6.6 km. In the Anisin graben it amounts up to 5.5 km, in the Chondon graben 3.5 and in the Bel'kov -Svyatonoskiy fault-attached trough 4 - 5.5 km. The minimum thickness of these deposits on the Central-Laptev height accounts for 2 km, the East-Laptev height 0.5 - 1 km, the Berelyekh height - 0.5 1 km, the Trofimov height 1.2 km. Within the Lena-Taymyr zone of marginal uplifts, the thickness of these deposits accounts for 0.1 - 0.5 km.

Judging by their peculiar structure, the Ust´-Lena and Omoloy grabens as well as the Bel'kov-Svyatonoskiy fault-attached trough seem to represent the continuations of the main negative structures of the Eurasian subbasin (the Nansen and Amundsen basins, the Gakkel Ridge rift valley) on the Laptev shelf. Their rifting nature is evident from a number of indications and features: the linearity and the total length of the structures (from 500 to 800 km) highly exceeding their width (from 20-25 to 50-60 km); the fault character of their margins expressed by the faults; the fill of grabens and depressions (the fill); the character of seismicity (surface and subsurface earthquakes) and its linearity ; the "M" surface rising within their limits up to 26-28 km. The formation of these structures is directly connected with the effect of the "continent-to-ocean" processes on the closing of the Eurasian basin.

The structural map of the sedimentary cover of the adjacent deep-sea part of the Eurasian subbasin (between 77° and 80° N) enables us for the first time to trace the junction of the shelf and oceanic structures, evaluating the role of fault dislocations in their formation and determining the thickness of the sediments. The thickness of the Upper Cretaceous-Cenozoic deposits on the western and eastern sides of the Gakkel Ridge (at its southern end) account for 3-4 and 2-3 km, respectively. The western side of the Ridge is observed along the strike up to 77° 30´ N. The eastern side is truncated by transform faults at 70° N, southward of which a marginal shelf trough of north-eastern orientation is established. In the rift zone, dislocated by transform faults and complicating the Gakkel Ridge, the thickness of sedimentary cover varies from 4 to 6.5 km. On the southern closing, the Nansen basin consists of two large coulisse-shaped depressions with a sediment thickness of up to 7-8

km; on the southern closing of the Amundsen basin the thickness of the sedimentary cover amounts to 4-5 km.

Seismicity

The data on the Laptev Shelf seismicity allow to distinguish four seismoactive zones and to correlate three of them with rift structures of the plate (Kim, 1994).

The first zone is distinguished within the coastal part and is confined to the Olenek aulacogen on its junction with the linear structure of the Lena-Taymyr marginal uplifts.

The second zone is virtually parallel to the first one and is on the shelf confined to the Ust´-Lena and the Ust´-Yana grabens. Near the eastern end of Taymyr Peninsula both zones merge together extending north-westward as a single zone confined to the western continental slope of the Eurasian subbasin.

The third zone is associated with the Omoloy graben and represent the continuation of the seismoactive zone, confined to the Gakkel Ridge rift valley, on the shelf.

The fourth zone has developed in the eastern part of the shelf and is traced from the northern end of Kotelny´y island to the southern end of the Bel'kovskiy island where it branches. The eastern part of the zone is confined to the eastern border of the Bel'kov-Svyatonoskiy fault-attached trough, the western has a meridional strike and reaches the Yana river delta. In the ocean its continuation is represented by a fragmentarily distinguished seismoactive zone associated with western continental slope of the Lomonosov Ridge.

Scientific problems

The analysis and interpretation of seismic profiles suggest that the formation of rift stuctures on the Laptev Shelf took place at the beginning of the Late Cretaceous and that the rift structures were mainly filled with Upper Cretaceous deposits. The complete fill of the graben was virtually finished at the end of Miocene. In this context, the time of origin of the Eurasian subbasin can hardly be assigned to the beginning of the Cenozoic as it accepted at present time. Most likely, it is Late Cretaceous or a bit older. Marine Cenomanian sediments with a visible thickness of 40-45 m found on Hofman Island (Franz Jozef Land, at the margin with western continental slope of the Eurasian subbasin) may serve as an indirect evidence of this conclusion. There, N. I. Shulgina has determined the remains of the ammonite *Schloenbachia aff. subvarian Spath.* which is abundant in the sublittoral zone at depths of 150-200 m, i.e. at the shelf edge. This species characterizes the "Varians" zone in Eastern Greenland which is there assigned to Lower Cenomanian.

Seismic works carried out by German and Russian scientists on the Lomonosov Ridge and Amundsen basin allow to establish that complete sedimentary cover section of small thickness (350-600 m) occur in the "pockets" and small grabens on the Lomonosov Ridge slopes (close to its near-dome part). A sharp wedging out of the reflectors and basement uplift occurs towards the Lomonosov Ridge. The depths where these zones have been observed do not exceed 1 - 1.3 km. The interpretation of the multichannel seismic profiling has led many scientists to the conclusion that the stratigraphic volume of sediments within the above-mentioned negative structures is not beyond the limits of Upper Cretaceous-Cenozoic. This permits the suggestion that the formation of the Amundsen basin (and, consequently, of the entire Eurasian subbasin) took place in Late Cretaceous (Jokat, 1994).

By analyzing the anomalous magnetic field (AMF) of the Eurasian basin it has been stated that it is the specific low-graident, weakly intensive field of the Gakkel Ridge which is the central part or the axis of symmetry for this system. Values of (ΔT), not exceeding 500 nTl, are characteristic of it and of adjacent basins. The dominant values of the magnetic field are $\pm$200 nTl. This feature distinguishes the Gakkel Ridge from parts of North Atlantic mid-oceanic ridge (except the Knipovich Ridge which also characterized by the low values of the magnetic field). An explanation of this feature is still not found. The suggestion, that it is caused by the reducing of the remnant magnetization with time which has a leading role in the formation of "spreading" anomalies results in the conclusion that linear anomalies of the Eurasian basin are older than 50 - 60 Ma (Verba et al., 1986).

The discussion of the above data raises the problem of the age correlation of linear magnetic anomalies of the Eurasian subbasin determined according to the Lamont scale.

Strategy of the drilling

The drilling strategy consists in collecting sections of the same age (Upper Cretaceous - Cenozoic deposits) both on the shelf and in the deep-sea part of the Eurasian subbasin for the subsequent analysis. It is determined by one purpose: to trace the evolution and interconnection of geological and tectonic development of the shelf and oceanic structures originated from the synoceanic stage. The drilling tactics consist in determining such zones on the Laptev shelf and in the Eurasian subbasin where these sections are can be recovered by drilling. The planned drilling includes two stages: drilling on the shelf and in the ocean.

For the Laptev shelf, a drilling along three profiles across the strike (Fig.1) is proposed taking into account the structural maps, which have been compiled, and those regions where Neogene - Quaternary deposits are absent. The first profile coincides with the seismic profile 86703 and the beginning of the seismic profile 90800. It extends from south-west to north-east. On this profile, the wells are planned to be drilled on the following structures: the South-Laptev basin, the Ust´-Lena graben, the Minin bar, the Central- and the East-Laptev heights, and the Anisin depression. The second profile coincides with seismic profile 247010 and is located in the central and eastern parts of the shelf. Along this profile, it is planned to located the wells at the southern end of Minin bar, on the East-Laptev height, the Omoloy graben, and the Bel'kov-Svyatonoskiy fault-attached trough. The third profile is situated in the south-eastern part of the shelf. The first well here is planned to be drilled in the eastern part of the Trofimov height (one from the islands on the north-eastern end of Lena delta), the second at the southern end of the Omoloy graben, and the third on the Berelyekh height. The two last wells are located on the seismic profiles. In the deep-sea part of the Eurasian subbasin, it is proposed to carry out the drilling within three zones which belong to the area where the Amundsen basin and the Lomonosov Ridge join. In this area, sedimentary formations are determined in lower depths (Fig.1). The first well is planned on the DSS - multichannel seismic profile which runs from the Makarov basin through the Lomonosov Ridge to the Amundsen basin. The second well is supposed to be located at the western end of the multichannel seismic profile carried out aboard RV "Polarstern" in 1991. The third well is planned in the zone where the Lomonosov Ridge and the seismic profile of the "North Pole - 28" ice-station intersect.

The analysis of the drilled wells will allow the solution of structural, stratigraphic, lithological, paleogeographic and other tasks and will also specify the stratigraphic correlation of the main reflectors within the sedimentary cover.

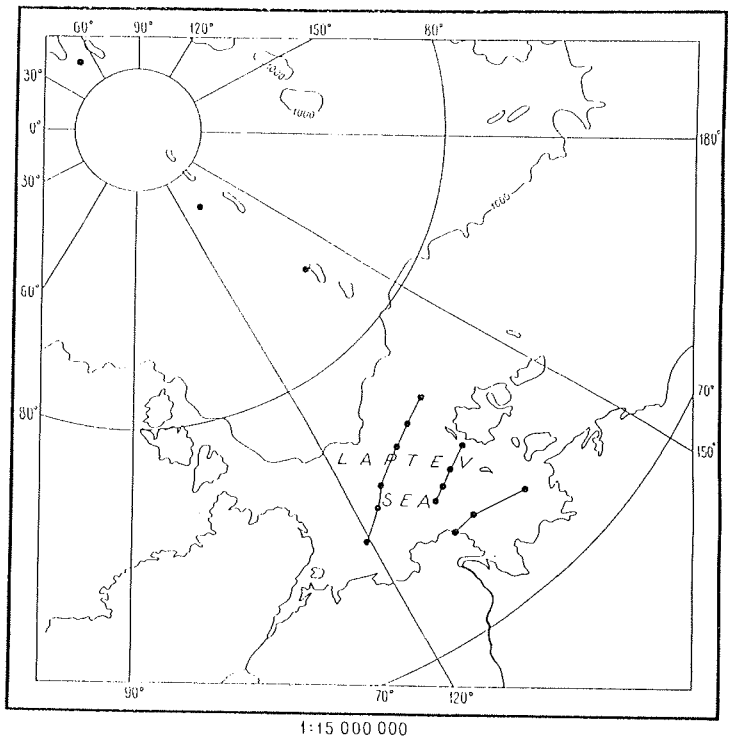

Fig. 1. Map of planned locations of wells on the Laptev Sea shelf and in the Eurasian basin.

References

Ivanova, N. M. et al., 1989. Data on geological structure of the Laptev Sea shelf by the data of seismic investigations. Oceanology, Vol. 29, N 5, p. 789-795.

Ivanova, N. M. et al., 1990. Structural complexes of the Laptev Sea shelf. (In Russian). Geology of the oceans and seas, Vol. 4. Abstracts of 9 All-Union School on marine geology, Moscow. p. 60-61.

Jokat, W., 1994. New results of geophysical studies in central Arctic and prospects of their development. (In Russian). Abstracts of VI. Conference on new achievements in marine geology. S.-Petersburg. p. 63-64.

Kim, B. I., 1986. Structural continuation of the Gakkel Ridge rift valley on the Laptev Shelf. (In Russian). In: Structure and history of development of the Arctic ocean, Leningrad, "Sevmorgeologia". p. 133-139.

Kim, B. I., 1994. New stratigraphic correlation of platform cover reflectors on the Laptev shelf. (In Russian). Abstracts of VI Conference on new achievements in marine geology, S.-Petersburg. p. 60-61.

Rusakov, I. M., Vinogradov, V. A., 1969. Eugeosynclinal and miogeosinclinal areas of the North-East of the USSR. (In Russian). Scientific notes of NIIGA. Regional Geology, Vol.5, p. 5-27.

Verba, V. V., 1986. Deep structure of the Arctic Ocean by the geophysical data. (In Russian). In: Structure and history of development of the Arctic Ocean, Leningrad, "Sevmorgeologia", p. 54-71.

Folgende Hefte der Reihe „Berichte zur Polarforschung" sind bisher erschienen:

* **Sonderheft Nr. 1/1981** – „Die Antarktis und ihr Lebensraum"
Eine Einführung für Besucher – Herausgegeben im Auftrag von SCAR

Heft Nr. 1/1982 – „Die Filchner-Schelfeis-Expedition 1980/81"
zusammengestellt von Heinz Kohnen

Heft Nr. 2/1982 – „Deutsche Antarktis-Expedition 1980/81 mit FS ‚Meteor'"
First International BIOMASS Experiment (FIBEX) – Liste der Zooplankton- und Mikronektonnetzfänge
zusammengestellt von Norbert Klages

Heft Nr. 3/1982 – „Digitale und analoge Krill-Echolot-Rohdatenerfassung an Bord des Forschungsschiffes ‚Meteor'" (im Rahmen von FIBEX 1980/81, Fahrtabschnitt ANT III), von Bodo Morgenstern

Heft Nr. 4/1982 – „Filchner-Schelfeis-Expedition 1980/81"
Liste der Planktonfänge und Lichtstärkemessungen
zusammengestellt von Gerd Hubold und H. Eberhard Drescher

* **Heft Nr. 5/1982** – "Joint Biological Expedition on RRS 'John Biscoe', February 1982"
by G. Hempel and R. B. Heywood

* **Heft Nr. 6/1982** – „Antarktis-Expedition 1981/82 (Unternehmen ‚Eiswarte')"
zusammengestellt von Gode Gravenhorst

Heft Nr. 7/1982 – „Marin-Biologisches Begleitprogramm zur Standorterkundung 1979/80 mit MS ‚Polarsirkel' (Pre-Site Survey)" – Stationslisten der Mikronekton- und Zooplanktonfänge sowie der Bodenfischerei
zusammengestellt von R. Schneppenheim

Heft Nr. 8/1983 – "The Post-Fibex Data Interpretation Workshop"
by D. L. Cram and J.-C. Freytag with the collaboration of J. W. Schmidt, M. Mall, R. Kresse, T. Schwinghammer

Heft Nr. 9/1983 – "Distribution of some groups of zooplankton in the inner Weddell Sea in summer 1979/80"
by I. Hempel, G. Hubold, B. Kaczmaruk, R. Keller, R. Weigmann-Haass

Heft Nr. 10/1983 – „Fluor im antarktischen Ökosystem" – DFG-Symposium November 1982
zusammengestellt von Dieter Adelung

Heft Nr. 11/1983 – "Joint Biological Expedition on RRS 'John Biscoe', February 1982 (II)"
Data of micronecton and zooplankton hauls, by Uwe Piatkowski

Heft Nr. 12/1983 – „Das biologische Programm der ANTARKTIS-I-Expedition 1983 mit FS ‚Polarstern'"
Stationslisten der Plankton-, Benthos- und Grundschleppnetzfänge und Liste der Probennahme an Robben und Vögeln, von H. E. Drescher, G. Hubold, U. Piatkowski, J. Plötz und J. Voß

* **Heft Nr. 13/1983** – „Die Antarktis-Expedition von MS ‚Polarbjörn' 1982/83" (Sommerkampagne zur Atka-Bucht und zu den Kraul-Bergen), zusammengestellt von Heinz Kohnen

* **Sonderheft Nr. 2/1983** – „Die erste Antarktis-Expedition von FS ‚Polarstern' (Kapstadt, 20. Januar 1983 – Rio de Janeiro, 25. März 1983)", Bericht des Fahrtleiters Prof. Dr. Gotthilf Hempel

Sonderheft Nr. 3/1983 – „Sicherheit und Überleben bei Polarexpeditionen"
zusammengestellt von Heinz Kohnen

Heft Nr. 14/1983 – „Die erste Antarktis-Expedition (ANTARKTIS I) von FS ‚Polarstern' 1982/83"
herausgegeben von Gotthilf Hempel

Sonderheft Nr. 4/1983 – "On the Biology of Krill *Euphausia superba*" – Proceedings of the Seminar and Report of the Krill Ecology Group, Bremerhaven 12.–16. May 1983, edited by S. B. Schnack

Heft Nr. 15/1983 – "German Antarctic Expedition 1980/81 with FRV 'Walther Herwig' and RV 'Meteor'" – First International BIOMASS Experiment (FIBEX) – Data of micronekton and zooplankton hauls
by Uwe Piatkowski and Norbert Klages

Sonderheft Nr. 5/1984 – "The observatories of the Georg von Neumayer Station", by Ernst Augstein

Heft Nr. 16/1984 – "FIBEX cruise zooplankton data"
by U. Piatkowski, I. Hempel and S. Rakusa-Suszczewski

Heft Nr. 17/1984 – „Fahrtbericht (cruise report) der ‚Polarstern'-Reise ARKTIS I, 1983"
von E. Augstein, G. Hempel und J. Thiede

Heft Nr. 18/1984 – „Die Expedition ANTARKTIS II mit FS ‚Polarstern' 1983/84",
Bericht von den Fahrtabschnitten 1, 2 und 3, herausgegeben von D. Fütterer

Heft Nr. 19/1984 – „Die Expedition ANTARKTIS II mit FS ‚Polarstern' 1983/84",
Bericht vom Fahrtabschnitt 4, Punta Arenas–Kapstadt (Ant-II/4), herausgegeben von H. Kohnen

Heft Nr. 20/1984 – „Die Expedition ARKTIS II des FS ‚Polarstern' 1984, mit Beiträgen des FS ‚Valdivia' und des Forschungsflugzeuges ‚Falcon 20' zum Marginal Ice Zone Experiment 1984 (MIZEX)"
von E. Augstein, G. Hempel, J. Schwarz, J. Thiede und W. Weigel